

Reconstructing the Arsenical Copper Production Process in Early Bronze Age Southwest Asia

Loïc C. Boscher

Thesis submitted to
University College London

For the degree of
Doctor of Philosophy (PhD)



UCL Qatar

November 2016

I, Loïc Boscher, confirm that the work presented in this thesis is my own. Where information has been derived from other sources, I confirm that this has been indicated in the thesis.

Date:

Signed:

Abstract

As the dominant alloy in much of the Old World for several millennia between in the Late Chalcolithic and Bronze Ages, surprisingly little work has been undertaken to understand how arsenical copper was produced and what led to its ubiquitous appearance in the archaeological record. Since arsenic and copper mineralizations often occur paragenetically, and due to the proximity of such deposits to a number of early production centres, it has often been assumed that the dominance of the alloy at the time was simply the result of the serendipitous smelting of widely available polymetallic ores. This thesis questions this narrative as overly simplistic and offers new evidence of intentional and advanced alloying techniques predating the rise of tin bronzes by several centuries.

The archaeometric study of metallurgical remains from two recently excavated sites is used as the basis for the reconstruction of arsenical copper's *chaînes opératoires*. The sites are Çamlıbel Tarlası in Central Turkey, dating to the mid-fourth millennium BC, and Arisman in West Central Iran, dating to the late fourth to early third millennium BC. The material under study consists of the full gamut of metal production remains, including ore minerals, crucibles, furnaces, slag, and finished objects, all of which were microscopically and compositionally characterised using optical microscopy and SEM-EDS. Other techniques, such as pXRF, EPMA, and ICP-MS were also employed to answer specific questions and in situations where the benchtop instruments were unsuitable.

The overall aim of the thesis was first and foremost to evaluate ways in which arsenical copper was produced. The results demonstrate unequivocally that both naturally occurring and synthetically produced arsenic minerals were alloyed with copper in stages entirely separate from smelting. These findings are then contextualised within the wider large scale societal developments occurring at the onset of the Bronze Age by looking at the impacts of these technological innovations on the emergence of settlement specialization, the organisation of labour, and wider networks of knowledge transfer and sharing.

Table of Contents

Abstract	3
Table of Contents	4
List of Figures.....	7
List of Tables.....	20
Acknowledgments	24
Chapter 1 A Contentious Alloy	26
1.1 Introduction.....	26
1.2 Current problems in our understanding of arsenical copper.....	29
1.3 Archaeometallurgy as Socio-economic and Cultural Interpretative Tool	34
1.4 Use of Production Remains in the Reconstruction of the Metallurgical Process.....	36
1.5 Aims of the Research.....	37
Chapter 2 Arsenical Copper Material Properties	39
2.1 Physical Properties	39
2.2 Casting Properties	41
2.3 Mechanical Properties.....	42
2.4 Volatility	45
2.5 Toxicity	48
2.6 Corrosion	51
Chapter 3 Arsenical Copper Production and Use.....	53
3.1 Production Technology, in Theory and Practice.....	53
3.1.1 Reduction of Copper Arsenates	53
3.1.2 Co-smelting of Copper Oxides with Copper Sulfarsenides.....	54
3.1.3 Co-smelting of Copper Oxides with Iron Arsenides or Sulfarsenides.....	55
3.1.4 Copper Arsenides or Arsenates to Molten Copper	56
3.1.5 Speiss.....	58
3.1.6 Interpretative Dilemma.....	60
3.2 Late Chalcolithic and Early Bronze Age Use	63
3.2.1 Origins of Metallurgy with Comments on Colour	63
3.2.2 Late Chalcolithic Innovations and Arsenical Copper Production	67
3.2.3 Onset of the Early Bronze Age.....	80
Chapter 4 Çamlıbel Tarlası.....	85
4.1 Geographic and Geological Context.....	85
4.2 Archaeological Context.....	87

4.2.1 Chronology	87
4.2.2 Çamlıbel Tarlası I	88
4.2.3 Çamlıbel Tarlası II	89
4.2.4 First Phase of Ephemeral Use (FPEU).....	91
4.2.5 Çamlıbel Tarlası III	91
4.2.6 Second Phase of Ephemeral Use (SPEU).....	93
4.2.7 Çamlıbel Tarlası IV	93
4.3 Previous and Related Research.....	95
Chapter 5 Arisman	96
5.1 Geographic and Geological Context.....	96
5.2 Archaeological Context	100
5.2.1 Chronology	100
5.2.2 Arisman I Area B.....	102
5.2.3 Arisman I Area D	103
5.2.4 Arisman I Area C.....	104
5.2.5 Arisman I Area A.....	105
5.2.6 Arisman I Area E	107
5.3 Previous and Related Research.....	108
Chapter 6 Methodology	110
6.1 Sampling Strategy	110
6.2 Optical Microscopy	111
6.3 Scanning Electron Microscopy – Energy Dispersive Spectrometry (SEM-EDS)	112
6.4 Portable Hand-held X-Ray Fluorescence (pXRF)	116
6.5 Multicollector Inductively Coupled Plasma Mass Spectrometry (ICP-MS)	116
Chapter 7 Analytical Results	119
7.1 Çamlıbel	119
7.1.1 Assemblage	119
7.1.2 Crucibles.....	122
7.1.3 Furnace Lining.....	132
7.1.4 Other Metallurgical Ceramics	136
7.1.5 Ores and Tailings.....	145
7.1.6 Slag.....	153
7.2 Arisman	200
7.2.1 Assemblage	200

7.2.2 Technical Ceramics	202
7.2.3 Ores and Tailings	218
7.2.4 Slag	221
Chapter 8 Lead Isotope Analysis	253
8.1 Arisman.....	253
8.2 Çamlıbel.....	256
Chapter 9 Discussion	271
9.1 <i>Chaînes Opératoires and Site Comparison</i>	271
9.1.1 Çamlıbel.....	271
9.1.2 Arisman.....	278
9.2 Changes in Production Technologies	289
9.3 Settlement Specialization	296
9.4 Arsenical Copper Alloying in the Southwest Asian Context	298
9.5 Iron in Copper.....	303
Chapter 10 Conclusions and Future Work	306
References.....	313
Appendices	336
Appendix A SEM-EDS Analysis of CRMs and RMs	336
Basalt	336
Metal	337
Appendix B Camlıbel.....	338
B.1 Technical ceramics	338
B.2 Bowl hearths	340
B.3 Other metallurgical ceramics	341
B.4 Slags.....	343
B.5 Copper prills in slag	350
B.6 Ore minerals and tailings	351
B.7 Lead isotopes.....	353
B.8 Objects	354
Appendix C Arisman	355
C.1 Technical ceramics	355
C.2 Minerals.....	359
C.3 Slags.....	360
C.4 Lead isotopes.....	371

List of Figures

Chapter 1

- Figure 1.1 Metallurgical chaîne opératoire extending beyond the deposition into the archaeological record (from Ottaway 2001). 35

Chapter 2

- Figure 2.1 Cu-As equilibrium phase diagram, after Subramanian and Laughlin (1988)..... 40
- Figure 2.2 Diagram of the effect of cold working on hardness of both Cu-As and Cu-Sn (after Lechtman 1996, p. 496)..... 44
- Figure 2.3 Increasing hardness of cold worked alloys with thickness reduced by 50% (after Lechtman 1996, p. 499)..... 44

Chapter 3

- Figure 3.1 Composition of Anatolian copper alloy objects according to period from Pulur, Yazılıkaya, Yortar, Tilmen, Kayapınarı, Horoztepe, Tarsus, Beycesultan and Bayındırköy, İkiztepe, Tepecik, and Tülintepe (Cukur and Kunç 1989, 229). Each dot represents a single object which can be present in several rows. 81
- Figure 3.2 Copper and arsenical copper bull from Horoztepe. Photograph from the Oriental Institute of the University of Chicago. 82

Chapter 4

- Figure 4.1 View from the northwest of Çamlıbel Tarlası excavations at the end of a ridge overlooking the Karakeçili Dere Valley..... 86
- Figure 4.2 Calibrated dates for Çamlıbel (from Schoop et al. 2009)..... 88
- Figure 4.3 Foundation of granary structure, elevated to avoid moisture (from (Schoop 2010a)). 89
- Figure 4.4 Alternating ashy layers in CBT I phase (from (Papadopoulou and Bogaard 2013)). 89
- Figure 4.5 Top view of 'bowl furnace' feature 3 (from (Schoop 2010a)). 89
- Figure 4.6 Section of 'bowl furnace' feature 3 (from (Schoop 2010a))..... 89
- Figure 4.7 CBT II structure plan (From (Schoop 2010a)). 90
- Figure 4.8 Infant burial dating to CBT II uncovered beneath a habitation structure (From Schoop forthcoming). 90
- Figure 4.9 Plan of the 'burnt house' of CBT III. Note the series of ring hearths surrounding bone features in the north-eastern corner (from Schoop forthcoming). 92
- Figure 4.10 Photograph of the CBT III ritual features. In the centre is an arrangement of bones which is surrounded by several small hearths (from Schoop forthcoming). 92
- Figure 4.11 Photograph of terracotta ring-shaped figurine casting mould (Schoop 2009). 93

- Figure 4.12 Plan of CBT IV courtyard with oven in south-eastern corner (from Schoop 2009).....94
- Figure 4.13 Photograph of large domed oven with plaster base from the CBT IV courtyard (from Schoop 2009).94

Chapter 5

- Figure 5.1 Location of Arisman with Karkas Mountain range in the background and the excavation of Area C in the foreground along with topographic map. Topographic map from Chegini 2000, 285, and photograph from Chegini 2004, 212.98

Chapter 7

- Figure 7.1 Bar chart distribution of the metallurgical remains from secure contexts at Çamlıbel Tarlası by period.....120
- Figure 7.2 Numbers of metallurgical remains at Çamlıbel Tarlası by chronological period (normalized to 100%).....120
- Figure 7.3 Weight of slag and ores at Çamlıbel Tarlası by chronological period (normalized to 100%).120
- Figure 7.4 Photograph of residue layer of crucible 139-6312. Photograph courtesy of Ulf-Dietrich Schoop.123
- Figure 7.5 Photograph of crucible fragment 62-6450.124
- Figure 7.6 Photograph of crucible fragment 242-6470.124
- Figure 7.7 Photograph of Crucible 636-6459. This crucible showed no evidence of high temperature use and was identified as a crucible purely based on its shape and similarity to other more fragmentary objects. Photographs courtesy of Ulf-Dietrich Schoop.....124
- Figure 7.8 Drawing of crucible 139-6312. This crucible's inner surface was strongly vitrified and had several areas of green copper oxide corrosion growth. Due to its excellent preservation, it was deemed too valuable for destructive analysis Drawing by Edward Rayner.124
- Figure 7.9 Cross section of sample 242-6470 showing the various layers present in the CBT III and IV group of crucibles.125
- Figure 7.10 Composition of refractories from Timna (Tite 2001), Los Millares (Freestone 1989), and Tal-i Iblis (Pigott 2012) to those of Çamlıbel. The outlined section to the bottom left delineates the composition of modern refractory firebricks while the one in the centre is of clays that bloat by 1300°C. Adapted from Freestone (1989).....127
- Figure 7.11 SEM image of the calcium arsenate layer on crucible fragment 107-6437.128
- Figure 7.12 SEM image of the calcium arsenate layer on crucible fragment 133-6376.128
- Figure 7.13 SEM image of the calcium arsenate layer on crucible fragment 136-6325.128
- Figure 7.14 SEM image of a copper oxide prill (bright phase) surrounded by copper corrosion (grey phase) with a thin layer of calcium arsenate (light grey, above). Small bright dense phases within the cuprite prill are arsenical copper.129
- Figure 7.15 Photograph of sample 956-6202.132

Figure 7.16 Photomicrograph of ceramic body and vitrified ceramic below metallic layer. Frame is 3.7mm wide.	132
Figure 7.17 SEM image of delafossite crystals just below the metallic layer. Note that the metal layer was lost during the polishing process.	132
Figure 7.18 Diagram of a typical bowl hearth cross-section.	133
Figure 7.19 Photograph of furnace feature number 4, sectioned and collected from the site for later analysis.....	133
Figure 7.20 Results of XRF analysis of soil contaminants within and outside experimental prehistoric copper furnaces (Radivojević and Boscher forthcoming).	136
Figure 7.21 Results of pXRF analysis of the different layers of the bowl hearths recovered at Çamlıbel.	136
Figure 7.22 Three examples of large pottery fragments with distinctive purple staining on the inner surface. Photograph courtesy of Ulf-Dietrich Schoop. In clockwork order starting in the top left, samples are 11-3, 651-16, and 100-3.	137
Figure 7.23 Pottery sample 758-6261 with large green and black corrosion staining.....	137
Figure 7.24 Pottery sample 200-6526 with 1cm thick crust of iron hydroxide corrosion on the surface.....	137
Figure 7.25 Sulphur, iron, copper, and arsenic content of clean ceramic fabric and associated purple staining as determined by pXRF. Each adjoining pair of results is from the same sample, demonstrating the consistent increase in the first three of these elements.	138
Figure 7.26 Photomicrograph of sample 108-6838 ceramic fabric under plane-polarized light. .	139
Figure 7.27 Photomicrograph of sample 108-6838 ceramic fabric under cross-polarized light...	139
Figure 7.28 Photomicrograph of sample 228-6870 ceramic fabric under plane-polarized light. .	139
Figure 7.29 Photomicrograph of sample 228-6870 ceramic fabric under cross-polarized light...	139
Figure 7.30 Photomicrograph of sample 108-6857 cross section showing the purple-coloured layer on the surface of the ceramic under plane-polarized light.....	140
Figure 7.31 Photomicrograph of sample 108-6857 cross section showing the purple-coloured layer on the surface of the ceramic under cross-polarized light.....	140
Figure 7.32 Photomicrograph of sample 720-6879 cross section showing the purple-coloured layer on the surface of the ceramic under plane-polarized light.	140
Figure 7.33 Photomicrograph of sample 720-6879 cross section showing the purple-coloured layer on the surface of the ceramic under cross-polarized light.....	140
Figure 7.34 Photograph of sample 21-6838 with the black layer on the inner surface.....	140
Figure 7.35 Photomicrograph of sample 21-6838 cross section showing the black layer on the surface of the ceramic under plane-polarized light.	140
Figure 7.36 SEM Image of iron copper oxide layer on ceramic from sample 720-6879.....	141

- Figure 7.37 SEM image of mineral inclusions within the iron copper oxide layer from sample 616-6922. The ceramic, seen in the bottom of the frame, is entirely detached from the layer..141
- Figure 7.38 SEM image of sample 228-6870 showing the needle-like delafossite crystals present in ceramic porosities and in crevasses on the surface.....143
- Figure 7.39 Photograph of various mineral fragments recovered from the site presumed to have been intended to be used as ores.....145
- Figure 7.40 SEM image of sample 799-5409. The bright grey angular crystals are chalcopyrite surrounded by light grey corrosion in a dark grey quartz matrix.146
- Figure 7.41 Photomicrograph of sample 637-4218 showing a mixture of pyrite (white) and chalcopyrite (yellow) in a quartz matrix (grey).146
- Figure 7.42 Photomicrograph of sample 585-4328A showing a network of elongated iron hydroxide crystals.146
- Figure 7.43 Photomicrograph of sample 753-5028 with both magnetite and iron hydroxides within the porosities.146
- Figure 7.44 Photomicrograph of sample 257-3130. The bright whitish phases are the remaining chalcopyrite crystals surrounded by corrosion. Entirely missing are the pyrite crystals which have largely corroded to iron oxides, leaving behind only the crystalline structure.....147
- Figure 7.45 Photomicrograph of sample 585-4328B. The black inclusions are iron oxides in a magnesium iron silicate matrix.....147
- Figure 7.46 Photomicrograph of sample 838-4870. The matrix is composed of fibrous magnesium silicate serpentinite but contains some rare chromite and iron sulphide minerals. No copper mineralizations were observed, although SEM-EDS analysis showed up to 2 wt% of copper present in the matrix.147
- Figure 7.47 Photomicrograph of sample 877-5695. The reddish matrix is plausibly clinocllore while the weathered cubic inclusions are the remains of pyrite crystals. The bright phases in the top centre of the frame are examples of the few pyrite crystals remaining. The grey veins are magnetite corrosion.147
- Figure 7.48 Photomicrograph of sample 727-4659 showing crushed agglomerated minerals sintered by corrosion.148
- Figure 7.49 SEM image of sample 727-4659. The interstitial area is copper and iron oxide corrosion binding the angular grains together.148
- Figure 7.50 Photomicrograph of sample 619-3497 showing the original pyrite and chalcopyrite mineral microstructure. The pinkish colours are chalcopyrite while the grey is iron silicate and the light grey is magnetite. Orange iron hydroxides can be seen throughout where the mineral has weathered post-depositionally.149
- Figure 7.51 Photomicrograph of sample 619-3497. The majority of the sample consisted of this type of microstructure showing a wide range of weathering products. Just visible are the network of highly stable magnetite 'fingers' and the dark grey inkblot blebs of what appear to be wüstite.149
- Figure 7.52 Scatterplot showing the main two chronological groupings of mineral types recovered from Çamlıbel.....150

- Figure 7.53 Photograph of the iron and copper sulphide extrusion from a serpentinitic ridge (photograph courtesy of Ulf-Dietrich Schoop)..... 152
- Figure 7.54 Photograph of the Karakaya ore sample. 152
- Figure 7.55 Photomicrograph of the ore outcrop sample. The bright phases are mixtures of chalcopyrite and pyrite surrounded by grey and yellow corrosion. The majority of the matrix is composed of magnesium iron silicate. 152
- Figure 7.56 Photographs of two complete slag cakes with flat base and semi-molten upper area. 155
- Figure 7.57 Samples 60-3094 and 722-7629 showing the formation and accumulation of iron sulphide corrosion..... 155
- Figure 7.58 Photograph of experimental copper oxide smelting products (Bamberger and Wincierz 1990, 133). Note the ingot on the left with its slightly curved upper surface and the inverted imprint on the base of the slag cake on the right with upraised meniscus caused by surface tension..... 157
- Figure 7.59 SEM image of sample 630-3866 showing both elongated skeletal chains of fayalite (light grey) and small feathery hedenbergite crystals (dark grey matrix). The bright prills are matte..... 158
- Figure 7.60 SEM image of sample 222-326A. The angular zoned polyhedral crystals are olivines approaching the composition of fosterite with an outer edge enriched in iron. The dark elongated crystals are calcium- rich monticellite and the small light grey blebs are magnetite. All of these phases lie within a microcrystalline matrix. 158
- Figure 7.61 SEM image of sample 637-4456 showing a typical microstructure of dark grey cored kirschsteinite crystals within a glassy matrix. The bright prill in the centre is matte, with both iron and copper sulphide phases. Light grey sub-angular blebs are magnetite. 159
- Figure 7.62 SEM image of sample 637-4225 showing a typical microstructure. The large dark angular cored crystals are diopside with light grey fayalite chains between the grains. The bright thin strings dispersed throughout are matte. 160
- Figure 7.63 SEM image of sample 846-5515. The large dark angular crystals are hedenbergite while the small lath-like crystals between the grains are fayalite. The bright phases are HSS of copper and iron sulphide and matte prills. 160
- Figure 7.64 Photomicrograph of sample 210-299 at 200X magnification. The dark grey angular crystals, half of which exhibit planar fracturing, are pyroxenes within the solid solution range of augite. The light grey crystal chains between them are the olivine fayalite, while the pink, blue, and yellow phases are solid solutions of copper and iron sulphide. Frame is 0.6mm wide. 160
- Figure 7.65 Diagram of pyroxene end-members..... 160
- Figure 7.66 SEM image of sample 443-3708 showing dark rectilinear anorthite and grey angular olivine crystals in a microcrystalline matrix. Bright prills are copper-iron sulphides..... 161
- Figure 7.67 SEM image of sample 890-5774 showing elongated lath-like barite/celestine crystals growing within a cavity. The surrounding matrix is composed of dark grey fayalite and light grey magnetite. 161

- Figure 7.68 Photomicrograph of sample 890-5774 showing large quantity of magnetite spinels. Note the association with reddish copper metal prills in the centre and larger blue-grey covellite surrounding what may have been copper before corroding away. Frame is 1.8mm wide.162
- Figure 7.69 SEM image of sample 846-5528a. Note the thick magnetite skin on the surface. The cored angular crystals are diopside, the large dark bleb is incompletely reacted quartz, while the bright phases in the bottom left are the remnants of HSS in the process of dissolution.162
- Figure 7.70 Photomicrograph of high temperature solid solution of covellite (blue), bornite (yellow), and pyrrhotite (bright yellow) in sample 836-4860. Frame is 0.9mm wide.....163
- Figure 7.71 SEM image of sample 630-3865 showing the various phases of partially corroded HSS. The bright grey angular phases are pyrrhotite and covellite while the small fine finger-like structures at the grain boundaries are magnetite.....163
- Figure 7.72 SEM image of sample 630-3866 showing the large incompletely reacted quartz fragments found throughout the sample, accounting for its high SiO₂ content.....164
- Figure 7.73 SEM image of sample 222-326A. The large angular grey cracked crystals are quartz while the surrounding microcrystalline matrix is mainly composed of magnetite and olivines.164
- Figure 7.74 Binary phase diagram of FeO_x and SiO₂ (Eisenhüttenleute 1995, 79).....165
- Figure 7.75 SEM image of copper prills surrounded by magnetite spinels in sample 629-3860. The long dark crystals are olivines.166
- Figure 7.76 SEM image of bright copper prills surrounded by long dark diopside crystals in a glassy matrix from sample 722-4629.166
- Figure 7.77 Monte Carlo simulation of 200 electron trajectories in pure copper at 20 KV. Blue trajectories indicate electrons that fail to escape the sample, while red reflect those that left the modelled sample and could be analysed by the detector. Diagram obtained using Win X-Ray 1.3 with conditions set to match those of the SEM-EDS instrument used.168
- Figure 7.78 Graph showing the penetration depth along the X axis and number of escaping electrons along the Y axis in pure copper at 20 KV. Note that the majority fall between 0.1 and 0.3 µm.168
- Figure 7.79 Fe-Cu binary phase diagram. From (Craddock and Meeks 1987).169
- Figure 7.80 Diagram of reaction dynamics of Pb, Fe, and Cu with sulphur at varying temperatures (Rehren et al. 2012).170
- Figure 7.81 This graph shows estimated temperatures and fO₂ in which various phases coexist in slag. Adapted from (Schreiner et al. 2003).171
- Figure 7.82 Biplot of two compounds commonly related to fuel ashes, potassium and phosphorous oxides. Samples which contained either element below the detection limit of the instrument were included with a value of 0.....176
- Figure 7.83 Biplot of titanium oxide and aluminium oxide. Samples which contained alumina or titanium below the detection limit of the instrument were included with a value of 0.177

- Figure 7.84 Biplot of titanium oxide and potassium oxide. Samples which contained alumina or titanium below the detection limit of the instrument were included with a value of 0..... 178
- Figure 7.85 Biplot of phosphorous oxide and aluminium oxide. Samples which contained alumina or titanium below the detection limit of the instrument were included with a value of 0. 178
- Figure 7.86 Equilibrium phase diagram of the CaO-FeO-SiO₂ system, with MgO added to FeO. Adapted from (Eisenhüttenleute 1995, 126). 182
- Figure 7.87 Photomicrograph of sample 97-3588 showing one isolated fragments of slag embedded in a conglomerate matrix. Frame is 2.4mm wide. 183
- Figure 7.88 SEM image of sample 97-3588's mixed matrix. In the bottom right is a large fragment of silicified charcoal while in the top right is a large fragment of copper-bearing goethite. Between them is fayalitic slag..... 183
- Figure 7.89 SEM image close up of slag inclusion in sample 97-3588. The zoned grey angular crystals are olivine while the light grey blebs are magnetite and the bright prills are metallic copper. The matrix is microcrystalline. 184
- Figure 7.90 SEM image of skeletal chains of pyroxenes in glassy matrix identified in the majority of the slag of the sample..... 184
- Figure 7.91 SEM image of ceramic area of sample 97-3588. The bottom fabric has only light bloating from heat while the top has been partially vitrified. 185
- Figure 7.92 SEM image of large piece of incompletely reacted charcoal found within the conglomerate. While this was the largest, several smaller examples were identified throughout the sample. 185
- Figure 7.93 Photograph of top view of a matte droplet. Sample 602-3411. 186
- Figure 7.94 Micrograph of sample 602-3411. The droplet is formed of a series of alternating crosshatch patterned grains of copper sulphide. The light blue is covellite encasing cracks which have filled with partially oxidized copper sulphide. The yellow space phase is a combine of both yellow bornite and bright yellow pyrrhotite. Frame is 0.9mm wide..... 187
- Figure 7.95 Close-up SEM image of sample 602-3411 showing clearly the two distinct phases of copper and iron sulphide. Also visible are the thin elongated darker phases of magnetite at the grain boundaries. The dark veins are corrosion. 187
- Figure 7.96 Photograph of cross section and top surface of sample 128-1083. Note the series of concave pits along the lower edge in the photograph where molten metal likely formed. 188
- Figure 7.97 SEM-EDS image of sample 128-1083 showing the largely corroded matte phases. Barely visible is the dendritic arrangement of the grains. 188
- Figure 7.98 Micrograph of sample 128-1083. Although highly corroded, some remains intact. In the left centre of the image can be seen the familiar crosshatch pattern of bornite and pyrrhotite. The dominant, slight corroded pinkish phase is chalcopyrite. 188
- Figure 7.99 Arsenic-rich slag samples identified by pXRF. Note that they were both recovered single fragments but were broken to expose a clean fracture for analysis. 191
- Figure 7.100 Quaternary phase diagram for the glassy phases of the slag approaching the composition of Al₂O₃-CaO-FeOx-SiO₂ with 10wt% FeO. The glassy matrix being quite rich in both arsenic and copper rich microcrystalline phases, the diagram poorly reflects the actual

- composition of the melt but still centres around the 1200°C low temperature trough in the centre of the diagram. Adapted from (Eisenhüttenleute 1995, 154).192
- Figure 7.101 Slag matrix of sample 740-6358. The dark polyhedral crystals are leucite, the grey blebs and the large grey angular crystal are magnetite, and the needle-like crystals are delafossite. Bright prills are arsenical copper. The underlying matrix is microcrystalline....193
- Figure 7.102 Closeup of slag matrix of sample 740-6358 with a cluster of black cubic aluminium silicate crystals. The dark grey angular crystals are diopside, the light grey blebs are magnetite, and the bright prills are arsenical copper. The underlying matrix is microcrystalline mainly composed of olivines and includes laths of delafossite visible in the top left corner of the image.....193
- Figure 7.103 Large incompletely dissolved fragment of gangue or ore within the arsenic-rich slag sample 740-6358.....195
- Figure 7.104 Close-up of the top left edge of the undissolved gangue in sample 740-6358.195
- Figure 7.105 SEM image of analytical areas across slag sample 740-6358. The gangue mineral can be seen in the bottom right while the copper rich areas are to the left of the SEM image. Results of the analyses can be seen in Table 7.19.197
- Figure 7.106 Slag matrix of sample 561-3957. The two main crystalline phases are the long thin needle-like grey delafossite and the angular polyhedral calcium arsenate. Light grey rounded prills are arsenical copper. All these phases are within a glassy silicate matrix.....198
- Figure 7.107 SEM image of small prills in sample 561-3957. The grey blebs are a combination of calcium arsenates and some magnetite within a glassy matrix.....198
- Figure 7.108 SEM image of typical large arsenical copper prill in sample 561-3957. The small dark inclusions are cuprite while the bright veinlet is filled with γ phase of Cu_3As198
- Figure 7.109 Photographs of sample FG-030119B. Image on the left is the base of the ceramic showing the organic matter impressions. Photograph on the right is a cross section. Note the slag scraped to the side.204
- Figure 7.110 Drawing of crucible base and wall (Helwing 2011d, small find no. 203, pp 280, 308). Note the slag dripping on the outside and the small edge extending outwards from the base.204
- Figure 7.111 Photomicrograph of furnace wall sample FG-030670 with typical organic temper voids. Although the matrix here is relatively fine grained and thus poor in mineral inclusions, the rest of the sample does contain significant quantity of them.....205
- Figure 7.112 Three furnace fragment samples with rims. All show extensive heat damage applied mainly to the inside but extending deep into the fabric. Note two distinct layers of slag on the leftmost example, with the top layer extending over the edge and most likely deposited after the ceramic had been broken and discarded.....206
- Figure 7.113 Photograph of sample FG-030113 showing the semi-circular hole running through the furnace wall interpreted as a tuyère or vent hole. The hole can be seen here in half-section in the center-left part of the photograph.....207
- Figure 7.114 Photograph of sample FG-012235A. This furnace lining fragment shows two smelting events and three ceramic linings, testifying to the reuse of the furnaces.....208

- Figure 7.115 Plane polarized photomicrograph of sample FG-012232 showing typical technical ceramic microstructure. 208
- Figure 7.116 Cross polarized photomicrograph of sample FG-012232 showing typical technical ceramic microstructure. 208
- Figure 7.117 Composition of technical ceramics from Arisman plotted according to elements known to greatly affect refractoriness. The outlined section to the bottom left delineates the composition of modern refractory firebricks while the one in the centre is of clays that bloat by 1300°C. Adapted from Freestone (1989). 212
- Figure 7.118 Photographs of exterior wall of two crucible fragments. Object on the left is sample FG-030116B while the one on the right is FG-030119A. Note the droplet downward direction of flow on the left sample helped in orienting the ceramic body sherd. 213
- Figure 7.119 Cross section photograph of crucible fragments FG-030119B on the left, and FG-030116B on the right. 213
- Figure 7.120 SEM image of sample FG-030113 showing typical slag matrix. The light grey blebs are magnetite, the skeletal chains are fayalite, the dark elongated crystals are pyroxenes, and the microcrystalline matrix is mainly composed of hedenbegite crystals. 214
- Figure 7.121 SEM image of sample FG-030113 showing ceramic body with matte and arsenic phases filling available porosity. 214
- Figure 7.122 SEM image of sample FG-012235A's bottom ceramic layer. 216
- Figure 7.123 SEM image of sample FG-012235A's top ceramic layer. 216
- Figure 7.124 SEM image of sample FG-012235A's bottom blueish-green deposit. 217
- Figure 7.125 SEM image of sample FG-012235A's top blueish-green deposit. 217
- Figure 7.126 Line graph comparing the compositions of the means of three distinct phases of sample FG-012235A. 218
- Figure 7.127 Photograph of sample FG-992864, a dense iron-rich mineral with green copper oxide staining. 219
- Figure 7.128 Photograph of sample FG-030663 showing typical dense iron-rich mineral with green copper oxide staining and white quartz veins. 219
- Figure 7.129 Photograph of sample FG-011992 showing once more a dense iron-rich mineral with green copper staining. In this case the sample also has metallic inclusions. 219
- Figure 7.130 Photograph of the iron-rich mineral lacking any green staining. Sample is FG-030125. 219
- Figure 7.131 Photomicrograph of Sample FG-011992 in cross-polarized reflected light. The dark angular crystals are magnetite while the matrix is mainly composed of greenish anorthite while the white blebs are calcium carbonate. Frame is 2.4mm wide. 220
- Figure 7.132 SEM image of FG-011992's matrix. The elongated crystals are iron oxide while the light grey subangular crystals anorthite and the darker phases are calcium carbonate. 220
- Figure 7.133 Photomicrograph of sample FG-030125 under cross-polarized reflected light. The grey phases are iron oxide while the yellow phases are iron sulphide. The sulphide phases

appear under the microscope mainly in the porosities, still visible through the clear resin. Frame is 1.2mm wide.....	221
Figure 7.134 SEM image of mineral sample FG-030125. Matrix is largely iron oxide with the occasional light grey phases of iron sulphide. Dark blebs are porosity filled with mounting resin.	221
Figure 7.135 Photographs of two samples showing the typical features associated with speiss slag. Note the orange and yellow corrosion staining on the surface and in the pores. Also note the layered and flowing surface features typical of tapped slag. The sample on the left is FG-010506 while that on the right is FG-030123B.	224
Figure 7.136 Cross section of speiss slag fragment with attached furnace remains. This specimen is the only one of the speiss slags to show minimal porosity. Sample FG-040919B.....	225
Figure 7.137 SEM image of sample FG-040920A showing typical slag matrix for speiss slags. The dark angular crystals and grey dendritic crystals are pyroxenes while the larger light grey crystals are kirschsteinite. The light grey dendrites are wüstite.....	226
Figure 7.138 Glassy speiss slag matrix on top of ceramic body. The bright phases are speiss prills while the light grey phases are magnetite clusters. SEM image of sample FG-011993.	226
Figure 7.139 SEM image of sample FG-012232 with the very bright metallic iron prills present in a single small area of the sample.....	226
Figure 7.140 SEM image of sample FG-010506's matrix. The bright prills are speiss while the light grey blebs are magnetite and the grey dendrites are kirschsteinite.	226
Figure 7.141 The Fe-As binary phase diagram (Raghavan 1988, 38).....	228
Figure 7.142 SEM image of corroded speiss prills in sample FG-040902A. The bright phases in the prill are FeAs while the corroded grey areas are likely Fe ₂ As based on the presence of both phases in un-corroded prills. Large dark crystals and grey dendrites are pyroxenes while the light grey phases and blebs are magnetite.	229
Figure 7.143 Arisman speiss slags plotted in FeO-CaO-SiO ₂ ternary diagram from Eisenhüttenleute (1995, 126).	231
Figure 7.144 Arisman speiss slags plotted in FeO-CaO-SiO ₂ -Al ₂ O ₃ quaternary diagram with 25% FeO. Results are represented by a red area because the iron content is never exactly 25% and therefore the slags cannot be accurately plotted. From Eisenhüttenleute (1995, 154).	231
Figure 7.145 Biplot of titanium oxide and aluminium oxide in Arisman speiss slags. Samples which contained aluminium below the detection limit of the instrument were included with a value of 0.....	232
Figure 7.146 Biplot of iron oxide and aluminium oxide in Arisman speiss slags.	232
Figure 7.147 Biplot of calcium oxide and potassium oxide in Arisman speiss slags.	233
Figure 7.148 Biplot of calcium oxide and iron oxide in Arisman speiss slags.	233
Figure 7.149 Biplot of calcium oxide and aluminium oxide in Arisman speiss slags.....	233

- Figure 7.150 Photograph of cross section of sample FG-012260B. The layering of metallic copper, matte, and slag can be clearly seen as it must have been in the larger slag cakes from Arisman. 234
- Figure 7.151 Photograph of large slag cake fragment. The left photograph is the fragment in cross section while on the right is the base of the fragment. The meniscus can be clearly seen in cross section. Also note the angle of the cake side against the base which does not match the shape of the large 'crucibles' recovered from Arisman..... 235
- Figure 7.152 Plate taken from (Boscher 2010, 39) showing the similarity in shape between some Arisman copper slags (far right, FG-030121) and Shahr-i Sokhta tapped copper slags (far left). The centre image is a photo diagram from (Hauptmann et al. 2003, 201). 235
- Figure 7.153 SEM image of sample FG-993152C showing typical dendrites in the solid solution between monticellite and kirschsteinite. The smaller dendrites are second generations of the same crystal. The grey blebs are magnetite spinels and the bright prills are arsenical copper. 236
- Figure 7.154 SEM image of sample FG-12260C showing mixed olivine crystalline matrix. The skeletal chains are fayalite while the dark angular crystals approach the composition of Kirschsteinite. The grey blebs are magnetite and the bright prills are copper sulphide and arsenical copper 236
- Figure 7.155 Arisman copper slags plotted in FeO-CaO-SiO₂ ternary diagram..... 242
- Figure 7.156 Arisman copper slags plotted in FeO-CaO-SiO₂-Al₂O₃ quaternary diagram with 25% FeO. Results are represented by a blue area because the iron content is never exactly 25% and therefore the slags cannot be more accurately plotted. 242
- Figure 7.157 Biplot of titanium oxide and aluminium oxide in Arisman green copper slags. 244
- Figure 7.158 Biplot of iron oxide and aluminium oxide in Arisman Green copper slags. 244
- Figure 7.159 Biplot of calcium oxide and iron oxide in Arisman green copper slags..... 245
- Figure 7.160 Biplot of calcium oxide and aluminium oxide in Arisman green copper slags. 245
- Figure 7.161 Biplot of calcium oxide and potassium oxide in Arisman green copper slags. 245
- Figure 7.162 Photograph of 5 typical glassy black slags. Note the flowing tapped pattern on the rightmost sample. 247
- Figure 7.163 SEM image of sample FG-012254 showing isolated calcium silicate crystal cluster in an overall glassy matrix..... 247
- Figure 7.164 SEM image of sample FG-030704B's glassy matrix showing typical flowing texture of most black glassy slags..... 247
- Figure 7.165 SEM image of sample FG-030974D's microcrystalline matrix. The dendrites are near hedenbergite in composition. The large porosity in the centre shows the three-dimensional structure of the dendrites. The small bright prills are copper metal and copper sulphide. 248
- Figure 7.166 Microstructure of FG-030116B under the SEM. The large angular crystals are calcium silicate while the grey blebs are magnetite and the bright prills are iron arsenide speiss. . 248
- Figure 7.167 SEM image of sample FG-030974F. The prill consists of a body of cuprite with frequent small blebs of chalcocite surrounded by a ring of chalcocite. 250

- Figure 7.168 Photograph of sample FG-030689's cross section. Note the large inclusions visible throughout.....250
- Figure 7.169 Photomicrograph of matte microstructure. The yellowish phase is bornite while the blue veinlets are copper sulphide corrosion. The bright phases in the centre are copper-zinc arsenate. The dark phases are a mixture of various lead compounds.250
- Figure 7.170 SEM image of Sample FG-030689. The large hexagonal pyramidal crystals in the porosity are mimetite while the grey grains in the upper right are chalcocite.251

Chapter 8

- Figure 8.1 Lead isotope ratios for the Arisman's slag and copper prills distinguishing between the different slag types. Diagram produced from data published in Pernicka et al. (2011). Analytical error was not available.....254
- Figure 8.2 Lead isotope ratios for copper objects recovered from Arisman, from (Pernicka et al. 2011, 679).255
- Figure 8.3 Mirror plots of lead isotope ratios for the various materials from Çamlıbel. Note the two strongly radiogenic minerals skewing the results.....261
- Figure 8.4 The same mirror plots as in Figure 8.1, but with the outliers removed.261
- Figure 8.5 Çamlıbel material within the context of well-defined Anatolian ore deposits. Reproduced from Lehner et al. (2009) from data gathered from a wide range of published sources. Note the wide range of the Çamlıbel material compared to the much narrower fields of individual ore deposits represented by numerous analyses each.264
- Figure 8.6 Lead isotope ratios of Çamlıbel material compared to known exploited deposits in the Near East and Eastern Mediterranean. This covers most of the deposits known to have been exploited during the Bronze Age and earlier periods. Data aggregated from several sources (Gale et al. 1990; Gale et al. 1985a; Hauptmann et al. 1992; Lehner et al. 2009; Pernicka et al. 2011; Stos-Gale and Gale 2011).267
- Figure 8.7 Biplots of lead isotope ratios measured for Çamlıbel's material against Faynan's DLS ores obtained from Hauptmann (1992).268
- Figure 8.8 Comparison of the lead isotope ratios of Çamlıbel material with that of Kaman-Kalehöyük Stratum III. The circled areas are those marked by Sayre et al. (2001).....270

Chapter 9

- Figure 9.1 Diagram of the shift in metallurgical activities being conducted in and around Çamlıbel.273
- Figure 9.2 Çamlıbel's arsenical copper chaîne opératoire. Note that dotted lines and transparent boxes represent operations which are suggested but for which only indirect archaeological evidence exists - namely the roasting of ores and the recycling of copper-rich slag.277
- Figure 9.3 Experimental results of arsenic losses from roasting arsenopyrite in various oxygen partial pressures at 798 K. Note that both high and low oxygen pressures result in increased arsenic losses. Adapted from Chakraborti & Lynch 1983.283
- Figure 9.4 Crucible rim from slagheap A embedded into clay as part of the joint between a furnace and a crucible. Note the speiss slag on the inner surface of the clay showing that it flowed into the crucible. Photograph from Steiniger (2011, 78).284

- Figure 9.5 Arisman's arsenical copper chaîne opératoire. Note that dotted lines and transparent boxes represent operations which are suggested but for which only indirect archaeological evidence exists. Fuel, fluxes and furnace material are not included in the diagram although they likely did contribute to the overall composition of the discarded slags. 288
- Figure 9.6 Comparison of pedestalled crucibles from the 5th and 4th millennium BC in Western Asia and the Eastern Mediterranean. All drawings and photos are to the same scale. 301
- Figure 9.7 Quaternary phase diagram of the Fe-As-S-O system at 973 K. Note that iron oxidizes at a much lower oxygen partial pressure than arsenic, which can remain as metallic gas for much longer, and also that a fairly high partial pressure of -9 to -3 is required to form FeAs. These conditions are approximately equivalent to those needed for FeS, and much more elevated than the pressure of oxygen required to form various iron oxides (Adapted from Chakraborti and Lynch 1983). 305

List of Tables

Chapter 2

Table 2.1 Effects of arsenic content and cold-hammering on alloy hardness. Reproduced from (Lechtman 1996, 494-495).....	44
--	----

Chapter 4

Table 4.1 Occupation phases at Çamlıbel with the two available radiocarbon dates (From Schoop et al. 2009).....	87
---	----

Chapter 5

Table 5.1 Comparison of analysis of Darhand copper mineralisation with ore and slag recovered from Arisman I. All data obtained by SEM-EDS and published in (Pernicka et al. 2011).	99
Table 5.2 Radiocarbon dates for the different areas of Arisman I (from Görsdorf, 2011). Dates in parentheses for area B are those given by Helwing (2011) taking into account stratigraphy and pottery assemblages indicating the probable re-use of old wood. Dates given for Area C represent two distinct occupations with approximately 100 years of abandonment. Areas are presented in this table chronologically.....	102

Chapter 7

Table 7.1 Distribution of the total metallurgical remains at Çamlıbel Tarlası by period.	119
Table 7.2 Çamlıbel Tarlası metallurgical samples analysed. Numbers in parenthesis indicate the number of samples which were macroscopically evaluated but not prepared for and analysed by SEM-EDS.....	122
Table 7.3 Bulk composition of alloying crucible and typical local pottery ware bodies as determined by SEM-EDS.	126
Table 7.4 Composition of the two types of arsenate phases in the crucible residue layers as determined by SEM-EDS.....	129
Table 7.5 Bulk composition of melting crucible or mould fragment 956-6202 as determined by SEM-EDS.	131
Table 7.6 Bulk elemental composition of bowl hearth fills using pXRF. The results are presented in ppm as the mean of three analyses across each layer of the six bowl hearths and the associated natural soil adjacent to the features.....	135
Table 7.7 Bulk elemental composition of typical domestic pottery fabric determined with pXRF. Results are presented in ppm as the mean of two analyses on three randomly selected fragments of pottery.....	135
Table 7.8 Composition of purple layer on surface of local domestic pottery as determined by SEM-EDS. Reported values are the mean of at least three area analyses normalized to a 100%.	142

Table 7.9 Composition of local domestic pottery fabrics which exhibited purple staining as determined by SEM-EDS. Reported values are the mean of at least three area analyses normalized to 100%.	142
Table 7.10 Bulk Composition of minerals recovered from Çamlıbel as determined by SEM-EDS. Results are the average of at least three area analyses taken at 100X magnification and presented in wt%.	149
Table 7.11 Bulk composition of minerals recovered from Karakaya outcrop as determined by four area analyses at 100X magnification by SEM-EDS.	153
Table 7.12 Composition of copper prills within the Çamlıbel slag as determined by SEM-EDS. Results are normalized to 100% and presented in wt%.....	166
Table 7.13 Result of microprobe analysis of copper prills within the slag matrix of two samples. Each row is the mean of spot analyses of 11 and 12 different copper prills. Reported results are not normalized although ZAF correction has been applied. The iron and copper account for more than 99wt% of the total.	169
Table 7.14 Normalized bulk composition of slag remains from Çamlıbel as determined by at least three area scans by SEM-EDS. All elements reported as oxides except for chlorine. Note that samples 602-3411 and 128-1083 are not included in this table as they essentially consists of highly corroded pure matte rather than slag and will be discussed separately. Data for sample 97-3588 are for the slag inclusions within the conglomerate only. Some elements found in only a few samples at levels near the detection limit of the SEM-EDS were not included in this table but can be found in the appendix.....	173
Table 7.15 Composition of the two samples of iron-copper sulphide material. Results are the means of 3 area analyses of the matte (the gangue material of sample 128-1083 is not included). Results are presented here as oxides since both samples had significant corrosion present in association with ubiquitous fractures throughout both samples. 30-40 wt% was detected in sample 128-1083, while 10-18 wt% oxygen by bulk was detected for sample 602-3411. Much of the iron and copper are therefore present as sulphide phases.	189
Table 7.16 Results of random bulk area and glassy matrix analyses by SEM-EDS. Results presented here are the means of three analyses each, normalized to 100%.	191
Table 7.17 Composition of large binary phased arsenical copper and pure copper prills and smaller single-phased prills in sample 740-6358 as determined by SEM-EDS spot analyses of a number of prills. All results are normalized to 100%.	194
Table 7.18 Composition of undissolved gangue as determined by SEM-EDS. Data presented here is the normalized mean of four area analyses.	195
Table 7.19 Area analyses of slag at regularly increasing distance from incompletely dissolved gangue as determined by SEM-EDS. All results are normalized to 100%.	197
Table 7.20 Composition of copper prills in sample 561-3957 as determined by SEM-EDS point analyses. Each result is the mean of several points taken from different prills, represented by the number in parantheses.	199

Table 7.21 List of metallurgical remains of Arisman I available for analysis and their provenience. Numbers in parentheses represent samples that were evaluated macroscopically but were not prepared or analysed by SEM-EDS.	201
Table 7.22 List of ceramic samples available for analysis arranged by function. Numbers in parentheses are the samples which have not been analysed by SEM-EDS.	203
Table 7.23 SEM-EDS bulk chemical results for Arisman technical ceramics. Results normalized to 100%.	210
Table 7.24 Bulk chemical composition of the slag and ceramic fabrics of furnace wall fragment FG-030113. The results are normalized totals resulting in each case from the mean of three area analyses using SEM-EDS.....	214
Table 7.25 Chemical composition of the two ceramic layers of sample FG-012235A as determined by SEM-EDS. Results are the mean of three area analyses and normalized to 100%.....	216
Table 7.26 Composition of layered deposits in on inner surfaces of furnace fragment FG-012235A as determined by three area analyses by SEM-EDS. Results are normalized to 100%.	217
Table 7.27 Bulk composition of two mineral fragments from Arisman as determined by SEM-EDS. Results are the means of three area analyses for each sample normalized to 100%.....	220
Table 7.28 Arisman slag samples available for analysis. Numbers in parentheses are the samples which were not analysed by SEM-EDS. Not included in this table are the ceramic samples with attached slag.	223
Table 7.29 Distribution of crystalline phases in the speiss slag of Arisman. The first six analyses are taken from Boscher (2010) while the bottom ten are newly obtained results.	227
Table 7.30 Normalized mean of the composition of speiss prills found in the speiss slags. The first six analyses are taken from Boscher (2010) while the bottom ten are newly obtained results.	229
Table 7.31 Normalized bulk compositions of Arisman speiss slags as determined by at least three area scans by SEM-EDS. All elements reported as oxides. The first six analyses are taken from Boscher (2010) while the bottom ten are newly obtained results.	230
Table 7.32 Normalized bulk composition of green copper slag remains from Arisman as determined by at least three area scans by SEM-EDS. All elements reported as oxides except for chlorine.....	240
Table 7.33 Normalized bulk composition of green copper slag remains with attached fragments of furnace walls from Arisman as determined by at least three area scans by SEM-EDS. All elements reported as oxides except for chlorine.	241
Table 7.34 Normalized bulk composition of glassy green copper slag remains from Arisman as determined by at least three area scans by SEM-EDS. All elements reported as oxides except for chlorine.....	241
Table 7.35 Microscopic and microstructural features of Arisman's black slags.	248

Table 7.36 Normalized bulk composition of black slag remains from Arisman as determined by at least three area scans by SEM-EDS. All elements reported as oxides except for chlorine and normalized to 100%.	249
--	-----

Table 7.37 Normalized bulk composition of matte samples as determined by SEM-EDS area analyses.....	251
---	-----

Chapter 8

Table 8.1 Distribution of Çamlıbel samples sent for lead isotope analysis. Numbers in parentheses represent samples analysed at NIGL in a parallel study.	257
--	-----

Chapter 9

Table 9.1 Mean composition of all speiss and copper slags from Arisman as determined by SEM-EDS.	281
---	-----

Acknowledgments

This PhD thesis would never have been possible without the help and encouragement of countless people over the course of the last four years. Their support has been invaluable and I feel a great debt of gratitude to all of them – not least for having to bear with me over these wonderful but trying times.

First I'd like to thank my supervisor, Thilo Rehren, who has been guiding me in my academic pursuits since the early days of my MSc research at UCL's Institute of Archaeology. He was the first to introduce me to the weird and wonderful speiss back in 2010 and suggested that I first work on the material for my MSc dissertation and to build that foundation for my PhD thesis. He kindly provided me with work as a laboratory technician in the gap year between my two degrees and has never failed to fully support me every step of the way. I am also most grateful for the critical engagement he has provided me over the years, something which I hope to continue for years to come.

Although his tenure as my secondary supervisor was short, I am thankful for the help provided by Ian Freestone at the Institute of Archaeology in my first year of study while Thilo was half a world away. Following in his Ian's, I am also grateful for the support of my other secondary supervisor, Rob Carter, who took over once I moved to UCL Qatar.

The generous financial support from Qatar Foundation and UCL Qatar played a large role in allowing this PhD research to come to fruition and for that I thank both organisations. In addition, I'd like to acknowledge the world class laboratory, academic, and support facilities of UCL Qatar, QF, and the Institute of Archaeology which have been a boon to my (and countless others') research - I will certainly be sad to leave them behind.

Equally essential to the success of this thesis have been those involved in providing the archaeological materials for analysis. For samples from Çamlıbel, I would like to thank Ulf-Dietrich Schoop of Edinburgh University. Not only did he supply me with resources from a wonderful archaeological site with a fantastic and thoroughly recorded metallurgical assemblage, but he also invited me to visit him at the site and provided me with additional samples as needed. For the material from Arisman, I would like to thank Ernst Pernicka at the Curt-Engelhorn-Zentrum Archäometrie (CEZA). In addition, I am grateful to Prof. Pernicka for his kind assistance in deciphering the lead isotope analysis his laboratory conducted for me.

I would like to thank the academic staff at the Institute of Archaeology and UCL Qatar, particularly Marcos Martín-Torres, Myrto Georgakopoulou, Voula Golfomitsou, Jose Carvajal-Lopez, and Brigitte Cech, for all their insightful discussions and critical advice. I am also grateful for all of the support staff in both departments, and in particular I would like to thank the extraordinary assistance from Philip Connolly, Kevin Reeves, Patrick Quinn, Harriet White, Stephanie Black, Stuart Laidlaw, and Lisa Daniels.

In addition, this research has benefited from countless conversations with colleagues over the course of the last four years. I especially would like to thank Barbara Helwing, Kunlong Chen, Bastian Asmus, Simon Timberlake, Tim Young, and Ben Roberts.

I am eternally grateful for the support of all of my fellow PhD colleagues who have contributed in one way or another to my research and to my life. I have learned much and more from them and for that I would like to thank Siran Liu, Maninder Singh Gill, Frederick Rademaker, P Vennunan, Anastasya Cholakova, David Larreina-Garcia, Matt Phelps, Kristina Franke, Mainardo Gaudenzi-Asinelli, Fernanda Kalazich, Rahil Alipour, Vana Orfanou, Oli Lown, Hania Sosnowska, Silvia Amivone, Carmen Ting, Ruth-Fillary Travis, Miljana Radivojević, Wenli Zhou, Qiyang Hong, Min Yin, Xiuzhen 'Janice' Li, Carlotta Gardner, Edwinus Lyaya, Thomas Thondhlana, Jelena Zikvovich, and Can Aksoy. I can only hope to keep encountering and stay in touch with all of these fantastic researchers throughout my career and feel honoured to have shared this right of passage with them. In particular, I want to thank the Institute of Archaeology's B52 tenants (and honorary tenants), with whom I shared my first year of PhD, for being such a great lot with boundless enthusiasm and an insatiable appetite for discovery.

Next I would like to thank my family, both far and less far away, without whose unwavering support this thesis would never have been written. My parents in particular have always encouraged me to seek out my life's dreams and in many ways this thesis is the culmination of the drive and commitment to that vision; words simply cannot express my gratitude.

My final acknowledgement and eternal gratitude goes to my wife Jill for believing in me, keeping me sane, and for being my lifeline throughout this grand adventure.

Chapter 1 A Contentious Alloy

1.1 Introduction

The study of ancient metals has formed an important aspect of archaeological interpretation since the early days of antiquarianism in the 19th century and continues well into the present day (Trigger 1989). While we have long moved away from early ideas of a direct systematic link between metallurgical technology and the development of cultural complexity (Pigott 1999b; Renfrew 1972; Thornton and Roberts 2009), the acquisition of metals and the knowledge required to exploit them have formed the basis of much cultural change in almost all societies of the last five thousand years. It is for these reasons that scholars have dedicated so much effort to understanding how mankind first developed the technology to extract metal from the earth, how artefacts were manufactured from such metals, and what roles they played in human society.

While the inception of metal use and extraction typically receive the greatest attention from both the public and scholars (Adams 1997; Caldwell 1968; Craddock 1995; Muhly 1988; Pigott 1999b; Radivojević et al. 2010; Thornton and Roberts 2009), other aspects of metallurgical technology have arguably had as much, if not more, impact on ancient societies. One such advance, the discovery and use of bronze has long been known to have had a widespread and tremendous effect on ancient economies and social structures. It was therefore quite surprising to early archaeological scientists to find that tin bronze was not the first prehistoric alloy it had been believed to be, but that many early objects were rather made of arsenical copper (Caley 1949; Coghlan and Case 1957; Forbes 1964; Tylecote 1962). The continued analytical study of metal objects in the second half of the 20th Century quickly led to the idea that the Late Chalcolithic and Early Bronze Ages of Southwest Asia, spanning roughly the fourth to the mid third millennia BC, were best described as having been largely dominated by the use of arsenical copper alloys (Bar Adon 1980; Charles 1967; Eaton and McKerrell 1976; Heskell 1983; Muhly 2006), something which has raised many new and interesting questions on the development of early technology.

Since this theory was first proposed, arsenical copper has been identified as an important alloy in almost every region of the world where copper smelting was discovered in prehistoric times. This includes regions that may have had some direct or indirect contact with Southwest Asia such as the Balkans (Paulin et al. 2000), the Caucasus (Courcier et al. 2012), the Aegean (Doonan and Day 2007; Muhly 2006), and India (Bhardwaj 1979), but also distant regions that are unlikely to have had any such interactions, including the Iberian Peninsula

(Fernández-Miranda et al. 1996; Hook et al. 1991; Müller et al. 2007), Britain (Budd 1993; Budd et al. 1992; Coghlan and Case 1957; O'Brien 1999), China (Mei 2012), and South America (Lechtman 1981; Lechtman 1991; Merkel et al. 1994). Developments seem to have occurred at widely different periods and for varying lengths of time in every region, and are so disjointed geographically that the distribution is unlikely to be entirely the result of technological diffusion. The arsenical copper production techniques were therefore more than likely developed independently several times, followed distinctive pathways, and had contrasting effects on their respective cultural contexts.

In Southwest Asia, the alloy first appeared in the highland regions of Anatolia and Iran where it seems to have had a tremendous impact on the socio-economic environment of the time (such as trade, warfare, wealth distribution, industrial development, etc.) and likely played a significant role in the outward expansion of Early Bronze Age state-level societies of the Mesopotamian and Susanian lowlands (Frame 2010; Pigott 1999a; Thornton 2010), although there is still considerable debate as to the nature of this lowland-highland interaction (Algaze 1993; Frangipane 2001; Stein 1999; Stein and Wattenmaker 1990).

Yet despite the prevalence of this material and the clearly important role it played in many prehistoric cultures, it remains largely misunderstood. While the physical properties of arsenical copper have largely been determined (Budd and Ottaway 1991; Charles 1967; Lechtman 1996; Meeks 1993; Northover 1989; Pollard et al. 1991), and we now have a large number of compositional analyses of finished objects relating chemistry to typology (i.e. Eaton and McKerrell 1976; Esin 1976; Hauptmann and Pernicka 2004), there are still a large number of issues that remain unresolved.

The object of the current study was to explore the various technological pathways to the production of arsenical copper alloys at their inception and to explore how this technology was adapted both socially and geographically across the Middle East. A premise was established that the later tin bronzes were unlikely to have appeared in a technological vacuum and that certain abilities, skills, and knowledge had to be available prior to its development in order to permit the dramatic spread of this alloy across the globe during the later Bronze Age. The isolated appearance of bronze alloy objects in Balkan contexts that predate the widespread production of arsenical copper, summarised by Radivojevic et al. (2013), are reportedly the results of the exploitation of rare tin-bearing copper mineralizations of stannite ($\text{Cu}_2\text{FeSnS}_4$). That these sporadic instances of bronze alloys did not lead to the widespread use of the alloy is likely largely due to the limited extent of the

geological deposits in question, and, to a lesser extent, perhaps because the resulting material was not perceived to be of enough value to warrant further exploitation. Although these objects predate the explosion in the use of tin-copper alloys by over a thousand years, they in fact highlight the long period of experimentation and exploitation of polymetallic ores resulting in the production of unintentional alloys prior to the Bronze Age. This observation opens the floor to the recognition that Chalcolithic smelters probably had at their disposition a much broader range of technological choices than previously thought.

This introductory chapter opens with the parameters under which the study was conducted, highlighting first the relative importance of arsenical copper in its cultural and historical context, followed by an overview of the lacunae in our understanding of it as a physical material and in regards to its socio-economic importance in prehistory. The theoretical framework under which this research was conducted is then discussed as well as how it will be applied to the analysis of production remains. The chapter ends with an outline of the intended goals of this doctorate research.

The second chapter gathers data from a range of sources to clearly define the physical properties of the alloy and draws attention to the various benefits of arsenical copper when compared to pure copper and tin bronze. The intended purpose is to serve as an interpretative tool when identifying cultural uses, both practical and symbolic, for the alloy. As will be shown, even in instances where the production of such a material is not seen as having been intentional, there is often an uneven distribution of arsenic content across artefact types which is hardly likely to have occurred without some kind of human agency. It will be shown that, until recently, most researchers have focused their attention on the hardness characteristic and casting properties of the alloy, but that efforts have now shifted to try to explain its use in more socio-economic terms since it is increasingly recognized that modern engineering and metallurgical views of materials may not be applicable to past practices.

The third chapter focuses on aspects of production technology and is divided into two parts. The first part explores the various techniques by which the alloy could be produced from a theoretical perspective. The second part covers the archaeological record itself and forms an overview of the production and use of arsenical copper in the Old World. In order to include as many potential known production processes, it was necessary to draw on material from a much broader scope of geographical and chronological data sets, often well outside of the study area. This approach allowed a wide range of production techniques to be described

and covers the full gamut of known uses for the material and creates a basis for comparison of our knowledge in the field. This chapter concludes with the development of a methodology to differentiate between diverse methods which in turn could be used to assess archaeological remains from relevant sites.

To test the hypotheses presented, materials from two archaeological sites were selected based on preliminary work which showed their potential for distinctive intentional alloying of arsenical copper. The two sites straddle the shift from the Late Chalcolithic (Çamlıbel) to the Early Bronze Age (Arisman), a period when massive socio-political and economic changes were taking place alongside great technological advances. Although very far from each other geographically, they represent evolving approaches to subsistence largely based on the exploitation of mineral resources on the margins of large urban socio-economic developments occurring in the Mesopotamian lowlands. The analysis of the metallurgical production remains will form the bulk of the research presented here, offering new data on the emergence of metallurgical innovations. Chapters 4 and 5 cover the geographical, geological, and archaeological contexts for these sites. Chapter 6 covers the methodological approach for the analysis of the material which is then presented in chapters 7 and 8. The discussion of these results, their implication to our understanding of arsenical copper and avenues for future work are then laid out in chapter 9 while overall conclusions are drawn in chapter 10.

1.2 Current problems in our understanding of arsenical copper

Several questions have dominated the study of arsenical copper since its earliest identification in the archaeological record. While some appear to have been resolved, most still require further investigation and will be defined here.

Without going into details of the physical properties of the alloy at this point as they will be thoroughly discussed in the next chapter, it is sufficient to note that, overall, the material behaves much like the low-tin bronze more familiar in the later bronze ages (Moorey 1999; Özbek et al. 2002) (Budd and Ottaway 1995; Charles 1967; Craddock 1995; Lechtman 1996; Northover 1989; Weeks 2003). It has been established that advantageous properties begin to be noticeable visually and physically with between 0.5 and 2 wt% arsenic content, a range which has been used by many authors as the minimum percentage required to denote intentionality of production. However, the large width of this range is the result of different approaches to the study of the material properties of the alloy and no consensus has been reached as to what constitutes a relevant minimum. For example, 0.5 wt% arsenic is defined

by Charles (1967, 25) as the “maximum figure which might be expected from the smelting of randomly selected ore without particular effort to remove or make additions of arsenic”, the same point at which Lechtman (Lechtman 1996) notes that the enhanced cold and hot working properties of the alloy become noticeable. Hardness as the prime advantageous marker over pure copper is argued by others (Eaton and McKerrell 1976; Northover 1989), suggesting 1 wt% as the minimum value for this property to be manifested after cold-working. Yet others have arbitrarily suggested 2 wt% as a basis for intentionality on the assumption that the smelting of complex ores is unlikely to yield consistently higher percentages (Branigan 1974; Hook et al. 1987). More pragmatically, Fernández-Miranda et al. reject the use of a minimum value, in particular in the low percentage range, as “the interpretation of the phenomenon can vary according to the geographic and cultural areas examined, the conditions of the available mineral deposits, and the technological knowledge behind the production of artifacts” (1996, 454).

Indeed, the concept of intentionality based on percentages is the result of applying well understood historical perceptions of ancient tin bronze metallurgy to interpretations of prehistoric arsenical copper production and use. This is questionable not least because we have little real understanding of which arsenical copper attributes were valued by ancient smiths. These are likely to be very different at the onset of the appearance of this new material than in the later periods when copper alloys were already common and widespread. It has, after all, been convincingly demonstrated that the introduction and adoption of a new material tends to be limited to the imitation of previously existing objects and it is only once that material has been firmly adopted by society that other uses begin to be explored (Pfaffenberger 1992; Shortland 2004). The contrasting use of metals in the early stage of adoption is apparent in the Near Eastern Chalcolithic when a large proportion of arsenical copper alloy objects were decorative pins and needles (Caley 1949; Eaton and McKerrell 1976; Esin 1976; Frangipane 1985; Thornton et al. 2002) rather than the more utilitarian tools and weapons of the later periods. These decorative objects were typically left as-cast and would therefore have gained little benefit from increased workability or hardness. It is possible that early metalworkers simply wished to make use of the other properties of arsenic such as its ability to lower the melting point of copper, its propensity to act as a deoxidant, or its silvering effect through inverse segregation (McKerrell and Tylecote 1972; Meeks 1993; Shalev and Northover 1993). It is also interesting to note that arsenic gives off a strong garlicky smell when heated from the release of arsenic trioxide (As_2O_3), a property that may have been significant to ancient peoples in much the same way that European brass

was deemed far more valuable to indigenous Carribean peoples of El Chorro de Maíta, Cuba, for its distinctive smell and colour (Cooper et al. 2008; Martinon-Torres et al. 2012).

Overall, and despite our thorough understanding of the various physical properties of the alloy, we still cannot identify which, if any, of its attributes were both visible and culturally valued during the Late Chalcolithic and Early Bronze Age. Hence, not only do we have little understanding of *how* arsenical copper was produced, but we still do not know *why* it was being produced so systematically during this period.

A major barrier to answering this last question has been the enduring doubt regarding the intentionality of the production process which has formed the crux of an on-going debate originating in the 1970s and lasting to this day. This uncertainty is largely caused by the common geological co-occurrence of arsenic and copper minerals. The smelting of such polymetallic ores produces arsenical copper and could account for its widespread use through unintentional production (Fernández-Miranda et al. 1996; Golden 2009; Hauptmann 2007; Pernicka 1999; Tylecote et al. 1977; Zwicker 1980). However, the archaeological evidence suggests that the situation was much more complex. Indeed, the chemical analysis of copper alloy objects often revealed patterns in the arsenic content correlated to certain functional artefact types, such as in the prestige items of the Nahal Mishmar treasure (Levy 1995), which has led many scholars to conclude that they were intentionally produced (Bar Adon 1980; Charles 1967; Charles 1980; Eaton and McKerrell 1976; Muhly 1973; Muhly 1988; Pigott 1999c; Tylecote et al. 1977). Further confusing the situation is the possibility that ancient metalworkers may have simply recognized the enhanced properties of copper smelted from certain deposits (Budd et al. 1992; Hook et al. 1991; Keesman et al. 1991-1992) and selected such alloys for specific uses rather than intentionally produced the alloy from them (Gale et al. 1985c; Palmieri and Sertok 1993).

Defining the concept of intentionality is therefore essential to the discussion. Since we have few clues as to which properties were sought after, the definition of such behaviour needs to be suitably encompassing to permit the inclusion of the different value systems of disparate groups of metalworkers and consumers. As such, Roberts et al (2009, 1017) define intentionality as the “deliberate choices made in the production process, whether in the selection of ores or the mixing of metals” and will therefore be used in this thesis. In addition, and to distinguish between intentional behaviours, the use of the term *alloying* will be limited to the deliberate addition of a material for the express purpose of enhancing or modifying the resulting product. This latter case is much more difficult to establish with any certainty

as it requires evidence in differential use of the finished product in addition to evidence relating to the production technology. In practice, *intentionality* is embodied in any metallurgical operation other than those which involve the direct smelting of complex ores containing all of the alloying elements and which result in the production of a noticeable alloy. The term *Alloying*, on the other hand, will be restricted to refer solely to the addition of a mineral or metal in a separate stage of production. Thus, alloys can be intentionally produced or accidentally produced at the smelting stage, but alloying itself applies only to more controlled and predictable instances typically only associated with silver or tin bronze metallurgy. In addition to this measure of intentionality, the notion of control versus uncontrolled (Weeks 2008, 343) is an important consideration in situations where the alloy is recognised and utilised distinctly from pure copper but control of arsenic content is not yet understood and achieved such as was the case in Iberia (see section 3.2). Potentially identifying formal alloying processes in Southwest Asian arsenical copper production is a main focus of this research and is a point which will be returned to throughout the thesis.

The difficulty in distinguishing between them archaeologically is evident, and particularly so when trying to apply the two concepts to arsenical copper for a number of reasons. First and foremost are issues relating to the retention of arsenic and recycling. Due to arsenic's low melting point and strong tendency to oxidize and volatilize, smelting of polymetallic ores, even under reducing conditions, is commonly thought to result in significant losses of arsenic of no less than 10% and usually more. In an oxidizing atmosphere, which is often present during melting and casting, up to 70% of arsenic can be lost (Tylecote 1991; Lechtman and Klein 1999; but also see section 2.4 and Mödlinger's forthcoming work on arsenic losses during casting). This obviously means that any recycling of an object would lead to a decrease in its arsenic content and thereby obscure efforts to understand the production technology. Furthermore, it has also been argued that large objects were less likely to be recycled and therefore the higher arsenic content in some objects were the result of preferential recycling of smaller objects, which would have resulted in a greater loss of arsenic content in certain object types (Kunç and Çukur 1987). There is therefore a clear disconnect between the finished objects and the additive process, something which has limited the validity of many analytical studies which have tended to focus on these end products, most obviously because their collection and study is also the main goal of archaeological research at the detriment of more mundane waste materials.

In an effort to put the intentionality debate to rest, over the last two decades, attention has shifted away from over-simplistic interpretations of the rather limited information obtained from the chemical composition of finished objects, and, during the 1990s, has concentrated on developing a theoretical understanding of the primary production process. This led to the formulation of various hypotheses on possible methods by which ancient metalworkers could have created arsenical copper (Budd et al. 1992; Lechtman and Klein 1999; Rostoker and Dvorak 1991; Thornton et al. 2009; Zwicker 1991). However, while useful in the development of our wider understanding of archaeometallurgy, these ideas are largely based on theoretical thermodynamics and have little archaeological backing.

In recent years, and in order to counter this paradigm, efforts have moved towards the analysis of primary production remains in order to identify the processes directly (ex: Bassiakos and Catapotis 2006; Bassiakos and Philaniotou 2007; Catapotis and Bassiakos 2007; Nezafati and Pernicka 2006; Pernicka et al. 2011; Thornton et al. 2009). The broader picture is only now beginning to emerge, and it is becoming increasingly clear that the arsenical copper production methods varied greatly between the different regions, based not only on the availability of raw materials, but also on technological and socio-economic contexts. This means that we cannot simply apply our understanding of arsenical copper from one area to another. It is therefore essential to continue to pursue research in this direction in order to understand *how* arsenical copper was produced.

Yet, even more troubling in some ways is that despite the many archaeometallurgical studies of the material itself, hardly any research has been undertaken to try to understand how it was perceived and integrated within the ancient societies that produced and used it (Doonan et al. 2007). Indeed, in contrast to the Late Bronze Age, little is as of yet known about the miners, smelters, and artisans who manufactured the Chalcolithic and Early Bronze Age arsenical copper artefacts. There have been scant publications on reconstructing the social organisation of production, the levels of craft specialization, or the value ascribed to this alloy. This dearth of anthropological analysis of the alloy is of course in large part due to the lack of consensus on intentionality as mentioned above. After all, how much impact could it have on these aspects of society if it was only incidentally produced? And yet this question in and of itself is worth exploring, especially within the context of the discovery and increasing use of a new material, whether intentional or not.

And lastly, one of the most enduring questions on arsenical copper use relates to its decline and replacement by tin bronze in the Middle to Late Bronze Ages. While early theories

ascribed the shift to the superior qualities of tin bronze, it has already been stated that this was not in fact true. Issues relating to the toxicity of arsenic (Charles 1967) have also been refuted (Merkel et al. 1994). Furthermore, the fact that regions such as Iran continued the almost exclusive production of arsenical copper up until the Iron Age despite the widespread adoption of tin bronze in surrounding regions is strong evidence in favour of a much more socio-political reasoning behind the change (Doonan et al. 2007). The shift to tin bronze is of course made much more enigmatic by the still unresolved questions relating to the Near Eastern sources of tin (Muhly 1985; Nezafati et al. 2008a; Penhallurick 1986; Yener 2008).

1.3 Archaeometallurgy as Socio-economic and Cultural Interpretative Tool

The study of technology is essentially the study of one of the most defining aspects of human knowledge and behaviour. As such, attributes of cultural, political, economic, and social behaviour are embedded in the ways in which we use the natural resources around us to produce material culture. Unlike earlier linear evolutionary (Thomsen 1836) or deterministic models (Childe 1936; Childe 1944), the current view is that the study of technology offers archaeologists a new venue to extract hidden facets of the human consciousness that are not easily obtainable by the study of objects alone. It is with this in mind that many archaeologists have borrowed heavily from anthropological theory to develop ways in which to use technological remains to make inferences on ancient cultural practices and the context within which they existed (Costin 1991; Dobres and Hoffman 1994; Lemmonier 1989; Pfaffenberger 1992).

In an effort to incorporate these ideas and to come to relevant anthropological results, this research will follow the concept of the *chaîne opératoire*. This theoretical framework is based on the work of the anthropologist Leroi-Gourhan (1943) which was formalized for archaeology more recently by Lemmonier for applications on lithic technology (1993) and later adapted for other technological disciplines such as ceramics and metallurgy (Roux et al. 2013). The concept outlines a methodology in which the various technical stages, gestures, motions, and behaviours, whether practical or purely socially defined, involved in an object's life cycle could be recorded and interpreted. Lemmonier remarked that every stage of this life-cycle represented a series of culturally defined choices that could be reconstructed by the technical study of the artefact. Subsequently, this particular methodology was further refined to include the full scope of technological choices and the long-term effects of environmental, functional, and cultural effects on the design, shape, and composition of the artefacts studied (Sillar and Tite 2000). In this way it is possible not only to reconstruct the

physical production process of an object from the technological remains left behind in its creation, but also to infer symbolic or cultural ancillary behaviours.

The application of the concept of the *chaîne opératoire* to archaeometallurgical remains therefore enables the reproduction of the entire life cycle of a metal object from the extraction of the ore mineral to its discard, and even beyond to its restoration and museum display (Ottaway 2001) (Figure 1.1). These *chaînes opératoires* can be expanded upon as new research is conducted and different regions of the broad diagram can be easily focused upon. Thus, the greatest value of this framework is that a wide range of cultural behaviours can be studied and compared as a whole or in part across different cultural contexts and thereby making it possible to identify where cultural choices differed across technospheres.

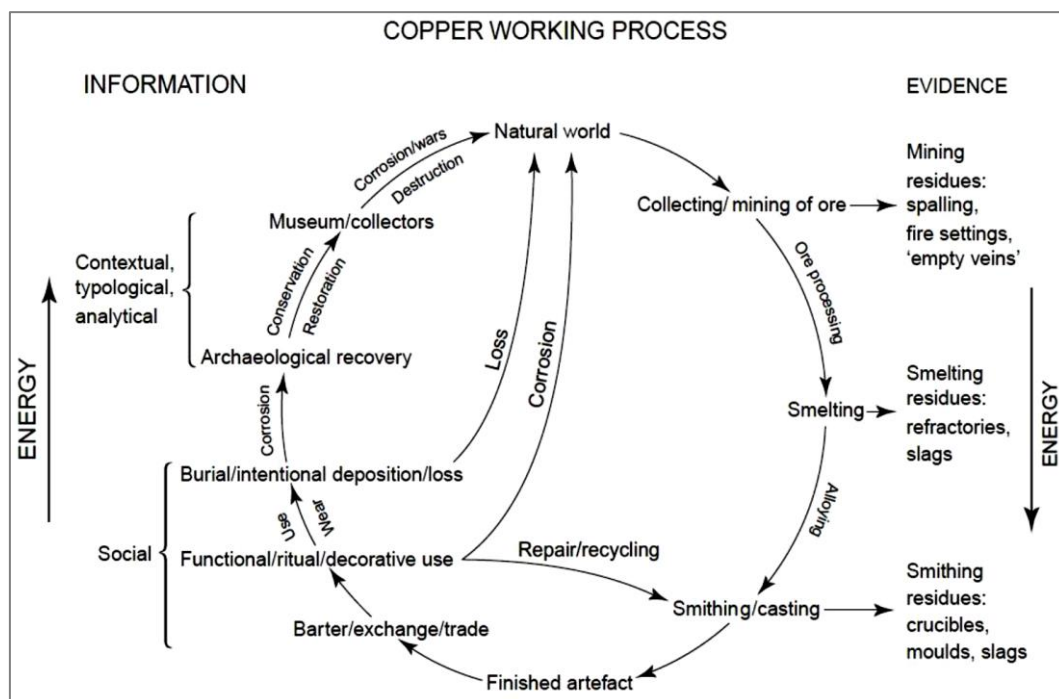


Figure 1.1 Metallurgical *chaîne opératoire* extending beyond the deposition into the archaeological record (from Ottaway 2001).

There are of course some drawbacks to the application of the *chaîne opératoire*. First and foremost is the risk of assigning cultural behaviour and intentionality to data which may in fact be caused by natural phenomena (Dobres 2010). At the other extreme is the risk of thinking of the *chaîne opératoire* as the end rather than the means of interpreting data. This latter is significant in that archaeological scientists often come to conclusions on the various technical steps of the process while making few or no inferences about past cultural behaviours (ex: Frame 2012; Pernicka 2010; Shalev et al. 2006). While these technical studies have their merits, the goal of archaeology should be to study human behaviour and their

interactions with their environment rather than the technical parameters in which they operate.

1.4 Use of Production Remains in the Reconstruction of the Metallurgical Process

Within this theoretical framework, this thesis makes use of several published methodologies when dealing with the various metallurgical finds. As the aim is to establish cultural and technological choice in the production of arsenical copper, it goes without saying that production remains form the main analytical corpus.

Of these, the most commonly recovered artefact, and arguably the most informative, is slag and as such forms the main material component of this project. This metallurgical waste product is generally considered of low aesthetic and perceived cultural value by the public and heritage professionals, which makes it relative easy to obtain for study and its destructive analysis permissible. It also inherently holds the highest potential for interpretation of the production process as it is formed of all the elements added to the system during a smelt or melt and therefore provides reliable information on the raw materials, the atmospheric conditions under which they were processes, and the intended product.

For example, slag often contains fragments of incompletely reacted material that can provide clear indications of the original charge composition and can inform on the type of ore, flux, and fuel used. Conversely, the fully molten and subsequently re-crystallized or amorphous phases are indicative of the atmospheric conditions within the reaction vessel, such that it is possible to identify the minimum temperature achieved, the oxygen fugacity present, and the length of cooling. Prills and other metallic or semi-metallic phases can be formed of partitioned elements absent in the slag and can further inform on the nature of the original charge. In addition, the oxidation state of certain transition elements (typically iron) can be fine indicators of the oxygen fugacity of a system.

Given a known quantity of slag and its composition, along with the known or deduced composition of the original ores, it is also possible to estimate the amount of ore processed and that of the metal produced. This can be calculated for any context, and can be invaluable in estimating the output of a single smelt to that of a slagheap.

Slag remains presented in the results chapters will be described following the steps outlined by Bachmann (1982) and Miller (Miller 2007) and will follow analytical principles laid out by Hauptmann (Hauptmann 2007; Hauptmann 2014).

Crucibles, moulds, and furnaces form the second major category of the assemblages under study. These technical ceramics, termed as such when manufactured explicitly for the use in specialized pyrotechnological industries regardless of their refractory behaviour (Rehren and Martín-Torres 2014), provide a parallel but vital aspect of technological choice in metallurgy. It has been said that the development of metallurgy often follows innovations in ceramic technology (Thornton and Rehren 2009), and indeed decision making during the manufacture of crucibles or furnaces, such as the type of clay used or the nature of temper added, often directly impacted the success of the metal extraction process. A measure of the various techniques used in their production therefore forms part of the overall cultural and technological package associated with metal extraction.

Chemical and petrographic characterization of these types of finds is helpful in identifying the presence or absence of specialist ceramic production when they differ significantly from other types of pottery found on site. Their refractoriness can be quantified by measuring the maximum temperature to which they can be subjected without losing their integrity, which in turn can be compared with domestic fabrics to gauge the ancient artisans' understanding of metallurgical necessities.

For the purpose of this thesis, crucible and furnace macroanalysis will follow the methodology of Bayley and Rehren (2007) and Whitbread (1995). Microscopic and chemical analysis of the finds will be based upon a number of case studies which have come to meaningful results (Bassiakos and Catapotis 2006; Catapotis and Bassiakos 2007; Georgakopoulou et al. 2011; Hauptmann 2007; Rehren et al. 2012) as there is currently no formalised methodology for these types of finds.

1.5 Aims of the Research

The research proposed herein will endeavour to address some of the problems and issues outlined above through the analysis of production remains from two recently excavated archaeological sites, Çamlıbel Tarlası in Turkey and Arisman in Iran. These sites straddled the shift from Late Chalcolithic to Early Bronze Age and it is believed that their metallurgical technology was reflective of wider regional trends. The study will first identify the technical parameters involved in the production of arsenical copper. Once this baseline for comparison is established, the research will focus more deeply on the cultural context within which this technology emerged. Broadly speaking, the proposed research will answer two main questions:

1. How was arsenical copper produced in Southwest Asia during the Late Chalcolithic and Early Bronze Age? Answering this question is essential in our understanding of the developments of the earliest alloying technology in the Old World. It should also finally shed some light on the intentionality of arsenical copper production in the region by isolating the nature of the alloying operation. In order to do so, the research will reconstruct the full production system at both sites by identifying and defining the types of ores, furnaces, crucibles, fuel, flux, as well as the intended output, through the study of the recovered slag and technical ceramics. Using these data, the arsenical copper *chaîne opératoire* will be reconstructed to develop a basis upon which to make socio-economic and cultural inferences.
2. How did arsenical copper alloying technology evolve from the Late Chalcolithic and how does it relate to contextual social, economic, political, and environmental factors? A large portion of this study is based on the assumption that arsenical copper production technology can act as a marker of technological changes and the emergence of new approaches to metal production between the smelting of pure copper and the production of bronze. As such, the study of the earliest form of alloying should inform on how and why this innovation occurred and how it relates to the wider regional cultural context. It is hoped that links can be made between the emergence of this technology with the increasing urbanization and social stratification occurring across the Near East at this time. It is expected that changes in the organization of production and settlement specialization may have been caused by the complex series of operations required to produce arsenical copper objects with any degree of control. How these ancient metalworkers were integrated into the wider regional trade networks and what roles these pathways played in the dissemination of metallurgical knowledge will also be explored.

Chapter 2 Arsenical Copper Material Properties

2.1 Physical Properties

The alloys of arsenic and copper have had very few uses throughout history since its decline in the Bronze Age except for a few exceptional instances. Indeed, until the advent of modern electronics, arsenic had only been added in small quantities (less than 1%) to copper alloys for locomotive fire-boxes, boilers, roofing and condenser tubes for its properties of raising the annealing temperature and protecting brass and copper from corrosion and wear (La Niece and Carradice 1989). However, since the decline of steam-powered locomotives in the early part of the 20th century and developments of new corrosion-resistant and less hazardous materials there has been little interest in the continued production of arsenical copper alloys. Today, modern metallurgists tend to treat arsenic as an undesirable impurity and great efforts are usually made to completely remove it because of its deleterious effect on electrical conductivity. This means that there has been little interest in arsenical copper alloys containing more than 1% arsenic since the mid-20th century, and therefore there is little to no modern industrial metallurgical data on the high arsenic alloys and their properties (La Niece and Carradice 1989). With increasing archaeological evidence of the use of the material in prehistoric times, there has been a push in the last few decades by archaeometallurgists to characterize these attributes. Unfortunately, work on this has been intermittent, with results often contradictory, incomplete, and scattered across dozens of publications. The following discussion will therefore group these strands together.

As has been pointed out by Budd (Budd 1991), our current theoretical knowledge of the copper-arsenic system is fairly recent and has undergone a number of revisions over the course of the last century. First established by Hanson and Marryat (1927), it was later added to by a number of researchers (Hansen 1958; Heyding and Despault 1960; Hultgren et al. 1973; Hume-Rothery 1949-50), culminating in the phase diagram used in this study (Subramanian and Laughlin 1988).

In their solid states, arsenic and copper are only partially soluble within each other (Figure 2.1), with a maximum of 7.8 wt% arsenic dissolvable in copper at the eutectic temperature of 685 °C, lowering to 6.9 wt% at room temperature. A eutectic is present at 21 wt% As from which a copper-rich β phase forms peritectoidally from Cu and γ' at 325°C. The γ -phase (Cu_3As) forms congruently from liquid at 827°C with a range of compositions between 25.5-27 at.% (wt% = 22.5-23.9) (Subramanian and Laughlin 1988).

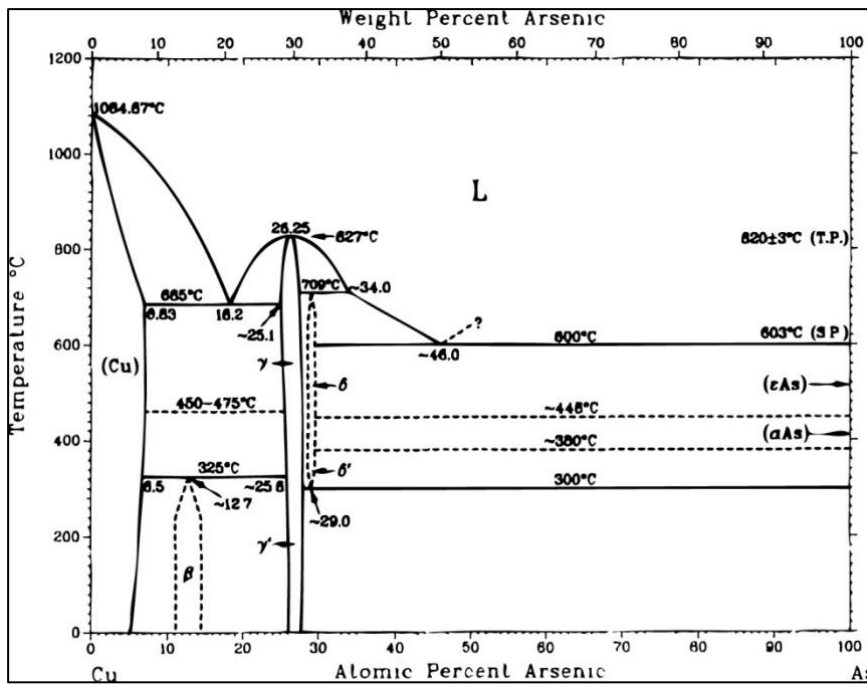


Figure 2.1 Cu-As equilibrium phase diagram, after Subramanian and Laughlin (1988).

However, it has been repeatedly reported that under non-equilibrium conditions the phase diagram should not be expected to be entirely accurate as this system is particularly prone to non-equilibrium cooling. It is indeed typical for a cored dendritic microstructure to form as a result of the steep gradient of the solidus-liquidus line (Budd and Ottaway 1995, 96). The higher melting point of copper leads it to solidify first as cored dendrites, and leaves behind an arsenic enriched inter-dendritic liquid with a lower melting point. These dendritic structures are preserved during rapid cooling due to the slow diffusion of arsenic ions in solid copper and results in the formation of a eutectic of copper-copper arsenic (domeykite, Cu_3As) which can contain upwards of 20 wt% As. The amount of arsenic required for Cu_3As phases to be present remains unclear, but these have been observed in alloys with as little as 1 wt% arsenic, well below the expected minimum of 7 wt% as suggested by the phase diagram (Budd and Ottaway 1991; Lechtman 1996; Meeks 1993; Ravich and Ryndina 1984; Shalev and Northover 1987). Regardless, the formation of this arsenic enriched eutectic occurs in a wide range of compositions and is likely to be highly dependent on the cooling rate.

Due to its lower melting point, the eutectic phase is usually forced to the surface by the solidifying dendritic network in a process identical to that of tin sweat but occurring at much lower concentrations of the alloying metal. This inverse segregation of arsenic rich phases leads to a concentration of arsenic towards the point of contact with the mould where the cooling rate is greatest (Charles 1967; McKerrell and Tylecote 1972). Some have suggested that the low boiling point of arsenic (613°C) may cause some arsenic metal to vaporize and

unavoidably form an enrichment layer upon cooling between the object and the mould surface during casting (Budd et al. 1992; Meeks 1993). However, this arsenic 'sweating' is unlikely to be a significant source of surface enrichment as arsenic appears to be strongly bound to the copper such that the arsenic partial pressure in non-oxidizing conditions is too low to cause significant loss of arsenic or surface enrichment, even at 1150°C (McKerrell and Tylecote 1972, 212). Regardless, inverse segregation is particularly relevant in the study of early metallurgical practices because it creates a distinctive silvery colour which has been found to tarnish less than silver metal (La Niece and Carradice 1989). It is therefore possible that ancient metalworkers were capable of exploiting this property by fast cooling low arsenic alloys to produce a silvery surface layer (Budd and Ottaway 1991; Eaton and McKerrell 1976; McKerrell and Tylecote 1972).

2.2 Casting Properties

In addition to these properties, the addition of arsenic also affects copper in a number of ways which are decidedly advantageous in casting of finished objects. The most obvious of these is the lower melting temperature provided by any alloying of two metals. Although according to the phase diagram the effect is rather minimal, the approximately 50°C drop in melting temperature from the addition of 3 wt% arsenic would have been enough to enhance casting success from improved flow and by granting just a few more critical seconds to complete the pour before the metal solidifies (Hook et al. 1991). Even more dramatic is the result of the addition of arsenic sulphide in the form of realgar which was found to reduce the melting point of copper to an astounding 830°C (Palmieri et al. 1992), although doing so also introduces significant quantities of sulphur to the final metal.

Furthermore, it has been often argued that arsenic acts as a deoxidizing agent in copper during the partial reducing conditions found in early smelting furnaces and crucibles or during fire-refining and casting (Charles 1967; Witter 1936). Oxygen is highly undesirable in copper metal as it forms cuprous oxide (Cu_2O) at the grain boundaries of the solidifying metal which makes the alloy much less ductile and drastically reduces cold-workability. Cuprous oxide can also react strongly with hydrogen during re-heating which results in blistering and cracking. The presence of arsenic prevents this from occurring as any excess oxygen will preferentially form arsenic trioxide, a highly volatile gas which is insoluble in copper (Charles 1967, 21). However, it may be that this benefit has been overstated as it has been pointed out more recently by Budd and Ottaway (1991, 134) that the formation of cuprous oxide only occurs when the alloy is slowly cooled. Furthermore, the detrimental aspects of cuprous oxide only occur when there is very little oxygen present and they disappear when oxides are

more evenly distributed in the metal as is typical in early smelting and casting technologies (Northover 1989). Low oxygen content, although it forms a tougher alloy, also leads to the rejection of dissolved hydrogen during solidification which can lead to increased porosity as reported from a range of sources (Budd and Ottaway 1991; Charles 1967; Hanson and Marryat 1927). Given that oxygen is not as deleterious as some authors suggested, and that its near complete removal could cause unsound casting, it is doubtful that the arsenic's deoxidizing behaviour was ever a characteristic actively pursued by ancient metal workers.

2.3 Mechanical Properties

There has been much debate about the mechanical properties of arsenical copper over the last several decades, culminating in a series of independent experiments which have attempted to provide a set of hardness, tensile strength, and cold/hot workability data comparable to the better known historic alloys. While these will be discussed below, it is critical to note that these properties were established using sets of modern arsenical copper alloys as well as archaeological material. As such, and given the propensity of the alloy to form non-equilibrium phases at various temperatures due to its steep cooling gradient, these data do not entirely adequately reflect the full range of microstructures, and thus properties, which could be produced in antiquity under non-equilibrium conditions. This point goes some ways in explaining the variability in the properties reported in the literature and indicates that such results should be read with some measure of caution.

One of the main physical trait of interest has been the increased hardness provided by the alloy. This property is imparted by the size difference between the atoms of smaller copper and larger arsenic atoms which together produce smaller grain sizes as well as distortions in the crystal lattice which impede dislocation in as-cast matrices (Hanson and Marryat 1927; Honeycome 1985). Although some researchers have dismissed the effect of this solution hardening as insignificant (McKerrell and Tylecote 1972), more recent work on Eneolithic artefacts from Britain has convincingly shown that there is a clear and noticeable increase in hardness beginning at concentrations of about 2 wt% arsenic (Budd 1991; Budd and Ottaway 1995; Budd and Ottaway 1991). Above the solubility level of arsenic of about 7% at equilibrium, the alloy becomes too brittle to be workable and this composition therefore forms the upper arsenic limit in objects which require working after casting. Heather Lechtman's (1996) more detailed experimental results (Table 2.1, Figures 2.2 and 2.3) confirm this and demonstrate that although arsenic concentrations of 2% or less have little effect on hardness in comparison to pure copper ($VHN_{Cu}=50$; $VHN_{Cu2\%As}=53$ [$VHN =$ Vicker's

Hardness Test, or kg/mm^2]), higher quantities of arsenic give significantly better results up to its solubility limit in copper ($\text{VHN}_{\text{Cu}3.5\%\text{As}}=62$; $\text{VHN}_{\text{Cu}7\%\text{As}}=72$).

Typical compositions for the Southwest Asian Late Chalcolithic and Early Bronze Age being around 3-5 wt% As, as-cast alloys would benefit from approximately 25% increase in hardness over pure copper. Although these increases may not seem particularly impressive, they are comparable to those achieved by low tin bronzes of about 4-5 wt% Sn (Figure 2.2) (Lechtman 1996; Ravich and Ryndina 1984) which were commonly produced at the onset of the Early Bronze Age (Esin 1969; Yener et al. 2003).

Also in line with tin bronzes is the ability of arsenical copper to be dramatically hardened through cold working thanks to its exceptional ductility (Hanson and Marryat 1927). Cold working, which is any mechanical stress applied to the objects below the recrystallization temperature (approximately 650°C), causes the formation and movement of defects within the lattice structure known as dislocations. These accumulate within the microstructure of the alloy as it is increasingly work hardened, leading to the formation of slip lines and eventually to the distortion of the grain boundaries expressed as a fibrous micro-structure (Ravich and Ryndina 1984). These can be easily observed metallographically and are important indicators of the amount of work hardening an object was subjected to. The dislocations interact with each other as well as the grains and inclusions until they ultimately restrict further motion and the alloy becomes significantly harder and resistant to further plastic deformation.

There is a point at which continued cold-working leads to the formation of cracks along the slip lines within the lattice, but the ductility of arsenical copper alpha solid solution means that it can be subjected to a relatively high amount of stress before this occurs. Indeed, if these phases are present, a reduction in thickness in excess of 99% can be achieved from cold reduction of alloys with just 1 wt% As (Hanson and Marryat 1927). This extreme ductility is maintained up to about 4 wt% As when it begins to taper off, from a maximum compression of 70-80% at 4-5 wt% As to a maximum of 40-60 between 6-8 wt% As, beyond which the alloy becomes too brittle to effectively cold work (Ravich and Ryndina 1984).

While no specific reduction in thickness constitutes the ideal balance between hardness and strength, it can at least be said that even low levels of arsenic concentrations can, in certain instances, have significant impacts on the hardness of an object when compared to pure copper. Following Lechtman's (1996) study, even low arsenic content and minimal cold working can lead to noticeably harder metal. For example, a reduction of thickness of 25% in

an alloy containing just 1 wt% As results in 33% increase in hardness versus pure copper ($VHN_{Cu}=85$; $VHN_{Cu1\%As}=113$), although it must be said that this improvement is almost entirely annulled upon reaching 50% reduction in thickness ($VHN_{Cu}=127$; $VHN_{Cu1\%As}=136$). However, typical alloy compositions of 3-5% arsenic benefit much more systematically from cold working and can easily be hardened by about 50% over pure copper with any reduction in thickness (Table 2.1).

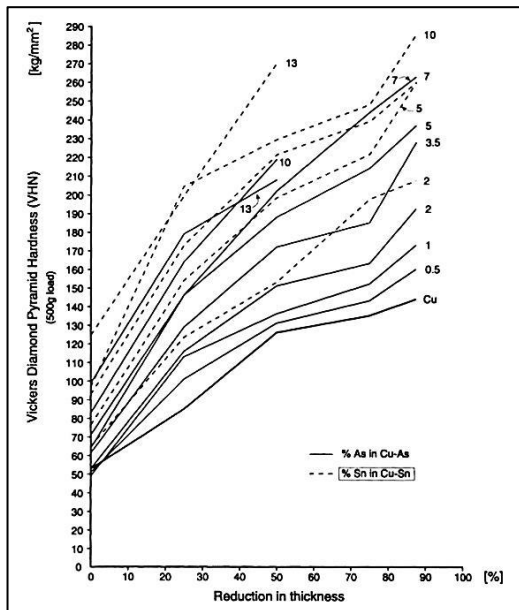


Figure 2.2 Diagram of the effect of cold working on hardness of both Cu-As and Cu-Sn (after Lechtman 1996, p. 496).

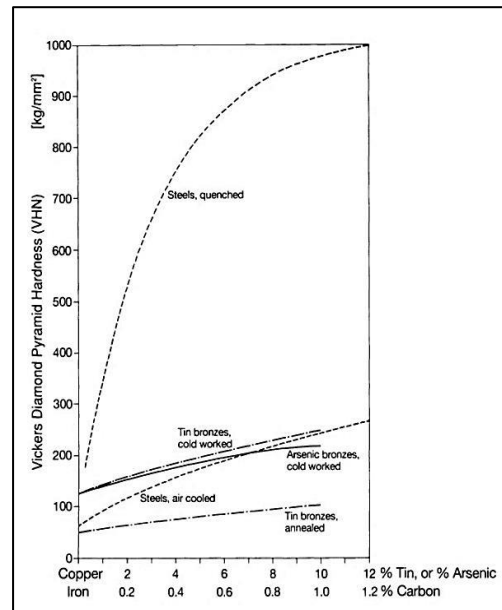


Figure 2.3 Increasing hardness of cold worked alloys with thickness reduced by 50% (after Lechtman 1996, p. 499).

Table 2.1 Effects of arsenic content and cold-hammering on alloy hardness. Reproduced from (Lechtman 1996, 494-495).

% reduction	Hardness in VHN (% Δ)						
	Cu	0.5% As	1% As	2% As	3.5% As	5% As	7%
25	85	101 (19)	113 (33)	116 (36)	129 (52)	145 (71)	145 (71)
50	127	131 (3)	136 (7)	151 (19)	179 (41)	188 (48)	201 (58)
75	135	143 (6)	152 (13)	163 (21)	184 (36)	214 (59)	243 (80)
87.5	144	160 (11)	173 (20)	193 (34)	229 (59)	236 (64)	262 (82)
Mean% Δ		10	18	28	47	60	73

It should be noted that the tendency of copper and its alloys to harden through cold working could also have been perceived as undesirable to ancient smiths who were equally concerned with malleability in order to work an object into its final shape. Fortunately, much like pure copper and bronze, arsenical copper can be softened through an annealing process to avoid the formation of cracks and failures during the manufacturing process. At low temperatures, this process removes stresses built up during cold working without affecting the material's

hardness. At slightly higher temperatures, new stress-free equiaxed grains with annealing twins begin to grow, eliminating the earlier dislocations and softening the metal. It allows the material to be shaped once more without the threat of cracks forming within the object but at the cost of loss of hardness.

The point at which this effect occurs is notoriously difficult to define due to compositional variability within the alloy, and depends on both time and temperature. The presence of solute atoms of arsenic within the copper solid solution is particularly effective in raising the recrystallization temperature of the alloy. Recrystallization of copper-rich dendrites begins at about 300°C (Budd 1991; Northover 1989), but complete recrystallization of both α and γ requires at least 600-650°C. It should be noted that even after recrystallization, the alloy retains much of its locally enriched dendritic and eutectic zones, and homogenization of materials containing 1-8% arsenic only occurs if a temperature above 650°C is maintained for 24 hours (Ravich and Ryndina 1984).

There has been some discussion of the hot-working properties of arsenic which suggests that high arsenic alloys can be easily worked while above the recrystallization temperature to allow a continuous forging process without risking the structural integrity of the object (Lechtman 1996; Ravich and Ryndina 1984). Although it was first suggested that deformation of oxide and sulphide inclusions might act as markers of hot forging alone (Tylecote 1987), it has subsequently been shown through experimental work that these could also be formed through cold working (Northover 1989). There is therefore no current way of distinguishing between hot working and cycles of cold working and annealing. Regardless, as Budd (1991, 56) points out, "restricting the shaping of artefacts to hot forging would seem to be an unnecessarily elaborate manufacturing process". In addition, the process of hot working would lead to unacceptable losses of arsenic through oxidation and volatilization under even the lightest of oxidizing atmospheres (see McKerrell and Tylecote 1972).

Little to no work has been done so far in assessing the subtler mechanical properties of the alloy, such as its tensile, fatigue, impact strength, or fracture toughness in relation to other available materials of the period. This lacuna will need to be addressed in order to provide a measure of comparability.

2.4 Volatility

Arsenical copper's Achilles heel is widely considered to be its volatility, although there remains some debate as to how much loss occurs in the various stages of smelting, melting, and annealing. This is largely due to the fact that we have little understanding of how arsenic

behaves in non-equilibrium high temperature systems. As a metal, its low boiling point of 613°C means that it could easily escape during smelting if conditions were reducing enough for it to exist. It is also strongly reactive to oxygen, and readily forms the highly toxic compound arsenic trioxide (As_2O_3) under oxidizing conditions. This compound is even more volatile, and with a boiling point of just 465°C will easily sublime from a smelt or melt. It should be mentioned that release of this arsenic trioxide can be easily noticed through its characteristically strong garlic-like odour which can easily warn metalworkers of its presence. Despite the lack of solid data on the topic, it is the easily volatilized and highly toxic nature of these two phases which has been interpreted as the main culprit behind arsenical copper's demise and ultimate replacement by tin bronzes (Branigan 1974; Charles 1967).

However, while these two phases are indeed highly volatile, they do not tend to be produced in significant quantities while smelting due to the prevalent reducing atmosphere (Bourgarit 2007) and arsenic's interactions with other phases present in the smelt. On one hand, such atmospheric conditions prevent the formation of arsenic trioxide, and on the other, like all elements of the 5th group of the Periodic Table, arsenic has a strong affinity for most transitional metals, often forming the intermetallic compounds 'speiss' when present in enough quantity (Thornton et al. 2009), rather than escaping as a metallic vapour. Under such conditions, low levels of arsenic will readily dissolve within copper metal while liquid and remain either as part of the α solution or as the eutectic γ upon cooling. Experimental smelts of cuprite sands with associated arsenic mineralizations in Heligoland showed that even when little arsenic is present in the ore body it is surprisingly easy to obtain elevated arsenic levels in the product (Lorenzen 1966). This has been further demonstrated by a series of experiments on a range of oxide ores from Israel's Timna Valley (Tylecote and Boydell 1978; Tylecote et al. 1977), Peru's Batan Grande (Merkel and Shimada 1988), and from the Caucasus (Pazuchin 1964) which has led the researchers to suggest that near total arsenic retention was possible. Experimental smelts of synthetic olivenite by Pollard et al. (1991) showed that it was relatively easy to produce arsenical copper of up to 4 wt% from the smelting of mixed copper arsenate ores below 1000°C. This finding was further tested a few years later by smelting southeastern Spanish copper arsenate ores (Fernández-Miranda et al. 1996). Their results confirmed that smelting such ores consistently led to the introduction of arsenic to the copper in quantities between 3.7 and 5.7 wt%, regardless of the original amount of arsenic in the charge. It therefore appears that beyond a threshold of about 4 wt%, and the closer one approaches the solubility limit, arsenic is most easily removed through sublimation, but that below this point arsenic losses in the same atmospheric

conditions tend to diminish. That being said, Pollard et al.'s experiments (1991) further concluded that once the copper was fully molten, arsenic could penetrate into the copper through a cementation process much more efficiently than in high temperature solid solutions. When added directly to molten copper under reducing atmospheres, less than 20% of the arsenic was lost. They add that such suitably reducing atmospheres could easily be produced within small charges simply by covering the ore with charcoal so that it was not particularly difficult to limit the escape of arsenic.

It should be noted that under smelting conditions, arsenic, whether as oxides or as metal, is not partitioned off with the rest of the gangue and very little is retained within the slag (Meliksetian et al. 2007).

During melting and casting, the opportunity for arsenic loss is much greater as the presence of oxygen is likely to cause the formation of arsenic trioxide. This happens through surface exposure to air, but also as a solid reaction with copper (I) oxide (Cu_2O) at lower temperatures (Budd and Ottaway 1995, 96). In the latter instances, evidence of the process can be observed under the microscope as spherical inclusions of arsenic trioxide which formed around reduced copper (I) oxide inclusions.

Much like the efforts undertaken to assess the behaviour of arsenic during smelting, a number of experiments have also been conducted in an effort to quantify arsenic losses of molten arsenical copper during melting and casting. These series of studies are particularly relevant given the common perception that arsenic is immediately removed when an oxidizing atmosphere, such as that present during casting or refining, are applied to liquid arsenical copper (Craddock 2000, 154). The most comprehensive of these found that under mildly reducing conditions arsenic losses were negligible - just 0.2 wt% decrease in arsenic content in a 9.8% As alloy after being molten for several hours in a low-oxygen environment (McKerrell and Tylecote 1972). However, under oxidizing conditions the loss was rather dramatic - from 9.7 wt% to 4.2 wt% after four melts and five episodes of hot working, and from 4.2 wt% to 0.8 wt% in just over 10 minutes of further hot working. Budd and Ottaway (1991), on the other hand, report that arsenic losses from arsenious oxide were elevated when arsenic was present above its solubility limit within copper, but negligible in low concentrations, even under oxidizing atmospheres. In addition, it has recently been shown that, at least theoretically, the presence of minor quantities of nickel results in lower arsenic vapour pressure and decreased losses through volatilization of arsenic and its oxides (Sabatini 2015, 2987).

These contrasting statements are difficult to reconcile without undertaking new studies of the behaviour of the alloy under systematically controlled conditions – something which is only now starting to be undertaken by Mödlinger (pers. com.) and for which results have yet to be published.

On a positive note, it has recently been demonstrated that the volatility of certain elements, particularly arsenic and zinc, offers opportunities in the tracing of inter- and supra-regional distribution and recycling patterns. This is based on the direct observable correlation between an archaeological object's distance from its metal source and the loss of volatile elements from remelting and recycling (Bray and Pollard 2012; Pollard et al. 2015).

In terms of metal production, it appears that arsenic can be readily retained under typical smelting conditions and its affinity for transition elements means that formation of speiss or arsenical copper is the norm rather than the exception even when arsenic is present only in low quantity. Furthermore, although hot working results in significant arsenic losses, melting and casting does not. As such, many researchers now feel that control of arsenic content in the final product was much easier to achieve than previously reported (Doonan et al. 2007; McKerrell and Tylecote 1972; Rapp 1988).

2.5 Toxicity

That arsenic is highly toxic to humans is of common knowledge, as anyone with a penchant for history and murder mysteries will know. However, arsenic can occur in both organic and inorganic forms, and with various oxidation states, all of which greatly affect the toxicity of the compounds. As several compounds can be formed through the smelting, casting, and working of arsenical copper, it is important to distinguish between these various compounds to understand the dangers and risks of the various metallurgical activities involved in the manufacture and use of the alloy.

While the organic compounds of arsenic, such as arsenobetaine found in fish, algae, and mushrooms, are known to be carcinogenic, they are not excessively dangerous to humans as they are not readily taken up by the body and undergo only limited metabolism (Cohen et al. 2006). Even today, they are still widely used in the agricultural and industrial sectors as pesticides.

In contrast, the inorganic compounds of arsenic are extremely hazardous to human health, and although exposure to these is most often associated with the use of water in regions with naturally arsenic-rich geology, the mining and smelting of arsenic bearing minerals is

certainly a major source of both groundwater contamination and airborne health hazards even today (Hughes et al. 2011, 308-309). These inorganic compounds occur in two main valence states, trivalent (III) and pentavalent (V). Although both of these states are toxic, trivalent arsenic compounds are more toxicologically potent due to their high reactivity with sulfur containing compounds and generation of reactive oxygen species (Hughes et al. 2011).

Arsenic entering the body through ingestion and/or inhalation is mostly flushed out through methylation in the liver and excreted in urine in just a few days. It is, however, considered a heavy element in that a significant amount of arsenic can be retained and incorporated into the body's keratin as well as into the bones (Özdemir 2010; Schoen 2004) and this can take several months to be removed. Long term exposure therefore can quickly lead to poisoning and a range of conditions ranging from dermatitis and hyperkeratosis, hair loss, liver and kidney problems, skin, bladder, and lung cancer, peripheral neuropathy which may lead to paralysis of the legs and feet, and eventual major organ failure and death (Hughes et al. 2011; Vahidnia et al. 2007).

It is unfortunate that the inorganic trivalent arsenic compounds are those most commonly produced in the smelting of arsenic bearing minerals, as arsenic reduced to its metal state (valence of 0) quickly re-oxidizes upon escape from the furnace to form the dangerous, and now airborne, arsenic trioxide (As_2O_3). The association of arsenic poisoning symptoms to metalworking has always been clear, and in particular it has often been pointed out that many ancient mythical metalworkers were afflicted by neuropathy, such as Greek Hephaistos, Roman Vulcan, Teutonic Wieland, Scandinavian Völunder, and the Finnish Ilmarinen who are all described as suffering from physical handicap (Harper 1987).

Health problems related to long term inhalation of arsenic trioxide gases produced during metallurgical activities are mentioned in the 17th Century Ming Dynasty's illustrated works of T'ien-Kung K'ai-Wu of Sung Ying-Hsing describing the arsenic calcination and sublimation process (I-Tu and Hsueh-Chuan 1966, 212):

For the calcination of [arsenic stones to make] arsenic, an earthen kiln is built which is faced with rocks on the outside. A chimney is built into the upper part [of this furnace], and the opening of the chimney is covered by an iron pot turned upside down. When fire is lighted beneath, the [arsenic] fumes will ascend through the chimney to become condensed in the pot. When the condensed layer is estimated to be about one inch thick, the fire is extinguished. After this layer is thoroughly cold, the fire is started again and the process is repeated until several layers have accumulated on the pot. This is the way to make white arsenic.

During the process of calcination, the operator must stand some 100 ch'ih to the windward of the kiln; all grass and trees close to the leeward side of the kiln will die. Arsenic workers must be transferred [to other work] after two years, otherwise all their hair will fall off.

Exposure to arsenic in ancient metalworkers has recently been determined in a number of instances where the preservation of organic material was exceptional. At Abu Matar, Israel, for instance, the analysis of bones from grave contexts showed that a number of low status individuals, as determined by their associated grave goods, had been exposed to elevated levels of arsenic when compared to bones from other nearby burials (Oakberg et al. 2000). These were buried as a single group and may represent a family or social group which have been interpreted as possible evidence of arsenical copper smelting and/or casting (Golden 2009). However, it should be mentioned that no analysis of the surrounding soil has been conducted, and the arsenic content could therefore still be the result of post-depositional accumulation through diagenesis.

Studies of hair obtained from mummified remains in South America have proved to be equally interesting, showing that many ancient Chileans suffered from chronic arsenic poisoning (Arriaza et al. 2010; Byrne et al. 2010). Although no link has yet been established with metalworking as the groundwater is known to be contaminated with arsenic in many parts of the Atacama Desert, evidence demonstrating that the arsenic was absorbed prior to burial rather than through taphonomic processes (Kakoulli et al. 2014) should prove relevant in future studies of arsenic-bearing human remains.

It is without doubt that ancient metalworkers were affected by arsenic's toxic effects, and this has been suggested as one of the reasons arsenic was phased out in favour of tin as an alloying agent (Charles 1967). However, given the generally rather small scale nature of smelting practices in the Late Chalcolithic and Early Bronze Age, the low life expectancy of individuals of that period, and the steps easily undertaken to minimize exposure, it is likely that the dangers of arsenical copper production and use have been largely overstated. Earl and Adriaens (2000) detail the experience of mid-20th century Cornish calciners where many tonnes of arsenic were burned off and arsenic sublimate collected in separate chambers. The workers simply covered their arms and face with fuller's earth to prevent arsenic sores and plugged their noses with cotton wool! Even modern archaeometallurgists undertaking a series of arsenical copper experimental smelts using blowpipes sitting less than two meters from a furnace suffered no ill effects (Merkel and Shimada 1988). Lastly, and perhaps a useful point to remember for potential experimental reconstructions, it has been demonstrated

medically that exposure to low doses of arsenic can increase tolerance to it (Gebel 2001; Schoen et al. 2004).

2.6 Corrosion

Like any alloying element, arsenic has some effect on the degradation and corrosion behaviour of copper objects which varies depending on the environmental conditions to which they are subjected. The topic of copper corrosion is, of course, one which has seen a tremendous amount of attention over the years from art historians, conservators, and archaeologists; it can, after all, so thoroughly affect and distort our understanding and preservation of such a large segment of our cultural heritage that it cannot be ignored in any discussion of the properties of arsenical copper.

Our modern understanding of the benefits and disadvantages of the presence of arsenic in copper tends to be limited to its well documented prevention of dezincification in alpha brasses containing less than 1% arsenic and about 30% zinc (Heidersbach 2011, 147). This is the main reason for its usage in locomotive fire boxes, boilers, roofing, and condenser tubes which were generally made of brass in the late 19th and early 20th centuries (La Niece and Carradice 1989).

In contrast, ancient arsenical copper alloys from the Chalcolithic and Bronze Ages tend to contain up to 5% arsenic and are often exposed to significant taphonomic processes over several millennia. Unfortunately, the corrosion behavior of such high arsenic alloys is poorly studied and little information is available on how they behave in various environmental conditions. Their heterogeneity in arsenic phase distribution and the disequilibrium in the phases caused by post depositional processes further compound the complexity of corrosion formation (Budd and Ottaway 1991). Scott (Scott 2002, 15-16) has suggested that the presence of any two distinct phases within arsenical (as well as antimonial and leaded) copper means that, at least theoretically, an electrochemical potential is formed between the anodic copper and the cathodic arsenic rich phases (typically domeykite, Cu_3As), which can lead to the movement of arsenic ions and the formation of various solid solution arsenic compounds within the alloy. As arsenic tends to be inversely segregated when cast, it is expected that the surface of the objects would be subject to drastically increased levels of corrosion and thus further concentrate the element on the outer surface (Craddock 1995; Hook et al. 1991).

This has been observed in archaeological objects in a number of instances. For example, at Abu Matar (Shugar 2003) it was noticed that surfaces of prills containing higher quantities of

arsenic tended to be more heavily corroded than those of purer copper. This was suggested to be caused by the inverse segregation of arsenical copper leading to the formation of domeykite phases along the outer surface. Shugar (2000, 207) further noted that arsenic's high mobility in oxidizing environments appeared to be controlled by co-precipitation with iron oxides, but that in iron poor or partially reducing environments, arsenic mobility was rather associated with higher levels of moisture and preferentially attacking the arsenic enriched phases along the surface of the object.

Overall, the multiple phases present in as-cast arsenical copper and the difficulty in homogenizing these phases, along with the relatively high electrochemical potential of arsenic, mean that arsenic-copper alloys have diminished corrosion resistance when compared to pure copper. This is in direct contrast to early archaeological thoughts on the matter (Caley 1949, 61). As few modern experiments have been conducted on this material, it is currently impossible to say exactly how susceptible it is to typical taphonomic processes and how it compares to tin bronze. Furthermore, since corrosion is highly dependent on environmental conditions, there are perhaps several situations in which arsenical copper could perform better than pure copper or other alloys. The preferential corrosion of pure copper phases over arsenical copper ones in Bronze Age bull figurine from Horoztepe (Smith 1973) certainly highlights this possibility.

Regardless, it remains unclear whether corrosion resistance was considered relevant to Late Chalcolithic and Early Bronze Age consumers or, for that matter, whether corrosion was rapid enough to be noticeable on a generational timescale. This area of research merits further attention.

Chapter 3 Arsenical Copper Production and Use

3.1 Production Technology, in Theory and Practice

Since it was first identified in the archaeological record, the production of arsenical copper has remained a thorny question which has confounded researchers for decades. Although some progress has been made in answering the question in some regions of the world such as South America (Lechtman 1991; Lechtman and Klein 1999; Merkel and Shimada 1988; Merkel et al. 1994) and the Iberian Peninsula (Hanning et al. 2011; Hunt-Ortiz 2003; Müller et al. 2007; Müller et al. 2004), there remains some doubt as to the process used in prehistoric Western Asia and the rest of Europe (Doonan et al. 2007; O'Brien 1999; O'Brien 2014; Thornton 2010). However, before discussing the archaeological record and what has been uncovered thus far, it remains useful to discuss the limited methods by which arsenical copper could theoretically have been produced in ancient times.

The distinction between these is critical in a discussion of the emergence of complex metallurgy since they denote varying degrees of ability and knowledge. While the first process described here denotes no concept of intentionality of production, this concept is implied in all subsequent theories presented here. However, it is only in the last two processes that true alloying in the modern sense is taking place.

3.1.1 Reduction of Copper Arsenates

With the notable exception of Central Iran, arsenic does not tend to be present in native copper in any significant quantities (Maddin et al. 1980, 213), and its alloy with copper therefore only begins to appear in parallel with the emergence of smelting activities in the 5th and 4th millennia BC and tend to contain over 1 wt% of arsenic (Esin 1967). As for Central Iran, where the deposits of Talmessi and Meskani in Anarak are known to contain rich native arsenic resources, little evidence has yet emerged to suggest that they were ever extensively exploited prior to the Early Bronze Age (Pigott 2004; Stöllner 2011; Stöllner et al. 2011a). Hence, it is generally believed that the earliest occurrence of these alloys is the result of the smelting of polymetallic ores containing both copper and arsenic. The simplest, and most likely origin for the earliest alloys, is the reduction of copper arsenates such as lammerite ($\text{Cu}_3(\text{AsO}_4)_2$) and olivenite ($\text{Cu}_2\text{AsO}_4\text{OH}$) (Budd et al. 1992; Charles 1967; Craddock 1995). The redox and temperature parameters required to smelt these arsenates are identical to those of purer copper oxide and hydroxides such as malachite and azurite and would not have required any additional skills or knowledge to extract. The ease of extracting arsenical copper from these types of ores has been demonstrated through a series of smelting experiments

which shows that a lightly reducing atmosphere led to the formation of fully molten copper metal with about 4% arsenic below 1000°C (Pollard et al. 1991).

These arsenate minerals tend to fall in the same green colour palette as copper oxide and hydroxide ores and could easily have been confused as such. Since the smelting of copper arsenates required no new mineralogical or pyrotechnological know-how, it is likely that the earliest arsenical copper objects were produced by this method through geological serendipity rather than as intended alloys. Certainly no specific systematic production processes had yet been established. This simple direct smelting process meant that the arsenic content of the final product was the direct result of the composition of local mineralizations and likely varied widely from smelt to smelt.

However, copper arsenate mineralizations such as these are quite rare as they are formed from the weathering of copper sulfarsenide minerals in the oxide enrichment zone where the arsenic is then easily leached out (Begemann et al. 1994; Blackburn and Dennen 1994; Yener et al. 1996). Thus, unlike what some earlier researchers had suggested (Charles 1967; Eaton and McKerrell 1976), it is doubtful that surface deposits of copper arsenates alone could be responsible for the ubiquity of the alloy in the Late Chalcolithic and Early Bronze Age. Although it is possible that such mineralizations were overexploited and depleted during this time period, their scarcity in regions where arsenical copper was never widely produced (such as Eastern Asia, North America, and Africa) seems to suggest otherwise.

3.1.2 Co-smelting of Copper Oxides with Copper Sulfarsenides

A second method involves the smelting of copper oxide along with sulfarsenide ores (Pazuchin 1964, 253; Ravich and Ryndina 1984; Rostoker and Dvorak 1991; Rostoker et al. 1989). Since it has been thoroughly demonstrated that roasting of copper sulfarsenides results in unacceptable losses of arsenic, it is now well understood that mixing these with copper oxides in a reducing atmosphere results in excellent arsenic retention while still permitting the removal of much of the sulphur (Budd et al. 1992; Eaton and McKerrell 1976; Lehner and Yener 2014; Meliksetian et al. 2007).

In many ways, this is simply an alternative to the previous technology to include the more common arsenic bearing minerals in a slag free to low-slugging process. These are much more complex and may have necessitated further technological innovations to successfully smelt. The easiest of these to deal with, the copper sulfosalts, can generally be divided into the tetrahedrite (or fahlerz) and enargite groups. While the enargite group is less common, it has a much more stable composition, ranging between enargite (Cu_3AsS_4) and famatinite

(Cu_3SbS_4) end-members. Fahlerz on the other hand is more common but has a complex microstructure with sites for uni-, di-, and trivalent cations following the general formula $\text{M}_{10}^+\text{M}_2^{2+}\text{M}_4^{3+}\text{S}_{13}^{2-}$, often containing copper sulfosalts of arsenic, antimony, or bismuth (Ixer and Patrick 2003; Yener et al. 1996). Copper cations can fill both the M^+ and M^{2+} positions and are commonly substituted by Ag, Fe, Zn, Cd, and Hg, of which only Ag and Zn readily partition into the final copper metal during typical copper smelting conditions (Yener et al. 1996). The composition of these minerals often varies within the same deposits, which makes them less than ideal for producing alloys with consistent arsenic content and sometimes difficult to smelt. Indeed, should more iron be present in the minerals, some fluxes may have been necessary and slag formation would be expected, thereby complicating the smelting process. Regardless, the relative abundance of such minerals in association with oxidized copper deposits (Ixer and Patrick 2003; Stos-Gale 1989), their noticeable grey-metallic colour, and the strong garlic smell of the arsenic-bearing members when heated would have made them easily identifiable and relatively easy to exploit (Craddock 1995, 289). There is much evidence to support the theory that this was one of the main ways of producing arsenical copper in many regions of the world (Hanning et al. 2011; O'Brien 1999). Although some researchers have cast doubt on the possibility of producing copper metal from sulphide minerals in crucibles as expected from Late Chalcolithic and Early Bronze Age contexts (Shugar 2003; Yalçin 2008), successful experimental tests suggest the opposite (Earl and Adriaens 2000; Özbal et al. 2002).

3.1.3 Co-smelting of Copper Oxides with Iron Arsenides or Sulfarsenides

In the same way, it is also possible to co-smelt oxidized copper ores with iron sulfarsenides or iron arsenides such as arsenopyrite (FeAsS), leucopyrite (Fe_3As_4), or löllingite (FeAs_2) (Merkel et al. 1994), although the higher iron content of such a mix would have necessitated an understanding of slagging technology. Despite this difficulty, mineralizations of arsenopyrite are relatively common and can be found in many of the largest copper deposits in the world. Indeed, smelting of such mixed ores has been attributed to many primary arsenical copper production sites dating to the prehistoric periods in both the Old and New Worlds. At Batan Grande in Peru, for example, it has been conclusively demonstrated that arsenopyrite and scorodite ($\text{FeAsO}_4 \cdot 2\text{H}_2\text{O}$) from nearby deposits were added to a mostly copper oxide charge (Lechtman 1996, 521-523; Merkel and Shimada 1988; Merkel et al. 1994). According to Lechtman (1996), this technology allowed the ancient smelters to avoid the roasting of ores and thereby prevent the release of toxic arsenic fumes since the smelt could be conducted either within a crucible or under strongly reducing conditions. This

technology appears to have been extensively used in the region and has been identified at several sites as far north as West Mexico, where arsenopyrite is thought to have been the primary source of arsenic, again mixed with copper oxide ores (Hosler 1988; Hosler 1994).

3.1.4 Copper Arsenides or Arsenates to Molten Copper

Perhaps more familiar to the metallurgy of bronze and more modern copper alloys, it is also possible to add arsenic rich material to molten copper to increase its arsenic content. This would be preferable over any type of smelting as it could potentially result in a predictable, consistent alloy composition (Craddock 1995). There is also evidence to suggest that arsenic is much more likely to enter copper when it is fully molten than through co-smelting or co-melting processes (Özbal et al. 2002, 437-438).

Given that arsenic as an element was not recognized or indeed isolated until the 13th century AD due to its extreme volatility (Wyckoff 1967) and given the difficulties in retaining the highly volatile element, metallic arsenic is highly unlikely to have been extracted prior the Medieval period. Although not abundant, native arsenic is known to form as a very late mineral at shallow depth in the intrusive magmatic sequence and those originating from sub-volcanic sequence (Ramdohr 1969). However, these occurrences, while not altogether rare, are typically rather limited to specific locations and generally present only as small mineralizations in the gossan. Together with the native arsenic, two further possible alloying agents exist: arsenic minerals similar to those described in the co-smelting methods (arsenates and sulfarsenides), and synthetic high-arsenic compounds (speiss) refined from these minerals.

The use of arsenic minerals added to molten metal after smelting has been widely acknowledged as a possible way by which arsenical copper could be both produced and its content controlled (Heskel 1983; Moorey 1999; Özbal et al. 2002; Özbal et al. 2008; Pigott 2008; Thornton et al. 2002). However, this suggestion is not as straightforward as it may first appear. The most obvious minerals to use for such a purpose would be copper arsenides, such as domeykite (Cu_3As) or arsenates, such as cornubite $\text{Cu}_5(\text{AsO}_4)_2(\text{OH})_4$, clinoclase $\text{Cu}_3(\text{AsO}_4)(\text{OH})_3$, olivenite $\text{Cu}_2(\text{AsO}_4)\text{OH}$, or calcium bearing conichalcite $\text{CaCu}(\text{AsO}_4)(\text{OH})$. In addition to what has already been discussed previously in co-smelting, these would be useful alloying agents in secondary production contexts as a way of increasing arsenic content once the copper had been extracted. This may have been an important source of arsenic in regions deficient in such mineralizations that required importation from further away. However, it should be noted that such a procedure would risk the oxidation of some of the copper from

the release of free oxygen and the inclusion of cuprite phases in the finished product unless strongly reducing conditions were maintained such as in a closed crucible.

More complex arsenides and sulfarsenides would be even more problematic as they would necessitate the removal of gangue and/or the loss of copper to matte. Despite this, experiments have been successful in creating arsenical copper from the cementation of copper with arsenic sulphide minerals such as realgar (AsS) and orpiment (As₂S₃) (Özbal et al. 1999; Özbal et al. 2008). However, these publications do not report the time necessary for the procedure or the mass balance of copper sulphide formation. Although it is certainly worth mentioning as a possible production process, the affinity of copper for sulphur, as discussed in the next section, means that the formation of matte is likely to be problematic under reducing conditions while unacceptable arsenic volatilization would be certain in an oxidizing atmosphere. Other experiments by the same author (Özbal et al. 2002) have also shown that it is possible to add significant amounts of arsenic to copper through the direct addition of arsenopyrite. By adding 1.5g of this mineral to 10g of molten copper, he produced an alloy containing 6-13 wt% arsenic. However, he does note that the final products also contained approximately 3-5 wt% iron and 1.5 wt% sulphur. This high iron content would have made the product nearly impossible to cold or hot work (Craddock and Meeks 1987). In fact, this elevated content is the direct result of the presence of sulphur, such that in a system at 1200°C, iron solubility in copper rises from approximately 3% in pure copper to more than 20% when just 2% sulphur is present (Craddock and Meeks 1987; Rosenqvist 1983). It is possible that the presence of sulphur and iron together also makes them more difficult to remove without also removing most of the arsenic, and this will be discussed further in the next section on speiss, but demonstrating this would require further experimentation. The absence of sulphur in iron arsenides (leucopyrite, or löllingite) could easily skirt the issue of increased iron solubility, and these minerals may therefore be more suitable for such an alloying process. However, their scarcity means that if they were ever used in such a fashion it was probably on a localized and small scale. The use of synthetic forms of these minerals, speiss, will be further discussed in the next section.

Regardless of which mineral is used, identifying such an alloying procedure in the archaeological record is extremely problematic as it would leave little to no archaeological traces. It has therefore never been conclusively identified archaeologically. However, this process has been recorded historically, albeit indirectly, in a number of passages in later periods. For example, Aristotle and his successor Theophrastus describe a technique for producing white copper which involved the addition of unusual 'earth' to molten copper

(Healy 1978, 210-212). As copper-silver alloys were already well known for millennia, it is likely that they are speaking of arsenical copper. Aristotle laments that such knowledge was tragically lost when the discoverer failed to transmit his innovation. In the well-known Leiden Papyrus, a kind of ancient metallurgical recipe book dating to the 3rd Century AD but referencing Alexandrian scholars from the 2nd Century BC, a formula is given for the production of white copper to imitate silver through the addition of decomposed *sandarach* to liquid copper. One of the original translators (Caley 1926) and other scholars (McKerrell and Tylecote 1972) have interpreted *sandarach* as the term used for the natural arsenic sulphide mineral realgar, and that decomposed *sandarach* likely refers to white arsenic trioxide which can be collected as a sublimate when arsenic sulphide is heated in air. A similar process involving the collection of sublimes has also been described more recently by Albertus Magnus in the 13th Century (Wyckoff 1967) and in Sung Ying-Hsing's illustrated T'ien-Kung K'ai-Wu published in 1637 (I-Tu and Hsueh-Chuan 1966). Although the Chinese example was probably conducted on a vast industrial scale and was likely associated with significant furnace structures, the other cases all describe small-scale processes that would have left little, if any, material remains behind.

It is also worth mentioning that arsenic can enter copper metal through solid state diffusion from arsenides at temperatures below 900°C. This has been demonstrated experimentally, but requires lengthy and extensive heat treatment and there is as of yet no evidence that this method was ever known or used (Pollard et al. 1991).

3.1.5 Speiss

The use of synthetic material was first proposed by Zwicker (1991) as speiss added to molten copper metal to produce arsenical copper. Although speiss technically refers to intermetallic compounds of any transition element with any element from the fifth group of the Period Table, in the context of the Early Bronze Age arsenical copper production only ferrous or base-metal arsenides, and to a lesser extent antimonides, are relevant. It should be noted that various forms of speiss are often observed in slag and tailings from the processing of lead, silver, and iron ores but that these are generally considered waste products formed incidentally and *in situ* in such instances (Broodbank et al. 2007; Kassianidou 1998, 74-75; Muhly et al. 1985; Özbal et al. 2002; Rehren et al. 1999). It has therefore been with some interest that recent discoveries in Iran at Shahr-i Sokhta (Hauptmann et al. 2003), Tepe Hissar (Thornton et al. 2009), and Arisman (Rehren et al. 2012) have led to a re-evaluation of the role of speiss as a useable product in the production of arsenical copper.

The use of speiss is likely to be the result of efforts to both control the arsenic content and to restrict copper losses to matte when introducing sulphide minerals in a process described by Rehren et al. at Arisman (2012), one of the two cases studies of this thesis. As oxidized surface deposits were depleted and copper exploitation shifted to the use of sulphidic ores, arsenic retention likely became increasingly problematic. Thoroughly roasting ores to drive off excess sulphur would invariably remove much of the desirable arsenic and so copper and arsenic sources had to be treated separately. This would have then left the smelters with oxidized copper ores and strongly sulphidic arsenic minerals, such as the abundant arsenopyrite. As previously discussed, these could be combined in the smelt in a co-smelting operation, but must have led to the loss of significant quantities of copper to matte since in reducing atmospheres and under temperatures expected during smelting sulphur has a stronger affinity to copper than iron (Willis and Toguri 2009). The solution presents itself in a separate smelting operation to produce speiss as an alloying agent, something which has been observed on a much larger scale at Arisman (Rehren et al. 2012).

Contrary to past understanding (Clark 1960), heating arsenopyrite at high temperature under poorly oxidizing conditions results in a series of transformation which ultimately leads to the preferential removal of sulphur from the system either as sulphur dioxide gas or its separation from the speiss as ferrous matte (Chakraborti and Lynch 1983; Raghavan 1988; Rehren et al. 2012). The remaining iron is thereby enriched in arsenic and ultimately melts and settles as a separate immiscible layer below any matte formed (see Fig. 1 in Thornton et al. 2009). However, this process is fraught with difficulty since the removal of sulphur exposes the arsenic to volatilization under oxidizing conditions, quickly leading to arsenic losses in the Fe-As system (Luyken and Heller 1938) as observed by numerous roasting experiments (Doonan and Day 2007; Meliksetian et al. 2007). Thus, the process had to be stopped immediately after the removal of sulphur, either by smothering the furnace, or through tapping the charge. Fortunately for our understanding of this technology, and unlike the addition of mineral copper arsenides to molten copper, this process leaves behind significant remains of slag. These slags are typically devoid of copper and rich in speiss and matte prills making them easily identifiable.

Once this iron speiss was produced, it could easily be added, either to a smelt or to molten copper, thereby increasing the arsenic of the finished copper in an easily repeatable and controllable fashion. When added to a smelt with copper oxides, the iron in the speiss, being less noble than the arsenic, would inherently act as a deoxidant in a co-smelting reaction (Marechal 1985). The resulting copper would then be enriched in arsenic, and to a very minor

extent iron. The same is true if speiss is added to molten copper, where a layer of iron oxide should form on the surface while arsenic ions migrate to the copper metal. Although it might be expected that some iron would enter the copper metal in such a process (Doonan et al. 2007, 112), the highly reactive nature of iron means that it is preferentially oxidized and precipitates out of the copper before the arsenic. This has been demonstrated experimentally by Pollard et al. (1991) who showed that the addition of synthetic löllingite to molten copper under reducing conditions resulted in 75% of the total arsenic present in the mineral being retained without significant increases in the iron content.

The added benefit of the production of a separate alloying agent such as speiss is that it could then in turn be traded over large distances much as tin was in later periods. Although we have definitive evidence that arsenical minerals were imported from outside sources to Chrysokamino in Crete (Bassiakos and Catapotis 2006), there is also some archaeological evidence suggesting that speiss was also being traded over long distances (Paulin et al. 2000; Thornton et al. 2009).

The unfamiliarity of archaeologists with these types of finds means that such minerals or objects are rarely recognized in the field and this may ultimately be responsible for the lack of data on the transport of non-metallic and non-ingot shaped alloying materials. Increasing awareness of the physical appearance of speiss may well reveal further evidence of its use. The re-evaluation of a fragment löllingite at the site of Poros Katsamba on Crete (Doonan et al. 2007) as a fragment of speiss (Thornton et al. 2009), the discovery of a large piece of iron arsenide/antimonide speiss ($\text{Fe}_2(\text{As,Sb})$) in a cremation burial context on the EBA site of Dhaskalio Kavos on the Cyclades island of Keros (Georgakopoulou 2013, 684-685; Georgakopoulou forthcoming), and the apparent inclusion of speiss material in melting slag from Çukuriçi Höyük in Western Turkey (Horejs et al. 2010; Mehofer 2014; Mehofer 2016) certainly suggest that we should expect further evidence of production and possibly long distance trade of this material.

3.1.6 Interpretative Dilemma

Problematic to our understanding of these technologies is the difficulty in distinguishing between them archaeologically, something which is necessary if one wishes to infer any human agency and make significant contributions to the study of ancient cultures.

Early attempts at discerning this tended to rely entirely on the chemical composition of finished objects, something which is fraught with analytical problems and which offers only limited insight into production technology. For example, Cayley (1949), while reporting on

the analysis of several objects from the Aegean, was the first to suggest that arsenical copper might represent an alloy produced specifically to exploit its work hardening properties and that it could potentially be used as a chronological marker. However, the study did not take into account the then relatively little known process of inverse segregation which may have greatly inflated the results, nor was any metallography attempted to confirm whether any cold working had indeed taken place. More fundamentally, Caley did not consider that such alloys could be produced from the direct smelting of complex geological deposits. Of course, Cayley's study should not be faulted for its limits but rather commended for identifying a distribution pattern which deservedly required further inquiry.

More in-depth studies of large artefact assemblages have since then led some to further consider the distribution of artefacts containing arsenic according to functionality. For example, in his wide ranging compositional and metallographic study of eneolithic arsenical copper artefacts from the British Isles, Budd (Budd 1991; Budd et al. 1992; Budd and Ottaway 1991) concluded that, despite a clear positive correlation between edged tools and high arsenic content (Northover 1989), there was no evidence to suggest any form of intentional *alloying*. He argued that because most objects had been annealed without further work hardening, ancient metalworkers could not have had any knowledge of the beneficial mechanical properties of the alloy. He therefore suggested that polymetallic ore deposits were simply exploited as found and that smelted prills of arsenical copper could be selected-for based on their lighter colour and reserved for the production of specific object types. This was done for reasons unknown, although it was pointed out that colour itself was unlikely to be the end goal as all of these objects were annealed and forged to shape, something which would have removed any strong colour differences through homogenization of the segregation layer with the body and overall arsenic loss. This view simply reaffirmed previously held beliefs that no form of alloying or conscious control was necessary to explain the typical composition of Bronze Age British assemblages (Coghlan and Case 1957; Tylecote 1962). Nearly identical conclusions have been drawn from artefact analysis alone at several other early consumption sites, and this methodology continues to be widely applied today (Palmieri and Sertok 1993; Pereira et al. 2013). Unfortunately, the disparity in arsenic content of the objects in these studies could just as easily be produced from differences in beneficiation or smelting practices as the preferential selection of arsenic rich prills. That no work hardening was undertaken does not constitute firm evidence of production technology.

Further information can, in some cases, be teased out of such assemblages and conclusively demonstrate some broad distinctions in production technology. Such is the case in the

Northern Italian Chalcolithic and EBA Remedello and Rinaldone cultures (Eaton 1980; Northover 1989). A comprehensive study of the composition of axes and blades from this region demonstrated a clear preference for high arsenic content in the blades but a consistent pattern of trace elements across both object types. This led the researchers to conclude that the same ore was being smelted and/or melted by different methods leading to more arsenic retention in the case of the blades. However, once recycling is taken into account, any such inference becomes untenable. As Kuņç and Çukur (Kuņç and Çukur 1987) proposed for the Iberian Chalcolithic, the differential arsenic content by functional types could be the result of preferences in the recycling of certain object types resulting in loss of arsenic during each melt. While the authors suggested that smaller objects may have had a greater chance of being recycled than larger objects in Iberia, shifts in perceived cultural values can be responsible for the retention of certain forms (and their arsenic) regardless of size. Regardless, these types of analyses likely form the upper interpretative limit of such data sets; it is certainly difficult to ascribe the concept of technological choice without a deeper understanding of the production *chaîne opératoire* for the alloy.

This is not to say that production remains always offer a clearer view of cultural behaviour, but they can certainly help in narrowing the range of possibilities. Indeed, although the production of speiss in a separate step leaves behind clear, distinct, and relatively long-lasting remains, most of the processes described above do not. How then can archaeologists differentiate between the reduction of copper arsenates, the co-smelting of copper oxides and copper sulfarsenides, or the addition of copper arsenides to molten copper since none of them is likely to have left much in terms of slag or other production remains? Similarly, slags produced from the co-smelting of copper oxide and speiss would be exceedingly similar to those produced from the co-smelting of copper oxides and native iron arsenide mineral. Furnaces and melting crucibles would be nearly identical and the final objects would most certainly be indistinguishable. However, the distinction implies a much more advanced industry or the trade in an entirely different material if synthetic speiss is used.

In many cases, knowledge of the ore minerals present at or near the production site along with the composition of the final objects can be sufficient in assessing whether co-smelting was the main means of production and if this was done intentionally or incidentally. Thus, the presence of complex copper arsenates and arsenides near and within several Chalcolithic sites of Southern Spain has led researchers to convincingly show that arsenical copper objects produced at Los Millares (Keesman et al. 1991-1992), El Malagon (Hook et al. 1987; Hook et al. 1991), Almizaraque (Delibes et al. 1991), and La Mancha (Bhardwaj 1979) were the result

of direct smelting without special beneficiation or mixing of different ores. This evidence does not exclude the further addition of arsenic minerals at any stage of the production process, but it is certainly less likely to have been necessary.

However, this was possible only because the technology was simple enough to be answered through the exclusive presence of complex ores on site. Where the technology involves mixing from two different sources, or when the nature of the ores remains unknown, reconstructing the production process becomes more difficult. In many cases it necessitates microanalysis of slag and technical ceramic remains. As the complexity of the dataset is then increased, so the resulting interpretations become less certain. For example, early analysis of Aegean slags from Kythnos pointed towards the accidental production of arsenical copper from complex ores (Gale and Stos-Gale 1989), something which has more recently been put into question (Bassiakos and Philaniotou 2007). More extensive analysis of material from a wider range of sites is now directing research towards the idea that arsenic minerals were imported from elsewhere and added to pure copper smelted on site (Catapotis and Bassiakos 2007; Doonan et al. 2007; Georgakopoulou et al. 2011).

There is no 'one size fits all' methodology here and to fully answer these questions it is often necessary to analyse every available aspect of the production process, from ore minerals to tailings, slag, and technical ceramics. Still, our understanding of alloying practices is expanding and archaeologists are continuously uncovering new production sites which help in testing the various theories offered thus far.

3.2 Late Chalcolithic and Early Bronze Age Use

3.2.1 Origins of Metallurgy with Comments on Colour

In the last decades there has been a dramatic rise in interest in the study of archaeometallurgy, which has led to a surge in the number of projects undertaken to answer many of the burning questions of the discipline. Despite this, the early use of metal-bearing minerals as pigments continues to be considered as the most likely origins of human interactions with such materials (Radivojević and Rehren 2015). The chronology may have been pushed back further in time, but our understanding of the sequence of technological development continues to remain static. This is due to the typical *longue durée* approach to innovative and socio-cultural development in the Neolithic which sees slow, incremental development over several millennia, followed by rapid Early Bronze Age urban expansion and dramatic changes in the fundamental structure of societies (Milevski 2013). Technological innovations occurring before the development of complex urban societies are often

perceived as following a linear evolutionary pathway prior to this period (Craddock 1995; Hauptmann 2007; Amzallag 2009). In that context, the use of copper-bearing mineral pigments is seen as part of a larger evolving package rather than a significant development in and of itself, and it is the use of the new colours associated with these that is very much of greater significance here.

Indeed, when compared to the earlier reliance on red and yellow ochres, the appearance of green and blue stones as beads for body adornments and as pigments in the Pre-Pottery Neolithic A (PPNA) marks the beginning of change in perceptions of aesthetics which has long term impacts on patterns of resource acquisition and cultural interactions (Bar-Yosef Mayer and Porat 2008; Roberts et al. 2009), what Yalçın (2008) has described as the 'pre-metallurgical phase' in his technological chronology. The earliest of these colourful minerals yet identified date to the 11th to 9th millennia BC. Green stones have been recovered from a number of cave sites throughout the Near East, but most notably at Hallan Çemi (Rosenberg and Davis 1992) and Çayönü Tepesi (Özdoğan and Özdoğan 1999) in southeastern Anatolia, a pendant from Shanidar Cave in Northern Iraq, and a perforated bead from Rosh Horesha in the Negev mountains (Bar-Yosef Mayer and Porat 2008).

Certainly by the Pre-Pottery Neolithic B (PPNB) there was an explosion in the use of green and blue minerals as beads and amulets with minerals such as apatite, malachite, chrysocolla, turquoise, amazonite, serpentinite, and lapis lazuli, being used with increasing frequency and traded over thousands of kilometres as seen by the large numbers of such beads found at a wide range of type sites such as Nahal Hemar (Bar-Yosef and Alon 1988), Jericho (Wheeler 1983), and Yiftahel (Gubenko and Ronen 2014). This has been remarked by some as a fundamental shift in the way settled peoples viewed their environment and a changing cultural value of aesthetics associated with sedentarism and the spread of agriculture (for an overview, see Bar-Yosef Mayer and Porat 2008). Links between the green colour and rebirth, fertility, health, and abundance have certainly been advanced a number of times, but never based on much concrete evidence. Regardless of whether one accepts these perspectives, the fact is that there was increasing demand for such colourful objects, and by the Late Neolithic green copper-bearing mineral adornments abound throughout the Near East.

Colourful minerals are thereafter part of the material assemblage of sedentary human societies and the frequency of use and extraction continuously increases throughout this period. It is during the PPNB that we have the first direct evidence of metal use, in the form of worked native copper beads and pins from late 9th Millennium BC Çayönü Tepesi in

Southeastern Anatolia, alongside perforated copper mineral beads (Maddin et al. 1999; Özdoğan and Özdoğan 1999; Stech 1990). It should be said that the site's exceedingly rich copper assemblage (over 50 copper objects weighing several kilograms) is unique at such an early period; other finds of native copper objects, dating to this period are few and far between. Early worked native copper objects have been identified in Anatolia at Aşıklı Höyük dating to the 8th Millennium BC (Yalçın and Pernicka 1999), at Çatalhöyük dating to the mid-8th to mid-6th Millennia BC (Birch et al. 2013), and Ali Kosh and Chogha Sefid in northern Kuzestan dating to the 8th Millennium BC (Hole 1977; Smith 1969). By the 7th Millennium, annealed and hammered native copper objects began to proliferate outwards towards the Balkans and throughout the Near East and were increasingly common over the course of the following two millennia. This long experimental period is considered by Yalçın (Yalçın 2008) as the 'beginning phase', which gave rise to the eventual 'development phase' with the advent of casting and extractive metallurgy in the Chalcolithic by the 5th Millennium BC (Yener 2000).

The topic of the earliest emergence of smelting technology is a hotly debated one which has seen the hypothetical innovative centre pinned at times in Mesopotamia, Anatolia, Iran, and more recently in the Balkans. Whether the near simultaneous emergence of extractive metallurgy across such a wide geographical expanse is due to independent indigenous developments or whether diffusion played a role remains unsettled. Smelting was certainly taking place in Eastern Serbia at the Vinča culture site of Belovode at the very onset of the 5th Millennium BC (Radivojević et al. 2010) as attested by a small number of slag, ore, and heat altered ceramic finds. However, there is also substantial evidence for smelting, in the form of slagged ceramic sherds interpreted as crucibles, at Tal-i-Iblis (Caldwell 1968; Caldwell and Shahmirzadi 1966; Frame 2012) and at Tepe Ghabristan (Majidzadeh 1979; Majidzadeh 1989). Both of these sites, situated in southwestern and northwestern Iran respectively, are dated to the 5th Millennium. Although an isolated find, a single slagged crucible fragment dating to 4600-4000 cal BC from Cheshmeh-ali in the central highlands may also prove to be indicative of early copper smelting technology in the region (Matthews and Fazeli 2004, 65). Similar production material has been unearthed at the site of Mentesh Tepe in Azerbaijan dating to the second half of the 5th Millennium BC (Courcier 2012).

Their near contemporaneity and distance from the Balkan evidence may indeed suggest independent centres of invention, but the scarcity of data on Chalcolithic sites in the Caucasus and Anatolia (Courcier et al. 2012; Schoop 2010b), largely due to a general enthusiasm for the Neolithic and Bronze Age period to the detriment of the Chalcolithic, may

also explain the large geographic void. The emergence of smelting technology from small-scale craft activities also bears responsibility in the ephemeral and rather limited nature of remains left behind by early smelting. Although it is often possible to identify whether the copper of a finished object is the result of extractive processes or the working of native copper based on increased impurities of arsenic, antimony, silver, nickel, and lead (Charles 1994; Maddin et al. 1980; Pernicka 1999; Krismer et al. 2012; Dussubieux & Walder 2015), direct and datable evidence, in the form of crucibles, furnace remains, and slag, is relatively rare.

Regardless of where smelting technology actually began, we have some ideas of the cultural and technological context under which it must have evolved. As previously mentioned, cultural association with colourful minerals played some role in their further processing and the discovery of their copper content. It is certainly well accepted that the earliest smelting most likely involved the reduction of rich oxidic copper ores found at or near the surface (most likely malachite) in open hearths in a non-slagging process (Craddock 1995; Hauptmann and Weisgerber 1996). This is certainly the case for the two earliest smelting sites known; oxidic manganese rich copper ores at Belovode and carbonate-hosted sulphides, arsenates, and chlorides for Tal-i Iblis (Pigott and Lechtman 2003, 294-295; Frame 2012). The heat treatment of lithic material and pigments were common in this period (Domanski and Webb 2007), thus heating of copper mineral adornments leading to the development of smelting is not unlikely. Experimental reconstructions of malachite and mixed oxide smelting in small furnaces abound, and it is without a doubt that producing copper from such rich copper ores is relatively simple (Bourgarit 2007; Bourgarit et al. 2003).

It has also been suggested that the development of early smelting typically occurred at, or near the ore deposits themselves (Levy and Shalev 1989; Nezafati et al. 2008b). However, there have been few early smelting sites identified in the vicinity of prehistoric mines, which Hauptmann and Wagner (2007) argue is because these coloured copper ores were well integrated into the wider exotic goods trade network. They propose that this trade in obsidian, which was conducted over distances of well over 100 km, resulted in experimentation with the materials at the point of consumption, some distance from the ore deposits. This would explain the focus on the copper production of high status objects such as pins and needles (Esin 1976; Thornton et al. 2002) rather than more utilitarian tools as well as the more domestic nature of early metalworking within settlements themselves. This theory appears to hold up not only in the Southern Levant where the study was undertaken, but also at early centres of metallurgical development such as Belovode in Serbia with

material likely originating from Majdanpek more than 100 km to the east (Radivojević et al. 2010, 2781-2782), in Anatolia at Arslantepe where ores came from several deposits in the Ergani-Maden area (Palmieri et al. 1999; Palmieri and Sertok 1993), at Norsuntepe (Hauptmann 1982; Zwicker 1980), Tüllintepe (Özbal 1986), Cayönü (Maddin et al. 1999; Özdoğan and Özdoğan 1999), and in Iran at Ghabrestan (Majidzadeh 1979; Majidzadeh 1989), and Tal-i-Iblis (Frame 2012). At each of the locales, evidence of early smelting and metalworking practices appears in settlement contexts, away from the sources of copper.

Ultimately, the separation between mineral and metal extraction may have been partly responsible for the eventual appearance and use of new and complex ores. The long range aspect of the exchange implies a disconnect between individuals involved in mining and those involved in smelting, not just geographically but also in their knowledge of technologies and techniques. Metal extraction and mineral extraction are, after all, fundamentally different processes requiring different skills. Throughout recorded history these activities have typically been conducted by entirely different people, and it appears that the earliest days of copper metallurgy were no exception given the distance between smelting remains and the ore sources.

In many ways this would have resulted in considerable competition to obtain the most productive ores through a highly decentralized system of prospection for new deposits. A variety of new ores must have thus occasionally (and increasingly) entered these distant settlements and preference for ores that resulted either in increased production success or in metal with desirable properties would have been quickly established. In essence the distance between mineral and metal production centres created a breeding ground for innovation which ultimately resulted in technological adaptation and innovation. Chalcolithic settlements were thus able to relatively quickly adopt novel sources of metal deposits, not just limited to copper, and to experiment with them. The scene was set for the development of lead, silver, 'gold', sulphide, mixed oxide-sulphide, and polymetallic smelting, for crucible-bound and furnace-bound pyrotechnology, for blowpipes and for bellows, and for the eventual rise of arsenical copper and other alloys in the Late Chalcolithic and Early Bronze Age.

3.2.2 Late Chalcolithic Innovations and Arsenical Copper Production

The currently accepted narrative on the rise of the Metal Ages has been well established over the decades since interest in ancient metallurgy began in earnest with Gordon Childe. It generally states that by the Late Chalcolithic, around the turn of the 4th Millennium BC, the

Near East and the Balkans witnessed a dramatic increase and outwards expansion of smelting activities which was to eventually reach Western Europe by the early 3rd Millennium BC and Eastern Asia by the late 3rd Millennium BC. Silver and lead smelting also proliferated at this time and metals quickly entered the realm of everyday life. As copper production increased, use shifted away from small luxury items to the manufacture of larger utilitarian objects, bringing with it a slew of socio-economic changes.

The increasing scale of these developments invariably led to the intensification of mining activities, which in turn quickly depleted the oxide enriched zone deposits near the surface, forcing the workers to dig ever deeper in search of copper-bearing ores (Craddock 1995; Yener 2000). It is this quest for copper which is thought to have forced ancient miners to exploit the more widely available but also more complex polymetallic ore deposits already mentioned, and consequently to the production of arsenical copper and other unusual alloys (Charles 1967; Wertime 1964).

As the name implies, polymetallic deposits typically contain several different metals and metalloids which have a tendency to partition into the copper product. These often include, but are not limited to, arsenic, antimony, nickel, zinc, bismuth, cobalt, and silver. They have several effects on the properties of the final copper alloy which may or may not have been sought after by early metallurgists. Interestingly, and regardless of whether past societies were aware of the deposits' impurities, the relative proportion of each element within polymetallic ores is often distinctive enough to be trackable in archaeological objects from certain periods and geographical regions (Chen et al. 2009; Northover 1983; Radivojević et al. 2013; Shalev 1999; Tadmor et al. 1995). However, these deposits are not ubiquitous to all regions and their complex chemistry means that metal could be difficult to extract efficiently with the technology of the prehistoric period. As such, only a few of these ore deposits appear to have seen mass exploitation during prehistoric times and it is unlikely that most 'special alloys' (Chen et al. 2009) were even recognized as distinctive during this time period, although some exceptions exist (Chakrabarti & Lahiri 1996; Kienlin et al. 2006). Apart from isolated instances such as the antimonial copper objects of the Nahal Mishmar Treasure and the silver alloys of the Royal Tombs of Arslantepe, arsenical copper is perhaps the only major exception as its early widespread production and use undeniably suggests at least some awareness that its properties were distinct from those of pure copper.

The extraction of such ores can be seen at a number of Chalcolithic and Bronze Age sites across the Old World and China and in the majority of these cases it is clear that the arsenic

content of finished objects is the result of the geological nature of the deposits rather than any wilful attempt at increasing it. It is generally thought that the complexity of such mineralizations undoubtedly caused some difficulties in the extraction of copper metal and likely initiated the development of innovative technologies to deal with them.

Foremost amongst these difficulties was the fact that deeper copper deposits were increasingly bound within gangue minerals which needed to be separated first by beneficiation, and then through the formation of slag from which copper could be extracted either through differential density or by mechanical means after cooling. For this reason, until the advent of slag tapping techniques, which are a hallmark of Bronze Age and subsequent metallurgy, the scale of copper production during the Chalcolithic was often restricted by the amount of gangue present in the mineralization and on the labour required to mechanically separate it. Due to limited understanding of slag liquefaction factors and optimal smelting conditions, the resulting copper prills were often trapped within a mass of semi-molten, viscous slag, which prevented them from coalescing into a billet (Bourgarit 2007). These amorphous lumps of slag had to be crushed to extract the enclosed copper prills. Furthermore, in order to achieve the temperatures required to achieve even this, Chalcolithic smelters had to include the fuel along with the charge in a relatively small reaction vessel, typically a crucible or bowl furnace, which further limited the scale of production. Fragments of crushed slag are characteristic of Chalcolithic smelting and are effectively found in all Chalcolithic copper-producing cultures across the Old World (Bourgarit et al. 2003; Georgakopoulou et al. 2011; Hauptmann et al. 2003; Müller et al. 2007).

Additionally, the increasing presence of sulphidic mineralizations in deposits approaching the water table and the secondary sulphide enrichment zone had to be dealt with, or risk forming unworkable copper sulphide (matte). For most of the prehistoric period, co-smelting of oxide and sulphides may have been sufficiently effective, but as the oxidic component was progressively depleted through mining, new approaches to extraction had to be developed. Conventionally, it is thought that this was achieved either by first roasting the ore to remove large portions of the sulphur or through a two-step matte smelting and conversion process. The combination of both oxide and sulphide ores, the so-called co-smelting discussed in sections 3.1.2 and 3.1.3, is seen as a technological form directly preceding the more complex sulphide technology (Valério et al. 2013; Rostoker and Dvorak 1991).

This is, however, where the story begins to show its oversimplicity and reliance on modern principles of economic geology to extrapolate ancient technology. The proposed methods of

metal extraction from complex and sulphidic ores assume highly reducing conditions within the smelting furnace, which promote the retention of sulphur as matte. This means that sulphur had to be removed either before hand (roasting) or following the smelt (conversion). Co-smelting is essentially a work-around to allow for an oxidation reaction to occur within a reducing atmosphere. However, it increasingly appears that early experimentation with polymetallic ores achieved some limited success following the same process as earlier direct-smelting techniques.

This is best exemplified at the site of Mariahilfbergl near Brixlegg in the Tyrolian Alps, and in particular in layer SE 6, dated to the late 5th to mid-4th Millennium BC. There, remains were found which suggest attempts were made to extract copper from fahlores through direct smelting (Bartelheim et al. 2002; Bartelheim et al. 2003; Höppner et al. 2005). Analysis of the slag fragments described them as highly porous, containing numerous relict quartz gangue fragments and copper prills, and confirmed their origin from local tetrahedrite deposits. However, lead isotope analyses of the copper objects from the site revealed them as having most likely originated in Serbia, with isotopic ratios compatible with those of the large deposits of Majdanpek (Höppner et al. 2005). The authors argue that this represents early attempts by peoples with links to the Carpathian basin at smelting fahlores in the Alpine region. Although they stop short of claiming that workers at this site were successfully producing copper objects, they acknowledge that fahlores were at least heated and smelted under *lightly* reducing conditions in an attempt to extract copper. The limited conclusions are no doubt the result of the small size of the assemblage, and it is probable that analysis of more objects from the region will show them to have been manufactured from local ores. Indeed, it is notable that the analysed slag did in fact contain significant amounts of recoverable arsenical copper prills and had been intentionally crushed to 0.5-2cm fragments (Höppner et al. 2005, 300), suggesting that copper had indeed been recovered from the slag in the characteristic fashion of Chalcolithic copper smelting.

Fahlore smelting under lightly reducing conditions, as that proposed at Brixlegg, is further attested at the site of La Capitelle du Broum, at La Cabrières in the French Alps, where the earliest smelting evidence has been found for this part of Western Europe (Bourgarit et al. 2003). Although the site is later in date, around the early 3rd millennium BC, this study and the one at Brixlegg reinforce the ease by which copper sulphide minerals could be smelted to produce both copper metal and matte prills without a need for roasting, or separation through slagging, a point which will be returned to in the context of early Southwest Asian arsenical copper.

Before discussing the Asian archaeometallurgical perspective, it is worth delving briefly into another European case which epitomizes the use of polymetallic ores: the Iberian Peninsula. Dating to a slightly earlier period than the rest of Western Europe, the Southern Iberian Peninsula is remarkable for its extensive use of mixed ores and preference for antimonial and arsenical copper alloys. As early as the 4th Millennium BC and extending well into the 3rd and in some places early 2nd Millennium BC, sites in Southern Spain and Portugal produced large quantities of objects of both pure copper and copper alloys. The early appearance of smelting remains and the distinctive character of their technology are often viewed as evidence that metal extraction was the result of indigenous development (Thomas 2009; Hunt-Ortiz 2003). The region has been the subject of a remarkably large body of analyses by scholars and its arsenical copper production is perhaps the most thoroughly investigated of all the regions of the Old World. These studies have concluded that the smelting of copper arsenate ores was taking place pan-regionally and is well attested at sites such as Vila Nova de San Pedro (Pereira et al. 2013), Zambujal (Müller et al. 2007), El Acequi6n and Mora de Quintanar in La Mancha (Bhardwaj 1979), Almizaraque (Delibes et al. 1991), El Malagon (Hook et al. 1987), Los Millares (Rothenberg 1989), and other Argaric culture sites (Coghlan and Case 1957; Selimkhanov 1982). Although the topic of intentionality has been more hotly debated for the Iberian Peninsula than in most places, with positions vacillating back and forth between these over the last few decades (for example Hook et al. 1987; Hook et al. 1991), it now seems well accepted that ancient smelters were selecting prills high in arsenic content based on their colour rather than following a conscious alloying process. The presence of copper arsenate minerals, typically containing several weight percent of arsenic, near remains of slag and in association with arsenical copper objects at the sites of Zambujal, Almizaraque, El Malagon, and Los Milares, is certainly suggestive of the direct smelting of such ores (Delibes et al. 1991; Fern6ndez-Miranda et al. 1996; Rothenberg 1989). Geological studies of Southern Iberian copper deposits certainly show them to be rich in polymetallic minerals. Furthermore, there is a clear connection between artefact function and arsenic content, but studies of the hardness of these objects has conclusively shown that there was no link between hardness and function, meaning that it was rather the characteristic colour or smell of arsenical copper which were perceived as valuable to ancient consumers (Pereira et al. 2013, 2055). All in all, metalworkers of the Iberian Peninsula had a clear preference for arsenical copper and were able to recognise it as distinct from pure copper even if alloying was not strictly taking place. These Central and Western European sites are important because they represent direct evidence in support of the commonly accepted view of the fortuitous smelting of

polymetallic ores and the perhaps intended but uncontrolled (Thornton and Roberts 2009) production of arsenical copper alloys. Archaeological remains at these sites leave little possibility for alloying of two different metals to have been practiced in any modern metallurgical sense. They fit the picture developed based on the elemental and trace analysis of a large body of artefacts dating from the Chalcolithic which shows the increasing dominance of this alloy without the compositional consistency observed in the later tin bronzes. It would, however, be an error to assume this to be the case in all situations, especially so in Southwest Asia where technological approaches to metal extraction appear to have been more varied.

Given that much of the archaeometallurgical literature has been written by European scholars, often with backgrounds in modern economic geological roots, and trained on Central and Western European archaeological contexts, it is doubtless that the prehistoric Near Eastern archaeometallurgical evidence has been viewed with a healthy measure of bias. Applying cross-cultural extrapolation is inevitable, and as such it appears that Near Eastern arsenical copper has more often than not been viewed as the product of the fortuitous smelting of polymetallic ores as it is understood to be in Europe. While some scholars have been more willing to accept the possibility of arsenical copper alloying as possibility (cf. Craddock 1995; Özbal et al. 2002; Rehren et al. 2012; Zwicker 1991), there has been little effort to interpret the archaeological record of Asia in this light.

Granted, the majority of primary production sites in the Near East dating to the Late Chalcolithic revolve around the extraction of pure copper even well into the 4th Millennium BC. This is evident at Wadi Fidan 4 (Hauptmann 1989; Hauptmann 2007), Abu Matar (Shugar 2003; Shugar 2000), Shiqmim (Golden et al. 2001; Shalev and Northover 1987), Tal-i Iblis I (Pigott and Lechtman 2003), Tepe Ghabristan (Majidzadeh 1979), and Çamlıbel, one of the sites discussed in this thesis.

This is surprising since there are many Chalcolithic sites, throughout the Old World where arsenical copper objects appear to have been in regular use but where the source of arsenic remains ambiguous, including at least two pure copper smelting sites, Çamlıbel (Rehren and Radivojević 2010) and Shiqmim (Golden et al. 2001). It seems that all such instances, researchers have tended to err on the side of caution and explained the production of these alloys as being the result of polymetallic ore smelting. It would of course be unwise to infer technological complexity where no evidence is present to suggest so, but the opposite is also dangerous and can easily lead to an oversimplification of the data.

Such is the case for Tülintepe and Tepecik, two multi-period occupation sites 10km apart in the Western Altinova region of Eastern Anatolia. Interpretation of the material remains from these sites has led researchers to conclude that polymetallic ores were being smelted without knowledge of their arsenic content (Çukur and Kunç 1989; Özbal 1986; Yalçin and Yalçin 2009). However, despite this matter-of-fact assertion, there does not seem to be any real evidence for this.

The analysis of ten Chalcolithic slag fragments from Tülintepe by AAS revealed that half contained no detectable arsenic (below instrumental detection limits of 8ppm) while the other half had between 2 wt% and 5 wt% (mean of 3.7 wt%) of the element (Çukur and Kunç 1989, 114). In contrast, the earliest relevant metallurgical material from Tepecik is dated to the Late Chalcolithic and consists of one fragment of crucible slag free of arsenic, one fragment of malachite bound to limonite gangue containing significant bulk arsenic (2 wt%), two pure copper objects, and a further two copper objects containing unusually high concentrations of lead and iron but again no arsenic (Çukur and Kunç 1989, 114). The authors then combine the datasets to suggest that the ores smelted at both sites likely consisted of rich oxidic copper mineralizations occasionally bound with an arsenical component and infer that arsenic content was a pure geological coincidence (Çukur and Kunç 1989, 119).

However, aspects of the interpretation are problematic, not least of which is the unlikely connection between the malachite fragment at Tepecik and the slag from Tülintepe from which they mainly draw their conclusion. The chemical analysis of the malachite revealed it to contain up to 18 wt% by bulk of iron. In contrast Chalcolithic slags from both sites are universally poor in iron (<4 wt%), but still described as crucible smelting slags with pyroxenes approaching the composition of Kirschsteinite ($\text{CaFe}^{2+}\text{SiO}_4$) as the main crystalline phase. Of course beneficiation could have removed much of the iron from the copper mineralization, but overall this iron deficient slag composition is much more suggestive of crucible melting than smelting. Furthermore, the extreme difference in arsenic content of the slags (over five orders of magnitude!) cannot be simply due to local variations in the same geological deposits, which, if arsenic bearing, would always contain significant amounts of arsenic throughout with concentrations in the copper mineralizations. The near complete removal of arsenic is known to be difficult even by modern standards (Rehren et al. 2012, 1724) and therefore the variation cannot be explained through production processes either. As such, even if they were sourced from the same region, the ores must have originated from two distinct deposits which were processed separately. Lastly, the authors do not comment on the fact all of the Chalcolithic and Late Chalcolithic objects uncovered at the sites are in fact

free of arsenic. Given how notoriously difficult it is to remove all vestiges of arsenic from copper, none of these objects are likely to have been produced from polymetallic ores containing arsenic.

While these data by no means suggest that alloying of arsenic and copper was occurring at these sites on any conscious level, they also most certainly do not exclude the possibility. Comments by researchers such as “the slags with high arsenic contents indicate that from the Chalcolithic Age arsenical copper ores were used as raw material” (Çukur and Kuş 1989, 119) and, in reference to a hoard of Chalcolithic objects near Tülintepe “in all of the objects the amount of arsenic lies between 0.5 and 3.1%. Only one sample (Tr-19/7) has 0.2% As. We can assume that arsenic comes from the extracted ores; thus it is not consciously alloyed with major copper”, may be inaccurate and oversimplified. In the latter example, the interpretation was an extrapolation of a previous study of Hassek Höyük material which linked objects to the nearby Ergani Maden deposits known to be polymetallic through lead isotope analysis (Schmitt-Strecker et al. 1992). A similar relationship between ores and objects using lead isotopes has never been established for either Tülintepe or Tepecik and is entirely based only on the presence of arsenic. The link to polymetallic ores and the rejection of conscious alloying practices thus remains purely conjecture.

Another prime example of confusion in the arsenical copper *chaîne opératoire* is the well-known site of Arslantepe, a deeply stratified multiple occupation settlement in southeastern Anatolia. In this case the arrival of new Mesopotamian cultural assemblages seems to be associated with the exploitation of new copper ore types, identified by characteristic impurities present in the final objects. Thus, indigenous Late Chalcolithic smelters of Arslantepe (level VII radiocarbon dated to 3700-3400 cal BC) made use of polymetallic ores containing antimony, nickel, and bismuth recovered from the site itself (Palmieri et al. 1993), which match the impurities found in the metallic objects of the period (Caneva and Palmieri 1983). In contrast to this, in the subsequent Late Uruk phase (level VIA, marked by the appearance of bevelled rim bowls), nickel-arsenic sulphide copper ores began to be in use. These new ores required new smelting techniques to deal with the increased sulphur while maintaining the elevated arsenic content (Palmieri et al. 1996a; Palmieri et al. 1996b) and therefore represent a change in smelting techniques as well as raw materials. By the Early Bronze Age I (level VIB), the ores recovered from the site were found to be either pure sulphides or oxides of copper and iron such as chalcopyrite/pyrite and cuprite/malachite/iron oxide/jarosites (Palmieri and Sertok 1993). The slags contain large quantities of iron and copper matte, and the ores contain very little, if any, amounts of As, Sb, or Ni (Palmieri et al.

1996b). Although many of the objects found on site are likely to have been imported from elsewhere, the intensive smelting activities present within the settlement suggest that much of the copper was produced on site and that the changes in the nature of ores reflect shifting patterns of trade and importation of ores from local to more distant sources in the Central Taurus or Northeastern Transcaucasia, an interpretation based on the prevalence of obsidian objects from that region found in related contexts at Arslantepe (Frangipane 2012; Hauptmann et al. 2002; Lehner and Yener 2014). The excavators stop short of making any conclusions on the alloying of these objects, and rather trust the ores to always have been arsenic-bearing despite the fact that no ores were recovered in the later occupation phases. However, regardless of the shifting patterns of ore sourcing, the final objects almost always contain consistently high levels of arsenic throughout all occupation periods (Yener 2000), which indicates that they had established ways of increasing the amount of arsenic independently of that present in the copper ores themselves.

Değirmentepe, a large 2.5-hectare mound site located on the southern floodplain of the Euphrates in Turkey, reveals a similar story, with clear evidence of experimentation with various ore sources presumed to be of polymetallic origins. Dating to the Ubaid period, Layers 9 to 6 at the site show a strong link to metallurgical activities, with hearth/natural draft furnaces, slag, ore, pigment, groundstone tools, and ceramics recovered throughout the site. The best preserved of these were found in level 7 (4166 +/- 170 cal BC) (Yener 2000, 34), typically within tripartite mudbrick architectural complexes lacking stone foundations, which are reminiscent of southern Mesopotamian architecture. Unlike most sites discussed here, metallurgical activities appear to have been limited to the melting and casting of copper objects based on the analysis of crucible slag and crucible remains (Özbal 1986; Özbal et al. 1999), with primary smelting likely undertaken at the mines themselves (Palmieri et al. 1992; Palmieri et al. 1993), despite the fact that these sites remain to be found. It has also been suggested that a secondary refinement of copper-rich slags and copper metal may have been undertaken at Değirmentepe itself (Lehner and Yener 2014; Yener 2000).

What is fascinating is that once more the vast majority of objects recovered from these phases were composed of arsenical copper which have been described as having been likely produced from polymetallic ores from nearby Malatya. However, problematically, there is no real understanding of the nature of these ores since none were recovered at the site, and no direct evidence for a link with the Malatya deposits has been demonstrated. It would therefore be useful to conduct lead isotope analysis, or at least an in-depth micro-phase analysis, of the assemblage of the site in an effort to relate it to known deposits. This lack of

data on the ores means that although analysis of the crucible slags has demonstrated that arsenic was a strong component of the charge, typically between 0.67 wt% and 2.33 wt% by bulk, it remains impossible to know whether this originated with the ores or was added in a separate stage. The only conclusion on production technology that can be drawn from Değirmentepe is that copper ores were smelted elsewhere and that arsenical copper objects were manufactured on site.

The ambiguity regarding the intent of these ancient metalworkers exists because it is often insufficient to relate intentionality and the concept of 'alloying' by relying exclusively on the correlations between ores and objects to infer past behaviour. In reality, it is likely that the concept of intentionality was much more complex in prehistoric times than we perceive it to be now. Ancient smelters had, after all, only incomplete knowledge of the physical properties of the metal they produced and while they probably had a practical understanding of what worked in terms of metal extraction processes, they certainly did not know why or how. Although this distinction may not have been relevant to the success of prehistoric smelting operations, the appearance of intentional alloying practices marks an important and archaeologically visible shift in metallurgical knowledge. The already discussed arsenical copper production of the Iberian Chalcolithic is a case in point. Not only did approaches to technology vary widely both locally and regionally, but what constitutes conscious production of a specific metal or alloy may also have.

Unlike later periods when extractive technologies are systematized and at times state controlled or sponsored, the Late Chalcolithic and, to a certain extent, the Early Bronze Age are characterised by an explosion in prospection of new metal deposits and consequently in experimentation. This created what has been termed a 'balkanized' landscape of approaches to copper extraction (Lehner and Yener 2014; Yener 2000), with each locale adapting first to their particular geological realities, and modifying known techniques to maximize benefit, explaining the uneven and disparate spread of arsenical copper smelting techniques across the Old World. Production remains may appear identical on the surface across any number of unrelated sites but represent completely different approaches to metal extraction and a simple one-size-fits-all model is inappropriate in this context.

Regardless, there is increasing archaeological evidence that arsenic content in copper was, if not directly manipulated, then at least recognized as creating a material which is distinctive from pure copper. Indeed, something of this nature can be observed at the last of the large mounds of Anatolia to show clear evidence of Chalcolithic arsenical copper production:

Norşuntepe. The excavation's deep sounding (levels 10-1) revealed Ubaid style ceramics dated to the mid-4th millennium BC and a number of structures reminiscent of the tripartite architecture identified at Değirmentepe and related to the Mesopotamian architectural traditions. Three rooms (3, 8 and 9) from the later Chalcolithic (levels 10-8) contained large quantities of metallurgical remains, several furnace features, copper slag, ores, and frustratingly vague remains termed "alloying material" by the authors (Hauptmann 1982; Hauptmann 1993; Zwicker 1980; Zwicker 1991).

Unlike the other large mound sites however, Norşuntepe holds strong evidence in favour of the distinction between pure copper and arsenical copper production. Although the archaeometallurgical report pointed to the use of polymetallic copper-antimony-arsenic oxide ores containing chalcopyrite as the main source of arsenic, the author also noted the presence of ores that were copper rich but free of arsenic and antimony (Zwicker 1980). Zwicker also states that the slag from the same Chalcolithic levels as these ores contained no traces of arsenic or antimony (Zwicker 1980, 17) which has been interpreted as evidence that arsenical copper production at Norşuntepe was based on the addition of arsenic minerals to pure copper in a secondary or final production stage (Lehner and Yener 2014, 541). Experimental co-smelting of As-Sb-Cu and copper oxide ores recovered from the site by Zwicker found that the resulting alloy was too brittle to be of use without removing excess arsenic and antimony. However, his experiments were conducted using modern materials in strongly reducing atmospheric conditions (Zwicker 1980, 15) which probably do not properly reflect expected losses of volatile elements of Chalcolithic technology (see section 2.4). Regardless, since the slag identified at Norşuntepe contained no arsenic, there is no evidence that such co-smelting was taking place. Unlike similar sites in the region, Norşuntepe's remains are unambiguous and form an effective contrast to the other sites already discussed. Certainly it demonstrates that some form of arsenic alloying was indeed taking place by the 4th millennium, and, as will be discussed further below, evolved into a reliable and large scale industry by the Early Bronze Age.

Smaller production sites located on the periphery of the Mesopotamian lowlands, as well as those further abroad in the Levant, Iran, and Transcaucasia offer contrasting evidence to that of the large mound sites and further highlight the diversity in Western Asian metallurgy in the Chalcolithic.

Even in regions devoid of arsenic mineralizations, such as the Levant (Bar Adon 1980; Golden 2009; Shugar 2000), some arsenical copper production, although limited, was undoubtedly

taking place during the Chalcolithic. Two well-known production sites in particular offer clues to the technology employed in the Levantine production of the alloy: Abu Matar and Shiqmim.

Evidence from the late 4th Millennium site of Abu Matar conclusively shows that arsenic ores were being imported and co-smelted with the explicit aim of producing arsenic enriched copper prills (Shugar 2003; Shugar 2000). In this case copper oxide/sulphide ores from the Faynan area are believed to have been co-smelted with arsenic-bearing copper ores imported from elsewhere. This is reflected in the lead isotope analysis of four 'ore' fragments from the site, three of which were strongly paralleled with the Faynan signature, and the fourth appears to have most closely related to deposits in North Central Anatolia (Shugar 2000, 178, 232-235), although the latter connection remains questionable given the distance. Regardless, the conscious addition of alloying material to a smelt to create synthetic copper arsenate charge was undoubtedly taking place at Abu Matar. Although not technically alloying, it certainly qualifies as the conscious production of arsenical copper given the trouble metalworkers went through to obtain distant arsenic-bearing ores.

In contrast, the Late Chalcolithic site of Shiqmim focused rather on the production of pure copper utilitarian objects while importing arsenical copper alloys (Golden et al. 2001; Levy and Shalev 1989; Shalev and Northover 1987). A clear preference for the alloy could be observed in the complex disc-shaped macehead which required the lost wax technique to manufacture and thus attests to the knowledge of the difference between the two materials (Golden et al. 2001). Slag, crucible, and ore remains uncovered at Shiqmim contained no traces of arsenic, so it is clear that arsenical copper objects or ingots had to be brought in from further afield, with polymetallic copper sources in Eastern Anatolia and Transcaucasia being commonly cited candidates (Hauptmann 2007; Tadmor et al. 1995). There is some osteological evidence to suggest that working, or melting of arsenic-bearing material was at least occurring at the site (Oakberg et al. 2000), but no primary production seems to have taken place.

This is also the usual origin given for the fabulous Nahal Mishmar hoard items which are mainly composed of antimonial copper and to a lesser extent arsenical copper (Moorey 1988; Shalev 1999; Shalev and Northover 1993; Tadmor et al. 1995) as well as to lesser known cave hoards, such as Peqi'in (Gal et al. 1996), Nahal Oanah (Gopher and Tsuk 1996), and Givat Ha'oranim (Scheftelowitz and Oren 1997). Overall the Chalcolithic Levant, while a voracious

consumer of copper alloys, engaged only in limited production due to the great distance from arsenic and antimony bearing sources.

The opposite is true for the region of Transcaucasia which is rich in polymetallic deposits (Courcier 2014, 621-622) and has resulted in the widespread appearance of arsenical copper metal in the Chalcolithic, exemplified by the late-5th millennium Azerbaijani site of Mentesh Tepe where ores, slag, and finished objects all contained minor elements typical of the use of complex As-Ni-Cu ores and later fahlores (Courcier 2012; Courcier et al. 2012; Lyonnet and Guliyev 2012). However, archaeometallurgical research in the Caucasus has thus far been rather limited and few production sites dating from this period have yet been excavated. Still, primary production remains have been uncovered but not yet thoroughly investigated at a number of Chalcolithic sites besides Mentesh Tepe, such as Tsiteli-Sopeli, Leilatepe, and Aratashen in Azerbaijan, and Göy Tepe in Armenia, which all point to the development of local copper production and to the widespread use of copper objects containing 1-3% arsenic (Courcier 2014). Further study in Transcaucasian metallurgy has tremendous potential in enhancing our understanding of the early spread of arsenical copper throughout Southwest Asia as the region has historically been used as catch-all origin for many of the unexplained occurrences of the alloy in distant sites such as the Aegean (Betancourt 1970), Iran (Berthoud et al. 1982; Vatandoust 1999; Yener 2000), and the Levant (Hauptmann 2007; Tadmor et al. 1995), particularly so in light of the suggestion that much of the production of arsenical copper could have been the result of the use of a high-arsenic copper 'master alloy' (Eaton and McKerrel 1976, 177-178) which could easily have originated from this region.

Much like in the rest of Western Asia, arsenical copper begins to appear within a large corpus of pure copper objects at a number of sites spanning the western highlands of Iran around the mid-5th millennium BC. This is reflected at sites such as Tepe Hissar (period IA-B) (Pigott et al. 1982), Susa (Period I) (Malfoy and Menu 1987), and Tepe Yahya (Periods VIA and VA/B) (Thornton 2010; Thornton et al. 2002) which all have assemblages dating to the 5th Millennium which include both pure and arsenical copper objects. Interestingly, two production sites from this early period in Iran have also been well investigated but offer little help in discerning the origins of these arsenical copper objects but are worth mentioning here.

Analysis of slag adhering to crucible fragments from Tal-i Iblis periods I and II (Caldwell 1967; Caldwell 1968; Caldwell and Shahmirzadi 1966) indicated the presence of some arsenic in copper prills, which was matched by the appearance of Cu-As mineralizations in ore

fragments recovered from the site beginning in late period I (Frame 2009; Frame 2012). However, despite the strong correlation to complex arsenic-bearing ore deposits, very few of the copper objects from Tal-i Iblis appear to have contained significant quantities of arsenic (Pigott and Lechtman 2003). This suggests that either these objects were being imported from elsewhere, or subsequent stages in the manufacture of finished objects resulted in the removal of much of the arsenic.

While we have little understanding of the origins of the earliest arsenical copper production process in Iran, the situation changes rather dramatically, as it does elsewhere in Western Asia, starting in the mid-4th Millennium BC when large-scale arsenical copper production begins to appear at Tal-i Iblis V (Frame 2009; Frame 2012), Arisman I (discussed later), and Tepe Sialk IV and later phases (Nezafati and Pernicka 2006; Pernicka 2004; Schreiner et al. 2003), and Tepe Hissar period II (Pigott 1989). In parallel to the emergence of these production sites, the use of the alloy expands exponentially throughout the region as exemplified by sites such as Godin Tepe's periods II and III (Frame 2010), Shahr-i Sokhta (Hauptmann and Weisgerber 1980), Tepe Yahya (Heskel and Lamberg-Karlovsky 1980; Thornton et al. 2002), and Susa's period II/IIIA (Malfoy and Menu 1987; Tallon 1987). Use of the alloy endures much longer in Iran than other regions, likely due to the well developed and consistent production techniques already discussed (see section 3.1.5) (Boscher 2010; Rehren et al. 2012).

3.2.3 Onset of the Early Bronze Age

Generally speaking, the 4th and 3rd Millennia can be described as dominated by arsenical copper alloys throughout Southwest Asia. While other copper alloys were certainly in use in more isolated contexts such as the copper silver of the royal tombs of Arslantepe (Caneva and Palmieri 1983; Hauptmann et al. 2002), the surprisingly early 5th millennium tin bronze of the Vinča culture (Radivojević et al. 2013), or the antimonial copper objects of the Nahal Mishmar hoard (Shalev and Northover 1993; Tadmor et al. 1995), it is arsenic which is the alloying agent of choice for at least a full Millennium (Figure 3.1). By this point there is a very clear recognition of arsenical copper as distinct from other alloys as evidenced by its preferential use for certain object types and functions.

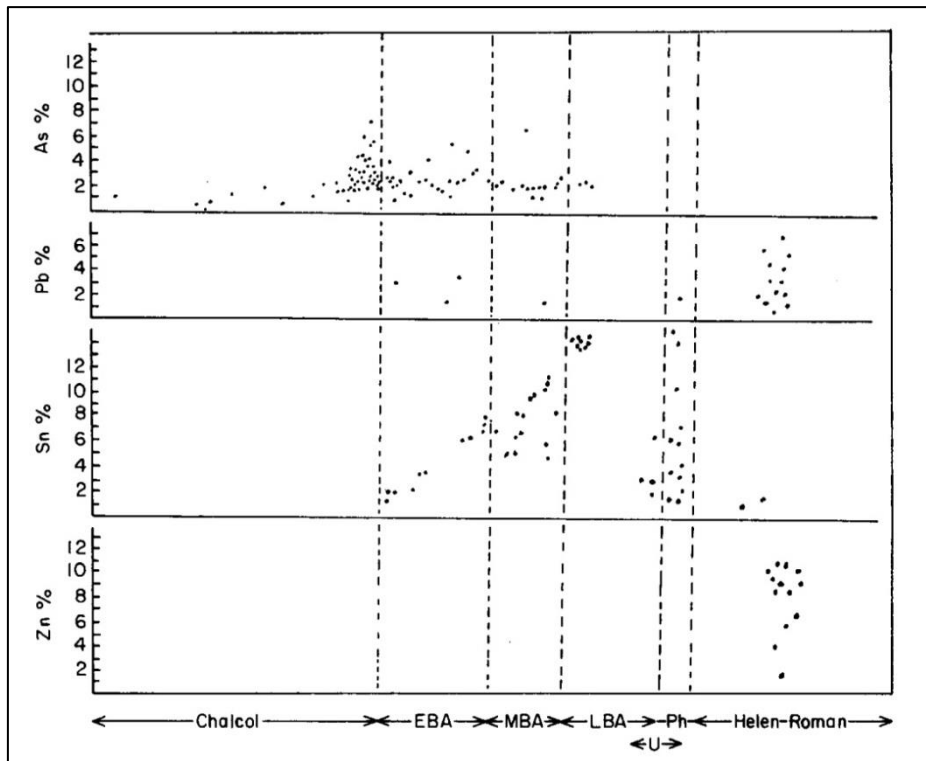


Figure 3.1 Composition of Anatolian copper alloy objects according to period from Pulur, Yazılıkaya, Yortar, Tilmen, Kayapınarı, Horoztepe, Tarsus, Beycesultan and Bayındırköy, İkiztepe, Tepecik, and Tülintepe (Cukur and Kunç 1989, 229). Each dot represents a single object which can be present in several rows.

Nowhere is this better represented than at the site of İkiztepe, along the Black Sea coast of Anatolia, which witnessed a dramatic shift from the almost exclusive use of pure copper in the Late Chalcolithic occupations dating between 4250 and 3200BC to an assemblage dominated by copper objects containing between 1 and 12% arsenic in İkiztepe's mound I dating to 2800-1900BC (Kunç 1986). It is during this period that a clear preference for the use of high arsenic alloys (above 9%) could be observed in jewellery and ceremonial objects found at the site. Lower arsenical copper (1-3%) on the other hand was more commonly used in the manufacture of more utilitarian weapons, needles, and awls. A similar shift is apparent at several other sites throughout Western Asia (Hauptmann et al. 2002, 51, Table 7; Thornton et al. 2002). Thus appreciation for the alloy's aesthetics rather than its mechanical properties appears to have driven demand in many instances (although see Eaton and McKerrell 1976), giving rise to the complex lost-wax castings of the Levant (Golden 2009; Levy and Shalev 1989; Moorey 1988; Shalev 1996; Shalev and Northover 1993), and culminating in the famous polychrome bull of Horoztepe dating to the mid-3rd millennium BC (Smith 1973) with contrasting bands of pure and arsenical copper (Figure 3.2).



Figure 3.2 Copper and arsenical copper bull from Horoztepe. Photograph from the Oriental Institute of the University of Chicago.

Intertwined with these developments in metallurgical technology are the emergence of increasingly complex societies and the rise of urbanism associated with the appearance throughout much of Southwest Asia of Uruk assemblages spreading outwards from Mesopotamia in the 4th and 3rd Millennia BC. The appearance of new architectural traditions and the introduction of distinct material assemblages to highland regions surrounding the Tigris and Euphrates river valleys has long been the source of much debate on the driving force of market economies and the conspicuous consumption of elites in driving demand for the acquisition of raw resources in more marginal areas (Algaze 1993; Frangipane 1993; Oates 1993). However, this position has been increasingly rejected in the highland regions of Anatolia, Transcaucasia, and Iran (Courcier et al. 2012; Stech 1999; Stein 1999; Stein and Wattenmaker 1990; Thornton 2009; Yener 2000; Frangipane 2012) and it is now apparent that significant levels of demand for and production of luxury metallic goods did indeed exist in earlier periods and played an important role in the indigenous development of these ‘peripheral’ regions.

Inseparable from concepts associated with the inception of Early Bronze Age models of subsistence has been the development of tin bronze metallurgy. Not only are the two bound etymologically since Christian Jürgensen Thomsen’s seminal work, but the two have often been synonymous with increasing technological and social complexity. Indeed, tin bronze has

often been seen as the earliest undeniable evidence of true alloying given the scarcity of geological deposits with both elements (with some exceptions, see Radivojević et al. 2013). This view is problematic as it ignores the growing body of evidence which shows that the emergence of alloying technology did not appear in a vacuum and most likely evolved from pre-existence knowledge obtained from experimenting with arsenical copper and other exotic alloys (Lehner and Yener 2014). The sophistication of metallurgical technology at the sites already mentioned here (Arslantepe, Norşuntepe, Abu Matar, or the objects of the Nahal Mishmar and other Levantine hoards) as well as the two sites which form the basis of the thesis certainly reinforce this view.

Indeed, there is increasing evidence to suggest that there is a direct link between the earliest occurrence of tin bronze production and existing known arsenic-bearing deposits. Without entering into the important debate on the earliest origins and most significant sources of tin in the Near East (Muhly 1973; Muhly 1979; Muhly 1985; Penhallurick 1986; Stöllner et al. 2011b; Yener and Vandiver 1993), it should be acknowledged that the Bronze Age site of Göltepe offers significant insight into tin production technology of the Near East. Although it may not have been directly responsible for supplying the tin necessary for the great surge in bronze production of the Bronze Age, the site does offer some clues as to the sequence of development leading to the exploitation of tin mineralizations around Kestel mine.

The first set of evidence appears as powdered ore found in one EBII house which was found to contain up to 3% tin as well as traces of arsenic (Adriaens et al. 1999). Secondly, several objects from the site were found to be composed of complex alloys, often containing tin, silver, and, crucially, arsenic (Yener et al. 2003). And thirdly, more recent unpublished surveys of the area around Kültepe in Hisarcik area northeast of Erciyes Dag have confirmed the existence of arsenic and tin mineralizations in close proximity to each other along with a number of Early Bronze Age sites reminiscent of Göltepe (Lehner, pers. com.). These tin oxide mineralizations (cassiterite) were often associated with occurrences of arsenic-bearing yazganite deposited superficially in fissures and fumaroles in the host andesitic and pyroclastic rocks. While the archaeological sites remain to be investigated and no firm connection has yet been made, the geological link between the two alloying elements is clearly present in the region and will necessitate further study.

The appearance of tin bronzes in the archaeological record marks the beginning of the end for arsenical copper use in most regions of Southwest Asia. Indeed, following a period in which both are used in parallel, production declines sharply in the Middle Bronze Age. This

can be seen by the increasing number of objects recovered which contain both arsenic and tin. This is generally seen to be due to the recycling of old arsenical copper which is then re-alloyed with tin. By the Late Bronze Age tin becomes the alloying agent of choice for much of the Old World and arsenical copper, with some few rare exceptions, all but disappears. In Eastern Anatolia this occurs around the 18th Century BC in what is termed the Assyrian Colonial period (Yener et al. 2003), while in Iran and in the Arabian Peninsula use persists a few more centuries and ends abruptly in the 12th century BC (Heskel 1983; Heskel and Lamberg-Karlovsky 1980; Thornton and Roberts 2009; Thornton 2010).

The evidence thus presented suggests a gradual evolution from polymetallic arsenical copper smelting to the intentional co-smelting of the alloy appear to have eventually led to the alloying of arsenic minerals with copper metal in the Late Chalcolithic. Although still tentative, there is also mounting evidence to suggest a connection between existing arsenical copper technology and the emergence of tin bronze in the Early Bronze Age. It is the period just prior to the introduction of tin which is the focus of this thesis, and two sites which show clear evidence of alloying will now be presented.

Chapter 4 Çamlıbel Tarlası

4.1 Geographic and Geological Context

The site of Çamlıbel Tarlası consists of a small intermittently occupied hamlet in the Central Highland region of Anatolia dating to the mid-4th millennium BC, and thus firmly in the Late Chalcolithic.

Excavations were undertaken at the site between 2006 and 2009 by Dr. Ulf-Dietrich Schoop from the University of Edinburgh as part of the on-going Hattuša/Boğazköy expedition of the Deutsches Archäologisches Institut (Schoop 2009; Schoop 2010a). The project was undertaken to answer a number of critical questions relating to the Central Anatolian Chalcolithic. It had been previously established through large surface surveys that, unlike other regions of Anatolia, land-use in Central and Northern Anatolia did not appear to be dominated by elevated mounds and permanent proto-urban settlements (Schoop forthcoming; Summers 1993; Summers 2002). It was therefore felt that, given the current archaeological focus on early mound sites and later Bronze and Iron Age sites in this region, excavations at the small, flat, archaeologically nearly invisible settlement of Çamlıbel would reveal new insight into the lives of a large, dispersed, and until now ignored, segment of Chalcolithic society. In addition, it was hoped that obtaining new Chalcolithic radiocarbon dates would settle the currently ambiguous and questionable pre-Bronze Age pottery seriation established for the region (Schoop forthcoming). It is through unexpected fortune that these excavations also revealed archaeometallurgical remains indicative of the early production and use of arsenical copper, thereby making the site of prime relevance to this study. Furthermore, it is likely that this group is representative of a common yet widely understudied Anatolian cultural tradition and Chalcolithic way of life (Schoop forthcoming) that may have been responsible for supplying the distant urban settlements with a small but steady supply of metal.

The site is situated on a low sloping plateau between two basaltic ridges at the end of a narrow valley (Figure 4.1). The plateau overlooks a small seasonal stream, Karakeçili Dere, fed by springs further upland. The site is approximately 3 km from the main river valley floodplain, and just 2.5 km west of the later Hittite capital of Hattuša. Parts of the site have been extensively eroded by seasonal runoff (Marsh 2010), but the local geomorphology rules out an original area greater than 50 x 50 m. Although today the climate is arid to semi-arid and rather barren, archaeobotanical analysis has shown that precipitation was much more

elevated in Chalcolithic times and that the site was situated in partially forested but well-established arable land (Papadopoulou and Bogaard 2013).

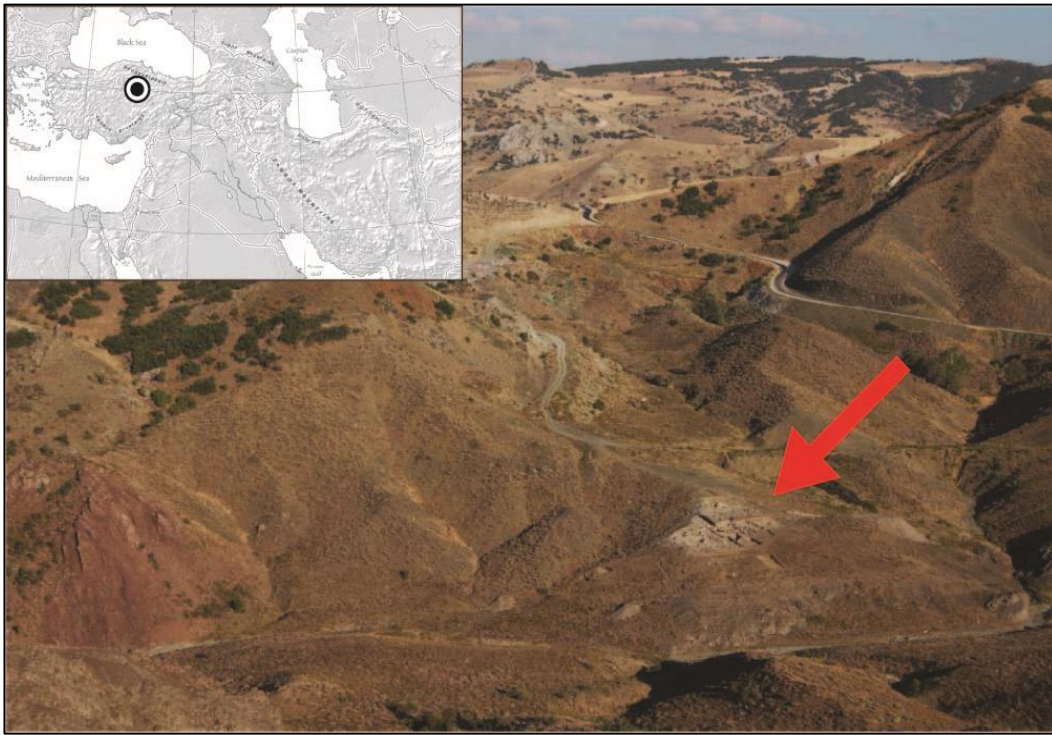


Figure 4.1 View from the northwest of Çamlıbel Tarlası excavations at the end of a ridge overlooking the Karakeçili Dere Valley.

The local landscape has been shaped by tectonic compression lifting the ocean crust to the surface to form complex geological formations of ophiolites, marine limestone, basalt, and deep-crust rocks such as serpentinite. This created a patchwork of low rolling hills on which clay and silt rich sediments were later deposited. The landscape is typified by mixed areas of arable land, where soils derived from basalt and limestone tended to be highly fertile while those formed onto serpentinite were characteristically poor and generally devoid of vegetation. Geochemically, these ophiolitic formations are generally associated with rich copper mineralizations such as can be seen in the famously rich copper deposits of Cyprus. A single small but rich chalcopyrite deposit dispersed in amorphous pyritic masses within weathered serpentinite beds was identified about 2 km north of Çamlıbel during a geomorphological survey of the area (Marsh 2010). Although this deposit has only recently been uncovered by erosional forces and could not have been itself used in prehistoric times, a few pottery sherds clearly belonging to the Late Chalcolithic were identified at the top of a nearby hill less than 50 m from this bedrock exposure. Marsh and others have hypothesized that deposits such as this one would have been much more common during the Chalcolithic (Hauptmann 2007; Marsh 2010) but that wide scale erosion of the hillsides due to agricultural activities has led to their long-term exposure to the elements leading to extensive leaching

and depletion of the copper sulphides. Although there are indeed a large number of limonite and haematite outcrops in the vicinity, the absence of significant copper oxide minerals does seem to put this theory into question. One would expect these minerals to be much more prevalent if large quantities of copper sulphides were exposed to the atmosphere for several thousand years. However, if rich copper deposits were present during prehistoric times, their close association to barren serpentinite ridges would certainly have increased their visibility in the landscape, greatly helping in their identification, and might explain why Çamlıbel is located in this particular valley. Regardless of whether these deposits were rich or poor, the presence of this copper mineral source within walking distance of Çamlıbel is of particular interest and will be further explored in this thesis.

4.2 Archaeological Context

4.2.1 Chronology

Excavations at the site have been quite extensive and revealed four occupation layers separated by two periods of intermittent ephemeral use (Table 4.1). Radiocarbon dates were obtained from cereal grains embedded in the settlement floors of two of the layers (CBT II and CBT IV) recovered through flotation from the 2007 excavations. Two radiocarbon dates were obtained for both of these stratigraphic layers and calibrated using Calib 5.0 (figure 4.2). The dates presented here are averages of each set. The occupation of Çamlıbel is therefore seen as relatively short lived, lasting at most 300 years (2σ), and most likely lasting just 120 years (1σ) between 3590 and 3470 cal BC once both pair estimates are combined (Schoop et al. 2009). Unfortunately, the 1σ and 2σ error margins are not reported for the calibrated radiocarbon dates, these are assumed to be approximately equivalent to the uncalibrated results.

Table 4.1 Occupation phases at Çamlıbel with the two available radiocarbon dates (From Schoop et al. 2009).

Phase	Sample	¹⁴ C BP (1 σ)	Calibrated Radiocarbon Date
Çamlıbel Tarlası IV	Lolium seed	4735 \pm 40	3470 cal BC
	Cereal grain	4790 \pm 30	
Second Phase of Ephemeral Use	-	-	-
Çamlıbel Tarlası III	-	-	-
First Phase of Ephemeral Use	-	-	-
Çamlıbel Tarlası II	Cereal grain	4725 \pm 35	3590 cal BC
	Cereal grain	4780 \pm 30	
Çamlıbel Tarlası I	-	-	-

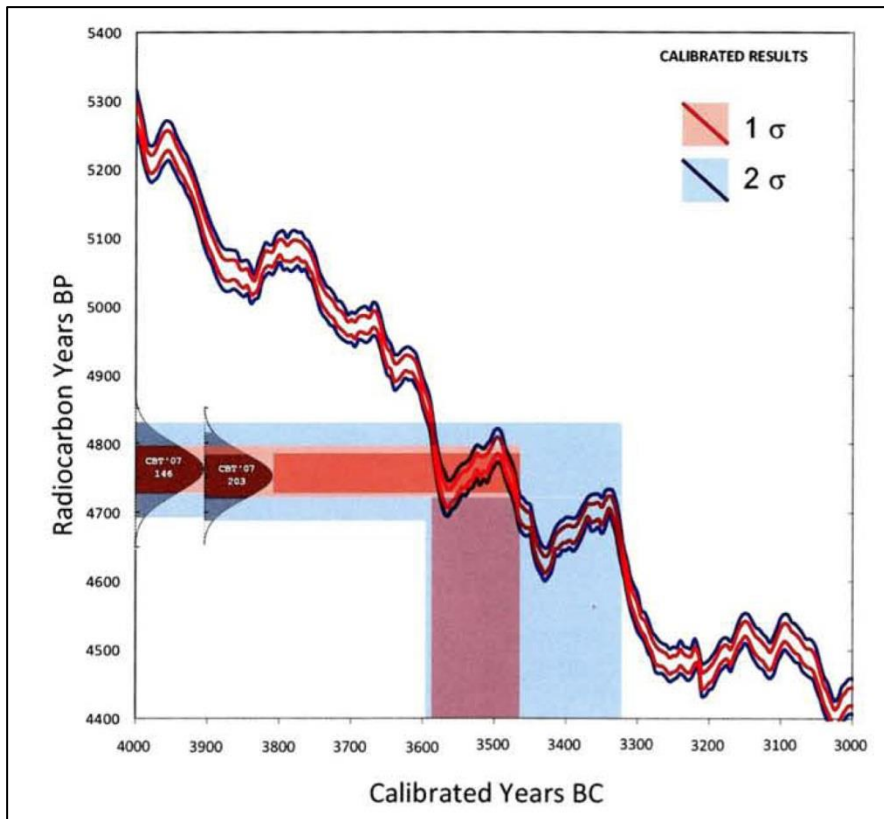


Figure 4.2 Calibrated dates for Çamlıbel (from Schoop et al. 2009).

4.2.2 Çamlıbel Tarlası I

The first phase of occupation at the site, Çamlıbel Tarlası I (CBT I), did not involve the construction of permanent habitation structures. It appears that the main activity conducted at this time was seasonal agriculture as demonstrated by the presence of a large granary (Figure 4.3) and several sickle blades. Agricultural use of the site is further evidenced by a thick deposit of black ash, in places as thick as 1m, containing burnt cereal seeds (Figure 4.4). In the later period of this phase, a small structure with a raised floor was constructed, interpreted as a grain storage silo.

In parallel to this activity, a few small pits exposed to intense heat were interpreted by the excavators as bowl furnaces (Figures 4.5 and 4.6). These pits were subjected to further analysis to assess whether they were indeed metallurgical furnaces and will be discussed more fully in the results section (see 7.1.3).



Figure 4.3 Foundation of granary structure, elevated to avoid moisture (from (Schoop 2010a)).



Figure 4.4 Alternating ashy layers in CBT I phase (from (Papadopoulou and Bogaard 2013)).



Figure 4.5 Top view of 'bowl furnace' feature 3 (from (Schoop 2010a)).



Figure 4.6 Section of 'bowl furnace' feature 3 (from (Schoop 2010a)).

Metallurgical finds from this phase included five small copper objects (two wires, two perforators, and one pin), 29 limonite or haematite mineral fragments (4345 g), 15 fragments of mixed iron and copper oxide minerals (1258 g), and two pieces of slag (112 g). One of the slag fragments had a flat base.

4.2.3 Çamlıbel Tarlası II

After a period of abandonment, Çamlıbel witnessed a second phase of occupation (CBT II). This layer was radiocarbon dated to 3590 BC Cal (Schoop et al. 2009). It is at this time that a number of stone-built houses are constructed in several clusters (Figure 4.7). The habitations always included well-built domed ovens with occasional signs of repairs. In addition, the remains of several infants and children were found buried beneath the floor of some of the houses (Figure 4.8). This phase ends in the complete abandonment of the site. Every house was emptied and well cleaned, leaving behind no finds from the occupational floors themselves.

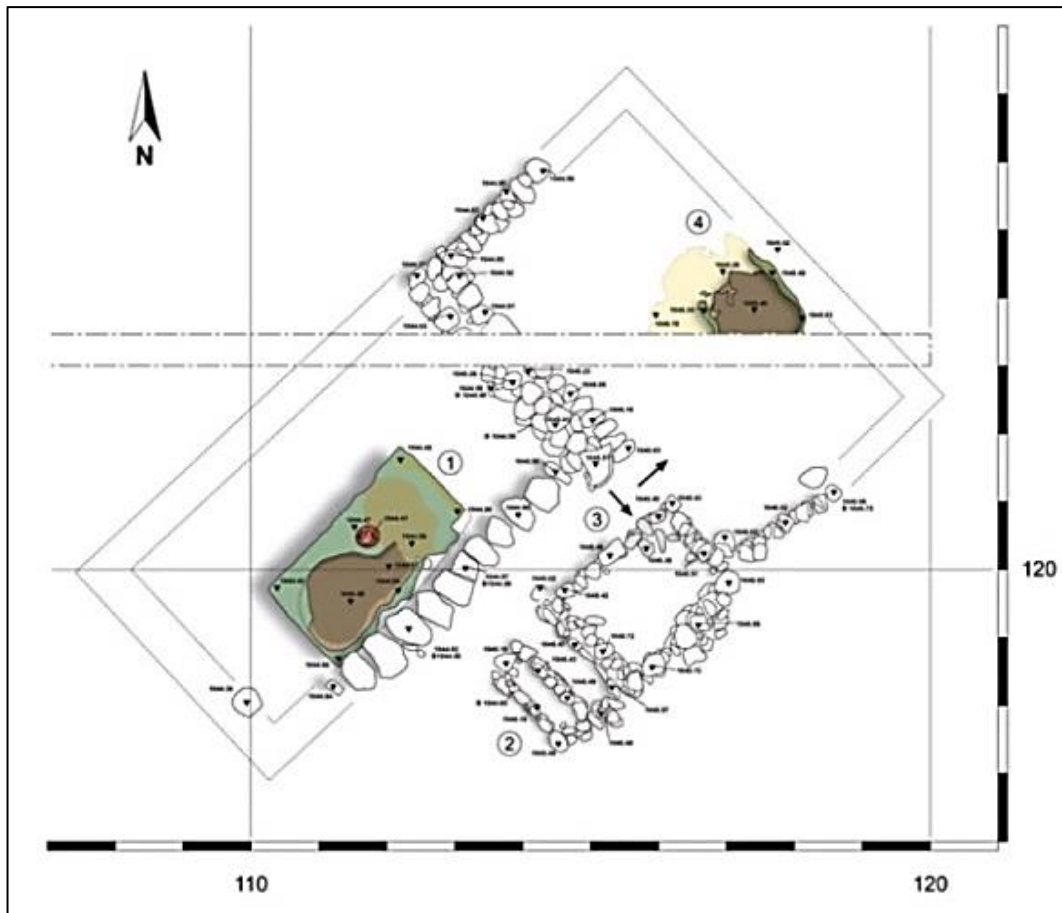


Figure 4.7 CBT II structure plan (From (Schoop 2010a)).



Figure 4.8 Infant burial dating to CBT II uncovered beneath a habitation structure (From Schoop forthcoming).

Clusters of bowl hearths seen in the first phase can once again be seen during this period. Metallurgical remains uncovered in this layer consist of four small copper objects (two intertwined wires forming a two-link chain, two needles, and a single pin), one small lead wire, 17 limonite or haematite mineral fragments (1809g), 9 fragments of mixed copper and iron oxide minerals (167g), and eight pieces of slag (260g), of which one had a flat base.

4.2.4 First Phase of Ephemeral Use (FPEU)

The site continued to be used sporadically for some time (First Phase of Ephemeral Use – FPEU) as testified by the presence of a few more bowl hearths dug into the abandoned floors. Two pieces of slag (37g), 12 iron oxide and sulphide mineral fragments (479g), 10 mixed copper and iron oxide mineral fragment (1359g), and four copper objects (a needle, a pin, and two perforators) were found in this layer. A small ceramic fragment with a layer of bright copper metal, likely a mould fragment, was also found in this layer. Metallurgical industries therefore clearly continued in this period in much the same way as in the previous two phases, only on a limited scale.

4.2.5 Çamlıbel Tarlası III

The next phase, Çamlıbel Tarlası III (CBT III), is characterised by the construction of much more substantial, rectangular, and widely spaced structures than in the previous stages (Figure 4.9). Several of the structures have stone wall foundations and in at least one structure a series of thick limestone floors were laid down. A number of ritual activities clearly took place as demonstrated by enigmatic bone installations ringed by small hearths (Figure 4.10). This period saw the hamlet's longest continuous occupation but the structures were ultimately cleaned out and at least one building was intentionally burned before the whole site was abandoned once again.

In terms of metallurgy, this phase shows a dramatic shift in site use. No intensely heated pits were identified in this period, but we see a dramatic increase in the amount of slag recovered (n=39, 1139g), and a decrease in the amount of iron oxide minerals (n=6, 180g) and mixed copper and iron oxide minerals (n=4, 22g). It is also the first phase in which crucible fragments begin to appear. These crucibles have distinctive tall and narrow oval perforated pedestals topped with a shallow oval bowl. Three copper pins and three copper perforators were also found in this layer.

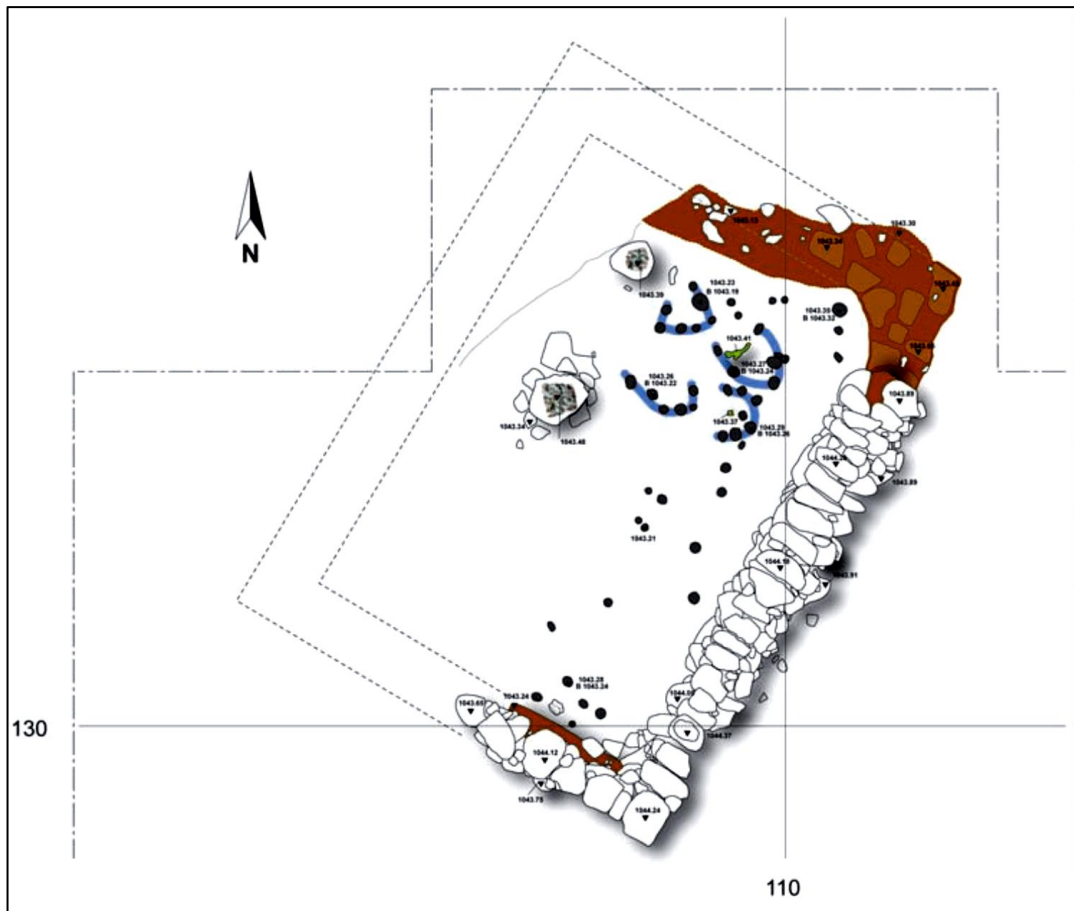


Figure 4.9 Plan of the 'burnt house' of CBT III. Note the series of ring hearths surrounding bone features in the north-eastern corner (from Schoop forthcoming).



Figure 4.10 Photograph of the CBT III ritual features. In the centre is an arrangement of bones which is surrounded by several small hearths (from Schoop forthcoming).

4.2.6 Second Phase of Ephemeral Use (SPEU)

Çamlıbel was then once more used only occasionally (Second Phase of Ephemeral Use – SPEU) and a new series of pit hearths were dug amidst the decaying ruins. Metallurgical remains were much less abundant in this phase than in any other. Just two copper objects were found (a pin and a needle), along with two pieces of iron oxide and sulphide minerals (8g), four pieces of mixed copper and iron oxide minerals (895g), and two fragments of slag (22g). The discovery of a ceramic casting mould for a ring-shaped figurine (Figure 4.11) proved to be the most exciting find from this period. These ritualistic types of artefacts are known to originate mainly from the Balkans, but are distributed as far east as Western and Northern Anatolian coastal regions (Zimmermann 2007). They are often thought of as a clear marker of contact between these regions during the Late Chalcolithic and Early Bronze Age. This object constitutes the first evidence that ring-idols were produced outside of the Balkans and may be indicative of metallurgical techniques linking the two regions.



Figure 4.11 Photograph of terracotta ring-shaped figurine casting mould (Schoop 2009).

4.2.7 Çamlıbel Tarlası IV

This was followed by the last period of occupation of the site, Çamlıbel Tarlası IV (CBT IV; 3470 cal BC), during which several new houses were constructed following the similar large rectangular plan of CBT III. However, unlike in CBT III, these were no longer isolated but rather clustered together once more as in the earliest periods. At the highest point of the site were two large structures connected by a covered courtyard (Figure 4.12 and 4.13). In the corner of this courtyard was a large rectangular oven installation measuring 2 X 2.3 m. It was covered by a large domed superstructure composed of several layers of mud and pottery sherds. The courtyard was strewn with a large quantity of broken slag fragments, hammerstones, and two flat anvil stones, which has been interpreted as a slag processing area where slag was crushed for the recovery of trapped copper prills (Schoop forthcoming).

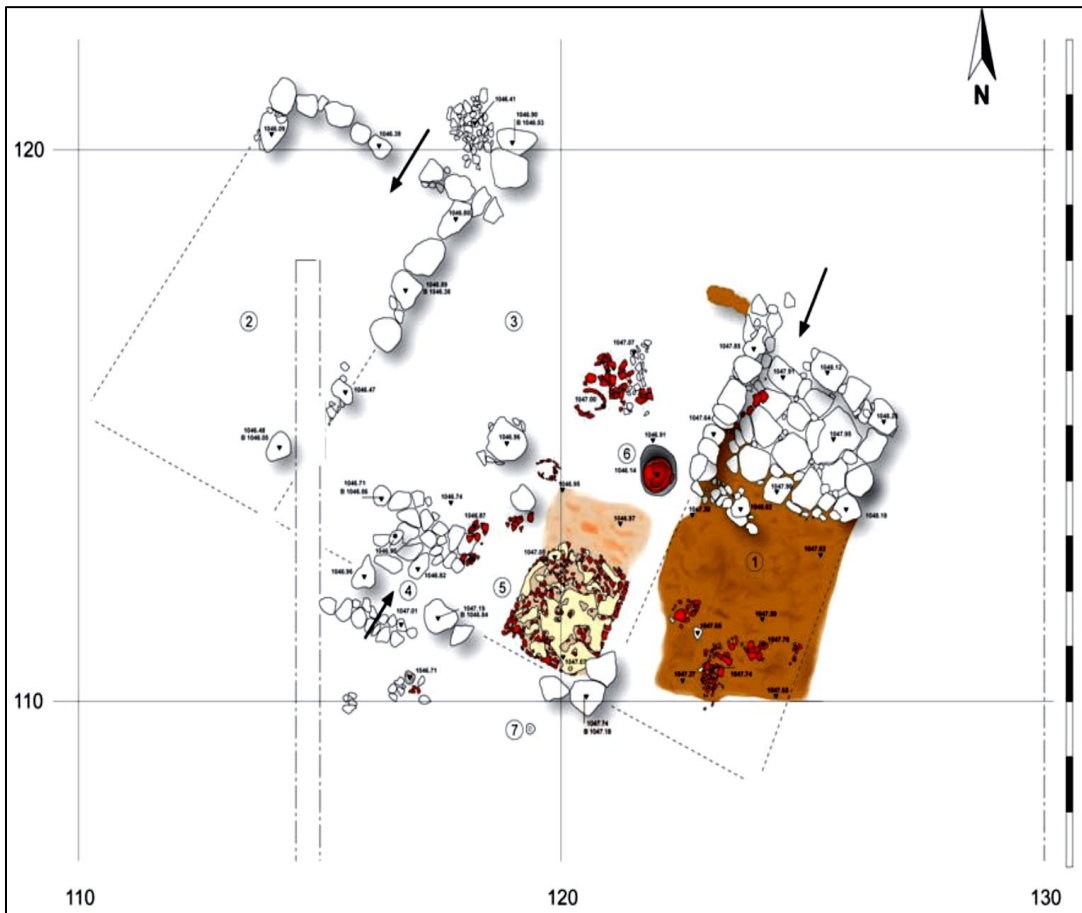


Figure 4.12 Plan of CBT IV courtyard with oven in south-eastern corner (from Schoop 2009).



Figure 4.13 Photograph of large domed oven with plaster base from the CBT IV courtyard (from Schoop 2009).

This phase saw a continuation and intensification of the metallurgical activities seen in CBT III. Finds included 63 fragments of slag (2811g), six crucible fragments, one iron oxide and sulphide mineral fragment (80g), 18 mixed copper and iron oxide mineral fragments (272g), a copper perforator, a copper pin, and an amorphous lump of copper.

The site was then abandoned for the last time, but no cleaning of interior spaces was undertaken.

4.3 Previous and Related Research

A preliminary study of some of the slag remains from Çamlıbel was previously conducted by Rehren and Radivojević (2010). Based on the characterisation of three samples by OM and SEM-EDS, the main conclusion was that copper bearing ore used at Çamlıbel was likely to be a copper oxide and hydroxides bound to a matrix of iron hydroxides as part of the gossan layer. The authors interpreted the presence of sulphide phases as the result of the use of sulphur bearing gangue minerals rather than any purposeful process. The authors acknowledge that they were limited in their conclusions since only two samples were analysed by SEM-EDS and proved to be compositionally very different. They highlighted the fact that no arsenic was identified in the slag but that unpublished analyses of copper objects were of arsenical copper. The authors encouraged further research to be conducted on the site in order to identify the origins of the arsenic content of the objects – part of the reason the assemblage was chosen for this research.

In addition to this current archaeometallurgical research project focusing on production remains, a parallel study of the finished objects from Çamlıbel is also being conducted (Weeks et al. forthcoming) and preliminary unpublished results have been made available for comparison (Appendix B.8). Their analysis does not form part of this thesis, but where relevant these results will be taken into account in the discussion.

Chapter 5 Arisman

5.1 Geographic and Geological Context

The site of Arisman was first identified by a local teacher with a background in geomorphology in 1996 and brought to the attention of the Iranian Cultural Heritage Organisation (ICHO). The discovery of this site occurred at a fortuitous time since the ICHO had taken steps in the previous few years at resuming scientific cooperation with western institutions with the aim of exploring Iran's significant role in the development of early metallurgy. This importance of the region had previously been highlighted through a number of excavations prior to the Iranian Revolution of 1979, but it was only with the formation of the "Early Mining and Metallurgy on the Western Central Iranian Plateau" project (EMWCIP), inaugurated in 1999, that research in this area was to recommence. The multidisciplinary study consisted of joint cooperation between the Iranian Cultural Heritage and Tourism Organisation (ICHTO), the German Archaeological Institute (DAI), the Geological Survey of Iran (GSI), the German Mining Museum Bochum (DBM), and the Department of Archaeometry of Freiberg Technical University (TU Freiberg) (Vatandoust et al. 2011a).

It was decided that a comprehensive study of the metallurgy of Arisman would form the core of the project, although the overarching goals were not limited in scope to the site itself. The study would also encompass all aspects of raw material acquisition, manufacture, and distribution of finished goods in as broad a regional basis as necessary. Since little work had been done on mining sites since the Wertime expeditions of the 1960s (Wertime 1968), the first goal of the project was to undertake an archaeometallurgical survey to identify potential mineral deposits responsible for supplying ores to the site of Arisman. Several samples were collected from various candidate deposits for lead isotope analysis, which were then compared to material remains recovered from Arisman. However, by far the greatest contribution to the project has been the result of the excavations of Arisman, conducted between 2000 and 2004, which uncovered a vast Early Bronze Age smelting workshop of industrial scale (Vatandoust et al. 2011b; Chegini et al. 2000; Chegini et al. 2004) that has provided half of the material analysed for this thesis. The term 'industrial' is used here to refer to metal production vastly greater than any possible local demand and where the site appears to have been specialized for this industry. The metallurgical production remains uncovered at Arisman are several orders of magnitude larger than those observed at other sites in the region, such as the contemporaneous and closely related site of Tepe Sialk.

Early surveys of the site revealed that it in fact consists of three distinctive activity areas covering several hectares named Arisman I, II, and III. Arisman I is the largest of the three sites, the only one to have been systematically excavated, and therefore the one which this thesis is referring to when discussing Arisman, unless otherwise specified.

The site is situated 1000 m above sea level, on a narrow corridor between the Karkas Mountains to the southwest and the Latif Massif to the northeast, along the western edge of the Central Iranian Plateau (Figure 5.1). This relatively flat region receives abundant water in form of seasonal runoff from Karkas Mountain range, which acts as a year-round reservoir. The water provided by snowmelt, historically tapped in underground Qanat irrigation systems, makes the region one of the most fertile in the generally inhospitable transition between the high mountains and the desert plateau. The continental climate is characterised by hot and dry summers and cold winters, receiving just 100-200 mm of precipitation a year, although the period in which the site was occupied is known to have been slightly wetter (Neef 2011). However, botanical evidence shows that vegetation around the site of Arisman was still quite sparse and comprised mainly of limited riparian forests of willow, poplar, tamarisk, maple, and ash, separated by wide areas dominated by drought resistant shrub steppe (Neef 2011). The foothills of the Karkas Mountains are thought to have been much more densely vegetated with a type of pistachio-almond steppe-forest which has today been destroyed by grazing and deforestation. Surprisingly, it is the more arid region immediately to the east of Arisman which is thought to have been the main source of fire wood for industrial activities at the site. Growing abundantly on sand dunes, and of excellent calorific value, were large steppe-forests of *haloxylon persicum* (white saxaul) (Neef 2011). The use of these shrubs as smelting fuel will be further discussed later.

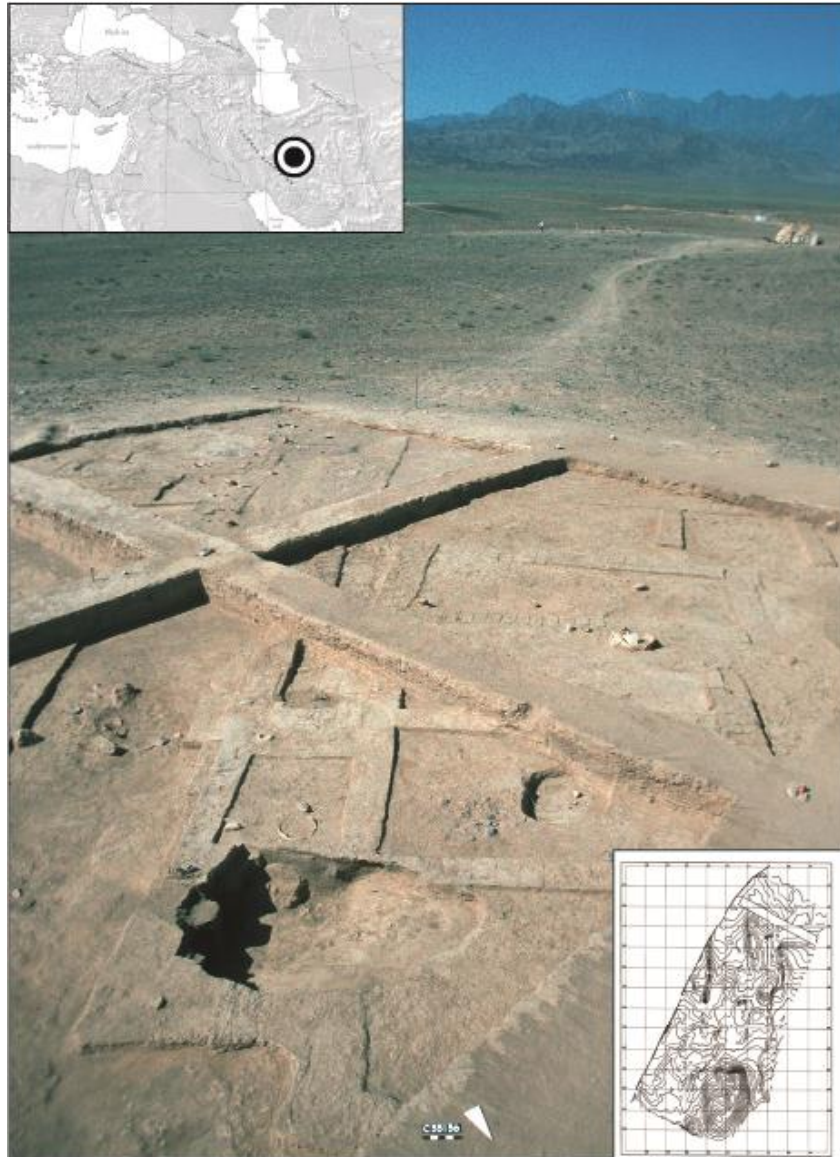


Figure 5.1 Location of Arisman with Karkas Mountain range in the background and the excavation of Area C in the foreground along with topographic map. Topographic map from Chegini 2000, 285, and photograph from Chegini 2004, 212.

Geologically, Iran's highland regions are rich in metal resources, with abundant copper deposits concentrated in the Orumiye-Doktar metallogenic zone, part of the Alpine-Himalayan metallogenic belt, that extends from Sistan in the southeast to Azerbaijan in the northwest (Stöllner et al. 2011a). The Karkas Mountain range, just a few kilometres to the southwest of Arisman and extending from Kashan to Ardestan, is part of this metallogenic belt and consists mainly of Tertiary magmatic and sedimentary rock units with a Pre-Cambrian basement that is prone to the concentration of metallic minerals such as porphyry copper deposits, volcanogenic massive sulphide deposits, hydrothermal lead-zinc-barium deposits and accumulations of gold, silver, arsenic, antimony, and mercury (Mansour 2013).

However, despite several mining surveys having been conducted around Arisman (Chegini et al. 2000; Pernicka et al. 2011; Stöllner 2011) uncovering several new ancient mines, none have been identified as dating to the Late Chalcolithic. Although dating mining sites is notoriously difficult, the latest survey, conducted as part of the same project as the Arisman excavations, was able to reject early dates for all of the identified mining sites based on the presence of iron tool marks and characteristic mining techniques known to have been developed in later periods. Stöllner (Stöllner 2011, 629) further suggests that the absence of slag at the mines may also be a marker of Chalcolithic exploitation, based on the dominance of such slagheaps at Tepe Sialk and Arisman and their absence from the, admittedly slightly younger, mining district of Vešnāve associated with Tepe Sialk. Predictably, mines surveyed in the Karkas Mountains were invariably associated with slag remains and therefore unlikely to be related to Arisman.

Ore samples obtained from several deposits in the Karkas and Latif mountains also proved to be disappointing in terms of copper content (typically less than 3.5%), and described as “hardly accessible to ancient miners” (Pernicka et al. 2011, 642). It should be noted that these conclusions were based on the microscopic analysis of just 11 samples and on the chemical analysis of just three of those, chosen on the basis of their proximity to Arisman and presence of associated mining galleries, hardly representative of such a large region. In addition, the composition and microstructure of the analysed samples from Darhand, a deposit within the Karkas Mountains, was found to be broadly comparable to that of two ore fragments and the slag recovered from Arisman if we assume that iron minerals were added as flux. The study also further acknowledges that this hydrothermal deposit is stratabound below the large Qom limestone formation together with vast Eocene amygdaloidal basalts which are expected to extend over a much larger area towards Natanz to the southwest. Relevant deposits and potential ancient mines may therefore remain unidentified further away from Arisman itself.

Table 5.1 Comparison of analysis of Darhand copper mineralisation with ore and slag recovered from Arisman I. All data obtained by SEM-EDS and published in (Pernicka et al. 2011).

	SiO ₂	Al ₂ O ₃	FeO	MnO	MgO	CaO	Na ₂ O	K ₂ O	TiO ₂	P ₂ O ₅	Cu ₂ O	As ₂ O ₃
Arisman I slags	38.5	7.5	23.7	0.3	2.3	16.3	1.8	1.9	0.3	0.3	4.7	1
Arisman ore	56	13	7.5	0.2	5.5	5.7	2.1	0.1	0.5	0.1	8.4	0
Arisman ore	59	12	4.4	0	0.2	3.4	5.5	0.8	0.8	0.2	11.5	n.d.
Darhand ore	49	14	4.4	0	0.1	32	0.1	<0.01	0.1	0	0.9	n.d.
Darhand ore	46	16	4.9	0.1	0.3	31	0	<0.01	0.1	0	2.7	n.d.

More distant, but rich in copper, are the Anarak and Talmessi/Meskani mining areas which had previously been highlighted as potential major sources of copper during the prehistoric period (Berthoud et al. 1982). This latter region is part of the Central Iranian Geological Block, situated on the southwestern edge of the Dašt-e-Kavir desert, approximately 200 km to the east of Arisman. Recent analyses of ore samples from these deposits have shown them to contain elevated nickel and cobalt content which rules out the region as a source of copper for Arisman since these elements are not found in any significant quantity in the slag or copper alloy objects recovered from the site (Pernicka et al. 2011).

The copper deposits exploited at Arisman have therefore not yet been identified, either because they have been destroyed by later activities, or because ores were brought from further afield than the surveyed areas. Alternatively, it has been suggested (Stöllner et al. 2011a) that the lack of large mining galleries dating to the Chalcolithic may be because several smaller deposits were exploited by small sporadic expeditions over a very large area and gathered centrally at settlement sites such as Arisman for further processing. These small-scale enterprises, when sufficient in number may account for the remains uncovered at Arisman and as well as the dearth of contemporaneously associated mines.

5.2 Archaeological Context

Thanks to the efforts of the members of the EMWCIP project, the results of excavations at Arisman are now well published, covering a thorough multidisciplinary approach to the site. It is not the aim of this section to reproduce the work that has already been carried out, but rather to highlight the relevant metallurgical elements of the site within their respective chronological and archaeological contexts. The chronology of the site will therefore be discussed first in broad terms, followed by an overview of each individual excavation area of Arisman I with a focus on the metallurgical remains.

5.2.1 Chronology

Arisman being a large occupation site, excavations were conducted on several large distinct features which have been designated areas A, B, C, D, and E which were occupied over several overlapping centuries but with distinct chronological developments. Typologically, the ceramics recovered from the various foci are associated with Sialk III and Sialk IV (also known as Proto-Elamite) styles, although there is little appreciable further deviations or evolution beyond these basic types (Boroffka and Parzinger 2011; Helwing 2011c). Rather than use the excavation nomenclature, activity areas will be presented here chronologically according to their radiocarbon dates (B, D, C, A, and E).

The Sialk III pottery assemblage, which is mostly concentrated in Area B, is defined by the use of local clays and shapes which have strong links with Tepe Sialk, Tal-i-Iblis, and Tepe Hesar, but also contain early bevelled rim bowls and nose-lugged jars which have parallels with Middle Uruk layers at Godin Tepe (V) and Susa (IIB) pottery types, linking Arisman to the Uruk influence sphere and Mesopotamia (Boroffka and Parzinger 2011, 133-143).

Sialk IV pottery, on the other hand, was mostly recovered from Area C and to a lesser extent Areas A, D, and E, showing a clear chronological shift in the site's focal points and a move away from ceramic industries towards metallurgical ones. Although contemporaneous with Late Uruk phases further to the west, it is much more obviously related with the assemblage recovered from the large Proto-Elamite center of Tal-i-Malyān in Fars in the southern Iranian highlands and other sites in Iran than with their Mesopotamian counterparts, although bevelled rim bowls and seal typologies still show continued interactions (Helwing 2011c, 219-220).

Radiocarbon dating is generally in agreement with the pottery seriation, although most of the lower Sialk III layers of Area B appear to suffer from the problematic use or re-use of old wood (see table 5.2), giving much older dates than the earliest strata on site (Helwing 2011a). Overall, the site appears to have been in use from the mid-4th to the mid-3rd Millennium cal BC (Görsdorf 2011). Based on stratigraphic realities rather than purely on radiocarbon dates biased by the old wood problem, the earliest part of the site to be occupied is Area B, lasting from the 36th to 34th centuries cal BC, with most structures alternatively used as pottery workshops and habitations. With some overlap, the focal point of the settlement later shifts to metallurgical production and the expansion of the large slagheap in Area D and associated settlement in Area C starting in the early 35th Century and lasting until the end of the 31st century cal BC. After a period of abandonment of up to two centuries, Area C was re-occupied by secondary workshops and used as a pithoi burial ground sometime in the first half of the third millennium as evidenced by a very small number of pottery fragments which hint at similarities with the Early Dynastic period of Mesopotamia. The secondary workshops of Area C appear to be related to a furnace in Area A which has been dated to the first two centuries of the 3rd millennium cal BC. Lastly, area E, which suffers from erosional damages and has poor stratigraphic integrity, has been dated to the 29th to 25th centuries BC, although the presence of a few pit furnaces suggests earlier use as well.

Table 5.2 Radiocarbon dates for the different areas of Arisman I (from Görzdorf, 2011). Dates in parentheses for area B are those given by Helwing (2011) taking into account stratigraphy and pottery assemblages indicating the probable re-use of old wood. Dates given for Area C represent two distinct occupations with approximately 100 years of abandonment. Areas are presented in this table chronologically.

Area	Sample	Sample No.	¹⁴ C BP (1 σ)	Calibrated Radiocarbon Date (1 σ)
B	Charcoal	4	5461 \pm 33 5177 \pm 36 4908 \pm 38 4700 \pm 29	4350-3370 cal BC (3630-3370 cal BC)
D	Charcoal	12	4666 \pm 39 4635 \pm 35 4633 \pm 39 4517 \pm 41 4495 \pm 48 4474 \pm 37 4564 \pm 33 4537 \pm 39 4522 \pm 37 4518 \pm 37 4514 \pm 36 4510 \pm 37	3520-3100 cal BC.
C	Charcoal	3	4437 \pm 33 4525 \pm 35 4317 \pm 42	3360-3110 cal BC 3010-2880 cal BC
A	Charcoal	3	4388 \pm 35 4367 \pm 34 4290 \pm 36	3080-2880 cal BC
E	Charcoal	2	4148 \pm 31 4114 \pm 38	2870-2580 cal BC

5.2.2 Arisman I Area B

Located on a small elevated spur in the central part of the site, Area B forms the earliest occupation of the site. Excavations revealed five phases of occupation spread over 13 stratigraphic layers, all of which were associated with Sialk III style pottery. The lowermost occupation layers (12-9) show little in terms of structural remains but rather scatters of lithic and ceramic fragments. It is only in layer eight that permanent structures are evident in the form of several rectangular buildings of pisé construction arranged on either side of a small alley. The architecture of these houses shows strong parallels with those of published for Tepe Sialk's layers III₅₋₇. From that period onwards, occupation consists of alternative layers of domestic pisé houses (layers 8 and 6) and pottery workshops (layers 7 and 3) (Boroffka et al. 2011). The kilns uncovered were well constructed, clearly permanent, and involved in large-scale production, certainly precursors to the industrial scale metallurgy which was to take place at the site in later periods.

Of special note is the presence of a number of small finds relating this part of the site to small scale metallurgical activities. Most obvious of these are 16 Ghabrestan-style pedestalled

crucibles as well as a single flat-bottomed crucible fragment, a slagged crucible rim sherd, six crucible lid fragments, and a possible tuyère fragment. In addition, four nearly complete shafthole axe moulds, seven fragments of rectangular moulds, a single triple ingot mould, and eight nondescript mould fragments were also found in this area. Silver cupellation is attested here by the presence of 13 litharge cakes, some of which are formed of several connected elongated cakes. Furthermore, and not necessarily indicative of metalworking activities, four anvils and 20 hammerstones were also recovered from various layers in this area (Helwing 2011d).

Surprisingly, very few copper objects have been recovered from this (n=22), or indeed any other area of Arisman, which has been suggested as strong evidence of the nature of Arisman as purely a production site intended for export rather than local consumption (Helwing 2011d). Objects recovered from Arisman mainly consist of small tools or implements, usually pins, chisels, awls, and rods, along with a few blade fragments, rather than the larger objects suggested by the shafthole axe and rectangular moulds.

The majority of objects clearly related to metallurgical production (40 of 58) were uncovered in layer 6, one of the habitation phases, indicating that metallurgical activities were typically conducted in domestic contexts. This has already been discussed in reference to Çamlıbel and other Late Chalcolithic sites (see section 3.2), but it is worth noting that Arisman demonstrates *in situ* the process of industrialisation and centralisation of metallurgical production. At no other time beyond the Sialk III period of Area B was this type of enterprise undertaken alongside domestic contexts. In all other instances, each area was either entirely devoted to metallurgical processes, or it was only after an area had been abandoned that such crafts were allowed to move in. This will be made evident from the description of the following Sialk IV period areas.

5.2.3 Arisman I Area D

Area D is divided in what appears to be two distinct focal points. On the surface, the area is dominated by a large slagheap 30 m in diameter, but a magnetometer survey revealed the presence of over 100 strong anomalies 50 m to the northeast of the slagheap and covering an area of 60X80 m (Helwing 2008; Steiniger 2011, 82-93).

The slagheap consists of complex alternating and intermixed layers of slag and sand extending to a depth of approximately 2m, underlain by a thick ash and charcoal deposit. Based upon the systematic recording of a cubic meter of slagheap remains, it was calculated that this slagheap contains roughly 88 tons of slag and 15 tons of furnace remains (Steiniger

2011, 93), representing production on scale even larger than the more thoroughly studied slagheap A (Boscher 2010; Rehren et al. 2012). A few pits and small mudbrick scatters were observed within the heap, but no significant structures or furnace remains were identified. In addition to slag and furnace fragments, the excavators recovered several mould fragments, a few pieces of litharge, anvils, and hammerstones. Although not particularly abundant, yet present throughout, were Sialk IV pottery fragments. Except for the presence of litharge, the distribution and deposition of the slag and other artefacts of slagheap D is remarkably similar in nature to the slagheap recorded in area A which will be discussed later.

A trench dug to investigate the magnetic anomalies revealed that they were in fact a series of circular pits with diameters ranging between 1.2 and 2.5m and generally preserved to a depth of 0.6m. The walls were sharply defined, either vertical or slightly concave, and sometimes covered in remains of plaster lining, while the bases were either flat or lightly depressed and always left bare. The surrounding gypsum appears to have been reddened and the plaster often exhibited flow textures, testifying to the presence of intense heat. Associated with these features were the typical slag and furnace fragments that litter the area in general, but marked here by a high proportion of litharge fragments and some metallic lead droplets, suggesting that the area was used in the smelting of lead and/or silver cupellation (Steiniger 2011).

5.2.4 Arisman I Area C

Area C consists of an urban settlement and composed of several mudbrick structures each containing several rooms (Chegini et al. 2011, 40-68). Five houses have been excavated, arranged around a north-south alley. The well organised grid-layout of the settlement, tightly packed around a main alley and leaving space only for drainage channels, has led the excavators to suggest that it was pre-planned rather organically grown. Each house was occupied for some length of time as attested by the presence of several occupation layers. Processing of copper is attested in at least two houses (house I room A and C, and house III room C) by the presence of pit furnaces next to 'fire platform' and related to copper residues and slag fragments. As this occupation is contemporaneous with the large slagheap in Area D, it seems that while primary smelting was a communal or outdoor affair, secondary processing of copper was taking place in more private indoors contexts.

The area was then abandoned for some time and re-occupied a several centuries later. The area appears to have first been reused as a metalworking workshop as evidenced by fire platforms constructed partly above the walls and the large number metal processing

artefacts uncovered such as flat axe and ingot moulds, grinding stones, and crushed slags (Chegini et al. 2000; Helwing 2008). The ruins must have provided some measure of shelter for these activities, as although it is likely that the roofs had collapsed, the walls were most probably still standing.

The area was then once again abandoned and pithos burials associated with the Sialk IV/2 period were later dug into the ruins. One pithos of note contained the remains of a small child buried with a single broken mould and the base of a crucible, although it is unclear whether that was intentional.

5.2.5 Arisman I Area A

Area A is dominated by a single large slagheap ca. 22m in diameter and a 1.2m in height, representing some 31 tons of slag, 5 tons of furnace linings, and 0.75 tons of stone, crucibles, and pottery fragments (Steiniger 2011, 69-82). This slagheap has been well investigated and sampled, and is therefore the main source of material studied in this thesis.

Although a modern irrigation channel has cut through the slagheap and destroyed about a third of it, the remainder is stratigraphically sound. Much like the slag deposit of Area D, this feature is composed of several layers of slag mixed with fragments of furnace lining and crucible, separated by thin, intermittent strata of loose reddish sandy lenses of varying thicknesses, all of which lies directly on virgin soil (Chegini et al. 2004, 294). Due to instability in the sections and the difficulties in differentiating between the various layers, these have not been reported and there is therefore no reported provenance for the various slag samples (Steiniger 2011, 69-70).

Although there is mention in the excavation monograph of the visual identification of three distinct slag types, there is no reported distinction in their stratigraphic provenance and they have been described as evenly distributed throughout the slagheap (Steiniger 2011, 80). These slag types are defined as (1) black glassy slag, almost obsidian in appearance, (2) coarse matt-brownish black slag, and (3) coarse and porous brownish-black slag with large quantities of green secondary copper mineralizations. The distinction between these has been studied in some depth and will be further discussed later as they form an integral aspect of early arsenical copper alloying technology at Arisman.

Most interestingly, the remains of a remarkably well preserved furnace were buried beneath the slagheap. The furnace was built first on a southeast-oriented mudbrick platform placed directly upon virgin soil. This platform measured 1.4 m wide, 1.8 m long, and 0.75 m high and

had a small extension protruding towards the southeast. A second platform was later built of clay to accommodate the increased height from succeeding furnace re-constructions. It appears that the front of the furnace was systematically broken open, re-lined with clay, and the superstructure rebuilt a number of times. These repairs could be observed from the presence of a sequence of between 33 and 40 distinct furnace linings, hinting at the original shape of the reaction chamber which was preserved up to a height of 40cm, an upper diameter ranging from 40-70cm, and a lower diameter of 30cm. The chamber appears to have been somewhat pear-shaped and always faced the northeast, with each repair and rebuilding of the furnace gradually extending it in that direction. Directly in front of the furnace, a pit feature filled with sand and smaller slag fragments was uncovered which has been interpreted as a working area kept clear during operation of the furnace. The slagheap appears to be partly composed of smaller dumps of slag deposited directly on virgin soil in a circle around the central furnace.

The excavators describe two different kinds of furnace lining which are critical to our understanding of the operations carried out here. The first group was sand tempered, approximately 2cm thick, and highly vitrified and glassy to a depth of about 1cm due to exposures to high temperatures. These formed a hemispherical shape which was open to the front where the structure seems to have been intentionally broken apart to extract the product. The second group of linings were just 0.5-1cm thick clay, and although partially reddened and burnt from heat, these were never exposed to the extreme temperatures of the first group and thus never vitrified. They are reported as forming a vertical U-shape about 15cm high, 30-40cm long, and 25-30cm wide. The base of these linings was generally flat or slightly inclined towards the northeast. It is noteworthy that neither of the linings is associated with any metal remains.

Steininger proposes that these two types of lining form distinct features of the same operating furnace. He suggests that a spherical firing chamber was constructed above a U-shaped hollow into which a crucible was slotted into and attached to the furnace by another lining of clay. Once the charge had fully reacted, it is suggested that an opening would be made and the slag and metal would be tapped into the crucible below.

This interpretation is somewhat problematic for a number of reasons. Foremost is that there is no direct archaeological evidence of a link between the two furnace linings, although the fact that the furnace was often lined with both types in alternative succession does suggest that they are related somehow. It is also difficult to envisage how such a system would be

advantageous over simply letting the charge cool inside the furnace unless the use of the crucible was designed to remove the slag from the furnace to keep the operation running while copper accumulated at the base, in which case simply tapping the slag downslope would have been simpler and probably more effective. It remains possible that the two linings are associated with entirely different operations, one of which may have required a slightly different shape and much lower temperatures. This possibility should be kept in mind in light of the two distinct speiss and copper smelting processes recently proposed for Arisman (Rehren et al. 2012).

Also of note is the fact that the furnace was buried under the slagheap, which suggests that metallurgical operations were ongoing at the site long after the furnace was abandoned. Although it is difficult to calculate how much slag was produced from a single smelt given that the slag may have been removed in a continuous operation, it is clear that a large number of such furnaces would have been required to produce such a large slagheap. Also of interest is the similarity in furnace design with those uncovered at Feinan in the Wadi Arabah in Jordan (Hauptmann 2007), although the comparison is somewhat tangential as few structural remains of furnaces from this period have been excavated anywhere, let alone closer to Arisman. The only notable exception is the workshop at Šahdād dating to mid to late 3rd millennium BC which has been described as a smelting furnace (Hakemi 1992), although the absence of slag or vitrified material has cast doubt on this (Pigott 2004).

In addition to the furnace, a number of small finds recovered from the slagheap are worth mentioning. Over three hundred fragments of Sialk IV pottery were found distributed evenly throughout the slagheap, evidently deposited in secondary context as refuse. These, in addition to the radiocarbon dates, suggest that the slagheap is contemporaneous with Area C's secondary workshop phase. Other finds included several crucible fragments, chaff-tempered mould fragments, one of which was clearly for a flat axe, and six hammer- and anvil stones. Problematically, no ingots, prills or any metallic finds were recovered from this slagheap so there is little direct archaeological evidence of the intended end product from such a large-scale operation.

5.2.6 Arisman I Area E

Three trenches were dug in Area E to investigate a shallow slagheap, a magnetic anomaly, and a surface scatter of furnace fragments (Steiniger 2011, 93-99), yielding little in terms of new data.

The slagheap appears similar to those reported for Area A and D, but the furnace lining fragments mixed within are described as lacking the vitrification and evidence of intense heat found on similar fragments in the other slagheaps. In addition, none of these exhibited the typical crucible contact faces often found on the more typical furnace fragments of Arisman, prompting the excavator to describe these artefacts as reminiscent of Area B kilns rather than smelting furnaces (Steiniger 2011, 95). In addition to pits and a small mudbrick wall, metallurgical finds from the slagheap included anvil-, hammer-, and grinding stones, the eponymous slag, litharge, mould fragments, and two crucible fragments. The only identifiable pottery associated with the slagheap was discovered within the mudbrick wall and belongs to the Sialk III period, which does not line up well with radiocarbon dates obtained from a pit below the slagheap which dates to the mid-3rd millennium, and which is therefore likely to be in secondary context.

A similar assemblage of small metallurgically-related finds was also uncovered buried in a small number of pit features in the trench covering the magnetic anomaly, although these are likely to be the result of secondary deposition rather than use.

The furnace fragment scatter proved equally disappointing to the excavators who had hoped them to be indicative of the presence of a buried furnace structure. These furnace fragments were similar to those found in association with the slagheap in the same area which have already been mentioned. The only feature of note was a large pit which is, albeit smaller, nearly identical to those found in Area D tentatively linked to lead and silver metallurgical operations. The range of small finds matches that of the rest of the area, with slag, litharge, furnace fragments, grinding and anvil stones, and a few fragments of pottery making up the assemblage.

All in all, Area E does not appear to be of great relevance to this project as the slag remains either date to a much later period, or are too fragmentary to be directly identifiable as metallurgical, although further efforts to identify the nature of the technical ceramics identified here would be of use to our understanding of the pyrotechnical processes present on site as a whole.

5.3 Previous and Related Research

Despite early hopes that excavations at Arisman would continue beyond the first five years in the early new millennium, it now appears unlikely that further work will be undertaken in the near future due to political reasons. Yet Arisman has been the focus of comprehensive

multidisciplinary study and is therefore one of the best understood metallurgical sites in the Late Chalcolithic/EBA transition period in the Near East.

A number of preliminary reports were published as the excavation was ongoing (Chegini et al. 2004; Chegini et al. 2000; Helwing 2005; Helwing 2006; Helwing 2008; Pernicka 2008), which, although of great use in reporting early results, have now been superseded by the site monograph, the source of most data presented in this chapter (Vatandoust et al. 2011b). In terms of metallurgy, this publication does not only report on the archaeological excavations and mining surveys conducted as part of the project, but also on the analysis of a large number of metallurgical finds. While this monograph was being prepared, a parallel study of the slag was undertaken by the author of this thesis as part of a Master's dissertation in order to assess the possibility of the use of speiss as an alloying agent at Arisman (Boscher 2010), the data of which was later published (Rehren et al. 2012). However, the excavation monograph was published just after the submission of the article and thus some new information came to light in each publication and a revision is in order.

For example, the excavation monograph inconclusively comments on the lack of distinction between copper and speiss slags (Pernicka et al. 2011, 654, 660) based solely on bulk analyses and only a handful of selected samples for micro-phase analysis. The lack of clear patterns was then shown by the parallel study to be the result of low analytical resolution due to the preliminary nature of the study (Rehren et al. 2012). On the other hand, data from the monograph has provided further details on some of the production remains which had until then gone unnoticed by the latter publication (black slags and crucible material) and form the basis for this research program.

Chapter 6 Methodology

6.1 Sampling Strategy

The material currently available for analysis consists of approximately 50 kg from Arisman, and approximately 10 kg from Çamlıbel Tarlası. Metallurgical remains from these sites consist of ores, slags, crucibles, and furnace remains. These form only small portions of much larger assemblages, particularly in the case of Arisman, which are currently in storage near the excavation sites themselves.

Sampling bias is a well-known problem inherent to all archaeological material which greatly affects the statistical representativeness of any assemblage relative to its original population (Shennan 1998, 361-362). There is, unfortunately, little that can be done to affect cultural discard practices or indeed reverse the preferential nature of taphonomic processes, but thankfully it is possible to sample the archaeological record in such a way as to maximize the effectiveness of probability analysis. To do this, sampling of these two sites followed a stratified random strategy, often considered one of the most representative ways of sampling archaeological assemblages (Baxter 2003; Orton 2000; Shennan 1998). Following this methodology, the number of random samples collected from each archaeological context is proportional to the size of the assemblage recovered from that particular phase relative to the overall site. Thus the analytical assemblage is representative of the original excavated population and retains more statistical strength. This sampling strategy was applied by the excavators (Dr. Schoop for Çamlıbel and Dr. Helwing for Arisman) who sent samples of each distinct metallurgical material type for laboratory analysis at UCL's Institute of Archaeology in London. Thus, periods of intense metallurgical activities resulted in greater number of samples and analyses overall but representing a lower percentage of the total assemblage than in layers with fewer metallurgical remains. This is because smaller assemblages require a large analysis of a larger proportion of the total population in order to remain statistically relevant (Baxter 2003).

It should be noted that one of the problems often associated with metallurgical remains is that they are often misidentified, incorrectly catalogued, or entirely missed by the excavators who may not be aware of the significance of small slag or mineral fragments (Jones 2001). This is particularly the case at primary copper production sites where there is a clear preference to recover common green copper oxide stained minerals, slag, and corrosion products at the expense of other less colourful ones. Furthermore, efforts to associate production remains from archaeological sites with geological ore deposits typically suffer

from the fact that ancient mineral resources have typically been exploited in later periods, often obliterating not only any archaeological remains, but also the mineralizations extracted by the ancient miners (Craddock 1995, 8). These difficulties complicate efforts to isolate the nature of the exploited ore, and it was hoped that the metallurgical focus of the excavations and excellent knowledge of metallurgical remains by the excavators at both Arisman and Çamlıbel would mitigate this sampling bias.

Following macroscopic analysis of the total assemblages, prepared samples were analysed using light optical microscopy (OM) and scanning electron microscopy with an energy dispersive spectrometer (SEM-EDS). Finally, samples which could only be accessed in the field were analysed using portable X-Ray Fluorescence (pXRF) in order to identify potential candidates for further export and analysis. The pXRF analysis was only conducted for Çamlıbel, since revisiting the site of Arisman was not possible, and resulted in the identification and export of an additional seven stained metallurgical ceramics and two fragments of crucible slag, categories of artefacts which had gone unreported prior to the campaign.

Bulk chemical analysis of the slag, such as those obtained from powdered or otherwise homogenised samples, was not undertaken because it was deemed of limited value to the aim of identifying technological choice given the large amount of variability identified both macroscopically and microscopically. The typical presence of partially unreacted gangue and the inclusion of large fragments of technical ceramics in many of the samples, compounded by difficulties in accurately quantifying minor and trace elements in iron-rich material, meant that there was little to be gained from such bulk analyses that could not be obtained more dependably through phase analysis in the SEM.

6.2 Optical Microscopy

Optical microscopy can be used in two main ways. Transmitted light microscopy, where light passes through a thinly prepared sample, is mostly used in determining crystalline compositions using the optical properties of minerals. It is useful when looking at natural minerals (MacKenzie and Adams 2011) or synthetic materials such as ceramic (Quinn 2009; Reedy 2008; Whitbread 1995), but much less so when used in the study of slag and metal which are generally isotropic and opaque. For this reason, reflected light microscopy has proven to be much more useful in the examination of microstructures of metals (Scott 1991), but also for slag, crucibles, and furnaces, and is now considered a standard first step in their analysis (Bachmann 1982; Jones 2001; Rehren and Pernicka 2008).

Samples to be analysed using OM were prepared following a standard procedure. The specimens were first cut into approximately 1cm³ using an abrasive tile cutter and mounted into an epoxy resin and cured. These were then ground using silicon carbide paper from 320 grit to 4000 grit, and then polished down to a near mirror-like finish using progressively finer polishing cloths and ending with 0.25 µm diamond paste. This sample preparation procedure being equally useful for SEM-EDS analysis, the same resin blocks were used for chemical analysis when deemed appropriate (Veldhuijzen 2003).

Samples were observed using a binocular Leica DM LM optical microscope with an external light source in order to gain a basic understanding of the chemical and crystallographic composition of the slag and technical ceramics. Plane polarized light (PPL) was used in order to determine the samples' crystalline phases, colour, homogeneity, porosity, and inclusions. Particular attention was given to trying to determine distinct categories or types of slag through phase analysis and the presence of distinct (semi)metallic prills. Cross polarized light (XPL) was also used to help in the identification of internal microstructures and phases as well as characterize the technical ceramic fabrics. Such examination also helped in locating areas of interest for further SEM-EDS. The microscope was equipped with a Nikon digital camera and photomicrographs were taken of both typical and atypical features within the samples.

6.3 Scanning Electron Microscopy – Energy Dispersive Spectrometry (SEM-EDS)

Widely used in the scientific study of various archaeological materials, the SEM-EDS enables both high resolution imaging as well as compositional analysis to be conducted both reliably and quickly. It is especially well suited for complex multi-phase characterisation and to identify spatial variations in composition of heterogeneous materials (Pollard et al. 2007; Pollard and Heron 1996) such as slag and technical ceramics (Rehren and Pernicka 2008).

The SEM-EDS is based on the principle that a beam of electrons aimed at a sample will cause vacancies in the inner shells of atoms along the surface forcing outer shell electrons to repopulate the inner shells, which causes secondary x-rays characteristic of the element to be emitted (Pollard and Heron 1996; Pollard et al. 2007). Low energy (less than 50 eV) secondary electron (SE), used to obtain a topographic image, and higher energy (more than 50 eV) back scattered electron (BSE), used to visualize compositional contrast between different phases, are both emitted when the sample is bombarded with electrons. It is the emitted x-ray energy levels which are characteristic of the elements present in the sample and which are therefore measured and counted by the energy dispersive spectrometer (EDS)

(Pollard et al. 2007). The downside of the technique is that the detection limits are rather elevated and thus only element concentrations above c. 0.1 wt% can be reliably measured, making the instrument unsuitable for trace element analysis.

A scanning electron microscope with an Oxford Instruments EDS was used along with INCA and Aztec software. Samples were prepared following the same methodology as for optical microscopy, but also coated with a thin layer of carbon to increase conductivity. The EDS was set up with an accelerating voltage of 20 kV, a spot size of 5.1, a working distance of 10 mm, and an operating dead time between 30 and 40%. The stability of the instrument was verified approximately every 30 minutes using a cobalt standard and kept within reasonable range to ensure adequate quantitative reliability. All results were normalized to 100% in order to facilitate comparison and reported either stoichiometrically for oxides such as ceramic, minerals, and slag bulk compositions or as elemental weight percentages for the metallic prills and objects. A ZAF correction procedure was applied to calculate the measured intensities of characteristic energy lines in order to obtain accurate chemical compositions. The use of several certified standards ensured acceptable quantitative reliability (Appendix A), with results believed to be accurate within ten percent relative of the measured value for concentrations above c. 5 wt%.

Since the arsenic content was deemed to be of crucial importance to this study special attention was paid to the instrument's accuracy and reliability in detecting it. The element is notoriously difficult to detect in the presence of lead as the arsenic K- α peak is overlapped by lead's L- α peak at ~ 10.5 KeV. This generally means that samples that have lead-to-arsenic ratios of 10 to 1 or more cannot be calculated efficiently because the lead peak overwhelms the arsenic peak. Thus, in the presence of lead, the arsenic levels may be calculated as higher than they really are, and precision is moderately decreased as a consequence. Spectra where arsenic and/or lead were detected by the instrument were individually assessed and in the rare cases where both elements were present lead was measured using its K- α peak and arsenic using its L- α . Two arsenical copper standards (BCR 691 Alloy C and 36X CuAs3A) were used to test the instrument's baseline reliability. However, due to BCR 691C's heterogeneous microstructure and its intended use in XRF analysis rather than microbeam analysis such as SEM-EDS, results were found to be largely overstated by over 40% relative to the certified value of 4.6 wt% As (Boscher 2010). It was therefore decided that only the results of the analysis of 36X CuAs3A would be relied upon despite small inconsistencies regarding the Sn content of this particular standard (Appendix A).

A few further limitations of the SEM-EDS are expected to affect the results presented in this thesis and are worth mentioning here. First and foremost are the errors in accuracy introduced by use of a micro-analytical instrument for bulk analysis of complex, multi-phased material. Slag, which is dominated by just a few major elements, such as iron and silicon, is particularly prone to this shortcoming. However, common alternatives, such as the bulk analysis of crushed samples by XRF, is even more problematic given that the complex crystalline phases are notoriously difficult to fully homogenize. In addition, the heterogeneous and incompletely molten aspect of the slags mean that in many of the cases minerals were not incorporated into the melt and their inclusion in the bulk results would not accurately reflect the prevailing atmospheric conditions of the smelt or melt. As such, it was deemed that the somewhat more subjective micro-analytical approach to bulk analysis of slag provided by the SEM-EDS was preferable to one based on powdered pellets.

Iron is typically present in most copper smelting slag in both of its oxidation states of Fe^{2+} and Fe^{3+} which cannot be accurately quantified using SEM-EDS alone, which leads to a certain amount of error in reporting this element. Without the use of mass spectrometry, or other techniques such as Mössbauer spectroscopy, it is only possible to qualitatively observe the relative presence of ferric and ferrous iron through its association with crystalline species such as magnetite or fayalite. Given this difficulty, iron oxides in this thesis are reported rather simplistically as Fe^{2+} , stoichiometrically as FeO. This overstates the ratio of iron to oxygen, since the iron is more likely to be present in slag as a combination of both oxidation states. This negatively affects the analytical totals and should be kept in mind when encountering both normalized and non-normalized results.

Loss on ignition (LOI) is another expected source of complication when conducting bulk chemical investigations using not only SEM-EDS but any other instrument. This effect is caused not by limitations in the instrument but by changes taking place in the material itself at the point of production involving high temperatures. The effect of escaping gases from the oxidation of reactive compounds, such as sulphur and carbon, and the volatilization of other elements such as antimony and arsenic, when exposed to thermodynamic conditions prevailing during smelting of ores or the firing of ceramics are particularly prominent.

At the point of SEM analysis, this problem translates into increased porosity which negatively influences the analytical totals due to the uneven, porous surface. This effect can be mitigated by crushing and homogenizing the samples, but as already discussed, this is a less than desirable compromise in highly complex material. Every effort was made during this

research to avoid overly porous regions in bulk and area analysis of the various samples in order to limit this problem. Bulk compositions of ceramic, slag, and other porous material will be presented in the body of this thesis as normalized totals in order to ensure comparability. Non-normalized totals are included in the appendices for reference.

That being said, it is worth noting that the greatest issue caused by LOI is not analytical but interpretative since the lost volatile elements create a large disparity between the original material which was gathered and transformed by human agency, and the final product and waste produced. For example, the addition of organic matter (chaff) to ceramics is only visible as characteristically shaped voids since the actual temper has long since been consumed during firing. More problematic for this particular thesis is the volatile nature of arsenic and its oxides. Although some arsenic, should it have been present during smelting or melting, should always remain present in detectable quantity, it should be kept in mind that significant amounts of the element were undoubtedly lost during the production process which will not be reflected in the material analysed here (see section 2.4).

The calculation of averages for several samples with elements at or near the instrument's detection limit is a commonly encountered problem. In order to obtain meaningful means, values below the detection limit must either be estimated or ignored, resulting in totals which are slightly inaccurate. This is particularly problematic when a few samples contain a few elements in significant concentrations while the rest of the assemblage does not. Prehistoric slags produced from inconsistent or variable charge and smelting conditions are especially prone to this issue. However, the error introduced into the mean values by the estimation of elements below the detection limit is generally smaller than the overall precision of the SEM-EDS and therefore has little impact on the interpretative value of the resulting data. For the purpose of this thesis, mean values and standard deviations of elements which were found to hover around the detection limit were calculated using the estimated minimum detection limit of the instrument for elements which fell below the detection limit. Exceptional cases where just a few samples have an extraordinarily high quantity of one element will not be averaged but will be discussed separately.

In order to obtain as meaningful results as possible, bulk analysis of the samples was conducted on a standardized area covered by 100x magnification at a working distance of 10 mm, which measures 1.2 mm by 0.8 mm whenever possible. In cases where samples were found to be exceedingly porous for rigorous analysis (analytical total of less than 80%), smaller areas were selected at increasingly high magnification.

6.4 Portable Hand-held X-Ray Fluorescence (pXRF)

The pXRF is an instrument which has seen increasing use in the last decades (Frahm and Doonan 2013) and which is quickly becoming a staple of archaeometallurgical analysis (Helmig et al. 1989; Karydas 2007). It is particularly well suited for non-destructive surface analysis of metallic objects. Although not designed for use with slag, analytical methods intended for mineral analysis are, to a certain extent, applicable for this use.

The portable XRF is based on the same principles as the ED-XRF but it does not require prior sample preparation or a vacuum to be present. However, the x-ray beam only penetrates the sample to a depth of a few tenths of a micron and therefore the analysis is essentially only a surficial one. For this reason, any sample should be cleaned of corrosion and preferably flat for the results to be meaningful. For this reason, field analysis of slag, minerals, ceramic, or soils was always performed on a freshly broken surface.

The Innovex Delta Premium instrument was set up using the 'alloys' mode for analysis of metal objects, and the 'soils' mode for all other materials. The results using the 'soils' mode were only valid as a basis of comparison between the remains on a broad qualitative scale and only used to identify trends or anomalies in the results rather than as quantitative data. The results of pXRF analysis will be presented only as supportive evidence to the analysis conducted by SEM-EDS since the data gathered from it were not deemed reliable enough for direct inferences.

6.5 Multicollector Inductively Coupled Plasma Mass Spectrometry (ICP-MS)

An investigation of the isotopic composition of metallurgical material from Çamlıbel was conducted in an effort to identify probable sources of copper ores for the site and to characterize local deposits for future comparison with other datasets. This now well established technique has been widely used to identify probable raw material sources (Begemann et al. 1989; Höppner et al. 2005; Lehner et al. 2009) and to infer the existence of trade networks over both local and inter-regional scales (Pryce 2011; Weeks et al. 2009). The advantageous nature of lead isotopes is that, unlike most trace elements, fractionation of lead during metallurgical processes insignificantly alters the relative quantity of each lead isotope (Cui and Wu 2011). This allows for a direct correlation to be made between the final metal product and the geological deposit from which it was produced and define unique groupings of artefacts which can be tracked over space and time (Artioli et al. 2008). In many ways, the use of lead isotope signatures has revolutionized our understanding of metal distribution and exchange.

The strength of these interpretations has been subject of much debate (Gale 2009; Pollard 2009) and has recently led to a resurgence of interest in trace element fingerprinting as an alternative or at least parallel method (Pollard et al. 2015). However, lead isotope studies are now well accepted and although any result must be considered within the context of the 'Provenance Hypothesis' (Wilson and Pollard 2001, 508), these types of studies remain the best tool in unravelling the conundrum of provenancing material that is produced through a transformative process.

For this thesis, sixteen samples from Çamlıbel were sent to the Curt-Engelhorn Zentrum Archäometrie for lead isotope characterisation under the supervision of Prof. Ernst Pernicka. The investigation was conducted using MC-ICP-MS, a technique now commonly used for relatively fast and accurate isotopic quantification of archaeological objects (Pernicka 2014; Pollard et al. 2007, 195).

The samples were taken from as wide a range of contexts as possible, and were intended to represent several steps in the production process. This involved the analysis of a few fragments of minerals, slag, and finished objects (two copper-based and the other a lead wire). Although the majority of LIA studies tend to focus on the analysis of finished objects with the aim of linking the isotopic profile to a well sampled and characterized ore deposit, the fact that isotopic ratios are little affected by the transformative smelting and melting processes (Pernicka 2014, 249) means that slag should have the same isotopic ratios of lead than that of the finished copper, and thus can be equally informative (Schreiner et al. 2003; Stos-Gale and Gale 2011).

This is especially true in the case of Çamlıbel where preliminary studies had already demonstrated a discrepancy in the arsenic content of the objects and the slag which had suggested either distinct sources or of an alloying operation. A comparison of the lead isotope ratios of the finished copper objects and slag could therefore offer supporting evidence for either scenario. If the ratios match, then the arsenic and copper come from deposits with the same geological age or the arsenic deposit contains too little lead to significantly impact the ratio. Should the objects and slag have noticeably distinct ratios, then either they have unrelated origins or the addition of an alloying agent has shifted the lead isotope ratios.

LIA using ICP-MS can be conducted on samples which have been either dissolved into solution, or using minimally destructive targeted technique of laser ablation. However, the laser ablation instrument of the Curt-Engelhorn Zentrum Archäometrie is coupled to a quadrupole ICP-MS which is much less precise in determining isotopic ratios. In addition, laser ablation likely

induces fractioning of isotopes which cannot be calculated or corrected for and thus may affect the results (Pernicka, pers. com.). Given that destruction of the material was not problematic in this case, and in order to maximize the accuracy of the analysis, the measurements were carried out in solution. Samples were first thoroughly cleaned and homogenized before being dissolved. In addition to the lead isotopic ratios, the total lead content was also determined to assess whether enough was present within the sample to provide meaningful results. Both of these results will be presented below in chapter 8.

Chapter 7 Analytical Results

7.1 Çamlıbel

7.1.1 Assemblage

The total metallurgical assemblage recovered from Çamlıbel Tarlası consists of material from all aspects of metal production and use, albeit with some caveats. For the purpose of this discussion, the term ‘object’ refers to finished metallic artefacts and is thus distinguished from all other artefacts which consist of production remains. Crucibles refer to either melting and/or smelting crucibles and this distinction will be further discussed in the next section. Lastly, it is rather difficult to distinguish between minerals, ores, and gangue without a thorough understanding of the economics of the extraction process, and, as such, this category of finds is left intentionally ambiguous. It should, however, remain broadly representative of varying mineral extraction and use in the settlement.

Although some metallurgical remains were found dating to each occupation period, they vary in their chronological distribution, with some periods marked by only limited production, while others witness a dramatic change in artefact distribution patterns. It is possible to identify a few trends in the frequency of these remains which are worth mentioning here as they may represent identifiable changes in cultural behaviour and may reflect technological developments at the site.

Table 7.1 Distribution of the total metallurgical remains at Çamlıbel Tarlası by period.

Phase	Objects	Crucibles	Minerals/Ores	Slag	Total
Surface	6	1	2	51	60
CBT IV	3	6	19	62	90
SPEU	2	0	6	2	10
CBT III/IV	0	0	2	1	3
CBT III	5	2	9	40	56
FPEU	4	0	21	2	27
CBT II/III	0	1	0	5	6
CBT II	5	1	25	8	39
CBT I/II	0	0	1	1	2
CBT I	5	0	42	2	49
Total	30	11	127	174	342

The table presented above lists all major metallurgical artefact categories found at Çamlıbel by stratigraphic layer (Table 7.1). Material which could not be securely assigned to a single phase were set in new categories (i.e. CBT II/III) by the excavators to reflect ambiguity while still being able to identify broad chronological trends without loss of resolution. Excluded from this list are the ‘bowl furnace’ features and purple-stained ceramics which remain poorly understood and will be discussed separately. It is however worth noting that the ‘bowl furnaces’ were found in all layers except for CBT III and CBT IV while the stained ceramics were found mainly in CBT IV, but that a few stray examples were found in deeper levels.

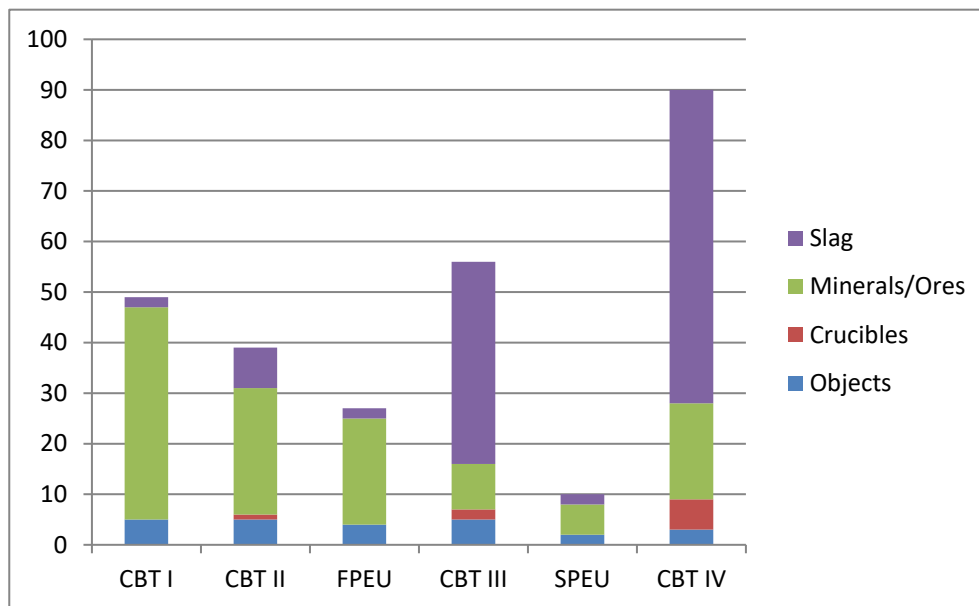


Figure 7.1 Bar chart distribution of the metallurgical remains from secure contexts at Çamlıbel Tarlası by period.

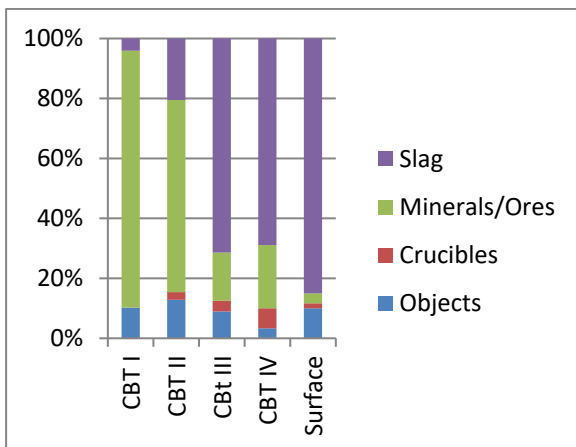


Figure 7.2 Numbers of metallurgical remains at Çamlıbel Tarlası by chronological period (normalized to 100%).

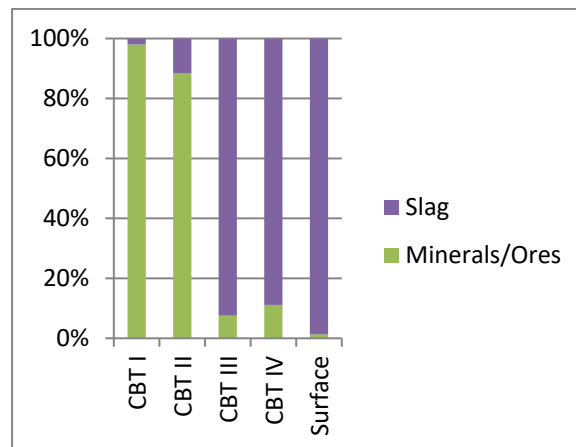


Figure 7.3 Weight of slag and ores at Çamlıbel Tarlası by chronological period (normalized to 100%).

Ignoring phases with unclear stratigraphy (CBT I/II, CBT II/III, and CBT III/IV), to focus rather on the more obvious copper producing periods, there appears to have been a shift in the nature of copper production starting in CBT III (Figures 7.1, 7.2, and 7.3). Prior to this period,

the metallurgical assemblage was dominated by oxide and sulphide minerals rich in iron and copper (n=89, 83%) and had relatively little slag (n=18, 17%). In contrast, after the site was re-occupied in CBT III, the assemblage contained fewer copper and iron minerals (n=38, 19%) and was increasingly composed of slag (n=156, 81%), from a ratio of mineral to slag of about 4:1 in CBT I and II to about 1:4 in CBT III and IV. Whether this represents a technological change or the relocation of ore processing and smelting activities remains to be established. It is worth noting that CBT III is also marked by the appearance of pedestalled type crucibles and coincides with the disappearance of bowl hearths from the site, and so there is a clear break in the metallurgical package at this time which will be discussed further in chapter 9.

Interestingly, despite this clear difference in the metallurgical assemblage of the later periods, there is no significant change in the discard rate of metal objects throughout these occupation phases (between 2-5 metal objects per stratigraphic layer). This occurs despite some very fundamental changes in the nature of the settlement during both periods of ephemeral use (FPEU and SPEU) as well as the increase in the number of permanent structures in the latest period (CBT IV). Furthermore, the distribution of the types of copper alloy objects does not appear to be affected by the rise and fall of metallurgical activity at the site (Schoop, pers. com.), suggesting that increased *in situ* metal production in later periods did not necessarily translate in a surge in metal use at the site. This may either indicate that although object use at the site remained stable, their production occurred at other locations in earlier periods, or alternatively, it may imply that the additional metal produced on site was destined for another market and thus used and discarded elsewhere.

Ninety-one samples from the total assemblage were selected for archaeometallurgical analysis and sent to UCL's Institute of Archaeology. With the exception of the two arsenic-rich slag samples and the six stained ceramic samples exported following the author's visit to the site in 2012, all of the samples were randomly selected by the excavator, Ulf-Dietrich Schoop, with the number of samples representing the total amounts recovered from each occupation phase. Of these 91 samples, five were found to be non-metallurgical upon closer inspection, consisting of quartz, asbestos, and heat-altered wall plaster, and will therefore not be discussed here. After microscopic and chemical analysis, a further seven samples were deemed to be of no relevance to the metallurgy of the site. Four of these were found to be molten ceramic with no evidence for use as crucibles, moulds, or furnace structures. The other three samples consisted of a bone splinter covered in copper corrosion, a ceramic

storage vessel, and a stone containing no copper-bearing minerals. As such, these twelve samples will also be excluded from these results presented here (Table 7.2).

All of the remaining 79 metallurgical samples have now been analysed through optical microscopy and 67 of them have also been analysed by SEM-EDS. This includes the revisiting of three samples (128-1083, 55-440, and 60-3094) previously analysed at UCL and published by Rehren and Radivojević (2010). Five soil samples and seven samples of the bowl hearth lining were not analysed by SEM-EDS and will be discussed separately. The metallurgical assemblage which remained in Turkey was analysed on site using a pXRF. These results will only briefly be discussed in the context of the bowl hearths since the reliability of the instrument is questionable on this type of multiphased material and results may not be accurate enough to make valid inferences unless further more quantitative testing can be conducted.

Table 7.2 Çamlıbel Tarlası metallurgical samples analysed. Numbers in parenthesis indicate the number of samples which were macroscopically evaluated but not prepared for and analysed by SEM-EDS.

Phase	Slag	Crucibles	Minerals /ores	Bowl hearths	Stained ceramic	Soil	Total
Surface	5	0	0	0	0	5 (5)	5 (5)
CBT IV	19	3	4	0	4	0	29
SPEU	2	0	2	0	1	0	5
CBT III	8	2	0	0	1	0	12
FPEU	1	0	0	0	0	0	1
CBT II/III	0	1	0	0	0	0	1
CBT II	2	1	4	0	0	0	7
CBT I/II	1	0	0	0	0	0	1
CBT I	2	0	3	7 (7)	0	0	12 (7)
Karakaya	0	0	1	0	0	0	1
Total	40	7	14	7 (7)	6	5 (5)	79 (12)

7.1.2 Crucibles

As mentioned, several fragments of metallurgical ceramics were collected from Çamlıbel. All fragments were identified as belonging to metallurgical activities based either on their distinctive flaring rims which did not match any of the local pottery wares or by the presence of what appeared to be high temperature greenish residues coating their inner surfaces near the rims (Figure 7.4).

These metallurgical ceramics were found in layers mostly dating to the last two periods of occupation at Çamlıbel (III and IV) and their appearance within the assemblage coincides with changes in the distribution of metallurgical finds previously discussed (see section 7.1.1). The only fragment to belong to an earlier period, 956-6202 from CBT II, has an entirely different morphology and will therefore be treated separately than the other pieces.

Although several large nearly complete examples were recovered by the site's excavators, these were deemed of too much cultural value for export. As such, seven fragmentary specimens (Figures 7.5 and 7.6) were made available for analysis for this research, all of which were sampled and fully investigated given that they were deemed of critical importance in developing a complete picture of the metallurgical activities at Çamlıbel. Particular attention was paid to the inner greenish coatings in order to identify whether the crucibles were used for smelting, melting, or alloying operations. The composition, microstructure, and refractory properties of the ceramic fabrics were also assessed with an eye towards their comparison with that of local pottery ware and the possibility of distinct specialised ceramic industries.



Figure 7.4 Photograph of residue layer of crucible 139-6312. Photograph courtesy of Ulf-Dietrich Schoop.

The overall morphology of these crucibles could be reconstructed thanks to the number of larger fragments recorded in the field but not available for analysis. They are best described as pedestalled (Figures 7.7 and 7.8), with flat bases and 10-15cm tall narrowing necks that flare outwards near the top to form shallow oval bowls 5-10cm long and 3-5cm wide. The depth of the bowls, in fragments where it could be estimated, was approximately 2-3cm, giving them a maximum volume of 0.15 litres. The oval pedestals are pierced along their narrow axis by a single hole approximately 1cm in diameter which is thought to have been made to facilitate transport of the crucibles and their content while hot. The crucibles were clearly heated from the top as no evidence of heat damage or vitrification could be seen on any of the crucibles' outer surfaces. This design would have ensured that the pedestals remained relatively cool throughout the operation and allowed it to be easily handled using organic material such as wooden shafts slotted through the hole with supporting shafts on either side.

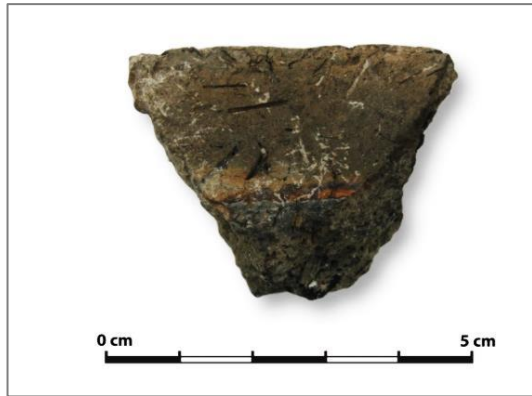


Figure 7.5 Photograph of crucible fragment 62-6450.



Figure 7.6 Photograph of crucible fragment 242-6470.



Figure 7.7 Photograph of Crucible 636-6459. This crucible showed no evidence of high temperature use and was identified as a crucible purely based on its shape and similarity to other more fragmentary objects. Photographs courtesy of Ulf-Dietrich Schoop.

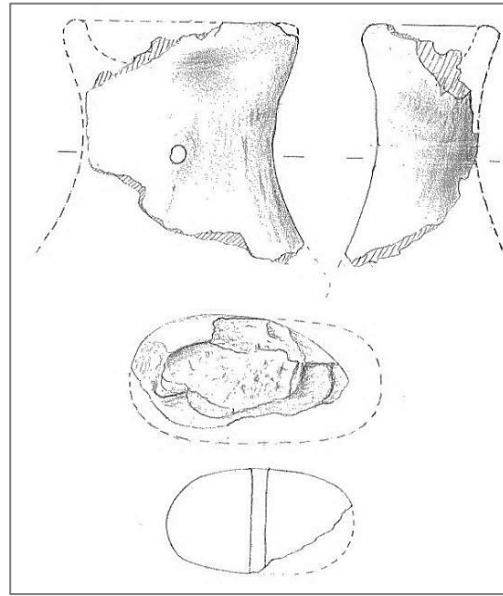


Figure 7.8 Drawing of crucible 139-6312. This crucible's inner surface was strongly vitrified and had several areas of green copper oxide corrosion growth. Due to its excellent preservation, it was deemed too valuable for destructive analysis. Drawing by Edward Rayner.

Interestingly, the crucible fragments were typically broken just below the rim, with the residue present only on a small area directly above the missing inner surface (Figures 7.5 and 7.6). It is unfortunately impossible to tell whether this was the result of an intentional effort to remove any traces of copper for re-processing, the result of damage caused by the metallurgical operation itself, or preferential post-depositional taphonomic processes.

Microscopically, the crucibles have fabrics with dark grey cores and light grey to beige inner and outer surfaces (Figure 7.9). These colours are an indication of the redox conditions during the metallurgical operation rather than any real compositional differences between the layers. The inner layer of the crucibles is usually greatly heat altered, with zones of

vitrification and bloating from intense heat, overlain by a dark residue left from the metallurgical operation. The ceramics are chaff tempered as evidenced by frequent elongated cavities throughout the bodies. In addition, occasional mineral inclusions of quartz, as well as iron, chromium, and titanium oxides were observed throughout the ceramic bodies. Other than the presence of chaff temper, these fabrics are macroscopically identical to that of the local pottery wares (Schoop, pers. com.). It should be noted that the use of chaff was advantageous in a metallurgical context as the elongated voids left by the burning organic material enhance ceramic's insulating property, stop cracks from spreading, and reduce the coefficient of thermal expansion (Rice 1987; Tylecote 1982).

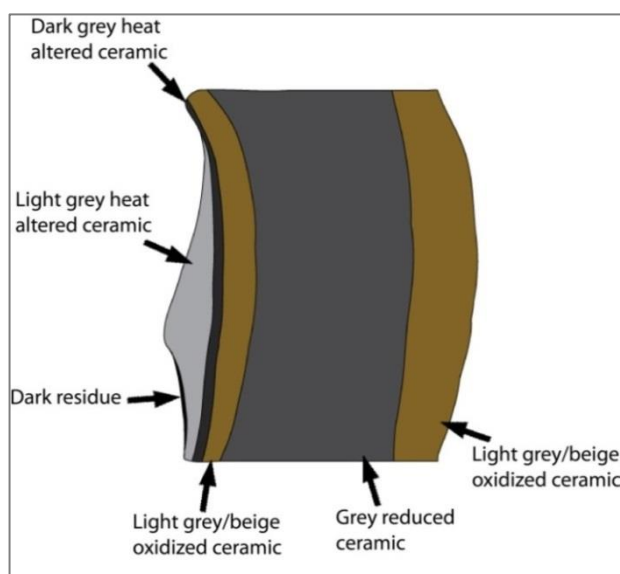


Figure 7.9 Cross section of sample 242-6470 showing the various layers present in the CBT III and IV group of crucibles.

The bulk chemical compositions of the ceramic samples show only slight variation, and certainly no chronological trends can be observed. The elevated arsenic content found in sample 133-6376 is probably due to contamination from volatile arsenic gas freed during the use of the crucibles, a point which will be discussed shortly. Overall, the consistent composition of the ceramics suggests that the potters were returning to the same clay source in both occupation periods and that although the crucible manufacturing and tempering was highly standardized at Çamlıbel, these are probably a feature of the overall pottery industry using local clay rather than a specialised refractory ceramic industry (Table 7.3). That being said, Çamlıbel's distinctive crucible shapes do suggest that some form of specialized manufacture aimed at metallurgical activities did indeed exist. This is in agreement with the observation by Bourgarit (2007) that Chalcolithic sites where smelting was conducted in domestic settings such as Al Claus, La Ceñuera and Almizaraque smelting tended to be conducted in non-refractory ceramic common wares.

Table 7.3 Bulk composition of crucible and typical local pottery ware bodies as determined by SEM-EDS. All results are the means of at least three area analyses, presented in oxide wt. %, and normalized to 100%.

Sample	Phase	Na ₂ O	MgO	Al ₂ O ₃	SiO ₂	K ₂ O	CaO	TiO ₂	FeO	As ₂ O ₃
107-6457	CBT IV	1.9	3.4	14.2	62.1	2.5	9	b.d.l.	7	b.d.l.
133-6376	CBT IV	1.5	5.5	13.7	58.9	2.1	9.1	0.7	7	1.4
136-6325	CBT IV	1.1	7.9	11.8	53.9	1.3	13	1.6	9.4	b.d.l.
242-6470	CBT III	1.7	6.6	13.9	61.2	1.3	4.3	1.4	9.6	b.d.l.
62-6450	CBT III	1.7	5.8	14.3	61.6	1.7	3.9	1.5	9.6	b.d.l.
79-6471	CBT II/III	1.6	5.7	13.7	61.3	2	4.9	1.2	9.6	b.d.l.
Mean		1.6	5.8	13.6	59.8	1.8	7.4	1.1	8.7	0.2
Std. dev.		0.3	1.5	0.9	3.1	0.5	3.6	0.6	1.3	0.6
Çamlıbel pottery mean of 6 samples	various	1.7	7.4	17.7	57.6	1.8	5.1	1.3	9.8	b.d.l.

The clay is rich in calcium, iron, and magnesium oxides and rather deficient in aluminium oxide, all of which are to be expected from the use of the local ophiolitic clays, but which would have made it poorly refractory (Figure 7.10). However, the use of such highly calcareous and ferruginous clays for technical ceramics appears to have been prevalent at this time period (Frame 2012; Freestone 1989; Thornton and Rehren 2009; Tite et al. 1990) and seems to have been sufficient for the purpose of smelting. In actuality, it is quite possible that the use of such poorly refractory material was actually somewhat beneficial to the crucible technology employed here. Since the crucibles were heated from above, the material's low thermal conductivity would have limited the amount of heat permeating through the crucible and therefore diminishing the chances catastrophic failures occurring from bloating and melting (Bayley and Rehren 2007; Hein et al. 2013). These crucibles would have therefore maintained their structural integrity, at least on the outside, but have a thin layer of vitrified ceramic on the inside which would interact strongly with the charge.

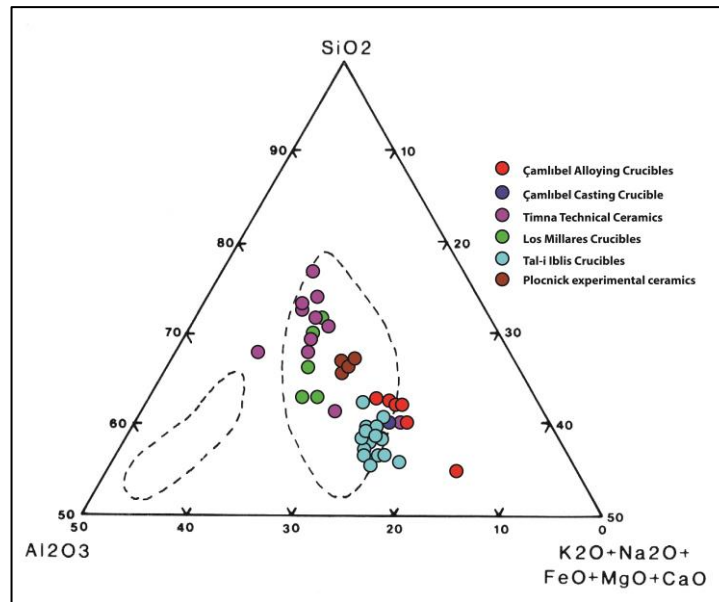


Figure 7.10 Composition of refractories from Timna (Tite 2001), Los Millares (Freestone 1989), and Tal-i Iblis (Pigott 2012) to those of Çamlıbel. The outlined section to the bottom left delineates the composition of modern refractory firebricks while the one in the centre is of clays that bloom by 1300°C. Adapted from Freestone (1989).

The most interesting aspect of these crucibles is the thin layer of calcium arsenate adhering to their inside surface (Figures 7.11 to 7.13). These residues appear to have been at least partially molten as they have a bubbly porous appearance from the escape of gases and adhere to the ceramics in a hot contact. They are typically composed of a single phase of calcium arsenate, although in some instances the layer is composed of magnesium calcium arsenate (Table 7.4). Four crucibles contained calcium arsenate exclusively, one contained only magnesium calcium arsenate, and one contained both types of arsenate phases. Both of these alkali earths are expected to behave similarly and are chemically interchangeable so that the final composition of the residues reflects the availability of each element in the system rather than any other atmospheric parameter.

Although the sample size is quite low, it is possible to notice a correlation between the elevated magnesium oxide phases and sodium, a compound commonly associated with fuel ash. On the other hand, the high calcium oxide phases appear correlated with increased silica and alumina and indicate greater interaction and input from the crucible fabric and charge, particularly in sample 79-6471. As already mentioned, the preference for one phase or the other is likely to be the result of local concentrations of each element.

Potash (K_2O) and soda (Na_2O) are also encountered in the arsenical layers. These are typical compounds found in virtually all crucible slags to some extent as they result from the interaction of fuel and ceramics (Tylecote 1987). However, in the case of about half of the Çamlıbel crucibles, potassium and sodium are only found in relatively low proportion, and in no instance do they appear

to correlate with each other. This is somewhat surprising as they would be expected to occur more or less in tandem.

However it should be remembered that these layers are not slag in the conventional sense and calcium/magnesium arsenates most likely do not interact with these fuel ash elements in the same way as iron silicates do. Furthermore, their location well above the reaction zones means that the layers did not come in direct contact with liquefied material, limiting contact with less volatile elements. In addition, a system very far from equilibrium, as can be assumed to exist here, would be expected to allow a much less constant interaction with the crucible and therefore a lower and more inconsistent content of these elements to enter the slag. It has also been suggested that since the vessel had to include both the charge and fuel, a bed of burning charcoal may often have isolated the 'slag' or (semi-)molten phases from the crucible walls, resulting in the lower presence of these elements as was surmised for the Early Bronze Age crucibles of Wadi Fidan 4 (Rothenberg 1988).

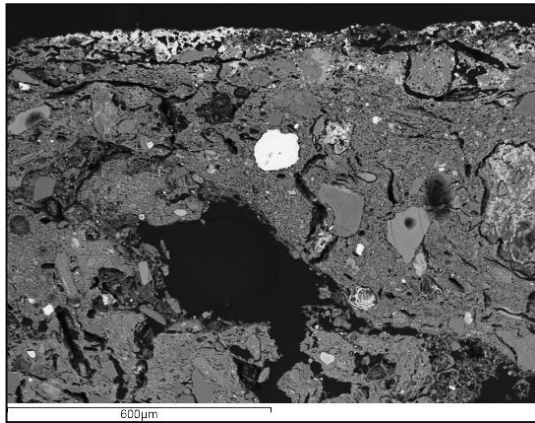


Figure 7.11 SEM image of the calcium arsenate layer on crucible fragment 107-6437.

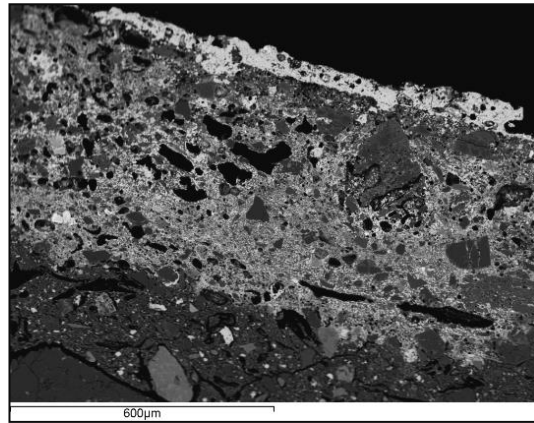


Figure 7.12 SEM image of the calcium arsenate layer on crucible fragment 133-6376.

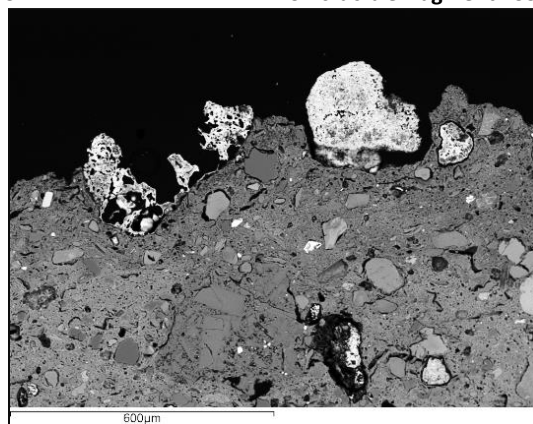


Figure 7.13 SEM image of the calcium arsenate layer on crucible fragment 136-6325.

Table 7.4 Composition of the two types of arsenate phases in the crucible residue layers as determined by SEM-EDS.

Sample	Phase	Na ₂ O	MgO	Al ₂ O ₃	SiO ₂	P ₂ O ₅	SO ₃	Cl	K ₂ O	CaO	MnO	FeO	CuO	As ₂ O ₃
107-6457	CBT IV	0.6	15.9	b.d.l.	3.1	2	b.d.l.	b.d.l.	2.5	14	b.d.l.	2.5	12.4	47
133-6376	CBT IV	b.d.l.	17.5	b.d.l.	2.1	0.4	b.d.l.	b.d.l.	2.8	18.4	b.d.l.	1.4	6.1	51.3
Mean		0.3	16.7	b.d.l.	2.6	1.2	N/A	N/A	2.6	16.2	N/A	1.9	9.2	49.2
133-6376	CBT IV	b.d.l.	2.6	b.d.l.	0.5	2.2	0.8	b.d.l.	0.7	37.9	b.d.l.	0.1	3.9	51.5
136-6325	CBT IV	b.d.l.	0.3	0.9	5.1	0.2	0.3	1.7	0.7	46.2	0.6	1.2	b.d.l.	42.5
242-6470	CBT III	1.1	3	0.5	4.9	4.5	1	b.d.l.	0.6	40	b.d.l.	2.5	0.9	41.1
62-6450	CBT III	b.d.l.	2.2	1.1	13.5	3.3	0.5	b.d.l.	1.2	32.6	0.3	2.9	4.2	34.9
79-6471	CBT II/III	b.d.l.	1.9	5.2	18.1	3.9	0.7	1.1	0.7	32.7	b.d.l.	4.4	b.d.l.	31.2
Mean		0.2	2	1.6	8.4	2.8	0.7	0.6	0.8	37.9	0.2	2.2	1.8	40.2

Most of the layers also contained significant quantities of copper oxide, varying from less than 0.1 wt% to 12.4 wt% and a mean of 3.9 wt%. In one crucible, 133-6376, a large prill of copper oxide was identified surrounded on all sides by calcium arsenate (Figure 7.14) and shows clear evidence that, unlike the smelting slags, these crucibles were operated in the presence of both copper and arsenic. It is therefore most likely that these crucibles were used for melting and/or alloying rather than any form of smelting.

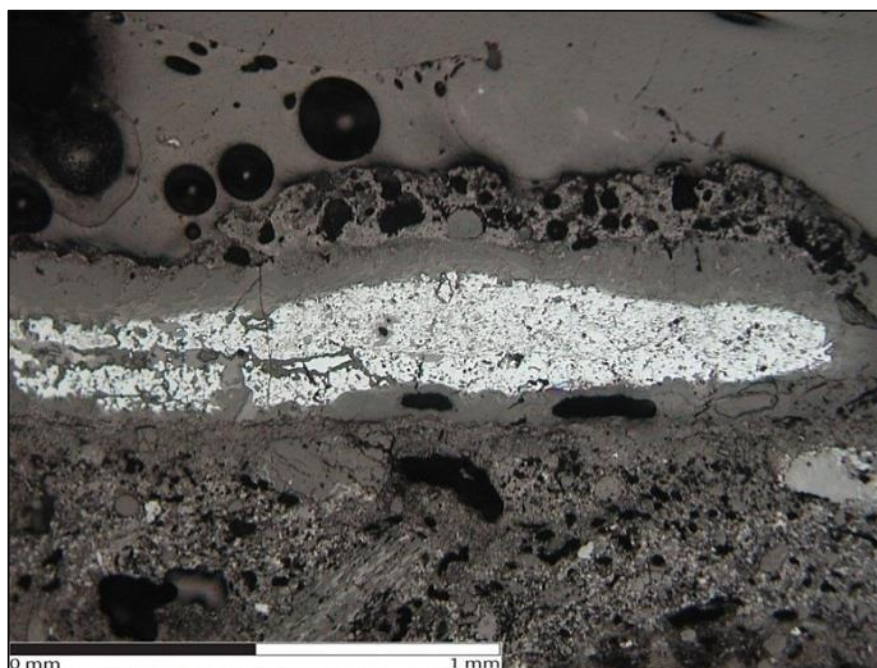


Figure 7.14 SEM image of a copper oxide prill (bright phase) surrounded by copper corrosion (grey phase) with a thin layer of calcium arsenate (light grey, above). Small bright dense phases within the cuprite prill are arsenical copper.

Although no arsenic minerals have been identified at Çamlıbel or in the immediate surrounding area, it is still possible to assess the probable nature of the alloying agent used in these crucibles. First and foremost, arsenic is unlikely to have been added as a metallic

product as the reduction of arsenic ores is inherently difficult given its low boiling point and strong tendency to oxidize. In fact, while later historical texts mention the use of various arsenical minerals (Caley 1926; Eaton and Mckerrell 1976; Healy 1978, , 158, 210-212; I-Tu and Hsueh-Chuan 1966; Wyckoff 1967), there is no archaeological evidence to suggest that metalworkers were aware of the existence of arsenic metal as a separate substance anywhere until the post-medieval period. We must therefore assume that the arsenic was added as a raw mineral to copper. Looking at the results presented here, it is possible to narrow the range of minerals which could have been employed at Çamlıbel. The small amount of sulphur present in the arsenate phases (mean 0.5 wt%) suggests that the original arsenic source mineral was most likely to have been an arsenate with only a minor sulphide component as has been already proposed by others (Craddock 1995; Zwicker 1991).

Arsenic-bearing mineral deposits where colourful arsenates could easily be identified as weathering products on arsenical sulphide minerals are indeed found in the wider region north of Çamlıbel (Enstitüsü 1970), well within 100 km of the site. Although it has been suggested that arsenic sulphides such as orpiment or realgar could also be used to make arsenical copper (Özbal et al. 1999; Özbal et al. 2008) the addition of such compounds would have been unsuitable in this context as it would have resulted in excessive losses of copper to matte (see section 3.1.4) and are therefore unlikely to have been used.

It is difficult to posit how the process functioned chemically without the original composition of the ores, but the calcium/magnesium arsenate phases offer some clues. The operation would certainly have required a reducing atmosphere in order to avoid arsenic losses to oxidation. The iron present in the copper as described above, would in this case act as a reducing agent for the arsenate mineral while itself being refined out of the copper as iron oxide. Under these conditions, the arsenate would be readily reduced to metallic arsenic gas which could then diffuse into the copper in a process similar to the well-known brass cementation process. Any escaping arsenic gases would have quickly oxidized above the charge to form arsenic trioxide (As_2O_3), which in turn combined with calcium oxide, typically introduced in crucibles as charcoal fuel ashes (Tylecote 1980), to form a compound with a composition between $3\text{CaOAs}_2\text{O}_5$ and $4\text{CaOAs}_2\text{O}_5$, much in the same way as modern arsenic-based pesticides are manufactured (Robinson 1918; Smith and Murray 1931). In this case the compound precipitated upon cooling above the crucible, forming the arsenate layers found near the crucible rims.

Similar arsenic-enriched layers deposited through the casting process have been observed on moulds and crucibles from El Malagon in Southern Spain where they have been interpreted as a typical effect of the release of arsenic gases during the melting of arsenical copper (Hook et al. 1987; Hook et al. 1991). It should be noted that the process of corrosion would also have a tendency to promote the enrichment of arsenic on the surface of these objects, but this is clearly not the case here as the layers show morphological traits distinctive of a hot process.

The earliest (CBT II) example of technical ceramics from Çamlıbel is sample 956-2602. This particular specimen exhibits a thin layer of reddish copper metal (Figure 7.15) and is therefore likely to have been part of a casting or melting/alloying crucible or mould. No discernible morphology could be tied to the underlying shape of the object other than the assumption that the metallic residue and heat alteration indentify the inside of the crucible.

The ceramic fabric is relatively fine grained with frequent large quartz inclusions but does not include any organic temper (Figure 7.16). Heat damage and vitrification is apparent directly below the metallic residue, extending into the ceramic body to an approximate depth of 2 mm. Compositionally, the unaltered ceramic fabric is virtually indistinguishable from that of the later alloying crucibles already described (Table 7.5). Immediately below the layer of metallic residue is a shallow region which has been generally fully vitrified, with only occasional clusters of thin copper iron oxides laths of delafossite (Figure 7.17). These crystals are very common in highly oxidizing atmospheres typically associated with re-melting of copper metal, reinforcing the original assumption that this particular sample is not a smelting crucible.

Table 7.5 Bulk composition of melting crucible or mould fragment 956-6202 as determined by SEM-EDS.

	Na ₂ O	MgO	Al ₂ O ₃	SiO ₂	P ₂ O ₅	K ₂ O	CaO	TiO ₂	FeO	CuO	As ₂ O ₃
unaltered ceramic bulk	1.4	6.4	15.1	59.4	b.d.l.	2.2	3.6	1.4	10.4	b.d.l.	b.d.l.
Heat altered ceramic bulk	0.8	7.3	10.4	59.4	1.1	2.7	4.6	1.3	10.6	1.8	b.d.l.
Glassy area without delafossite	1.2	7.2	12.9	54.2	1.9	7.7	4.5	1.2	9.2	b.d.l.	b.d.l.
Glassy area with delafossite	1.2	7.1	12.6	47.8	2.4	3.7	7.4	1.6	11.2	5.0	b.d.l.

Unfortunately, because the metallic layer does not appear to have truly meshed with the ceramic fabric it was largely broken away during sample preparation and could not be analysed by SEM-EDS. However, the complete absence of any arsenic in the ceramic fabric and the clearly reddish colour of the surface residue mean that the metal was most probably pure copper.

Bulk composition of the heat altered areas of ceramic fabric shows a nearly identical composition to that of the unaltered ceramic which has been slightly enriched in copper where delafossite is present and more generally in elements commonly related to fuel ash. This suggests that the glassy layers were not formed from interaction with slag and confirms that the ceramic was likely not used for smelting. Furthermore, delafossite crystals are commonly observed in oxidizing atmospheres typical of exposure to open air during the melting, refining, alloying, or casting of copper metal and confirms the first impression of this sample as either a melting crucible or mould fragment.

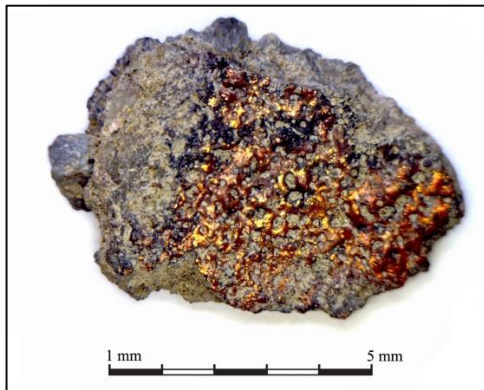


Figure 7.15 Photograph of sample 956-6202.

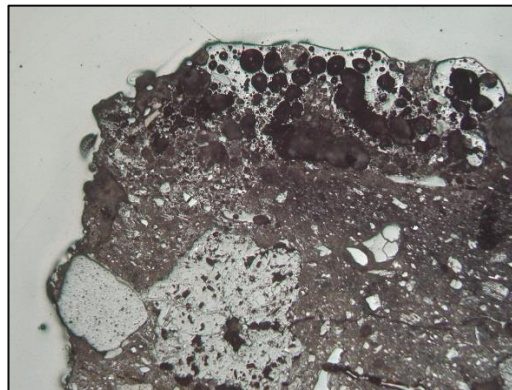


Figure 7.16 Photomicrograph of ceramic body and vitrified ceramic below metallic layer. Frame is 3.7mm wide.

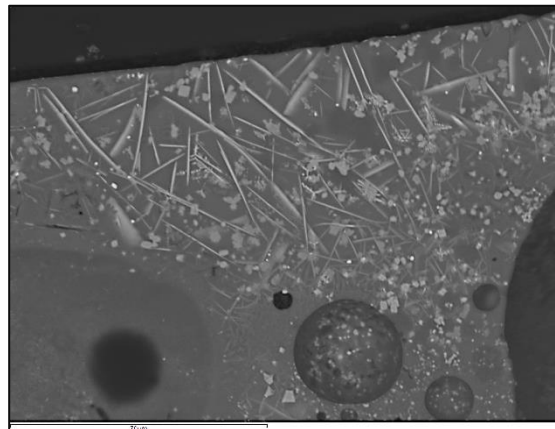


Figure 7.17 SEM image of delafossite crystals just below the metallic layer. Note that the metal layer was lost during the polishing process.

7.1.3 Furnace Lining

A number of small shallow bowl shaped pits with evidence of extensive heat application were uncovered, mostly in the earliest two levels of Çamlıbel (I and II). Large deposits of charcoal and ash were observed directly adjacent to them, testifying to their pyrotechnical use. The fills and surrounding ashy soil contain abundant fragments of iron rich minerals such as limonite and haematite which led to them to be described as bowl furnaces involved in the processing of copper ores (Schoop 2010a, 72-73). However, a number of questions remained as to their actual function

and process and therefore a sample of ash (629-4416) was obtained from the lining of one of the features from Çamlıbel I for detailed laboratory analysis. In addition, several of these pit features, which had been removed as sectioned blocks by the excavators for preservation, were also analysed in the field using a pXRF in order to identify and compare minor and trace elements between the various component layers. The morphology of the bowl pits will first be described followed by a discussion on their chemical composition.

The features were approximately 15-25cm in diameter and 10 to 20cm in depth (Figure 7.18). They were haphazardly lined with small stones and broken pottery sherds in an ashy soil and the base was invariably covered by a hard fired clay cap 2 to 5 cm thick. The few identifiable fragments of pottery were found to be of the local domestic ware type (Schoop, pers. com.), suggesting that they were reusing old broken pots to line the pit, although the purpose of this remains unknown. The clay caps are shaped like concave lenses and appear to have been fired *in situ* from elevated temperatures within the pit and the soil surrounding the pits was reddened to some depth extending between 5 and 10cm beyond the edges of the feature, indicating that heat was sustained for a protracted period of time. In some instances, a cluster of larger stones was buried beneath the layer containing the pottery sherds, although no plausible explanation for this could be ascertained.

Above the clay caps, the pits were filled with several distinct deposits, identical in texture to the surrounding natural soil but rich in ash causing them to be lighter in colour. In some cases stones had been laid directly on top of the features as markers, prompting the excavators to suggest that the pits were backfilled intentionally to preserve their structure between seasonal occupations.

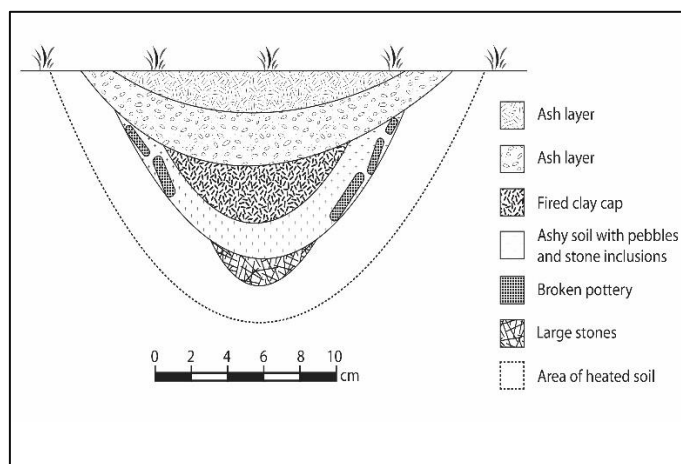


Figure 7.18 Diagram of a typical bowl hearth cross-section.



Figure 7.19 Photograph of furnace feature number 4, sectioned and collected from the site for later analysis.

As previously mentioned, the excavators recovered several of these features as sectioned blocks during excavation (Figure 7.19) and these were cleaned and analysed in the field using a pXRF.

The mean results of the various layers from six of these features are presented in Table 7.6. The surface of the clay cap was treated as a separate layer in an attempt to confirm the nature of these bowl furnaces by identifying any increase due to pollutants derived from the process. It was hoped that the outer layer would show the increased presence of certain volatile elements such as copper and arsenic when compared to the underlying body of the cap as well as to the surrounding natural soil.

The results clearly show that most elements are tightly clustered and appear to be precise even if not quantitatively accurate. While lighter elements (notably phosphorous, potassium, and calcium) show large standard deviations, this is most probably due to the limitations of the instrument and should not be taken to represent real compositional differences. Many trace elements, on the other hand, have much lower relative standard deviations and should be considered reliable for comparison between the layers analysed here.

It is clear that, at least compositionally, there is little difference between the fills, clay cap, and underlying natural soil. The hard clay cap is therefore likely to be the result of the simple firing of the clay-rich surrounding soil rather than a ceramic lining applied to the inside of the pits. Analyses of three random fragments of domestic pottery using the exact same settings on the pXRF instrument confirm this (Table 7.8). Although quite a few elements do overlap, the pottery is lower in calcium and potassium, while consistently higher in titanium, manganese, and barium.

Of significance to this study are arsenic and copper contents which are much lower than one would expect from contamination due to copper related activities. Although taphonomic processes such as leaching are known to affect the concentration of such contaminants, there is sufficient evidence to suggest that enough pollutants remain within the soil to enable the identification of metallurgical activities even after several thousand years. For example, Bronze Age mining and smelting at Copa Hill in Wales resulted in an increase in the copper content of the surrounding peat from 30ppm to 90ppm at Copa Hill 2, a site located some 600m distant from the main activity area (Mighal et al. 2002). Such contamination should have been even more dramatic within the confines of the firing chamber where leaching would also have been minimized by the insulating ceramic. This was certainly observed in prehistoric copper smelting experiments which were aimed at reproducing Vinča culture technology where soil copper content was increased by between 100% and 2600% within remains of the furnace (Figures 7.20 and 7.21). This difference is large enough that it should overshadow any resolution issues arising from the semi-quantitative nature of the pXRF instrument used.

Table 7.6 Bulk elemental composition of bowl hearth fills using pXRF. The results are presented in ppm as the mean of three analyses across each layer of the six bowl hearths and the associated natural soil adjacent to the features.

	P (%)	S (%)	Cl (%)	K (%)	Ca (%)	Ti (%)	Mn (%)	Fe (%)	Cr (ppm)	Co (ppm)	Ni (ppm)	Cu (ppm)	Zn (ppm)	As (ppm)	Rb (ppm)	Sr (ppm)	Zr (ppm)	Sb (ppm)	Ba (ppm)	Pb (ppm)
Top Fill	b.d.l.	b.d.l.	b.d.l.	0.8	12.8	0.7	0.1	6.0	570	610	640	100	80	b.d.l.	20	280	120	b.d.l.	280	5
Bottom Fill	3.3	b.d.l.	0.8	0.8	8.1	0.6	0.1	6.3	630	650	830	80	70	b.d.l.	20	220	120	b.d.l.	280	6
Clay Surface	4.3	0.8	0.9	1.1	12.5	0.5	0.1	5.3	520	620	560	130	90	5	30	310	150	b.d.l.	290	8
Clay	2.6	b.d.l.	0.6	1.1	8.3	0.5	0.1	4.7	390	430	500	80	80	5	30	320	140	b.d.l.	280	10
Natural	3.9	b.d.l.	0.7	0.8	9.1	0.7	0.1	6.1	640	630	660	100	90	4	20	310	130	40	300	6
Mean	3.5	0.8	0.7	0.9	10.1	0.6	0.1	5.7	550	588	638	98	82	5	24	288	132	40	286	7
Std Deviation	0.7	0.0	0.1	0.2	2.3	0.1	0.0	0.6	102	90	125	20	8	1	5	41	13	N/A	9	2
Relative std deviation (%)	21.0	0.0	14.3	17.8	23.0	13.4	4.5	11.3	18	15	20	21	10	12	23	14	10	N/A	3	29

Table 7.7 Bulk elemental composition of typical domestic pottery fabric determined with pXRF. Results are presented in ppm as the mean of two analyses on three randomly selected fragments of pottery.

Sample	P (%)	S (%)	Cl (%)	K (%)	Ca (%)	Ti (%)	Mn (%)	Fe (%)	Cr (ppm)	Co (ppm)	Ni (ppm)	Cu (ppm)	Zn (ppm)	As (ppm)	Rb (ppm)	Sr (ppm)	Zr (ppm)	Sb (ppm)	Ba (ppm)	Pb (ppm)
mean	2.8	b.d.l.	1.3	2.1	5.3	0.9	0.2	6.7	500	640	440	240	100	7	37	310	200	b.d.l.	500	10
Std dev	0.5	N/A	0.5	0.4	0.9	0.0	0.0	0.3	57.7	78.1	41.6	108.2	9.8	1.8	5.5	72.3	20.0	N/A	23.1	0.0
Relative std dev (%)	17.1	N/A	38.6	18.2	16.1	4.4	0.4	4.9	11.6	12.2	9.4	45.1	9.8	26.8	15.1	23.6	10.0	N/A	4.7	0.0

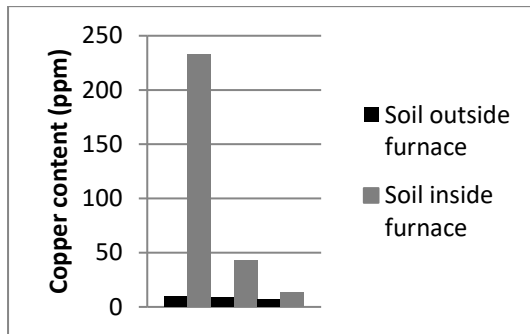


Figure 7.20 Results of XRF analysis of soil contaminants within and outside experimental prehistoric copper furnaces (Radivojević and Boscher forthcoming).

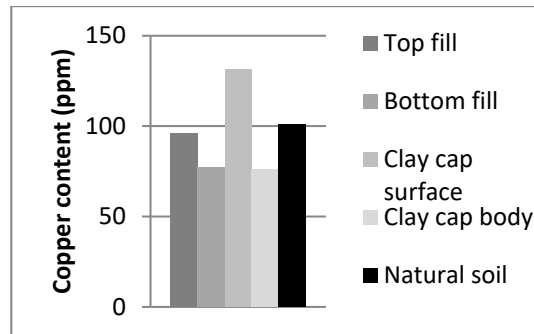


Figure 7.21 Results of pXRF analysis of the different layers of the bowl hearths recovered at Çamlıbel.

Given that arsenic is significantly more volatile than copper, an even more striking increased contamination of the surrounding soil would have been observed had these installations been used for the melting or smelting of arsenical copper. Even using crucibles, the ash-rich fills should have contained significant quantities of one or both of these elements if they were related to metallurgical processes. That they were not present in significant amounts, that no crucibles are associated with these layers, that little slag was found in association with these same deposits, and that no evidence of ceramic vitrification could be observed within the features suggests that they are not metallurgical installations.

As an alternative purpose, it is plausible that the features were used in the manufacture of the micro-beads composed of synthetic steatite also recovered from Çamlıbel (Pickard and Schoop 2013). This can unfortunately not be confirmed from these analyses since the pXRF was not calibrated to accurately quantify silica and magnesium, the two main constituents of steatite-derived minerals.

7.1.4 Other Metallurgical Ceramics

Post-excavation pottery cataloguing and analysis by the excavation team led to the identification of a large number of broken pottery fragments which showed odd purple staining (Figure 7.22). The team was intrigued by the fact that the staining appeared mostly on broken body sherds of thick and wide vessels tempered with organic material and concentrated in an area around the central courtyard of Çamlıbel IV's flagstone house. The breaks appear to have occurred prior to the staining of these objects given that the colour at times ran over the broken edges. The stains are generally, although not exclusively, found on the inner concave surface of the pots, and in some instances appear to be elongated as though they were the result of a liquid dripping downwards. In some samples, the purple colour is associated with a slight bulging of the ceramic, likely due to distortions and bloating caused by high temperatures.

It is worth noting that a few fragments of similar pottery recovered from the same area had thick copper and iron corrosion layers (Figures 7.23 and 7.24). Given that they exhibited no evidence of bloating or vitrification, it was assumed that this was caused by post-depositional processes rather than metallurgical operations.



Figure 7.22 Three examples of large pottery fragments with distinctive purple staining on the inner surface. Photograph courtesy of Ulf-Dietrich Schoop. In clockwork order starting in the top left, samples are 11-3, 651-16, and 100-3.



Figure 7.23 Pottery sample 758-6261 with large green and black corrosion staining.



Figure 7.24 Pottery sample 200-6526 with 1cm thick crust of iron hydroxide corrosion on the surface.

During the fieldwork campaign of 2013, eight purple-stained broken pieces of pottery were ear-marked for pXRF analysis aimed at identifying the nature of these stains and whether they were pigments or the consequence of some other effect. The results showed very clearly that the affected areas were enriched in copper, iron, and sulphur (Figure 7.25) with little effect on other elements. Since there was no similar increase in arsenic, the enrichment in other elements probably did not involve arsenical copper, although it is possible that the

element could have been leached out by taphonomic processes. It was therefore thought probable that these remains were associated with smelting or ore processing activities. Given these preliminary data, it was decided that seven samples should be exported for microscopic and quantitative analysis to determine their role, if any, in the metallurgical *chaîne opératoire* of Çamlıbel. These seven specimens were thus integrated into the analytical program of this thesis.

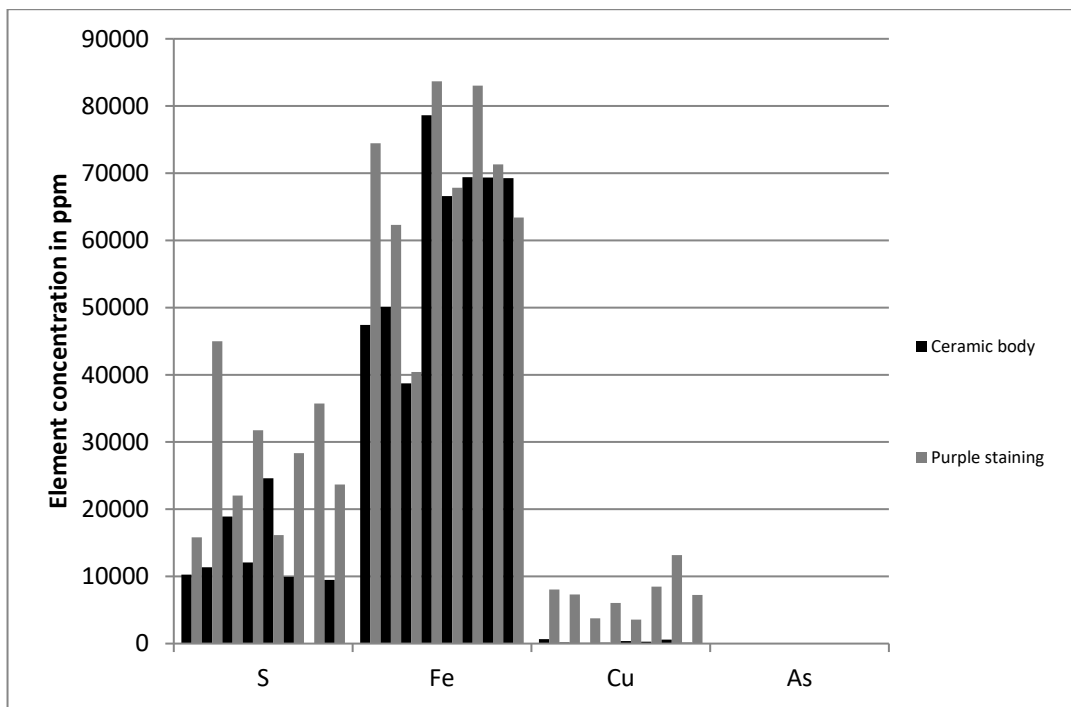


Figure 7.25 Sulphur, iron, copper, and arsenic content of clean ceramic fabric and associated purple staining as determined by pXRF. Each adjoining pair of results is from the same sample, demonstrating the consistent increase in the first three of these elements.

The samples provided were from as wide a range of contexts as possible, and are therefore not representative of the actual distribution of the finds. As previously mentioned, the vast majority of these artefacts were found in CBT IV (Schoop, pers. Com.), but a few fragments were found in strata belonging to the SPEU and CBT III. Thus, the two samples analysed from CBT III and the one from SPEU are representative of only a very small number of examples recovered from those layers.

The provided fragments are mostly body sherds, although two pieces have rounded rims (108-6857 and 819-7020). Their thicknesses vary consistently between 1.52 and 1.76 cm, with the exception of one of the rim sherds (108-6857) which is too damaged for an accurate measurement. They are generally mottled orange and brown showing mixed redox firing conditions, although several fragments also show an even beige colour on one of the surfaces. This is typical of the appearance of local pottery vessels identified at the site.

The fabrics are rather coarse, with significant amounts of organic chaff temper evident from the presence of elongated cavities and occasional inclusions of quartz and other minerals which may also have been added as temper (Figures 7.26 to 7.29). This is again typical of the local domestic pottery types.



Figure 7.26 Photomicrograph of sample 108-6838 ceramic fabric under plane-polarized light.

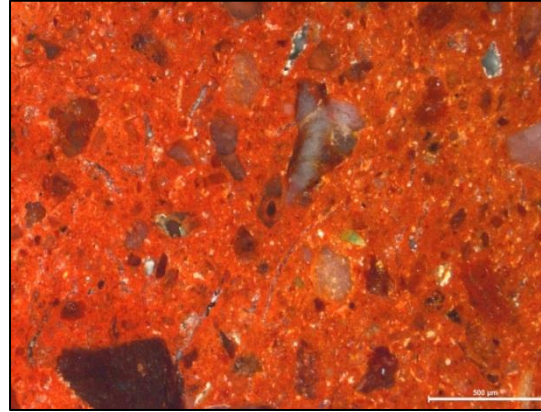


Figure 7.27 Photomicrograph of sample 108-6838 ceramic fabric under cross-polarized light.

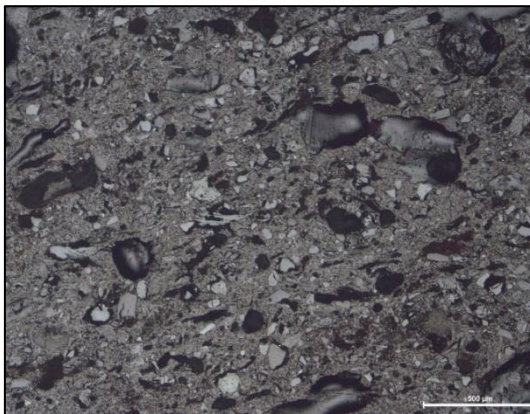


Figure 7.28 Photomicrograph of sample 228-6870 ceramic fabric under plane-polarized light.

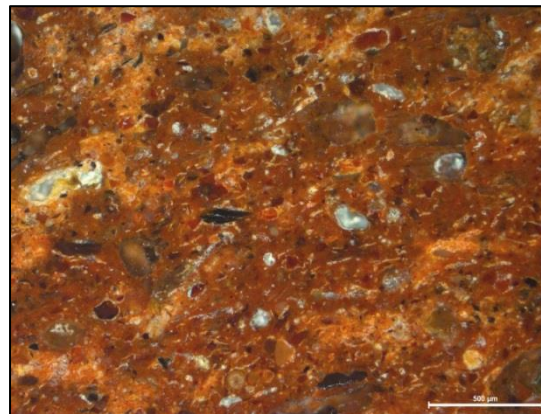


Figure 7.29 Photomicrograph of sample 228-6870 ceramic fabric under cross-polarized light.

Special attention was given during sample preparation so that the purple stained areas could be seen in cross section at their thickest extent, typically in the centre of the discolouration. Once mounted, the areas under question were very obvious under the microscope in all cases (Figures 7.30 to 7.33) except for sample 21-6838 which proved to have a highly bloated vitrified black inner layer which was completely different than the others (Figures 7.34 and 7.35) and will not be further discussed as it showed no evidence of metallurgical use.



Figure 7.30 Photomicrograph of sample 108-6857 cross section showing the purple-coloured layer on the surface of the ceramic under plane-polarized light.

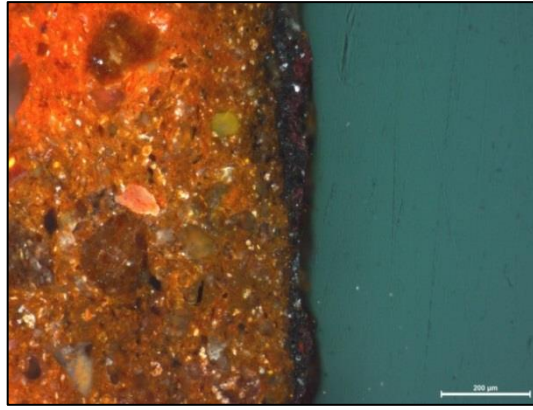


Figure 7.31 Photomicrograph of sample 108-6857 cross section showing the purple-coloured layer on the surface of the ceramic under cross-polarized light.

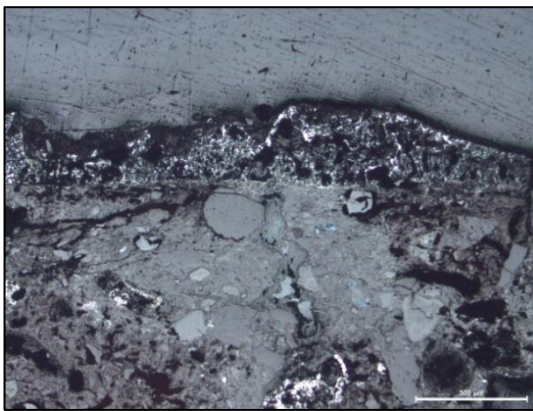


Figure 7.32 Photomicrograph of sample 720-6879 cross section showing the purple-coloured layer on the surface of the ceramic under plane-polarized light.

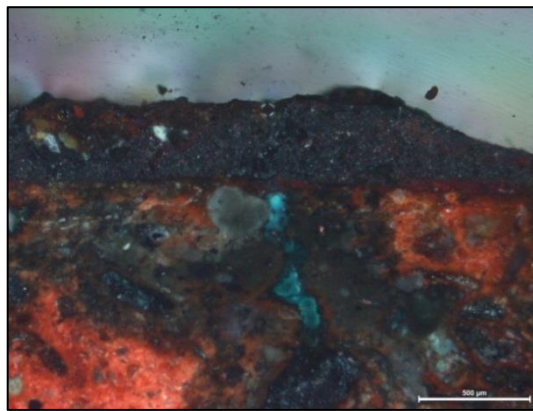


Figure 7.33 Photomicrograph of sample 720-6879 cross section showing the purple-coloured layer on the surface of the ceramic under cross-polarized light.



Figure 7.34 Photograph of sample 21-6838 with the black layer on the inner surface.

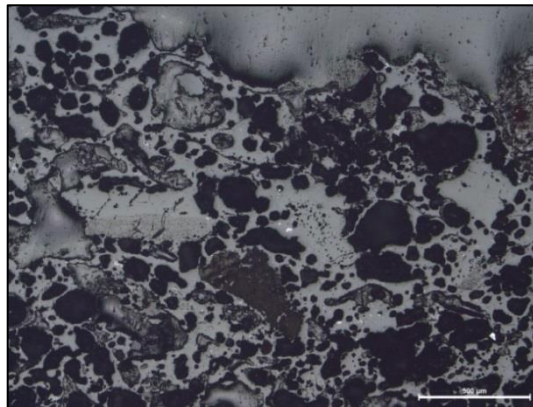


Figure 7.35 Photomicrograph of sample 21-6838 cross section showing the black layer on the surface of the ceramic under plane-polarized light.

In all other cases, the discolourations consisted of a single layer resting directly on the ceramic body, although separated by a gap of up to 2µm in some places. The layers were thin and intermittent, ranging from a thickness of just 9µm in sample 819-7020 to 150µm in sample 720-6879. These were clearly not the result of very high temperatures as was

apparent from the distinctively cold contact with the underlying ceramic body (Figure 7.36). Some of the layers were slightly diffused into the ceramic fabric down to a depth of 1mm but those areas still did not show any evidence of bloating or heat alteration, suggesting that this was the result of post-depositional corrosion and the migration of ions to fill porosities within the ceramics. The layers themselves were always quite porous and in one instance (sample 616-6922) several mineral inclusions were present within the layer itself (Figure 7.37).

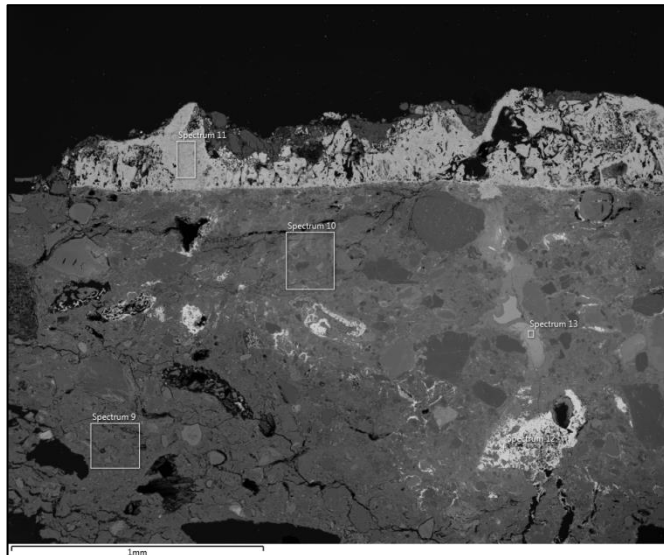


Figure 7.36 SEM Image of iron copper oxide layer on ceramic from sample 720-6879.

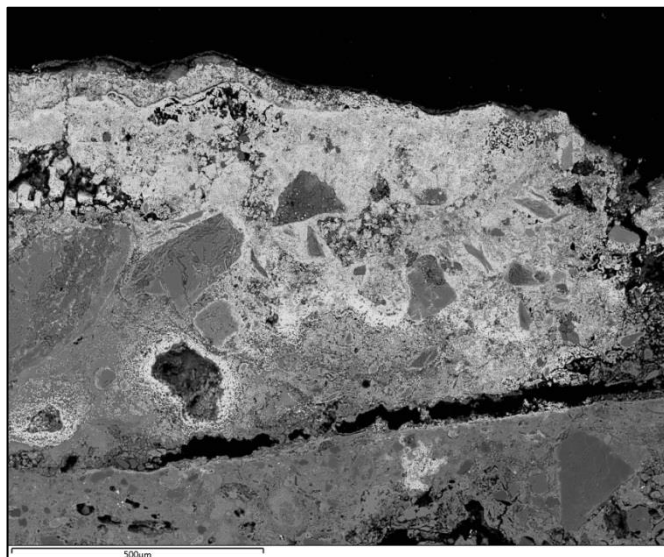


Figure 7.37 SEM image of mineral inclusions within the iron copper oxide layer from sample 616-6922. The ceramic, seen in the bottom of the frame, is entirely detached from the layer.

Compositionally, the layers can broadly be described as copper and iron oxides and hydroxides (Table 7.9) and quite distinct from the underlying ceramic fabrics (Table 7.10). Three samples have elevated Al_2O_3 and SiO_2 ; in two cases (228-6870 and 819-7020) this can be attributed to the fact that the layers are relatively thin ($9\mu\text{m}$ and $17\mu\text{m}$ respectively) and

to the difficulty in analysing such small areas with the SEM-EDS, while in the third case (616-6922) the layer is much less clearly defined and corrosion appears to have migrated into the ceramic to a greater extent than in other samples. In both cases, the reported composition is in part the result of the difficulty in analysing the layers without including the background ceramic rather than compositional reality. In contrast, the presence of MgO, K₂O, and TiO₂ in all of the samples cannot be caused by analytical influences from the ceramic since these elements do not correlate with the amount of Al₂O₃ or SiO₂ present. They are more likely to be present in the layers themselves, introduced either from soil contamination within porosities, or from the same source as the iron and copper.

Table 7.8 Composition of purple layer on surface of local domestic pottery as determined by SEM-EDS. Reported values are the mean of at least three area analyses normalized to 100%.

Sample	Na ₂ O	MgO	Al ₂ O ₃	SiO ₂	SO ₃	K ₂ O	CaO	TiO ₂	FeO	CuO
108-6857	ND	1.8	0.6	1.2	b.d.l.	0.1	0.2	0.3	69.3	27.8
147-6832	ND	b.d.l.	b.d.l.	0.4	b.d.l.	b.d.l.	0.1	b.d.l.	89.2	8.5
228-6870	ND	0.6	5.3	7.8	b.d.l.	0.3	0.3	1.2	36	47.7
616-6922	ND	2.3	4.4	7.1	0.3	0.2	0.4	0.5	73.6	14.4
720-5879	ND	2.1	b.d.l.	0.6	b.d.l.	b.d.l.	0.3	b.d.l.	70.3	26.7
819-7020	ND	2.7	5.3	11.2	0.3	0.4	0.5	0.8	45.1	32.3
Mean	ND	1.6	2.6	4.7	b.d.l.	0.2	0.3	0.5	63.9	26.3

Table 7.9 Composition of local domestic pottery fabrics which exhibited purple staining as determined by SEM-EDS. Reported values are the mean of at least three area analyses normalized to 100%.

Sample	Na ₂ O	MgO	Al ₂ O ₃	SiO ₂	SO ₃	K ₂ O	CaO	TiO ₂	FeO	CuO
108-6857	1.9	4.2	17.2	60.9	0.2	3.1	2.9	1	8.1	b.d.l.
147-6832	1.7	6.4	15.2	59.8	0	1.8	2.7	1.2	10.1	b.d.l.
228-6870	0.7	9.9	12.8	55.3	0.3	1.4	7.2	1.6	10.2	b.d.l.
616-6922	1.7	7.4	14.6	58.1	0.3	1.7	3.7	1.2	10.5	0.1
720-5879	1.8	6.5	15.7	58.1	0.2	1.8	3.7	1.4	10.2	b.d.l.
819-7020	0.8	10.1	12.5	53.2	0	1.1	10.5	1.5	9.9	b.d.l.
Mean	1.4	7.4	14.7	57.6	0.3	1.8	5.1	1.3	9.8	b.d.l.

The sulphur content of the layers proved to be much lower than first reported by the pXRF. Although it is possible that the sulphur was present only as loose secondary sulphosalts which were washed away during sample preparation, this would not have resulted the complete absence observed here, and it is much more reasonable to infer that the pXRF instrument was reporting false positives for such a light element.

In the samples where the layer was clearly defined and thick enough to exclude potential interference from the ceramic body (108-6857, 147-6832, 720-5879), iron and copper oxide accounted for more than 95% of the total weight of these layers. The only naturally occurring

secondary mineral close to these compositions is delafossite ($\text{CuFe}^{3+}\text{O}_2$) which generally forms as well defined black tabular crystals found in association with iron and copper minerals. These have also been known to occur in anthropogenically formed glass and slag, typically crystallizing as needle-like structures from glassy matrices containing sufficient copper oxide during cooling (Radivojević et al. 2010). This crystalline microstructure appears in only one sample (228-6870) and is mainly concentrated within the ceramic porosities where tiny crystals, measuring approximately 1-2 μm in length, evidently grew as secondary corrosion (Figure 7.38). In every other sample, the layers appear as botryoidal masses typical of haematite and malachite crystal growth patterns.

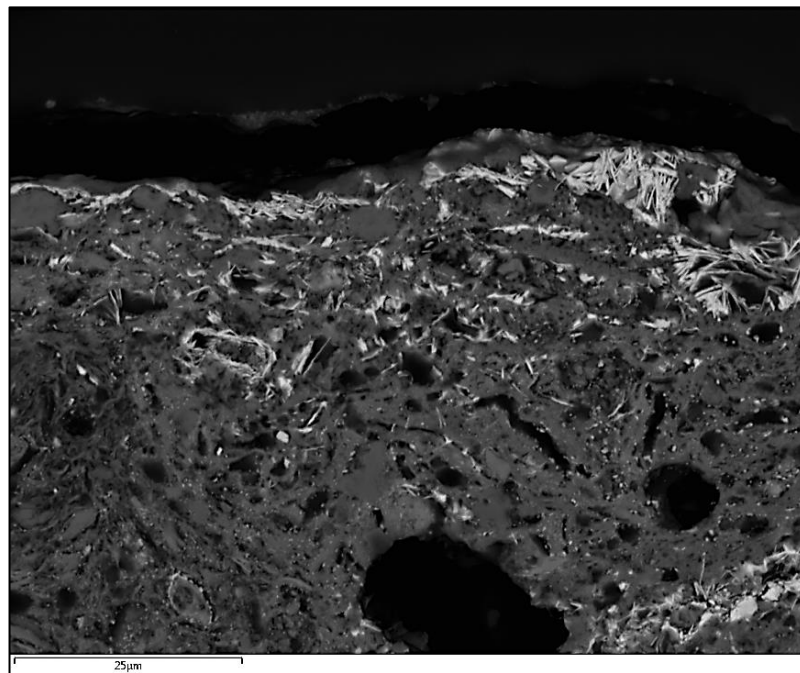


Figure 7.38 SEM image of sample 228-6870 showing the needle-like delafossite crystals present in ceramic porosities and in crevasses on the surface.

It is the origin of the iron and copper oxide which is the main point of interest in this instance. As there is little mention of such features in the archaeological literature, assessing what created these mineral layers is problematic and requires the elimination of several possibilities.

On the one hand the layers could be caused by natural post-depositional processes such as the leaching of such elements in the soil and their deposition as hydroxides on the surface of the ceramic, or from the formation of secondary minerals from the corrosion of elements within or next to the objects. Distinguishing between these is important because, in the latter case, the hydroxides may reflect culturally driven choices made in the production of the

pottery (i.e. temper or clay source) or in its discard while the former may simply reflect naturally occurring elements in the surrounding soil.

Alternatively, the layers may be entirely anthropogenic and could be directly representative of a human process such as copper smelting or the storage of raw materials.

Leaching from soil is perhaps the least likely to have formed the discolouration. These appear as discreet features on the surface of just a few ceramics at the site and not on the entire surface of every pot as would be expected from leaching. Iron itself is known to be very stable when well crystallized in clays and soils, and although some amorphous Fe^{3+} ions can be dissolved and leached in acidic solutions (Dousova et al. 2014), this cannot explain the limited localization of the iron-rich layers. Although only approximately 100ppm of copper could be detected in the soil (see the results of the pXRF analysis of the 'natural' soil in table 7.7 in section 7.1.3 and Appendix B.2), copper ions tend to be highly mobile and susceptible to leaching, which could account for the concentration of the elements in the levels observed here (8-48 wt% CuO), but again the very limited extent of staining makes this unlikely.

For the same reasons, the copper-iron oxide layers are unlikely to have formed from corrosion processes of the ceramics themselves. In addition to ceramic being a largely stable material, the Çamlıbel pottery fabrics contain very little to no copper (<0.1 wt%) and relatively little iron (~10 wt%).

This leaves the two previously mentioned probable sources for the iron and copper oxides deposited on the ceramics: the formation of corrosion from natural processes from iron and copper rich material directly abutting the ceramics post-depositionally, or, alternatively, originating from culturally-derived processes.

The lack of visible heat alteration in the ceramics immediately below the layers seems to suggest that they were not the result of a high temperature metallurgical operation such as smelting or melting, and are rather more likely to be formed through lengthy process of oxidation and corrosion. However, the exposure of these ceramics to material high in copper and iron is most probably the result of an association with metallurgical activities more generally. Whether this is simply from chance discard in a courtyard where slag and ore minerals were also disposed of, or whether it is something more intentional has several implications which will be further discussed in chapter 9.

7.1.5 Ores and Tailings

The assemblage of metallurgical finds at Çamlıbel includes several fragments of what appear to be iron and copper rich minerals, mostly found in the earlier occupations of the site (see section 7.1.1). These were first identified in the field based upon their red, yellow, and green coloured surfaces (Figure 7.39), which contrasted strongly with the site's geology (Schoop, pers. com.) and which were catalogued as the remains of ores processed on site. A total of 127 fragments of minerals were recovered from the site. About half of these showed evidence of green oxidation suggesting significant copper content (n=62). The minerals were usually quite small, ranging from less than 1 cm³ up to a maximum of 10 cm³. Thirteen random fragments were made available for sampling and analysis for this thesis in addition to a large mineral fragment recovered from a copper-bearing mineral outcrop near Karakaya, 2km upstream from Çamlıbel (Marsh 2010).

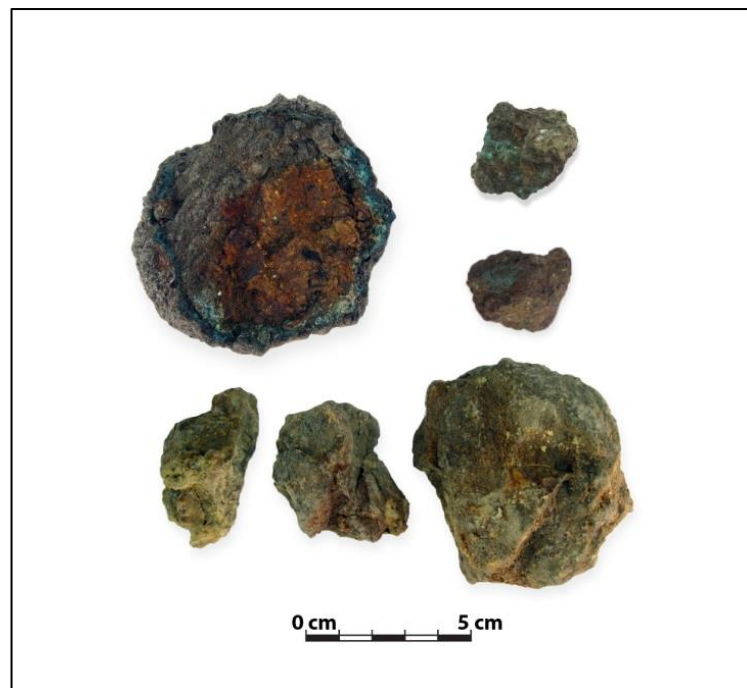


Figure 7.39 Photograph of various mineral fragments recovered from the site presumed to have been intended to be used as ores.

Microscopic analysis of these samples revealed some patterns in the types of minerals in use at Çamlıbel. Five fragments (934-5409, 799-5218, 637-4221B, 637-4222, and 637-4218) consisted of highly degraded minerals of mixed sulphide and iron silicates with frequent inclusions of pyrite and a few rare chalcopyrite mineralizations (Figures 7.40 and 7.41). These tended to be found in the later phases of the site (CBT III and IV). Notably, a small inclusion of sphalerite ((Zn,Fe)S) was observed in one sample (799-5218), which is consistent with the presence of traces of zinc in some of the slags (see copper smelting slags in section 7.1.6).

This comes as no surprise as these sulphide minerals are typically encountered in association with pyrite and other sulphide deposits.

Another four samples (257-3130, 753-5028, 585-4328A, and 585-4328B) could be grouped together as they are formed mostly of iron hydroxides with occasional pyrite and chalcopyrite inclusions (Figures 7.40-7.43). Sample 257-3130 is interesting in that it is essentially a solid 1 cm³ fragment of weathered pyrite with corrosion still maintaining the mineral's cubic crystal microstructure (Figure 7.44). One of these samples, 585-4358B, also contains large magnesium silicate crystals with iron oxide inclusions (Figure 7.45), a feature common of metamorphosed serpentinite. Most of these iron rich minerals appear to have been concentrated in the earliest levels of the site (CBT I and II).



Figure 7.40 SEM image of sample 799-5409. The bright grey angular crystals are chalcopyrite surrounded by light grey corrosion in a dark grey quartz matrix.

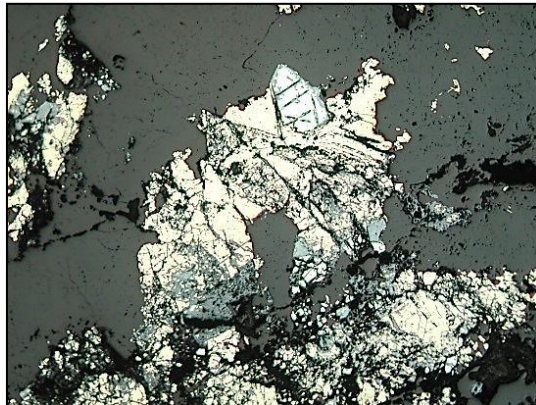


Figure 7.41 Photomicrograph of sample 637-4218 showing a mixture of pyrite (white) and chalcopyrite (yellow) in a quartz matrix (grey).



Figure 7.42 Photomicrograph of sample 585-4328A showing a network of elongated iron hydroxide crystals.



Figure 7.43 Photomicrograph of sample 753-5028 with both magnetite and iron hydroxides within the porosities.



Figure 7.44 Photomicrograph of sample 257-3130. The bright whitish phases are the remaining chalcopyrite crystals surrounded by corrosion. Entirely missing are the pyrite crystals which have largely corroded to iron oxides, leaving behind only the crystalline structure.

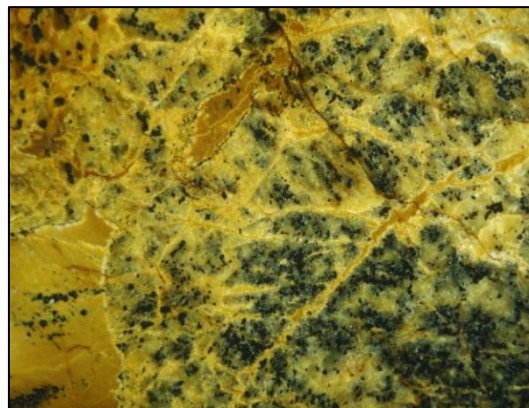


Figure 7.45 Photomicrograph of sample 585-4328B. The black inclusions are iron oxides in a magnesium iron silicate matrix.

Samples 877-5695 and 838-4870 (from CBT I and II respectively) consist of highly weathered chlorite minerals, both of which contain frequent remnants of oxidized pyrite inclusions.

While sample 838-4870 is the typical green colour commonly seen in much of this group of minerals (Figure 7.46), 877-5695 is yellowish brown (Figure 7.47), suggesting higher iron content. Chlorite minerals are largely expected from the surrounding ophiolitic geology as they tend to form in a wide range of metamorphic contexts. They may well have been associated with any copper ore deposit in the area, but despite their green colour they are not copper-bearing minerals themselves.

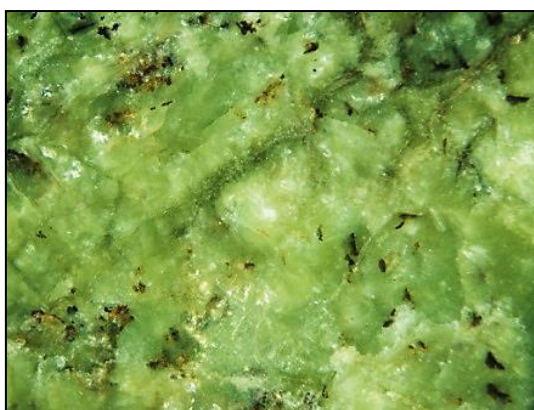


Figure 7.46 Photomicrograph of sample 838-4870. The matrix is composed of fibrous magnesium silicate serpentinite but contains some rare chromite and iron sulphide minerals. No copper mineralizations were observed, although SEM-EDS analysis showed up to 2 wt% of copper present in the matrix.

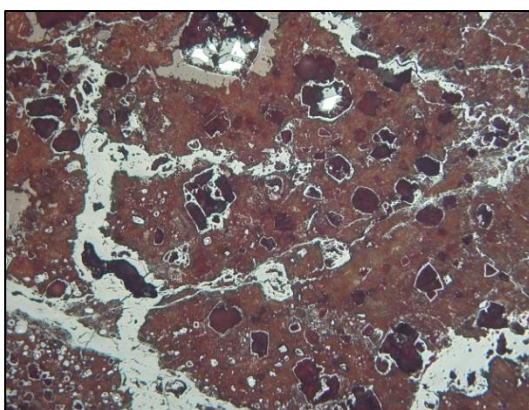


Figure 7.47 Photomicrograph of sample 877-5695. The reddish matrix is plausibly clinocllore while the weathered cubic inclusions are the remains of pyrite crystals. The bright phases in the top centre of the frame are examples of the few pyrite crystals remaining. The grey veins are magnetite corrosion.

The last two samples are very different than the rest and are suggestive of some form of ore processing being undertaken on site. Sample 727-4659 was found to be extremely fragmentary and appears to be mostly composed of crushed angular grains of chlorite, ranging between 20 μm and 200 μm , with frequent pyrite, chromite, and chalcopyrite mineral inclusions (Figures 7.48 and 7.49). This conglomerate texture and microstructure is suggestive of ore beneficiation processes where minerals are crushed and sorted to remove the metal bearing fraction and left to corrode and sinter post-depositionally.

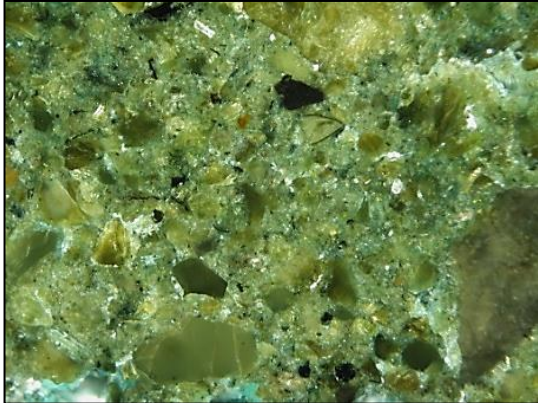


Figure 7.48 Photomicrograph of sample 727-4659 showing crushed agglomerated minerals sintered by corrosion.

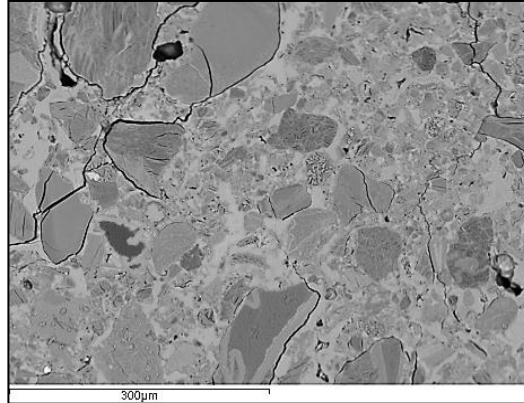


Figure 7.49 SEM image of sample 727-4659. The interstitial area is copper and iron oxide corrosion binding the angular grains together.

Under the microscope, the last sample (619-3497) proved to be composed of highly weathered iron hydroxides but with the remains of a network of magnetite crystals (Figure 7.50). These crystals take either the shape of long thin intermittent finger-like structures, or of globular petal-shaped crystals resembling blobs of ink (Figure 7.51). The long thin finger-like crystals of magnetite are known to form as oxidizing high temperature solid solutions (HSS) from pyrite and chalcopyrite. They indicate that the temperature was not elevated enough for the copper sulphide to have fully dissolved or liquefied, but that a strong oxidizing atmosphere was present which was in the process of removing much of the sulphur. This type of microstructure, although highly corroded here, is common when iron and copper sulphide minerals are exposed to an open fire (Bachmann 1982, 23). Although a single specimen is certainly not strong evidence, but it is plausible that this represents a conscious attempt at roasting the ores prior to smelting.



Figure 7.50 Photomicrograph of sample 619-3497 showing the original pyrite and chalcopyrite mineral microstructure. The pinkish colours are chalcopyrite while the grey is iron silicate and the light grey is magnetite. Orange iron hydroxides can be seen throughout where the mineral has weathered post-depositionally.

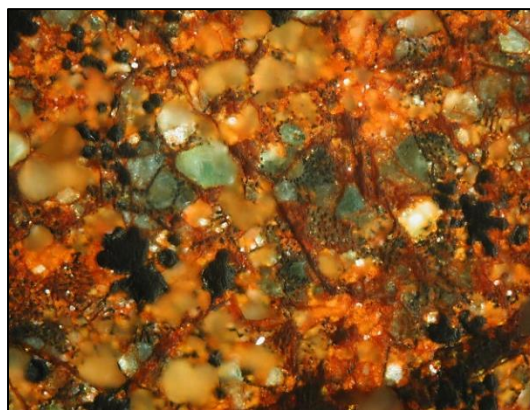


Figure 7.51 Photomicrograph of sample 619-3497. The majority of the sample consisted of this type of microstructure showing a wide range of weathering products. Just visible are the network of highly stable magnetite 'fingers' and the dark grey inkblot blebs of what appear to be wüstite.

Chemical analysis reflects the heterogeneity of the microstructures of these minerals, and although the compositions reported here are more or less in agreement with the groupings identified using optical microscopy, the results show a high degree of variability within each group (Table 7.11). The lack of clear trends in the data is likely caused by the low sample count. Given that the sampling was random, they should nevertheless be roughly representative of the full gamut of mineral types found within the assemblage, even if the results do not accurately reflect their distribution across the site.

Table 7.10 Bulk Composition of minerals recovered from Çamlıbel as determined by SEM-EDS. Results are the average of at least three area analyses taken at 100X magnification and presented in wt%.

Sample	Phase	Na ₂ O	MgO	Al ₂ O ₃	SiO ₂	P ₂ O ₅	SO ₃	K ₂ O	CaO	TiO ₂	Cr ₂ O ₃	MnO	FeO	CuO	As ₂ O ₃
934-5409	CBT I	b.d.l.	b.d.l.	b.d.l.	15.6	b.d.l.	29.6	7.6	b.d.l.	b.d.l.	b.d.l.	b.d.l.	47.2	b.d.l.	b.d.l.
257-3130	CBT I	b.d.l.	0.2	b.d.l.	6.4	b.d.l.	4.2	0.9	0.5	b.d.l.	b.d.l.	0.2	84.1	3.7	b.d.l.
877-5695	CBT I	2.2	5.4	12.1	33.2	0.4	0.7	1.8	0.6	2.1	b.d.l.	b.d.l.	41.5	b.d.l.	b.d.l.
753-5028	CBT II	b.d.l.	5.1	b.d.l.	11.8	b.d.l.	b.d.l.	b.d.l.	b.d.l.	b.d.l.	b.d.l.	b.d.l.	83.1	b.d.l.	b.d.l.
838-4870	CBT II	b.d.l.	33.3	1.9	48.5	b.d.l.	b.d.l.	b.d.l.	0.4	b.d.l.	0.7	0.2	13.2	1.9	b.d.l.
585-4328A	CBT II	b.d.l.	0.8	b.d.l.	6.7	0.4	0.5	b.d.l.	1.4	b.d.l.	b.d.l.	0.3	89.5	0.5	b.d.l.
585-4328B	CBT II	b.d.l.	7.3	0.2	17.8	0.4	0.4	b.d.l.	0.7	b.d.l.	0.5	b.d.l.	72.5	0.3	b.d.l.
727-4659	CBT III / SPEU	b.d.l.	13.3	6.9	49.7	b.d.l.	b.d.l.	0.5	5.3	1.3	b.d.l.	b.d.l.	8.8	14.2	b.d.l.
799-5218	SPEU	b.d.l.	b.d.l.	3.1	41.2	b.d.l.	21.1	5.6	1.3	b.d.l.	b.d.l.	b.d.l.	27.8	b.d.l.	b.d.l.
637-4218	CBT IV	b.d.l.	1.0	2.1	77.1	b.d.l.	4.7	b.d.l.	0.2	0.2	b.d.l.	b.d.l.	11.9	2.8	b.d.l.
619-3497	CBT IV	b.d.l.	b.d.l.	0.4	6.1	0.1	0.9	0.1	0.5	b.d.l.	b.d.l.	b.d.l.	70.1	21.9	b.d.l.
637-4221B	CBT IV	b.d.l.	b.d.l.	0.1	39.6	b.d.l.	9.9	b.d.l.	0.2	b.d.l.	b.d.l.	b.d.l.	41.2	8.9	b.d.l.
637-4222	CBT IV	b.d.l.	3.6	7.2	43.7	b.d.l.	6.9	b.d.l.	b.d.l.	1.4	b.d.l.	0.6	33.1	3.9	b.d.l.

Despite this caveat, it can be tentatively stated that minerals recovered from the earlier periods of CBT I and II tend to be ultramafic rocks high in iron and magnesium and poor in copper (mean of 1.6 wt%), while later periods were dominated by silica rich sulphide minerals with a higher copper content (mean of 11.9 wt%) in the form of chalcopyrite. This distinction can be seen in the ratio of $\text{SiO}_2:\text{FeO}+\text{MgO}$ which demonstrates a slight chronological divide, with the exception of sample 619-3497 from CBT IV which consists of a fragment of possibly roasted ore (Figure 7.52).

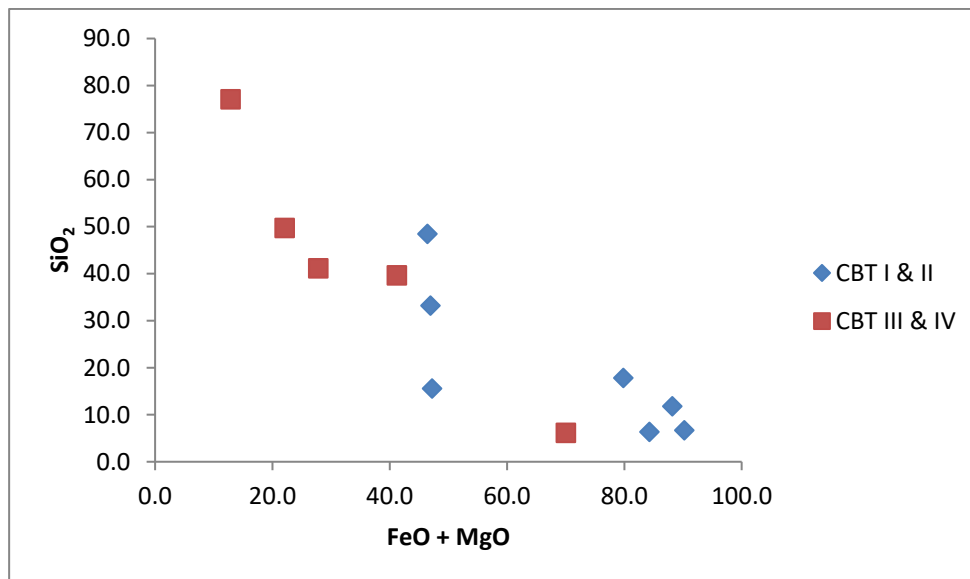


Figure 7.52 Scatterplot showing the main two chronological groupings of mineral types recovered from Çamlıbel.

Although the two broad categories appear separated chronologically, it should be mentioned that in either cases the compositions of the minerals are either too rich in silica or in iron and magnesium to form fully liquid slag at temperatures attainable during the Chalcolithic. As such, mechanical separation of copper through differential density would not have been possible without the addition of some flux. That being said, the combination of both of these mineral types together would form a composition which approaches the fayalite eutectic (2:1 Me:Si). However, given the distribution of these minerals across distinct occupation phases, there is little evidence to show that they were indeed mixed. Furthermore, these results do not reflect the composition of the slag reported in the next section, which contain much higher amounts of calcium oxide, which is notably low in these mineral samples.

The copper content is also problematic when describing these as ores. Most samples, with the exception of 619-3497 (21.9 wt% Cu), 727-4659 (14.2 wt% Cu), and perhaps 637-4221B (8.9 wt% Cu) contain too little copper to have been economically recoverable by Late Chalcolithic extraction technology. As will be discussed in the next section, the slags

themselves retained significant amounts of copper (3.6 wt% mean, and rarely less than 1 wt%). As such, an ore would need to contain significantly more than 3% copper in order to be viably extractable, and therefore most of the minerals presented here cannot be considered ores according to the modern definition of the term. Given that they were transported to the site by human agency, that they do contain some copper, and are generally associated with metallurgical debris, most of these samples are best described as discarded tailings from the removal of gangue minerals during beneficiation to concentrate the copper minerals before the smelt.

In contrast, sample 727-4659 represents the likely intended product of such operations, being a conglomerate of crushed copper-rich particles mixed with a variety of gangue minerals. Similarly, the most elevated copper content analysed was found in the highly heat altered pyrite and chalcopyrite of sample 619-3497, which should therefore be also considered an ore, albeit already processed by roasting.

The chemical analysis of the material confirms that the minerals are generally sulphidic and ultramafic, which comes as no surprise in a landscape dominated by ophiolitic serpentinite ridges. These geological formations are commonly associated with copper mineralizations, such as is the case in the famous Troodos Mountains of Cyprus, and the minerals recovered from Çamlıbel were most likely sourced from the immediately surrounding area.

The copper mineral source identified near Karakaya has therefore also been analysed in the hopes of confirming the nature of the copper sources exploited at Çamlıbel. The outcrop consists of an isolated extrusion of iron sulphide, roughly 2m in diameter, eroding from a serpentinitic ridge (Figure 7.53). It is composed of a yellowish orange core with weathered bands of iron and copper hydroxides (Figure 7.54). Sampling of this mineral source was predominantly concerned with the green oxide formation and it was therefore the focus of the analysis. The matrix was found to be mostly composed of a mixture of serpentinite and iron hydroxides. Chromite crystals (FeCr_2O_4) surrounded by shells of magnetite corrosion as well as a few crystals of phosphate rare earth compounds between the composition of monazite-(Ce) and monazite-(La) were also identified throughout the sample. A few isolated pyrite and chalcopyrite minerals were also observed (Figure 7.55), which may suggest that some parts of the outcrop may be richer in copper than this particular sample. Spot analyses of some of these chalcopyrite phases showed the presence of minor amounts of zinc, although no zinc minerals such as sphalerite were observed.



Figure 7.53 Photograph of the iron and copper sulphide extrusion from a serpentinitic ridge (photograph courtesy of Ulf-Dietrich Schoop).

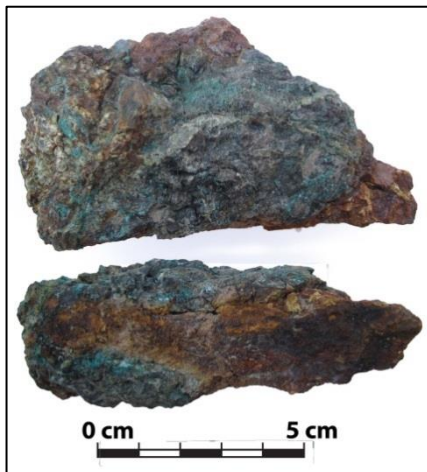


Figure 7.54 Photograph of the Karakaya ore sample.

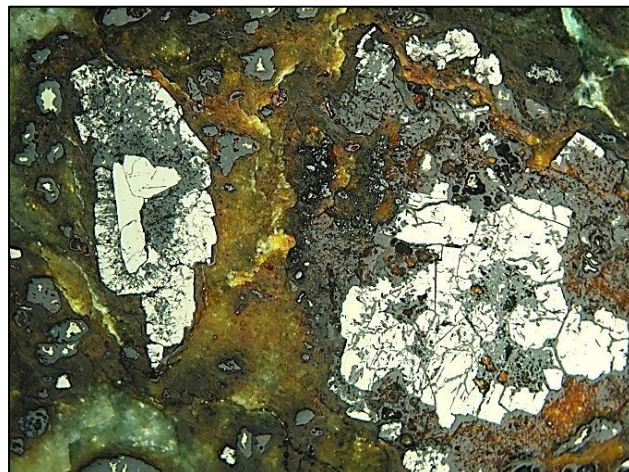


Figure 7.55 Photomicrograph of the ore outcrop sample. The bright phases are mixtures of chalcopyrite and pyrite surrounded by grey and yellow corrosion. The majority of the matrix is composed of magnesium iron silicate.

Bulk analysis (Table 7.12) demonstrated an expectedly low copper content of just 1.7 wt%, once again too low to be efficiently extracted by available techniques of the time. The composition of the Karakaya source was found to be very similar to that of at least one of the minerals recovered from Çamlıbel (838-487), although the aluminium content is significantly higher in this case.

The lack of a clear relationship between the composition of this sample and those from Çamlıbel certainly puts in question whether this type of deposit was indeed exploited at the time, however this likely reflects the fact that only one sample was taken from a single

outcrop, which is entirely too limited to characterize a geological deposit. Lead isotope data, which will be discussed further in chapter 8, was also inconclusive in attempting to tie this deposit to the minerals and slag from Çamlıbel due to the near complete absence of lead in the sample.

Table 7.11 Bulk composition of minerals recovered from Karakaya outcrop as determined by four area analyses at 100X magnification by SEM-EDS.

	MgO	Al ₂ O ₃	SiO ₂	SO ₃	Cl	CaO	TiO ₂	Cr ₂ O ₃	MnO	FeO	CuO	As ₂ O ₃
Karakaya outcrop	28.7	12.2	41	b.d.l.	b.d.l.	b.d.l.	0.6	0.2	b.d.l.	15.6	1.7	b.d.l.

7.1.6 Slag

Slag cakes and slag fragments form the bulk of Çamlıbel's metallurgical assemblage and also contain the most informative clues towards the reconstruction of the extractive process. As such, this section will thoroughly describe the full assemblage recovered from the site macroscopically as well as the analysis of the 39 samples of slag and related material exported for further study.

Most of the slag, although highly variable, will be described as a single group of samples since no compositional or typological patterns could be identified which clearly defined separate clusters amongst them. Regardless of the wide range of morphologies and compositions of these samples, they can all be broadly categorized as smelting slag and will therefore be presented together. Their macroscopic descriptions will focus on the characteristic of the few complete slag specimens recovered from the site. This data will include samples measured, weighed, and photographed during fieldwork conducted in 2013 to discern any general morphological patterns in their distribution and compare this to their archaeological and chronological contexts. Macroscopic descriptions of the slag will thus include information obtained from samples which were unavailable for more in-depth microscopic and chemical study.

Microscopic descriptions of exported samples will cover the entire spectrum of crystalline phases present in the majority of the available assemblage of slag. Special attention will be paid to sulphide and metallic phases as they are most relevant when discussing the intended smelting products. Individual samples will only be discussed when specific features relate to only a small subset of the main slag assemblage which highlight specific aspects of the smelting process.

This will be followed by a discussion of the bulk chemical composition of these slags to once again assess the presence of trends in the data. Bulk compositions will also be used to gauge

thermodynamic conditions of the smelts as well as to relate the slags to their original ore charges.

In addition to this main category encompassing the majority of the slag assemblage, four samples will be discussed in two separate groups as they do not conform to the general morphology and composition of the rest. These results will be presented in the same order as that of the rest of the slag – macroscopically, microscopically, crystallographically, and chemically. Two samples of matte and two samples of arsenic-rich slag will thus be described separately from the rest. The matte will be useful in describing a waste or secondary product of the smelting process, while the arsenic-rich samples represent an entirely separate process and can best be described as crucible slags.

Copper smelting slag

Without those few notable exceptions, there is little to distinguish macroscopically between the majority of the various lumps and fragments of slag recovered from Çamlıbel. The main discerning factor seems to be the level of fragmentation of the slag, although this does not correlate with any microscopic or compositional differences. While most of the slag fragments were recovered as small crushed pieces of 1-10 cm³, at least ten specimens were identified as complete or nearly complete (Figure 7.56), which were of great help in assessing the slag's original morphology.

Overall they can be described as slag cakes with a flattened base and heterogeneous top surface. The bases are slightly convex and have sand and soil adhering to them, and therefore likely formed by rapid cooling on a rough surface. Their upper surfaces are heterogeneous and bubbly, with large fragments of unreacted gangue. No other features commonly seen in typical tapped slags could be observed, confirming the initial interpretation that the slags flowed from above (Rehren and Radivojević 2010) and were likely dumped onto the ground or other surface as a lump rather than a continuous flow. Many of the smaller fragments also have convex bases or heterogeneous surfaces, attesting that they were originally of the same shape as the complete specimens.

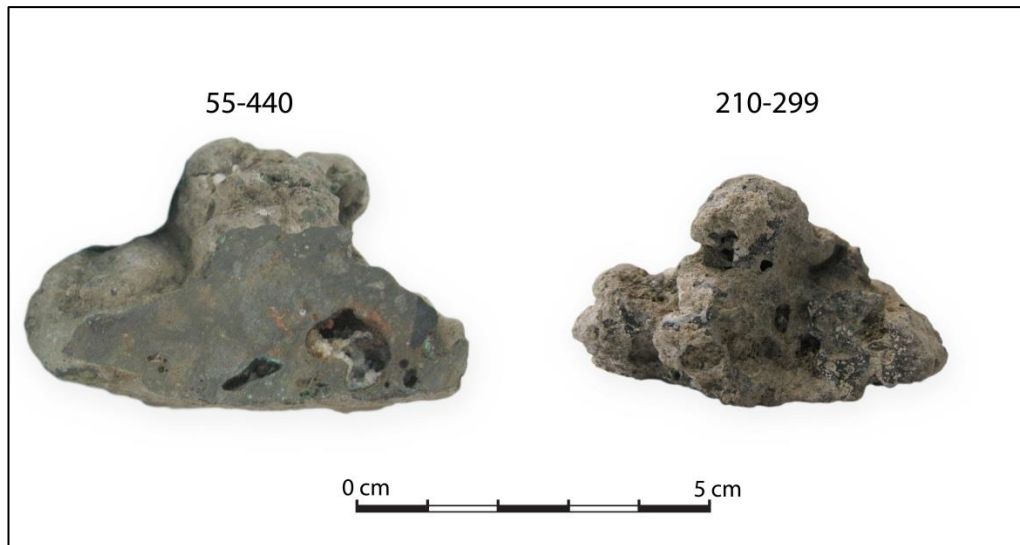


Figure 7.56 Photographs of two complete slag cakes with flat base and semi-molten upper area.

The slags are generally greyish brown in colour with copper oxide staining commonly present on the outside and dark grey in in cross section. Approximately a tenth of the slag assemblage had clear sulphide corrosion on the surface which suggests that sulphur was rarely completely removed and remained an important component of the smelting charge. In two fragments (60-3094 and 722-4629) the amount of sulphur was so extreme it is unlikely that copper metal could have been produced (Figure 7.57).

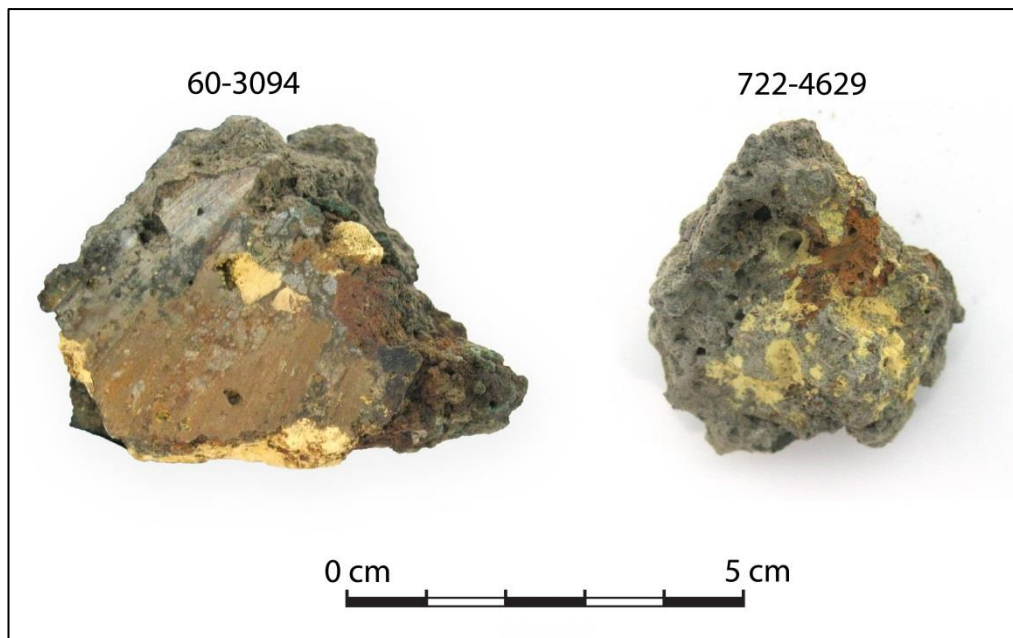


Figure 7.57 Samples 60-3094 and 722-7629 showing the formation and accumulation of iron sulphide corrosion.

The cakes are roughly circular in shape, have a diameter of 5-10 cm, are typically less than 5cm in height, and weight between 50 g and 200 g. Of the entire slag assemblage of 174 pieces (7098 g), 71 (4792 g) have clear evidence of having a flat base (41%). Furthermore,

those with identifiable bases also tend to be larger (mean 67.5 g) than amorphous fragments (mean 22.4 g) and are therefore responsible for a larger portion of the total weight of slag for the site (68%). Although this size range is well within the limits of what could be produced within bowl furnaces, their characteristic shape indicates that they likely formed in crucibles which could be emptied while hot. It is therefore unlikely that the small bowl hearths found throughout the site could have produced them without the added use of crucibles (see section 7.1.3). The slags do not appear to have been fully molten but rather achieved only a highly viscous and heterogeneous state during smelting.

The macroscopic appearance of these fragments is well in line with the typical appearance of Chalcolithic slags in general. These are usually defined as highly viscous, partially fused material which contains frequent remains of incompletely reacted minerals and large numerous millimetre-sized metallic copper prills resulting in relatively high copper content (Bachmann 1980; Palmieri et al. 1992).

It is worth noting that in no instance was the negative impression of a regulus observed on any of the slag bases. Such a feature would be expected should the metal have fully separated into a solid metal or matte ingot below the slag (Figure 7.58). That it did not suggests that either the slag solidified into these shapes after having been mechanically separated from the product (such as by tapping or scraping the slag off), or that the copper remained trapped as prills which had to be extracted by manual crushing and sorting due to the overly viscous nature of the semi-liquid slag. Since no evidence for the former of these two exists and because most of the recovered slag appears to have been crushed and processed, the latter of the two explanations seems to be the most plausible. The presence of a flattened base is in agreement with this since it appears to have rested directly on a hard surface rather than on a bed of solid material which could have allowed the metal or matte to flow away from the slag without forming the characteristic negative impression below the slag.

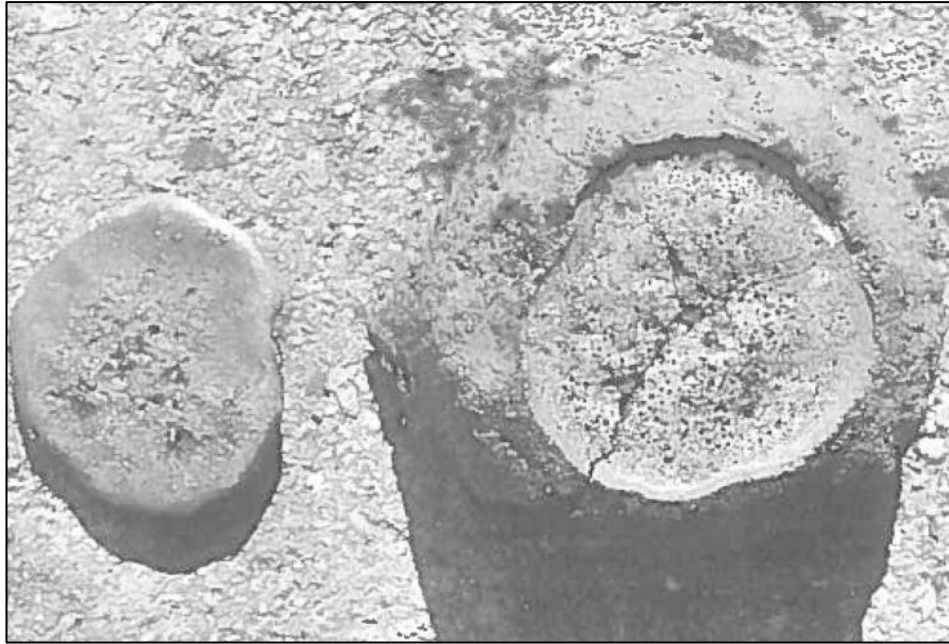


Figure 7.58 Photograph of experimental copper oxide smelting products (Bamberger and Wincierz 1990, 133). Note the ingot on the left with its slightly curved upper surface and the inverted imprint on the base of the slag cake on the right with upraised meniscus caused by surface tension.

In all instances the samples contain frequent porosities ranging in size from 5 μm to 50 μm , with the occasional larger voids measuring up to 1cm in size. Slag porosity is known to be largely caused by the formation and entrapment of gases caused both by the oxidation of some elements and the reduction of volatile transition elements such as arsenic. In addition to being dependent on atmospheric conditions which are responsible for the production of gases, the amount of porosity is also directly dependent on the viscosity of the slag.

In fragments that could be orientated by the presence of a base, a clear difference in microstructure could be distinguished between the top and bottom areas. In such cases, the top areas were typified by large fragments of incompletely molten gangue minerals while the bases were usually much more homogenized and composed of fully formed silicate crystals in a microcrystalline matrix. This is caused by less than optimal charge compositions and non-equilibrium conditions which prevented the slag from being fully molten. The denser and more liquid slag invariably flowed down while the lighter, semi-molten or incompletely dissolved mineral fragments remained floating on the upper surface. This has had the effect of creating much heterogeneity, not only between slag samples, but within each sample.

As such, a wide range of crystalline structures could be observed in many of the samples which are not commonly found in association with each other in later, more standardized smelting operations (Bachmann 1982). The strong localisation of diverse silicates within the slag is in part due to the highly variable mineral sources used by early smelters, but mostly

the result of the partially molten state of the slag where the compositions, temperatures, and free-oxygen pressures varied widely within the same smelt, something which comes as no surprise in this context. In essence, the heterogeneity observed here epitomizes the trial and error approach to smelting and its small scale, domestic nature commonly associated with Chalcolithic metallurgy.

Generally speaking, the microstructure of the samples tends to be dominated by the olivine group of minerals found in 35 of the analysed slags, with most samples containing either fayalite crystal chains (Fe_2SiO_4) ($n=12$; Figure 7.59) or crystals approaching the composition of forsterite (Mg_2SiO_4) ($n=15$; Figure 7.60), and in some instances, both ($n=6$). The majority of olivines were present as angular to sub-angular crystals, often exhibiting some coring with the center being closer to the ideal mineral composition of end-members and the outer edges enriched in Mg, Fe, or Ca depending on the overall bulk composition of the melt. In addition to these two main minerals present, many of the samples also contained significant calcium and can therefore be more accurately classified as belonging to the solid solution spectrum ranging between kirschsteinite ($\text{CaFe}^{2+}\text{SiO}_4$) ($n=9$; Figure 7.61) and monticellite (CaMgSiO_4) ($n=4$) end-members (Figure 7.60). These minerals reflect quite accurately geological specimens which are expected to be present in basic igneous rocks such as the ophiolites found around Çamlıbel.

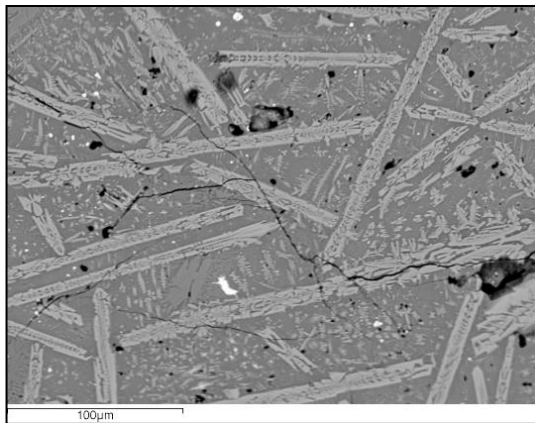


Figure 7.59 SEM image of sample 630-3866 showing both elongated skeletal chains of fayalite (light grey) and small feathery hedenbergite crystals (dark grey matrix). The bright prills are matte.

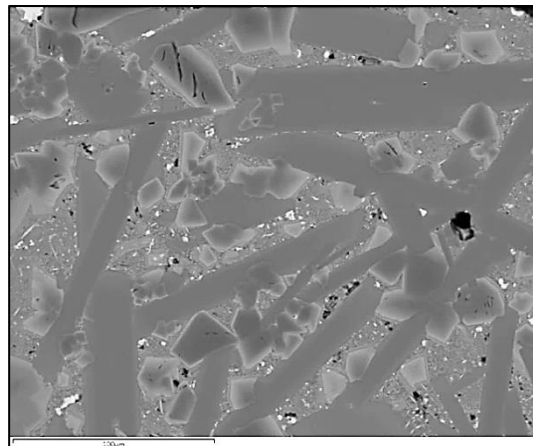


Figure 7.60 SEM image of sample 222-326A. The angular zoned polyhedral crystals are olivines approaching the composition of forsterite with an outer edge enriched in iron. The dark elongated crystals are calcium-rich monticellite and the small light grey blebs are magnetite. All of these phases lie within a microcrystalline matrix.

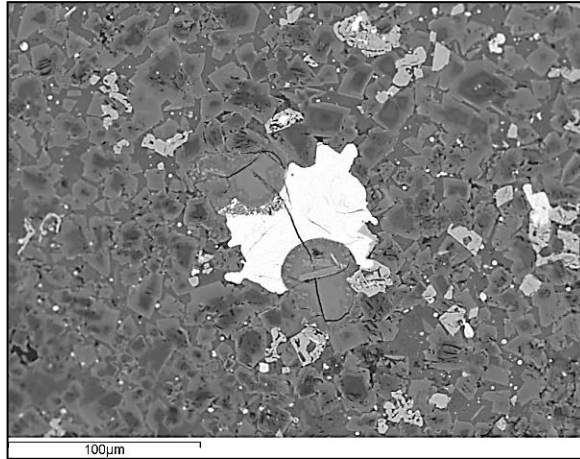


Figure 7.61 SEM image of sample 637-4456 showing a typical microstructure of dark grey cored kirschsteinite crystals within a glassy matrix. The bright prill in the centre is matte, with both iron and copper sulphide phases. Light grey sub-angular blebs are magnetite.

It should be mentioned that although the presence of silicon, iron, and magnesium and their relative ratios in each of these slags must have been introduced from the ore charge or originated with the inclusion of vitrified ceramic, it is probable that a significant proportion of the variability in calcium was rather related to the amount of fuel ash present in the system and thus a consequence of both the type of fuel used and of the duration of the smelt. As such, the presence of minerals enriched in calcium, such as those approaching the compositions of monticellite and kirschsteinite, may not reflect differences in the charge but rather in the smelting technology or technique.

In only three samples (561-3957, 722-4629, and 846-5515) were olivine group minerals entirely absent.

Approximately half of the slag samples ($n=22$) contained pyroxene group minerals in addition to the olivines, although generally occurring with lesser frequency. These tended to fall within the solid solution range between diopside ($\text{MgCaSi}_2\text{O}_6$) (Figure 7.62) and hedenbergite ($\text{FeCaSi}_2\text{O}_6$) (Figure 7.63) or falling within the broad composition spectrum of augite ($(\text{Ca},\text{Na})(\text{Mg},\text{Fe},\text{Al},\text{Ti})(\text{Si},\text{Al})_2\text{O}_6$) (Figures 7.63 and 7.65). These crystals appear angular and often show clear zoning on their outer edges where they are richer in iron.

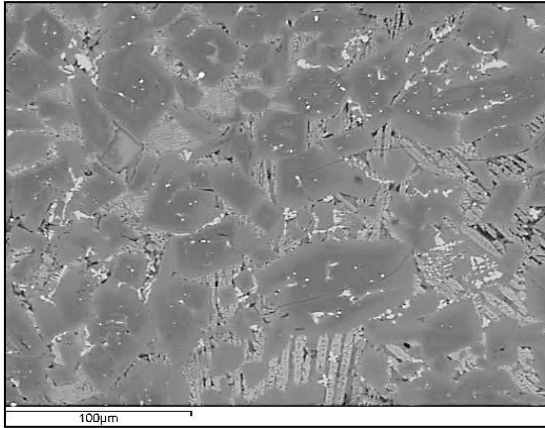


Figure 7.62 SEM image of sample 637-4225 showing a typical microstructure. The large dark angular cored crystals are diopside with light grey fayalite chains between the grains. The bright thin strings dispersed throughout are matte.

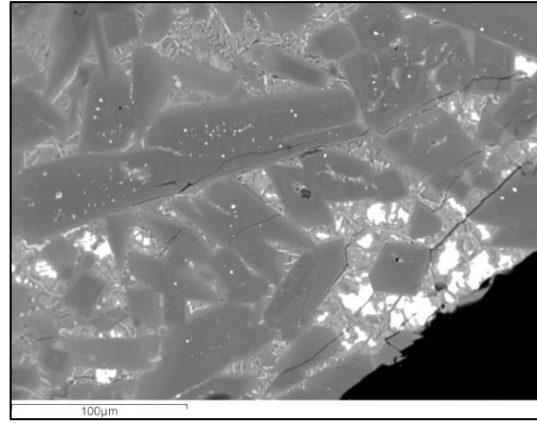


Figure 7.63 SEM image of sample 846-5515. The large dark angular crystals are hedenbergite while the small lath-like crystals between the grains are fayalite. The bright phases are HSS of copper and iron sulphide and matte prills.

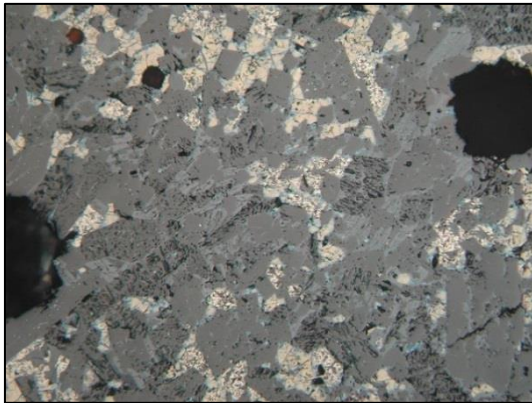


Figure 7.64 Photomicrograph of sample 210-299 at 200X magnification. The dark grey angular crystals, half of which exhibit planar fracturing, are pyroxenes within the solid solution range of augite. The light grey crystal chains between them are the olivine fayalite, while the pink, blue, and yellow phases are solid solutions of copper and iron sulphide. Frame is 0.6mm wide.

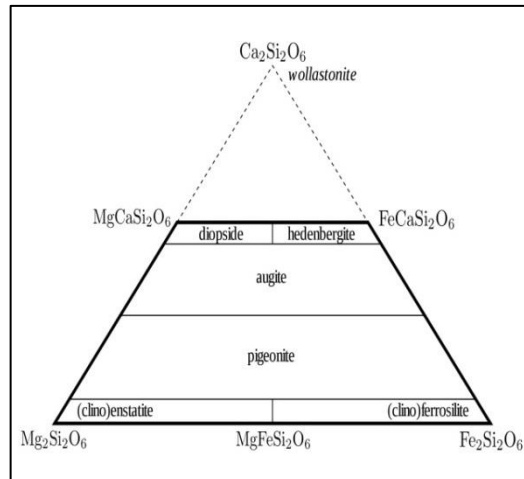


Figure 7.65 Diagram of pyroxene end-members.

These common crystalline phases are useful when trying to determine the operating temperatures reached by the smelting operations as they act as markers since they only form and remain stable under specific atmospheric conditions. For example, pyroxenes are known to crystallize at 1150 °C to form minerals in the augite range (Huebner and Turnock 1980), while hedenbergite is only stable subsolidus at temperatures below 980 °C (Schreiner et al. 2003).

The intergranular matrix of all slag samples was composed of the full spectrum of micro- to cryptocrystalline, usually too minute to be analysed by scanning electron microscope, giving them the appearance of glass. Area analyses of these phases revealed them to be generally composed of silicates with varying ratios of Ca-Mg-Fe.

In addition to the more typical crystalline structures, some outlier minerals were observed in a few samples, such as anorthite ($\text{CaAl}_2\text{Si}_2\text{O}_8$) in two samples (Figure 7.66), and occasional occurrences of barites/celestine ($\text{BaSO}_4/\text{SrSO}_4$; Figure 7.67). Chromite ($\text{Fe}^{2+}\text{Cr}_2\text{O}_4$) crystals were also occasionally present in small quantity, as were rare earths.

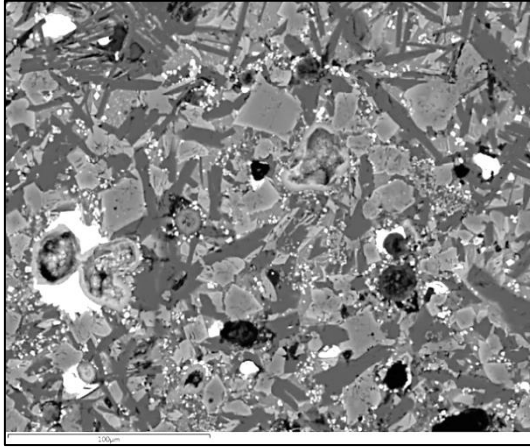


Figure 7.66 SEM image of sample 443-3708 showing dark rectilinear anorthite and grey angular olivine crystals in a microcrystalline matrix. Bright prills are copper-iron sulphides.



Figure 7.67 SEM image of sample 890-5774 showing elongated lath-like barite/celestine crystals growing within a cavity. The surrounding matrix is composed of dark grey fayalite and light grey magnetite.

Almost every specimen contained large amounts of magnetite spinels present in clusters throughout the matrix (Figure 7.68) and as skins on the outside surfaces (Figure 7.69), which testifies to the only lightly reducing atmospheric conditions present in most of the slags, and to the contact of the slag to ambient air while still hot. Furthermore, there is a strong correlation between the presence of magnetite and that of metallic copper prills. Spinel is known to generally increase slag's viscosity, thus preventing the formation of large copper prills, and in so doing inversely affect copper yields (Gilchrist 1989). However, since separation of slag and metal was never intended here, the formation of magnetite is not thought to have greatly affected the success of the extraction process.

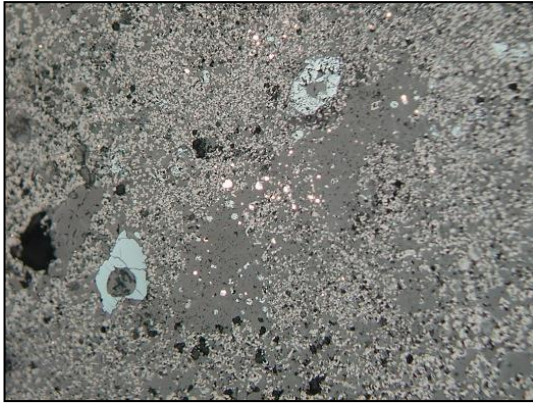


Figure 7.68 Photomicrograph of sample 890-5774 showing large quantity of magnetite spinels. Note the association with reddish copper metal prills in the centre and larger blue-grey covellite surrounding what may have been copper before corroding away. Frame is 1.8mm wide.

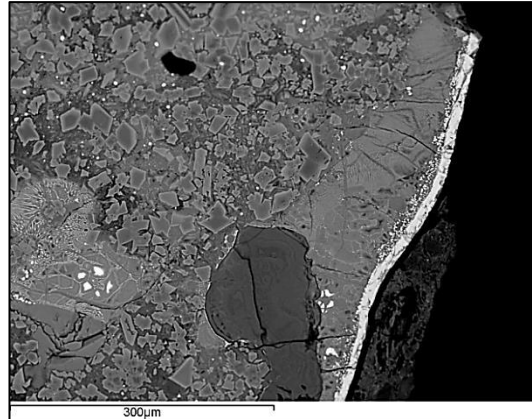


Figure 7.69 SEM image of sample 846-5528a. Note the thick magnetite skin on the surface. The cored angular crystals are diopside, the large dark bleb is incompletely reacted quartz, while the bright phases in the bottom left are the remnants of HSS in the process of dissolution.

The most striking features of the slag are high temperature solid solutions (HSS) of copper, iron, and sulphur in the process of reduction (Figures 7.70 and 7.71), present in all of the samples analysed. These phases are mainly composed of pyrrhotite (FeS) and covellite (CuS), but also bornite (Cu_5FeS_4) and chalcocite (Cu_2S), and more rarely, the original minerals chalcopyrite (CuFeS_2) and pyrite (FeS_2). They are often abutting large porosities caused by release of sulphur dioxide and other gases.

Although not ubiquitous to every sample or to every HSS bleb, many of the analysed sulphide phases revealed some minor component of nickel and, more rarely, of zinc in solution. This is in line with expectations as sulphides of both elements are geologically associated with iron and copper sulphide deposits, and particularly so in ultramafic rocks. Given the propensity of zinc to partition into the slag and for nickel to remain with the copper, the presence of both of them in the HSS phases confirms that these sulphides originated directly from the ore deposits and did not form secondarily in the melt.

Indeed, the various phases observed in the HSS commonly form from an original charge of chalcopyrite or other iron-copper sulphide minerals under mildly oxidizing atmospheres. The process involves first the formation of eutectoid magnetite 'fingers' at the grain boundaries and the consequent loss of iron from the sulphidic body at elevated temperature. In parallel to this reaction, a large portion of the sulphur is oxidized and escapes the melt as sulphur dioxide gas. However the removal of sulphur is rarely complete in the typically reducing conditions of a smelt. As the iron continues to be oxidized and dissolved into the surrounding iron silicate slag melt, the remaining phases are enriched in copper while maintaining roughly the same ratio of metal to sulphur. This process occurs unevenly and results in the

characteristic phases seen here when the reaction is interrupted during cooling. When the iron is allowed to be fully slagged, the remaining copper sulphides form discrete prills of matte typical of these and other prehistoric copper smelting slags. These can then be further reduced to copper metal in an oxidizing atmosphere or in the presence of copper oxides in a co-smelting operation.

That being said, these HSS phases described here are generally associated with rounded prills of copper sulphide, but rarely found in association with those fully reduced to copper metal. In fact, only about a quarter of the analysed slag samples contained identifiable metallic copper prills, which will be described in more detail below.

All in all, the consistent presence of HSS phases demonstrates that atmospheric conditions prevailing during smelting, although lightly reducing, did not contain enough free oxygen to fully remove the excess sulphur and may be largely responsible for the failure to produce copper in many instances observed here. That is not to say that copper was not being systematically produced at Çamlıbel, but only that most of the slag samples analysed here do not exhibit the elevated copper metal content typical of early smelting slag and that sulphur was commonly present in levels which drastically limited the copper yield.

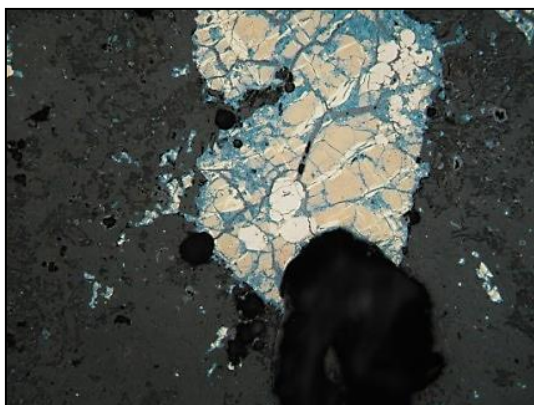


Figure 7.70 Photomicrograph of high temperature solid solution of covellite (blue), bornite (yellow), and pyrrhotite (bright yellow) in sample 836-4860. Frame is 0.9mm wide.



Figure 7.71 SEM image of sample 630-3865 showing the various phases of partially corroded HSS. The bright grey angular phases are pyrrhotite and covellite while the small fine finger-like structures at the grain boundaries are magnetite.

Continuing with the description of the main microstructural characteristic of the slags, eight samples, representing a fifth of the analysed slag, contained large pieces of semi-reacted quartz gangue throughout the matrix (Figures 7.72 and 7.73). The quartz remnants were usually fairly large and although some measured less than 50 μm , most were between 1 mm and 1 cm in size. They show the characteristic cracks and gas porosities of thermal damage

and often appear to have been in a partial state of dissolution into the surrounding melt at the moment of crystallization.

Four of the quartz-rich samples also contained large quantities of magnetite and metallic copper prills were observed in two of them. Olivines are the main crystalline component of these slags, with fayalitic chains present in five of them, kirschsteinite in two, and monticellite in a further two. Pyroxenes were present in four, but only in minor quantities. No correlation could be found between the presence of these large quartz particles and the surrounding slag microstructure.

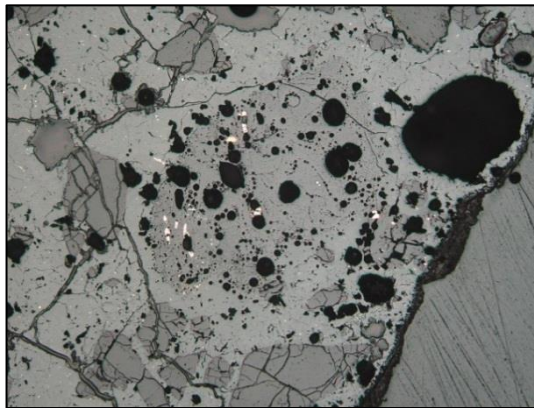


Figure 7.72 SEM image of sample 630-3866 showing the large incompletely reacted quartz fragments found throughout the sample, accounting for its high SiO₂ content.



Figure 7.73 SEM image of sample 222-326A. The large angular grey cracked crystals are quartz while the surrounding microcrystalline matrix is mainly composed of magnetite and olivines.

These quartz inclusions in the slags have been recognized in a variety of contexts and are usually described as ‘free silica slag’ (Hauptmann 2007, 167-169). These features are widely understood as the result of the addition of quartz to a charge, but the reasons for this are still debated. They have been interpreted in a variety of ways which include the intentional cooling of lead/silver smelting slags (Tylecote 1987) or the formation of a layer acting as a sieve to facilitate liquefaction (Lutz et al. 1994). However, the inconsistency of the presence of such inclusions at Çamlıbel and the clear absence of a fully molten slag means that these are unlikely to have been added to optimize the formation or handling of the slag, which are rather recent technical innovations.

Bulk analysis revealed that many of the samples containing quartz fragments were generally too rich in silica (>50wt% SiO₂) to form a fully molten slag and could never have been entirely liquid at temperatures typical in Chalcolithic furnaces of less than 1200 °C. Although it does not fully describe the complex composition of iron silicate slags, the binary diagram for FeO_x and SiO₂ clearly shows the low eutectic that allows most slags to be liquid at typical operating temperatures and the steep liquidus line gradient in such silicates containing beyond 40%

silica (Figure 7.74). It is much more likely these inclusions are the remains of quartz-rich host rock as described for other early slags in Oman, the Faynan area of Jordan, and the Austrian Alps (Hauptmann 2007). In addition, it seems likely, although this was not verified empirically for these samples, that the remaining quartz particles had undergone partial structural transformation to cristobalite much as has been observed in similar slags from Tepe Sialk and Faynan (Hauptmann 2007; Schreiner et al. 2003). Fine fern-like tridymite were not observed in any of the slags, probably due to the large size of the quartz grain particles introduced into the charge (Hauptmann 2007).

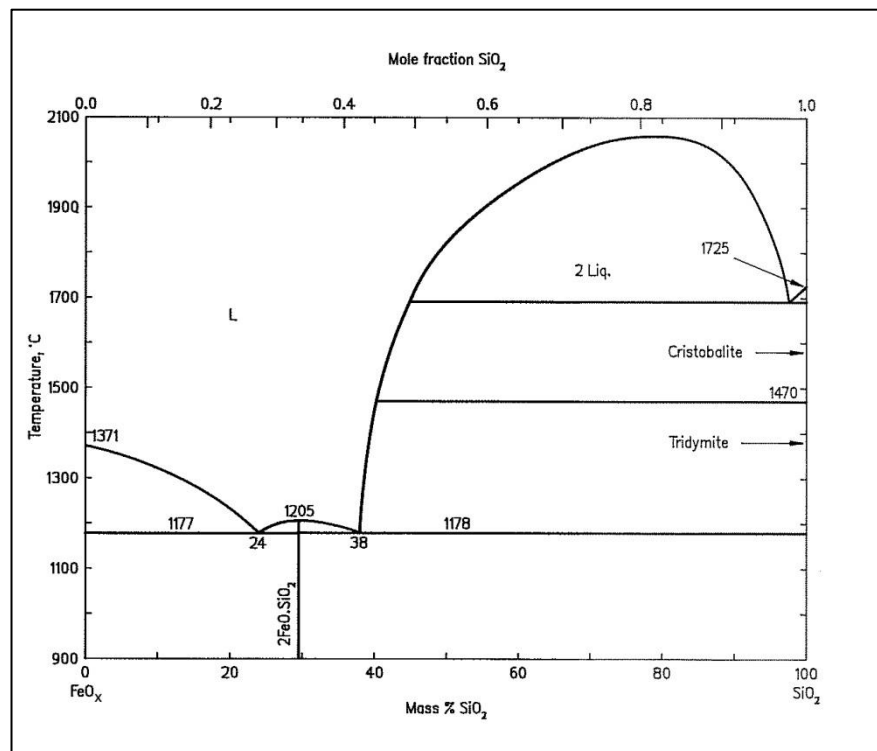


Figure 7.74 Binary phase diagram of FeO_x and SiO₂ (Eisenhüttenleute 1995, 79).

Only 11 samples, representing 27.5% of the analysed slags, contained metallic copper prills, mostly less than 5 μm in size but occasionally up to 50 μm . The scarcity of metallic phases means that the bulk copper content of the slag is largely due to the prevalence of sulphide phases. As sulphide phases are less dense than copper metal, it is possible that much of the copper produced accumulated in the lower region of the slag cake which was later processed to extract the copper prills and thus absent from the archaeological record. This would certainly explain the fragmentary nature of much of the slag remains uncovered at Çamlıbel. Thus, the remaining nearly complete slag cakes were likely those which were considered to have too little copper to be of use and discarded as failed smelts.

Although 11 samples contained metallic copper prills (Figures 7.75 and 7.76), two of them consist of the arsenic-rich slags previously mentioned (740-6358 and 561-3957) and will therefore be reported separately. The means of the analysis of several metallic copper prills in each of the nine remaining samples are reported in Table 7.13.

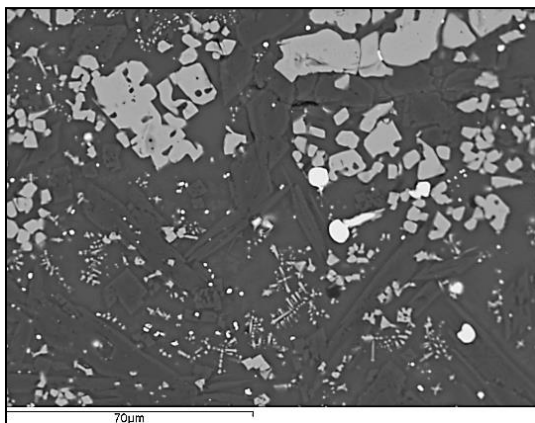


Figure 7.75 SEM image of copper prills surrounded by magnetite spinels in sample 629-3860. The long dark crystals are olivines.

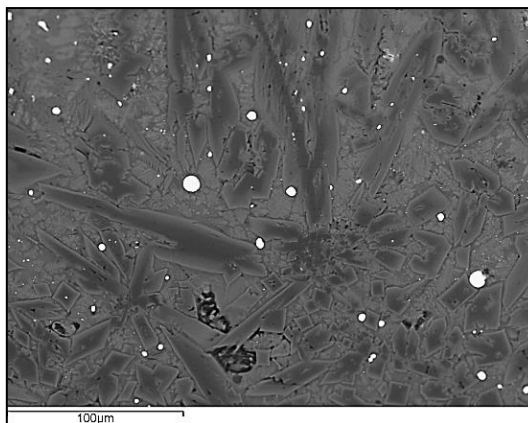


Figure 7.76 SEM image of bright copper prills surrounded by long dark diopside crystals in a glassy matrix from sample 722-4629.

Table 7.12 Composition of copper prills within the Çamlıbel slag as determined by SEM-EDS. Results are normalized to 100% and presented in wt%.

Sample	# prills	S	Fe	Cu	Ni	As
222-326A	2	0.1	5.1	93.7	0.4	b.d.l.
527-4329	6	0.1	1.5	97	0.9	b.d.l.
629-3860	8		2.8	96.5		b.d.l.
637-4226B	2	0.3	2.3	94.8	1.8	b.d.l.
722-4629	5		2.8	96.1		b.d.l.
777-5161	3		3	97		b.d.l.
846-5528b	3		5	95		b.d.l.
890-5774	8		6.5	93.3	0.2	b.d.l.
97-3588	12	0.4	4.9	94.3		b.d.l.

In all instances the prills were composed of nearly pure copper metal with arsenic well below the detection limit of the SEM-EDS, estimated at 0.1 wt%. Further analysis of two samples by WDS confirmed this and showed arsenic present near the detection limit of this second instrument, reporting values between 10 ppm and 100 ppm, with a mean of 74 ppm (Appendix B.5). Arsenic has a strong affinity for copper and should any arsenic have been present during the smelt, significant detectable amounts would be expected in at least some of the metallic copper prills. The difficulty in entirely removing arsenic from copper, even under strongly oxidizing conditions, has been reported several times (Özbal et al. 2002; Rehren et al. 2012, 1724) and it is therefore unlikely to have entirely escaped the system if it had been present to begin with. The absence of such impurities in all instances suggests that no arsenic was introduced with the charge and thus the intended product was unalloyed copper metal. This point has been alluded to several times

already and has several implications regarding the alloying of copper and arsenic at Çamlıbel which will be discussed in more depth in later sections.

Four of the samples contained prills with detectable levels of nickel present. Nickel typically partitions into copper metal during smelting and is thus easily concentrated in metallic prills. That only half of the copper-bearing samples had significant amounts of nickel suggests some variability in composition of the charge.

Zinc, which is present in one of the slags bearing copper metal (722-4629) is notably absent from the metallic prills. This is likely due to zinc's tendency to partition mainly into the slag during smelting and easily lost to volatilization and oxidation (Tylecote et al. 1977). It appears that unless zinc is present in the ores in the low percent level, only insignificant amounts end up in the metallic copper phases. The previously discussed tailings recovered from the site showed that zinc mineralizations were likely present in the ores, but only inconsistently and in very minor quantity.

Analysed metallic prills found in the remaining nine samples were composed of nearly pure copper with an average of 4 wt% iron, none of which were found to contain less than 1 wt%. It can be questioned whether the iron being reported here is caused by analytical errors introduced by the incidental interaction of the electron beam with the surrounding iron silicate matrix as has been reported elsewhere (Georgakopoulou et al. 2011, 133), however this was found to be rather unlikely in this case for a number of reasons.

Firstly, it can be confidently established that the electron beam did not reach the underlying iron silicate matrix. The analysed prills were all larger than 10 μm in diameter, which, assuming that the prills are more or less spherical should insure that the copper extended well into the matrix. It is then possible to estimate the depth of penetration based on empirical data using an equation offered by Potts (Potts 1987, 336-337) in order to verify that little unintended beam interaction occurred:

$$X(\mu\text{m}) = \frac{0.1 E_o^{1.5}}{\rho}$$

Where E_o = accelerating voltage (KV)

ρ = density (g/cm^3)

This calculation provides an estimated electron penetration depth of 1 μm in pure metallic copper with an accelerating voltage of 20 KV and is largely in agreement with theoretical calculations which yield a maximum straight line distance of electrons travelling through copper at 20 KV of 1.46 μm based upon work by Kanaya and Okayama (Kanaya and Okayama 1972, 46). In addition, a number of electron trajectory simulations were run using the Monte Carlo method in the Win X-Ray program. These simulations very rarely produced electrons travelling more than 1 μm ; those that escaped the sample and could be analysed by the detector had typically travelled a distance of between 0.1 μm and 0.5 μm within the sample (Figures 7.77 and 7.78). Since iron has a similar atomic mass and density to copper, it is not expected that its presence had much impact on the penetration depth.

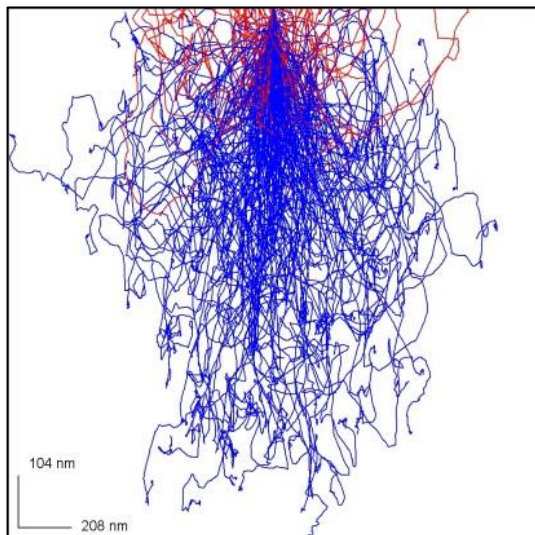


Figure 7.77 Monte Carlo simulation of 200 electron trajectories in pure copper at 20 KV. Blue trajectories indicate electrons that fail to escape the sample, while red reflect those that left the modelled sample and could be analysed by the detector. Diagram obtained using Win X-Ray 1.3 with conditions set to match those of the SEM-EDS instrument used.

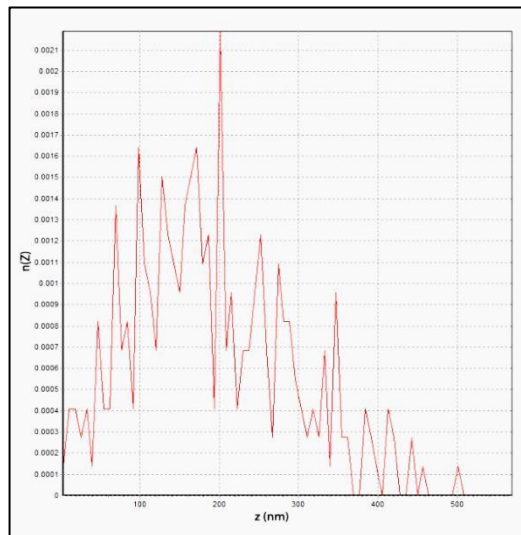


Figure 7.78 Graph showing the penetration depth along the X axis and number of escaping electrons along the Y axis in pure copper at 20 KV. Note that the majority fall between 0.1 and 0.3 μm .

Secondly, two samples which contained copper metal were analysed by an SEM-WDS at UCL's Wolfson Archaeological Science Laboratories in order to minimize the effects of pulse pileup. The WDS instrument is also much better suited for detecting low concentrations of silicon and oxygen which could be used to infer whether iron silicates were being analysed. Much like the methodology employed for the SEM-EDS analysis, a series of several spots were taken on various copper prills at a relatively low accelerating voltage of 20 KV to keep the interaction volume low. All analysed prills were once again larger than 10 μm . The presence of only trace amounts of both oxygen and silica and the consistently elevated level of iron (Table 7.14) is largely in agreement with the EDS data and confirms that the background matrix was not responsible for the detection of iron in the prills since much

higher ratios of iron to oxygen and iron to silicon would be expected should that have been the case. A single analytical spot taken from a prill in sample 629-3860 showed that it was partly corroded and contained oxygen above 10%. Although no silicon was detected in that prill, it was excluded from the means reported here as it strongly skewed the other results.

Table 7.13 Result of microprobe analysis of copper prills within the slag matrix of two samples. Each row is the mean of spot analyses of 11 and 12 different copper prills. Reported results are not normalized although ZAF correction has been applied. The iron and copper account for more than 99wt% of the total.

Sample	O	Si	S	Cu	Fe
629-3860 (11)	0.06	0.01	0.01	96.7	3.5
722-4629 (12)	0.22	0.13	0.05	96.3	2.8

Although the conditions in the smelt were far from equilibrium and phase diagrams should not be overemphasized, it is worth pointing out that iron is soluble in copper up to a few percentage points at high temperatures typical of copper smelting (Figure 7.79). Thus, at 1200 °C, up to about 6 wt% iron can be in solution. As the temperature drops, so does the solubility of iron, down to approximately 0.2 wt% at room temperature (Salje and Feller-Kniepmeier 1978), causing α iron dendrites to precipitate. Although these dendrites were not observed in the prills, this is likely due to the instrument's limited resolution at high magnification.

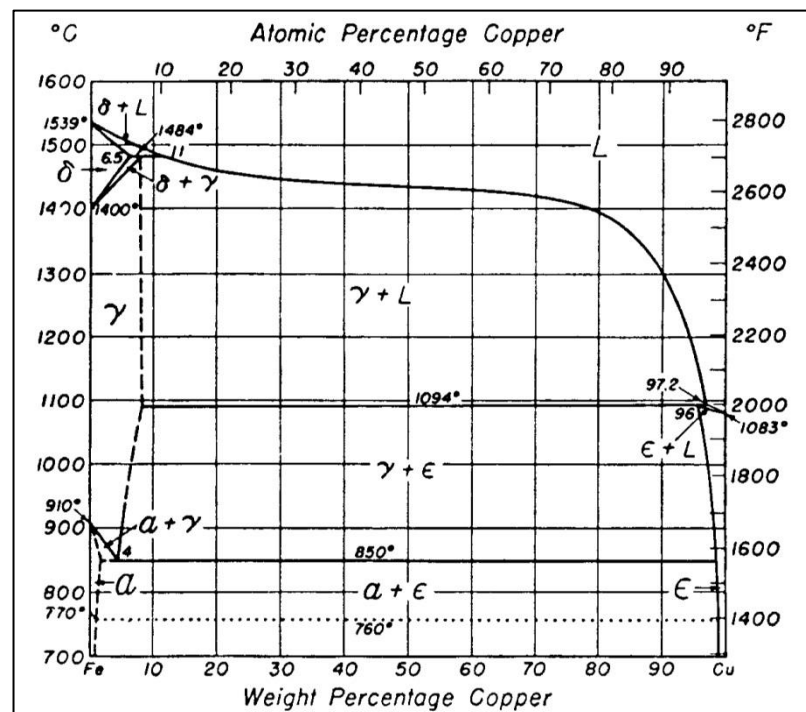


Figure 7.79 Fe-Cu binary phase diagram. From (Craddock and Meeks 1987).

It has been pointed out by Craddock and Meeks (1987, 198) that the presence of minor amounts of sulphur (in the low percent levels), as copper sulphide or iron-copper sulphide,

However, for the former of these two pathways to the formation of iron to have occurred, one would expect iron to be mainly present in its lower oxidation state of Fe^{2+} , usually observed in later Bronze Age copper smelting slag as dendrites of wüstite (FeO). The reduction of magnetite to wüstite is generally considered a precursor to the reduction of wüstite to iron metal, a process which requires strongly reducing atmospheres (Figure 7.81) that are generally thought to only be achievable in much later shaft furnace designs (Killick and Gordon 1988; Tylecote 1976). Since every slag sample which contained metallic copper also exhibited abundant Fe^{2+} in the form magnetite, pyroxene, or both, it is clear that fairly reducing conditions were indeed present. As such, the absence of wüstite but the presence of metallic iron in the prills is difficult to explain without pointing to the highly variable and far from equilibrium atmospheric conditions prevalent during the smelts. It should be noted that metallic iron, either in copper prills or as discrete phases, has been observed in a number of prehistoric copper smelting contexts (Bourgarit 2007, 9; Georgakopoulou et al. 2011, 132-133; Hauptmann 2007) and it therefore appears to be a common feature of such slags.

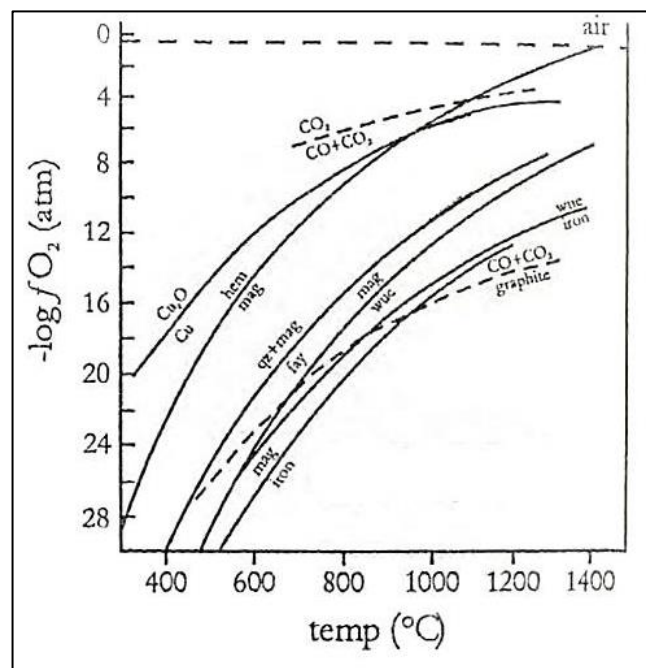


Figure 7.81 This graph shows estimated temperatures and $f\text{O}_2$ in which various phases coexist in slag. Adapted from (Schreiner et al. 2003).

Bulk chemical composition of each sample was determined using a series of at least 3 SEM-EDS area analyses at 100X magnification, each covering an area 1.2 mm by 0.8 mm. Whenever possible, the analyses avoided exceedingly heterogeneous regions rich in metal or gangue. In cases where the sample exhibited extreme heterogeneity, such as was the case in some of the free-silica slags, the analytical areas were shrunk to 200X magnification as it

was felt that this would be more representative of the smelting conditions than analyses which included large parts of gangue or metallic phases.

The results presented below are normalized to 100%, but the analytical totals were generally lower due to factors discussed in the methodology (section 6.3). These mostly ranged between 70 and 94, with the greatest variability attributable to porosity which could not be avoided in bulk area analyses. The mean compositions of these areas are shown in table 7.15.

Table 7.14 Normalized bulk composition of slag remains from Çamlıbel as determined by at least three area scans by SEM-EDS. All elements reported as oxides except for chlorine. Note that samples 602-3411 and 128-1083 are not included in this table as they essentially consists of highly corroded pure matte rather than slag and will be discussed separately. Data for sample 97-3588 are for the slag inclusions within the conglomerate only. Some elements found in only a few samples at levels near the detection limit of the SEM-EDS were not included in this table but can be found in the appendix.

Sample	Phase	MgO	Al ₂ O ₃	SiO ₂	P ₂ O ₅	SO ₃	K ₂ O	CaO	TiO ₂	MnO	FeO	CuO	As ₂ O ₃	ZnO
527-4329	Surface	12.6	4	45.7	1.1	1.2	1.5	11.4	0.4	b.d.l.	20.4	2	b.d.l.	b.d.l.
846-5515	Surface	3.8	0.5	47.7	b.d.l.	0.7	b.d.l.	17.2	b.d.l.	0.5	26	3.6	b.d.l.	b.d.l.
846-5528a	Surface	8	2.4	36.9	0.8	1.5	1.1	8.9	0.1	b.d.l.	39.3	0.9	b.d.l.	b.d.l.
846-5528b	Surface	4.2	0.7	46.9	b.d.l.	1.4	b.d.l.	16.4	b.d.l.	0.3	28.6	1.6	b.d.l.	b.d.l.
222-326A	CBT IV	9.4	1.8	41.4	1	1.2	1	19.7	0.2	0.7	23.2	0.4	b.d.l.	b.d.l.
222-326B	CBT IV	1.6	6.5	28.3	0.4	3.4	0.2	1.8	0.4	b.d.l.	55.5	1.6	b.d.l.	0.3
443-3708	CBT IV	6.6	17.3	30.7	0.2	5.7	0.3	4.5	1.5	0.3	29.2	3.7	b.d.l.	b.d.l.
443-3710A	CBT IV	9.7	2.3	30.7	0.8	1.8	0.8	12.2	0.2	0.2	40.1	1.4	b.d.l.	b.d.l.
443-3710B	CBT IV	1.8	3.3	42.8	b.d.l.	0.9	0.2	8.3	0.3	b.d.l.	41.1	1.4	b.d.l.	b.d.l.
445-3716	CBT IV	4.2	8.6	51.9	b.d.l.	0.5	0.2	12.6	0.7	0.2	20.9	0.2	b.d.l.	b.d.l.
446-3722	CBT IV	4.3	1.1	45.1	0.1	0.8	0.1	17.4	b.d.l.	0.6	27.9	2.6	b.d.l.	b.d.l.
466-4118	CBT IV	3	0.4	50.9	0	1.4	b.d.l.	15.6	b.d.l.	0.5	25.8	2.4	b.d.l.	b.d.l.
629-3860	CBT IV	10	2.9	47.6	0.9	b.d.l.	1.3	4.8	0.3	b.d.l.	27.1	5	b.d.l.	b.d.l.
630-3865	CBT IV	5.5	13.2	34.3	0.2	2.7	0.1	10.7	1.1	b.d.l.	29.4	2.6	b.d.l.	b.d.l.
630-3866	CBT IV	1.2	2.5	68.2	b.d.l.	0.9	0.2	4.9	b.d.l.	b.d.l.	21.5	0.5	b.d.l.	b.d.l.
637-4219	CBT IV	12	1.4	34.7	0.7	1.6	0.3	13.8	0.2	0.5	32.5	2.4	b.d.l.	b.d.l.
637-4221A	CBT IV	9.4	3.4	48.7	0.2	0.5	0.5	12.2	b.d.l.	b.d.l.	21.9	1.6	b.d.l.	1.6
637-4225	CBT IV	4.4	0.4	46.1	b.d.l.	3.1	b.d.l.	15.7	b.d.l.	b.d.l.	27.8	2.5	b.d.l.	b.d.l.
637-4226a	CBT IV	3.2	0.7	45.5	b.d.l.	0.3	b.d.l.	16	b.d.l.	0.6	31.8	1.9	b.d.l.	b.d.l.
637-4226B	CBT IV	4	3.3	26.8	0.7	1.2	1.3	6.4	0.3	0.3	52.6	2.4	b.d.l.	b.d.l.

Sample	Phase	MgO	Al ₂ O ₃	SiO ₂	P ₂ O ₅	SO ₃	K ₂ O	CaO	TiO ₂	MnO	FeO	CuO	As ₂ O ₃	ZnO
637-4456	CBT IV	11.3	2.4	38.9	0.7	1.5	0.6	13.6	0.1	b.d.l.	30.3	0.8	b.d.l.	b.d.l.
646-4500	CBT IV	3.1	1.6	46.3	b.d.l.	0.5	0.2	15.9	b.d.l.	0.6	30.3	1.6	b.d.l.	b.d.l.
722-4629	SPEU	2.3	2.3	55.8	b.d.l.	2.6	0.7	2.6	b.d.l.	b.d.l.	30.3	2.6	b.d.l.	0.4
740-6358	SPEU	7.2	6.1	34.6	1.4	b.d.l.	2.3	9.3	0.6	b.d.l.	16.5	17.5	4.5	b.d.l.
55-440	CBT III	4.1	0.2	49.8	b.d.l.	0.8	b.d.l.	18.9	b.d.l.	0.5	25.2	0.6	b.d.l.	b.d.l.
60-3094	CBT III	2.5	14.4	38.7	b.d.l.	5.1	0.9	1.8	0.5	b.d.l.	34.7	1.4	b.d.l.	b.d.l.
440-3566	CBT III	11.4	3	40.1	0.8	1.9	1.1	19.2	0.2	b.d.l.	21.8	0.4	b.d.l.	b.d.l.
440-3567A	CBT III	10	2.7	37.9	0.8	1.3	1.2	22.5	0.2	0.3	22.7	0.2	b.d.l.	b.d.l.
440-3567B	CBT III	11.1	3	39.1	0.9	1.2	1.3	20.7	0.3	0.3	21.8	0.2	b.d.l.	b.d.l.
561-3957	CBT III	b.d.l.	3.3	15.5	1.3	0.2	0.5	11.4	0.3	b.d.l.	25.8	23	18.3	b.d.l.
643-4264	CBT III	13.7	2.2	39.1	0.8	1.7	0.4	7.6	0.3	0.4	33.4	0.8	b.d.l.	b.d.l.
890-5774	CBT III	5.5	0.6	25.2	0.3	1	0.3	2.2	b.d.l.	b.d.l.	59.6	5.1	b.d.l.	b.d.l.
777-5161	FPEU	16.5	2.8	37	0.7	1.8	0.8	14.4	b.d.l.	b.d.l.	25.6	1.3	b.d.l.	b.d.l.
836-4860	CBT II	3.8	0.8	44.4	b.d.l.	1.8	b.d.l.	14.6	b.d.l.	0.5	32.3	1.9	b.d.l.	b.d.l.
842-4890	CBT II	1.2	6	37.6	b.d.l.	3	0.3	2.1	0.6	b.d.l.	48.8	0.4	b.d.l.	b.d.l.
97-3588	FP (I) / OSP (II)	9.4	2.7	40.5	0.8	b.d.l.	1	4.3	0.3	0.2	38.3	2.1	b.d.l.	b.d.l.
210-299	CBT I	3.8	0.7	45.9	b.d.l.	1.3	b.d.l.	17	b.d.l.	0.5	28.9	1.9	b.d.l.	b.d.l.
251-984	CBT I	13	4.8	43.4	0.7	0.4	0.7	14.3	0.4	b.d.l.	17.6	4.7	b.d.l.	b.d.l.
Mean		6.5	3.7	40.5	0.4	2	0.6	11.5	0.2	0.2	30.1	3.6	1.3	0.1
Min		b.d.l.	b.d.l.	3.9	b.d.l.	b.d.l.	b.d.l.	0.1	b.d.l.	b.d.l.	1.3	0.1	b.d.l.	b.d.l.
Max		16.5	17.3	68.2	1.4	21.5	11.5	22.5	1.5	3.6	60.5	23	18.3	1.6
Std. dev.		4.6	4	13.2	0.4	3.6	0.6	6.3	0.3	0.2	11.4	5.8	4.4	0.4

The slag's copper content is the first and most obvious observation to be made from these results. With a mean of 1.8 wt%, it is just below typical expectations for Early Bronze Age slags which have been described as usually containing between 2.0 and 4.6% copper (Gale et al. 1985a). The mean is somewhat misleading given how variable the copper content truly is, ranging from 0.2 to 5.1 wt% with a standard deviation of 1.3. This is easily explained by the extremely high viscosity of the slag and lack of equilibrium conditions in the smelt which prevented copper prills from freely travelling within the melt. The distribution and copper content of the samples therefore represent a much broader normal distribution than in the later fully liquefied tapped slags (Bachmann 1980).

The most relevant result is the confirmation of the absence of arsenic in any appreciable amount within the bulk of the Çamlıbel slag, which is in accordance with preliminary results from the previous study (Rehren and Radivojević 2010). The two notable exceptions (740-6358 and 561-3957) are discussed in greater detail below. While trace element analysis has not been conducted, the lower detection limit for arsenic of the SEM-EDS in an oxidic matrix such as this is estimated to be 0.1 wt%. The absence of significant quantities of lead, which tends to cause problems when detecting arsenic due to overlaps in energy levels, means that the instrument's measurement of arsenic is reliable. Although a bulk arsenic content lower than the detection limit does not necessarily indicate the absence of arsenic, the instrument should be adequate enough to identify arsenical phases within the slag and metallic prills. That none of these phases were observed in any of the slag except for two distinctive samples discussed separately below, suggests that arsenic was never present in high quantity within the typical smelting charge and that these slags are therefore unlikely to be the result of smelting of arsenic-rich polymetallic ores. The metal produced from them certainly could not have been used to manufacture the arsenical copper objects found at Çamlıbel without the subsequent addition of arsenic from a secondary source.

Looking at the results more broadly, the bulk analysis shows highly variable compositions throughout every period. There does not appear to be any correlation between the occupational phases and the composition of the slag, although the limited number of available samples predating period CBT III may be partly responsible for this.

The majority of the variability in composition is represented in fluctuations in the aluminium, magnesium, and calcium, which is likely caused by strong influences from fuel ashes and, to a lesser extent, molten ceramic (Tylecote 1980; Tylecote et al. 1977) on what was clearly a relatively small, possibly crucible-bound, charge.

The influence of elements introduced by charcoal on the composition of the slag is attested by the correlation between potassium and phosphorous, elements commonly known to enter the slag through the formation of fuel ash. As expected, they are positively correlated when plotted against each other (Figure 7.82), and consequently they have a high coefficient of determination (R^2) of 0.829 if one excludes result below the detection limit of the instrument. Although there appear to be two distinctive clusters, this is probably due to sampling bias as there does not appear to be any distinctive characteristics associated with either group which matches the clusters visible here.

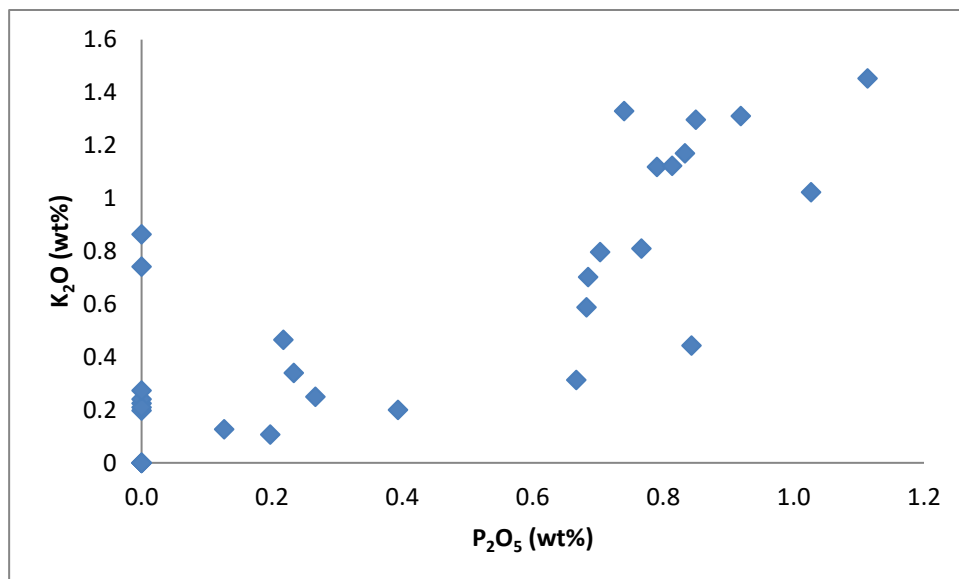


Figure 7.82 Biplot of two compounds commonly related to fuel ashes, potassium and phosphorous oxides. Samples which contained either element below the detection limit of the instrument were included with a value of 0.

Aluminium and titanium are typically used as a measure of the absorption of furnace or crucible ceramic material into the slag since they tend to be more commonly associated with clay deposits than fully beneficiated ores. Although it is expected that the ore charge would contain some quantity of both elements, elevated amounts are taken to indicate the inclusion of clay minerals into the slag. When plotted against each other for the Çamlıbel slag, a clear correlation can be observed (Figure 7.83). Indeed, R^2 between TiO_2 and Al_2O_3 is very high at 0.901, suggesting a strong correlation between the two. The cluster near the bottom left likely represents cases where there was little or no interaction between the ceramic and the slag, while those with higher amounts of both represent instances where ceramic melted and was absorbed into the slag to a greater extent. The single outlier from the otherwise neat line of best fit, sample 60-3094, is most probably the result of inclusion of aluminium rich mineral to the charge rather than solely originating from the ceramic. It also contains

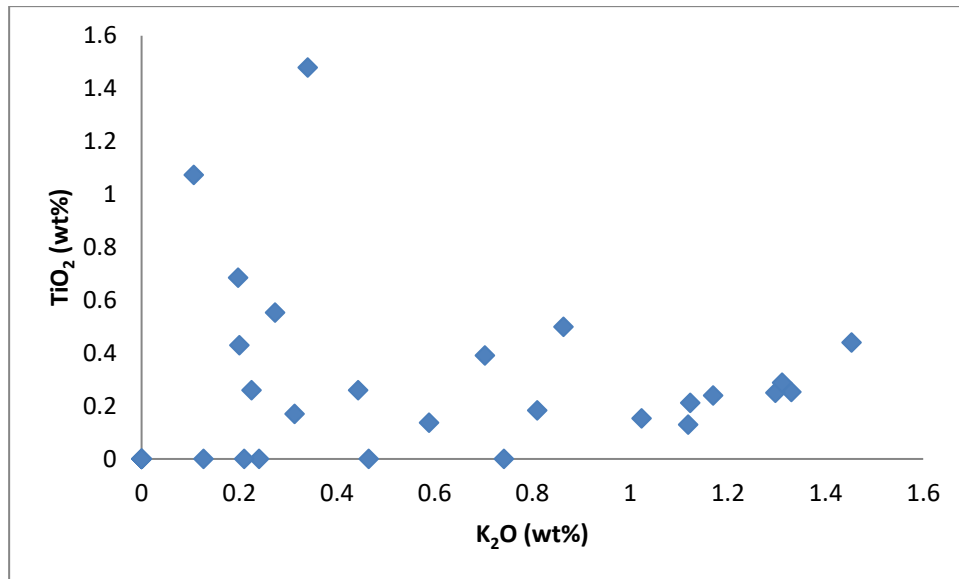


Figure 7.84 Biplot of titanium oxide and potassium oxide. Samples which contained alumina or titanium below the detection limit of the instrument were included with a value of 0.

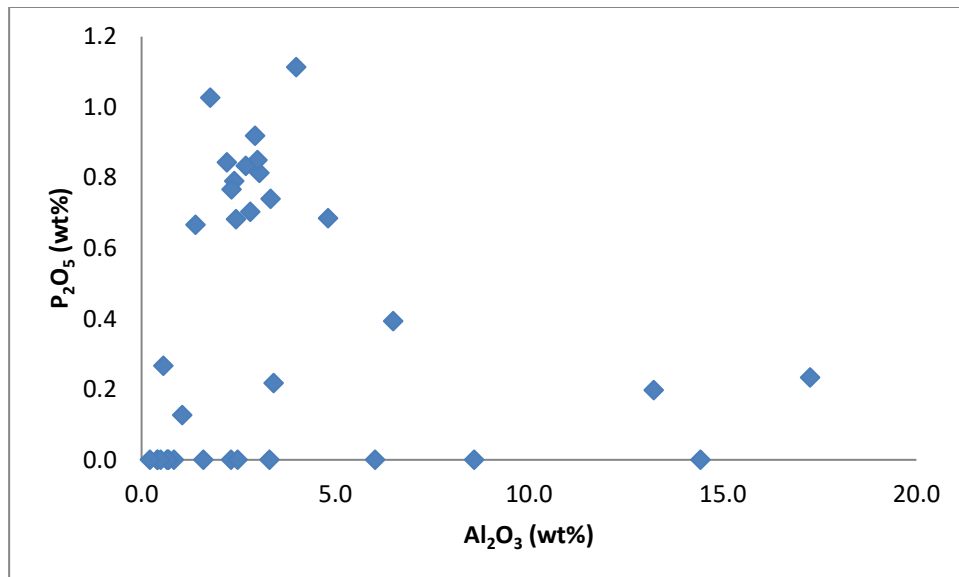


Figure 7.85 Biplot of phosphorous oxide and aluminium oxide. Samples which contained alumina or titanium below the detection limit of the instrument were included with a value of 0.

Experimental reconstructions of 5th millennium BC Vinča smelting techniques using blowpipes and mixed oxide copper ores in bowl furnaces have yielded similar results (Radivojević & Boscher, forthcoming) and can help explain this discrepancy. Despite the fact that the tempered clay used in the reconstruction was even less refractory than Çamlıbel's (Figure 7.10), little ceramic material entered the slag. This was due to two factors. The first is that the slag was only in direct contact with the blowpipe nozzles for brief intervals at a time, resting rather in the coals above the charge. Constant changes in the position of the blowpipes from the addition of fresh charcoal and the alternating blowers means that it was doubtful that contact between the slag and blowpipes ever lasted longer than a few minutes. The second, rather surprising factor is that the slag never reached the bottom of the bowl

furnace even with the operations lasting well over an hour and regularly reaching temperatures up to ~ 1100 °C. This is understood to have been the case because of the localized nature of the air flow from above the charge which largely prevented the charcoal below the slag to fully combust. Thus the slag never interacted directly with the furnace base or walls. A similar situation occurred when crucible smelting was attempted, with only the edge closest to the air inlet, bag bellows in this case, showing any signs of vitrification. This is in line with observations made by other experiments involving smaller reaction vessels such as crucibles (Tylecote and Boydell 1978).

Although purely hypothetical in the case of Çamlıbel, it can be posited that the localized heat applied to the small charge can limit interactions with the ceramic despite the intensity and length of the smelt. Small, open vessels such as bowl furnaces and lid-less crucibles are not efficient at heat retention and while high temperatures can be produced in them, this heat dissipates too quickly to greatly affect the surrounding ceramic.

Also noteworthy from the bulk analysis is that the calcium oxide content is rather more elevated (11.9 wt% mean and up to 20.7 wt%) than one would usually expect from contamination from fuel ashes alone. In the fully flowing tapped copper slag of later Bronze Age periods, fuel ashes typically only introduce up to 8 wt% calcium to fayalitic slag (Tylecote et al. 1977). In Çamlıbel's slags there seems to be little correlation between calcium and other fuel ash elements. The measure of correlation r -square gives values of 0.2 between CaO and K_2O and 0.1 between CaO and P_2O_5 .

This would seem to suggest that calcium was entering the smelt from some other source. However, the analysis of ores and tailings (section 7.1.5) yielded little evidence of high lime content, making it unlikely to have been a typical component of the ore charge.

The addition of lime as flux from some other source also seems improbable at such an early period given that the technology relied on the extraction of prills from crushed slag rather than the complete separation of fluid slag and molten copper. It has furthermore been demonstrated that the presence of lime above 15% becomes detrimental to the free-running temperature of iron silicate slag (Tylecote et al. 1977), which is the case in 12 of the 34 slag samples analysed. The addition of calcium-rich flux would therefore have been counter-productive in the separation of metal from slag had that have been the intended aim.

The lack of correlation between CaO and other elements is thus problematic since no source for the oxide can be clearly identified from the analysed material. It is most likely that calcium

entered the system through a combination of highly variable ore charges and highly inconsistent fuel consumption.

The limited number of ores and tailings recovered from Çamlıbel, and their recovery from excavations mainly based on their iron and copper oxide colouring may well have created a strong sampling bias in favour of iron and magnesium rich minerals at the detriment of the more faded colours usually associated with calcium-bearing minerals.

In addition, the small open-aired nature of furnaces and/or crucibles used for smelting at Çamlıbel may have required a relatively large ratio of fuel to ore in order to achieve and maintain the temperatures required for the reduction of metal. Certainly this ratio would have been much greater than in the efficient Bronze Age and later shaft furnaces upon which much of the archaeometallurgical literature is based. It is quite probable that in Chalcolithic cases fuel ash played a much more important role in the formation of slag, thus leading to the increased absorption of calcium. In that respect, elevated lime content in the slag may have been unavoidable, but did not have an overly detrimental effect on the recovery of copper prills since slag fluidity was not essential.

The combination of these two factors is therefore most likely responsible for the lack of clear patterns in relating the calcium content to other elements and adds to the overall heterogeneity observed in the composition of the slag.

Magnesium is also highly variable and elevated in some of the slag. This comes as no surprise as it is a major component of the local ultramafic geology (Marsh 2010) and likely entered the slag with the ore charge. Indeed, ores and tailing previously discussed (see section 7.1.5) show magnesium oxide as ranging between less than 1 wt% to 33 wt%. The high degree of fluctuation in the magnesium content of the slags (ranging from 1.2 wt% to 16.5 wt%, with a mean of 6.6 and a standard deviation of 4.2) is thus probably mainly a reflection of the mineralogy of local ore deposits. It is also worth noting that many naturally occurring magnesium minerals are green, which may have led to their accidental inclusion as part of the charge due to their confusion with copper minerals

Its presence makes it a major factor in the thermodynamic reactions occurring during the smelt in about half of the slag and will be considered accordingly.

The main components of the system are therefore SiO₂, Fe oxides, CaO, and MgO, together forming between 80 and 98% of the total weight of the bulk slag. Given the crystallo-chemical

behaviour of Mg in iron silicate melts, it was observed that MgO behaves in much the same way as FeO as described in similar cases (Bachmann 1982; Hauptmann 2007), although in reality Mg^{2+} ions can easily replace both Fe^{2+} and Ca^{2+} ions in the various pyroxene end-members (Figure 7.65). Regardless of which form the magnesium takes, the effect on smelt thermodynamics would be similar, bringing the slag compositions nearer to the eutectic region.

The melting behaviour and firing temperature was therefore estimated using the ternary diagram often applied to copper slag, CaO-FeO-SiO_2 with MgO combined with FeO (Figure 7.86). Given the relatively low alumina content of most of the slag, it was deemed that the $\text{Al}_2\text{O}_3\text{-FeO-SiO}_2$ diagram used in many of the studies of Bronze Age fayalitic slags would not be representative of the compositions observed here. It is of note that all samples appear to be somewhat silica-rich, moving the system away from the eutectic, particularly in samples 722-4629 and 630-3866. This is generally caused by the already described large incompletely reacted quartz grains which were unavoidably analysed as part of the bulk. In reality, the glassy phases are lower in silica than the bulk analysis suggests, and therefore closer to the low temperature trough of the ternary diagram.

The presence of incompletely reacted material also points to the conditions in the melt being very far from the assumed equilibrium modelled in the ternary diagrams. As such, it would be a mistake to make any overly literal interpretation of these diagrams and they should be used for rough estimates rather than reliable inferences. With this warning in mind, it can be estimated that the firing temperature was between 1100 and 1200 °C, which is typical of copper slag from this period and easily achieved in small furnaces or crucibles (Georgakopoulou et al. 2011; Hauptmann 2007; Merkel et al. 1994; Shugar 2000). This temperature is slightly higher than the minimum that had to be reached in order to fully melt the metallic copper prills (1083 °C) observed in the slag cakes.

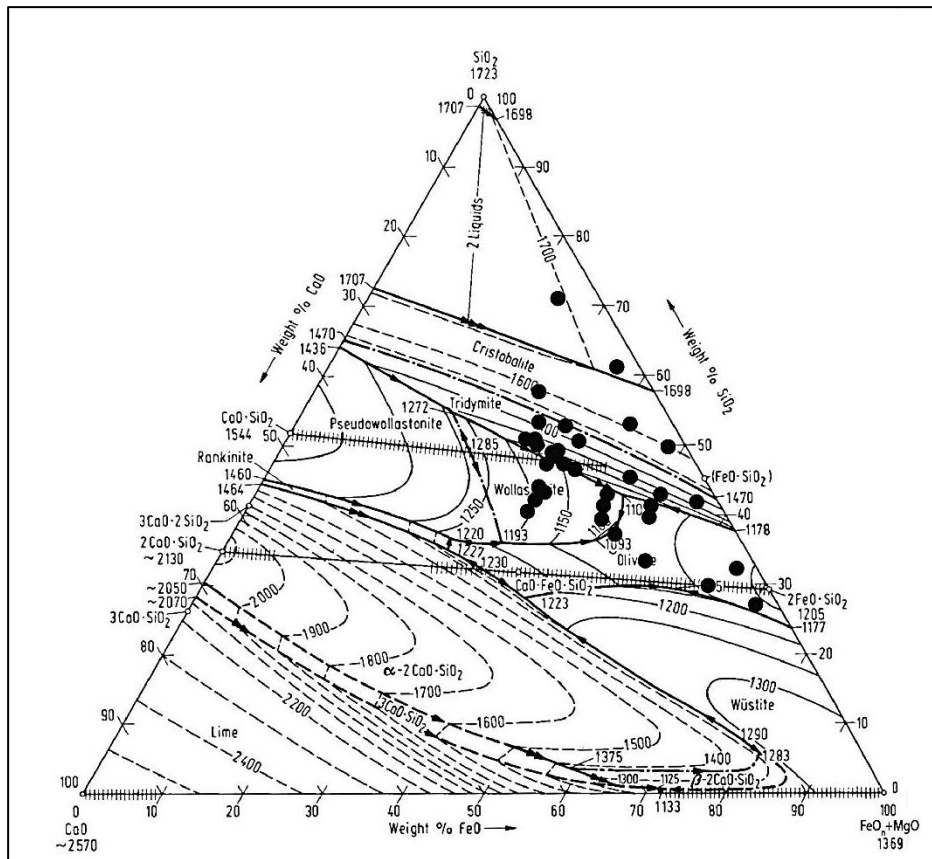


Figure 7.86 Equilibrium phase diagram of the CaO-FeO-SiO₂ system, with MgO added to FeO. Adapted from (Eisenhüttenleute 1995, 126).

Soil, slag, charcoal conglomerate

It is clear from the slag discussed thus far that there is a large amount of compositional and microstructural variation between the different slags produced at Çamlıbel. While most of these specimens have some features which can be used to describe the samples in subsets, none are consistently distinctive enough to formally group them into separate categories. They are thus best described generally as smelting slags.

That being said, there are a number of samples which cannot be clearly described as smelting slag and are worth describe in more detail as they highlight particular aspects of the metallurgical technology employed at Çamlıbel.

Sample 97-3588, which is one of two specimens recovered from the earliest levels of Çamlıbel, is quite distinct from the rest in that it consists of several fragments of slag embedded within a conglomerate of a variety of oxide minerals, fired clay, and pieces of silicified charcoal (Figures 7.87 and 7.88). The sample appears to be highly degraded and many of the metal-bearing phases are present as corrosion in porosities or as veins.

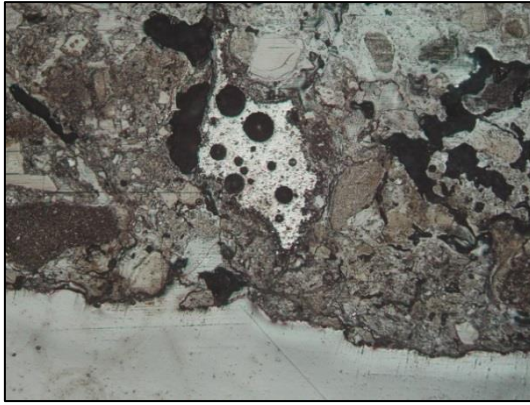


Figure 7.87 Photomicrograph of sample 97-3588 showing one isolated fragments of slag embedded in a conglomerate matrix. Frame is 2.4mm wide.



Figure 7.88 SEM image of sample 97-3588's mixed matrix. In the bottom right is a large fragment of silicified charcoal while in the top right is a large fragment of copper-bearing goethite. Between them is fayalitic slag.

One particularly interesting aspect of this sample is the presence of discrete angular pieces of slag in cold contact with the surrounding matrix (Figure 7.89). Based upon their morphology and context, they do not appear to have formed in situ but rather to consist of fragments of slag mixed in with the conglomerate. Other phases of slag within the conglomerate clearly show a large amount of interaction with the surrounding material, with both hot and cold contacts, while these are isolated and stand out in their angularity.

They are also very distinct in their microstructure and compositions. The microstructure of the angular slag is dominated by large cored angular olivine crystals generally in the composition range of the forsterite endmember (Figure 7.89), clusters of magnetite, microcrystalline dendrites too small to analyse, and large numbers of metallic copper prills ranging in size from 2 μm to 10 μm . It is worth noting that analysis of these prills showed iron content to be appreciably higher (4 wt% to 6 wt%) than in the other slags so far described, but that results also showed oxygen and sulphur to be present in this case. This suggests that some of the iron being reported is likely present as either copper-iron sulphide or the background iron silicate matrix is being accidentally included in the analysis. These prills also contained around half a percent of nickel. Overall, these angular slag inclusions have up to 30 wt% copper in their bulk.

The other phases of slag identified in the sample were entirely devoid of copper prills, although they did contain up to 10 wt% of the element in bulk, present as oxides bound in the microcrystalline matrix. Their microstructures are dominated by pyroxenes rather than olivines, with skeletal chains in the solid solution range of augite within a very fine microcrystalline to glassy matrix (Figure 7.90).

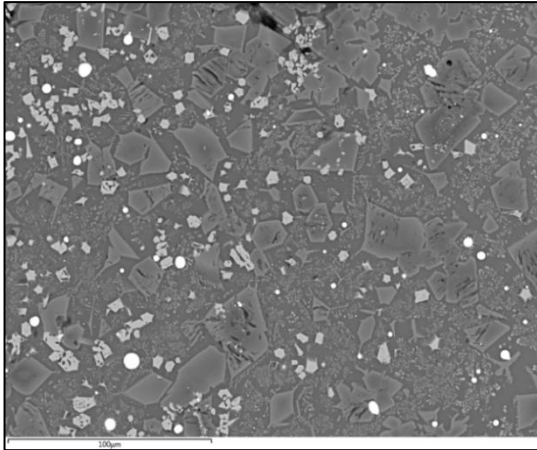


Figure 7.89 SEM image close up of slag inclusion in sample 97-3588. The zoned grey angular crystals are olivine while the light grey blebs are magnetite and the bright prills are metallic copper. The matrix is microcrystalline.

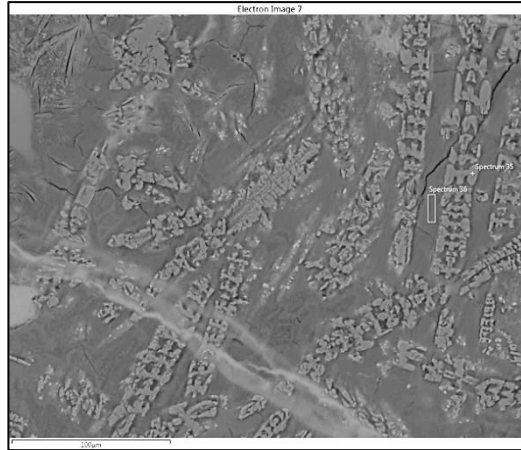


Figure 7.90 SEM image of skeletal chains of pyroxenes in glassy matrix identified in the majority of the slag of the sample.

The composition of these more common pyroxene slags is very much in line with that of the minerals identified and analysed in the rest of the conglomerate. These were mainly iron-magnesium-aluminium silicates along with some iron oxides and hydroxide. Very occasional minerals of pyrite and chalcopyrite were also identified within the mass, suggesting that the charge likely originated from the gossan and included remnants of the primary sulphide deposit. However, most of the identified minerals had undergone significant weathering, with the bulk of the copper-bearing phases identified as copper silicates, containing between 2 and 30 wt% copper.

The similarity in the composition of these minerals with the slag formed in places seems to suggest that it was in essence self-fluxing – that is to say, they could be fully liquefied at reachable temperatures without the addition of anything else to the charge. This is in contrast to the gangue and tailings minerals already discussed in the previous section which were typically too high in either silicon or iron to be fully molten at reasonable temperatures. The rich copper content also indicates that the mineral phases identified in this sample more likely to reflect the true ore minerals used at Çamlıbel.

About a third of the sample is made of what appears to be ceramic or sintered clay included in the charge. In some areas this clay has been nearly completely vitrified while in others it appears to have suffered little heat damage (Figure 7.91), testifying to highly variable heat applied across the material. Where vitrified, it appears to have had strong interaction with the copper rich material as analyses of these areas showed a large increase in copper content.

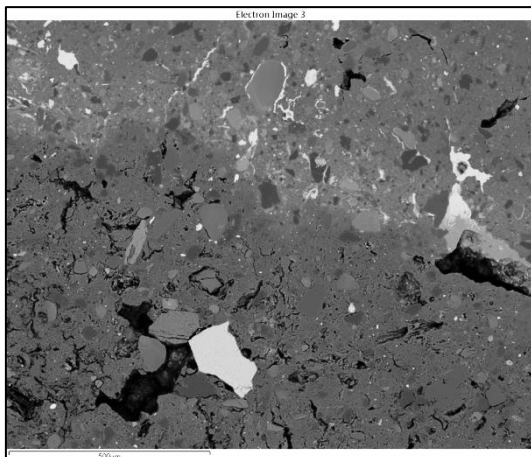


Figure 7.91 SEM image of ceramic area of sample 97-3588. The bottom fabric has only light bloating from heat while the top has been partially vitrified.

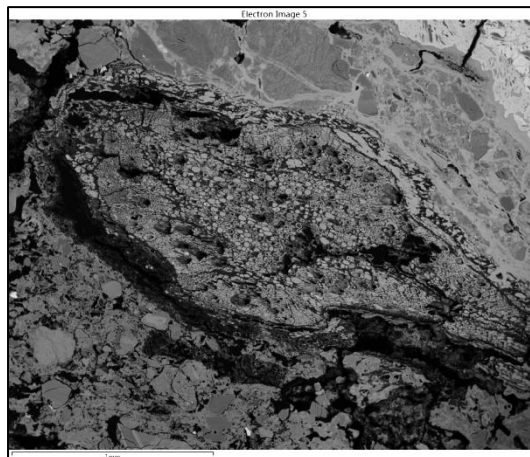


Figure 7.92 SEM image of large piece of incompletely reacted charcoal found within the conglomerate. While this was the largest, several smaller examples were identified throughout the sample.

The presence of charcoal directly associated with some of the slag (Figure 7.92) suggests that the whole mass was subjected to fairly high temperatures and formed in situ rather than through post-depositional corrosion processes. It was unfortunately not possible to identify the species of plant which was used due to the highly degraded nature and limited nature of the charcoal preserved within the slag. They do, however, clearly belong to angiosperm (leaved) trees since the microstructure is clearly that of heteroxylous wood (Gale and Cutler 2000).

The conglomerate nature of this sample is unlike any other slags observed at Çamlıbel and thus does not represent a typical smelting process. The limited amount of slag indicates that while it was indeed exposed to high temperatures it never attained a fully molten state. It likely never formed the major constituent of a smelting charge, but rather is composed of several associated remains fused together due to the proximity of heat.

Despite not being a true slag, the partially reacted nature of this sample provides insight into the original copper ore minerals of Çamlıbel. In addition, although beyond the scope of this thesis, further study of this sample may provide appropriate charcoal remains to enable the identification of the wood type used as smelting fuel at Çamlıbel.

Copper sulphide droplet and cake

Looking at the other end of the smelting process, samples 602-3411 and 128-1083 are composed largely of copper sulphide and represent either intermediary or waste products of the operations. The first of these two specimens consists of a droplet of matte, while the second appears outwardly as a dense fragment of slag and only revealed itself as matte when

cross sectioned. Although these samples are not strictly slag, they are included in this section as they form one of the products, intended or otherwise, of the smelting process.

Sample 602-3411 (Figure 7.93) measures just over 1 cm³ and weighs 9 g, although the old break suggests it was larger when first produced. The droplet has a flattened base and a rounded top surface which implies that it was fully molten at one point and therefore cannot be geological in origin. Interestingly, this particular shape is typical of a regulus which would have formed below another liquid, with a flat surface and rounded sides caused by surface tension. This is surprising since, as has been previously mentioned, none of the slag fragments showed any evidence of such negative impressions. It remains doubtless that this material was at one point fully liquid, and thus must have completely separated from the slag without being in contact with it. This seems probable given the low melting point of copper sulphide and the highly viscous slag preventing it from pooling on top of the matte.



Figure 7.93 Photograph of top view of a matte droplet. Sample 602-3411.

Although the sample has significantly corroded, forming iron and copper oxide veins throughout the samples, many sulphide phases remain free of corrosion. These have been identified as covering a range of composition similar to the sulphide phases found in the rest of the slag, mainly bornite and pyrrhotite, with some occurrences of chalcocite (Figure 7.94). The body of the matte droplet is composed of a series of small grains with a crosshatch pattern of iron sulphide pyrrhotite and iron-copper sulphide bornite phases (Figure 7.95). Large cracks appear throughout the sample which have filled with corrosion and are surrounded by a halo of covellite, likely formed by the loss of iron and sulphur ions by corrosion. Surrounding the grain boundaries are networks of elongated phases of magnetite, much like the high temperature solid solutions previously discussed for the slag.

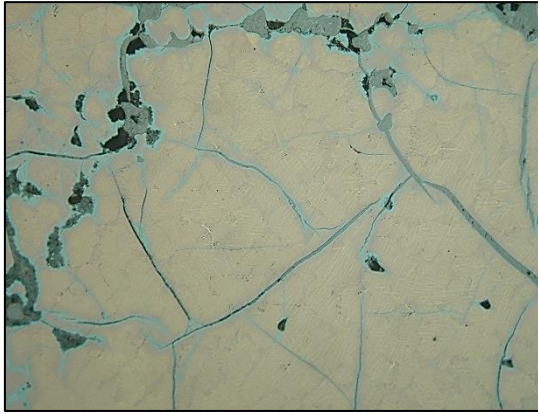


Figure 7.94 Micrograph of sample 602-3411. The droplet is formed of a series of alternating crosshatch patterned grains of copper sulphide. The light blue is covellite encasing cracks which have filled with partially oxidized copper sulphide. The yellow space phase is a combine of both yellow bornite and bright yellow pyrrhotite. Frame is 0.9mm wide.

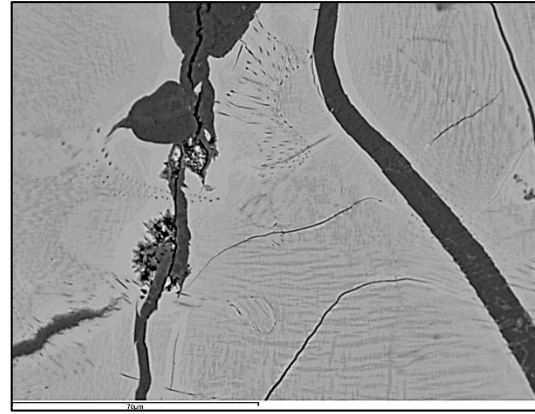


Figure 7.95 Close-up SEM image of sample 602-3411 showing clearly the two distinct phases of copper and iron sulphide. Also visible are the thin elongated darker phases of magnetite at the grain boundaries. The dark veins are corrosion.

Sample 128-1083 on the other hand appears, at first glance, to be an amorphous lump of dense material. Although some results have been published for 128-1083 (Rehren and Radivojević 2010), it was not described as a fragment of matte but rather as slag with a large sulphide component. Having revisited the sample for this thesis, it is clear that phases which first appeared to be iron silicates to the naked eye were in fact highly corroded copper and iron sulphides very similar in appearance to the roasted ore (619-3497) described in the previous section. The main distinction with the roasted ore lies in that this sample was at one point nearly completely liquid and therefore exposed to higher temperatures than typical of a roasting hearth, somewhere between the melting points of CuS (500 °C) and Cu_2S (1130 °C).

It weighs 20 g and measures 3 cm by 4 cm and is 1.5 cm thick. It has a somewhat flat base and a rough upper surface. One of the edges is very slag-like, having a rather heterogeneous appearance. In contrast, the opposite edge is composed of a series of concave pits giving the appearance of either large trapped gas bubbles or a liquid-liquid interface. In cross section, the sample appears mainly metallic grey with a pinkish hue around the edges. A few large undissolved mineral fragments are also visible in cross section.

The microstructure of this sample is in many ways similar to the matte droplet. Although highly corroded (Figure 7.97), it is still possible to identify phases which are identical to those previously identified, consisting of grains of bornite with crystals of pyrrhotite arranged in regular crosshatch patterns (Figure 7.98). The halos of covellite could also be found along cavities and fractures throughout the sample. However, unlike in the droplet, the sample is

much richer in iron than copper, with grains of pyrrhotite dominating the matrix. Most of these phases have to a large extent oxidized, with many small pores throughout.

Also striking are the large fragments of gangue minerals, which consists of iron oxide/hydroxide. It seems that the scarcity of silicon in the charge prevented the iron from forming iron silicate slag, and thus, while the sulphides could melt at relatively low temperatures, the iron oxide remained solid throughout.

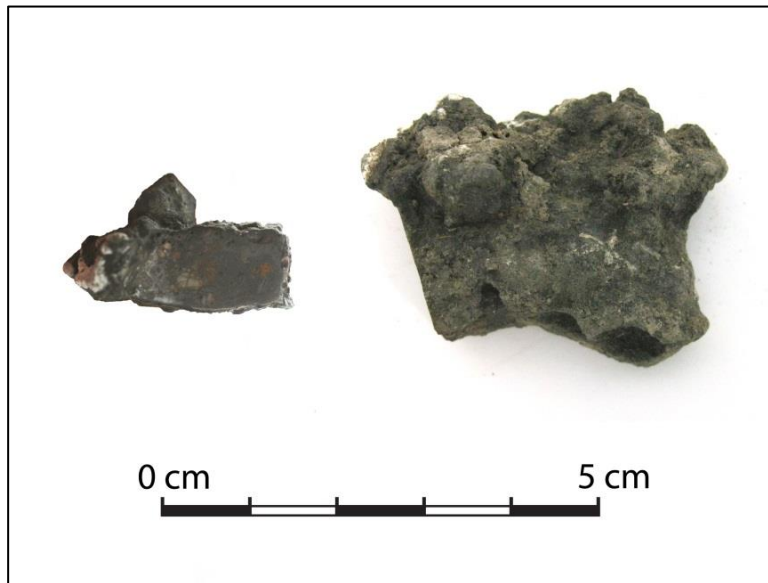


Figure 7.96 Photograph of cross section and top surface of sample 128-1083. Note the series of concave pits along the lower edge in the photograph where molten metal likely formed.

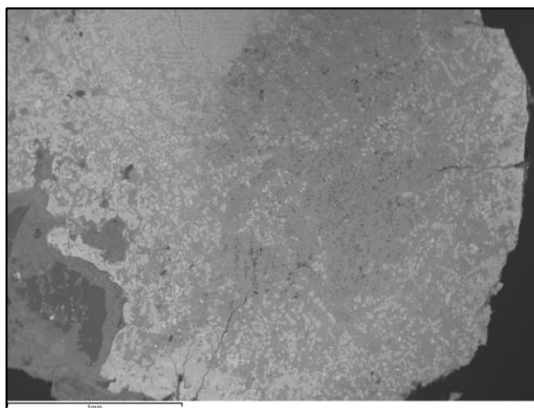


Figure 7.97 SEM-EDS image of sample 128-1083 showing the largely corroded matte phases. Barely visible is the dendritic arrangement of the grains.

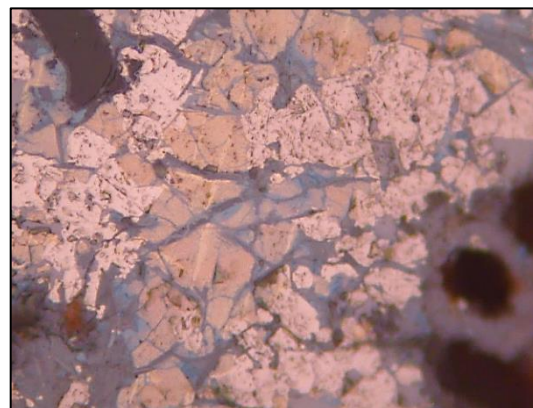


Figure 7.98 Micrograph of sample 128-1083. Although highly corroded, some remains intact. In the left centre of the image can be seen the familiar crosshatch pattern of bornite and pyrrhotite. The dominant, slight corroded pinkish phase is chalcopyrite.

The composition of both of these fragments is not overly informative beyond what could be surmised microscopically (Table 7.15). The iron content of the matte droplet is in line with expectations given that the body is mainly composed of bornite along with some pyrrhotite and magnetite.

In contrast, the slag-like matte cake is much richer in iron and contains significant amounts of silicon. Area analyses avoided all regions with gangue minerals, so the increased iron and silicon does not indicate the inclusion of such material in the area under investigation. Rather it marks the greater prevalence of iron sulphide in this material, much of which has been oxidized by corrosion, along with only a minor component of iron silicates in the intergranular matrix. This composition confirms that the operation which formed this material was unlikely to have resulted in much slag. Instead, it seems that the sulphide phases, in this case mainly pyrrhotite, simply melted and formed a cake in which much of the gangue remained solid. This is completely distinct from the appearance of the slag cakes already described which do not show any evidence of liquid-liquid interfaces. The concentration of gangue minerals along one edge indicates some form of manipulation of the charge while semi-molten.

Table 7.15 Composition of the two samples of iron-copper sulphide material. Results are the means of 3 area analyses of the matte (the gangue material of sample 128-1083 is not included). Results are presented here as oxides since both samples had significant corrosion present in association with ubiquitous fractures throughout both samples. 30-40 wt% was detected in sample 128-1083, while 10-18 wt% oxygen by bulk was detected for sample 602-3411. Much of the iron and copper are therefore present as sulphide phases.

Sample	Phase	SiO ₂	SO ₃	FeO	CuO
128-1083	CBT IV	3.6	10.2	74.7	11.5
602-3411	CBT IV/Surface		31.6	14.6	53.9

The presence of discrete lumps of matte is not surprising given the sulphur-rich smelting charge suggested by the common presence of sulphide corrosion products on many of the slag fragments, tailings, and lump minerals which have already been described. In fact, it is likely that matte was a common by-product of smelting these types of mixed sulphide-oxide ores, and as such one would expect matte cakes and droplets to be much more common remains at the site. This would be in line to the evidence uncovered at Shahr-i Sokhta (Hauptmann et al. 2003) where matte, an undesirable product, was consistently discarded along with the slag. That these two pieces of matte were the only recovered specimens from smelting operations dominated by mixed sulphide and oxide ores tentatively points towards matte having been reintroduced into later smelting charges to extract the remaining copper as has been suggested elsewhere (Bourgarit et al. 2003). Although this negative evidence is by no way sturdy proof, and despite the fact that copper sulphide was clearly not the

intended product of smelting activities at Çamlıbel, the site may yet represent one of the earliest examples of matte conversion, albeit via co-smelting.

Arsenic-rich slag

During the 2013 season of fieldwork, an analytical program of surface pXRF analysis was conducted on all available material in order to identify the presence of broad distinctive compositional groupings. Although the pXRF is not an ideal instrument for the analysis of corroded, geometrically complex, multi-phased material and the results show an extreme range of results, the analysis did succeed in the identification of two small fragments of slag which, unlike the rest of the assemblage, contained significant amounts of arsenic. This led to the export of two samples (740-6358 and 561-3957) for further analysis which will be discussed here, but separately from the other slag fragments as it will be argued that they belong to an entirely different set of activities.

The two arsenic-rich pieces of slag are macroscopically indistinguishable from the rest of the assemblage (Figure 7.99). Both samples were collected from the field as single fragments of what must have been larger pieces, but were broken in order to expose a fresh surface for pXRF analysis. The two fragments are small, measuring 1-2 cm³ and weighing 1-2 g, and both have the same beige oxidized exterior as the other slag cakes and fragments. They are roughly spherical yet angular in appearance, and seem to have been crushed or processed in some way rather than in their original shape. In cross section they are slightly darker with noticeably greater porosity, although not so different from the smelting slag to set them clearly apart. Both fragments exhibit significant amounts of green copper corrosion in cross section.

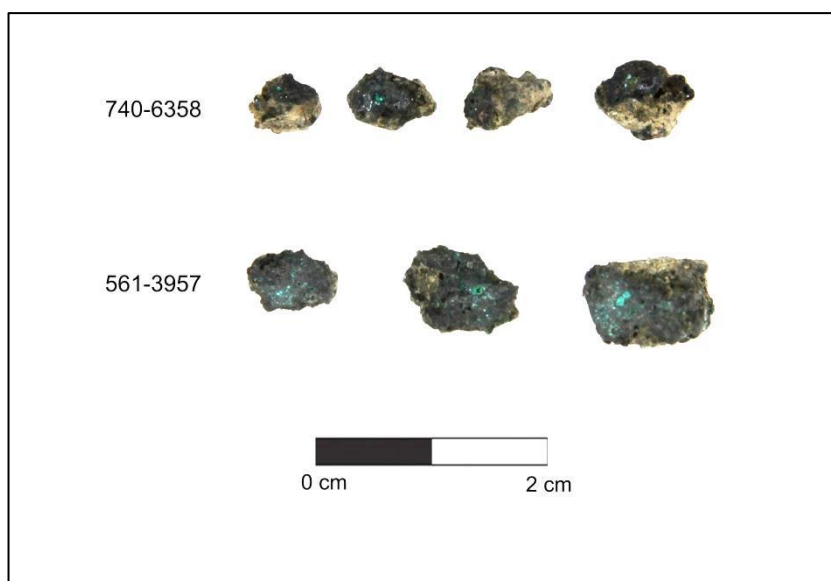


Figure 7.99 Arsenic-rich slag samples identified by pXRF. Note that they were both recovered single fragments but were broken to expose a clean fracture for analysis.

Arguably the most interesting samples from the whole assemblage, the microstructure of these two specimens is considerably different from the rest and worth describing in some detail.

Both slag samples have largely heterogeneous microstructures with very frequent occurrence of magnetite and magnesioferrite spinels. They also both contain large quantities of arsenical copper and pure copper prills embedded throughout the matrix. However, although the composition of the glassy phases in the samples is roughly comparable, the bulk composition and the main crystalline phases present in each sample do not match up well (Table 7.16). This is most likely due to the limited nature of the slag produced from the operations which caused just slight variations in the charge, fuel, length and intensity of the fire, and the amount of interaction with the crucible walls, to have a large impact on the final composition of the samples. Furthermore, the highly heterogeneous nature of the sample made the acquisition of a representative bulk difficult without first homogenizing the samples.

Table 7.16 Results of random bulk area and glassy matrix analyses by SEM-EDS. Results presented here are the means of three analyses each, normalized to 100%.

Sample	Area	Na ₂ O	MgO	Al ₂ O ₃	SiO ₂	P ₂ O ₅	SO ₃	Cl	K ₂ O	CaO	TiO ₂	FeO	CuO	As ₂ O ₃
740-6358	Bulk	b.d.l.	7.2	6.1	34.6	1.4	b.d.l.	b.d.l.	2.3	9.3	0.6	16.5	17.5	4.5
561-3957	Bulk	b.d.l.	b.d.l.	3.3	15.5	1.3	0.2	0.3	0.5	11.4	0.3	25.8	23	18.3
740-6358	Glassy matrix	2.4	5	7.4	35.5	2.4	b.d.l.	b.d.l.	4.6	20.3	0.9	7.6	9.5	4.5
561-3957	Glassy matrix	1.5	2.1	6.2	40	b.d.l.	b.d.l.	b.d.l.	0.8	21.6	b.d.l.	11.4	5.5	10.9

The glassy phases appear to have formed in the low temperature trough of the quaternary $\text{Al}_2\text{O}_3\text{-CaO-FeO}_x\text{-SiO}_2$ diagram (Figure 7.100), with the balance crystallizing out of the melt upon cooling. Copper and arsenic identified in the glassy phases are assumed to be present as oxides rather than as metallic prills since at such high concentrations metallic prills should be readily identifiable. The difference in bulk composition is thus mainly expressed through the variety in the microcrystalline phases prominent in each sample. These being quite different for each specimen, they will be discussed separately below.

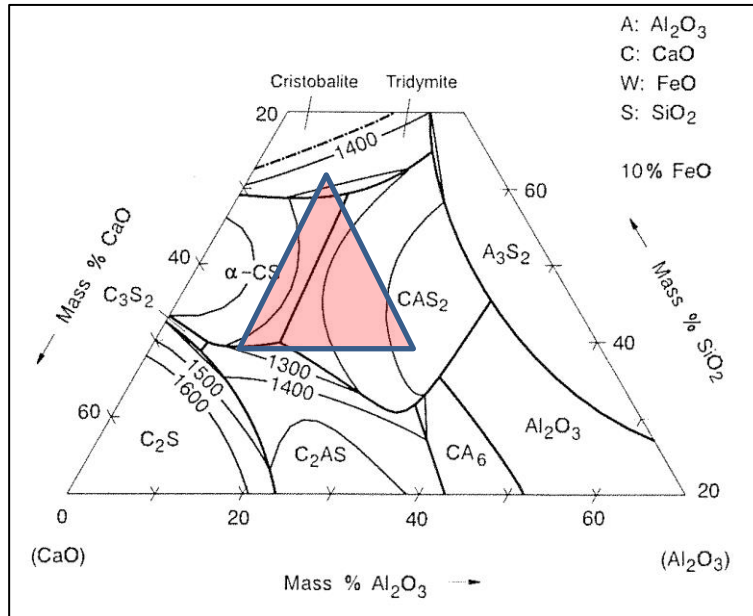


Figure 7.100 Quaternary phase diagram for the glassy phases of the slag approaching the composition of $\text{Al}_2\text{O}_3\text{-CaO-FeO}_x\text{-SiO}_2$ with 10wt% FeO. The glassy matrix being quite rich in both arsenic and copper rich microcrystalline phases, the diagram poorly reflects the actual composition of the melt but still centres around the 1200°C low temperature trough in the centre of the diagram. Adapted from (Eisenhüttenleute 1995, 154).

The most prominent feature of these specimens when compared to other samples is the large number of metallic copper prills present, which amounts to 23 wt% by bulk for 561-3957 and 18 wt% for 740-6358, easily an order of magnitude above all other slag samples. While many of the metallic prills appear reddish under plane polarised light, suggesting nearly pure copper, others have a clear whitish tint which is caused by elevated arsenic content. The larger prills tend to be encased in a ring of cuprite, and in a few instances these also have small copper oxide inclusions trapped within and likely formed while molten due to a relatively oxidizing atmosphere. A few prills of copper sulphide could also be found in both samples, although they are rather uncommon and certainly do not dominate the matrix in the same manner as seen in the slag cakes. The composition of these prills will be discussed separately for each sample.

Equally significant is the arsenic content which exhibits a strong presence in the bulk values of both samples, a marked contrast from its complete absence, or at least in such low concentrations as to be undetectable by SEM-EDS, in every other recovered slag fragment of the assemblage. Although sample 561-3957 has four times more arsenic content than sample 740-6358, discrepancy comes as no surprise given the strong volatility of the element and should still have resulted in a consistent arsenic content in the final copper product if enough of the element was present to reach the solubility limit of arsenic in copper.

Each sample will now be described in more detail individually as some fine points are relevant to the arsenical copper *chaîne opératoire*.

Sample 740-6358 is iron deficient and contains angular crystals of diopside, needle-like delafossite, as well as the distinctively cubic icositetrahedra-shaped potassium-aluminium silicate leucite (KAlSi_2O_6) (Figures 7.101 and 7.102), all of which are associated with a microcrystalline matrix largely dominated by olivines. Overall, although many of the phases are typical of smelting slag, the bulk composition is far from one typical of smelting slags given the low iron content. The delafossite points at atmospheric conditions which were much more oxidizing than was present in the operations which resulted in the formation of the previously described slag cakes. These conditions can be best described as only lightly reducing. It can also be said that, given the low amount of sulphur present, these atmospheric conditions probably resulted in significant oxidation and loss of arsenic during the operation.

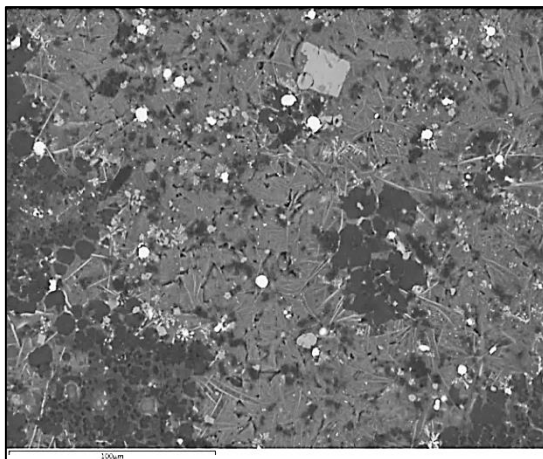


Figure 7.101 Slag matrix of sample 740-6358. The dark polyhedral crystals are leucite, the grey blebs and the large grey angular crystal are magnetite, and the needle-like crystals are delafossite. Bright prills are arsenical copper. The underlying matrix is microcrystalline.

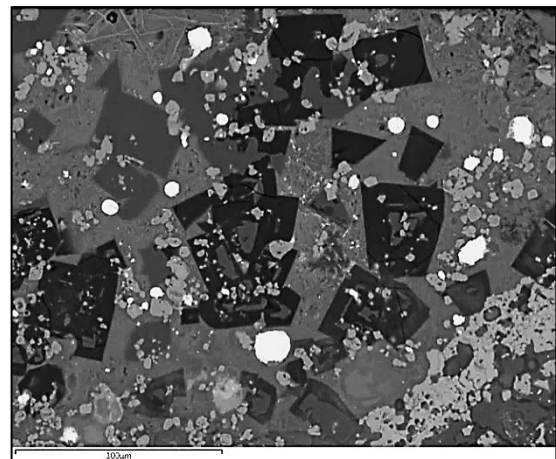


Figure 7.102 Closeup of slag matrix of sample 740-6358 with a cluster of black cubic aluminium silicate crystals. The dark grey angular crystals are diopside, the light grey blebs are magnetite, and the bright prills are arsenical copper. The underlying matrix is microcrystalline mainly composed of olivines and includes laths of delafossite visible in the top left corner of the image.

The matrix of this sample contains a large number of small, nearly pure, copper prills measuring between 5 μm and 25 μm that include impurities of iron between 0.5 wt% and 2 wt%. Larger copper prills, measuring over 50 μm and up to 500 μm , tend to be arsenical, usually containing up to the limit of arsenic's solubility in copper of around 6.5 wt% but entirely free of iron (Table 7.17). Most of the larger such prills also contain the γ Cu_3As phase which commonly forms in arsenical copper rapidly cooling below 827 °C (See section 2.1). A few exceptions from this trend were observed where large prills were composed of pure copper with just traces of iron; in all these instances no arsenic could be detected.

Table 7.17 Composition of large binary phased arsenical copper and pure copper prills and smaller single-phased prills in sample 740-6358 as determined by SEM-EDS spot analyses of a number of prills. All results are normalized to 100%.

Prill size	Phase	S	Fe	Cu	As
>100 μm (4)	Prill matrix			93.32	6.68
>100 μm (7)	γ Cu_3As phase	0.1	0.2	70.8	28.9
>100 μm (3)	Prill matrix		0.4	99.6	
<25 μm (6)	Prill matrix		1.7	98.3	

Some of the copper prills also contain rare sulphide inclusions, often along with both selenium and tellurium, and in rare instances also included traces of silver. These elements were identified in only one other sample (133-6376), but are known to be ubiquitous to copper deposits worldwide, and to concentrate within sulphide inclusions (Rehren 1991). Although difficult to remove entirely, these elements are usually mostly partitioned out of the copper through refining or re-melting processes. Although these elements indicate nothing unusual or unexpected, their presence in detectable quantity here suggests that the copper had not been previously refined and was probably either added directly after production or was formed within the same operation.

The most interesting features of this sample is the remnants of a large fragment of gangue (Figure 7.103) which gives clues as to the nature of the arsenic minerals employed. The amorphous fragment of gangue measures approximately 3 mm across and has a large number of gas-formed porosities, indicating that it was in the process of being dissolved when the operation was halted. The main body of the fragment consists of calcium-magnesium-iron silicate with up to 3 wt% arsenic oxide by bulk (Table 7.18). In some places, the gangue has vitrified and a few crystals of the pyroxene hedenbergite could be observed there. Although clearly heat altered, the bulk composition shows it to be mainly silicon with nearly equal parts of magnesium, aluminium, calcium, and iron. Interestingly, the gangue

contains detectable, albeit low, amounts of copper. This indicates some geological relation between the mineral and copper deposits.

Table 7.18 Composition of undissolved gangue as determined by SEM-EDS. Data presented here is the normalized mean of four area analyses.

Sample	Na ₂ O	MgO	Al ₂ O ₃	SiO ₂	P ₂ O ₅	K ₂ O	CaO	TiO ₂	CrO	MnO	FeO	CuO	As ₂ O ₃
740-6358	2.4	9.5	10.7	47.8	0.5	6	8.9	1.8	0.2	0.1	11.3	0.3	0.5

Around the edge of the gangue, close to the interaction zone with the surrounding slag, the frequency of pyroxene crystals increases and exsolved metallic phases begin to appear (Figure 7.104). These metallic blebs can best be described as iron-arsenic (FeAs) and copper-arsenic (CuAs) speiss. Analysed ferrous speiss contained traces of sulphur (0.3 wt%), minor quantities of copper metal (2.5 wt%), and, in about half the analysed phases, some minor amounts of nickel (1.7 wt%). Cuprous speiss on the other hand usually had slightly higher levels of nickel (2.1 wt%) while retaining significant quantities of iron (8.23 wt%), but did not have any detectable sulphur.

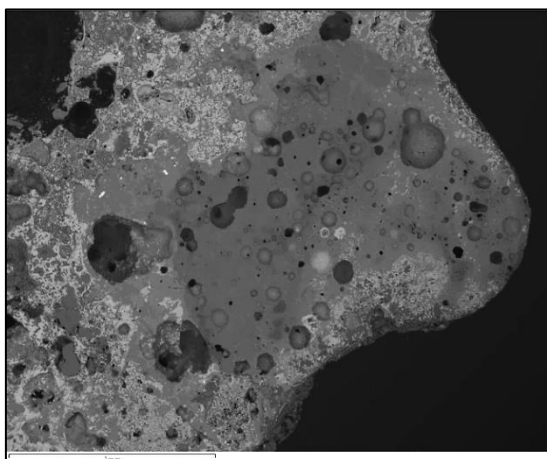


Figure 7.103 Large incompletely dissolved fragment of gangue or ore within the arsenic-rich slag sample 740-6358.

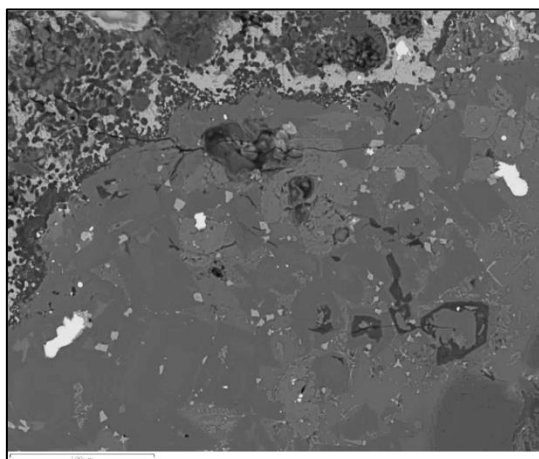


Figure 7.104 Close-up of the top left edge of the undissolved gangue in sample 740-6358.

These phases indicate that the partial pressure of arsenic in the melt near the gangue was at least equivalent or higher than that of sulphur, but much greater than that of oxygen as the presence of iron speiss excludes these possibilities (Chakraborti & Lynch 1983, 243-244). The same is true for copper, and it is clear that both ferrous and cuprous types of arsenic speiss form under these atmospheric conditions as long as sulphur is not a major constituent of the charge. This suggests that the arsenic-bearing mineral was not a primary sulphide but rather an arsenide or arsenate associated with some minor copper-bearing component.

Since under lightly reducing conditions iron-speiss is readily slagged to form iron silicate, it is understood that as the gangue dissolved, arsenic bound within ferrous speiss was released

and free to combine with the copper as has been described in a previous section (3.1.5) in a manner similar to that suggested for Arisman (Rehren et al. 2012). Although arsenic losses were likely substantial, given that the larger copper prills in the main body of the slag are all strongly arsenical, it does not appear that arsenic loss due to oxidation and volatilization was overly problematic as long as enough arsenic was present in the system.

The iron content of the cuprous speiss is also relevant here in distinguishing between arsenical copper produced directly from the arsenic-bearing ore or that which has been added separately. According to Chakraborti and Lynch (1983), under equilibrium conditions iron is preferentially oxidized before arsenic. This means that it is impossible for the arsenic to be entirely removed from cuprous speiss without also oxidizing most if not all of the iron also present within these phases. In other words, exposing cuprous speiss to the lightly oxidizing conditions found in the melt here would first result in the formation of arsenical copper free of iron impurities, and only then would the remaining arsenic be potentially oxidized. While this process could have resulted in the large arsenical copper prills observed in the main slag body, it is not possible for the small pure copper prills containing detectable amounts of iron found throughout to have been produced directly from the arsenic-bearing minerals. This distinction counters the common observation that arsenic will often segregate unequally in copper prills during smelting leading to the presence of both prills with high arsenic content along with pure copper prills (Bourgarit 2007; Gale et al. 1985a; Selimkhanov 1982). Although there is little doubt that this is the case in most far-from-equilibrium smelts, the divergent iron content of the prills here suggests two distinct sources.

Identifying the mineral from which the arsenic originates remains difficult beyond what has already been surmised since much of the microstructure of the gangue has recrystallized and due to loss of material on ignition. Bulk analysis of the least altered parts of the undissolved gangue shows that it has a much less basic composition than other minerals recovered from Çamlıbel (see section 7.1.5). However, a series of four area analyses taken at regular intervals across the sample show an increase in iron and arsenic and a proportional decrease in copper nearer to the gangue (Figure 7.105 and Table 7.19), which suggests that the arsenic-bearing mineral was originally richer in iron than is now apparent from the remnants of gangue. Indeed, the gangue is surrounded by a large area rich in magnetite spinels. Thus, the lower Mg and Fe contents of the undissolved material are likely largely due to their removal by oxidation and slagging.

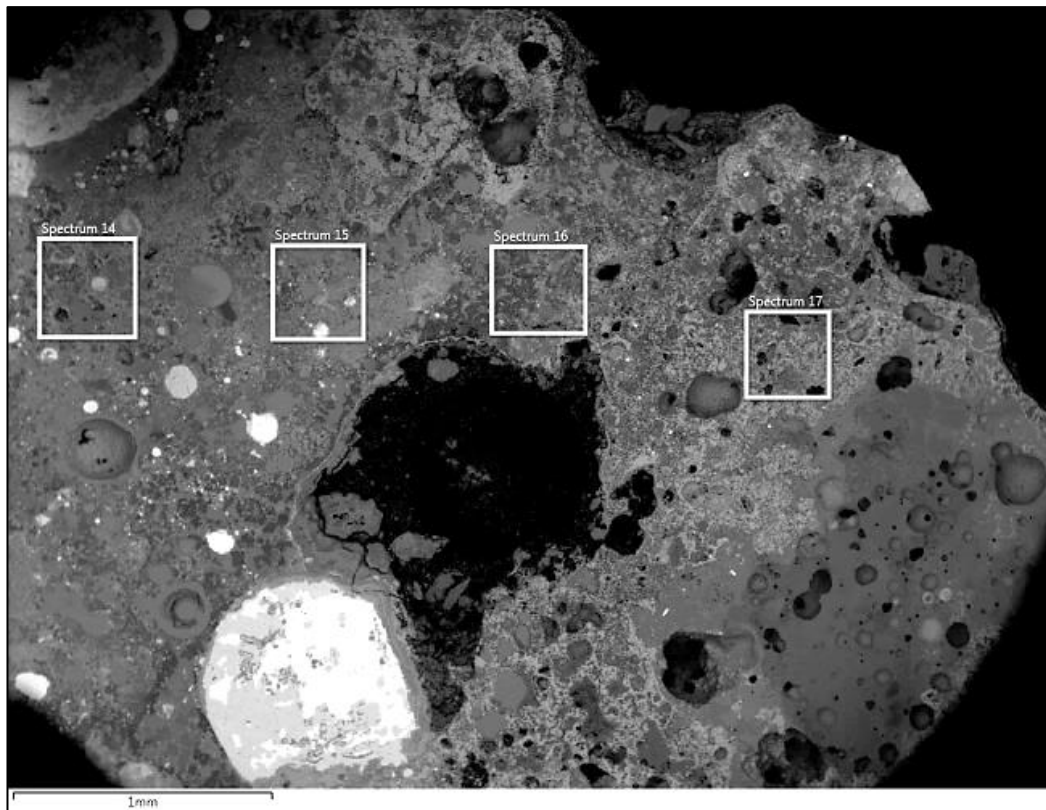


Figure 7.105 SEM image of analytical areas across slag sample 740-6358. The gangue mineral can be seen in the bottom right while the copper rich areas are to the left of the SEM image. Results of the analyses can be seen in Table 7.19.

Table 7.19 Area analyses of slag at regularly increasing distance from incompletely dissolved gangue as determined by SEM-EDS. All results are normalized to 100%.

Distance from gangue (mm)	MgO	Al ₂ O ₃	SiO ₂	P ₂ O ₅	K ₂ O	CaO	TiO ₂	FeO	CuO	As ₂ O ₃
1	5.3	6.2	32.2	1.4	1.9	9.9	0.5	24	12.4	5.9
2	3.2	5.7	29.1	2	1.4	11.2	0.6	14.5	23.1	9.2
3	4.8	6.3	39.4	1.5	0.8	12.2	0.7	23.9	7.7	2.8
4	3.1	4.8	24.1	1.8	0.2	10.2	0.9	49	2.1	3.7

Sample 561-3957, on the other hand, contains more iron and comparatively little silicon. In addition, the bulk is very rich in copper, containing between 15 and 24 wt% of the element, and up to 10 wt% arsenic. The main silicon-bearing phase consists of a glassy matrix with elevated calcium. The crystalline makeup of the sample is thus characterised by an unusual assemblage of needle-like delafossite (CuFeO_2) and angular polyhedral calcium arsenate crystals approaching the composition of johnbaumite ($\text{Ca}_5(\text{AsO}_4)_3(\text{OH})$), although these are unlikely to be present as hydroxides given the high temperature present in the melt (Figure 7.106). Much like the other arsenic-bearing slag sample, this particular specimen is unlikely to have originated as a smelting slag. The high copper and low iron content along with presence of phases formed under relatively elevated oxygen partial pressures is rather suggestive of a refining or melting slag under oxidizing conditions.

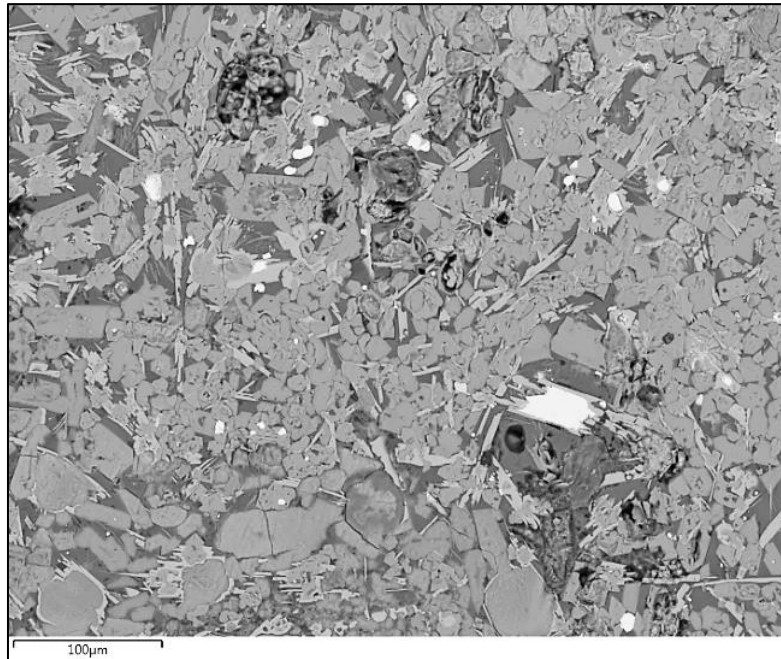


Figure 7.106 Slag matrix of sample 561-3957. The two main crystalline phases are the long thin needle-like grey delafossite and the angular polyhedral calcium arsenate. Light grey rounded prills are arsenical copper. All these phases are within a glassy silicate matrix.

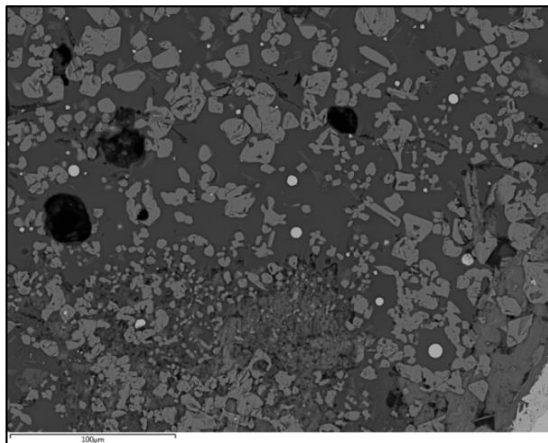


Figure 7.107 SEM image of small prills in sample 561-3957. The grey blebs are a combination of calcium arsenates and some magnetite within a glassy matrix.

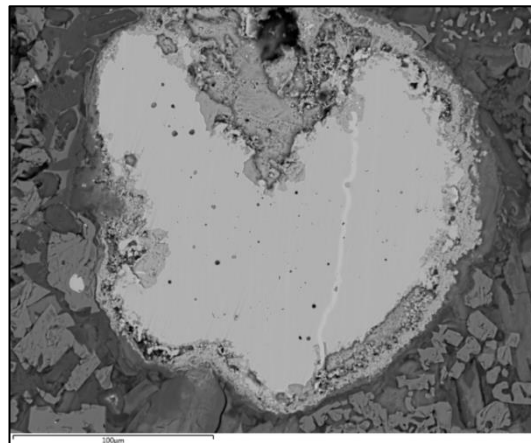


Figure 7.108 SEM image of typical large arsenical copper prill in sample 561-3957. The small dark inclusions are cuprite while the bright veinlet is filled with γ phase of Cu_3As .

The calcium arsenate crystalline phases identified here are of particular relevance as their composition is clearly reminiscent of the crucible residues (see section 7.1.2). They appear here in large tight clusters throughout the sample and are always observed along with small copper prills and delafossite. It appears that under these thermodynamic conditions arsenic is quickly oxidized and will not combine with other metal oxides, but rather has a tendency to form calcium arsenate compounds similar to those observed in the crucible residues.

Despite the prevailing oxygen rich atmosphere, a large number of small metallic copper prills were identified throughout the body of the sample (Figure 7.107). Much like sample 740-

6358, the prills identified here could be categorized into two distinct compositions: small prills containing between 2 and 4 wt% of iron impurity and less than 2 wt% or no arsenic, and large prills containing little iron (less than 1 wt%) and between 3 and 6 wt% arsenic along with the expected γ Cu_3As phase (Figure 7.108, Table 7.20). Small prills are defined here as measuring less than 25 μm , while large prills as those found to be greater than 100 μm . Although not as clearly defined as in the previous sample, the inverse relationship between the iron and arsenic is still very much present and suggests distinct origins for the copper and arsenic. Had they been introduced to the melt together, prills containing high iron should also contain high arsenic since the arsenic should, in theory, be retained until most of the iron is removed.

Table 7.20 Composition of copper prills in sample 561-3957 as determined by SEM-EDS point analyses. Each result is the mean of several points taken from different prills, represented by the number in parentheses.

Prill size (# analyses)	Phase	S	Fe	Cu	As
>100 μm (3)	Prill matrix		0.1	95.9	4
>100 μm (4)	γ Cu_3As phase	0.1	0.1	70.3	29.5
<25 μm (19)	Prill matrix		3.3	95	1.7

Notably, a few copper prills were found to contain traces of silver. Although the area analyses of the prills revealed no silver, small concentrations of the element could be seen within the copper corrosion products surrounding some of the larger prills. Although definitively present, the bulk content of silver within the copper prills must therefore be lower than the detection limit of instrument, estimated at 0.1 wt%. Such silver concentrates were found in corrosion phases associated with both pure copper and arsenical copper and thus likely originated with the copper metal rather than with the arsenic. Only three other samples in the entire assemblage also contained traces of silver (133-6376, 251-984, and 740-6358), and in two of these cases the silver was found to be related to selenium and tellurium inclusions.

Although this particular sample does not have any undissolved gangue material to conveniently point at the original charge, it seems reasonable to suggest that the process was similar to the one proposed for the previous sample given the same relationship between the arsenic and iron in the copper prills.

Overall, it appears that these fragments of slag resulted from operations which combined unrefined copper metal, which included several weight percent of iron impurity, with iron arsenide or arsenate minerals containing minor quantities of copper. For reasons already discussed, the arsenical minerals are unlikely to have been rich in sulphur and therefore were probably not the more common arsenic-bearing types (realgar, orpiment, and arsenopyrite).

Although rare, löllingite, scorodite, or leucopyrite are the most likely candidates. Since no such minerals have been recovered from the archaeological assemblage or identified in the general vicinity of the site, it is not currently possible to confirm this.

The size, morphology, and composition of these slag fragments are consistent with the expected waste produced from small crucible-bound operations. Although they cannot be directly matched to the residue layers found on the crucible fragments recovered from Çamlıbel, this is probably because they were formed through distinct but parallel chemical reactions. While the slag was thus formed directly from the melting and reactions within the crucible charge, the crucible residues were formed by the re-depositions of volatile elements from the same operation.

7.2 Arisman

7.2.1 Assemblage

Unlike Çamlıbel, where only a preliminary study of the metallurgical material had been conducted, the metallurgical assemblage from Arisman has already been the subject of several studies and publications. It was therefore not necessary to entirely revisit much of the already well-characterized samples and the focus was instead placed on the poorly understood ceramic technology and the black glassy slags previously described as containing both ferrous speiss and arsenical copper prills (Boscher 2010).

The material of interest was obtained from the Curt-Engelhorn Zentrum Archäometrie, in Mannheim, Germany, where samples from the excavations had been sent by the German Archaeological Institute for preliminary analysis (Pernicka et al. 2011). Following encouraging results from the thorough micro-phase analysis of a small subset of 15 samples (Boscher 2010; Rehren et al. 2012), approximately 50 kg of metallurgical materials from 88 distinct contexts were made available for this analytical program with the aim of completely characterizing the speiss and arsenical copper production processes at Arisman.

These 50kg were collected by the excavators as a representative sample of several tons of material recovered from the various excavated areas of Arisman I. A few additional samples collected from the surface of Arisman II and III, which remain unexcavated to this day, were also included in the shipment.

Unfortunately, it proved difficult to obtain provenance data for just over half of the material obtained and as such it was not possible to assign them to specific areas of the site. However, and despite the fact that Arisman's occupation layers span several centuries and are spread

across a number of loci, it should be noted that copper and arsenic production remains appear to be consistent across all seven areas of the site, with only the slag originating from Area D showing slightly higher calcium content (Pernicka et al. 2011, 644-654). This is broadly suggestive of some measure of standardized ore extraction, beneficiation, and smelting technology across the site. Slags associated with melting and casting operations from the so-called workshop in Area C proved to be clearly distinctive from the rest of the assemblage. These were found to be rather poor in iron (<20 wt%) and much richer in copper metal (>10 wt%) than smelting slag and could be easily identified as such (Pernicka et al. 2011, 650-651). Data obtained from smelting slags originating from any of the production areas should therefore be broadly, although cautiously, comparable. The lack of provenience information should thus not be overly problematic in the interpretation of the Arisman results.

In order to remain objective and avoid the introduction of false information, samples without provenience which were found to be isolated or form distinct compositional groupings will be discussed separately. In addition, because Arisman II and III have not been excavated or dated, remains known to have originated from these sites were not included in this research.

Several of the sample bags contained multiple fragments of materials collected from the same archaeological contexts and bagged together but not necessarily representative of a single process or even material type. The assemblage was therefore sorted in order to enable a complete catalogue of the different materials available for analysis. Where individual contexts contained several distinctive types of material, these were separated and given catalogue numbers with a new suffix (e.g. FG-000118 became FG-000118A and FG-000118B). This resulted in a complete list of 119 individual or groupings of identical specimens available for analysis (Table 7.21). Upon closer examination, eight of these were found to consist of material not relevant to this research (soil, ash, plaster, and small stones) and will therefore not be discussed.

Table 7.21 List of metallurgical remains of Arisman I available for analysis and their provenience. Numbers in parentheses represent samples that were evaluated macroscopically but were not prepared or analysed by SEM-EDS.

	Slag	Technical ceramics	Minerals/ores	Other	Total
Area A	23 (6)	5	-	-	28 (6)
Area B	5 (3)	-	-	-	5 (3)
Area C	1 (1)	-	2	-	3 (1)
Area D	7 (4)	2	-	-	9 (4)
Unknown	35 (11)	17 (6)	14 (12)	8 (8)	74 (37)
Total	71 (25)	24 (6)	16 (12)	8 (8)	119 (51)

7.2.2 Technical Ceramics

The analysis of Arisman's technical ceramics was of particular interest when this research was proposed as a means to clarify the distinction between the ferrous speiss and arsenical copper *chaînes opératoires* and to shed more light on the use of the vaguely described tapping receptacles (Rehren et al. 2012). While it was one of the aims of this research to sample some of the early Qabrestan-type crucibles from Area B, access to these for sampling could not be obtained and could thus not be included in this study. The technical ceramics described and analysed here are divided morphologically between ceramics described as flat-based crucibles (Helwing 2011d, 262-263,306-309) and furnace linings.

Twenty-four samples received for this thesis had been marked as ceramics in one way or another associated with metallurgy. Upon closer inspection, four specimens were found to be unrelated to metallurgical processes. Two of these consisted of molten lime plaster (FG-000117D and FG-012274), while one was comprised of a number of fragments of molten ceramic showing no recognizable metallurgical features (FG-012272), and the last was described by the excavation report as coarse black ceramic lining a pit (FG-030707). Although no heat alteration was evident on this last sample, the excavators had suggested that it may be related to charcoal production and thus fell outside the scope of this study. Only one of these four samples was analysed (FG-000117D) and it was confirmed to be composed entirely of lime plaster. Since none of these were found to be directly related to the metallurgical processes of Arisman they will not be further discussed.

Although the remaining 20 samples of technical ceramics could easily be classed as either crucible or furnace fragments, it was at this stage unclear whether they were related to speiss or copper smelting or both. Since the crucibles and furnace linings were mainly recovered from the slagheaps of Areas A and D and only rarely from workshop Area C, they were assumed to be related to either ferrous speiss or arsenical copper production. This assumption was confirmed by the analysis of slag residues attached to the ceramic or by the presence of prills embedded within the ceramic and is summarized in Table 7.22. In only three furnace samples was it impossible to determine the intended product due to a lack of appropriate analytical targets.

Table 7.22 List of ceramic samples available for analysis arranged by function. Numbers in parentheses are the samples which have not been analysed by SEM-EDS.

	Crucible		Furnace			Other	Total
	Speiss	Copper/Black	Speiss	Copper	Unknown		
Area A	2	1	1	1	-	-	5
Area D		-	2	-	-	-	2
Unknown	1	-	-	9	3 (3)	4 (3)	17 (6)
Total	3	1	3	10	3 (3)	4 (3)	24 (6)

The first group of technical ceramics, the flat-based bowl crucibles, was mainly identifiable through the ceramics' macroscopic appearance. Although they show a high degree of variability in their shapes and sizes it is still possible to make a general description which encompasses the full range of morphologies. In all instances the bases are flat to slightly concave and clearly show the negative impression of soil and organic matter embedded on their underside (Figure 7.109). Similarly consistent across the entire assemblage are the vessel walls which are invariably at right angles from the bases and between 2 cm and 2.5 cm thick. Although all base fragments analysed for this thesis were broken and missing the rims, at least one piece reported in the excavation monograph had a full cross section extending from the base to the rim (Helwing 2011d, small find no. 203, pp 280, 308) and measured 13.8 cm in height. The crucibles' inner diameters are reported as rather small, ranging between 8 cm and 10 cm (Helwing 2011d, 262), but at least one fragment analysed during the MSc research (FG-030119A) was found to have a diameter of 16 cm (Boscher 2010). Most fragments had small spurs or ledges extending outwards from the base (Figure 7.110) which is likely to have been used to join the crucibles to the furnace superstructure (Steiniger 2011) or to increase stability.

Assuming a perfect cylindrical shape, the maximum capacity of the crucibles can be estimated at ranging roughly between 700 cm³ and 1100 cm³. If these were filled with copper metal, their total capacity would equate to approximately 6-10 kg. However, since some slag is also known to have been present in the crucibles and because the crucibles are unlikely to have ever been filled to the brim, the volume of copper produced in them was probably significantly lower.



Figure 7.109 Photographs of sample FG-030119B. Image on the left is the base of the ceramic showing the organic matter impressions. Photograph on the right is a cross section. Note the slag scraped to the side.

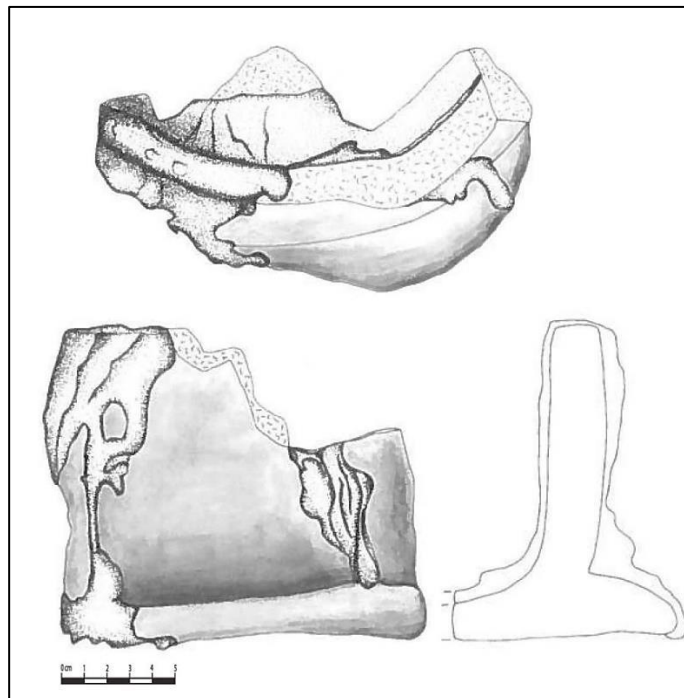


Figure 7.110 Drawing of crucible base and wall (Helwing 2011d, small find no. 203, pp 280, 308). Note the slag dripping on the outside and the small edge extending outwards from the base.

The crucible fabrics are well fired, suggesting that these were manufactured and fired prior to smelting. This is no surprise given Arisman's large pottery industry evidenced by a number of kilns recovered from Area B (Boroffka et al. 2011). Macroscopic observations of the ceramic cross sections revealed them to be relatively dense and lacking any form of temper. The redox conditions are difficult to pin down as the bodies range in colour from beige to grey, probably reflecting changing conditions between the initial firing and the later smelting operations. The darker grey colour was probably caused by reducing conditions present during the original manufacturing stage, while the lighter reddish and yellowish tones were likely the result of oxidation during and directly following the metallurgical process. The

crucibles appear to have largely retained their initial shapes and integrity despite exposure to high temperatures. The outside surfaces are in fact largely unaffected by heat, indicating that the source of heat was inside the crucibles. Given the lack of bloating in general, it is unlikely that heat was applied for any length of time. Rather than being used for smelting or casting, it seems more likely that these vessels were intended to capture a molten mass which was allowed to cool gradually.

The furnace fragments are macroscopically distinctive from the crucibles in several ways. Firstly they tend to be much thicker, typically measuring 3 cm to 5 cm in thickness. They are also much rougher in texture and always have a large organic temper component clearly visible in cross section as elongated voids (Figure 7.111). Most of these fragments have thick layers of slag attached to their inner surfaces. In all instances heat damage was extensive, resulting in strong bloating, vitrification, and slagging of the ceramic body. Chemical interaction between slag and ceramic was the norm and resulted in thick layers of mixed compositions. Given the amount of vitrification which clearly took place on much of the inner wall, furnace ceramic must have greatly contributed to overall slag formation during smelting.



Figure 7.111 Photomicrograph of furnace wall sample FG-030670 with typical organic temper voids. Although the matrix here is relatively fine grained and thus poor in mineral inclusions, the rest of the sample does contain significant quantity of them.

Unlike the crucibles, most of the furnace ceramic bodies appear to have been fired *in situ* as evidenced by the poor preservation of non-vitrified furnace walls. Indeed, the outer surface rarely survives on most samples due to being poorly fired. In most cases only the slagged, and thereby much more weathering resistant, inner surface of the furnace wall survived.

In three furnace samples (FG-030669, FG-030671, and FG-030672A), and in several examples in the excavation report (Helwing 2011d, small finds nos. 237-242, figure 84, p312) rims could be identified which were in some cases covered by slag that had spilt over and covered the edge. This is somewhat unusual since it would be nearly impossible to add enough ore and fuel to the point that slag could spill over the top. This is therefore either the result of manipulation of the charge during smelting or the sherds first broken and discarded and only later covered in slag in subsequent operations.



Figure 7.112 Three furnace fragment samples with rims. All show extensive heat damage applied mainly to the inside but extending deep into the fabric. Note two distinct layers of slag on the leftmost example, with the top layer extending over the edge and most likely deposited after the ceramic had been broken and discarded.

In one previously reported sample (FG-030113) (Boscher 2010, 41), a large semi-circular hole piercing the width of a fragment of furnace wall was identified (Figure 7.113). Although no further analysis was conducted on the sample, the 5.7 cm diameter hole was tentatively interpreted as a vent or tuyère inlet. It should be noted that no tuyère fragments have been reported from any of the activity areas of Arisman. This does not exclude the possibility of the use of more perishable materials as sources of forced air but it does open the floor to the more unconventional 'draft furnaces' reported elsewhere (Juleff 1996). As such, wind patterns and the orientation of the furnace recovered from slagheap A may be worth exploring as an added reason for Arisman's location.

Analysis of this sample has now been conducted and will be discussed below; suffice it to say for now that the prills embedded in the furnace walls were arsenical copper and thus it is assumed that this was the intended product of this particular furnace.

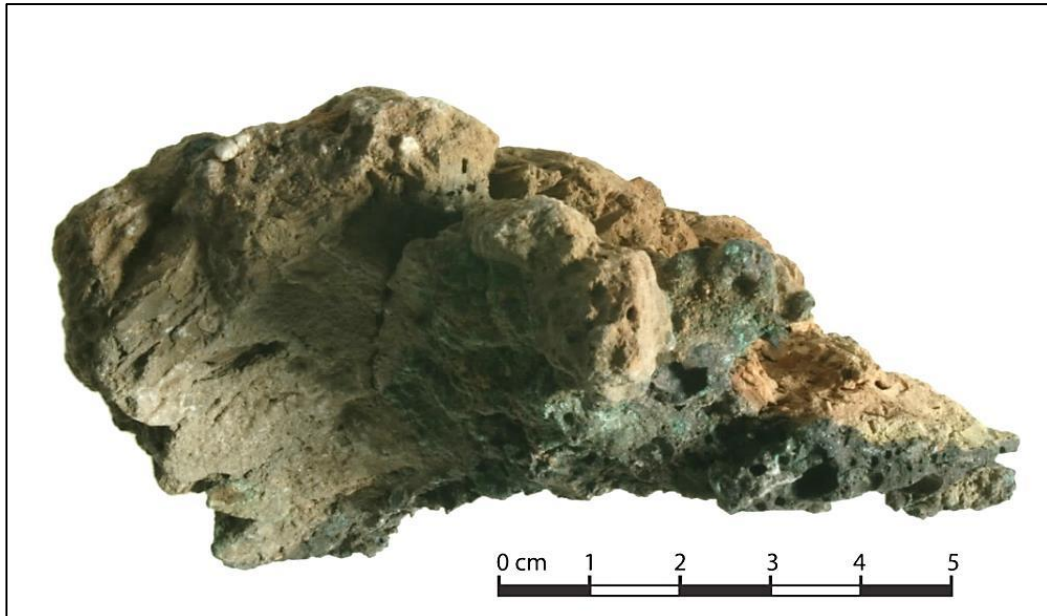


Figure 7.113 Photograph of sample FG-030113 showing the semi-circular hole running through the furnace wall interpreted as a tuyère or vent hole. The hole can be seen here in half-section in the center-left part of the photograph.

Another sample of note is FG-12235A, a roughly cubic shaped furnace fragment measuring 5 cm on each side which is essentially composed of two furnace linings (Figure 7.114). The specimen has two well-defined layers of blueish-green corrosion measuring 0.3 mm to 0.5 mm overlying reddened ceramic which fade into the more typical organic-tempered orange-beige furnace fabrics. A thin layer of ceramic at the bottom of the sample also shows evidence containing the same greenish corrosion as the two distinct layers. The layers therefore testify to at least three separate smelting events and at least two repairs. The fragmentary nature of the specimen means that more layers may have been present originally but have since broken away. Evidently, Arisman's smelters re-used the same furnace structure several times as was already discussed in the archaeological background for the site in relation to the furnace structure from slagheap A which had been re-lined up to 33 times (See section 5.2.5). This sample will be discussed in more depth at the end of this section.

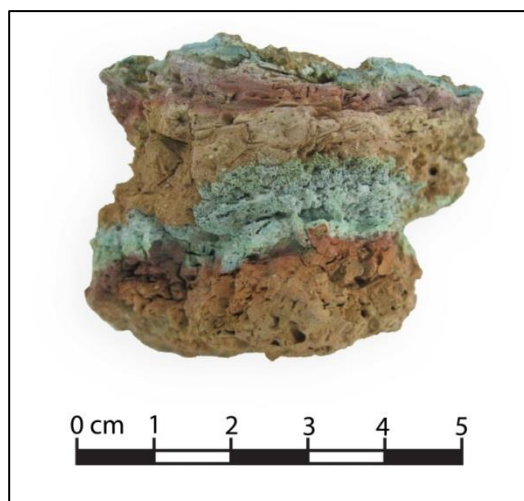


Figure 7.114 Photograph of sample FG-012235A. This furnace lining fragment shows two smelting events and three ceramic linings, testifying to the reuse of the furnaces.

Microstructurally, all furnace and crucible samples are very similar except for the presence of organic temper in the former and its absence in the latter. Mineral grains range from $5\mu\text{m}$ to $250\mu\text{m}$ and consist mostly of quartz in a lime rich clay matrix (Figures 7.115 and 7.116). Little porosity is present in non-heat altered parts of the ceramics. There does not appear to be any difference between speiss and arsenical copper furnace fragments. Every sample with attached slag also exhibited intensive alteration from heat damage to a depth of at least 1cm and at times penetrating the entire thickness of the furnace walls, resulting in bloating, increased porosity, vitrification of the ceramic, and mixing with the slag at the point of interaction. Volatile elements clearly penetrated the ceramic in many instances, as shown by the presence of increased metallic phases embedded in the bloated ceramics.



Figure 7.115 Plane polarized photomicrograph of sample FG-012232 showing typical technical ceramic microstructure.

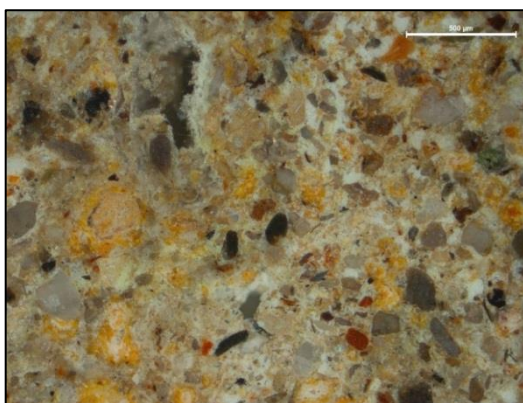


Figure 7.116 Cross polarized photomicrograph of sample FG-012232 showing typical technical ceramic microstructure.

Bulk chemical data for the ceramics were obtained through a series of area analyses conducted at a standard 100X magnification covering areas of approximately 400 μm by 500 μm (Table 7.23). Analytical totals were quite variable due to porosity inherent in ceramic fabrics, ranging from just about 60% in highly porous and heat altered samples up to 80% in the denser ceramic crucibles. The amount of computer modelling necessary to normalize these totals is expected to account for some of the variability observed in the results.

Despite this, much of the bulk data, with a few notable exceptions, appears consistent across all sample types. The only pattern between function and composition which could be identified is the relatively elevated calcium oxide content of the crucibles (mean 17.2 wt%) when compared to the furnace fragments (mean 8.6 wt%). However, it should be noted that four furnace fragments also contained elevated calcium oxide content that reached levels similar to those of the crucibles. This variability is assumed to represent the natural range found in the clay sources rather than differences in function or metallurgical technique. That being said, there is a clear correlation between high calcium content and known provenience: all technical ceramics uncovered from slagheap A were high in calcium oxide ($n=4$; mean of 17.6 wt%), while the only two objects from slagheap D had very little calcium (mean of 1.9 wt%). Since no other samples could be assigned to any specific area, it is difficult to ascertain whether this is indeed representative of the original distribution of technical ceramics or due to sampling bias.

Table 7.23 SEM-EDS bulk chemical results for Arisman technical ceramics. Results normalized to 100%.

Function	Type	Sample	Area	No. analyses	Na ₂ O	MgO	Al ₂ O ₃	SiO ₂	P ₂ O ₃	SO ₃	Cl	K ₂ O	CaO	TiO ₂	MnO	FeO	CuO	As ₂ O ₃	SrO
Crucible	Copper/Black	FG-030116B	1A47	3	2.3	2.9	13.1	53.7	b.d.l.	0.3	0.4	2.7	17.7	0.5	b.d.l.	5.9	0.1	0.4	b.d.l.
	Speiss	FG-0111993		6	2.1	3.4	13.9	52	0.4	0.5	0.3	3	17.8	0.6	0.1	5.4	b.d.l.	0.6	b.d.l.
		FG-030119A	1A50	5	1.5	3.4	12.4	45.8	b.d.l.	7.8	0.6	2.2	19.4	0.1	b.d.l.	5.3	b.d.l.	1	b.d.l.
		FG-030119B	1A50	3	2.9	3.9	14.6	54	b.d.l.	b.d.l.	b.d.l.	1.3	14.3	0.8	b.d.l.	7.4	b.d.l.	0.7	b.d.l.
		Mean				2.2	3.6	13.6	50.6	0.4	4.1	0.4	2.2	17.2	0.6	0.1	6	b.d.l.	0.8
Furnace	Copper	FG-012235A		6	1.9	4.2	14.2	51	0.4	2.7	0.5	3.3	10.6	0.7	0.1	5.7	0.3	4.3	b.d.l.
		FG-0301113	1A45	6	1.9	3.5	13.8	59.9	b.d.l.	b.d.l.	0.3	2.8	9.1	0.8	b.d.l.	5.9	1.3	0.7	b.d.l.
		FG-030665		3	2.9	3.1	14.5	66.7	b.d.l.	b.d.l.	0.2	3.2	3.3	0.6	b.d.l.	5.6	b.d.l.	b.d.l.	b.d.l.
		FG-030669		3	2.5	2.4	14.4	63.8	b.d.l.	b.d.l.	0.3	3.7	5.6	0.7	b.d.l.	6.5	b.d.l.	b.d.l.	b.d.l.
		FG-030670		3	2.4	4.5	15.7	51.6	b.d.l.	b.d.l.	0.3	1.3	16.9	0.7	b.d.l.	6.7	b.d.l.	b.d.l.	b.d.l.
		FG-030671		3	2.1	4.5	16.5	53.5	b.d.l.	b.d.l.	0.2	1.6	13.9	0.7	0.2	6.8	b.d.l.	b.d.l.	b.d.l.
		FG-030672A		3	2.6	2.5	14.4	68.5	b.d.l.	b.d.l.	0.2	3	2.2	0.6	b.d.l.	6.1	b.d.l.	b.d.l.	b.d.l.
		FG-030672B		3	2.5	2.6	14.8	67.7	b.d.l.	b.d.l.	b.d.l.	3.2	1.9	0.7	b.d.l.	6.6	0.3	b.d.l.	b.d.l.
		FG-993152A		3	2.2	2.9	13.8	55.1	0.2	0.4	0.2	2.7	15.6	0.6	0.2	5.7	0.2	0.3	b.d.l.
		FG-993152B		3	1.9	2.3	13.1	49.8	b.d.l.	1.3	0.1	2.4	7	0.7	0.3	17	3.7	0.5	b.d.l.
	Mean				2.3	3.3	14.5	58.8	0.3	1.5	0.3	2.7	8.6	0.7	0.2	7.3	1.2	1.5	b.d.l.
	Speiss	FG-012232	1D45	3	2.4	3.5	13.3	53.9	0.3	0.8	0.6	3.3	16.1	0.7	0.2	5.0	b.d.l.	b.d.l.	b.d.l.
		FG-012234	1D45	3	2.4	2.7	15.3	66	b.d.l.	b.d.l.	0.1	3.3	2.4	0.8	b.d.l.	7	b.d.l.	b.d.l.	b.d.l.
		FG-030117B	1A48	3	1.7	3.1	11.5	56.3	b.d.l.	b.d.l.	b.d.l.	2.6	18.9	b.d.l.	b.d.l.	5.2	b.d.l.	0.7	b.d.l.
		Mean				2.2	3.1	13.3	58.7	0.3	0.8	0.4	3.1	12.5	0.7	b.d.l.	5.7	b.d.l.	0.7
	Other	Lime plaster	FG-000117D	surface	1		2.2	0.5	1.4	b.d.l.	0.7	b.d.l.	b.d.l.	94.7	b.d.l.	b.d.l.	0.3	b.d.l.	b.d.l.

Another distinction which could be tentatively seen is the difference in sulphur content between the crucible and furnace fragments. However, this difference is largely due to a single high sulphur crucible fragments (FG-030119A) which contained 7.8 wt% of SO_3 and largely skewed the results. Although no sulphur was detected in any of the furnace fragments related to speiss production, this could again be due to sampling bias rather than any real trend. Given that the current interpretation of speiss production at Arisman assumes the ore source to be arsenopyrite, one would expect there to be detectable amounts of sulphur present in the ceramics relating to these operations. That there is none is surprising but does not invalidate the theory since the sample count is so low.

Although arsenic is clearly more consistently present in the speiss-related furnace and crucible fragments, it is still present in detectable levels in many of the copper smelting ceramics. This is assumed to be caused by arsenic's strong tendency to volatilize and penetrate within the ceramics even when present in low quantity. It is also possible that the post-depositional proximity of arsenic-bearing material to porous ceramics may have led to the leaching of the element into ceramics which were not related to speiss smelting. However, and as will be discussed in the section on Arisman's slag, many of the metallic copper prills associated with copper smelting also contained detectable amounts of arsenic, so its presence in the ceramic is likely to be the direct result of human activity rather than taphonomic processes.

Conversely, the presence of copper is limited to ceramics involved in copper smelting. This comes as no surprise since speiss smelting is not thought to have involved the use of copper-bearing ores. Given copper's low volatility and strong surface tension, the element was only detected in ceramics bodies which had strongly interacted with the adjacent copper smelting slag.

In all other respects (Na_2O , MgO , Al_2O_3 , P_2O_3 , K_2O , TiO_2 , MnO , and FeO) the ceramics are consistent across functional types, occupation periods, and activity areas.

In order to assess the refractoriness of Arisman's technical ceramics, their compositions were plotted according to a diagram proposed by Freestone (1989). The diagram clearly shows the two separate clusters formed by the high and low calcium clays already discussed (Figure 7.117). What is interesting is that the low calcium clays plot in the zone typical of low refractory prehistoric ceramics which bloom by 1300°C , but that most of the Arisman material actually plot quite far from this region. They are indeed very poorly refractory and, as could be surmised by the amount of vitrification apparent in furnace material, probably could not

handle extended periods of operation. The melting of the furnace walls thus assuredly contributed to slag formation.

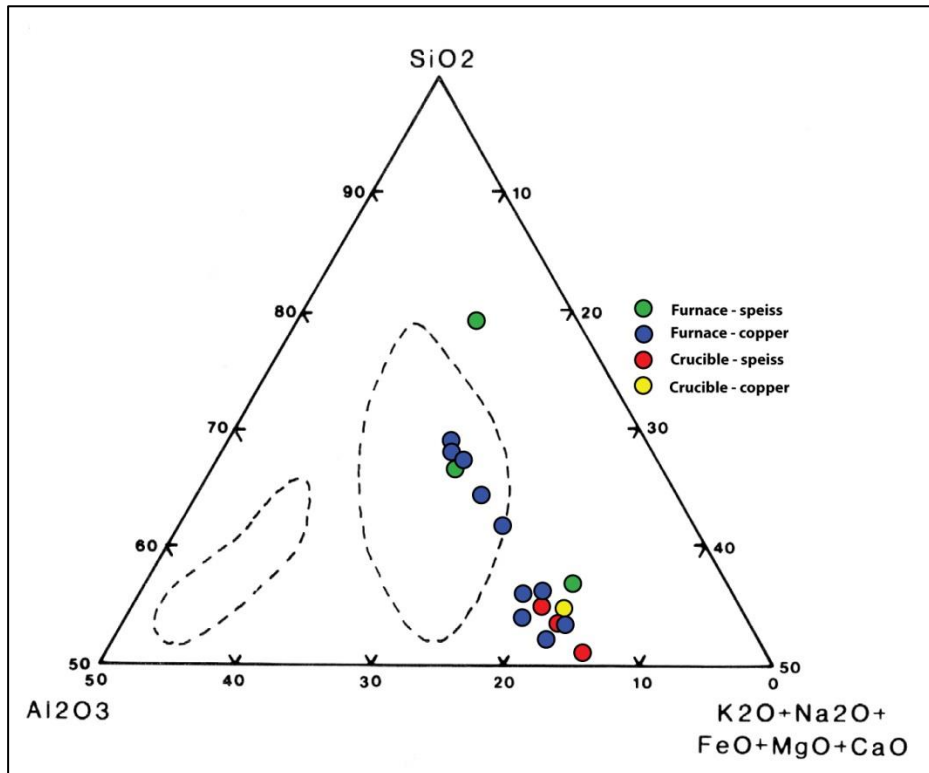


Figure 7.117 Composition of technical ceramics from Arisman plotted according to elements known to greatly affect refractoriness. The outlined section to the bottom left delineates the composition of modern refractory firebricks while the one in the centre is of clays that bloat by 1300°C. Adapted from Freestone (1989).

The evidently poor refractory properties of the clays also further reinforce that the crucibles could not have been exposed to long periods of extreme heat or they would also have experienced the same level of alteration as the furnace fragments. In many cases, slag was present as thick 0.5-2 cm layers covering the inside of the crucible fragments and occasionally also as drippings on the outside of the vertical walls (Figure 7.118). Although these fragments usually showed some clear heat damage on the contact surface with the slag, such as bloating and discolouration, the interface between the two does not appear to have sustained high temperatures over extended periods. In fact the interface between the slag and ceramics exhibits only minimal interaction and thus appears to have been relatively cold (Figure 7.119).

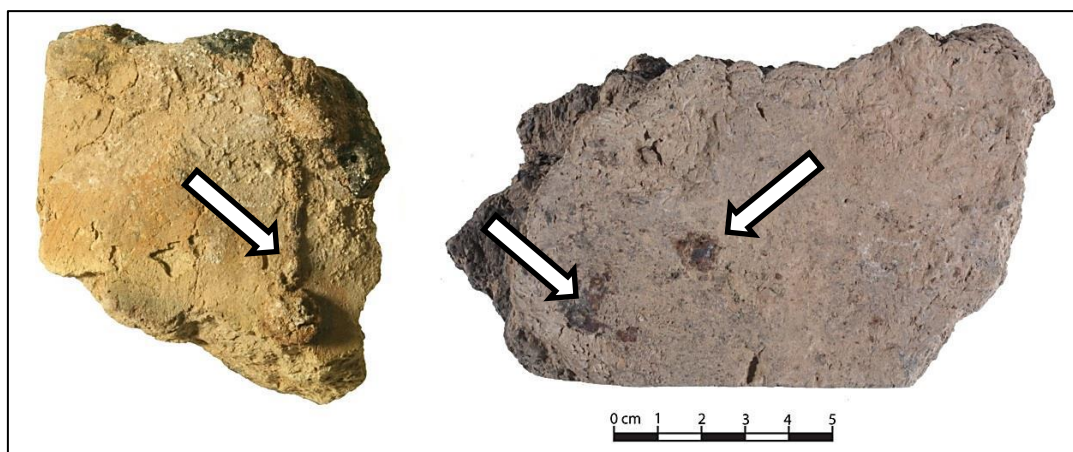


Figure 7.118 Photographs of exterior wall of two crucible fragments. Object on the left is sample FG-030116B while the one on the right is FG-030119A. Note the droplet downward direction of flow on the left sample helped in orienting the ceramic body sherd.



Figure 7.119 Cross section photograph of crucible fragments FG-030119B on the left, and FG-030116B on the right.

In an effort to avoid repetition and because the slag attached to most of these technical ceramics is essentially identical to the rest of the slag samples recovered from the site, they will be discussed together in section 7.2.4 rather than separately here. Two samples, however, are worth discussing here as the findings relate more to the nature of the technical ceramics than to the slag.

The first of these two samples is the piece of furnace wall with the tuyère or vent hole already mentioned (FG-030113) found within slagheap A. Two distinct areas of the specimen were mounted together to obtain a picture of the scale of vitrification and interaction with the slag. As can be expected, areas closest to the hole are highly vitrified and contain abundant phases commonly associated with prevailing oxidizing conditions. Magnetite spinels, often clustered in elongated bands could be observed throughout the slag, indicative of the formation of a sequence of oxidized surfaces continuously covered by new layers of slag. The slag is further dominated by skeletal fayalite chains, dark elongated pyroxene crystals rich in calcium and aluminium and smaller angular crystals approaching the composition of

hedenbergite (Figure 7.120). The bulk analysis of the slag showed it to be almost identical to the ceramic body but with an increase in iron and magnesium and an equivalent decrease in silicon (Table 7.24). This is understood to be the direct result of interaction with an iron-rich ore body causing the ceramic to vitrify and form slag.

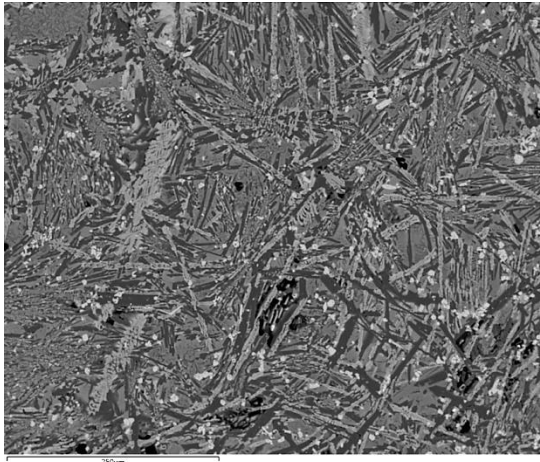


Figure 7.120 SEM image of sample FG-030113 showing typical slag matrix. The light grey blebs are magnetite, the skeletal chains are fayalite, the dark elongated crystals are pyroxenes, and the microcrystalline matrix is mainly composed of hedenbergite crystals.

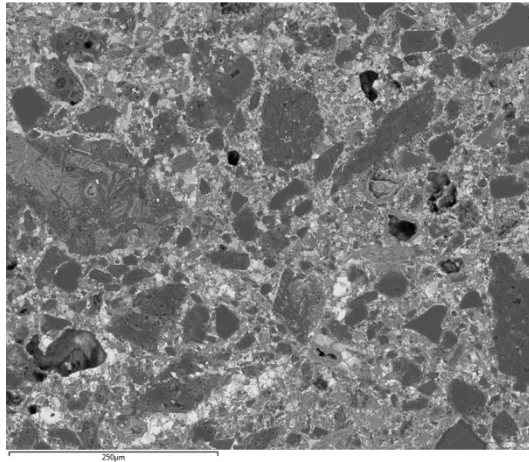


Figure 7.121 SEM image of sample FG-030113 showing ceramic body with matte and arsenic phases filling available porosity.

What is particularly interesting is the presence of detectable levels of arsenic in much of the lightly heat altered ceramic body (Figure 7.121) but absence in the heavily vitrified phases and slag. This reinforces how arsenic gases, in the absence of copper metal, tend not to partition into the slag but rather to escape through any available porosity, in this case ceramic, where they can then condense and precipitate upon cooling. In this case the ceramic body also contained minor quantities of copper oxide in association with this arsenic, presumably also volatilized and redeposited in the ceramic in the same way as the arsenic. The penetration of these elements is relatively low, entering the ceramic only up to a maximum depth of approximately 1 cm.

Table 7.24 Bulk chemical composition of the slag and ceramic fabrics of furnace wall fragment FG-030113. The results are normalized totals resulting in each case from the mean of three area analyses using SEM-EDS.

Phase	NaO ₂	MgO	Al ₂ O ₃	SiO ₂	P ₂ O ₃	SO ₃	Cl	K ₂ O	CaO	TiO ₂	MnO	FeO	CuO	As ₂ O ₃
Ceramic	1.8	4.0	13.8	60.6	b.d.l	b.d.l	0.3	2.8	10.9	0.8	b.d.l	5.1	b.d.l	b.d.l
Heat-altered ceramic	2.0	3.1	13.8	59.3	b.d.l	b.d.l	0.3	2.9	7.2	0.8	b.d.l	6.7	2.7	1.3
Vitrified ceramic	2.2	3.8	14.5	56.4	b.d.l	0.4	0.1	2.7	13.3	0.7	b.d.l	6.0	b.d.l	b.d.l
Slag	1.4	3.3	15.2	41.3	0.5	0.4	0.1	2.1	9.5	0.3	0.6	24.8	0.6	b.d.l
Matte-infused ceramic	1.5	1.3	8.9	35.3	b.d.l	14.3	0.9	1.2	1.8	0.4	b.d.l	8.7	25.8	b.d.l

In some areas of the sample, copper sulphide and oxide appears to have also entered the ceramic body up to approximately 0.5cm deep. The penetration in of itself is not surprising

given matte's relatively low surface tension compared to both slag and metallic copper (Donald 1997; Hamuyuni et al. 2012), but the presence of sulphide phases so close to the oxidizing atmosphere created by the tuyère is remarkable. It seems that the matte must have suffused the ceramic body first as it melted out of the charge and that the sulphur simply remained trapped within the ceramic porosity despite the prevailing atmospheric conditions. Given that the tuyère is unlikely to have been right at the base of the furnace, a higher amount of matte likely penetrated the furnace bottom to a much greater depth, which would have resulted in significant copper losses during the smelting process. Unfortunately, no such furnace base samples were identified or analysed as part of this thesis to confirm this.

The second piece of technical ceramic with interesting slag attached is sample FG-012235A. This sample, already described macroscopically as a series of two furnace linings with three greenish layers, provides the only available analytical evidence of sequential smelting events occurring over a presumably short period of time. Since all other samples are disconnected fragments representing just a single event, this particular sample offers a unique opportunity to assess the consistency in smelting and furnace building technology and materials of a single furnace. Of course, there remains the possibility that an old furnace was relined at a much later date, but given the relatively short occupation of each area and the intensity of industrial activities this is highly unlikely. It should be noted that the find location for this sample is not known but given the similarity in fabric to the other furnace fragments recovered from areas A and D and the nature of the slag remains attached to it, it is believed to have originated from one of those two areas.

Microscopic comparison of the two ceramic layers immediately revealed differences in the grain sizes. The bottom (older) layer is composed of very fine clay with only a few larger mineral grains mainly in the 15-30 μm range (Figure 7.122), while the top (younger) layer is dominated by larger grains measuring 20-100 μm (Figure 7.123). While both of these fabrics are extreme variants of what is typically seen throughout the assemblage, most samples are rather similar to the topmost layer observed here and no other analysed ceramic was as fine grained as the bottom furnace lining. Given the range of mineral inclusions seen in all furnace samples, it does not appear that mineral temper was being added, but rather reflects the natural range of grains found in the clay. The bottom layer's microstructure is therefore unique amongst the Arisman technical ceramics analysed.

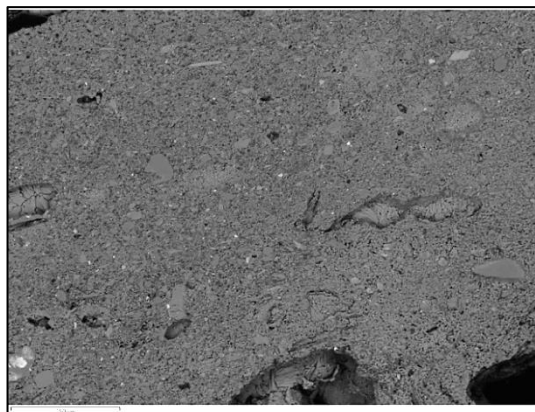


Figure 7.122 SEM image of sample FG-012235A's bottom ceramic layer.

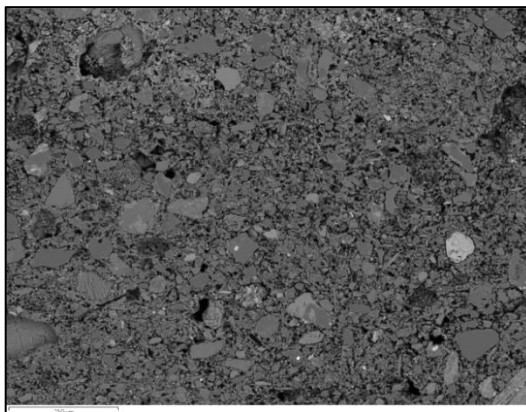


Figure 7.123 SEM image of sample FG-012235A's top ceramic layer

Despite the clear microstructural differences between the two layers, their chemical compositions are in actuality nearly identical (Table 7.25), with most of the elemental variability well within the expected range of natural soil fluctuations, differences potentially introduced by the levigation process, or instrumental detection range. The only notable difference which cannot be thus explained is the arsenic content, which, along with copper, are assumed to be introduced by the smelting process rather than originally present in the ceramic.

Table 7.25 Chemical composition of the two ceramic layers of sample FG-012235A as determined by SEM-EDS. Results are the mean of three area analyses and normalized to 100%.

Area	Na ₂ O	MgO	Al ₂ O ₃	SiO ₂	P ₂ O ₃	SO ₃	Cl	K ₂ O	CaO	TiO ₂	MnO	FeO	CuO	As ₂ O ₃
Bottom ceramic	1.2	4.7	15.2	50.9	0.4	2.2	0.3	3.5	10.5	0.8	0.2	6.6	0.4	3.1
Top ceramic	2.7	3.8	13.2	51.1	0.4	3.2	0.3	3.1	10.6	0.6	0.1	4.7	0.3	5.5
Vitrified ceramic	2	1.2	5.8	59.7	b.d.l.	b.d.l.	b.d.l.	9.1	2.8	0.4	b.d.l.	9	0.7	9.4

Not only is this sample unique amongst the analysed technical ceramic assemblage for having a very fine ceramic body, but also for the blueish green layers that separate the furnace linings. Upon closer inspection, the first impression of these as copper corrosion or slag layers proved false. They are in fact ceramic bodies which have been infused with metal or metal oxide gases which have later undergone minimal corrosion (Figures 7.124 and 7.125). Since these layers are not formed of slag but rather of volatile elements, it seems most probable that this particular sample originated from an upper area of the furnace wall. That it was re-lined also suggests that it belonged somewhere along the back of the furnace since the front is known to have been destroyed after each smelt.

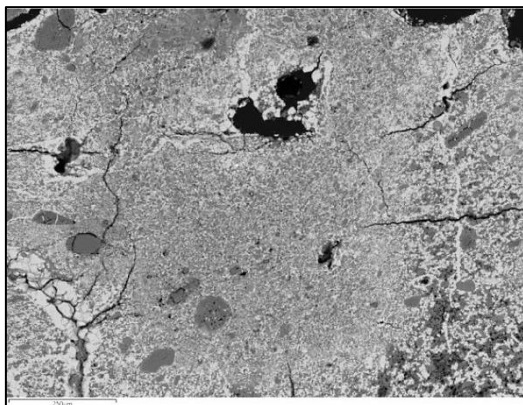


Figure 7.124 SEM image of sample FG-012235A's bottom blueish-green deposit.

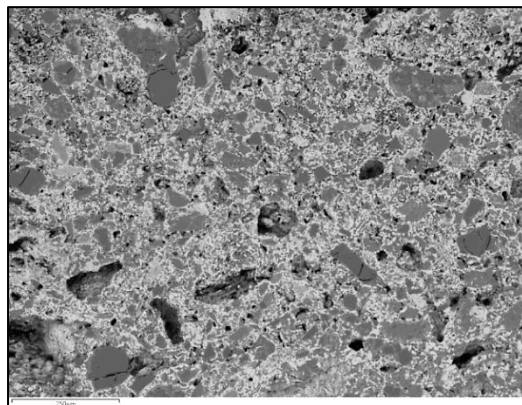


Figure 7.125 SEM image of sample FG-012235A's top blueish-green deposit.

Bulk chemical analysis confirmed that these layers were mainly composed of ceramic which had been greatly enriched in arsenic and to a lesser degree with zinc and copper (Table 7.26), all elements known to be volatile under typical smelting conditions. Spot and area analyses of the bright phases filling the ceramic voids showed them to be rather complex compounds of arsenic, calcium, iron, and copper oxide. Although no known naturally occurring minerals have a composition that matches these phases, calcium and arsenic form a wide variety of compounds which readily combine with all of the elements represented here (such as in nickenichite $(\text{Na}_{0.8}\text{Ca}_{0.4}(\text{Mg}, \text{Fe}^{3+}, \text{Al})_3\text{Cu}_{0.4}(\text{AsO}_4)_3)$ and lukrahnite $(\text{Ca}(\text{Cu}, \text{Zn})(\text{Fe}, \text{Zn})(\text{AsO}_4)_2(\text{OH}, \text{H}_2\text{O})_2)$ for example) (Robinson 1918, Hughes et al. 2011).

Table 7.26 Composition of layered deposits in on inner surfaces of furnace fragment FG-012235A as determined by three area analyses by SEM-EDS. Results are normalized to 100%.

Area	Na ₂ O	MgO	Al ₂ O ₃	SiO ₂	P ₂ O ₃	SO ₃	Cl	K ₂ O	CaO	TiO ₂	MnO	FeO	CuO	ZnO	As ₂ O ₃
Top deposit	2	1.8	10.2	41.5	b.d.l.	0.7	b.d.l.	6.4	6.2	0.5	b.d.l.	3.5	6.9	0.2	20.3
Middle deposit	4.2	2.4	11.2	33.3	b.d.l.	1.2	b.d.l.	6.4	8.1	0.6	b.d.l.	4.7	4.1	0.3	23.7
Bottom deposit	3.7	1.7	6.5	37.4	0.2	0.2	0.14	3.1	8	0.2	0.2	12.2	6.2	1.9	18.4
Bright phases	5.2	5.4	b.d.l.	0.4	0.3	0.2	b.d.l.	1.7	13.9	b.d.l.	0.3	9.7	8.9	0.5	53.5

These blueish-green deposits cannot therefore be described as slag surfaces but rather redeposited volatile elements in a high temperature environment which precipitated upon cooling within the ceramic porosities. A comparison of the composition of the ceramic, enriched ceramic, and the bright phases reveals which elements were thus introduced into the ceramic fabric during smelting (Figure 7.126). The composition of the enriched ceramic is generally bound between that of the original furnace wall and the bright arsenic oxide phases. Some exceptions exist, however, in that the magnesium and calcium in the enriched ceramic are notably lower while potassium is higher than both other phases. This is most likely the result of post-depositional corrosion causing ions to migrate between the ceramic

and metallic oxide phase. The comparison between the bulk compositions of the original ceramic with that of the enriched ceramic is therefore much more representative of the addition of material occurring during smelting.

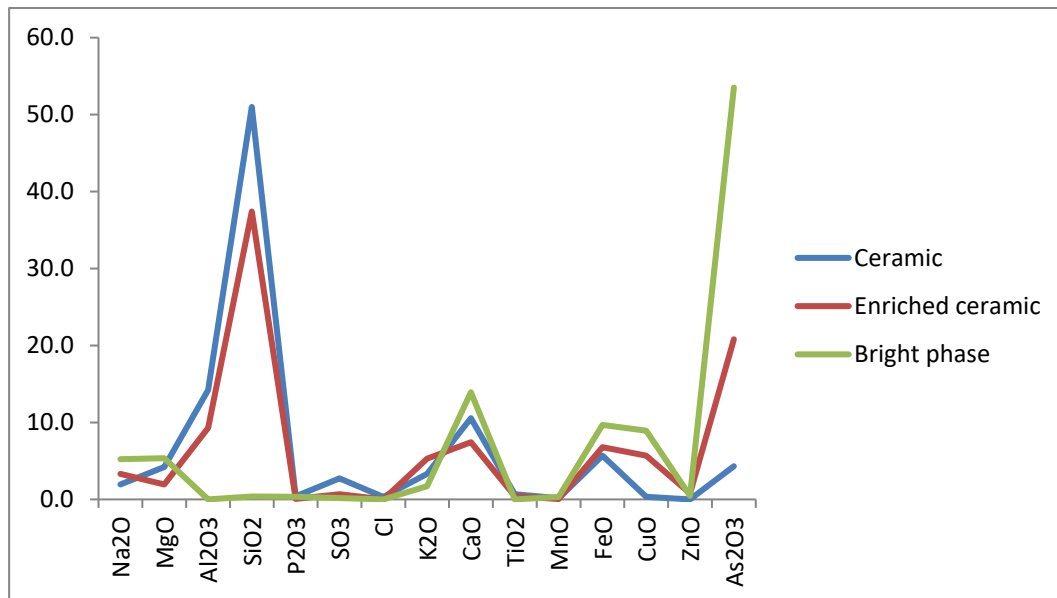


Figure 7.126 Line graph comparing the compositions of the means of three distinct phases of sample FG-012235A.

7.2.3 Ores and Tailings

A total of 16 specimens made available for this research can best be described as mineral fragments recovered from Arisman I. While two of these are known to originate in the secondary processing centre of Area C, the rest are unfortunately of unknown provenience, severely limiting their interpretative value.

That being said, all but two samples appear to have been collected based upon the presence of green staining on otherwise unremarkable stones. Such field identification and sampling of green minerals was, of course, based upon the assumption that copper smelting was the main metallurgical activity of Arisman and thus largely biased in favour of minerals perceived to be related to it. Since the exposed areas of the site have not only revealed copper smelting but also ferrous speiss extraction as well as silver cupellation and possible lead smelting, this collection bias is problematic as it does not offer any potential analytical evidence of non-copper bearing deposits.

Fourteen of the minerals can be classified as a single group composed mainly of a dense iron rich matrix with a surface layer of greenish to blueish copper mineralization (Figure 7.127). Exactly half of these have white quartz veins (Figure 7.128), which in some cases also have a

greenish tint. Only one of these samples (FG-011992) stands out particularly from the rest for its grey metallic-looking inclusions throughout the matrix (Figure 7.129).

Two samples were found entirely distinct from the rest of the assemblage. One of these, FG-030126, is very light, entirely yellow, and therefore most probably composed of sulphur compounds. The other, FG-030125, is very dense, dark grey, and shows no green staining at all but instead some reddish iron corrosion and yellow sulphide inclusions in cross section (Figure 7.130).

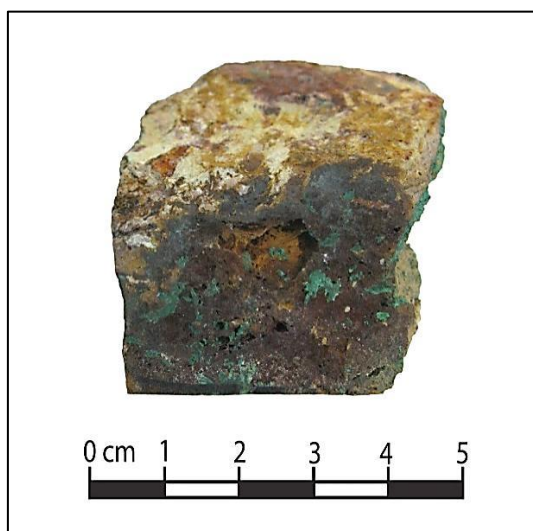


Figure 7.127 Photograph of sample FG-992864, a dense iron-rich mineral with green copper oxide staining.

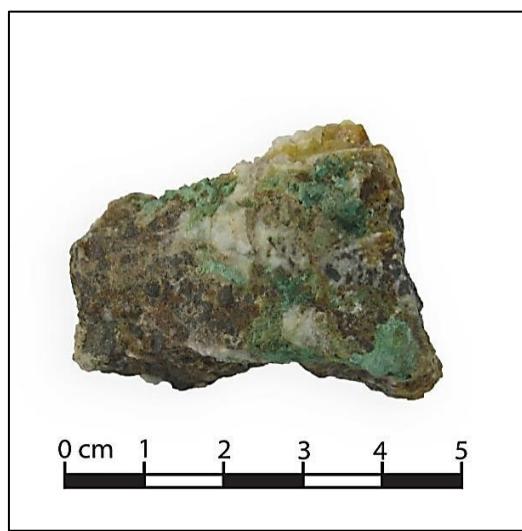


Figure 7.128 Photograph of sample FG-030663 showing typical dense iron-rich mineral with green copper oxide staining and white quartz veins.

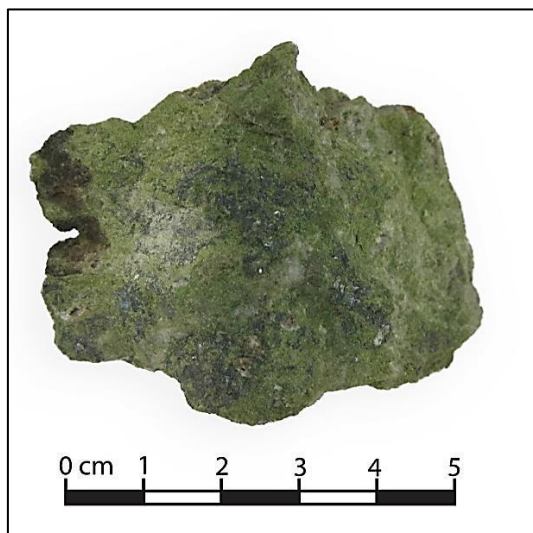


Figure 7.129 Photograph of sample FG-011992 showing once more a dense iron-rich mineral with green copper staining. In this case the sample also has metallic inclusions.

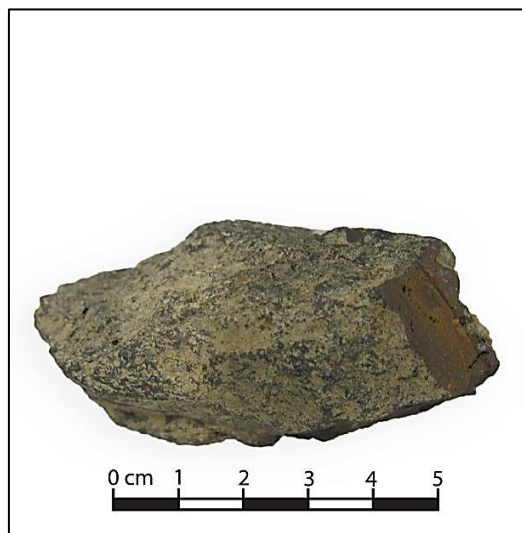


Figure 7.130 Photograph of the iron-rich mineral lacking any green staining. Sample is FG-030125.

Since most of the samples were nearly identical macroscopically, and because much has already been done on the analysis of minerals in and around Arisman (Pernicka et al. 2011;

Stöllner 2011; Stöllner et al. 2011a) only two specimens were prepared for more detailed microscopic and chemical analysis. These two samples (FG-011992 and FG-030125) were selected because they were atypical and it was hoped that they would help in identifying the nature of arsenic-bearing deposits exploited at Arisman.

Sample FG-011992 is characterized by magnetite laths in matrix of green plagioclase feldspar approaching the composition of anorthite and calcium carbonate (Figures 7.131 and 7.132, Table 7.27). No arsenic or copper was detected by bulk or in any phases present. Although it may have been brought to the site because its green colour was mistakenly thought to be indicative of copper content, there is no concrete evidence of it actually having been smelted or processed. The mineral is too rich in aluminium to have been useful as an effective calcium or silicon flux and if it had been added in any quantity to the smelting charge the increased aluminium content would be reflected in the slag. That this is not so suggests that this mineral is unlikely to have been related to metallurgical activities at the site.



Figure 7.131 Photomicrograph of Sample FG-011992 in cross-polarized reflected light. The dark angular crystals are magnetite while the matrix is mainly composed of greenish anorthite while the white blebs are calcium carbonate. Frame is 2.4mm wide.

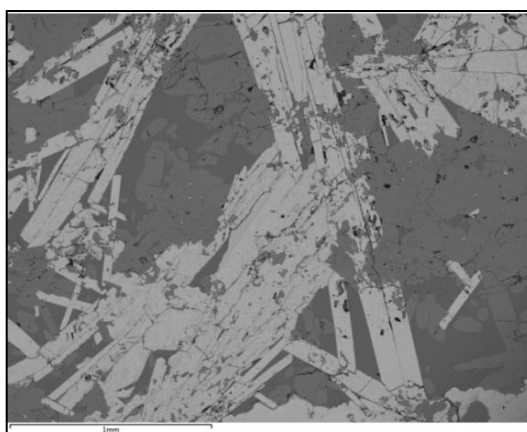


Figure 7.132 SEM image of FG-011992's matrix. The elongated crystals are iron oxide while the light grey subangular crystals anorthite and the darker phases are calcium carbonate.

Table 7.27 Bulk composition of two mineral fragments from Arisman as determined by SEM-EDS. Results are the means of three area analyses for each sample normalized to 100%.

	Al ₂ O ₃	SiO ₂	P ₂ O ₅	SO ₂	Cl	CaO	TiO ₂	MnO	FeO	CuO	As ₂ O ₃
FG-011992	19.7	30.5	b.d.l.	b.d.l.	b.d.l.	27.7	0.8	0.4	20.9	b.d.l.	b.d.l.
FG-030125	0.7	3.3	0.3	0.7	0.1	0.3	b.d.l.	b.d.l.	94.3	0.1	0.3

The second specimen in this category, FG-030125, is mainly composed of iron oxides and hydroxides with remnants of primary iron sulphide (Figures 7.133 and 7.134). Although no discrete copper-bearing or arsenic-bearing particles were observed, the bulk composition shows that trace amounts of both elements are present in the sample (Table 7.27), but in

such low quantity that they could hardly have been economically recoverable. Although this particular sample cannot be considered an arsenic or copper ore, it may have originated from a deposit suitably rich in either or both elements to have been a viable source of chalcopyrite, arsenopyrite, and their associated secondary oxidation minerals. This sample is therefore best described as tailings, discarded during beneficiation. Given its high iron content, it could also potentially have been used as a fluxing agent if the charge was too rich in silicon, but once more there is little direct evidence of this at Arisman.



Figure 7.133 Photomicrograph of sample FG-030125 under cross-polarized reflected light. The grey phases are iron oxide while the yellow phases are iron sulphide. The sulphide phases appear under the microscope mainly in the porosities, still visible through the clear resin. Frame is 1.2mm wide.

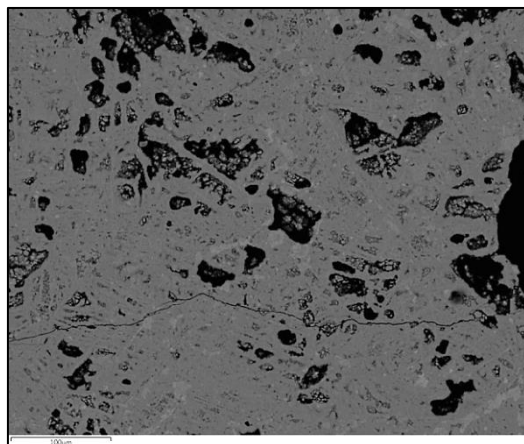


Figure 7.134 SEM image of mineral sample FG-030125. Matrix is largely iron oxide with the occasional light grey phases of iron sulphide. Dark blebs are porosity filled with mounting resin.

7.2.4 Slag

The slag material from Arisman has been subjected to two previous studies which focused on different aspects of reconstructing the metallurgical processes of Arisman. The investigation conducted as part of the post-excavation analysis by the DAI mainly revolved around the bulk chemical characterization and superficially covered the microstructural nature of the slags (Pernicka et al. 2011) as the research followed conventional archaeometallurgical practice for very large industrial slagheaps assumed to be of fairly homogenous compositions. The smaller and more focused parallel study (Boscher 2010; Rehren et al. 2012) highlighted diversity in the slag remains which could only be explained through two separate metallurgical processes – arsenical copper smelting and iron-arsenic speiss smelting. However, this second publication was based on analytical work conducted as part of an MSc dissertation which acknowledged limitations due to the small number of samples. Just fifteen specimens were analysed, divided evenly between speiss and arsenical copper processes. In addition to this concern, two samples of dense glassy black slag containing copper sulphide, arsenical copper, and iron arsenide phases identified during that study remained ambiguous and their place in the smelting

technology of Arisman was left largely hypothetical. The aim of revisiting the slag from the site was therefore twofold: to expand the number of speiss and arsenical copper slag analyses, and to try to clarify the formation process for the dense black slag and its role in the arsenical copper *chaîne opératoire*.

The three slag categories described in this section are mainly defined by their intended product as established through macroscopic, microscopic, and chemical analysis. The three types are 'green', 'brown', and 'black', referring to arsenical copper slag, ferrous speiss slag, and glassy black slags respectively. Arisman's slag deposits are mainly composed of green and brown slag in roughly equal proportions, while black slags are much less common although these were not identified as distinct by the field archaeologists and therefore of unknown total quantity (Pernicka, pers. com.). Each type encompasses a series of characteristics which do not necessarily apply to every one of the samples in that category. For example, while the vast majority of green slags are greyish in cross section, dense, and have green corrosion on the surface, some samples may lack one or more of these attributes but are considered arsenical copper slags based on the presence of specific phases observed microscopically or chemically. As such, while macroscopic evidence was an adequate preliminary indicator of the slag type, chemical and microscopic analysis are necessary in order to confidently assign them to any category (Boscher 2010, 60-63). Bulk ratios of arsenic to copper and the presence and absence of certain prills and phases are much stronger indications of the intended output of the operation than density, colour, and surface corrosion alone.

Slag samples were first categorized according to their macroscopic characteristics and then re-assessed after microscopic and chemical investigations. Samples which did not undergo further analysis may therefore be incorrectly categorized. However, since there was no increased prevalence of false identification in one category versus any other, this potential reporting error should cancel itself out and is thus not expected to have any significant impact on the distribution patterns. The Arisman I slag samples available for analysis are summarized in Table 7.28. In addition to the samples listed below, 16 fragments of technical ceramic (see section 7.2.2) had adhering layers of slag, the analysis of which will be included in this section.

Table 7.28 Arisman slag samples available for analysis. Numbers in parentheses are the samples which were not analysed by SEM-EDS. Not included in this table are the ceramic samples with attached slag.

	Brown	Green	Black	Matte	Total
Area A	7 (1)	15 (5)	1	-	23 (6)
Area B	2	3 (3)	-	-	5 (3)
Area C	-	1 (1)	-	-	1 (1)
Area D	3 (2)	2 (2)	2	-	7 (4)
Unknown	3 (2)	24 (9)	6	2	35 (11)
Total	15 (5)	45 (20)	9	2	71 (25)

It would be a mistake to try to assess the distribution of the slag types according to their provenance given that just under half of the available samples come from unknown contexts and since field-sampling was conducted prior to the identification of the three slag types. Regardless, samples from the different known contexts will be contrasted in order to assess whether there is any variation linked to activity areas. This should provide a basic understanding of whether technological continuity existed across the activity foci of Arisman.

The results of the slag analysis will be presented separately for each category of slag and follow the same format in each case. The macroscopic characteristics of the samples will first be presented and will include a description of their morphology, density, surface corrosion, and colour. This will be followed by an overview of findings obtained from optical microscopy and SEM imaging to discuss the slag's full range of crystalline phases. Lastly, the bulk chemical compositions of the samples will be presented and discussed. The detailed analytical methodology is identical to that already used for Çamlıbel and will thus not be further discussed.

Microscopic descriptions of the exported samples will cover the entire spectrum of crystalline phases present in the majority of the available assemblage of slag. Special attention will be paid to sulphide and metallic phases as they are most relevant when discussing the intended smelting products. Individual samples will only be discussed when specific features relate to only a small subset of the main slag assemblage which highlight specific aspects of the smelting process.

In addition to these three categories, two fragments of matte were also analysed and will be briefly discussed below.

'Brown' Speiss Slag

Of the 15 slag samples categorized as speiss-bearing, three had previously been analysed in preliminary MSc research (Boscher 2010) while seven new samples were prepared and

investigated as part of this doctoral thesis. In addition to these ten slag fragments, three crucibles and three furnace fragments (which includes three previously analysed samples) had adhering slag which has been identified as speiss slag and will therefore also be discussed in this section. This brings the total of analysed speiss slags to 16.

Speiss slag is defined as slag which was formed in the production of iron arsenide (speiss). It has previously been referred to as 'brown' slag because of the tendency of the material to be covered by iron corrosion and contrasts starkly against the green copper-bearing slag. This is in fact a bit of a misnomer as the slags themselves are not brown but rather dark grey in cross section. Additionally, most of the samples which fall into this category also exhibit a number of yellow sulphide phases, usually located within the slag's cavities and pores.

Speiss slags are relatively low in density due to their highly porous nature, with large gas-formed cavities often visible to the naked eye. The majority of pores ranged between 1mm and 2mm in size but in some cases could reach several centimetres in diameter. Nearly all of these samples have flowing surface textures on the upper surface and several overlapping layers typical of tapped slags (Figure 7.135). Only one speiss slag specimen, FG-040919B, was found to diverge from this general description in that it was free of large porosity and did not show any of the typical characteristics of tapped slag (Figure 7.136). This particular sample is clearly associated with a small fragment of furnace wall (as determined by the presence of organic temper) and likely solidified within the furnace itself.



Figure 7.135 Photographs of two samples showing the typical features associated with speiss slag. Note the orange and yellow corrosion staining on the surface and in the pores. Also note the layered and flowing surface features typical of tapped slag. The sample on the left is FG-010506 while that on the right is FG-030123B.



Figure 7.136 Cross section of speiss slag fragment with attached furnace remains. This specimen is the only one of the speiss slags to show minimal porosity. Sample FG-040919B.

The microstructure of the newly analysed slag is largely consistent with those already described in previous publications (Boscher 2010; Rehren et al. 2012) although one of the major crystalline phases appears to have been wrongly identified. In the previous research, the authors determined that the most prominent crystalline phases belong to the melilite group. However, upon review of the composition of these previously reported phases and the newly acquired data, it appears that these crystalline phases would more accurately be described as pyroxenes in the solid solution range between augite $((\text{Ca},\text{Na})(\text{Mg},\text{Fe},\text{Al},\text{Ti})(\text{Si},\text{Al})_2\text{O}_6)$ and hedenbergite $(\text{CaFeSi}_2\text{O}_6)$ (Figure 7.137, Table 7.29) rather than melilite. Although alkaline pyroxenes are rather rare in typical smelting slags (Bachmann 1982, 14) due to the minor amount of aluminium usually present, the Arisman speiss slag appear to be rich enough in the element (9.2 wt% of Al_2O_3 by bulk) to allow their formation. These phases are unlikely to be of the melilite group since such minerals always contain calcium oxide above 30 wt%, something which has not been observed in any of the analysed crystalline phases of the speiss slags. Although the metal to silicon atom percent ratio does not always exactly match the typical pyroxene ideal of 1:1, it does come close in most instances. The microstructure of the speiss slag is thus mainly dominated by a mixture of two types of pyroxene crystals: large rhomboid crystals approaching the composition of iron-rich augite, and smaller fern-like dendritic crystals nearer to the composition of hedenbergite. In one sample (FG-993154) augite crystals were found to be composed of smaller dendritic crystals but these still roughly extended to a rhomboid shape.

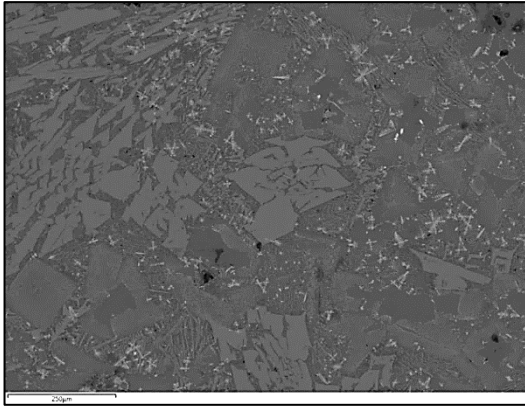


Figure 7.137 SEM image of sample FG-040920A showing typical slag matrix for speiss slags. The dark angular crystals and grey dendritic crystals are pyroxenes while the larger light grey crystals are kirschsteinite. The light grey dendrites are wüstite.

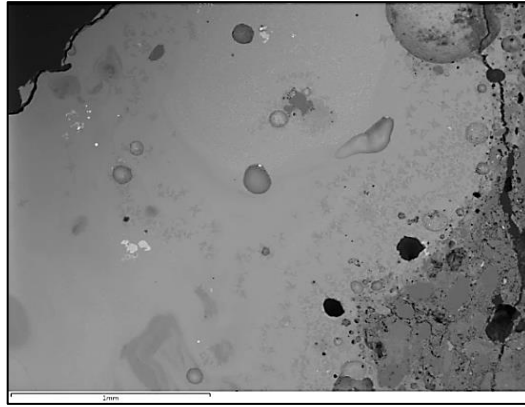


Figure 7.138 Glassy speiss slag matrix on top of ceramic body. The bright phases are speiss prills while the light grey phases are magnetite clusters. SEM image of sample FG-011993.

Magnetite clusters appear throughout all samples (Figure 7.138), as do occasional smaller clusters of wüstite in regions where more strongly reducing conditions prevailed. In one sample, FG-012232, the conditions were so reducing that iron prills also formed (Figure 7.139). These iron prills were rare, isolated, and in such small quantity that it is highly unlikely that a larger consolidated mass or bloom ever formed. Since iron prills were also observed in Çamlıbel slags and in other Late Chalcolithic slags produced in the most rudimentary of furnaces (Radivojević, pers. com.), it does not appear that the formation of small amounts of iron metal is a particularly unusual occurrence even in early copper smelting slags.

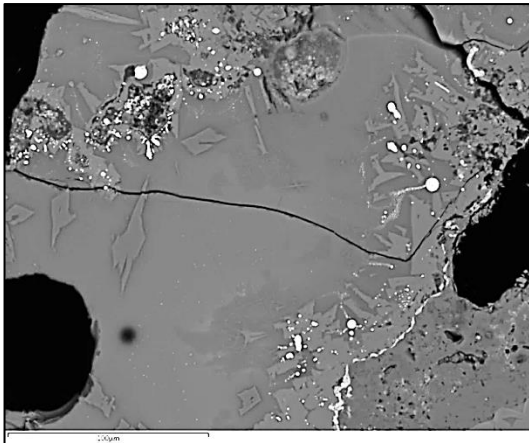


Figure 7.139 SEM image of sample FG-012232 with the very bright metallic iron prills present in a single small area of the sample.

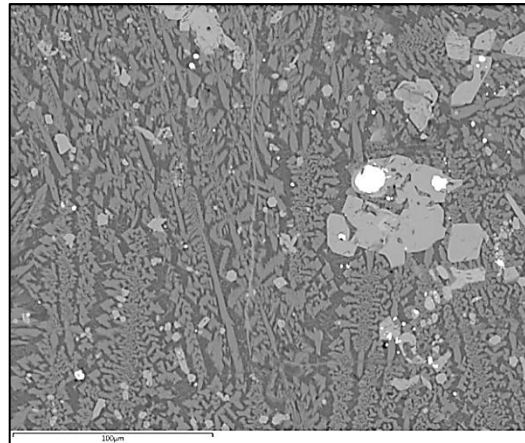


Figure 7.140 SEM image of sample FG-010506's matrix. The bright prills are speiss while the light grey blebs are magnetite and the grey dendrites are kirschsteinite.

In addition to these phases, four of the speiss slags also contained a few isolated olivines, mostly in the form of kirschsteinite. One speiss sample (FG-010506) stood out from the others in that it contained no pyroxene crystals at all but was mainly composed of

kirschsteinite in a microcrystalline matrix. This did not, however, result in significant bulk compositional differences (Table 7.31).

One previously analysed sample (FG-030119B) (Boscher 2010) also contained dark lath-shaped calcium aluminium silicate crystals which have no analogous naturally-occurring minerals. Once again, their presence did not affect the overall composition of the slag and is likely the result of micro-conditions in the smelt rather than representing a shift in technology.

No matte and very few sulphide-bearing phases were identified during the analysis, suggesting that either the ores were not sulphidic or that most of the sulphur had been removed through a roasting stage. As discussed in section 3.1, sulphur is highly detrimental to the formation of copper metal and difficult to remove from copper without also removing any arsenic. Since it is easier to separate iron and sulphur without excessive losses of arsenic than doing the same with copper and sulphur, the absence of sulphide in the resulting speiss would have been highly desirable to ancient smelters (Rehren et al. 2012).

Table 7.29 Distribution of crystalline phases in the speiss slag of Arisman. The first six analyses are taken from Boscher (2010) while the bottom ten are newly obtained results.

	Dendritic pyroxenes	Angular pyroxenes	Kirschsteinite	Dark laths	Glassy	Attached crucible	Attached furnace
FG-030116A	X	X	X				
FG-030117	X	X					X
FG-030119A					X	X	
FG-030119B	X	X	X	X		X	
FG-040919	X	X					
FG-040919B	X	X	X				
FG-011993					X	X	
FG-012232					X		X
FG-012234	X	X					X
FG-000116A		X					
FG-000116B		X					
FG-030118	X						
FG-030123B	X	X					
FG-040920A	X	X	X				
FG-993154	X	X					
FG-101506			X				

Although the microstructure just described is representative of the majority of the speiss slag, three speiss-bearing slags lacked any visible microstructure, being entirely glassy in appearance. All three of these slag samples were attached to either crucibles or furnace remains and would therefore likely have been strongly influenced by the addition of ceramic to the melt. However, the bulk composition of these three samples does not reflect this possibility since an increase in aluminium and decrease in iron typically caused by the greater

presence of clay cannot be clearly observed (Table 7.31). That being said, the Arisman slags, with their high calcium and low iron contents, may be relatively prone to forming very fine microstructures or glass, particularly given the slightly different cooling rates next to the furnace walls or crucibles.

As has been already shown in previous publications, these brownish slags are dominated by the presence of iron-arsenic speiss prills (Figure 7.140) ranging from 5 μm to over 2000 μm . The majority of smaller prills are composed of either a single phase of FeAs or FeAs₂. Larger prills have a more complex microstructure consisting of a eutectic of FeAs and Fe₂As. This binary structure is the result of the decomposition of an unstable phase, Fe₃As₂, upon cooling between 825 °C and 1000 °C (Figure 7.141).

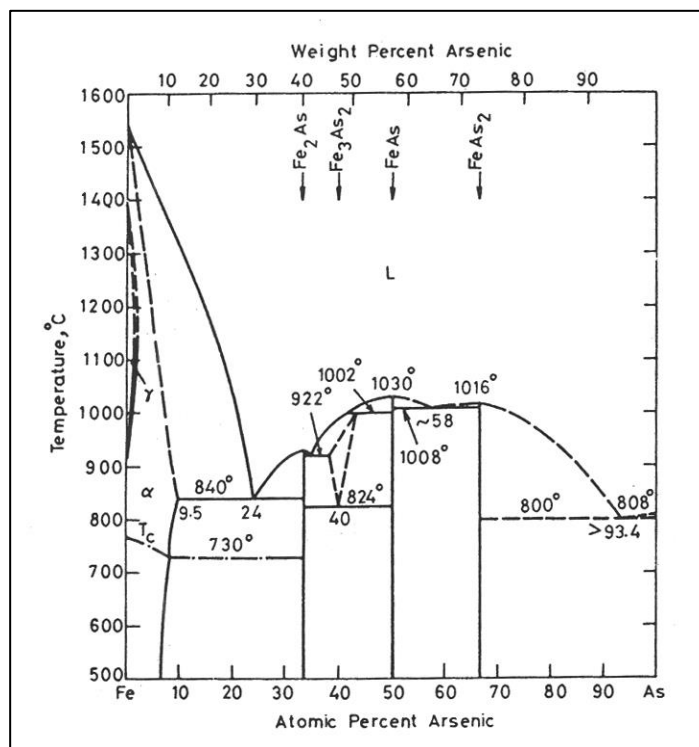


Figure 7.141 The Fe-As binary phase diagram (Raghavan 1988, 38).

Interestingly, the newly analysed speiss prills revealed low but consistent levels of copper (Table 7.30). While some prills analysed in the preliminary MSc research did also show some copper content, in the majority of cases the element was well below or only just above the SEM-EDS' detection limits and always below 1 wt%. (Boscher 2010, Appendix 5). In the new analyses, traces of copper were identified in the speiss prills of two thirds of the slag samples and in one third of all analysed speiss prills. Copper content in these prills ranged between 1-3 wt%. This, in and of itself, is not very revealing other than as evidence that the arsenic-bearing minerals are possibly paragenetic with the copper ores but not bound together. It also shows the strong affinity of copper for these speiss phases and confirms the absence of any significant

quantity of copper in the speiss slags. The same is true for sulphur which, although almost always present, rarely exceeds 3 wt%. Since sulphur cannot be removed under reducing conditions, very little must have been present in the ore charge itself. One speiss prill in sample FG-30123B contained detectable levels of nickel.

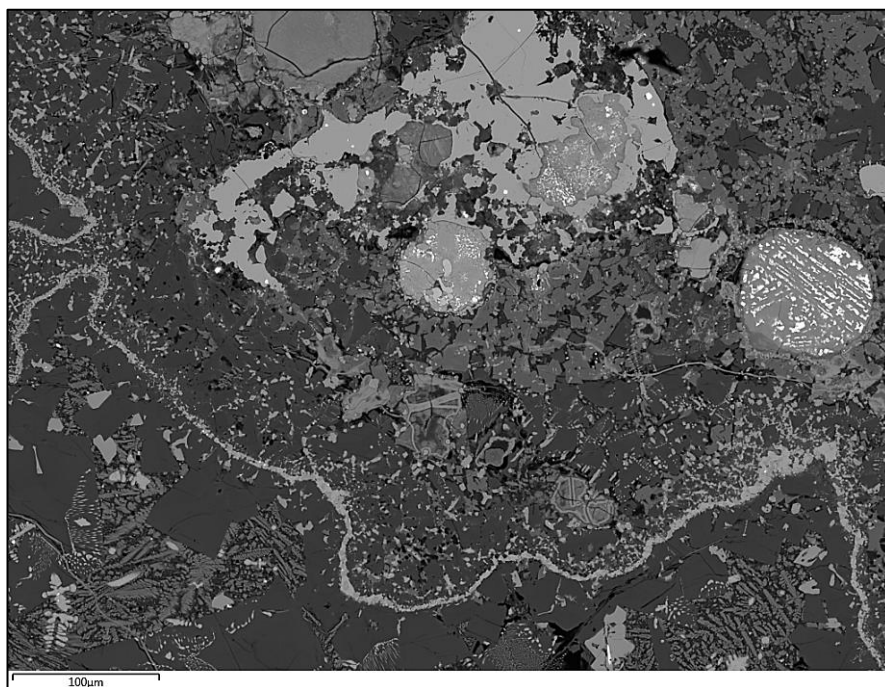


Figure 7.142 SEM image of corroded speiss prills in sample FG-040902A. The bright phases in the prill are FeAs while the corroded grey areas are likely Fe_2As based on the presence of both phases in un-corroded prills. Large dark crystals and grey dendrites are pyroxenes while the light grey phases and blebs are magnetite.

Table 7.30 Normalized mean of the composition of speiss prills found in the speiss slags. The first six analyses are taken from Boscher (2010) while the bottom ten are newly obtained results.

	# of prills analysed	O	S	Fe	Ni	Cu	As
FG-30116A	19	b.d.l.	1	45.5	b.d.l.	b.d.l.	53.2
FG-030117	3	1.2	0.8	42.7	b.d.l.	0.2	55.1
FG-030119A	4	b.d.l.	2.7	40.8	b.d.l.	0.4	56.1
FG-030119B	9	b.d.l.	0.8	38.1	b.d.l.	0.1	61.1
FG-040919	1	1.3	2.1	44.4	b.d.l.	b.d.l.	52.4
FG-040919B	4	1	0.5	49.4	b.d.l.	0.2	48.9
FG-011993	5	b.d.l.	1.1	48.7	b.d.l.	1.2	48.9
FG-012232	3	b.d.l.	1.3	62	b.d.l.	b.d.l.	36.6
FG-012234	5	b.d.l.	3.2	55.4	b.d.l.	1.4	39.9
FG-000116A	7	b.d.l.	1.8	45.8	b.d.l.	0.6	52.3
FG-000116B	8	b.d.l.	1.3	42.4	b.d.l.	b.d.l.	56.3
FG-030118	5	b.d.l.	0.5	48.2	b.d.l.	b.d.l.	51.3
FG-030123B	8	b.d.l.	0.4	46.8	0.5	0.5	51.8
FG-040920A	5	b.d.l.	2.6	44.6	b.d.l.	b.d.l.	52.8
FG-993154	5	b.d.l.	1.2	51.2	0.1	0.7	46.8
FG-010506	5	b.d.l.	1.6	45.6	b.d.l.	b.d.l.	52.8

The bulk composition of the speiss slags is fairly consistent across all samples (Table 7.31), with a standard deviation for most minor elements well below 0.5 wt%. Major elements

(calcium, silica, and iron) vary more widely, but not unaccountably so given the limitations of the use of the SEM-EDS for bulk analysis and expected variability in prehistoric slag compositions. Although efforts were made to analyse areas which were fully molten and avoid regions rich in metallic elements or undissolved gangue minerals, this was not always possible and may also account for some of the range of results.

Table 7.31 Normalized bulk compositions of Arisman speiss slags as determined by at least three area scans by SEM-EDS. All elements reported as oxides. The first six analyses are taken from Boscher (2010) while the bottom ten are newly obtained results.

	Na ₂ O	MgO	Al ₂ O ₃	SiO ₂	P ₂ O ₅	SO ₃	Cl	K ₂ O	CaO	TiO ₂	MnO	FeO	Cu ₂ O	As ₂ O ₃
FG-030116A	2.2	1.2	9.2	43.8	b.d.l.	b.d.l.	b.d.l.	2.4	14.4	0.4	1	24.2	b.d.l.	1.2
FG-030117	2.3	1.8	8.5	39.6	b.d.l.	b.d.l.	b.d.l.	1.6	14.9	b.d.l.	0.9	28.9	b.d.l.	1.4
FG-030119A	1.9	2.3	10.5	48.3	b.d.l.	b.d.l.	b.d.l.	2.5	16.1	0.5	1.1	15.7	b.d.l.	1.1
FG-030119B	2.3	1.5	7.8	38.7	b.d.l.	b.d.l.	b.d.l.	1.6	19.1	b.d.l.	1.2	23.7	b.d.l.	3.4
FG-040919	2.1	1.8	9.2	43.3	b.d.l.	0.6	b.d.l.	2.2	19.3	0.6	0.5	19.5	b.d.l.	0.8
FG-040919B	2	1.6	8	35.8	b.d.l.	b.d.l.	b.d.l.	1.8	14.5	0.4	b.d.l.	34.1	b.d.l.	1.6
FG-011993	2	2.1	8.3	35.9	0.4	0.6	0.1	2.1	20.4	0.5	0.4	26.9	b.d.l.	0.5
FG-012232	1.8	3.3	12.6	49.2	0.3	b.d.l.	0.1	2.5	16	0.8	0.2	12.8	b.d.l.	0.5
FG-012234	3.7	2	9	37.1	0.4	0.7	0.1	1.5	22.1	0.4	0.2	22.2	0.1	0.5
FG-000116A	2	2.6	7.9	48	0.5	0.5	0.1	2	22.6	0.4	0.1	12.8	b.d.l.	0.4
FG-000116B	3.2	3.5	9.2	38.9	0.6	0.8	b.d.l.	1.7	28.9	0.5	0.2	12.2	b.d.l.	0.4
FG-030118	2.9	1.6	10.6	40	0.5	0.3	0.1	1.7	13.2	0.6	0.2	27.8	b.d.l.	0.4
FG-030123B	2.2	1.9	9.2	39.7	0.3	0.3	0.2	2.1	18.6	0.5	0.5	23	b.d.l.	1.5
FG-040920A	2.4	1.3	7.6	34.2	0.6	0.5	0.3	1.8	20.7	0.4	0.5	29.3	b.d.l.	0.5
FG-993154	2.2	1.5	9.1	40.7	0.4	0.4	0.1	2	16.1	0.5	0.6	26.1	b.d.l.	0.4
FG-010506	2.7	1.4	8.7	35.1	0.5	0.4	0.1	1.7	14.3	0.4	0.3	33.4	b.d.l.	0.9
Mean	2.4	2	9.1	40.5	0.4	0.5	0.1	1.9	18.2	0.5	0.5	23.3	0.1	1
Min	1.8	1.2	7.6	34.2	0.3	0	0	1.5	13.2	0.4	0.1	12.2	0	0.4
Max	3.7	3.5	12.6	49.2	0.6	0.8	0.3	2.5	28.9	0.8	1.2	34.1	0.1	3.4
Std. dev.	0.5	0.7	1.3	4.8	0.1	0.2	0.1	0.3	4.1	0.1	0.4	7.1	0	0.8

Despite these analytical shortcomings, it remains possible to note several trends which are largely in agreement with the previously obtained data. Foremost is the fact that the bulk composition is generally too high in calcium and aluminium to fall in the typical prehistoric slag range. Regardless, as they of course must have, the slags reached a fully molten state at temperatures which were achievable in Arisman's furnaces. When plotting the results in a typical ternary diagram of FeO-CaO-SiO₂, which accounts for 82 wt% of the total composition, the results are rather widespread (Figure 7.143). Although most samples fall within the wollastonite range with an estimated melting temperature of about 1200 °C, a few samples appear entirely too rich in silicon and could not have reached a molten state according to this

diagram. A more accurate representation of the theoretical behaviour of these slags can be obtained when the aluminium is taken into account in a quaternary FeO-CaO-SiO₂-Al₂O₃ diagram (Figure 7.144) which includes over 90% of the total elements in the slag. Admittedly, the iron oxide is more highly variable than the 25% represented in the diagram, but it highlights the effects of 10% aluminium in approaching the low temperature trough in the system.

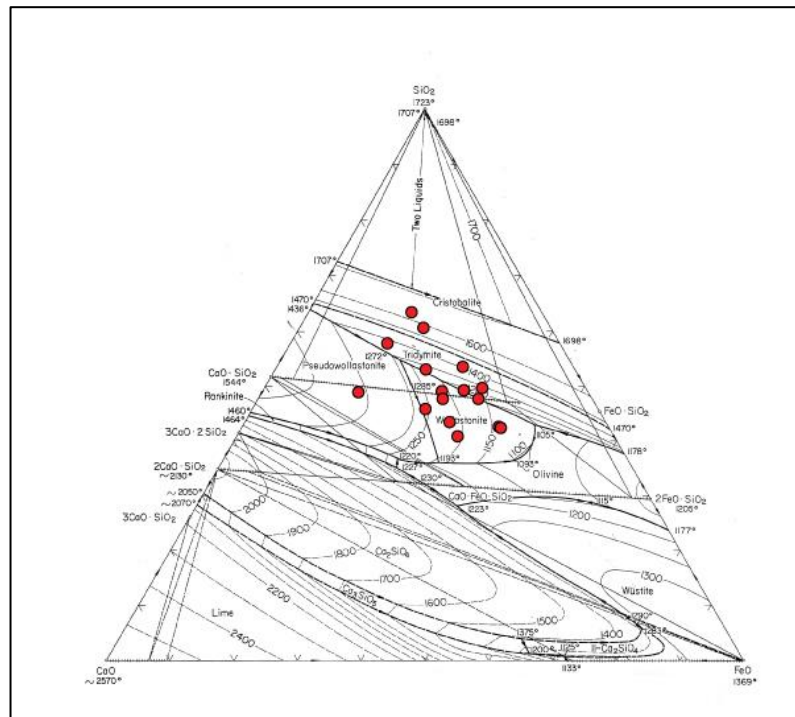


Figure 7.143 Arisman speiss slags plotted in FeO-CaO-SiO₂ ternary diagram from Eisenhüttenleute (1995, 126).

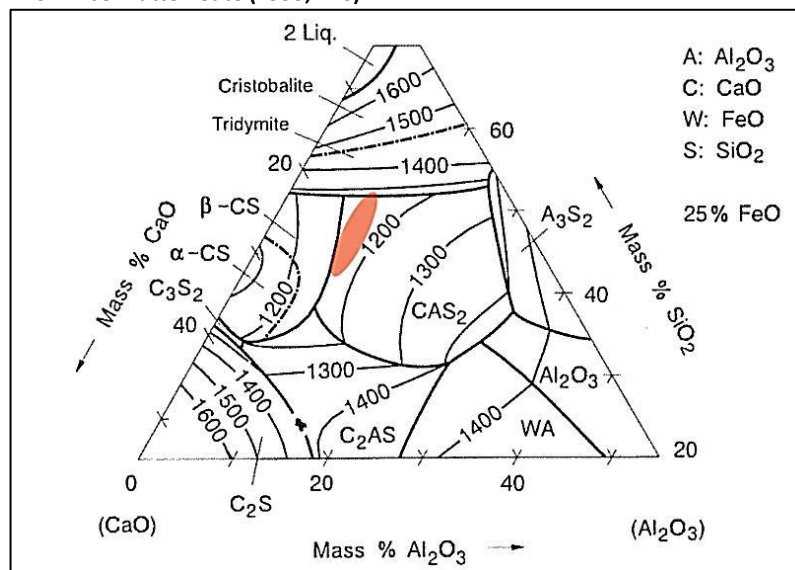


Figure 7.144 Arisman speiss slags plotted in FeO-CaO-SiO₂-Al₂O₃ quaternary diagram with 25% FeO. Results are represented by a red area because the iron content is never exactly 25% and therefore the slags cannot be accurately plotted. From Eisenhüttenleute (1995, 154).

Interestingly, the aluminium is relatively elevated when compared to other prehistoric slags which tend to hover around 5 wt% and almost always below 7 wt% (Bassiakos and Catapotis 2006; Georgakopoulou et al. 2011; Hauptmann 2007; Rovira 2003). This is even the case for the related and contemporaneous site of Tepe Sialk (Schreiner et al. 2003, 491, Table 1). Since aluminium and titanium in the Arisman slags are strongly correlated ($R^2= 0.87$, Figure 7.145) and aluminium and iron are roughly inversely correlated ($R^2=-0.45$, Figure 7.146), the elevated presence of the element appears to be caused by a high degree of influence from the melting and integration of furnace walls into the slag. This appears to have positively affected the fluidity of the slag and was probably highly desirable, and may account for the regular relining of the furnaces as suggested by the recovered archaeological remains of Arisman (see section 5.2.3).

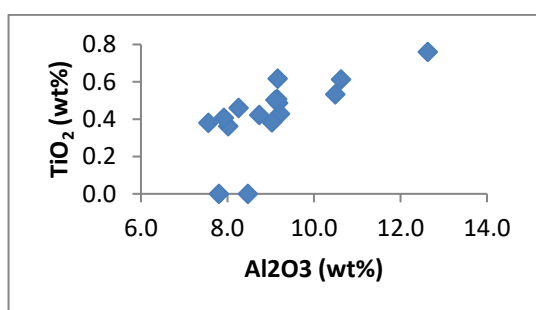


Figure 7.145 Biplot of titanium oxide and aluminium oxide in Arisman speiss slags. Samples which contained aluminium below the detection limit of the instrument were included with a value of 0.

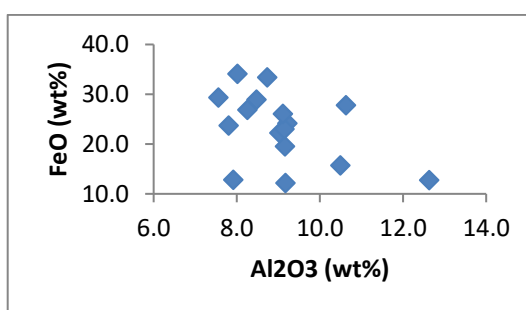


Figure 7.146 Biplot of iron oxide and aluminium oxide in Arisman speiss slags.

The high calcium content does not appear to be correlated to elements commonly introduced by fuel ashes (Figure 7.147), nor is it strongly related to iron introduced from the ores (Figure 7.148), nor to the titanium introduced by the ceramic (Figure 7.149). It therefore seems likely that the calcium originated from a combination of all three, blurring any observable parallel between the elements. Since fuel ash would have a similar effect on slag regardless of geology between most prehistoric sites, and since Arisman slags have relatively high calcium content, it can be safely inferred that the calcium mainly originated from the ores and furnace walls.

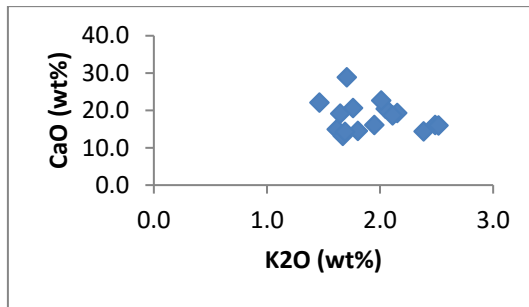


Figure 7.147 Biplot of calcium oxide and potassium oxide in Arisman speiss slags.

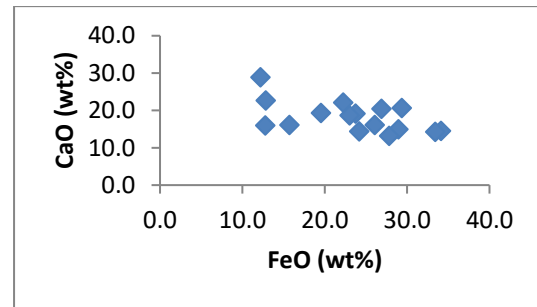


Figure 7.148 Biplot of calcium oxide and iron oxide in Arisman speiss slags.

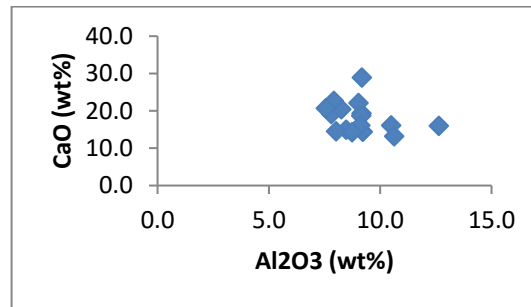


Figure 7.149 Biplot of calcium oxide and aluminium oxide in Arisman speiss slags.

Despite the higher amount of copper identified in the speiss prills, the trend of extreme paucity of copper by bulk in the speiss slags identified in previous research is still very much true in the newly analysed results. Only two samples had detectable amounts of copper, and then only at the lowest detection limit of the SEM-EDS of around 0.1%. In all instances arsenic was high enough to be identified in the bulk analysis, with a mean of 1.1 wt% and a standard deviation of 0.9 wt%.

'Green' Copper Slag

Although the green copper slags have already been described in some depth previously through the detailed analysis of five samples (Boscher 2010; Rehren et al. 2012), it is worth reiterating some of the previous findings along with the newly obtained results from 20 slag samples belonging to this category. In addition to these 25 samples, nine ceramic samples with related attached slag will also be discussed.

Generally speaking, the green copper slags are much denser than the speiss slags. They are grey in cross section and fairly homogeneous, but almost always contain large particles of incompletely reacted quartz or other gangue minerals. In cases where the slag could be orientated, relics of the original charge were found to be typically near the top of the sample due to the lower density of quartz-rich material than the surrounding slag.

In addition to density, corrosion, and general colouration, there is a clear morphological difference between the copper bearing slag and the speiss slag in that the former often has

a clear meniscus where they solidified above a liquid while the latter slags do not. One sample in particular (FG-012260B, Figure 7.150) beautifully demonstrates the layering of metal, matte, and slag resulting from the smelting process. Furthermore, some of the large fragments of arsenical copper slag have a truncated conical shape which is believed to be the negative impression of the furnace superstructure (Figures 7.151 and 7.152) since the shape does not match that of the associated crucibles which tend to have straight walls at 90° from their base. The large slag cakes are therefore clear evidence that much of the arsenical copper slag solidified in situ within the furnace. This is in contradiction to the earlier interpretation that the slag had been tapped out to settle into a separate receptacle (Boscher 2010). That few of the arsenical copper slags show any flowing tapped slag features reinforces this point, as does the sequential destruction and rebuilding of the furnace recovered under slagheap A in order to remove the slag and copper metal. In light of this, the interpretation of the ‘tapping crucibles’ will need to be revised somewhat and will be further discussed later.



Figure 7.150 Photograph of cross section of sample FG-012260B. The layering of metallic copper, matte, and slag can be clearly seen as it must have been in the larger slag cakes from Arisman.

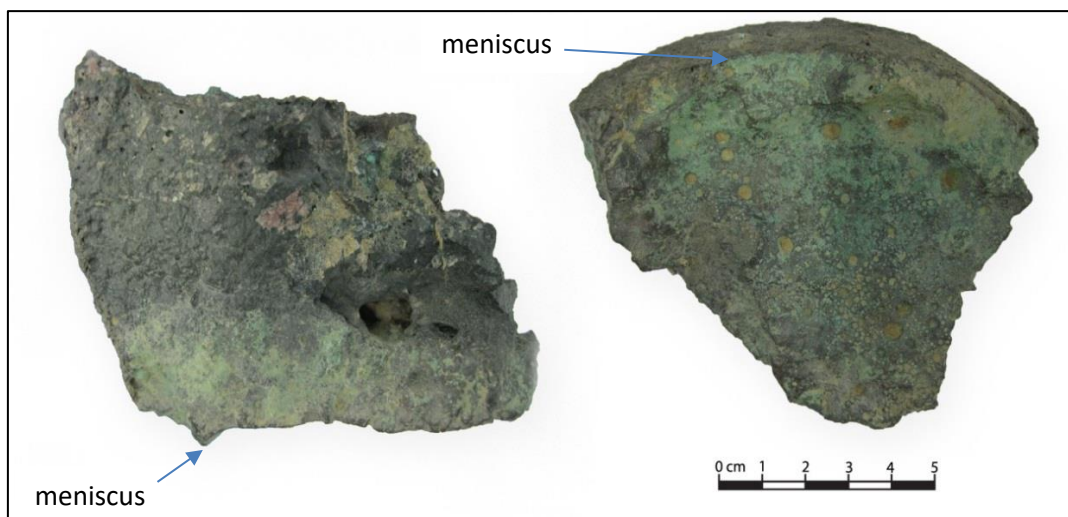


Figure 7.151 Photograph of large slag cake fragment. The left photograph is the fragment in cross section while on the right is the base of the fragment. The meniscus can be clearly seen in cross section. Also note the angle of the cake side against the base which does not match the shape of the large 'crucibles' recovered from Arisman.

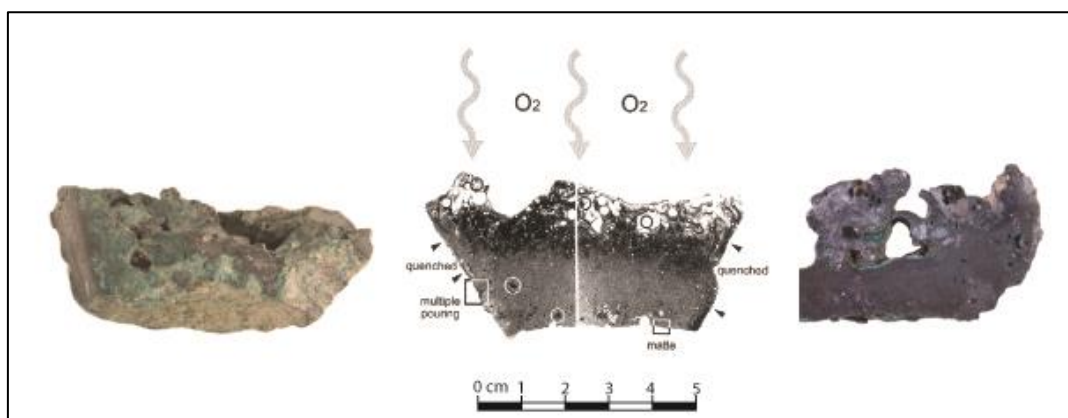


Figure 7.152 Plate taken from (Boscher 2010, 39) showing the similarity in shape between some Arisman copper slags (far right, FG-030121) and Shahr-i Sokhta tapped copper slags (far left). The centre image is a photo diagram from (Hauptmann et al. 2003, 201).

The microstructure of the green slags is consistent across most samples, with olivine dendrites within the solid solution between monticellite and kirschsteinite as the most commonly occurring silicate crystal in 22 of 34 green slags (Figure 7.153). Three slags were mainly fayalitic in microstructure. In five cases the slags contained fayalite along with a variety of other olivines (Figure 7.154), likely due to slight variations in the slag composition at the time of cooling. Three slag fragments with attached ceramic fabric were dominated by large dark angular calcium silicate olivine crystals low in both magnesium and iron. In all of these microcrystalline slags magnetite spinels could be found either grouped in clusters or dispersed throughout the matrices.

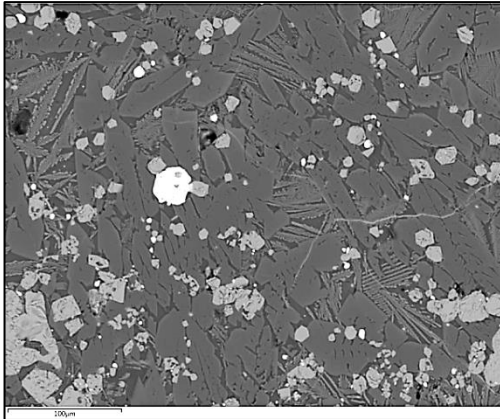


Figure 7.153 SEM image of sample FG-993152C showing typical dendrites in the solid solution between monticellite and kirschsteinite. The smaller dendrites are second generations of the same crystal. The grey blebs are magnetite spinels and the bright prills are arsenical copper.

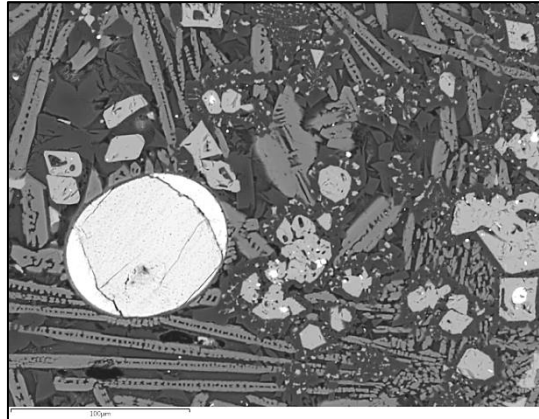


Figure 7.154 SEM image of sample FG-12260C showing mixed olivine crystalline matrix. The skeletal chains are fayalite while the dark angular crystals approach the composition of Kirschsteinite. The grey blebs are magnetite and the bright prills are copper sulphide and arsenical copper

The last six analysed specimens were found to be largely glassy. It should be mentioned that three of the glassy slags were in fact associated with furnace lining and thus probably include a large component of ceramic and do not accurately represent the microstructure of most of the slag. The other three glassy slags were all recovered from the same unknown context and consist of an accumulation of small (<math><1\text{ cm}^3</math>) slag fragments. While all three contained arsenical or pure copper prills, they will be shown to be largely deficient in iron and therefore may better be described as crucible slags and therefore probably related to later stages of production such as refining, casting, or alloying processes.

It can therefore be said that the main crystalline phases in the non-glassy green slags belong to the olivine group. The consistency in the nature of the slag matrix suggests a somewhat standardized charge and smelting process. All slags known to have originated from slagheap A fall within the monticellite-kirschsteinite solid solution range. Other slag microstructures are either due to the close proximity, and likely incorporation, of ceramic fabrics, or related to other stages of metal production.

Out of the 34 green slags analysed, all but three contained copper sulphide prills. Unlike Çamlıbel's HSS phases, the matte present in Arisman's green slags had all clearly been fully molten during smelting but had failed to reduce to copper metal. Although matte is less dense than metallic copper and thus prone to stay within the slag, the homogenous and fully liquefied appearance of the slags suggests that a significant amount of matte would have been produced and pooled below the slag during smelting. This is further attested in the cross section of fragment FG-012260B already mentioned (Figure 7.150). That few discrete

lumps and cakes of matte were recovered from the site is a pertinent point which will be returned to later.

The majority of the green slags (n=27) also contain arsenical copper. These prills were not necessarily found in direct association with matte, but mostly occur together in 24 of the green slag samples. Although the prills contain variable arsenic concentrations, they generally have between 1 and 5 wt% of the element. In some of the larger prills this led to the formation of the γ -phase of Cu_3As already discussed (See section 2.1) and in exceptional cases in the presence of a few small prills of copper-arsenic speiss. In one third of the samples (n=11) nearly-pure copper prills were also observed, but only as a few isolated cases.

Particularly interesting is the fact that seven specimens were free of arsenic-bearing phases entirely, suggesting that pure copper may have been the intended product. This includes one sample (FG-030123B) known to have been recovered from slagheap A. Although the absence of arsenic phases in the slag does not strictly mean that no arsenic was present in the charge, it does strongly suggest that pure copper was being produced or at least melted at Arisman. It is also worth mentioning two arsenic-free glassy slag fragments (FG-030974B and FG-030974E) which have been identified as possibly crucible slags from re-melting operations which will be further discussed below.

Much like the prills from Çamlıbel, the arsenical copper and pure copper prills of Arisman typically contain several percentage points of iron in solution. As was already discussed (see section 7.1.6), this appears to be a common occurrence of copper production under even lightly reducing atmospheres and is not the result of analytical error. This point is further reinforced by the presence of metallic iron prills produced under similar conditions in the speiss slags.

Also worth mentioning is that many of the copper prills contained minor or trace amounts of other elements such as antimony, zinc, lead, and nickel. Rarer are the appearance of copper bismuth inclusions (FG-000117C) and silver chloride concentrated within corrosion products of copper prills (FG-030669). The presence of these elements is not surprising given their common geological association in copper mineralizations. That they were only detected in some samples but not all is likely due to the limitations of the SEM-EDS rather than representing any real distribution patterns. Nevertheless, and although the possibility is remote, the use of ore minerals from several distinctive deposits cannot be wholly discounted without confirming the ubiquitous presence of these trace elements using more precise instruments, something which was out of the scope of this research.

Bulk chemical compositions of the green slags are reported here in three tables. The first table (7.32) shows the results for the majority of copper-bearing slags which form one large corpus of mostly consistent compositions. The second table (7.33) includes the green copper slags which were associated with fragments of furnace wall and thus have been greatly influenced by the inclusion of molten ceramic. The third table (7.34) solely includes the three glassy green slag fragments from context FG-030974 since they are significantly different both in compositions and microstructure from the bulk of the green slags. These will be discussed in parallel with the rest of the assemblage.

Much like the other prehistoric slags presented in this thesis and elsewhere, the green copper slags of Arisman have a large degree of variability in their bulk chemistry. Although the dominant crystalline phases are consistent across most samples, it appears that these crystal phases form over a wide range of compositions. While in absolute terms iron, calcium, and silicon have the largest standard deviations, it is the minor elements which show the most variation relative to their means. Although some of the variation is probably due to instrumental difficulties in analysing porous, heterogeneous, and multi-phased material with polished blocks by SEM-EDS, most of this variability is still likely to have originated from inconsistent composition of the smelting charges. Soda, phosphorous, potassium, and calcium are all prone to wide compositional differences due to the variable influence from the fuel ash. The values of alumina on the other hand are largely dependent on the amount of furnace wall or crucible fabric which melted into the slag, in turn partly dependent on the length and intensity of the smelting or melting operation.

Excluding slags attached to furnace walls and glassy slags, the green slag samples contain appreciable levels of copper, averaging 2.1 wt%. Although only two thirds of samples have detectable arsenic in the bulk, arsenic phases were observed in all of the more typical ceramic-free green slags except for two (FG-000117C and FG-030123B). The ratio between arsenic and copper in these new analyses (10:1) is even more pronounced than previously reported ratio of 2:1 by Boscher (2010, 61). The large discrepancy may in fact be due to the use of different instruments for the preliminary bulk analysis of used to determine the 2:1 ratio and thus the newly obtained ratio is more reliable in this regards.

Interestingly, most of the samples also contained traces of zinc which were not always detected in the individual phase analyses, most likely because zinc tends to form small interstitial crystals rather than segregate into the metallic prills or major silicate phases which were the focus of this study. Barium was also present in some quantity in a few of the

samples, typically present in the glassy or microcrystalline matrix, but occasionally forming large barite crystals (BaSO_4).

In contrast to this, two of the three glassy slags contained arsenic and zinc below the SEM-EDS detection limits and no trace of these elements was found in any of the phases. In addition, the glassy slags are much poorer in iron and have much higher silicon and aluminium content than the typical green slags. Although the sample count is low, at this stage it is safe to say that they are unlikely to have been formed by the same process as the rest of the green slags. Their overall bulk compositions confirm that they are likely to be crucible slags rather than smelting slags. Although their provenance is unknown, their distinctive size, morphology, microstructure, and composition points at melting and/or casting activities taking place in a different part of the site.

Table 7.32 Normalized bulk composition of green copper slag remains from Arisman as determined by at least three area scans by SEM-EDS. All elements reported as oxides except for chlorine.

	Area	Na ₂ O	MgO	Al ₂ O ₃	SiO ₂	P ₂ O ₅	SO ₃	Cl	K ₂ O	CaO	TiO ₂	Mn	FeO	CuO	ZnO	As ₂ O ₃	BaO	PbO
FG-000115	A	1.8	2.6	8.5	39.6	b.d.l.	b.d.l.	0.1	1.9	13.2	0.3	b.d.l.	29.1	2.9	0.1	0.1	b.d.l.	b.d.l.
FG-000117A		3	1.9	10.3	47.2	0.4	b.d.l.	0.2	2.9	13.9	0.4	0.3	16.7	2.2	0.1	0.8	b.d.l.	b.d.l.
FG-000117B		1.8	2.2	8.4	37.4	0.3	0.3	0.1	2.2	13.8	0.4	0.3	32.4	0.4	b.d.l.	b.d.l.	b.d.l.	b.d.l.
FG-000117C		1.4	2.1	6.4	41.6	0.2	0.2	0.6	1.5	16.8	0.3	0.9	25.6	2.3	0.1	0.1	b.d.l.	b.d.l.
FG-000118A	A	1.2	2	5.2	41.5	b.d.l.	b.d.l.	0.1	0.9	10.7	b.d.l.	b.d.l.	36	2.4	0.1	b.d.l.	b.d.l.	b.d.l.
FG-000119	A	1.1	2.5	8.4	39.9	0.6	b.d.l.	0.3	1.3	15.1	0.2	2.4	27.2	1	0.1	0.1	b.d.l.	b.d.l.
FG-000123		0.8	2	8.8	41.9	b.d.l.	b.d.l.	0.1	2	14.2	0.4	0.4	26	2.2	b.d.l.	0.9	b.d.l.	b.d.l.
FG-012260A		1.1	2.2	6.3	34.4	b.d.l.	0.3	0.3	1.2	11.2	0.3	2.8	37.3	2.1	b.d.l.	b.d.l.	b.d.l.	b.d.l.
FG-012260B		1	2.1	6.3	33.7	b.d.l.	0.4	0.3	1.2	10.4	0.3	2.9	38.9	2	b.d.l.	b.d.l.	b.d.l.	b.d.l.
FG-030114	A	2.5	2.3	8.2	42.6	b.d.l.	0.2	0.3	2.3	14.4	0.4	0.5	23.6	2.4	0.1	0.3	b.d.l.	b.d.l.
FG-030115	A	1.9	3.7	12.1	41.9	0.3	b.d.l.	0.1	3.1	14.1	0.6	0.2	20	1.7	0.1	0.3	b.d.l.	b.d.l.
FG-030120	A	1.2	2.2	9.6	47.2	b.d.l.	b.d.l.	0.3	2.6	13.6	0.4	0.2	20.2	2.6	0.1	b.d.l.	b.d.l.	b.d.l.
FG-030121		0.7	1.4	4.7	40.3	0.1	0.4	b.d.l.	1.4	7.1	b.d.l.	b.d.l.	42.2	1.7	0.1	b.d.l.	b.d.l.	b.d.l.
FG-030122B	A	1.7	2.9	8	43.9	0.5	b.d.l.	0.2	2	15.3	0.5	0.3	23.9	0.6	b.d.l.	b.d.l.	b.d.l.	b.d.l.
FG-030123A	A	0.9	1.6	5.9	44.1	0.4	b.d.l.	0.4	1	8.1	0.2	0.2	35.7	0.7	0.1	b.d.l.	0.7	b.d.l.
FG-030124A	A	1.2	4	6.9	42	b.d.l.	b.d.l.	0.3	1.6	12.9	0.3	b.d.l.	28.6	2.2	0.1	b.d.l.	b.d.l.	b.d.l.
FG-030124B	A	1.8	2.3	7.7	38.5	0.4	b.d.l.	0.2	1.9	13.3	0.4	0.4	29.2	2.9	0.1	0.6	0.5	b.d.l.
FG-030664		1.1	1.8	4.7	27.9	b.d.l.	0.9	0.2	0.9	16.6	0.3	b.d.l.	41.9	3.1	b.d.l.	0.3	b.d.l.	b.d.l.
FG-030673		1.5	2.4	6.4	33.1	b.d.l.	0.6	b.d.l.	1.4	23	0.3	b.d.l.	30.2	0.7	0.1	b.d.l.	0.3	b.d.l.
FG-993152C		1.2	2.1	7	37.9	0.4	0.1	0.6	1.4	9.9	0.3	0.3	35.1	3.3	0.1	0.2	b.d.l.	b.d.l.
FG-993152D		2.2	1.9	7.8	41.4	0.4	0.5	0.2	2.2	14.7	0.3	0.2	24.4	1.8	0.1	0.5	1.5	b.d.l.
FG-993155		1.4	4.1	7.7	38.8	0.3	b.d.l.	0.8	1.6	15.6	0.5	0.4	23.5	5	0.1	0.3	b.d.l.	b.d.l.
Mean		1.5	2.4	7.5	39.9	0.2	0.2	0.3	1.8	13.5	0.3	0.6	29.4	2.1	0.2	0.2	0.2	b.d.l.
Min		0.7	1.4	4.7	27.9	0.1	0.1	0	0.9	7.1	0.1	0.1	16.7	0.4	0.1	0	0.1	b.d.l.
Max		3	4.1	12.1	47.2	0.6	0.9	0.8	3.1	23	0.6	2.9	42.2	5	0.5	0.9	1.5	b.d.l.
Std. dev.		0.6	0.7	1.8	4.6	0.2	0.2	0.2	0.6	3.3	0.1	0.9	7.2	1.1	0.1	0.2	0.3	N/A

Table 7.33 Normalized bulk composition of green copper slag remains with attached fragments of furnace walls from Arisman as determined by at least three area scans by SEM-EDS. All elements reported as oxides except for chlorine.

	Area	Na ₂ O	MgO	Al ₂ O ₃	SiO ₂	P ₂ O ₅	SO ₃	Cl	K ₂ O	CaO	TiO ₂	Mn	FeO	CuO	ZnO	As ₂ O ₃	BaO	PbO
FG-030113	A	1.4	2.4	14.2	43.1	0.5	0.1	0.1	2.3	9.9	0.3	0.5	24.6	0.5	b.d.l.	b.d.l.	b.d.l.	b.d.l.
FG-030665		1.7	3.4	9.9	42.2	0.4	0.2	0	1.7	21.9	0.5	0.3	16.3	0.6	b.d.l.	0.9	b.d.l.	b.d.l.
FG-030669		1.6	4.7	6.5	29.7	0.6	0.5	0.4	1	22.5	0.3	b.d.l.	6.9	12.4	b.d.l.	10.1	b.d.l.	3
FG-030670		1	6.7	6	44.6	b.d.l.	b.d.l.	b.d.l.	1.4	10.6	0.3	0.8	24.9	2	0.2	b.d.l.	b.d.l.	b.d.l.
FG-030671		1.6	3.6	12.6	50.8	b.d.l.	b.d.l.	b.d.l.	3.1	19.8	0.7	0.2	5.2	2.4	b.d.l.	10	b.d.l.	b.d.l.
FG-030672A		2.2	3.1	11.6	49	b.d.l.	b.d.l.	b.d.l.	2.6	17.5	0.7	0.1	13.1	0.2	b.d.l.	b.d.l.	b.d.l.	b.d.l.
FG-030672B		1.4	1.5	5	29.8	0.2	0.8	0.2	1.1	17.1	b.d.l.	b.d.l.	41.3	1.6	b.d.l.	b.d.l.	b.d.l.	b.d.l.
FG-993152A		1.6	3.8	13.1	52.5	0.3	b.d.l.	b.d.l.	2.7	17	0.8	0.2	6.3	1.7	b.d.l.	b.d.l.	b.d.l.	b.d.l.
FG-993152B		1.5	3.6	14.4	51.6	0.1	0.3	0.1	2.7	16.5	0.7	0.2	8.2	0.3	b.d.l.	0	b.d.l.	1.5
Mean		1.6	3.7	10.4	43.7	0.3	0.3	0.1	2.1	17	0.5	0.3	16.3	2.4	0.1	2.4	b.d.l.	0.6
Min		1	1.5	5	29.7	0.1	0.1	0	1	9.9	0.1	0.1	5.2	0.2	0.1	0	b.d.l.	0.1
Max		2.2	6.7	14.4	52.5	0.6	0.8	0.4	3.1	22.5	0.8	0.8	41.3	12.4	0.2	10.1	b.d.l.	3
Std. dev.		0.3	1.5	3.7	8.8	0.2	0.2	0.1	0.8	4.4	0.2	0.2	12	3.8	0	4.3	N/A	1

Table 7.34 Normalized bulk composition of glassy green copper slag remains from Arisman as determined by at least three area scans by SEM-EDS. All elements reported as oxides except for chlorine.

	Area	Na ₂ O	MgO	Al ₂ O ₃	SiO ₂	P ₂ O ₅	SO ₃	Cl	K ₂ O	CaO	TiO ₂	Mn	FeO	CuO	ZnO	As ₂ O ₃	BaO	PbO
FG-030974A		3.1	3.4	8.9	41.5	0.3	0.2	b.d.l.	3.2	17	0.4	0.1	17.1	4.3	b.d.l.	0.3	b.d.l.	b.d.l.
FG-030974B		2.7	2.6	10.3	48.5	0.6	0.3	b.d.l.	2.4	12.8	0.6	0.2	18.7	0.3	b.d.l.	b.d.l.	b.d.l.	b.d.l.
FG-030974E		1.9	4.6	13.3	52.1	0.4	b.d.l.	0.2	3	16.1	0.7	0.2	7	0.5	b.d.l.	b.d.l.	b.d.l.	b.d.l.
Mean		2.6	3.5	10.8	47.4	0.4	0.19	0.1	2.8	15.3	0.6	0.2	14.3	1.7	0.1	0.16	b.d.l.	b.d.l.
Min		1.9	2.6	8.9	41.5	0.3	0.1	0.1	2.4	12.8	0.4	0.1	7	0.3	0.1	0.1	b.d.l.	b.d.l.
Max		3.1	4.6	13.3	52.1	0.6	0.3	0.2	3.2	17	0.7	0.2	18.7	4.3	0.1	0.3	b.d.l.	b.d.l.
Std. dev.		0.6	1	2.3	5.4	0.1	0.1	0.1	0.4	2.2	0.1	0	6.3	2.2	0	0.1	N/A	N/A

Overall, the composition of the green copper slags is similar to that of Arisman's speiss slags and thus the same ternary diagrams can be used to try to visualize groupings and estimate the temperature of liquefaction (Figures 7.155 and 7.156).

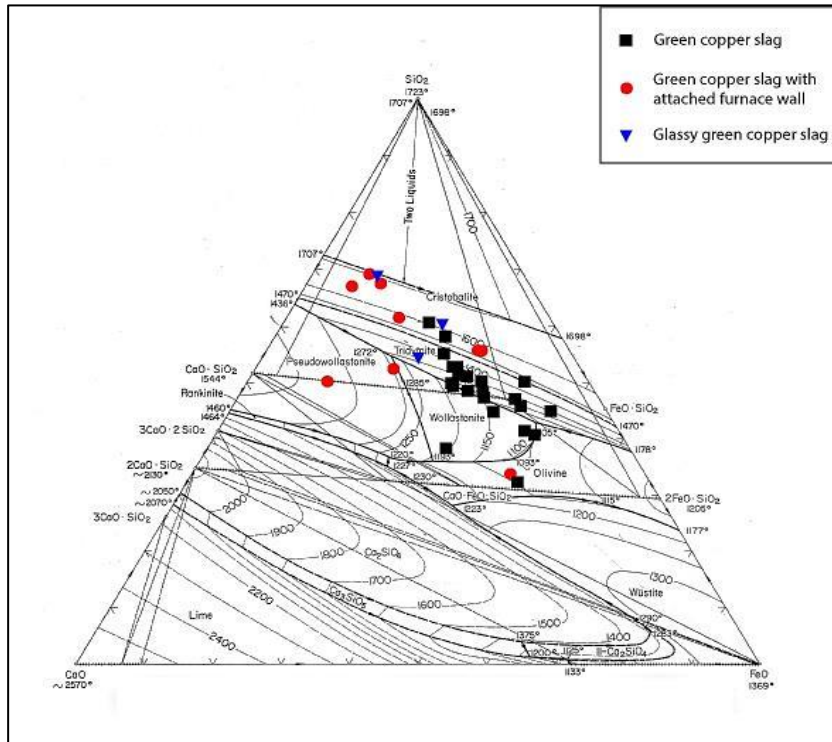


Figure 7.155 Arisman copper slags plotted in FeO-CaO-SiO₂ ternary diagram.

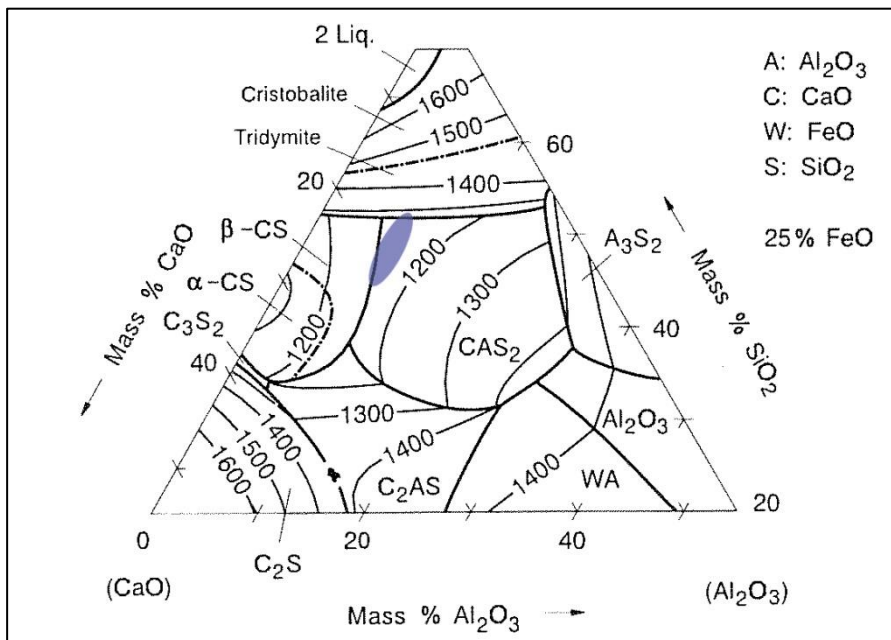


Figure 7.156 Arisman copper slags plotted in FeO-CaO-SiO₂-Al₂O₃ quaternary diagram with 25% FeO. Results are represented by a blue area because the iron content is never exactly 25% and therefore the slags cannot be more accurately plotted.

The first point to be made is the clear difference in the composition of the three subcategories of green copper slag. The main body of the corpus is relatively well concentrated, with only two stray outliers (FG-030664 and FG-030673) with lower silicon and higher iron and calcium contents. The slags with attached ceramic fabrics are generally significantly richer in silicon, calcium, and, although not represented in the first ternary diagram, also richer in aluminium. Conversely, they have much lower iron content. This is due to the increased ceramic content caused by the proximity of the molten slag to the furnace walls during smelting. The uneven and non-equilibrium conditions at the slag/ceramic interface also resulted in the much wider distribution of the furnace wall associated slags. The compositional spread is the main reason that these were separated from the main body of green slags as they are most likely not truly representative of the makeup of typical green copper slags. The glassy slags are also evidently distinct from the main green slag assemblage. In actuality they are very similar in composition to the slags attached to furnace walls, being rich in aluminium and silicon and poor in iron. This is likely caused by an equally strong influence from the inclusion of clay bodies, although in this case from crucible fabrics rather than furnace walls.

While the first diagram shows that the slag appears too rich in silicon to be fully molten at temperatures attainable using prehistoric technology, when the slags are plotted into the FeO-CaO-SiO₂-Al₂O₃ quaternary diagram they fall into the same 1100-1200 °C low-temperature trough as the speiss slags. This is significant as it implies either similar geological origins for the arsenic and copper ores or the use of fluxing agents. Preliminary results had been interpreted as indicative of the former rather than the latter purely based on the early dating of the material (Boscher 2010, 64), but the presence of relic quartz gangue fragments in nearly all of the copper slag samples implies that fluxing may in fact have been a common slagging strategy at Arisman. This is reinforced by the narrow compositional range of the slags uncovered across the site (Figure 7.156).

When looking at some of the elemental relations in biplots, a few points of interest can be further identified. First is the clear influence of ceramic bodies on the composition of both the green slags and those attached to furnace wall as evidenced by the fact that titanium and aluminium plot much higher than the typical green slags in Figure 7.157. The inverse relationship between iron and aluminium (Figure 7.158) further attests to that these elements did not originate with the iron-rich ore but from another source, in this case the technical ceramics.

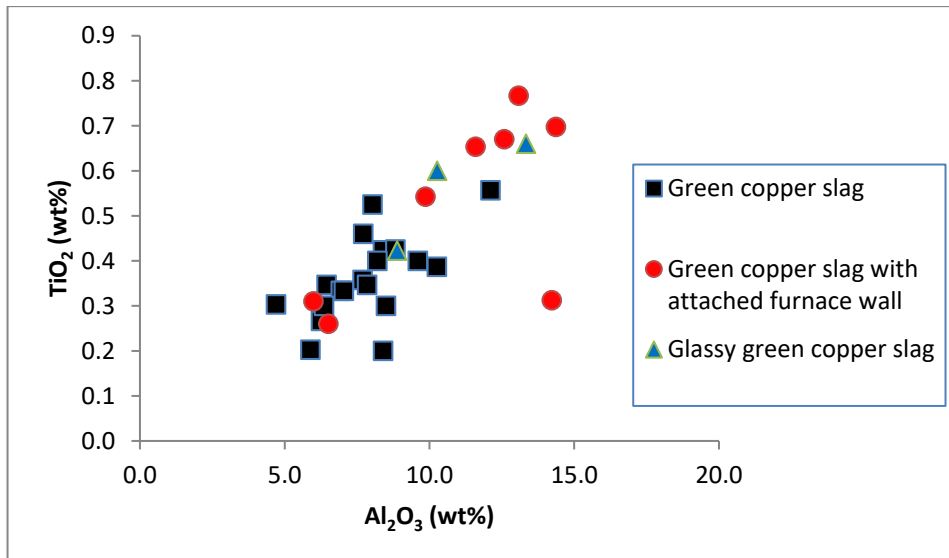


Figure 7.157 Biplot of titanium oxide and aluminium oxide in Arisman green copper slags.

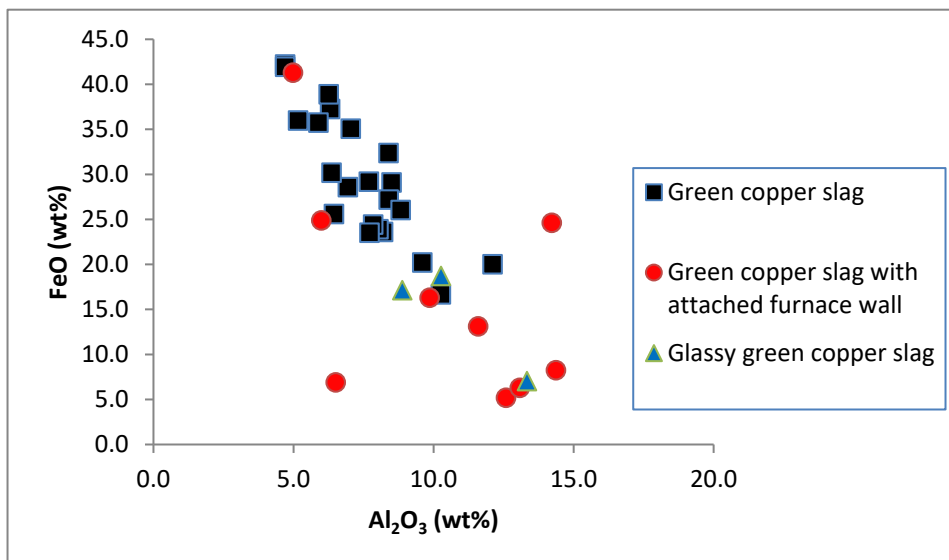


Figure 7.158 Biplot of iron oxide and aluminium oxide in Arisman Green copper slags.

The calcium and iron on the other hand show a very distinct inverse correlation (Figure 7.159) suggesting once more than calcium did not enter the slag from the same source as the iron. There does not appear to be a clear direct link between the quantity of calcium present in the slag and elements typically associated with technical ceramics (Figure 7.160) or fuel ashes (Figure 7.161). Therefore, much like the speiss slag, the relatively high calcium content must be the result of a combination of the two. This is significant because, unlike Çamlıbel, the ore deposit exploited by Arisman's smelters remains uncertain and a cursory study of the high calcium slag may have suggested a dolomitic origin for the ores. The data presented here refutes that possibility.

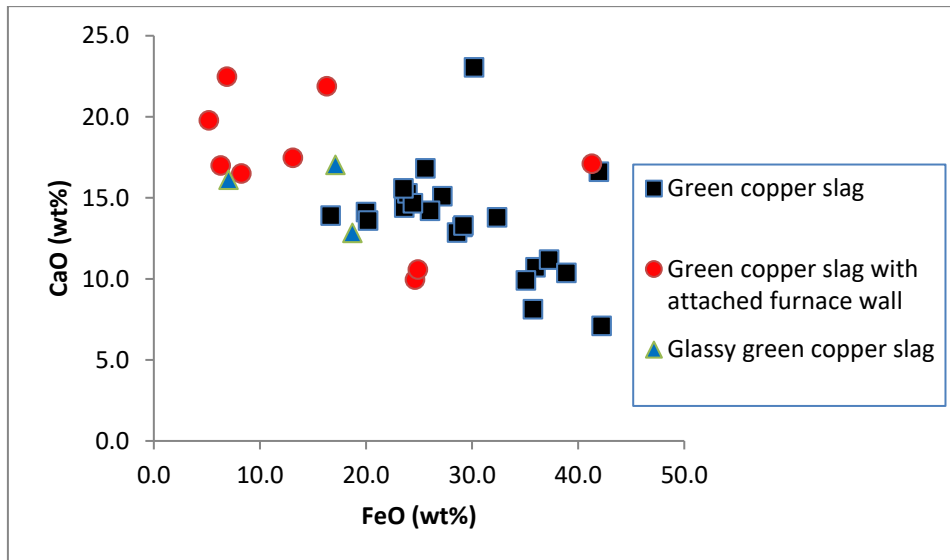


Figure 7.159 Biplot of calcium oxide and iron oxide in Arisman green copper slags.

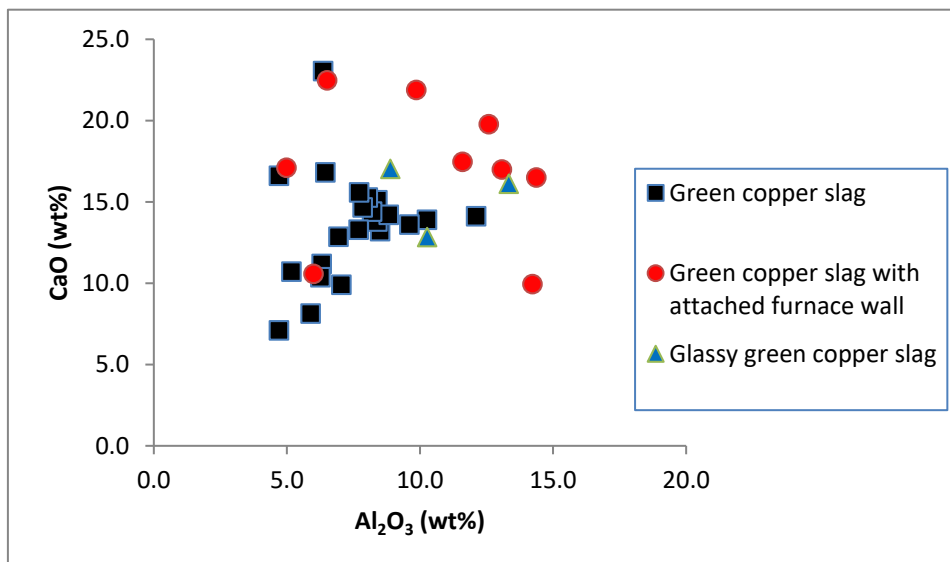


Figure 7.160 Biplot of calcium oxide and aluminium oxide in Arisman green copper slags.

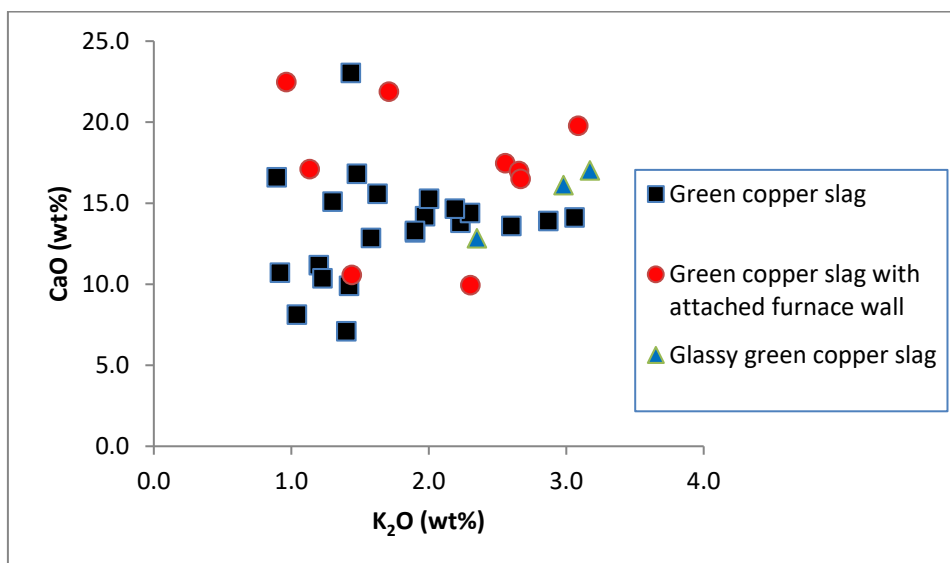


Figure 7.161 Biplot of calcium oxide and potassium oxide in Arisman green copper slags.

Black Slag

Just two samples of black slags have previously been studied in microscopic detail as a subcategory of the typical copper smelting slags (Boscher 2010), interpreted as the result of co-smelting of copper ores and poorly beneficiated arsenopyrite or speiss. Since one of the main goals of this research was to confirm, or at least clarify, the role of this type of slag in the arsenical copper production process, special efforts were made to analyse as many specimens of black slags as possible. This type of slag, however, proved to be much less common than was expected from preliminary work. Ignoring the single fragment uncovered at Arisman III, only 6 further fragments could be identified in the entire available assemblage sampled from Arisman I. These were mostly small pieces pulled from large crushed bags of slag originating from just two contexts (FG-030704 and FG-030974). All of these were analysed by optical microscope and by SEM-EDS. They will be discussed together with the two previously analysed samples.

The specimens are generally black in appearance both on their outer surface and in cross section and they are distinguished from other slags mainly in their glassy appearance (Figure 7.162). Larger pieces clearly exhibit flowing textures on their upper surface, suggesting they had been tapped.

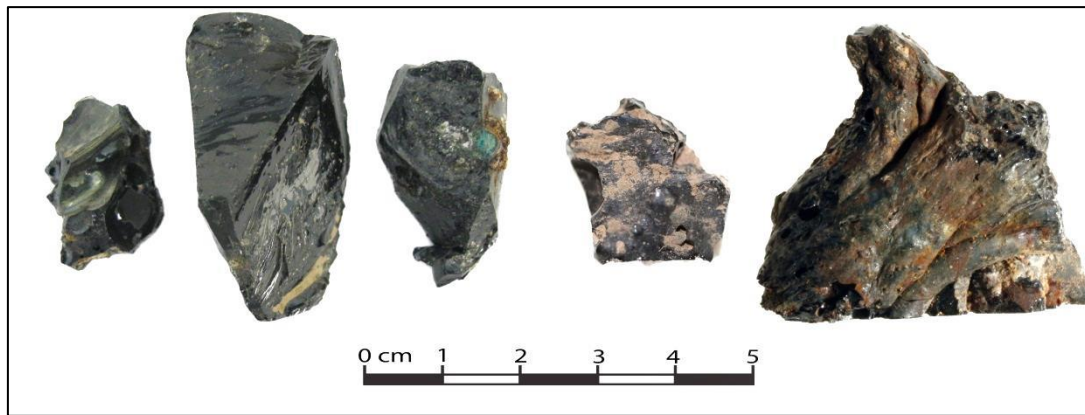


Figure 7.162 Photograph of 5 typical glassy black slags. Note the flowing tapped pattern on the rightmost sample.

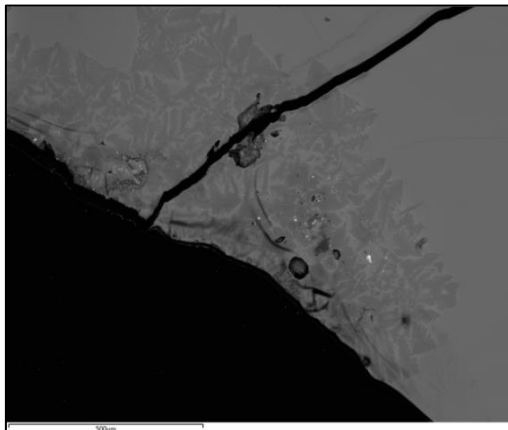


Figure 7.163 SEM image of sample FG-012254 showing isolated calcium silicate crystal cluster in an overall glassy matrix.

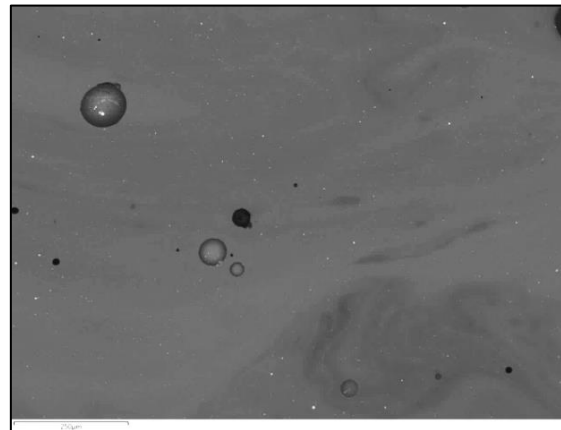


Figure 7.164 SEM image of sample FG-030704B's glassy matrix showing typical flowing texture of most black glassy slags.

Expectedly, nearly all black slags have glassy matrices with only occasional isolated clusters of crystallization in some samples due to localized compositions and cooling speeds (Figure 7.163). The glass itself is usually two-phased, which gives the matrix a 'flowing' texture (Figure 7.164). The brighter of the two phases is slightly richer in CaO and FeO and inversely poorer in both Al_2O_3 and SiO_2 than the darker phase.

Two black slag samples, FG-030974D and FG-030116B, proved to be microcrystalline in nature rather than glassy. The main crystalline phases present in FG-030974D consist of pyroxene dendrites approaching the composition of hedenbergite surrounded by a glassy matrix (Figure 7.165). Also setting this sample apart from the other black slags is the presence of isolated but frequent chromite particles. FG-030116B, on the other hand, contains mostly large angular calcium silicate crystals and magnetite blebs set in a microcrystalline matrix (Figure 7.166).



Figure 7.165 SEM image of sample FG-030974D's microcrystalline matrix. The dendrites are near hedenbergite in composition. The large porosity in the centre shows the three-dimensional structure of the dendrites. The small bright prills are copper metal and copper sulphide.

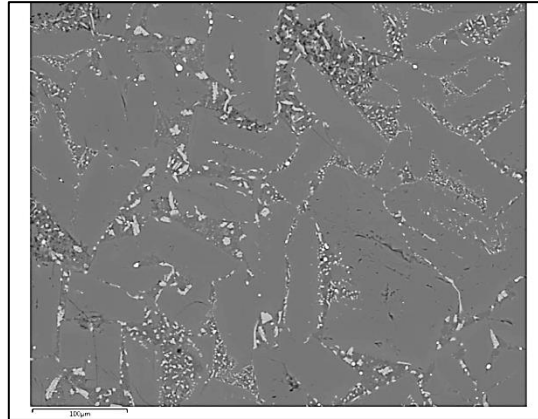


Figure 7.166 Microstructure of FG-030116B under the SEM. The large angular crystals are calcium silicate while the grey blebs are magnetite and the bright prills are iron arsenide speiss.

Of more interest is the presence of a variety of metallic, metalloid, and sulphidic prills in the samples (Table 7.35). Four of the analysed samples contained iron arsenide speiss. In two of these four samples (FG-030116B and FG-010505) iron and copper matte prills were also observed, while in one (FG-010505) arsenical copper prills were identified. No speiss was found in the remaining four samples which are dominated by copper sulphide and arsenical copper prills.

Table 7.35 Microscopic and microstructural features of Arisman's black slags.

	Glassy matrix	Crystalline phases	Arsenical copper	Speiss	Matte
FG-030116B		X		X	X
FG-010505	X		X	X	X
FG-012007A	X	X		X	
FG-012254	X	X		X	
FG-030704A	X		X		X
FG-030704B	X		X		X
FG-030704C	X			X	X
FG-030974C	X		X		X
FG-030974D		X			X
FG-012255	X	X		X	X

Despite the large variability in the nature of the prills associated with the black slags, their bulk chemical composition is comparatively consistent (Table 7.36), even between the glassy and non-glassy types. With just two exceptions (FG-012007A and FG-012254), all of the black slags contained both copper- and arsenic-bearing phases, although not always in enough quantity to be detectable by the SEM-EDS bulk analyses. The composition of all of the black slag is generally similar to that of both the green and brown slags already discussed and,

other than the glassy nature of the matrix, show little microscopic distinction from these. This is significant because it conclusively refutes the earlier assessment of these as the result of mixing a copper bearing ore (chalcopyrite) with an arsenic-bearing ore (arsenopyrite) or poorly beneficiated speiss (Boscher 2010, 57). These black slags are thus much more likely to have formed from the production of either speiss or copper rather than representing a third process entirely. Since both speiss and copper slags have similar overall compositions, the glassy black slags appear to be formed from both processes without being particular to either. Although four samples contained both arsenic and copper by bulk, only the two samples analysed in the preliminary research contained discrete copper prills and speiss prills. The original interpretation was therefore erroneous due to sampling bias and the two samples are likely anomalies perhaps caused by the reuse of crucibles or furnaces.

Table 7.36 Normalized bulk composition of black slag remains from Arisman as determined by at least three area scans by SEM-EDS. All elements reported as oxides except for chlorine and normalized to 100%.

	Na ₂ O	MgO	Al ₂ O ₃	SiO ₂	P ₂ O ₅	SO ₃	Cl	K ₂ O	CaO	TiO ₂	MnO	FeO	CuO	As ₂ O ₃
FG-030116B	3.2	3.5	9.2	38.9	0.6	0.8	b.d.l.	1.7	28.9	0.5	0.2	12.2	b.d.l.	b.d.l.
FG-010505	2.4	2.2	10.5	48.5	0.2	0.1	b.d.l.	2.6	17.2	0.6	0.1	15.2	0.2	0.4
FG-012007A	1.8	2.8	10.9	47.3	0.4	0.2	0.1	2.5	19	0.6	0.4	13.7	b.d.l.	0.3
FG-012254	2.2	2.2	9.8	42	0.3	0.2	0.1	2	22.3	0.6	0.6	16.8	b.d.l.	0.8
FG-030704A	3	3.5	9	41	0.4	0.2	b.d.l.	3.1	16.6	0.5	b.d.l.	17.9	4.6	0.2
FG-030704B	2.5	2.4	9.2	51.3	0.5	b.d.l.	b.d.l.	2.2	12.3	0.6	0.2	18.4	0.3	b.d.l.
FG-030704C	1.9	3.1	13.1	51.2	b.d.l.	b.d.l.	0.1	2.8	16.3	0.8	0.2	10.1	0.1	0.3
FG-030974C	1.9	3.1	13.1	51.2	b.d.l.	b.d.l.	0.1	2.8	16.3	0.8	0.2	10.1	0.1	0.3
FG-030974D	1.2	2.8	8.9	45.4	0.4	b.d.l.	0.2	1.5	15.8	0.6	0.3	21.6	1.3	0.1
FG-012255	2.1	2.5	10.2	42.8	0.5	0.4	0.1	2.3	22.1	0.6	0.3	15.7	b.d.l.	0.6

Matte

Just two fragments of matte were collected from the assemblage of Arisman for analysis. Given that copper sulphide phases are ubiquitous to all arsenical copper slags, it is no surprise that some of it may have pooled and formed discrete cakes during typical smelting operations. In fact, it is somewhat unusual that so little of the material was found at Arisman and may suggest that, unlike other prehistoric sites (Pryce et al. 2007; Hauptmann et al. 2003), much of it was re-processed to extract the remaining copper.

The first of the samples in question (FG-030974F) comes from the same context as the three glassy green copper slags just presented. It consists of a single small 7mm spherical droplet of what at first appeared to be corroded copper metal. Only after microscopic analysis did it become clear that the sample is composed of small blebs of chalcocite in corroded matrix of cuprite (Figure 7.167). Although it may appear that the object was originally a copper prill

with matte inclusions, the large thick ring of copper sulphide (Table 7.37) surrounding it suggests that much of it must have been matte prior to deposition.

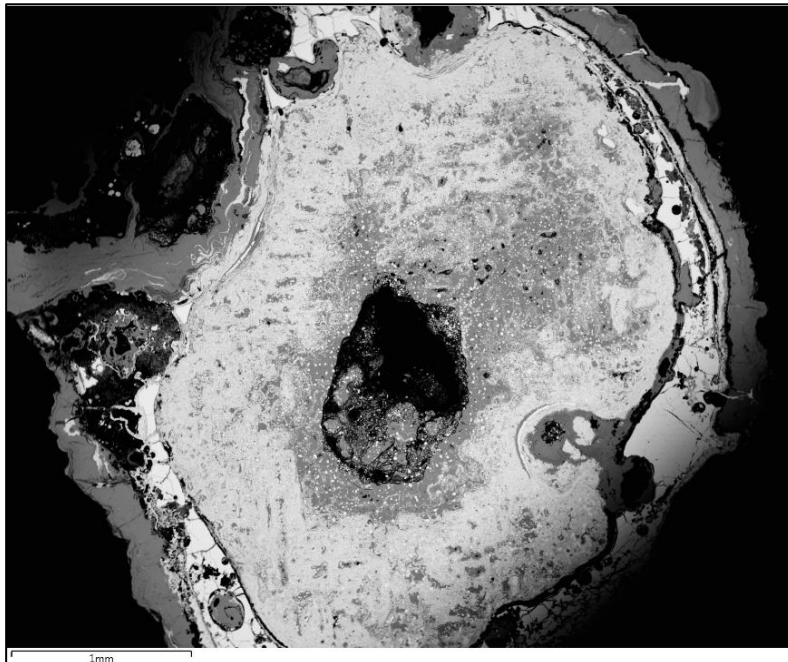


Figure 7.167 SEM image of sample FG-030974F. The prill consists of a body of cuprite with frequent small blebs of chalcocite surrounded by a ring of chalcocite.

The other sample, FG-030689, measures roughly 4 cm by 4 cm by 4 cm. It is metallic grey in cross section and several large quartz and copper oxide and lead-rich inclusions are visibly trapped within the matrix (Figure 7.168).



Figure 7.168 Photograph of sample FG-030689's cross section. Note the large inclusions visible throughout.

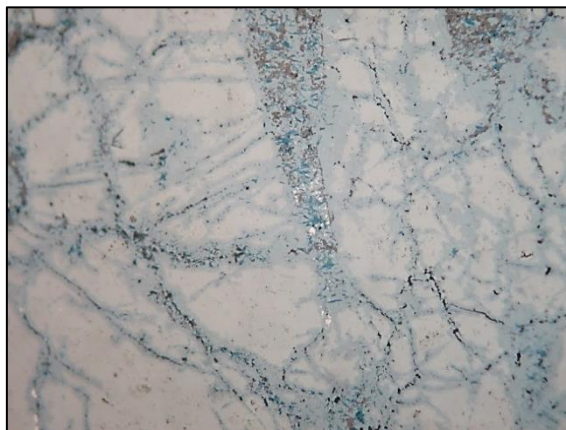


Figure 7.169 Photomicrograph of matte microstructure. The yellowish phase is bornite while the blue veinlets are copper sulphide corrosion. The bright phases in the centre are copper-zinc arsenate. The dark phases are a mixture of various lead compounds.

Crystallographically, the sample proved to be surprisingly complex under the microscope (Figure 7.169). In addition to the yellowish copper sulphide grains of bornite and their associated blue corrosion products which make up the majority of the matrix, discrete

particles of copper zinc arsenate, copper arsenate, arsenic-lead speiss, as well as fully formed wulfenite (PbMoO_4) and mimetite ($\text{Pb}_5(\text{AsO}_4)_3\text{Cl}$) crystals (Figure 7.170) could be observed throughout the matrix.

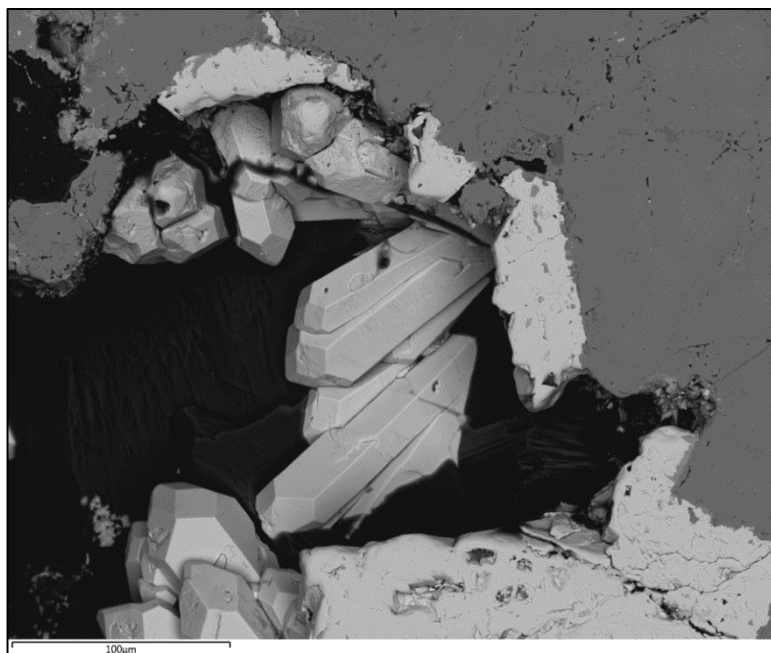


Figure 7.170 SEM image of Sample FG-030689. The large hexagonal pyramidal crystals in the porosity are mimetite while the grey grains in the upper right are chalcocite.

Bulk analysis of the sample shows the complex nature of the matte lump. While sulphur and copper are in ratios which approach that of common copper sulphide phases, the presence of nickel and iron in trace amounts and zinc, arsenic, and lead is responsible for the various phases and crystals observed in the matrix.

Table 7.37 Normalized bulk composition of matte samples as determined by SEM-EDS area analyses.

	O	S	Fe	Ni	Cu	Zn	As	Pb
FG-030974F		21.6			78.4			
FG-030689	3.5	21.6	0.9	0.3	60.2	1.9	7.4	4.4

The composition and microstructure of this intriguing sample is unlike any other analysed as part of the wider analytical program (Table 7.37). Rounded prills in the matrix suggest that this material was at one point entirely molten, and thus cannot be a mineral or ore but is definitely the product of a pyrotechnical process. It was likely formed by the direct smelting of complex copper sulphide ores which already contained significant amounts of arsenic, lead, and zinc.

The presence of arsenic is at first glance quite exciting in regards to identifying sources of the element for the production of arsenical copper, but as this is mainly a sulphidic material it is

unlikely to have been possible to extract the copper without also removing most of the arsenic through oxidation (See section 3.1.4). Its direct addition to metallic copper would also have been equally fruitless as the sulphide and lead phases which contain the arsenic are insoluble in copper.

More telling is that although some nickel and zinc has occasionally been detected in some matte phases in other slag samples, lead has generally been noticeably absent, or at least only in quantities below the SEM-EDS's approximate detection limit of 0.1 wt%. As such, and since the provenance of this particular specimen is unknown, it is likely that it did not originate from the same metallurgical contexts as the rest of the analysed slag assemblage. This is partly in line with results presented in the excavation monograph which suggests that slag from Arisman's areas II and III were richer in zinc, lead, and, although less relevant in this case, antimony (Pernicka et al. 2011, 654). It certainly hints at the use of a significantly different source of copper ores, and may also be indicative of an entirely different copper extraction process undertaken elsewhere at Arisman. As this sample is the only one of its kind analysed, little else can be stated about the implied distinctive *chaîne opératoire*.

Chapter 8 Lead Isotope Analysis

8.1 Arisman

A number of lead isotope studies of metallurgical material (slag, ore deposits, and objects) have already been conducted for Arisman (Pernicka et al. 2011) as well as a number of related sites in the Iranian highlands (Chegini et al. 2000; Schreiner et al. 2003). Unfortunately, these have not been able to identify the copper deposits supplying for either Arisman or for the nearby related and contemporaneous site of Tepe Sialk (Pernicka 2011, p 675). Since both minerals and objects from Arisman have already been characterised isotopically, it was deemed unnecessary in the thesis' design stage to obtain new data from the slag which would add little to the ongoing discussion. No isotopic analysis was therefore undertaken on this Iranian material, although the topic remains one of significant interest to questions relating to arsenical copper production for the region.

That being said, one small point is worth discussing in light of the fact that lead isotope data from the excavation monograph (Pernicka et al. 2011) were not available during the preliminary analysis of the speiss slag (Boscher 2010; Rehren et al. 2012). Since the authors do not make the case for a strong distinction between the 'grey-green' and 'brown' slags through their chemical compositions, they did not distinguish between the types in their discussion of lead isotopic distribution (Pernicka et al. 2011, 679, Figure 45).

When re-plotted to take the various types into account, the only slag outlier (FG-010506) proved to belong to the 'brown' slag category and is closer in its isotopic ratios to many of arsenical copper prills than the 'green slags' (Figure 8.1). The only other 'brown' slag for which lead isotope ratios were obtained (FG-012233B) plots much closer to the rest of the 'green' slag samples. However, and unlike sample FG-010506, this particular specimen has been identified as 'brown' based upon its outward appearance and its bulk chemical composition as determined by ICP-AES, and not upon the presence or absence of ferrous speiss or copper-bearing phases. Since bulk composition alone is not always a reliable marker of the type of slag under scrutiny, the identification of FG-012233B as speiss-bearing may be problematic. In contrast, the presence of speiss prills in FG-010506 means that it is unquestionably distinct from the arsenical copper slags. In addition, lead content in sample FG-012233B, as determined by ICP-AES, has been reported in the monograph as below detection limits which may be a source of errors in the lead isotope ratios.

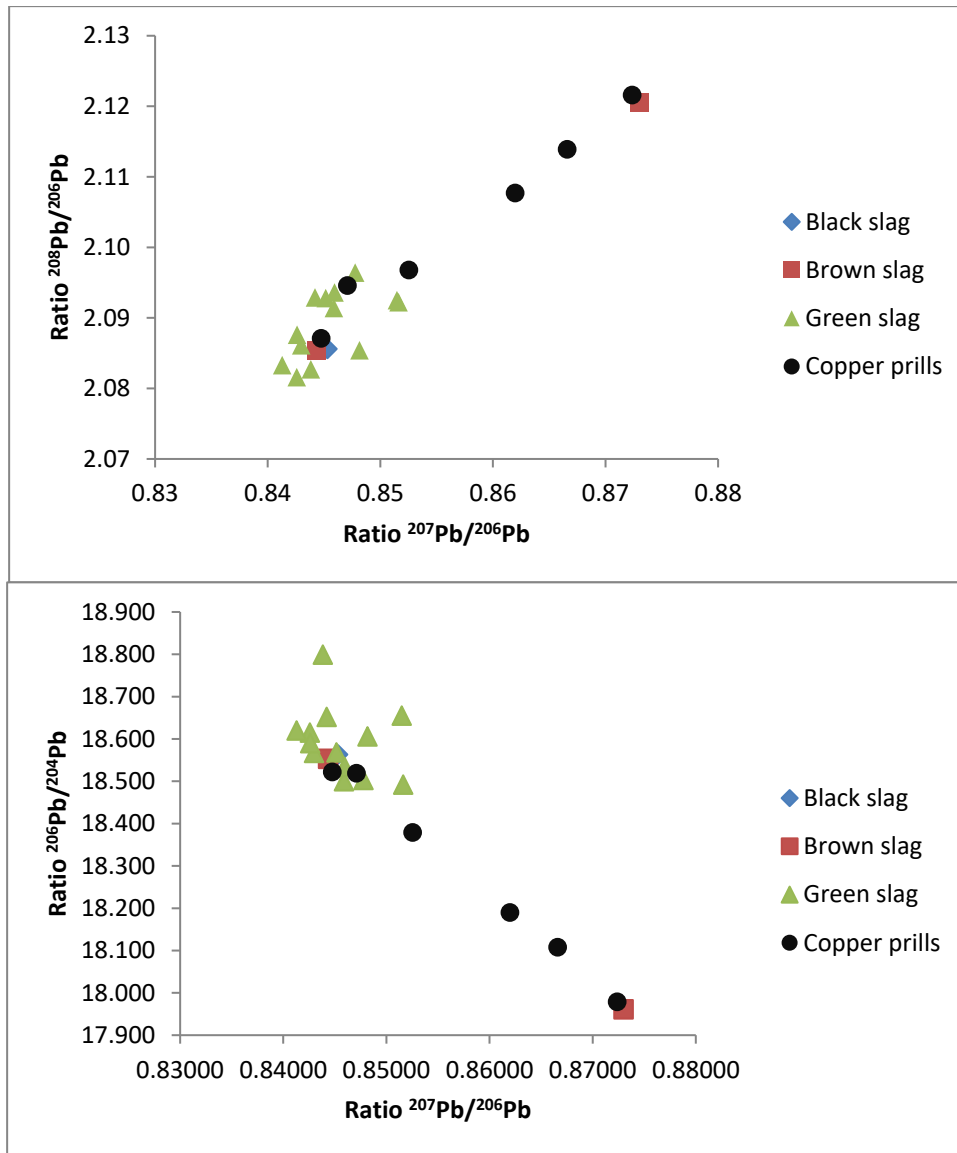


Figure 8.1 Lead isotope ratios for the Arisman's slag and copper prills distinguishing between the different slag types. Diagram produced from data published in Pernicka et al. (2011). Analytical error was not available.

The additional division of the lead isotope results according to their slag types is by no means unambiguous, but it does hint at a significant distinction in the provenance of the arsenical ore material. This may explain the difference between the lead isotope signature of the arsenical copper slags and that of many of the copper prills and objects recovered from Arisman. This is particularly true of a large grouping of objects recovered from Area B which plot between the cluster formed by the green copper slag and the outlying speiss slag (Figure 8.2).

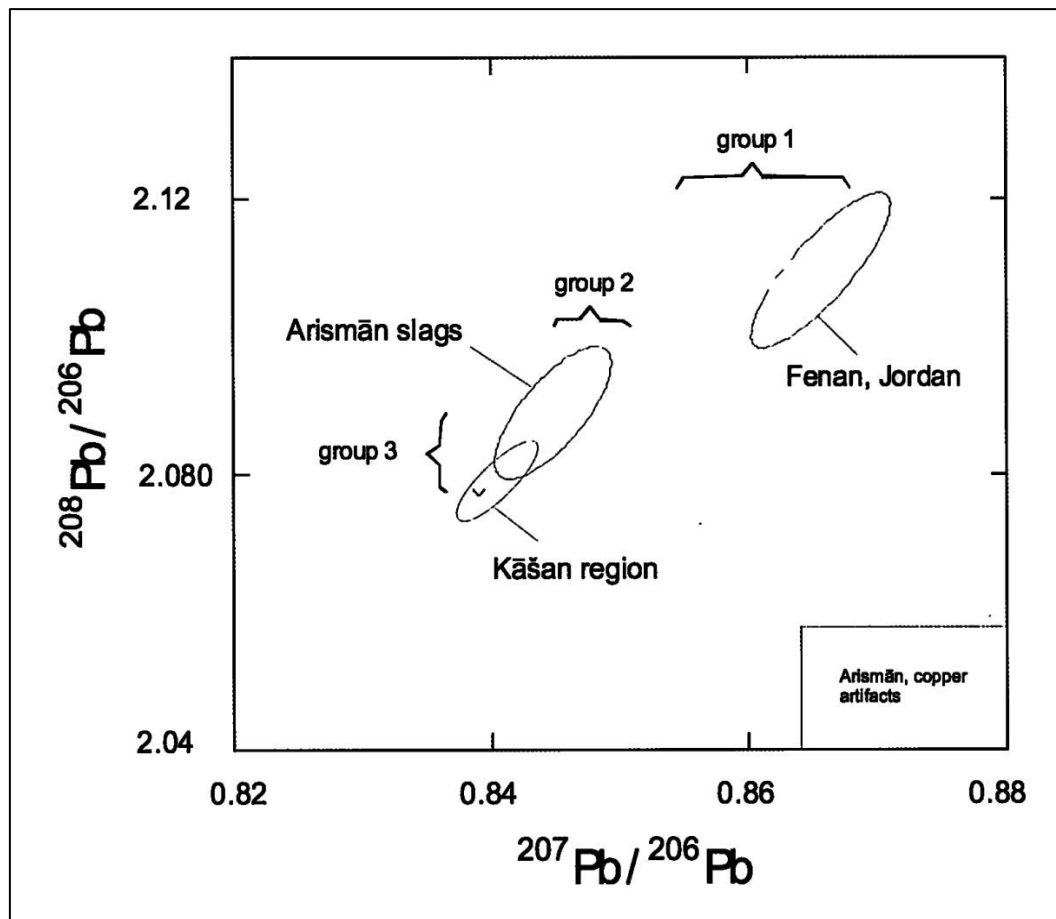


Figure 8.2 Lead isotope ratios for copper objects recovered from Arisman, from (Pernicka et al. 2011, 679).

It is tempting to infer that much of the arsenical copper slags may have been produced using arsenic and copper bearing ore of a particular signature, while the speiss producing ores are derived from a completely different source. If this is the case, it would explain the presence of arsenical copper objects at Arisman which match the lead isotope signature of the ‘green’ slag (group 2) as well as those which would better be described as a mixture between speiss produced from geologically older arsenic-bearing deposits with the younger mainly copper bearing deposits for the purpose of increasing the final arsenic content (group 1).

The lead isotope data therefore point towards the use of two distinctive ores with unique lead isotope signatures. One type is geologically younger and contains both arsenic and copper and produced arsenical copper metal, while the other, older deposit, is mainly arsenic-bearing and produced iron-arsenide speiss. The latter of these two appears to have been added, in some cases, to copper metal to increase the arsenic content of the final product. It does not appear that speiss was added to the smelting charge of the former of the two ores since they form discrete lead isotope groups rather than a long ‘mixing’ trail between two isotopic extremes.

However, these inferences should be taken with some measure of caution given both the small sample size of the brown slags, and the fact that the lead content appears relatively low in most slag samples. Indeed, only 21 of 58 slag samples analysed by ICP-AES contained detectable levels of lead (Pernicka et al. 2011, 650-651, Table 3a). Those that contained detectable levels had a mean lead content of just 0.05 wt%, with many specimens having significantly less than 100 ppm of the element. Although lead content is only really problematic below 10 ppm, as will be discussed much more depth in the following Çamlıbel lead isotope section, the lack of information on the amount of lead present in the published slag samples is cause for some concern.

Taking all of this into account, it is fair to say that while the green arsenic and copper bearing slags are well characterized isotopically, the picture of alloying and speiss alloying would be much clearer with the further analysis of several more samples of speiss slag from Arisman.

8.2 Çamlıbel

In contrast to Arisman, no lead isotope analysis had been conducted on the Çamlıbel material prior to this study. In fact, very little such work had as of yet been undertaken on material from Late Chalcolithic Central Anatolia, the majority of the research having focused on the Cyclades, Western and Eastern Anatolia, and the Levant (Yener et al. 1991). Despite this, some data is available for the central highlands and it was hoped that the well characterised copper deposits of Anatolia would provide fertile ground for comparisons of isotopic datasets and provide a clue to the sources exploited by the inhabitants of Çamlıbel.

As already mentioned in the methodology, samples were sent for LIA at the Curt-Engelhorn Zentrum Archäometrie. The specific samples were chosen from as wide a range of stratigraphic phases as possible in order to cover as many of the occupation periods of Çamlıbel as feasible within the limited research budget.

Although several mineral fragments were recovered from the site, their association with the copper production process was at that stage still ambiguous. Therefore, only four mineral samples were included for LIA while the slag remains were deemed to be the best candidates for meaningful results and formed the bulk of the package with eight samples. Six finished objects samples were kindly provided for LIA by Prof. Lloyd Weeks following their trace element and microstructural study. In addition, a single large fragment was also sampled from the copper mineralization protruding from a hillside at Karakaya and sent for LIA.

Given the encouraging results from the geomorphological study of the area it was thought that the Karakaya mineralization was a likely source of copper ores for Çamlıbel and thus worth characterizing. Unfortunately, sampling of the mineralization had not originally been taken with isotopic analysis in mind and as such only a single large sample was taken from the outcrop. This is generally considered too little to define the entirety of the variability within a single deposit, which, at best, should require at least five to ten analyses and sometimes well over 50 (Pernicka 2014, 249; Pernicka et al. 1993). However, given the relatively small size of the mineral outcrop near Karakaya, barely qualifying as more than a single boulder, lead isotope ratios are not expected to exhibit much variability and therefore the single sample was considered adequate to represent this particular mineralization.

In total 19 samples from five of the six Çamlıbel contexts were subjected to LIA (Table 8.1) as part of this thesis. With the exception of CBT III, all main occupation phases are represented by at least one sample from each material type. In addition to these new analyses, the lead isotope ratios of three copper alloy objects had previously been investigated by LA-MC-ICP-MS at the NERC Isotope Geosciences Facility (NIGL). These results will be included here.

Table 8.1 Distribution of Çamlıbel samples sent for lead isotope analysis. Numbers in parentheses represent samples analysed at NIGL in a parallel study.

Phase	Slag	Minerals	Objects	Total
Surface		1	(3)	1(3)
CBT IV	3	1	1	5
SPEU				
CBT III	2		2	4
FPEU			1	1
CBT II	2	2	1	5
CBT I	1	1	1	3
Total	8	5	6(3)	19(3)

Unfortunately, several factors have had a notable impact on the results and limited their interpretative value. Firstly, the object analyses were expected to be problematic as the objects had been sampled specifically for metallographic analysis. As such, the samples had been previously prepared and mounted in resin for such observations and etched with a variety of acids to accentuate annealing and work hardening features (Weeks, pers. com.). Regardless, it was hoped that meaningful results could be obtained, and in the end only a single object sample (543-6370) was too small and too greatly affected by the prior work for the lead isotope ratios to be determined.

More problematic was the exceedingly low lead content of many of the samples (Appendix B.7), with the obvious exception being that of the lead wire. Only four samples had above 10 ppm of lead and most had well below 5 ppm, as determined by MC-ICP-MS. One slag fragment (440-3567), two objects (773-5138 and 877-5692), and the Karakaya copper mineralization had such low lead content that it was in fact impossible to extract meaningful isotopic ratios from them. This was also the case for two of the three specimens sent for separate analysis at NIGL (624-3828 and 624-3831). In all, although meaningful results could be obtained for the majority of the slag and mineral samples, this was only the case for three out of the eight copper alloy objects sent for analysis. Unfortunately, it also means that it was not possible to characterize the local copper mineralization at Karakaya isotopically, which still leaves a clear gap in our understanding of the site. It should be noted that the extreme paucity of lead in both the Karakaya outcrop and the slags and copper alloy objects from Çamlıbel strongly suggests that these ancient smelters exploited local geological deposits.

In addition to preventing lead isotope characterization of many samples entirely, the low lead content in the slags and objects is further troubling as it implies the use of ore deposits with equally low lead concentrations. This has been recognized as a cause of large variability in the isotopic signature of such deposits due to the influence of newly formed radiogenic lead and the heterogeneity of uranium and thorium distribution in any mineral body (Pernicka 2014). Indeed, while in deposits with greater lead concentrations new lead isotopes formed by the decay of these radioactive elements have little impact on the overwhelming proportions of lead already amassed during geological formation, the opposite is true when lead content is low. In deposits such as those implied by the Çamlıbel LIA results, the production of new lead isotopes can significantly alter the isotopic ratios well after formation of the ore deposits, but does so inconsistently across the body according to the distribution of thorium and uranium. Lead isotope ratios of the Çamlıbel materials are therefore expected to be extremely variable. The low number of successful analyses also means they are less likely to be reflective of the breadth of variation present in the original ore deposits.

Despite these limitations, patterns in the lead content distribution which only became clear thanks to the low detection limit of the MC-ICP-MS instruments are worth mentioning here. It was observed that the three copper alloy objects containing sufficient lead content for isotopic analysis (6324621, 709-4551, and 523-3368) also contained either trace or minor quantities of nickel. Samples which lacked enough lead for ratios to be determined had nickel

contents below the detection limits of the EPMA used for bulk compositional analysis, reported as 77 ± 4 ppm (Appendix B.8).

Of course, this trend may be largely due to the low sample count and must therefore be taken with some reservation, especially since a similar pattern could not be identified in the slag remains, although in that case instrument detection limits were the main constraint.

Indeed, of the seven slag samples where lead isotopes ratios could be determined, only two were found to contain detectable amounts of nickel. However, since the analysis of slag remains was conducted with SEM-EDS, it was only possible to identify the presence of the element when it had been concentrated within sulphidic or metallic prills above the detection limit of the instrument (estimated at 0.1 wt%) and thus the lack of pattern may be partly due to analytical limitations. That being said, there is no correlation between the amount of lead present in the slag and the presence/absence of nickel. In fact, the only slag sample with insufficient lead for LIA was found to contain traces of nickel in some of the prills embedded in the matrix, contradicting the pattern observed in the objects.

Furthermore, mineralizations containing both nickel and lead are rather uncommon geologically (only 6 mineral species with both elements are known to exist) but both co-occur frequently in copper-bearing deposits.

Given that the traces of both nickel and lead were near the detection limits of the instruments used, that their correlation in the finished objects was not reflected in the slag, and that nickel and lead have little geological affinity, it seems most probable that the discrepancy in their content is due to natural variation in the ore deposits. It is unlikely that this reflects the use of distinct sources of ore minerals.

Despite these shortcomings in the sampling and difficulties in dealing with these low lead materials, much of the data remains useful to the discussion. For the purpose of the presentation of the results, three isotope ratio plots ($^{208}\text{Pb}/^{206}\text{Pb}$ and $^{206}\text{Pb}/^{204}\text{Pb}$ versus $^{207}\text{Pb}/^{206}\text{Pb}$, and $^{207}\text{Pb}/^{204}\text{Pb}$ versus $^{206}\text{Pb}/^{204}\text{Pb}$) will be used as they are sufficient in fully characterizing the samples (Gale et al. 1985b); data embodied by further combinations of the lead isotopes are already implied by these ratios and therefore superfluous. Although just two bilplots are often considered to adequately represent the isotopic ranges, because many publications report findings using different sets of ratios this thesis will present the data in the three most commonly used diagrams. When comparing datasets, the published data will be presented according to the system used by the authors. Despite the fact that some of the

relationship data are lost when not presented in three dimensional space (Pryce 2011; Sayre et al. 2001), they are much more clearly understood when defined in the mirrored bi-plots more widely published. When plotted against each other, the different isotopes show a number of promising features (Figures 8.3 and 8.4).

The most obvious result is that two mineral samples are markedly radiogenic when compared to the rest of the assemblage. Both of these mineral samples, 585-4328 and 753-5028, have markedly low lead with 1.4ppm and 2.2ppm respectively and therefore their radiogenic nature is no surprise. The fact that one of the other mineral fragments located in the larger cluster has just 0.8ppm of lead shows how much variability can result from the analysis of samples so deficient in lead. As such, although these extreme values may at first glance appear useful in defining the Çamlıbel material, they are in essence the result of relatively common geological realities which could exist in any number of deposits. Furthermore, they appear in the $^{206}\text{Pb}/^{204}\text{Pb}$ vs $^{207}\text{Pb}/^{204}\text{Pb}$ plot to be on a different alignment than the rest of the assemblage. As such they probably did not contribute greatly to the lead isotope fields of the slag and objects identified at Çamlıbel. Since they do not appear related and because their strong radiogenic nature is likely caused by the lack of lead rather than the age of the deposit, these ratios have little value in comparisons with other datasets and will therefore largely be ignored. Biplots in Figure 8.4 presents the same data shown Figure 8.3 but without the two mineral outliers and focused into the area dominated by the rest of the Çamlıbel material.

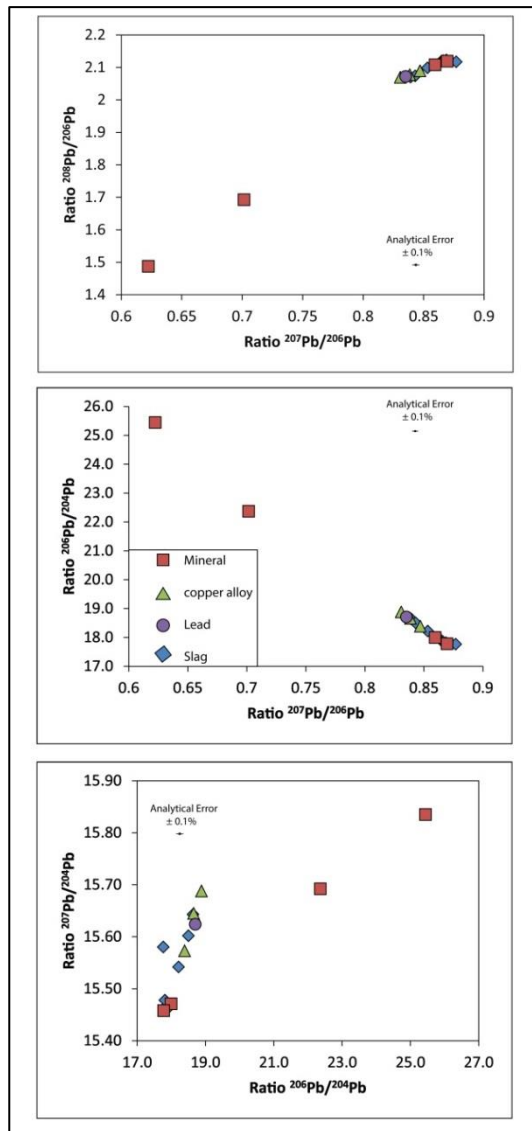


Figure 8.3 Mirror plots of lead isotope ratios for the various materials from Çamlıbel. Note the two strongly radiogenic minerals skewing the results.

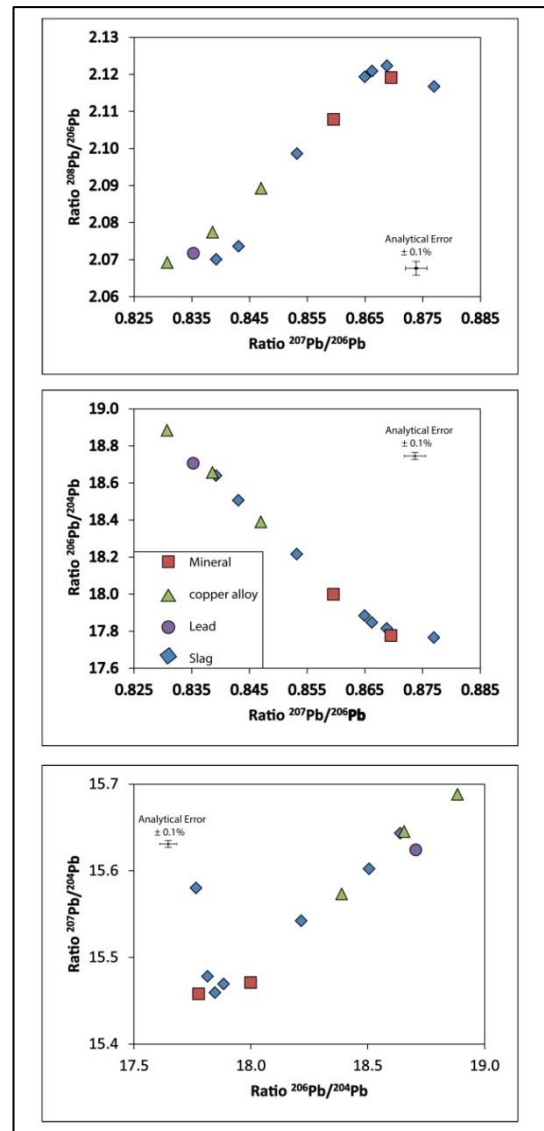


Figure 8.4 The same mirror plots as in Figure 8.1, but with the outliers removed.

The remaining materials have a very widespread distribution, with a rough separation between the majority of the slags and minerals at one end and the copper alloy, the lead wire and two slag fragments at the other.

It should be remembered that the slags and minerals are associated only with pure copper, while the copper objects all contain consistently elevated arsenic. The general clustering seen in the lead isotope data seems to largely fit this observation as it suggests that the copper alloys' isotopic signatures have been consistently shifted to positions intermediate between that of the copper ore and that of an undefined alloying agent. This is similar to case studies where the alloying or recycling of copper could be directly inferred from isotopic distributions (Stos 2009, 168-169). However, the long linear arrangement of the results could also easily reflect isotopic diversity due to the low lead problem already described rather than the

mixing of different materials, as has been highlighted for the site of al-Midamman in Yemen (Weeks et al. 2009) or Mondsee Culture artefacts in the Austrian Alps (Frank and Pernicka 2012). The two fragments of slag which plot close to the copper alloy artefacts (210-299 and 836-4860) certainly reinforce this possibility, especially given that there is little to differentiate these two specific samples microstructurally or compositionally from the rest of the assemblage. They certainly do not originate from unique or isolated contexts, but rather belong to the main activity areas of the earliest and latest occupational phases respectively. As such, they are roughly representative of the typical Çamlıbel slag and the fact that they plot so close to the objects is most likely due to natural variability in the isotopic ranges. It is unfortunate that the two slag samples with high arsenic content (740-6358 and 561-3957) were identified as such only after the program of lead isotope analysis had been concluded and could therefore not be included in this study. Their isotopic characterization would have helped in clarifying their nature as possible alloying slags and their future analysis remains a possibility.

At first glance, the lead content of the copper alloys (~3 ppm mean for all samples, including those below detection limits), slag fragments (5.6 ppm mean) and minerals (8.4 ppm mean) make it less likely, although not impossible, that the shift in ratios is due to the addition of an arsenic alloy. However, for such a shift in isotopic ratios to occur from the combination of two metals, a significant amount of lead must be present in the alloying agent to affect, if not entirely overwhelm, the isotopic composition of the receiving material. Since the alloying material only forms a small proportion of the total composition of the new alloy (up to ~5 wt% for Çamlıbel's arsenical copper objects) and since lead does not preferentially partition into metallic elements, the incoming charge would need to contain a significant fraction of lead in order to affect change in the final product. This should at least result in a noticeable bump in lead content in the final composition of the objects. The Çamlıbel data do not demonstrate this increase.

While arsenic often occurs in complex fahlor deposits along with lead, copper, nickel, bismuth, antimony and a wide range of other impurities, when found in its relative pure forms derived from primary sulphide deposits such as arsenopyrite, realgar, or orpiment, it does not tend to be associated with lead. Given that the objects are not enriched in the elements commonly introduced by fahlors beyond what is observed in the slag, it is likely that the source of arsenic was derived from one of these more 'pure' oxidized primary mineralizations. Thus, if arsenic minerals were indeed alloyed to pure copper produced on site, they did not introduce significant amounts of lead to the melt, and as such could not

have had much impact on the isotopic ratios witnessed here. The fact that a larger proportion of the objects had lead below the detection limit of the MC-ICP-MS than the slag and minerals further reinforces this point.

It should also be noted that the crucible fabrics themselves and perhaps even the fuel ashes can have some impact on lead isotope ratios with extreme lead deficiencies. Such skewing effects from crucible fabrics have indeed been proposed in the context of crucible-bound melting and casting of low-lead copper from Apliki, Cyprus at the site of Pi-Ramesse in Egypt (Rademakers 2015, 228). That being said, the minimal interaction witnessed between the crucible fabrics and the slag at Çamlıbel (see section 7.1.2) means that the crucible and furnace walls probably did not greatly affect the material in this case. The effects of fuel ash on the other hand are poorly understood and thus far undocumented. Given the small-scale nature of the metallurgical operations undertaken at Çamlıbel it is unlikely that significant amounts of lead, in absolute terms, could be introduced into the slag and metal by that pathway. However, given the extreme paucity of lead in the slag, it is indeed possible that even minute quantities of lead introduced from fuel ashes could have had a measurable impact on the isotopic ratios, a possibility which requires experimental investigation.

One is therefore forced to the conclusion that the apparent linear distribution separating the primary production material from the finished product is purely the result of natural variations within the isotopic field rather than the mixing of metals. While it remains possible that arsenic and copper were alloyed together, neither the arsenic nor the copper source appear to have had any noticeable lead in them, which makes it impossible to state with any degree of confidence whether they came from different or the same source.

Another point of interest in the data is that the lead wire plots in the same region as the copper alloy objects. These two metals must have originated from different ores entirely given the extreme paucity of lead in the copper alloys, and yet they have similar isotopic signatures. There is no way of explaining this connection other than through coincidence as any link between the two deposits should be reflected in the lead content. Although it is possible that both the copper and lead ores have the same geological age, it is highly unlikely that they formed in the same geological reservoir. As will be discussed shortly, all objects, whether lead or copper alloy, fall within the range of a number of Anatolian ore fields and thus it is quite likely that the lead and copper originated from completely unrelated fields.

In order to place the data within the wider archaeological context of the region, the results were plotted against available published lead isotope datasets. The first biplot graph (Figure

8.5) compares the isotopic signature of the Çamlıbel material to that of a wide range of well-characterised Turkish copper and lead ore deposits (Begemann et al. 1989; Begemann et al. 2002; Gale et al. 1985b; Hirao et al. 1995; Sayre et al. 2001; Wagner and Öztunalı 2000; Wagner et al. 1986; Yener et al. 1991).

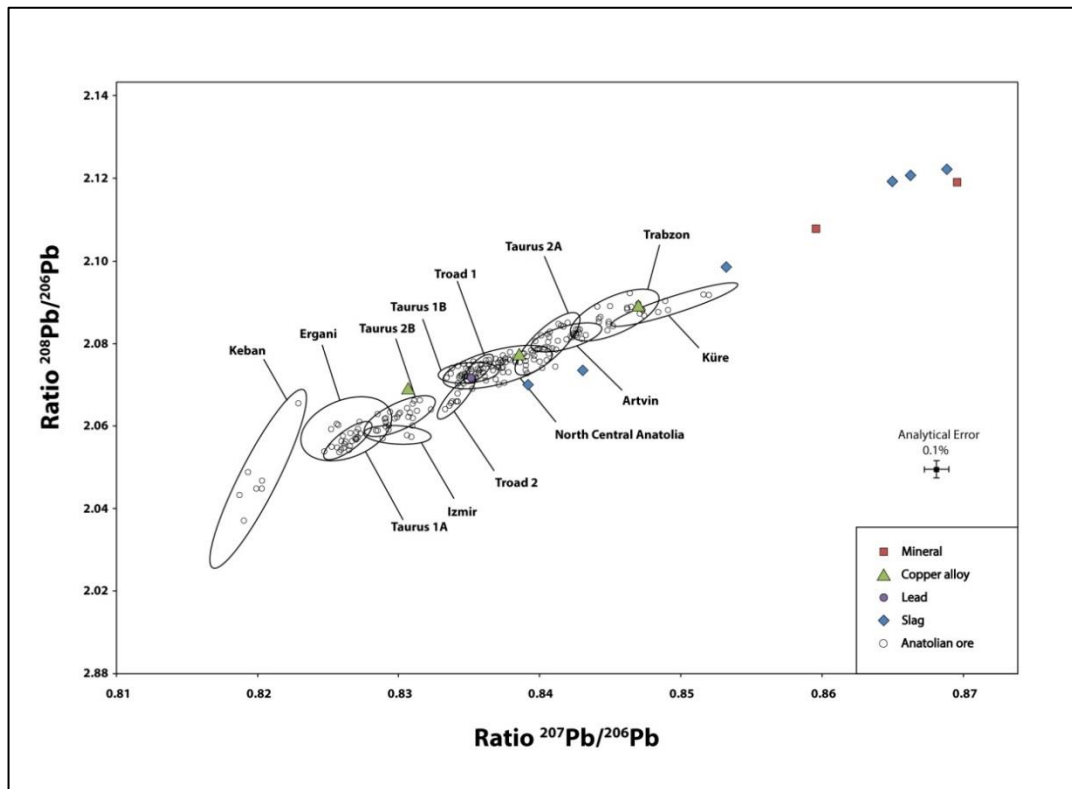


Figure 8.5 Çamlıbel material within the context of well-defined Anatolian ore deposits. Reproduced from Lehner et al. (2009) from data gathered from a wide range of published sources. Note the wide range of the Çamlıbel material compared to the much narrower fields of individual ore deposits represented by numerous analyses each.

Given the socio-cultural and technological context of Çamlıbel, it would be highly dubious to suggest that ores were sourced from areas very distant from the site itself, let alone beyond the Anatolian plateau. As such, this set of isotopic fields represents the most probable associations for the production remains. Furthermore, while it is possible that the finished objects originated from further afield, the region defined by these deposits represents an approximate 300-500 km radius around the site and should be considered their likeliest provenance should they not have been manufactured at Çamlıbel itself.

As can be clearly seen, extreme variability continues to plague the interpretative value of the dataset. The results are spread across several known ore fields with a cluster of slag and minerals beyond the typical Anatolian isotopic ranges. These outliers are highly relevant as they appear to be geologically older than any of the well characterized ores for the region and may form a uniquely identifiable isotopic signature. On the other hand, all of the objects

and two slag fragments plot within and in the vicinity of regions covered by several overlapping isotopic fields.

The copper alloy objects probably do not in fact belong to any of these geological deposits for the reasons already explained, but rather likely relate to the slags and minerals found at the site. Even assuming that they are unrelated to primary production remains at Çamlıbel, they do not cluster in any identifiable field or even the same general area as each other which might have facilitated in provenancing them. One sample plots near the Taurus 2B deposit, one in the area of overlap between the Küre and Trabzon fields, and the third plots in both the North Central Anatolian and Troad 1 regions. The central location of Çamlıbel means that all the deposits (except the north central Anatolian field), are situated 300 km or more from the site. Some areas can, however, be completely discounted. This includes the Ergani Maden, the Izmir region, the Taurus 1A field, the mining district around the town Artvin, and the Keban area, all geological deposits of younger age. The object typologies are equally unhelpful, consisting of two needles and a casting droplet, further preventing any assignation to any cultural source region. Overall, although it is possible that these objects originated in the various regions observed above, it is not very probable, especially given the use of the site as a primary production centre and the problems caused by paucity of lead. It is much more likely that they plot in a wide region which includes the two fragments of slag near the North Central Anatolian field and extends all the way to the cluster with the rest of the production material.

In contrast to this ambiguity, the lead object is certainly not related to the Çamlıbel minerals or slag and its position within the biplot is much more trustworthy. Unfortunately, it lies in the single area with the greatest amount of overlap between geological deposits. This includes the large area of North Central Anatolia, both Troad deposits, and the Taurus 1B. Although geographically the North Central Anatolian region is the most logical source for the lead, objects from this time period are known to have been extensively traded across vast distances which means the other three origins cannot be entirely ruled out. The nature of the object, a simple lead wire, provides no insight into distinguishing between the regions.

Interestingly, the clustering of primary material at one end of the array may represent the more 'typical' signature for the geological deposit exploited at Çamlıbel, but with a long diffuse tail extending through the lower ratios of more commonly exploited Anatolian deposits. The cluster of older primary production material is still significant in that it lies far beyond the usual isotopic ranges and is therefore quite unique and may form a discriminating

grouping. Although the variability of the deposit is indeed high and can be cause of confusion and interpretative error, archaeological objects with lead isotope signatures that fall within the isolated field may convincingly be associated with the Çamlibel area since no Anatolian deposits come even remotely close to that range.

This characteristic holds true well beyond Anatolia alone. Broadly speaking, the vast majority of ore deposits from Anatolia, the Aegean, and the Near East plot in clusters with $^{208}\text{Pb}/^{206}\text{Pb}$ below 2.09, with the important exception of those from the so called dolomite-limestone-shale (DLS) ores of Faynan, Jordan (Hauptmann et al. 1992), and their counterpart in Timna, Israel (Gale et al. 1990), which are geologically older (Figure 8.6) and will shortly be discussed.

Despite the somewhat disappointing isotopic results from which so few conclusions can be drawn, there is one further point which offers a glimmer of redemption. It emerges from the comparison of the production remains' lead isotope ratios against those of known archaeological objects from other sites in the region. As previously touched upon, although the distribution of the Çamlibel isotopic field is very large, there is a noticeable clustering in of material at one end of the array which is distinctive enough from other known geological deposits in Anatolia to define an isolated grouping (see Figure 8.5). This separation also holds true for well-characterized lead isotope ratios of ore deposits from Greece and the Aegean (Stos-Gale 1989; Stos-Gale and Gale 2011) (data obtained from the Oxalid online database [accessed 06/08/2015]), as well as those of Western Iran (Pernicka et al. 2011) exploited during the Bronze Age and earlier (Figure 8.6).

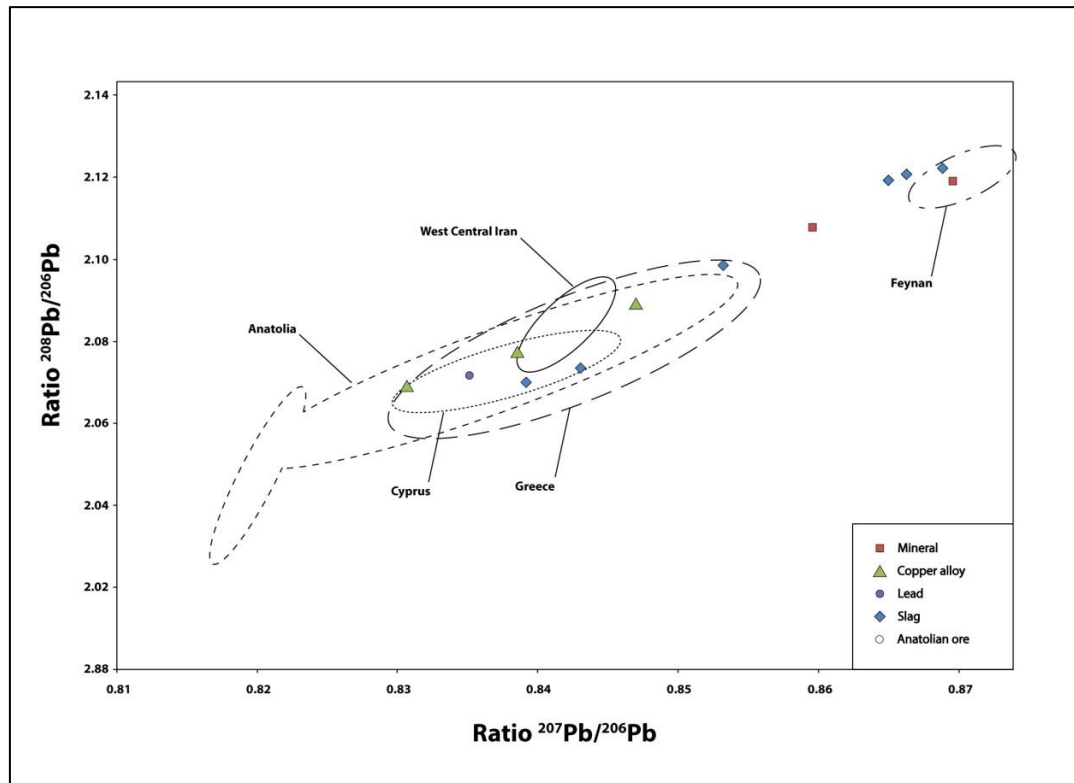


Figure 8.6 Lead isotope ratios of Çamlıbel material compared to known exploited deposits in the Near East and Eastern Mediterranean. This covers most of the deposits known to have been exploited during the Bronze Age and earlier periods. Data aggregated from several sources (Gale et al. 1990; Gale et al. 1985a; Hauptmann et al. 1992; Lehner et al. 2009; Pernicka et al. 2011; Stos-Gale and Gale 2011).

The only deposits which come close in terms of LI ratios are those of Faynan and Timna, although these are known to have been exploited much later, between the late 4th and the early 3rd millennium BC for Faynan (Hauptmann 2007) and the Early Iron Age for Timna (Ben-Yosef et al. 2010). Although the primary material from Çamlıbel appears deceptively close to that of the DLS ores of Faynan in the $^{207}\text{Pb}/^{206}\text{Pb}$ versus $^{208}\text{Pb}/^{206}\text{Pb}$ and the $^{207}\text{Pb}/^{206}\text{Pb}$ versus $^{206}\text{Pb}/^{204}\text{Pb}$ dimensions, they are entirely different when plotting $^{206}\text{Pb}/^{204}\text{Pb}$ against $^{207}\text{Pb}/^{204}\text{Pb}$ (Figure 8.7).

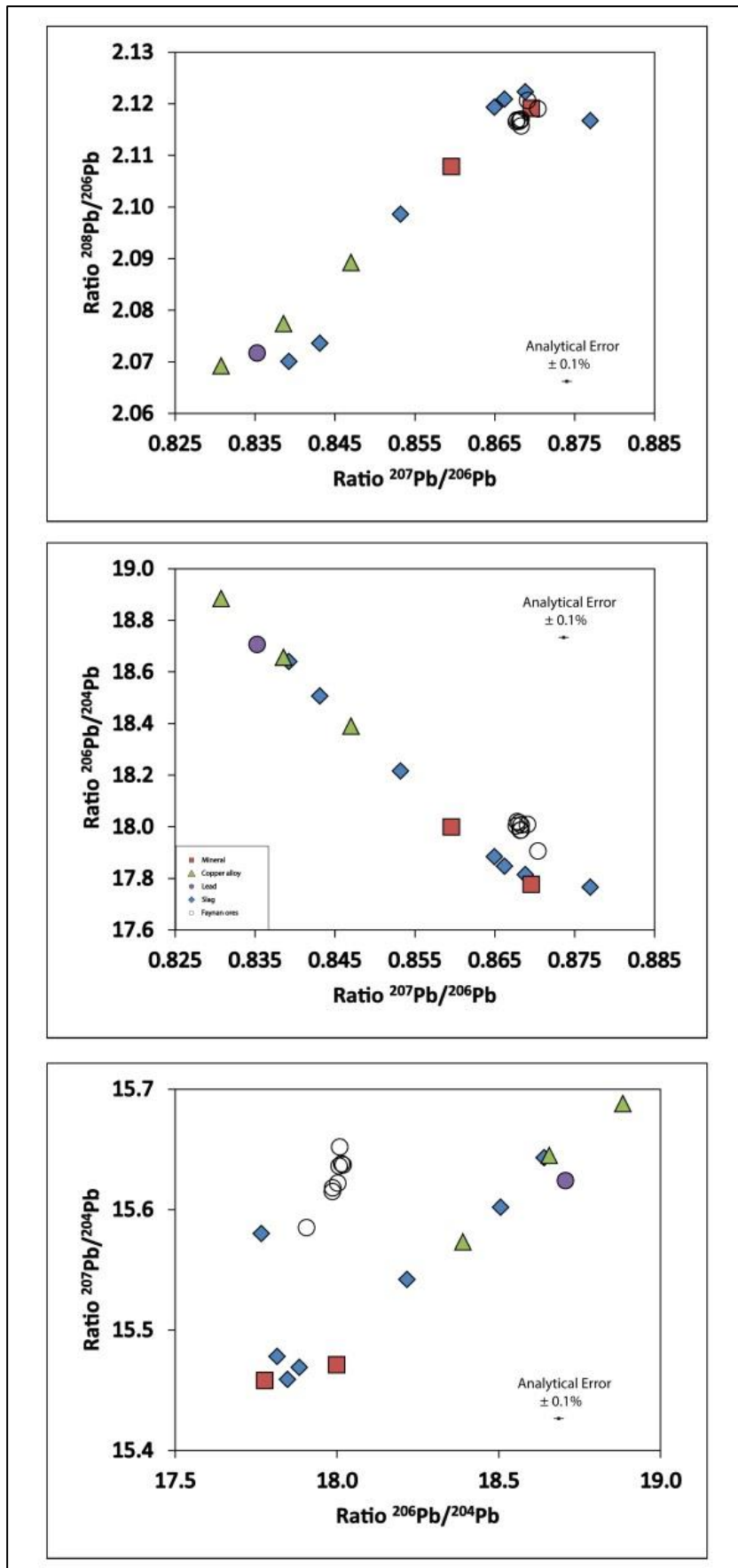


Figure 8.7 Biplots of lead isotope ratios measured for Çamlıbel's material against Faynan's DLS ores obtained from Hauptmann (1992).

Therefore, despite a large spread, one cluster of primary material from Çamlıbel defines an isotopic signature which is unique to the vicinity and does not overlap with any other regionally known copper deposits exploited during the period in question. While objects produced from these ores may appear to originate from other deposits due to the low lead content, artefacts which fall within the Çamlıbel cluster have a high probability of originating from the same deposits.

While the limited nature of the copper deposits near Çamlıbel mean that they were unlikely to ever have been extensively or industrially exploited at any point, it would not be surprising for some intermittent local metal production to have taken place throughout the prehistoric periods until imports from more distant lands in the 3rd millennium BC superseded local production (Yener et al. 1991). To this effect, a study of the lead isotopes of copper artefacts from the region reveals a number of objects within or near Çamlıbel's isotopic field which are worth exploring in more detail.

More specifically, a group of objects from Central Northern Anatolia, conveniently named the Central Artefact Group, have been highlighted in a number of publications as having high $^{207}\text{Pb}/^{206}\text{Pb}$ ratios that do not match any known deposits (Hirao et al. 1995; Sayre et al. 2001). This series of seven copper alloy objects, all belonging to the same Hittite layer of Kaman-Kalehöyük (Stratum III, dating to the 20th to 12th Centuries BC), all have lead isotope ratios that match those of the cluster of production material from Çamlıbel (Figure 8.8). They were originally thought to belong to the 'North Central Anatolian Exceptional Copper ores' group (Hirao et al. 1995) as they plot together when comparing $^{207}\text{Pb}/^{208}\text{Pb}$ against $^{208}\text{Pb}/^{206}\text{Pb}$. However, Sayre et al. (2001) have pointed out that this is simply a coincidence as they are not relatable in the $^{206}\text{Pb}/^{204}\text{Pb}$ versus $^{207}\text{Pb}/^{204}\text{Pb}$ dimension. When comparing these results to Çamlıbel's production material, it can clearly be seen that they have the same geological age and match in all projections of the LIA data space. Unfortunately, lead contents for these objects, which could cement the association should they prove to be equally deficient in the element, could not be obtained from the authors. As has already been discussed however, no other geological deposit overlaps that of Çamlıbel's production cluster and therefore the Kaman-Kalehöyük objects were most likely produced from ores issued from the same or related geological deposits.

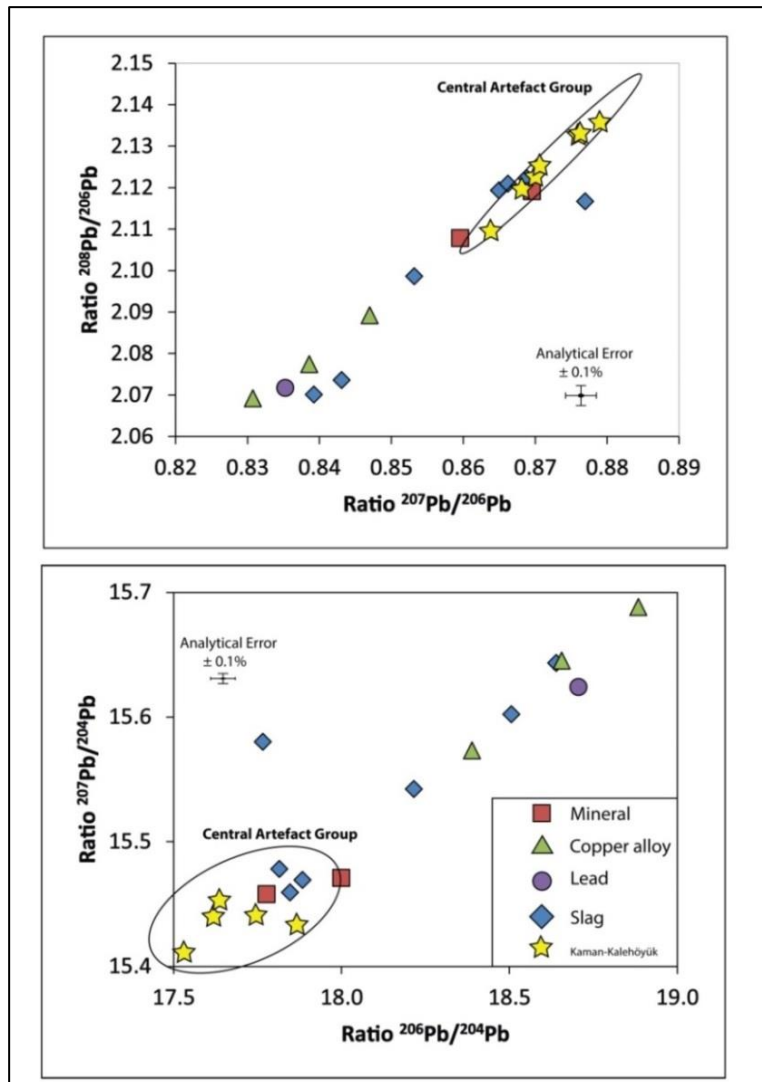


Figure 8.8 Comparison of the lead isotope ratios of Çamlıbel material with that of Kaman-Kalehöyük Stratum III. The circled areas are those marked by Sayre et al. (2001).

Since Hattusa, the Hittite capital, is located very close to Çamlıbel, it would not be surprising for local ores or locally produced metal to be traded the relatively short 100 km distance to this culturally related site. Although unlikely to be linked to metal production of Çamlıbel itself given the centuries that separate the occupation of the two sites, the use of the same ore deposits at a later period is certainly archaeologically and geographically sound.

Overall, although limited insight has been gained on the provenance of the Çamlıbel material itself, it has been possible to characterise the unique attributes of the geological deposit from which it was produced and relate it to artefacts from at least one other site despite problems caused by the paucity of lead in all but one sample analysed and the high variability resulting from it. Furthermore, despite the fact that alloying of arsenic and copper could not be confirmed through lead isotope analysis, it remains a possibility that can be corroborated by other lines of evidence.

Chapter 9 Discussion

9.1 Chaînes Opératoires and Site Comparison

In light of the results obtained by this thesis, it is now possible to reconstruct several aspects of the arsenical copper *chaîne opératoire* at both Çamlıbel and Arisman. This section synthesizes the results of the analytical program undertaken during this thesis for each site and then compares these results in order to assess whether supra-regional development in alloying technology did in fact exist.

9.1.1 Çamlıbel

Before discussing the smelting and alloying technologies of Çamlıbel, it is important to start with the current state of knowledge of the nature of the ores exploited by the site's inhabitants. While the preliminary report stated that the primary copper ore mineral was malachite or another oxidic mineral (Rehren and Radivojević 2010), the large overabundance of matte in nearly every analysed slag sample and the ubiquitous presence of high temperature solid solutions of iron and copper sulphides indicate, at least, a large sulphidic and iron-rich component. Given that chalcopyrite was the dominant copper-bearing phases in the Karakaya ore source as well as in several minerals recovered from the site, iron-copper sulphides are likely to have formed an important if not the main copper-bearing ore mineral exploited at Çamlıbel. These would then have had to either be co-smelted with an oxidic copper mineral charge or partially roasted in order to ultimately produce copper metal under the lightly reducing conditions known to have been achieved by Çamlıbel's smelters. Since very few fragments of roasted ore or partially reduced matte were found, products commonly associated with the smelting of largely sulphidic minerals, a source of oxygen in the form of oxidic ores used in a co-smelting operation is highly likely. As such, the main ore forming minerals were neither oxidic nor sulphidic but most probably the combination of both but with an excess of sulphur (Lechtman and Klein 1999; Rostoker and Dvorak 1991; Rostoker et al. 1989). While not widely recognized for this early time period, the use of mixed sulphide and oxide copper ores has been noted in much earlier contexts, such as the Varna Culture of the Balkans (Ryndina and Kolosova 1999) and Shar-i Sokhta in Southern Iran (Hauptmann et al. 2003), and should come as no surprise here.

That being said, it is important to note that the inhabitants of Çamlıbel appear to have viewed matte as waste rather than an intermediate product, much as has been described for the Early Bronze Age site of Shahr-i Sokhta (Hauptmann et al. 2003). This is evidenced by the lack of further processing of slag cakes rich in matte to extract the remaining copper. This fact is

problematic in that it may have created a depositional, and therefore also sampling, bias in favour of sulphide rich slag. Indeed, since all of the slag fragments sampled are essentially discarded waste products, it is possible that slag produced from more successful and 'typical' smelts was then further processed to extract all available copper metal. Such an operation may have revolved around the crushing of the slag to a very fine fraction or recycling them in later smelts, which would have essentially made them archaeologically invisible. Alternatively, the absence of this material in the record may be the result of efforts to avoid the loss of copper prills by conducting the processing of copper-rich slags over a skin or other fabric which could then be shaken loose elsewhere in secondary context away from the site as has commonly been suggested for flint knapping activities (Behm 1983, Olausson 1986). If this was indeed the case, then the sulphide-rich slags do not reflect the 'typical' smelting technology of Çamlıbel and cannot be used to accurately infer the original charge. Problematically, the selective discard and preservation of only some of the waste products, were it to have taken place at Çamlıbel, is rather difficult to demonstrate archaeologically since it is based on the absence of evidence. Therefore, although deposition bias remains a possibility, all available data point towards the use of mixed ores with a strong sulphidic component, and this is therefore the favoured interpretation.

Given the nature of the Karakaya mineral outcrop as highly iron-rich, it appears likely that the ore exploited by the inhabitants of Çamlıbel was first crushed and processed to remove much of the iron sulphide fraction and to mechanically concentrate the copper-bearing minerals. The presence of discrete lumps of corroded high temperature solid solutions of chalcopyrite at the site suggest that some efforts were made to roast the ores prior to mechanical beneficiation but that the sulphide component was never entirely removed.

It is interesting to note that the ratio of slag to mineral increased dramatically following period CBT III. This may be indicative of a change in the location of beneficiation away from the site and smelting activities edging closer to the site (Figure 9.1). Such a change was conceivably caused by the depletion of ore deposits close to Camlibel itself and thus the processing of ores at the mine or at the smelting site becoming more attractive. This interpretation fits in well with the nature of copper mineralizations in the area which are rich but small and dispersed. Alternatively, the observed changes in the composition of the assemblage could represent a shift towards less beneficiation leading to a decrease in the amount of gangue minerals discarded and an increase in the production of slag. However, had ores undergone less processing in the later periods, the decrease in the ratio of copper

to gangue minerals would have resulted in a proportional decrease in the concentration of copper in the resulting slag, so long as the smelting process remained identical. That no such change could be observed in the bulk copper content of earlier and later slag means that, although not impossible, it is unlikely that beneficiation practices underwent any great change. Therefore it is safe to conclude that the rise in total slag quantity and weight implies an increase in the production volumes at this period resulting in a greater copper output. That this does not correlate with an increase in the number of copper alloy objects recovered from the site may suggest that a greater proportion of the produced metal made its way out of the settlement in the later periods.

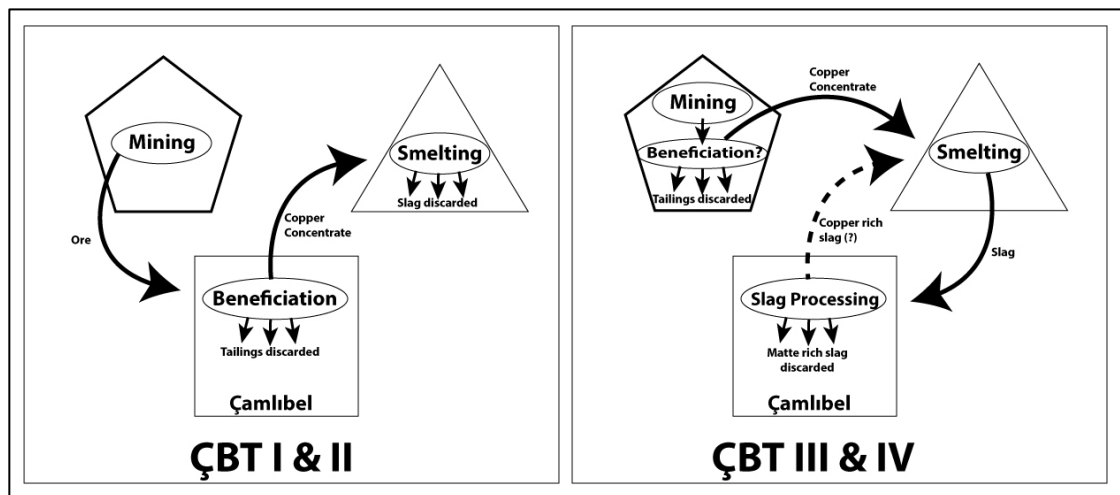


Figure 9.1 Diagram of the shift in metallurgical activities being conducted in and around Çamlıbel.

Since the nature of the bowl hearth installations has been put into question, there is no clear evidence that smelting was indeed taking place at the site of Çamlıbel itself. While the association of the bowl-shaped hearths with a copper producing site certainly seems to fit at first glance, the low temperature nature of the operations carried within them and the lack of copper and arsenic contaminants within the fills make this an improbable relationship. In addition, the slag morphology clearly shows that they were dumped from above onto a cold surface, which could not be accomplished in features such as these without the use of crucibles. That no such crucibles were identified in layers containing bowl hearths makes it even less likely that they were involved in copper metallurgy. The hearth features, with the associated deep deposition of ash and charcoal, are more likely to be related to either charcoal making or to the synthetic bead industry previously identified at the site (Pickard and Schoop 2013).

Smelting was therefore likely conducted away from the main site and most probably in small crucibles. These crucibles were most likely made of the non-refractory clay used in common

pottery but with the addition of organic temper and using specialised shapes more suitable for the retention of heat. Although common pottery wares are known to have been used as pyrotechnological ceramics in some early instances (Bourgarit 2007, 11), specialized shapes and fabrics intended for use in smelting activities were the norm rather than the exception even during the Chalcolithic (see section 9.4). This is certainly the case for the alloying and melting crucibles as well as the casting mould. Since smelting was not likely conducted directly on site, it is no surprise then that no blowpipe nozzles or tuyères have so far been uncovered. The nature of the air supply therefore remains enigmatic. The presence of large quantities of matte along with patches of magnetite spinels within the slag suggests that while the conditions were relatively oxidizing, they were still too reducing to effectively remove all the sulphur from the charge. That being said, recent studies have demonstrated that oxygen present in the solid state and iron sulphide, introduced via the ore charge, play much larger roles in dictating the redox conditions of the system than gaseous oxygen alone (Burger 2008; Liu 2014), making any assessment of airflow based on the microstructure of the slag nearly impossible. Although it has long been established that the mixed sulphide/oxide nature of the ore charge would have generally been greatly beneficial to the production of copper by providing a self-regulating system reducing copper to metal while providing free oxygen for the sulphides to be oxidized out of the charge while providing an additional source of heat (Rostoker and Dvorak 1991; Rostoker et al. 1989), the importance of using adequate ratios of sulphide/oxide minerals is only now becoming apparent. As has already been discussed, the temperature within the furnace must have reached up to 1200 °C, well within the limits of what is expected to be achievable with simple bellows or even blowpipes. No evidence for the addition of flux was identified and, in any case, none was required given the nature of the ore which appears to have been largely self-fluxing. Indeed, the nature of the tailings identified at the site and that of the Karakaya mineralization suggests that the ore used contained a proportion of iron and silica which is consistent with that found in the slag, and could easily have formed the pyroxenes observed in the slag without requiring the addition of any flux.

Under these conditions, prills of copper and matte were formed and remained floating within a semi-molten, tacky slag. These slags were then dumped onto a cold slightly convex surface such as sherds of domestic pottery. The product of these operations, as evidenced by the analysis of copper prills embedded within slag, was clearly pure copper with some measure of iron impurities. That being said, only about a quarter of all slags contained pure copper, suggesting three possibilities: that the success rate was rather low, that the copper-bearing

slags were crushed to extract trapped copper prills, or that slag from relatively unsuccessful smelts was preferentially brought to Çamlıbel for further processing or beneficiation. It is nevertheless clear that, no matter the success rate of such smelting operations and where the slag was transported, the inhabitants of Çamlıbel thought it economically viable and continued to produce pure copper for several generations.

The results from the crucible analyses show that, once enough pure copper was produced, it was re-melted and alloyed with arsenic just prior to casting it. In all likelihood an iron arsenate or arsenide mineral with minor quantities of copper, as inferred from the composition of the two identified fragments of crucible slag, was added to molten copper where the arsenic dissolved and entered the metal through a process of cementation. Keeping this operation separate from smelting offered several benefits to ancient smelters. On the one hand it would have prevented excessive losses of arsenic through oxidation and volatilization by limiting the number of high temperature reactions. Furthermore, adding the arsenic only just before casting would also have helped in granting more control over the resulting composition of the alloy, a control which is clearly demonstrated by the consistent arsenic content of final products (Appendix B.8). In addition, in the case of an arsenate, the reduction of the mineral would have led to the release of free oxygen which would have helped in refining much of the remaining iron out of the copper as crucible slag much as the well-known process of fire refining (Tylecote et al. 1977) with the added benefit that the reactions occurred within the melt rather than just at the surface. That little iron or sulphur was identified in the finished objects (Appendix B.8) certainly corroborates this, as the addition of the more common arsenopyrite minerals are known to increase the presence of both of these elements which would then need to be refined out (Özbal et al. 2002, 436, table 4). The resulting arsenic-enriched copper, free of iron impurities and with a significantly reduced melting point, could then be easily cast directly into an available mould such as the mould fragment recovered from the site (Schoop 2009, 65).

It is worth noting a number of prehistoric sites in the Iberian Peninsula have been interpreted wholly differently than the reconstruction proposed despite highly similar assemblages. The site of El Malagon, for example, was first interpreted as demonstrating clear evidence of the intentional alloying of arsenic minerals with copper based on the analysis of ores which showed little or no arsenic, but its enrichment both in final objects and on the inner surface of mould fragments (Hook et al. 1987). This was, however, later refuted when it was discovered that the ores did contain some arsenic after all and that the arsenic rich refractory surfaces were simply the result of enrichment from arsenic volatilization during casting (Hook

et al. 1991). Such a scenario clearly does not apply for the site of Çamlıbel which shows an irrefutable lack of arsenic in the primary production remains of copper metal. Arsenical copper here was clearly the result of an intentional alloying of pure molten copper

It is interesting to note that some large fragments of broken local pottery wares exhibited strong evidence of localized heating which proved to also contain elevated levels of copper contaminants. Since it has been demonstrated that smelting was not conducted directly at Çamlıbel, it is most likely that these objects were involved in the melting, alloying, and casting of metallic copper and arsenical copper. None of these ceramics show signs of exposure to extreme temperatures for prolonged periods of time. As such, it is unlikely that they are fragments of technical ceramics and thus much more likely to have been used either as opportunistic tools to manipulate hot slag and metal or as rough floor tiling around the activity area onto which, occasionally, molten material dripped and dribbled. Either way, they do not themselves provide new information on the metallurgical activities themselves, but they do paint an overall picture of the metalworker's workspace and inventive use of available scrap material.

Tellingly, the vast majority of melting crucibles, fragments of 'stained' ceramics, and slag were recovered from the central courtyard of the site in the layer dating to the last occupation period of the site, CBT IV. In addition to these finds, hammerstones, anvils, and a large structure described as a large domed oven situated on an elevated platform were also identified as having originated from this context. The close association between the 'oven' and these objects suggests that the feature was most probably related to metallurgical activities rather than used for more domestic purposes. Despite the presence of large quantities of slag, the lack of highly vitrified furnace remains or of identifiable smelting crucible remains suggests that smelting was not likely taking place here. Instead, copper was probably smelted elsewhere and slag cakes brought to this location to extract any remaining trapped copper prills on site. Pure copper appears to then have been melted, refined, and alloyed with arsenic to be finally cast into moulds in this central courtyard.

This series of processes, up to the production of arsenical copper, can be summarised as the arsenical copper *chaîne opératoire* of Çamlıbel (Figure 9.2).

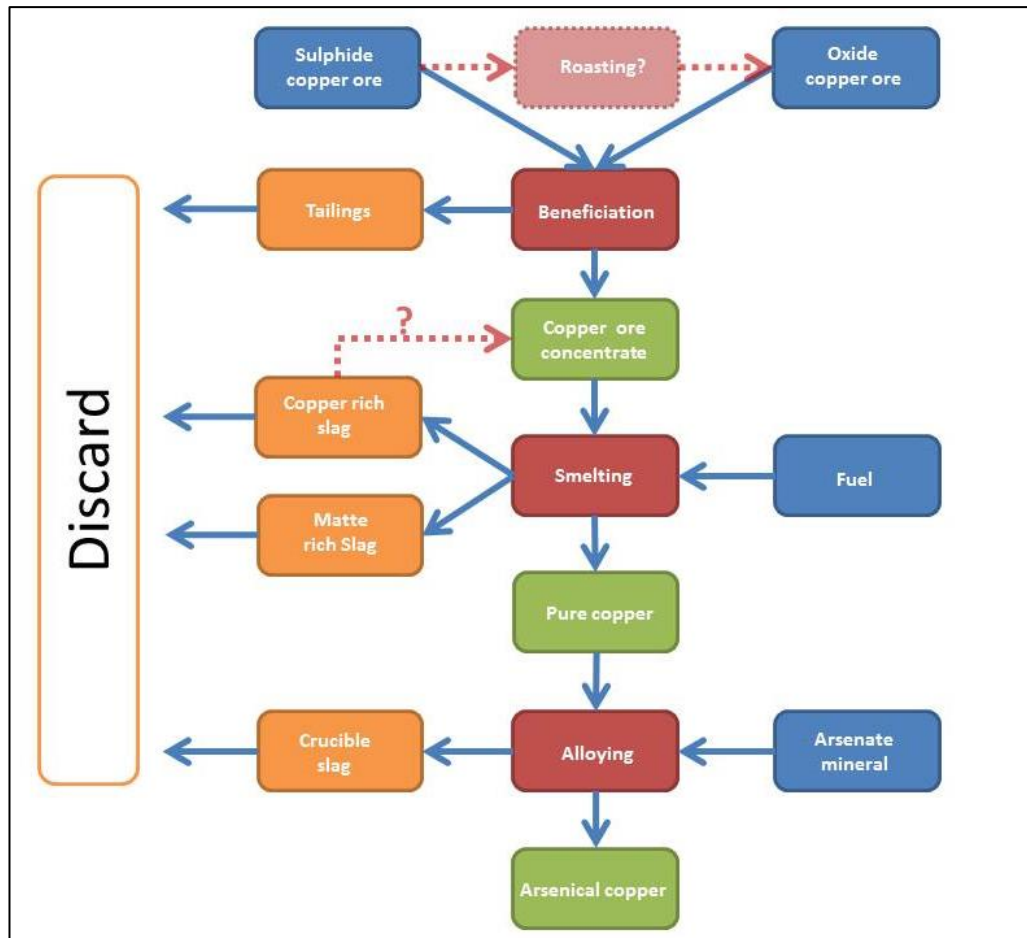


Figure 9.2 Çamlıbel's arsenical copper chaîne opératoire. Note that dotted lines and transparent boxes represent operations which are suggested but for which only indirect archaeological evidence exists - namely the roasting of ores and the recycling of copper-rich slag.

What makes this site quite remarkable is that, unlike most other Chalcolithic arsenical copper production sites in Western Asia where the intentional alloying of arsenic has been proposed as only a possibility (Özbal et al. 2008; Rehren et al. 2012; Thornton et al. 2009), Çamlıbel forms the earliest direct evidence of the conscious mixing of these two elements as a distinctive step. The only other site to demonstrate similar evidence in the wider region is that of Poros Katsamba in northern Crete dating to Early Minoan II and perhaps as early as Early Minoan I (Doonan and Day 2007; Doonan et al. 2007), roughly half a millennium to a full millennium later than Çamlıbel's material. In that context, however, the alloying material appears to have been ferrous speiss (Thornton et al. 2009, 309). Although the smelters of Çamlıbel and Poros Katsamba were on a similar footing in terms of alloying technology, the latter is much more closely related to approaches developed in Iran around the same time period as typified by the site of Arisman discussed in this thesis and previously published preliminary work (Boscher 2010; Rehren et al. 2012).

9.1.2 Arisman

Since two separate but related metal extraction processes have been identified at Arisman, the reconstruction of the arsenical copper *chaîne opératoire* there is more complex than Çamlıbel's. This section will first discuss the production of copper as inferred from the analysis of green slags and their related finds, followed by a discussion of the speiss slags and their interpretation, and finally an overview of how these two technologies relate to each other. In light of these findings, a re-assessment of the furnace uncovered beneath slagheap A will also be discussed.

Given the composition of the majority of copper bearing slags discussed in section 7.2.4, it appears that copper was mainly produced from mixed oxide/sulphide mineralizations, most probably chalcopyrite and its secondary minerals which are common throughout the Orumiye-Doktar metallogenic zone of Western Iran (Mansour 2013). Much like Çamlıbel, this is based on the common presence of copper sulphide phases within the slag and the lack of material remains commonly associated with the roasting of sulphidic ores and the matte smelting and conversion processes.

The relatively low arsenic content present in the bulk of the copper slags but its presence in many of the copper prills suggests that some arsenic-bearing minerals were usually present during smelting. Whether this arsenic was introduced along with the copper ores or through the addition of another material is difficult to establish. The lead isotope data (see section 8.1) show that the synthetic speiss, or the ore from which it was produced, was most probably not added to the charge here as they have isolated lead isotope signatures. Had they been mixed in the charge, the copper slags would have exhibited an extended mixing trail (Weeks 2003) which should have matched that of the finished objects. The arsenic in the copper slags therefore most likely originated with the copper ores themselves. The fact that the copper prills contained highly variable amounts of arsenic and that approximately a quarter of the copper slags contained no significant quantities of arsenic suggests that the arsenic content of the copper produced at Arisman was highly variable. This point is highly pertinent as it suggests the existence of a secondary reliable source of arsenic added to the finished products to produce an alloy of consistent composition and is central to our understanding of alloying practices at Arisman.

Depending on the amount of sulphur present, the copper ores may have required roasting prior to smelting. However, given the scarcity of data on the original mineralization, it is at this stage impossible to state with any degree of certitude whether this step was undertaken

at Arisman. Regardless of whether they were roasted or not, significant amounts of sulphur remained in the charge during smelting, resulting in the formation of fully liquid matte in the slag. This is typical of this period's exploitation of mixed sulphide/oxide sources and has been observed at a number of near-contemporaneous sites throughout the Near East and the Eastern Mediterranean (Georgakopoulou et al. 2011; Hauptmann et al. 2003; Schreiner et al. 2003).

These copper ores appear to have been smelted under lightly reducing conditions as exemplified by the abundant presence of magnetite. The furnaces' running temperature, necessary for the slag and copper prills to be fully molten, is estimated to have been approximately 1100-1200 °C based on equilibrium phase diagrams.

Interestingly, the truncated-cone shapes of the few near-complete slag cakes have clear menisci on their base, suggesting a liquid-liquid interface at the time of solidification. This, along with the lack of tapping features observed on the green stained slags categorically demonstrates that these were left to cool in the furnace. This would have required the front of the furnace to be broken apart to extract the metal product. While at first glance this last point matches the description of the furnace excavated beneath slagheap A, the reconstruction by Steiniger conclusively shows that the operation of this particular furnace involved the tapping of the slag and product into a crucible placed on a clay lined shelf below the furnace (Steiniger 2011, 77-79). Although the reconstruction fits well with all of the available archaeological data, such as the two types of linings and the joined furnace and crucible fragments, such an elaborate tapping feature does not match the morphology of the green stained slags. Steiniger himself makes the point that no green staining was observed on any of the structure's surfaces (Steiniger 2011, 73-74). It therefore appears that slagheap A's furnace was not used for the smelting of copper, and as such we do not currently have any available example of such a furnace at Arisman.

The analysis of the layered furnace fragment (FG-012235A) presented in section 7.2.2 highlights an interesting possibility for the recovery and re-use of arsenic precipitates formed during smelting. Such arsenic-rich material accumulations usually form when arsenic volatilizes and is allowed to condense in contact with the cooler surfaces of the furnace's upper reaches, much as has been described in 17th century Chinese texts (I-Tu and Hsueh-Chuan 1966).

Hypothetically, this material could be recovered and added to subsequent smelts to increase the arsenic content of any copper produced. Given that the arsenic is likely to exist as an

oxide and since it is physically entrapped within the ceramic it would not have been suitable as a true alloying agent to be added directly to molten copper. It could, however, be added to a copper smelt under reducing conditions to increase the arsenic content of the produced copper metal. Since the material contains only traces of sulphur, little or no matte would be produced from mixing it with copper. Since this arsenic infused ceramic likely has the same isotopic signature as the copper slags associated with it, it is unlikely to relate to speiss production. This is however a avenue which would need further investigation.

Although there is no direct archaeological evidence of the use of such an arsenic concentrate, its use must be at least considered as a potential source of arsenic in the arsenical copper *chaîne opératoire* and should not be discounted out of hand. It is highly likely that the ancient smelters of Arisman were at least aware of its existence given that they were well versed in a wide range of metallurgical substances as evidenced by the lead smelting and silver cupellation taking place in Area B for several centuries prior to the expansion in the copper extraction industry of Areas A and D (Pernicka 2004).

In contrast to the well-known copper-extraction process exemplified by the green slags, the speiss slags are representative of a much less well understood arsenic extraction process. One of the most elusive aspects of speiss production highlighted by previous studies remains the nature of the arsenic-bearing minerals. This lacuna is in large part due to the fact that speiss extraction was only recognized long after excavations at Arisman had been concluded. Minerals that did not appear linked to copper smelting or lead/silver cupellation were not collected since these were thought to be the only metallurgical activities conducted at the site. Despite this, some broad inferences on the nature of arsenic mineral exploitation can still be made based on available analytical data which narrow the field of possibilities.

The use of arsenates can be rejected as highly unlikely for two reasons. Firstly, the smelting of such minerals would generally lead to unacceptably high arsenic losses and secondly because such minerals could easily be added directly to a copper-smelting charge or molten metal to produce arsenical copper without the need for a separate smelting stage. Most arsenide minerals can also be rejected because any efforts to smelt them would result in a speiss slag and speiss prills which are clearly enriched in associated metals commonly found in such minerals (iron, nickel, copper, cobalt, and to a much lesser extent platinum). Certainly the hypothesized exploitation of copper arsenides, such as domeykite, could not be responsible for the formation of the brown speiss slags since only trace amounts of copper were found in them. Since the speiss slags always contain very low amounts of these

elements relative to arsenic, the more exotic arsenides are unlikely to have been extensively used at Arisman. The only exception to this is the systematic presence of high levels of iron in all of the speiss slags. Although it is possible that iron and silicon fluxes were both added to the charge, it is much more likely that either an iron arsenide, such as löllingite, or a sulfarsenide, such as arsenopyrite, was smelted at Arisman.

Furthermore, other than the absence of copper, the composition of the speiss slags is nearly identical to that of the copper slags (Table 9.1). This suggests that both speiss and copper smelts involved very similar charge compositions and points at arsenopyrite, which has similar iron content to the chalcopyrite used in the copper smelting process, as the most probable ore. Since arsenopyrite is known to have widespread distributions throughout Western Iran's Zagros Mountains as well as the more central Anarak region (Mansour 2013, 141-143), it could certainly have formed an abundant source of arsenic for this industry. The similarity in bulk analysis results is also highly suggestive of a standardized slag forming process which likely involved the addition of fluxes to nudge the slag's composition towards a more manageable melting temperature.

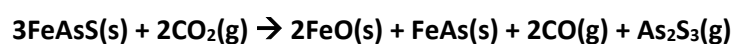
Table 9.1 Mean composition of all speiss and copper slags from Arisman as determined by SEM-EDS.

	Na ₂ O	MgO	Al ₂ O ₃	SiO ₂	P ₂ O ₅	SO ₃	Cl	K ₂ O	CaO	TiO ₂	Mn	FeO	CuO	ZnO	As ₂ O ₃	BaO
Copper	1.6	2.7	8.5	41.6	0.2	0.2	0.2	1.9	14.2	0.4	0.5	25.8	1.8	0.1	0.2	0.1
Speiss	2.4	2	9.1	40.5	0.4	0.5	0.1	1.9	18.2	0.5	0.5	23.3	b.d.l.	b.d.l.	1	b.d.l.

Two types of sulphide ores were thus mined from unknown geological deposits and brought to Arisman. Both types were similar in nature in that they were both iron rich sulphide minerals. The critical innovation of Arisman's smelters was the realization that sulphur had to be removed from the two ores through different processes. Since sulphur has a stronger affinity to copper than does arsenic (Earl and Adriaens 2000), desulphurization of arsenic-bearing copper ores through oxidation (i.e. roasting) unavoidably results in the removal of most of the arsenic and both low and highly variable arsenic content in the final copper metal. The addition of arsenic from a sulphur-free source at a later stage was therefore highly advantageous in manufacturing a consistent arsenical copper alloy while minimizing copper losses. It is in this context that Arisman's metalworkers developed speiss smelting technology which revolved around the removal of sulphur from iron sulfarsenides to produce an arsenic-enriched ingot of ferrous speiss.

The thermodynamic principles of speiss smelting have already been explored in some depth before (see section 3.1.5; Boscher 2010; Rehren et al. 2012) and will only be briefly reiterated

here since little new information has come to light in this regard. According to the work conducted on the roasting of arsenopyrite by Chakraborti and Lynch (1983), the retention of arsenic and the removal of sulphur can only be achieved together under relatively controlled atmospheric conditions that promote the following reactions:



According to the experimental parameters used by the authors (Chakraborti and Lynch 1983, 248-249), these two reactions occur under reducing atmospheres with a CO_2/CO ratio of around 50. More strongly reducing conditions are undesirable as they lead to the release of arsenic sulphide gases (As_4S_4 , As_2S_3 , and AsS) and therefore to the removal of arsenic along with the sulphur. These overly reducing conditions are marked by the formation of wüstite crystals in the remaining slag – phases which have occasionally been observed in Arisman's speiss slag. In contrast, as the oxygen partial pressure is increased towards the ideal CO_2/CO ratio, both sulphur and wüstite tend to oxidize preferentially, forming SO_2 gas and magnetite. Under these conditions, arsenic remains with the iron to form iron arsenides. The nature of these arsenides depends largely on the availability of arsenic, but covers the range between Fe_2As , FeAs , FeAs_2 , along with the unstable compound Fe_3As_2 which only exists at higher temperatures. When PCO_2/PO_2 exceeds the ideal ratio of 50, such as those common in an open-hearth roast, losses of arsenic rise dramatically as much of the available arsenic is oxidized and removed as As_2O_3 or As_2O_5 gas. Overly oxidizing atmospheres are marked in the slag by the formation of some FeAsO_4 phases. Although some of these phases have been identified in the Arisman speiss slag, they appear to be secondary corrosion products in binary phased prills of FeAs and FeAs_2 . The retention and loss of arsenic caused by these atmospheric conditions are summarised in Figure 9.3. That being said, it is important to remember that these reactions are reported at roasting temperatures of around 600 °C rather than the higher temperatures expected in speiss smelting. However, although the higher temperatures would result in higher arsenic losses due to increased reaction areas, the middle range of partial pressure facilitating arsenic retention should remain consistent.

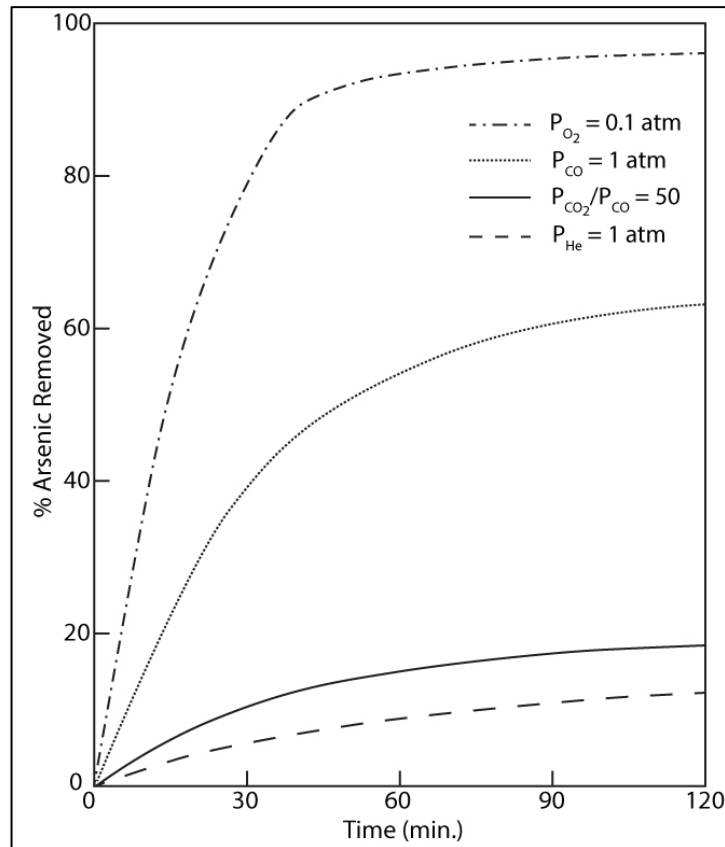


Figure 9.3 Experimental results of arsenic losses from roasting arsenopyrite in various oxygen partial pressures at 798 K. Note that both high and low oxygen pressures result in increased arsenic losses. Adapted from Chakrabarti & Lynch 1983.

Since the Arisman speiss slags contain all three stable iron arsenide compounds and the iron oxides are dominated by magnetite with only the occasional cluster of wüstite, it appears that the atmospheric conditions which maximize the retention of arsenic as well as the removal of sulphur were the intended goal of Arisman's speiss smelters. It is perhaps no coincidence that such oxygen partial pressures are very similar to those commonly inferred for prehistoric copper extraction from mixed oxide/sulphide deposits (Bourgarit 2007), and yet it shows quite clearly that these ancient smelters, as elsewhere, were quite capable of achieving controlled redox conditions to suit their needs (Müller et al. 2004).

Copper smelting technology could therefore be directly transferred to speiss smelting with little need for drastically new innovations. The main distinction appears to have been the need to stop the reaction once most of the sulphur had been removed in order to avoid the oxidation and volatilization of arsenic. Although the theoretical diagram just discussed shows relatively low arsenic losses when redox conditions are ideal (<20%), these may not have been easily maintained during cooling, and thus explains why the ancient smelters felt the need to tap the slag and speiss while still molten. In order to do this, the smelters of Arisman

appear to have developed the ingenious solution of tapping the slag and speiss into an open crucible which could be quickly removed from below the furnace and covered. Indeed, while the tapping features of the furnace underneath slagheap A do not match the morphology of the green stained copper slags, they fit perfectly with the shape and appearance of the speiss slags. The two types of furnace linings identified by the excavators of the furnace and the cold-contact nature of the ceramic vessels associated with speiss smelting scattered throughout the slag heap indicate that tapping of the speiss charge into cold-receptacles was indeed taking place in this particular furnace. Fired fragments of clay moulded around crucible rims with attached speiss slag (Steiniger 2011, 78)(Figure 9.4) further illustrate the connection between the furnaces and crucibles. All in all, it appears doubtless that the furnace recovered underneath slagheap A exemplifies the typical setup used to extract speiss and that the reconstruction proposed by Steiniger appears accurate.



Figure 9.4 Crucible rim from slagheap A embedded into clay as part of the joint between a furnace and a crucible. Note the speiss slag on the inner surface of the clay showing that it flowed into the crucible. Photograph from Steiniger (2011, 78).

Where Arisman's two smelting technologies converge is also worth exploring as it highlights the intended market and use for both products. Ferrous speiss can, in theory, be added to either the smelting stage or to molten copper in a separate alloying stage (perhaps at the time of melting and casting). Although both of these possibilities would result in the production of copper with increased arsenic content, they also both have their drawbacks. The addition of speiss to a smelting charge would result in less control of the final arsenic content and to poorer overall arsenic retention. The addition of ferrous speiss to molten

copper on the other hand would result in a consistent arsenic content but also in the inclusion of a significant amount of iron into the copper metal (Doonan et al. 2007; Rehren et al. 2012). This iron would need to be removed through oxidation or risk embrittlement (Craddock and Meeks 1987). Fortunately, however, iron is much more reactive to oxygen than arsenic is and would thus act as a strong deoxidant in the system (Luyken and Heller 1938), which has the added benefit of preventing much of the arsenic from volatilizing.

Pinpointing the role of speiss in the arsenical copper *chaîne opératoire* of Arisman is somewhat difficult for a number of reasons. Firstly, the copper ores appear to have contained some arsenic and thus the presence of the element alone cannot be taken to demonstrate the addition of an alloying agent in the same fashion as it can in the case of Çamlıbel. Secondly, the speiss slags are as of yet still isotopically poorly defined which means that inferences based on such isotopic ratios should be taken with a measure of caution. And thirdly, while the lead isotope signature of the green stained copper slags cluster nicely together, there are several groupings visible for the finished objects which could either indicate different alloying practices or distinct ore sources altogether.

Notwithstanding these obstacles, several inferences can be suggested which should be easily testable in future studies. The first is that it is highly unlikely that speiss was added directly to the copper smelting charge. This can be deduced from the fact that although some of the green stained copper slags contain little to no arsenic, their isotopic fields form a tight cluster with those that did contain the element. Had speiss been added to some of the charges, then one would have expected the arsenical copper slag and pure copper slags to form discrete groupings. Since they do not, either the speiss contains so little lead as to have had no impact on the isotopic ratios or the copper ores naturally contain variable amounts of arsenic mineralizations, which is not an unreasonable assumption. Clearly, the single sample of speiss slag thus far characterized isotopically is insufficient to justify inferences of any strength and will need to be supplemented by further analyses in the future to confirm or refute these preliminary results.

Furthermore, it has already been established that a large proportion of the copper alloy artefacts uncovered at Arisman (three copper alloy prills and object group 1 as defined by Pernicka et al. 2012) do not have the same lead isotopic signature as either the green stained copper slags or the brown speiss slags (see section 8.1). Based on the spread of these ratios between those of the speiss and copper slags, it appears likely that these objects were produced from the mixing of metallic copper with speiss. Group 2 appears to be also

clustered between the two slag types, albeit in this case much closer to the green copper slags. Although much more tentative, this could also be indicative of the smaller addition of speiss to molten copper. Group 3, along with another 3 prills, have lead isotope ratios which are much closer to those of the green arsenical copper and likely represent objects which have not been further alloyed.

These interpretations can be verified to a certain extent through an assessment of the arsenic content of the copper alloy objects in the various clusters. One would expect artefacts with lead isotope ratios that plot closest to the speiss slags to be richer in arsenic than those further away. Unfortunately, these data have not been published and is not currently available but would be worth obtaining in the future. Another way by which the use of speiss as an alloying agent could be tested is through the increased presence of iron in solution within copper artefacts (Doonan et al. 2007). Although this is somewhat blurred by the fact that copper prills in the copper-bearing slags typically already contained a few percentage points of iron and also because much of the iron would be oxidized regardless during refining/casting, a correlated increase in both iron and arsenic together may be indicative of the addition of speiss to molten metal. Indeed, this can be observed in the analysis of prills previously published where the two elements are clearly correlated (Pernicka et al. 2011, 675, Table 14).

Arisman's arsenical copper and speiss chaînes opératoires are summarized in Figure 9.5 and can be described as follows:

Synthetic speiss was most likely smelted from arsenopyrite under mildly reducing conditions in order to expel as much sulphur as sulphur dioxide as possible while retaining arsenic as iron arsenide. Once most of the sulphur was removed, the reaction was stopped by opening the furnace base and allowing the slag and speiss mass to flow into a straight-walled, flat-bottomed crucible which was then quickly removed and covered. Speiss was then collected either as prills or as a small ingot pooled below the slag. Whether the speiss was recovered as an ingot or through the collection of prills remains enigmatic, particularly in the absence of any negative imprints on the base of the speiss slags matching that found in the copper slags. The different density of speiss and slag suggests that it should separate out given enough time to do so (Thornton et al. 2009), but no evidence has been found at Arisman. The collection of prills from crushed slag cannot be ruled out, but there is again little evidence that the speiss slag was crushed to a larger extent than the copper slag. Experimental work

on the smelting of speiss would be useful in highlighting how this process could operate in practice.

Copper was produced from mixed sulphide and oxide ore deposits containing some arsenic mineralizations. These may have been roasted or directly smelted in a co-smelting operation, both of which would have resulted in the uneven retention of arsenic. The charge was at one point fully molten and copper metal, matte, and slag allowed to fully separate within the furnace where it was left to cool. The furnace was then broken apart and the copper and matte were recovered. It is unclear whether the matte was recycled in later smelts but its notable absence from the archaeological record suggests as much. The upper reaches of the copper smelting furnaces appear to have been infused with enough arsenic that this material may have been a useful resource for further arsenic enrichment but no direct evidence of this has as of yet been identified. Based on the analysis of prills within the slag, metallic copper produced from such smelts typically contained up to 1-3% arsenic.

Lead isotope data suggest that some objects were manufactured from this raw copper without the addition of speiss while others were cast from metal which had been enriched with arsenic using the available speiss. In addition, although there is no direct evidence yet, there remains the possibility of the use of arsenic-infused ceramic from the smelting of arsenic-bearing copper ores in the alloying process. Since Arisman does not appear to have been involved in the production of finished objects, it is quite possible that much of the alloying was conducted offsite. As such, and unlike Çamlıbel, there is as of yet no direct material evidence of how the alloying process was conducted using Arisman's speiss, but the addition of speiss to molten copper has already been shown to be similar to the process described for at Çamlıbel (see section 3.1.5).

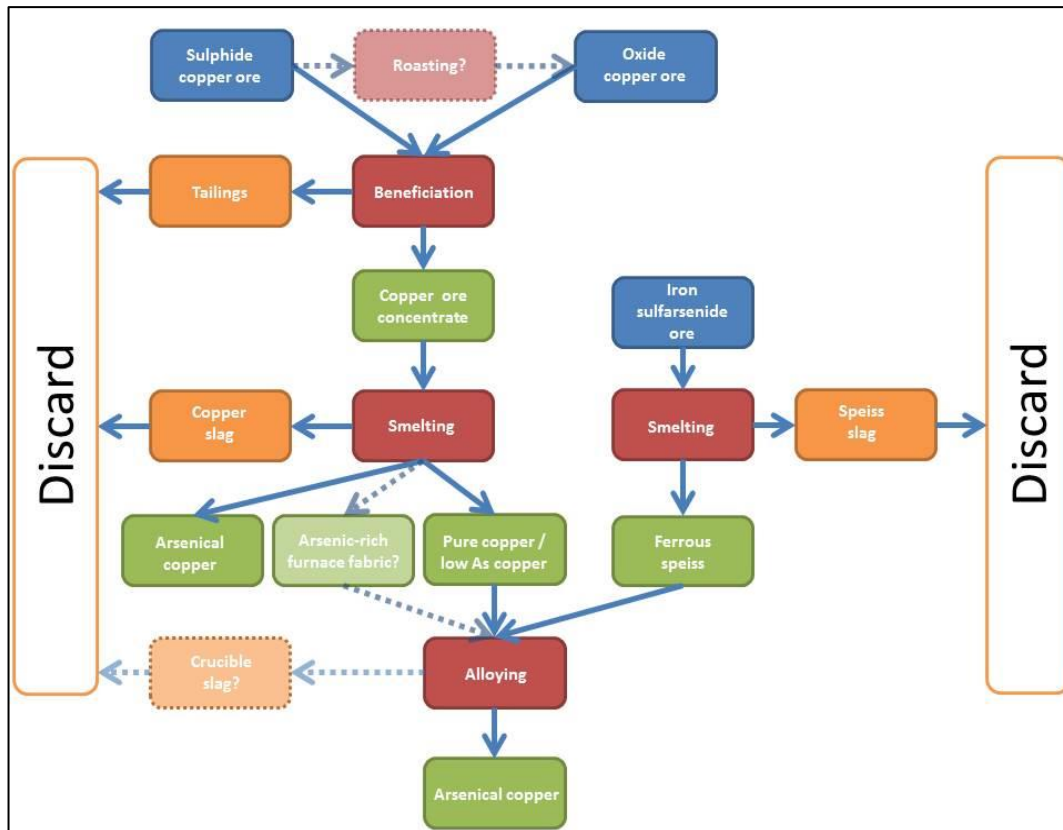


Figure 9.5 Arisman's arsenical copper chaîne opératoire. Note that dotted lines and transparent boxes represent operations which are suggested but for which only indirect archaeological evidence exists. Fuel, fluxes and furnace material are not included in the diagram although they likely did contribute to the overall composition of the discarded slags.

Although recent evidence has largely corroborated our growing understanding of the use of speiss as a potential alloying material at a number of sites (Doonan et al. 2007; Georgakopoulou 2013; Mehofer 2014; Thornton et al. 2009), Arisman remains the only known location where the production of speiss has been directly identified.

9.2 Changes in Production Technologies

The parallel study of Çamlıbel and Arisman together offers a unique opportunity to observe a fundamental shift in the emergence of social, economic, and technological complexity occurring at the onset of the Early Bronze Age. The two sites may be separated by several centuries and nearly two thousand kilometres, yet they reflect the wider developmental patterns of their times such as the often-debated nature but undeniable increasing influence of the Mesopotamian lowlands on highland communities (Algaze 1993; Frangipane 2001; Stein 1999). Despite increasing diverse approaches to practicalities of copper extraction (Lehner and Yener 2014; Yener 2000), similarities between the highland regions of Anatolia and Iran have been highlighted by a number of scholars (Avilova 2008; Chernykh 1991; Chernykh et al. 2002).

The most notable change appears to be the switch from crucible-bound smelting producing just a few hundred grams or less of metal at a domestic or craft-industry scale to the much larger industrial scale furnace smelting which could produce several kilograms of copper each smelt. The use of such larger installations which could sustain high temperatures for much longer lengths of time meant that the slag and metal could reach a fully molten state, allowing for the complete separation of the immiscible liquids. This resulted in a much more efficient recovery of metal from the ores and abolished the tedious process of prill extraction from slag through mechanical means. The technological shift is well represented archaeologically at numerous sites dating to around the same period in the Near East (Adams 1997; Craddock 1995; Hauptmann 2007; Hauptmann and Weisgerber 1996; Müller et al. 2007; Shalev and Northover 1987; Shugar 2003). On a practical level, this technical leap allowed for a dramatic expansion of metal output while increasing fuel efficiency (Craddock 1995; Tylecote 1980). From an economic perspective, it also reflects a dramatic increase in demand and the emerging appeal of metal in the manufacture of an increasingly wider range of object types. Since the regions of central Anatolia and West Central Iran saw only modest increases in settlement densities (Hopper and Wilkinson 2013; Schoop 2010b; Schoop 2010c), it appears that much of this increasing production may have ultimately been destined for emerging distant markets; certainly, this possibility exists and is worth further discussion.

Çamlıbel's crucible-bound copper production likely satisfied local needs and only a small proportion of the output was traded over long distances. Indeed, while the total copper production of Çamlıbel over the course of the century and a half of occupation probably did not exceed a few kilograms (just 9 kg of slag were recovered), a relatively large number of functional objects were recovered from there, suggesting that much of the copper produced

at the site was intended for domestic use. Although the site is clearly part of a wider regional cultural tradition and trade network as evidenced by the red and black pottery which extends all the way to the Malatya region (Schoop 2009; Schoop 2010a) to the east and as evidenced by the ring-shaped idols which are commonly associated with the Balkans and Western Anatolia (Schoop 2009; Zimmermann 2007), the site is also significant as employing a number of unique pot morphologies found only at the site and in the general vicinity (Schoop 2011, 65). The site appears to have been a producer of arsenical copper without being a major supplier. The industry was part of a subsistence economy which involved the exploitation of local resources. That being said, since Çamlıbel belongs to a relatively archaeologically invisible type of sites (Schoop 2010b; Schoop 2010c), if a large number of settlements of this type of settlements existed throughout the region it is plausible that together they could have produced a significant enough amount of copper to have been an important supplier to more distant regions.

In contrast, based on the estimated 120 tons of slag scattered around the different foci of the site (Steiniger 2011, 92-93), Arisman's total copper output was probably around several tons. This is orders of magnitude more than could possibly have been necessary for the inhabitants of a site covering just a few hectares at any one time. This point is reinforced by the fact that very few finished metal objects were found anywhere at the site (Chegini et al. 2004; Helwing 2011d, 271). The few copper alloy objects which were found mainly consisted of small scrap pieces with only a few occasional rings or spirals. Larger objects, evidently produced at Arisman in some quantity as suggested by the number of mould fragments found throughout the site, were noticeably absent. By and large, this suggests that the site was mainly used as a manufacturing hub and that most objects produced there were intended to be exported to other proto-Elamite centres of consumption such as Susa, Malyān, Yahyā and Northern Mesopotamia with whom several cultural links could be established (Helwing 2011b, 529-530).

It should be mentioned that while it is possible to comment on the scale of copper output from Arisman, it is as yet still impossible to assess how much speiss was produced on site. Although the estimate of slagheap A as containing roughly equal proportions of 'green' and 'brown' slags is significant, without more information of the nature of the ores used and without conducting experimental speiss smelts it remains impossible to tell how much speiss was produced from any quantity of speiss slag. This experimental work has already been started by the author and should further inform on this topic in the near future.

From its very foundation Arisman appears to have been intended as a specialized industrial centre responsible for meeting external economic needs. Indeed, the industrial focus of Arisman appears to have been in place for some time prior to the peak copper production which occurred during the Proto-Elamite period, but centred rather on ceramic production, on the manufacture of finished copper alloy objects, and, to a lesser extent, on silver cupellation (Boroffka et al. 2011; Chegini et al. 2011; Pernicka 2004). The late 4th millennium BC saw a dramatic increase in the metallurgical activities of Arisman which appears to coincide with the introduction of furnace-bound smelting. Copper was extracted in these furnaces without tapping the slag, a feature commonly associated with the use of such structures in the early 3rd millennium (Craddock 1995, 146-149). In essence, the furnaces were used in the same fashion as large crucibles, allowing the smelting of larger volumes but without the increased fuel and time efficiency obtained from slag tapping. It appears that tapping only occurred in the speiss production process, but once again this was not done to increase output but to maximize arsenic retention. The dramatic scale of copper production in Arisman's later periods is therefore not the result of the use of new technology but rather simply a case of the intensive use of larger reaction vessels. That is not to say that the introduction of furnaces at Arisman is not significant, only that it did not have a large impact on production output. Moreover, it has often been pointed out that the evolution of extractive metallurgy typically occurs in tandem with that of ceramic technology since the knowledge and skill sets of both industries are related and interchangeable (Craddock 2000; Rehren and Martín-Torres 2014). It is therefore perhaps no coincidence then that Arisman's metallurgical peak followed a period of intense pottery production in the Sialk III and earlier periods.

Of course, the ultimate destination of the metal produced at both Çamlıbel and Arisman will need to be verified through further lead isotope and trace element studies potentially linking these two sites to finished objects across their respective geographic regions.

Another major shift in production technology hinted at by the Çamlıbel and Arisman material is the rise of sulphidic ore exploitation. While Çamlıbel appears to have been largely reliant on the secondary oxidation of small isolated nodules of chalcopyrite, exploitation at Arisman was aimed squarely at sulphidic ores. Although the Çamlıbel slags contain significantly more sulphur in their bulk (mean 2 wt%) than do Arisman's copper (mean 0.2 wt%) or speiss (mean 0.5 wt%) slags, this is not reflective of the original ore composition. Indeed, minerals found at both sites suggest that copper sulphide and oxide minerals both played an integral part of

the ores of both sites but that their proportion and treatment varied. Since the inclusion of sulphide minerals in a well contained shaft or enclosed furnace under reducing atmospheres results in the retention of most of the available sulphur (Merkel 1990), it appears that Arisman's smelters spent much effort in reducing the sulphur content of the charge prior to smelting. On the other hand, the largely mixed sulphide/oxide charge proposed for Çamlıbel, smelted under the variable and only marginally reducing conditions common of crucible smelting (Bartelheim et al. 2003; Bourgarit 2007; Bourgarit et al. 2003) means that there would have been more opportunities for the removal of sulphur during smelting than in the later furnace-bound smelting techniques. As Bourgarit (2007, 9-10) suggests, while weakly reducing atmospheres caused by charcoal burning were likely consistent across the Chalcolithic world, the variability in the ore charge's O:S ratios created micro-conditions within the smelt which could greatly encourage sulphur removal. That being said, much of the sulphur identified in Çamlıbel's slag is present as incompletely reacted high temperature solid solutions. Had conditions approached equilibrium and the charge allowed to fully melt, it is likely that much more of the sulphur would have had a chance to escape the charge as SO₂ gas.

Although the trend towards the increasing exploitation of sulphide deposits is well known across the Old World (Craddock 1995; Muhly 1999), the inhabitants of Arisman are thus far the earliest known to have developed the ingenious smelting of ferrous speiss in order to efficiently produce arsenical copper from sulpharsenides. Speiss smelting thus not only exemplifies a major change in the approach to the production of metallic alloys but also informs on the evolving sulphide-smelting technology.

It is, however, the innovations surrounding the production of arsenical copper, both at Çamlıbel and at Arisman, which are by and large the most interesting aspects of the metallurgical technology of the two sites and the focus of this thesis. Although archaeological evidence had so far hinted at some measure of awareness of arsenic content in the Late Chalcolithic and Early Bronze Age (see section 3.2), these two sites provide the most concrete evidence of the practicalities of arsenical copper alloying known to date.

Within the context of the emergence of the use of polymetallic deposits in southeastern Anatolia (Çukur and Kunç 1989; Özbal 1986; Yalçın and Yalçın 2009; Palmieri et al. 1992; Palmieri et al. 1993), it appears that sites such as Çamlıbel were beginning to experiment with mineral additives to alter the properties of metals. These innovations did not happen in a vacuum and it appears that arsenical copper was only one of several different special alloys

which began to be created in the late 4th/early 3rd millennium BC such as the silver and antimonial copper (Caneva and Palmieri 1983; Hauptmann et al. 2002; Palmieri et al. 1999; Shalev and Northover 1993; Tadmor et al. 1995). The difficulty in creating alloys of copper and arsenic was neatly circumvented by the mixing of arsenate minerals to molten copper in a manner similar to the brass cementation process involving the use of the zinc carbonate mineral calamine, a practice which was developed and widespread a few millennia later during the Roman period (Dungworth 1997; Ponting 2002; Rehren 1999). Çamlıbel provides an important case study of such a practice, demonstrating that the intentional production of copper alloys predates that of tin bronzes and provides an alternative technological narrative which is not dependent on the geological determinism implied by referring to the use of polymetallic ores, a distinction which had been advocated over a decade ago by Yener (2000).

Arsenical copper production at the site of Arisman serves as an excellent example of a mixture of incremental technological development and large innovative leaps. Early forays into metallurgy at the site as exemplified by Area B appear to have focused on the casting and manufacture of finished objects in a largely domestic context within a wider industrial landscape. Such crucible-bound secondary production has been reported frequently from urban settlements large and small from this period (De Ryck et al. 2003; Palmieri et al. 1999; Weeks 2013; Yener 2000). In the late 4th millennium BC, slagheaps in Areas D and A testify to a dramatic expansion of the primary production which is generally associated with the introduction of several new technologies such as the use of furnaces for smelting and the development of speiss production.

Since neither copper nor speiss furnaces were used to tap slag in the conventional sense, they do not represent a major leap forward in the technological approach to smelting. Essentially, the use of furnace structures permits a larger reaction volume and therefore a linear increase in output per operation but little in the way of increased efficiency. In that sense, the furnaces represent a small evolution of design rather than the revolution usually ascribed to their introduction. Likewise, the use of increasingly sulphidic ores may have been a gradual change over time which did not necessitate entirely new methods of ore processing but simply an intensification of known beneficiation and preparation steps (Craddock 1995, 167).

Speiss smelting on the other hand can be considered revolutionary in a number of ways. Firstly, it is the first example of an entirely new method of sulphur removal without resorting to fully oxidizing roasts. Secondly, it demonstrates a hitherto unknown awareness of the

ongoing reaction process within the reaction vessel and of the conscious steps taken to stop this reaction at a critical moment. In all previous known metal extraction processes, the reaction was always allowed to continue for as long as practically possible. While equilibrium was rarely reached (due to limitations of time, fuel, airflow, manpower, etc.), the charge was ideally intended to fully react. The retention of arsenic, however, required the oxidizing process to be stopped once most of the sulphur had been removed. Tapping of the reactants into a crucible which could be closed and quickly cooled was thus a critical innovative solution. The timing of such an operation could be roughly estimated by the changes in both the colour of the smoke (from yellowish to white) and from the smell (from that of rotten eggs to garlic). Such qualitative assessments have been noted by the author's own experimental smelting and will be further tested in the future.

The isolation of arsenic as an alloying material was an entirely new concept at the time and predates the earliest known extraction of metallic tin by several centuries (Lehner et al. 2009; Yener 2008). Given that investigations at Çamlıbel revealed the mixing of arsenate minerals with pure copper predating Arisman's speiss smelting by approximately half a millennium, it is reasonable to suggest that the alloying of speiss with copper forms an integral step in a general trend towards the increasing control of arsenic content. In other words, the conceptualization of 'alloying' as a distinctive and intentional process separate from smelting had already been established for some time prior to the unique metallurgical developments of Arisman. It would indeed be difficult to fathom the production of synthetic speiss without prior knowledge of arsenic as an additive which modified the properties of copper, something which could not be apparent from the use of polymetallic deposits alone.

Broadly speaking, speiss smelting allowed for much greater control of the arsenic content of finished products by systematizing the process and removing the uncertainty associated with geological variability. In doing so, the scale of production could be increased through the use of abundant arsenopyrite deposits without having to rely on arsenic bearing copper deposits. Since, as has already been discussed, Arisman was clearly a manufacturing hub controlled by a distant polity, the production of an alloying agent which could be traded long distances would have been seen as being of significant value - particularly so given the tendency of arsenic content to diminish with every casting (Mödlinger, pers.com.; Bray and Pollard 2012).

It is probable that speiss was exploited and traded in very similar ways to tin, which was then just beginning to be available across the region (Pigott 2012; Stöllner et al. 2011b; Yalçın and Yalçın 2009) and which ultimately replaced arsenic as the element of choice in copper

metallurgy. It remains unclear whether speiss smelting formed a precursor technology or a parallel one to tin exploitation at this stage since Arisman is the only known speiss production centre and dates for the earliest tin bronzes are still debated (Lehner et al. 2009; Yener 2008).

9.3 Settlement Specialization

Certain broad aspects of metallurgical production technology are known to have spread nearly simultaneously over larger regions and tend to offer large one-time increases in productivity or offer access to new materials. These can take many forms, such as the far-reaching shift from crucible-based smelting to the use of furnaces (Craddock 2000), or from blowpipe driven air supply to bellows (Rehder 1994), or be limited to the development of new object types as markers of contact or influence over long distances (Chernykh 1991). Regardless of the form of the innovation, they are invariably manifested by the introduction of new functional object typologies in the archaeological record which may or may not quickly spread beyond the culturally-defined boundaries of the point of invention. The diversification in the types of alloys produced in the Near East in the 4th millennium BC, based on the exploitation of new mineral resources, constitutes another one of these broad trends (Weeks 2013). However, unlike the artefact typology, composition, and fabrication technique commonly used by Chernykh to define the various supra-cultural provinces (Chernykh 1991), the production of new alloys is largely dependent on the local geological realities which cannot be exploited in exactly the same manner at every production locality. So while the emergence of alloying technology may be manifested in the archaeological record by the appearance and dominance of a few new artefact compositions and typologies, such as those defined by Chernykh's metallurgical provinces, they in fact reflect local adaptation to geological realities and the diversification of technological choice and style (Lechtman 1977; Lemmonier 1993). In other words, the homogenization of metallurgical preferences does not necessarily occur in parallel with the systematization of metal production technology.

This is particularly evident when considering the two production sites presented in this thesis which exemplify local adaptive technological choice. Çamlıbel's exploitation of small isolated mixed oxide/sulphide copper deposits alongside arsenate mineralizations and Arisman's sulphidic copper and speiss smelting both show innovative use of resources.

Such a system of settlement specialization and technological divergence has been proposed to describe the emergence of Bronze Age copper mining districts in the Alps based on the Law of Comparative Advantage (Shennan 1999). Although this model has never been applied to earlier prehistoric societies, which are often thought of as too distant to be rationalized in purely economic terms, it does offer some insight on possible mechanisms which might have enabled the rise of new varied technologies at the time. At its most fundamental level, the

theory is based on the idea that a settlement must facilitate the survival of its members, whether that is through mutual protection, control of resources, or any other means that offer advantages over alternative settlements or relocation. In isolation, variations in environmental and 'social-technical' factors determine the viability of the community, but where networks of long-distance trade exist allowing the exchange of goods of variable values, new avenues for settlement success evolve from local economic constraints and opportunities.

Settlement specialization has been recognized as often arising from "autonomous individual or household-based production units, aggregated within a single community producing for unrestricted regional consumption" (Costin 1991, 8). White and Pigott (1996) have offered that such a system of production involving independent producers and suppliers providing goods to a flexible group of consumers would minimize production and transaction costs and would be characterized by flexible hierarchy and lateral differentiation, something which at first fits well with Çamlıbel's situation.

However, applying Shennan's economic model and Costin's definition to Çamlıbel's archaeological context, one quickly comes to the conclusion that the production of a few kilograms of arsenical copper probably offered negligible increases to the community's chances of survival, whether directly or through advantageous exchange. For all intents and purposes, Çamlıbel's inhabitants may have exploited local mineral resources but the settlement cannot be described as one specialized in the production of arsenical copper. Innovative use of alloying technology or not, the scale of the metal production industry at Çamlıbel could not provide sufficient economic leverage to offer competitive advantages within the context of Anatolian Chalcolithic subsistence patterns. The same is also true of the agricultural, ceramic, and bead industries, which together all provided the inhabitants of Çamlıbel with the means of survival but which were limited to a local and domestic scale.

That being said, the slight ramping up of copper production evidenced by the increase in metallurgical waste material starting in CBTIII without an associated increase in the number and weight of discarded copper metal suggests that the metal output was increasingly in use elsewhere. While this does not necessarily imply an increase in the export of surplus production, it certainly points at the growing importance of this industry to the inhabitants of Çamlıbel and may hint at a nascent but unfulfilled settlement specialization.

Arisman on the other hand exemplifies the nature of a specialized metallurgical settlement. Located in an inhospitable environment with little to no arable land, the site's settlers must

have relied upon their industrial outputs in exchange for food necessary for survival (Helwing 2011b). The earliest occupation phases appear to have focused only partly on secondary metal production and much more heavily on pottery production as evidenced by the relatively large number of kilns uncovered in Area C. In later periods approaching the turn of the 3rd millennium, activities appear to have shifted to the large scale primary production of arsenical copper metal using the methods described in this thesis. The shift towards primary production is likely partly due to the development of speiss smelting which allowed for metal output to jump significantly by exploiting sulphidic deposits while being able to maintain an elevated arsenic content. This technology allowed the settlement to fulfil consumer demand in the home market, thus guaranteeing Arisman's continued existence.

Of course in Arisman's case the relationship between producers and consumers does not conform to our modern economic models. By the time arsenical copper production peaked around 3000 BC, Arisman appears rather to have been an industrial outpost under the direct control of a Proto-Elamite polity (Helwing 2011b) which does not quite fit the model of the free exchange of goods proposed by Shennan. Nevertheless, the relationship between Arisman and its 'parent culture' is still dependent on the same concepts of uneven distribution of resources providing benefits according to the Law of Comparative Advantage. After all, even under the most unfavourable and uneven of exchange relationships, the cost of maintaining a settlement such as Arisman must be less than the perceived value of the settlement's output. It is only when the situation is reversed that the settlement must either be reinvented, as it was when it switched its industrial focus in the mid-4th millennium BC, or be abandoned, as happened in the early 3rd millennium BC.

9.4 Arsenical Copper Alloying in the Southwest Asian Context

The results presented thus far demonstrate unequivocally that arsenic and copper were being intentionally alloyed starting in the mid-4th millennium. This has a number of implications for our understanding of Late Chalcolithic and Early Bronze Age societies and interaction spheres which need to be further explored.

It is important to note that Çamlıbel's arsenical copper production was most probably not a unique technological development or indeed the earliest occurrence of this particular innovation. Given the broad Chalcolithic trend towards increasing metallurgical exploitation and 'balkanisation', it is likely that the evidence uncovered here simply marks the first record of a technology which was already in use for some time. The widespread circulation of arsenical copper objects at the time (Muhly 2006) means that the introduction of new

manufacturing methods would not necessarily be very visible archaeologically other than through an overall more consistently elevated arsenic content, something which can most definitely be seen in the thousands of object analyses already conducted (Esin 1976; Lehner 2012). The alloying technology of Çamlıbel alone cannot therefore provide a one-size-fits-all view of intentional arsenical copper production for Southwest Asia's Late Chalcolithic and it is important to assess how this particular site fits into the wider technological context. Of particular importance are questions relating to the origins of the technology uncovered at Çamlıbel and whether it relates in any way to the emergence of speiss smelting and tin bronze a few centuries later.

The evidence from Çamlıbel demonstrates a well-developed alloying technology associated with a still largely inefficient smelting process where control of atmospheric conditions remained the main difficulty. Once pure copper was produced, Çamlıbel's metalworkers were proficient at both enriching it with arsenic and casting it into complex shapes. Indeed, the arsenic content of finished objects from the site which have been analysed is relatively consistent, mostly in the range of 3-4 wt% (mean of 3.7 and Std. Dev. of 1.2, Appendix B.8). As such, Çamlıbel was probably not the birthplace of arsenical copper alloying. However, geological circumstances and pre-existing metallurgical knowledge similar to that inferred at Çamlıbel were likely necessary to provide a suitable environment for this technology to develop: most notably the absence of polymetallic ores but the availability of both arsenic and copper mineralization in relative proximity to each other. We can thus eliminate many of the more typical deposits thought to be exploited at this time period, such as Majdanpek and other sites in the Southern Carpathians, Ergani Maden in Eastern Anatolia, the abundant polymetallic deposits of Transcaucasia, and the Anarak and Talmessi/Meskani deposits of Central Iran. Marginal areas - where copper mineralizations are present but in smaller and more isolated deposits - appear to have been a prime breeding ground for experimentation with new ores, and it is likely that the Central Anatolian Plateau was at the forefront of these innovations given its geological situation.

Regardless of where it actually first occurred, arsenical copper alloying was not developed in a vacuum and several pieces of evidence suggest that a large network of interactions or movement of people facilitated the dissemination of metallurgical knowledge over vast distances.

This is best exemplified by the links in early crucible technology across Anatolia and Iran (Figure 9.6). Although there is no clear cultural connection between the sites of Çamlıbel and

Arisman in the more typical archaeological finds such as pottery or architectural styles, morphological similarities between the perforated pedestalled crucibles of Çamlıbel and those of Ghabrestan style in the earlier occupation layers of Arisman tentatively hint at a communal or connected past. The Ghabrestan style crucibles are typically found across the Iranian Highlands and appear to have evolved from shorter and shallower forms identified at Tal-i Iblis level II dating to the late 5th millennium BC (Caldwell 1968; Frame 2012) although these are much shorter, wider, and do not have the characteristic hole. The shape appears to have been formalized at Tepe Ghabrestan in the first half of the 4th millennium BC (Majidzadeh 1979; Majidzadeh 1989) and spread across Western Iran. Other than Ghabrestan's level II and Arisman I Area B (Helwing 2011d), pedestalled crucibles were also identified at Tepe Sialk and Qal'e Guše (Helwing 2005). In all cases the crucibles were found in layers associated with Sialk III pottery, providing a likely date of approximately late 5th to mid-4th millennium BC. Unlike the earlier Tal-i Iblis crucibles, these are morphologically much more similar to the ones from Çamlıbel, being taller, narrower, and with the expected round perforation in the mid-shaft. The first appearance of these crucibles pre-dates those of Çamlıbel, but their use in Iran continued over several centuries and likely overlaps the central Anatolian evidence. A further example of melting crucible with similar attributes was identified at Aghia Photia on Crete dating to the Early Minoan I to IIA transition (roughly 3000-2500 BC), although in this case the hole was squared and the crucible had a spout (Betancourt and Muhly 2007). Other pedestalled crucibles have been found in other contexts such as Late Bronze Age Boğazköy-Hattuša (Lehner 2015, 91), the Phoenician site of La Fonteta in southeastern Spain (Renzi 2013, 370-373, Group 7), or even the strange 'eggcup crucible holders' from Broom Quarry in the UK (Doonan 2006), but these always lack the transverse hole and shallow bowl and are likely simply coincidences rather than the continuation of a stylistic tradition across millennia and continents.

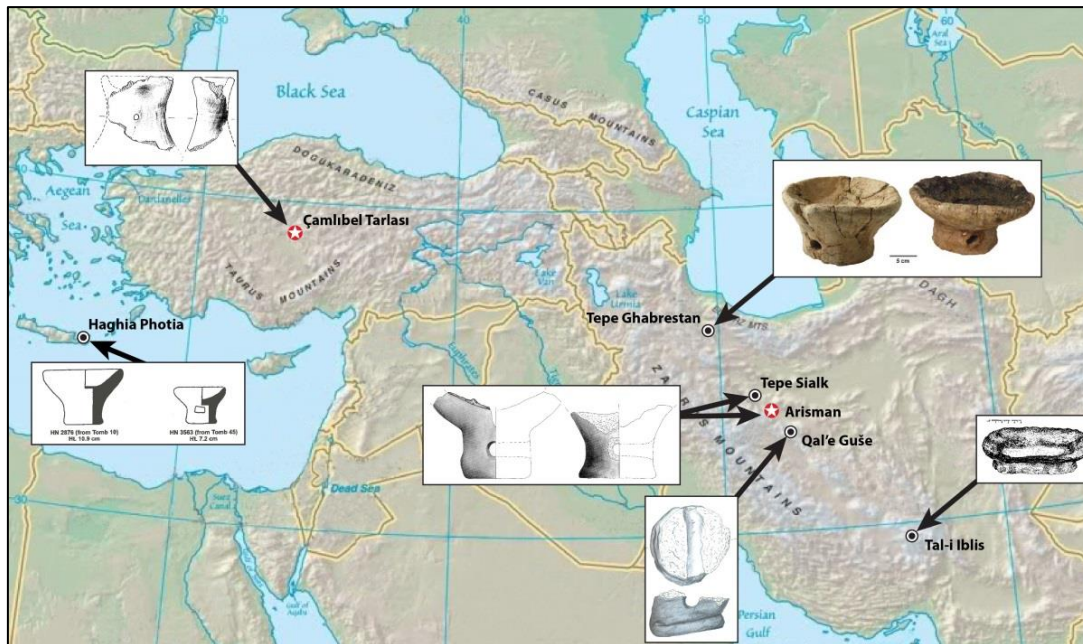


Figure 9.6 Comparison of pedestalled crucibles from the 5th and 4th millennium BC in Western Asia and the Eastern Mediterranean. All drawings and photos are to the same scale.

Despite the current unpopularity of diffusion models in archaeological thoughts and theory (Davis 1983; Ottaway 2001; Pfaffenberger 1992), particularly in terms of metallurgical technology (Craddock 1999; Radivojević et al. 2010, although see Roberts et al. 2009), the link between the early aspects of crucible-bound copper metallurgy and pedestalled-shaped crucibles appears to be fairly tangible. Indeed, while the heavy temper, the shallow bowl-shaped opening, the thick walls, and the internally-heated aspects of the crucibles are typical of crucible-bound smelting across the Old World, stylistic variation in the way such vessels were handled often appear to vary according to cultural traditions (Bayley and Rehren 2007; Rehren et al. 2015, 113). As such, it is reasonable to suggest that some cultural exchanges, however indirect, did indeed take place across the two regions and that knowledge of arsenical copper alloys was part of a technological package that probably included stylistic and/or functional aspects of crucible design around the mid-4th millennium BC.

Further reinforcing this connection, the spread of the use of arsenical copper alloys itself, in both Southeast Europe and Anatolia, has been highlighted as one of several defining attributes of the emerging Circumpontic Metallurgical Province (CMP) dating to the Early Bronze Age (Chernykh 1991; Chernykh et al. 2002, 91) and indicative of the reconstructing of relationships across supra-cultural regions (Weisgerber and Pernicka 1995). Included in the CMP are the steppe areas of Western Asia, the northern Balkans, the southern Balkans or Carpatho-Balkans, the Aegean, Anatolia, Mesopotamia and Susa (inclusive of the Zagros Mountains), and the Caucasus.

In addition to arsenical copper as the material of choice, typological links in the use of axes, adzes, daggers, and spears also highlight common elements of this metallurgical province. Although the region around Arisman has not typically been included in the CMP by Chernykh, it has recently been pointed out that adzes and axe-adzes identified from Mejkop and Kura-Araxes sites of the Caucasus show clear similarities with others uncovered from Tepe Ghabrestan and Tepe Sialk (Courcier 2014, 607-614) as well as Arisman. Çamlıbel, on the other hand, shows leanings towards both the Balkan and Caucasus regions based on the presence of a ring idol mould found on site (Zimmermann 2007) and the typology of awls and the shape of the single blade recovered (Schoop forthcoming).

Overall it appears that Arisman and Çamlıbel both formed part of a wider supra-regional pattern of arsenical copper exploitation and use. It would therefore come as no surprise for technological innovations to spread by the same pathways as that leading to common metal object typologies.

In many ways what is more surprising is that speiss smelting is not more commonly seen in production sites of the Early Bronze Age across Southwestern Asia. Although fragments of speiss have occasionally been recovered from the archaeological record (see section 9.1.2), the smelting of speiss does not appear to have been particularly common practice in the Early Bronze Age. In fact, the abandonment of Arisman in the first half of the 3rd millennium may well indicate shifting consumption patterns and the introduction of tin bronzes which may have made Arisman's technology obsolete. Indeed, Doonan and Day (Doonan and Day 2007, 113) see arsenical copper as a superior product to tin bronze that was only replaced by the latter due to the socio-political context of the Early Bronze Age. They argue the intensification of production and exchange observed in the 3rd millennium would have made the complex smelting and alloying procedures required to control the arsenic content too difficult and unreliable when compared to the simplicity and efficacy of tin bronze alloying. Furthermore, it may well be that in the increasingly politicized landscape of the Bronze Age, the control afforded by the exploitation of just a few isolated mineralizations of tin ores over the rather more common and thus difficult to restrict arsenic-bearing deposits played an important role in favouring state-sponsored exploitation of tin.

Although these explanations remain hypothetical, it is doubtless that this time period witnessed the rise of tin and the downfall of arsenic as the alloying element of choice. This can be seen quite clearly in nearly all archaeological sites dating to the Bronze Ages, but it particularly well exemplified by Tell Beydar (De Ryck et al. 2003) and Boğazköy/Hattusa

(Lehner 2012; Lehner 2015). That being said, certain regions, such as Iran (Thornton and Lamberg-Karlovsky 2002; Thornton 2010; Cuenod et al. 2015), Anatolia (Özbal et al. 2002), and Arabia (Liu et al. 2015) continue the exploitation of arsenical copper well into the Bronze Age, with production occurring sporadically into the Iron Age and perhaps even as late as the Roman period in some regions.

9.5 Iron in Copper

It is widely known that copper containing iron in the 1-5% range would have led to an overly brittle metal with inferior physical properties to pure copper. It would have needed to be removed in a separate 'fire refining' step, something which is well recorded in the Bronze Age when the use of iron rich copper sulphide ores that required the formation of slag and the development of well contained shaft furnaces caused much of the copper produced in that period to be very rich in iron (Catapotis and Bassiakos 2007; Craddock and Meeks 1987; Merkel 1990; Papadimitriou 2001; Thornton et al. 2009). There is however no evidence of this refining technique being applied in earlier periods.

That being said, it is interesting to find that the finished objects from Çamlıbel contain much less iron than the prills found in the slag from the site. Results of a study of the finished objects showed that most had bulk iron in concentrations below the detection limits of the WDS instrument used to analyse them, estimated at c. 120 ppm (Weeks et al. forthcoming) (Appendix B). Just two artefacts had iron above the detection limit, containing just 240 ppm and 410 ppm respectively, and representing just a tenth of the analysed assemblage. These quantities are much lower than what would normally be expected to result from Bronze Age refining technology, let alone from an earlier period. Indeed, while objects from the Late Chalcolithic often contain less than 500 ppm of iron, this is generally thought to be the result of smelting rich oxidic copper ores in a relatively slag-less process under only marginally oxidizing atmosphere. Under such circumstances, little to no iron could enter the metallic copper since the ores contained none. It was not until the Early Bronze Age shift to a fully slagging process that iron tended to enter the copper much more readily and had to be refined out, leading to finished objects with about 0.3 wt% iron (Cooke and Aschenbrenner 1975; Craddock and Meeks 1987; Tylecote et al. 1977).

It is clear that while the low iron content of the finished objects of Çamlıbel appears to confirm the hypothesis outlined above, the composition of the copper prills within the slag tell a different story. First of all, it is clear that iron could easily enter the metallic copper despite the poorly reducing conditions, and therefore the simple presence of iron in the

charge may be all that is needed to produce a copper metal with 1-3 wt% iron content. The discrepancy in the iron content of finished objects is therefore not exclusively indicative of a slagging process, but rather of the presence of iron rich ores or the addition of iron fluxes.

Furthermore, if we assume that the objects used at Çamlıbel were also manufactured there, then it is necessary to try to understand by what process the iron was removed. Since alloying, casting, and refining also took place in the Bronze Age but still resulted in a relatively high residual iron content, simple surface exposure to oxidizing conditions cannot have been solely responsible for the iron depletion process at Çamlıbel. An explanation should therefore be sought in the step involving the addition of the arsenic to the metal. An explanation could be found in the use of arsenate minerals as alloying agents. The addition of such a mineral to molten copper under lightly oxidizing conditions would result in the release of both arsenic vapour and free oxygen gas. Thermodynamically, this would result in the rapid oxidation of the iron (Chakraborti and Lynch 1983; Luyken and Heller 1938) (Figure 9.7), which would form a layer of iron oxide that could be easily removed or separated from the underlying metal, much like the conventional fire refining process. In addition, this would also have freed the arsenic vapour to enter the copper to form arsenical copper in a process similar to that described for Tepe Hissar (Thornton et al. 2009), Arisman (Rehren et al. 2012), and Hacınebi (Özbal et al. 1999). This is unlike the production of tin bronze in later periods in that tin was typically added to copper in its metallic form rather than as an oxide, and therefore would not have resulted in the additional chemical removal of iron.

Regardless, it puts in question the theory proposed by Craddock and Meeks that copper with significant iron impurity is a marker of Bronze Age furnace designs but may rather be entirely due to the increased presence of sulphur in sulphidic ores. In no way do the smelting conditions of Çamlıbel's slag resemble the more reducing conditions seen in typical Bronze Age furnace smelts. Since the copper produced at the site does appear to contain significant quantities of iron, it appears that strongly reducing conditions alone cannot be an adequate explanation for the presence of iron in the copper.

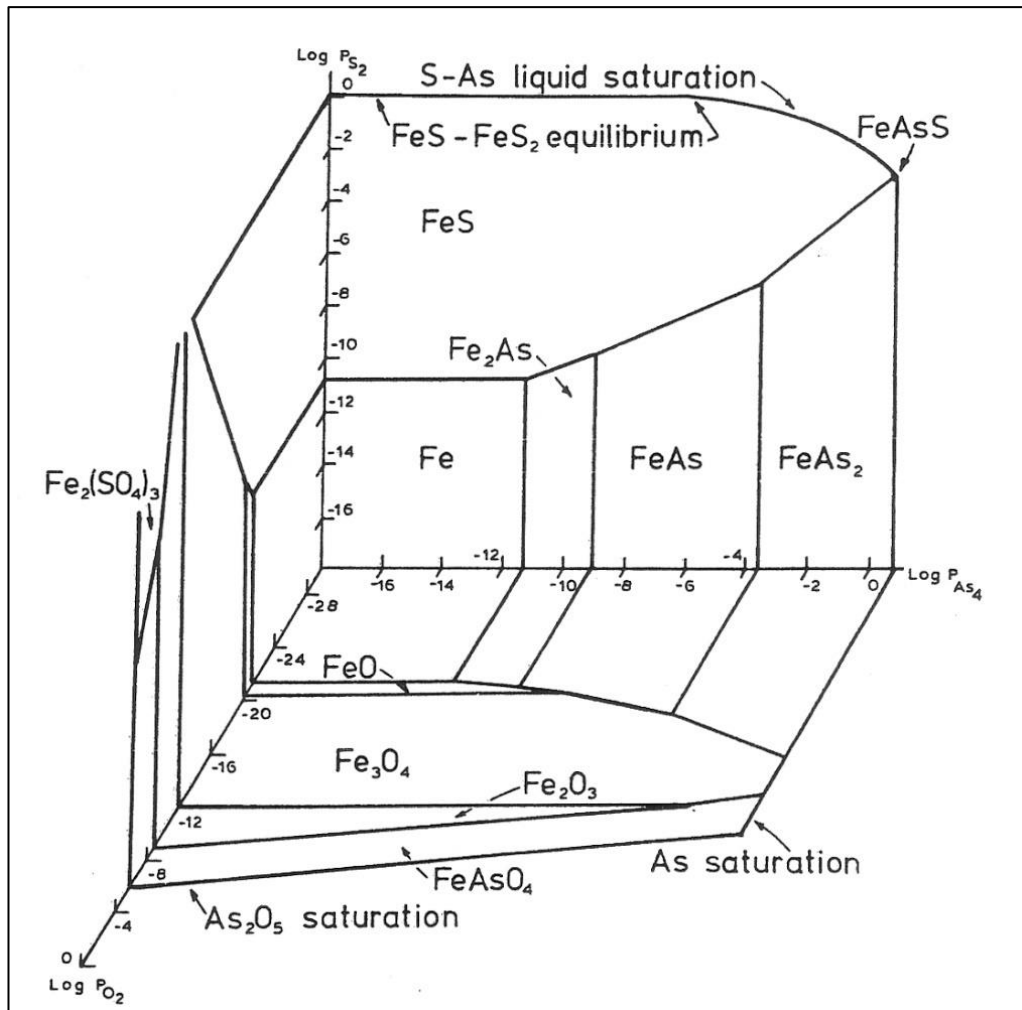


Figure 9.7 Quaternary phase diagram of the Fe-As-S-O system at 973 K. Note that iron oxidizes at a much lower oxygen partial pressure than arsenic, which can remain as metallic gas for much longer, and also that a fairly high partial pressure of -9 to -3 is required to form FeAs. These conditions are approximately equivalent to those needed for FeS, and much more elevated than the pressure of oxygen required to form various iron oxides (Adapted from Chakraborti and Lynch 1983).

Chapter 10 Conclusions and Future Work

The aim of this thesis was to investigate the production of arsenical copper alloys during South West Asia's shift from Chalcolithic to Early Bronze Age with the ultimate goal of understanding whether the production was intentional and how it related to the underlying cultural context of the time.

Using a well-established archaeometallurgical framework to highlight technological choice from archaeological data, the arsenical copper *chaînes opératoires* of two sites dating to the mid- to late-4th millennium BC were reconstructed using material evidence from metal extraction, alloying, and casting processes. Samples were taken from the full range of production activities, including primary ores, crucibles, furnace walls, slag, as well as finished objects, and subjected to various analytical techniques to retrieve their chemical, microstructural, and isotopic compositions. After detailed investigation of the data to characterize these technologies, the results were contextualized within the region's broader socio-economic backdrop.

The earlier of the two sites, Çamlıbel, dates to the mid-4th millennium BC and consists of a small settlement, most likely inhabited by a small nuclear or extended family, engaging in farming activities but maintaining an essentially subsistence-based lifestyle. A number of domestic-scale craft industries, such as pottery, bead, and metal production appear to have been intended mainly for local consumption. Although they also likely aided in mitigating periods of economic hardship by providing alternative resources which could be traded for necessities, surplus appears to have been rather limited. Despite the limited scale of production and ephemeral nature of the metallurgical industry of Çamlıbel, this thesis has revealed it to be surprisingly sophisticated.

Indeed, rather than the well-known exploitation of polymetallic ore deposits which resulted in the fortuitous production of arsenical copper without much effort, it now appears clear that Çamlıbel's copper smelters made exclusive use of local mixed oxide/sulphide copper deposits devoid of any arsenic mineralization to produce nearly pure copper metal. Analysis of crucibles and crucible slag revealed that it was not until a later stage that arsenic was added to the molten copper in the form of mineral arsenate. This afforded several benefits such as much increased control of the final arsenic content of the product, a significant decrease in potential losses of the element from the reduced instances of heating, and in the removal of iron impurities from the copper through the release of oxygen. Unavoidably, the heating of arsenic-bearing minerals resulted in the volatilization of some of the arsenic as an

oxide then bonded with calcium oxide from fuel ash to form thin residues visible along the upper rims of the melting crucibles.

In addition to innovations relating to alloying practices, the study of the metallurgical assemblage of Çamlıbel also revealed a shift in the organization of the industry which occurred following the first abandonment of the site. Whereas in the early two occupation periods of the site ores were brought to the site for sorting and beneficiation before being smelted outside the settlement, in the later periods ore processing and smelting both took place elsewhere while the slag was brought back to Çamlıbel for further handling. Since this change correlates directly with an increase in copper production, it has been argued that it was caused by a depletion of ore resources in close proximity to the site and therefore a move towards beneficiation, and perhaps smelting, away from Çamlıbel and closer to the ore deposits themselves. This shift in organization and increase in production offers a glimpse at a settlement which was increasingly specialized in pyrotechnologies at a period where economic divergence between regions was driving the rise in urban settlements elsewhere, parallels which may be inexorably linked through networks of interactions suggested by the emergence of the Circumpontic Metallurgical Province.

Although a programme of lead isotope analysis was undertaken on samples of minerals, slag, and copper alloy objects recovered from Çamlıbel, the results have been somewhat disappointing. Although it was possible to characterise the unique lead isotope ratios of the copper ore deposits exploited by the inhabitants of the site, the provenance of these ores could not be identified due to large variations caused by the paucity in lead in all but one sample. Despite these problems, this limited information did indicate a probable connection to a series of copper artefacts from at least one other site in the vicinity. Although culturally unrelated, it is highly likely that the metal used to produce the Central Artefact Group objects from Kaman-Kalehöyük originated from the same deposit as that exploited by Çamlıbel's smelters. Furthermore, although the alloying of arsenical copper from two distinct mineral deposits could not be confirmed through lead isotope analysis, the data do not contradict the possibility.

The second case study under scrutiny for this thesis was the site of Arisman in West Central Iran dating to the Late 4th to Early 3rd millennia BC. It is assumed that, although wetter in the Early Bronze Age, the region's arid climate and poor soils could not sustain such a large settlement without support from somewhere else. Although the nature of this support is still poorly understood, in all likelihood the site operated as an industrial outpost and

pyrotechnological hub supplying raw materials to more distant urban settlements of the Uruk and Proto-Elamite cultures because it was situated in close proximity to preferred high-calorie wood sources suitable for fuel-intensive industries. Not only does this archaeological site offer many insights into the complex and rich cultural interaction spheres of the period, but analysis of the archaeometallurgical remains also revealed the clearest and strongest evidence for the smelting of iron arsenide as an intermediate step in the systematic alloying of arsenic with copper.

Although some preliminary analysis had previously been undertaken on the archaeometallurgical material of Arisman which had brought to light the use of speiss smelting at the site, the aim of revisiting the material was to confirm our existing knowledge and to uncover more details of the process through the analysis of still little-understood remains. For this purpose, and in addition to the study of samples of the more common copper and speiss slags, the new analysis largely focused on technical ceramics and black glassy slag.

While the analysis of 'brown' and 'grey' slag largely confirmed previous results, the technical ceramics revealed that the speiss smelting process made extensive use of cold 'crucibles' to retrieve the molten speiss charge. This led to the reinterpretation of the furnace uncovered beneath slagheap A as a speiss smelting rather than copper smelting and the U-shaped slot beneath it as the position of the crucibles which could quickly remove and cover the smelting charge from the furnace. This fits in well with the known behaviour of arsenic, sulphur, and iron in controlled experiments conducted by industrial metallurgists some three decades ago. It has been argued that in order to produce ferrous speiss from arsenopyrite without excessive losses of arsenic, it is necessary to first remove excess sulphur and then quickly end the operation, hence the need to remove the charge from the furnace and quickly cover it. This system has been shown to match the range of technical ceramics recovered from Arisman's slagheaps.

The analysis of the black glassy slags revealed them to be the result of both speiss and copper smelting processes rather than representing a third mixing process as had previously been suggested. This reinterpretation is based on a much more reliable number of analyses and therefore much more robust than the inferences previously made on just two samples. Although it was hoped that this wider sampling strategy would reveal a separate stage of arsenical copper production, the new results do not significantly alter the suggested *chaîne opératoire* for the alloy at Arisman.

Indeed, much of the copper-bearing slags have now been shown to include low but significant quantities of arsenic, suggesting that arsenical copper was typically produced at Arisman as a single co-smelting stage. Whether arsenic-bearing minerals or synthetic iron arsenide were used as the co-smelting alloying material remains a critical question which could not be answered by this study. Although ferrous speiss would be an ideal candidate, it could not be unequivocally shown to have been used here. Regardless, and while there is no direct evidence of this, it is likely that the material's value as a transportable alloying agent meant that it was favoured for export while arsenical copper was produced directly on site from mixed charges.

In addition to clarifying our understanding of the arsenical copper *chaînes opératoires* and the broader archaeometallurgical technologies of both Çamlıbel and Arisman, the parallel study of the material from the two sites has drawn attention to a number of important cultural trends relevant to our perceptions of Late Chalcolithic and Early Bronze Age societies. Indeed, this study has highlighted how the alloying technology employed at Çamlıbel represents an important advance in our ancestors' approach to the production and use of metals. Control over composition of the finished alloys granted by the innovative use of arsenate minerals paved the way for further experimentation and exploitation of an increasingly diverse array of alloys appearing near the end of the Chalcolithic. As such, although arsenical copper production itself may not have been an essential precursor to the later tin bronzes, this thesis has made the case that the concept of alloying as distinct from smelting probably evolved from efforts to produce arsenical copper in regions where polymetallic ores were absent.

It has also been argued that these technological developments did not occur in isolation but were part of a series of related trends associated with the Circumpontic Metallurgical Province which extended over much of the region under discussion at the time. It is highly likely that knowledge of alloying was thus propagated across a vast region relatively quickly and ultimately played a formative part in the development of more advanced forms of alloying, particularly that proposed for site of Arisman.

It is at this latter site, and potentially others like it, that arsenical copper production technology appears to have achieved its apogee. This thesis has demonstrated that knowledge of speiss smelting was developed to resolve several issues inherent in the combination of two metallurgical realities at the time: the increasing reliance on sulphidic copper ores and the difficulty in retaining arsenic in the final copper product. The highly

specialized speiss smelting furnace design of Arisman permitted the extraction of arsenic from non-copper bearing ores and as such offered a new highly dependable and consistent source of alloying material. The settlement appears to have become specialized in this pyrotechnology very quickly and probably supplied both arsenical copper metal and iron arsenide speiss to distant polities. It has been suggested that this technology was so well established that it provided a valid alternative to tin bronzes and is in part responsible for the protracted use of arsenical copper in Iran up to the Iron Age.

Finally, the commonly accepted correlation between minor quantities of iron in finished copper objects with the emergence of larger, more highly reducing furnace designs in the Bronze Age has been put into question by the results of this research. Indeed, given the ubiquitous presence of iron impurities within copper prills trapped in slags predating the appearance of large shaft furnaces, such a theory now appears to oversimplify the situation. It now appears much more likely that the use of sulphide minerals played a much more important role in allowing a larger proportion of reduced iron to enter the finished copper product than the redox conditions themselves. It has therefore been suggested that, prior to the Bronze Age, the use of arsenate minerals as alloying material may have played a hand in reducing the iron content of finished objects through the release of free oxygen gas which favoured the formation of an iron oxide layer which could easily be separated from the copper during the alloying or casting process. Archaeologically, the end result of such a process was the lengthening of the period of time in which low-iron copper objects were produced well past the beginning of the use of sulphide minerals.

No doubt like all doctorate theses, this research has answered a number of interesting questions but has also opened up several new lines of inquiry which will be worth exploring in the future.

First and foremost is the need to test the hypotheses proposed in this thesis in order to better understand the behaviour of arsenic when smelting and alloying. The proposed alloying of molten pure copper with arsenate minerals could easily be tested to confirm the absorption rate of arsenic under various redox conditions. Such an experiment could also be used to test the effects of arsenates on iron impurities and offer a basis of comparison against the known effects of fire refining processes or direct melting and casting. The processes proposed for Arisman also warrant experimental testing. Since speiss smelting from arsenopyrite has not been conducted in several millennia, it is essential to experimentally demonstrate the viability of the process and assess real-world ideal redox conditions to confirm whether this

was indeed possible. Furthermore, the addition of speiss directly to molten copper also needs to be examined as the inclusions of iron in the melt may be problematic. Although it is assumed that much of the iron would form an oxidized layer on the surface, this will also need to be confirmed experimentally.

The revisiting of the lead isotope data from Arisman has highlighted a potential distinction between arsenic and copper ore sources. In order to investigate this, it will be first necessary to obtain a larger sample count of speiss slags to confirm the pattern hinted at by the available data. Should these trends turn out to hold true, then a survey of the vicinity of the site with the aim of collecting arsenic-bearing minerals would be of great interest in efforts to provenance the ores exploited there. A similar effort should also be undertaken in the vicinity of Çamlıbel in order to locate the arsenic source there as well. If the data from such surveys and analyses fit with the results presented here, it would greatly expand our knowledge of early alloying practices and justify the inclusion of such field methodology when dealing with any Late Chalcolithic and Early Bronze Age sites.

More ambitiously, it would be of further great interest in our understanding of our past relationship with early alloys to excavate and analyse the material from any number of metal production sites dating to the Late Chalcolithic. Particularly interesting would be the recovery of primary production from small sites such as Çamlıbel in other localities across Southwest Asia. Of course such sites are not widely recognized and even more rarely excavated due to their limited remains, but a potential initial target would be Qal'e Guše in Western Iran where perforated pedestalled crucibles and Sialk III pottery have been recovered.

Overall, it is hoped that this thesis and the proposed future research have and will shed more light on humanity's first tentative steps towards mastering control over metallic alloys. The data presented here have demonstrated that while the earliest copper-arsenic alloys were most certainly produced from polymetallic ores, by the Late Chalcolithic efforts were being made to reproduce the alloy under more controlled conditions. Experimentation with different minerals quickly led to innovation and to emergence of highly diversified technological approaches to metallurgy and the appearance of several new alloys in the archaeological record. The existence of a specialized Early Bronze Age production site at Arisman shows unequivocally the importance of the alloy at this period. However, despite the development of speiss smelting providing a reliable and systematic mode of production and the continued use of arsenical copper throughout Iran's Bronze Ages, its steady decline

and ultimate replacement in favour of tin bronzes could not be reversed. The nature of the competition between these two alloys and the reasons for the obsolescence of one and the rise of the other remains enigmatic. Although this research has provided concrete evidence for the state of metallurgical technology at this critical period, exploring the underlying economic, political, and social causes for the technological choices presented here will be an ongoing challenge but of great importance in furthering our understanding of the rise and development of Bronze Age societies.

References

- Adams, R. 1997. On early copper metallurgy in the Levant: A response to claims of Neolithic metallurgy. In: Gebel, H. G., Kafafi, Z. & Rollefson, G. (eds.) *The Prehistory of Jordan II. Perspectives from 1997*. 651-655. Berlin: Ex Oriente.
- Adriaens, A., Veny, P., Adams, F., Sporcken, R., Louette, P., Earl, B., Özbal, H. & Yener, K. a. B. 1999. Analytical investigation of archaeological powders from Göltepe, Turkey. *Archaeometry* 41, 81-89.
- Algaze, G. 1993. *The Uruk World System: The Dynamics of Expansion of Early Mesopotamian Civilization*. Chicago: University of Chicago Press.
- Amzallag, N. 2009. From metallurgy to Bronze Age civilizations: The synthetic theory. *American Journal of Archaeology*, 113, 497-519.
- Arriaza, B., Amarasiriwardena, D., Cornejo, L., Standen, V., Byrne, S., Bartkus, L. & Bandak, B. 2010. Exploring chronic arsenic poisoning in pre-Columbian Chilean mummies. *Journal of Archaeological Science*, 37, 1274-1278.
- Artioli, G., Baumgarten, B., Marelli, M., Giussani, B., Recchia, S., Nimis, P., Giunti, I., Angelini, I., & Omenetto, P. 2008. Chemical and isotopic tracers in Alpine copper deposits: geochemical links between mines and metal. *Geo.Alp*, 5, 139-148.
- Avilova, L. 2008. Regional models of metal production in Western Asia in the Chalcolithic, Early and Middle Bronze Ages. *Trabajos de Prehistoria*, 65, 73-91.
- Bachmann, H.-G. 1980. Early copper smelting techniques in Sinai and in the Negev as deduced from slag investigations. In: Craddock, P. T. (ed.) *Scientific Studies in Early Mining and Extractive Metallurgy*. London: British Museum.
- Bachmann, H.-G. 1982. *The Identification of Slags from Archaeological Sites*. London: Institute of Archaeology.
- Bamberger, M. & Wincierz, P. 1990. Ancient smelting of oxide copper ore. In: Rothenberg, B. (ed.) *The Ancient Metallurgy of Copper*. 123-157. London: Institute for Archaeo-Metallurgical Studies.
- Bar-Yosef Mayer, D. C. & Porat, N. 2008. Green stone beads at the dawn of agriculture. *Proceedings of the National Academy of Sciences*, 105, 8548-8551.
- Bar-Yosef, O. & Alon, D. 1988. The Excavations in Nahal Hemar Cave. *Atiqot*, 18, 1-30.
- Bar Adon, P. 1980. *The cave of the Treasure*. Jerusalem: Israel Exploration Society.
- Bartelheim, M., Eckstein, K., Huijsmans, M., Krauß, R. & Pernicka, E. 2002. Kupferzeitliche Metallgewinnung in Brixlegg, Österreich. In: Bartelheim, M., Pernicka, E. & Krause, R. (eds.) *The beginnings of metallurgy in the Old World*. 33-82. Rahden/Westf.: Forschungen zur Archäometrie und Altertumswissenschaft.
- Bartelheim, M., Eckstein, K., Huijsmans, M., Krauss, R. & Pernicka, E. 2003. Chalcolithic metal extraction in Brixlegg, Austria. *Archaeometallurgy in Europe, 2003 Milan*. 441-447. Milan: Associazione Italiana di Metallurgia.
- Bassiakos, Y. & Catapotis, M. 2006. Reconstruction of the Copper Smelting Process Based on the Analysis of Ore and Slag Samples. *Hesperia Supplements*, 36, 329-353.
- Bassiakos, Y. & Philaniotou, O. 2007. Early copper production on Kythnos: Archaeological evidence and analytical approaches to the reconstruction of metallurgical process. In: Day, P. & Doonan, R. (eds.) *Metallurgy in the Early Bronze Age Aegean*. 19-56. Oxford: Oxbow Books.
- Baxter, M. J. 2003. *Statistics in Archaeology*. London: Arnold.
- Bayley, J. & Rehren, Th. 2007. Towards a functional and typological classification of crucibles. In: Niece, S., Hook, D. & Craddock, P. T. (eds.) *Metals and Mines: Studies in Archaeometallurgy*. 46-55. London: Archetype Publications.

- Begemann, F., Pernicka, E. & Schmitt-Strecker, S. 1994. Metal finds from Ilıpınar and the advent of arsenical copper. *Anatolica*, 20, 203-211.
- Begemann, F., Schmitt-Strecker, S. & Pernicka, E. 1989. Isotopic composition of lead in early metal artefacts. In: Hauptmann, A., Pernicka, E. & Wagner, G. A. (eds.) *Old World Archaeometallurgy*. 269-278. Bochum: Deutsches Bergbau-Museum.
- Begemann, F., Schmitt-Strecker, S. & Pernicka, E. 2002. On the composition and provenance of metal finds from Beşiktepe (Troia). In: Wagner, G. A., Pernicka, E. & Uerpman, H.-P. (eds.) *Ancient Troia and the Troad: Scientific Approach*. 173-201. New York: Springer.
- Behm, J.A. 1983. Flake concentrations: distinguishing between flintworking activity areas and secondary deposits. *Lithic Technology*, 12, 9-16.
- Ben-Yosef, E., Tauxe, L. & Levy, T. E. 2010. Archaeomagnetic dating of copper smelting site F2 in the Timna Valley (Israel) and its implications for the modelling of ancient technological developments. *Archaeometry*, 52, 1110-1121.
- Berthoud, T., Cleuziou, S., Hurtel, L. P., Menu, M. & Volfovsky, C. 1982. Cuivres et alliages en Iran, Afghanistan, Oman au cours des IVe et IIIe millénaires. *Paléorient*, 8, 39-54.
- Betancourt, P. & Muhly, J. D. 2007. The crucibles from the Aghia Photia. In: Day, P. & Doonan, R. (eds.) *Metallurgy in the Early Bronze Age Aegean*. 146-153. Oxford: Oxbow Books.
- Betancourt, P. P. 1970. The Majkop copper tools relationship to Cretan metallurgy. *American Journal of Archaeology*, 74, 351-358.
- Bhardwaj, H. C. 1979. *Aspects of Ancient Indian Technology*. Delhi: Motilal Banarsidass.
- Birch, T., Rehren, Th. & Pernicka, E. 2013. The metallic finds from Çatalhöyük: a review and preliminary new work. In: Hodder, I. (ed.) *Substantive Technologies at Çatalhöyük*. 307-316. Los Angeles: Cotsen Institute of Archaeology Press.
- Blackburn, W. H. & Dennen, W. H. 1994. *Principles of Mineralogy*. Dubuque: Wm. C. Brown.
- Boroffka, R., Chen, J. & Parzinger, H. 2011. Excavations at Arisman, Area B. In: Vatandoust, A., Parzinger, H. & Helwing, B. (eds.) *Early Mining and Metallurgy on the Western Central Iranian Plateau: The First Five Years of Work*. 28-39. Mainz: Verlag Philipp Von Zabren.
- Boroffka, R. & Parzinger, H. 2011. Sialk III pottery from Area B. In: Vatandoust, A., Parzinger, H. & Helwing, B. (eds.) *Early Mining and Metallurgy on the Western Central Iranian Plateau: The First Five Years of Work*. 100-195. Mainz: Verlag Philipp Von Zabren.
- Boscher, L. 2010. A Reconstruction of Early Bronze Age Arsenical Copper Production at Arisman on the Iranian Plateau. Unpublished MSc Dissertation. UCL Institute of Archaeology.
- Bourgarit, D. 2007. Chalcolithic copper smelting. In: La Niece, S., Hook, D. & Craddock, P. T. (eds.) *Metals and Mines: Studies in Archaeometallurgy*. 3-14. London: Archetype Publications.
- Bourgarit, D., Mille, B., Prange, M., Ambert, P. & Hauptmann, A. 2003. Chalcolithic fahlore smelting at Cabrière: Reconstruction of smelting processes by archaeometallurgical finds. *Archaeometallurgy in Europe*. 431-440. Milan: Associazione Italiana di Metallurgia.
- Bourgarit, D., Rostan, P., Carozza, L., Mille, B. & Artioli, G. 2010. Vingt ans de recherches à Saint-Véran, Hautes Alpes: état des connaissances de l'activité de production de cuivre à l'âge du Bronze ancien. *Trabajos de Prehistoria*, 67, 269-285.
- Branigan 1974. *Aegean Metalwork of the Early and Middle Bronze Age*. Oxford: Clarendon Press.
- Bray, P. & Pollard, A. M. 2012. A new interpretative approach to the chemistry of copper-alloy objects: source, recycling and technology. *Antiquity*, 86, 853-867.
- Broodbank, C., Rehren, Th. & Zianni, A.-M. 2007. Scientific analysis of metal objects and metallurgical remains from Kastri, Kythera. *The Annual of the British School at Athens*, 102, 219-238.

- Budd, P. 1991. *A Metallographic Investigation of Eneolithic Arsenical Copper*. PhD thesis, University of Bradford.
- Budd, P. 1993. Recasting the Bronze Age. *New Scientist*, Oct 23, 33-37.
- Budd, P., Gale, D., Pollard, A. M., Thomas, R. G. & Williams, P. A. 1992. The early development of metallurgy in the British Isles. *Antiquity*, 66, 677-686.
- Budd, P. & Ottaway, B. S. 1991. The properties of arsenical copper alloys: Implications for the development of Eneolithic metallurgy. In: Budd, P., Chapman, B., Jackson, C. M., Janaway, R. & Ottaway, B. S. (eds.) *Archaeological Sciences 1989: Proceedings of a Conference on the Application of Scientific Techniques to Archaeology*. 132-142. Oxford: Oxbow Books.
- Budd, P. & Ottaway, B. S. 1995. Eneolithic arsenical copper: chance or choice? In: Jovanovic, B. (ed.) *International Symposium, Ancient Mining and Metallurgy in Southeast Europe*. 95-102. Belgrade: Archaeological Institute.
- Budd, P. & Ottaway, B. S. 1991. The properties of arsenical copper alloys: Implications for the development of Eneolithic metallurgy. In: Budd, P., Chapman, B., Jackson, C. M., Janaway, R. & Ottaway, B. S. (eds.) *Archaeological Sciences 1989: Proceedings of a Conference on the Application of Scientific Techniques to Archaeology*. 132-142. Oxford: Oxbow Books.
- Byrne, S., Amarasiriwardena, D., Bandak, B., Bartkus, L., Jones, J., Kane, J., Ya'N'ez, J., Arriaza, B. & Cornejo, L. 2010. Were Chinchorro exposed to arsenic? Arsenic determination in Chinchorro mummies' hair by laser ablation inductively coupled plasma-mass spectrometry (LA-ICP-MS). *Microchemical Journal*, 94, 28-35.
- Caldwell, J. R. 1967. *Investigations at Tal-i Iblis*. Illinois State Museum Preliminary Reports No. 9. Springfield: Illinois State Museum Society.
- Caldwell, J. R. 1968. Tal-i Iblis and the beginning of copper metallurgy at the fifth millennium. *Archaeologia Viva*, 1, 145-150.
- Caldwell, J. R. & Shahmirzadi, S. M. 1966. *Tal-i Iblis. The Kerman Range and the Beginnings of Smelting*. Springfield: Illinois State Museum.
- Caley, E. R. 1926. The Leyden Papyrus x. *Journal of Chemical Education*, 3, 1154.
- Caley, E. R. 1949. On the prehistoric use of arsenical copper in the Aegean region. *Hesperia Supplements*, 8, Commemorative Studies in Honor of Theodore Leslie Shear, 60-63.
- Caneva, C. & Palmieri, A. M. 1983. Metalwork at Arslantepe in Late Chalcolithic and Early Bronze I: The evidence from metal analyses. *Origini*, 12, 637-654.
- Catapotis, M. & Bassiakos, Y. 2007. Copper smelting at the Early Minoan site of Chrysokamino. In: Day, P. & Doonan, R. (eds.) *Metallurgy in the Early Bronze Age Aegean*. 68-83. Oxford: Oxbow Books.
- Chakraborti, N. & Lynch, D. C. 1983. Thermodynamics of roasting arsenopyrite. *Metallurgical Transactions B*, 14B, 239-251.
- Chakraborti, D.K., Lahiri, N. 1996. *Copper and Its Alloys in Ancient India*. New Delhi : Munshiram Manoharlal.
- Charles, J. A. 1967. Early arsenical bronzes - a metallurgical view. *American Journal of Archaeology*, 71, 21-26.
- Charles, J. A. 1980. The coming of copper and copper-base alloys and iron: a metallurgical sequence. In: Wertime, T. A. & Muhly, J. D. (eds.) *The Coming of the Age of Iron*. 151-181. New Haven: Yale University Press.
- Charles, J. A. 1994. Determinative mineralogy in the early development of metal. *Historical Metallurgy*, 28, 66-68.
- Chegin, N. N., Fahimi, H. & Helwing, B. 2011. Excavations at Arismān, Area C. In: Vatandoust, A., Parzinger, H. & Helwing, B. (eds.) *Early Mining and Metallurgy on the Western Central Iranian Plateau: The First Five Years of Work*. 40-68. Mainz: Verlag Philipp Von Zabren.

- Chegini, N. N., Helwing, B., Parzinger, H. & Vatandoust, A. 2004. A prehistoric industrial settlement on the Iranian Plateau - research at Arisman. In: Stöllner, T., Slotta, R. & Vatandoust, A. (eds.) *Persia's Ancient Splendour; Mining, Handicraft and Archaeology*. Bochum: Deutsches Bergbau-Museum.
- Chegini, N. N., Momenzadeh, M., Parzinger, H., Pernicka, E., Stöllner, T., Vatandoust, R. & Weisgerber, G. 2000. Preliminary report on archaeometallurgical investigation around the prehistoric site of Arisman near Kashan, Western Central Iran. *Archäologische Mitteilungen aus Iran und Turan*. Berlin: Band 32, 281-318.
- Chen, K., Rehren, Th., Mei, J. & Zhao, C. 2009. Special alloys from remote frontiers of the Shang Kingdom: Scientific study of the Hanzhong bronzes from southwest Shaanxi, China. *Journal of Archaeological Science*, 36, 2108-2118.
- Chernykh, E. 1991. *Ancient Metallurgy in the USSR: The Early Metal Age*. Cambridge: Cambridge University Press.
- Chernykh, E., Avilova, L. & Orlovskaya, L. 2002. Metallurgy of the Circumpontic area: from unity to disintegration. In: Yalçın, Ü. (ed.) *Anatolian Metal II*. 83–100. der anschnitt Beiheft 15. Bochum: Deutsches Bergbau Museum.
- Childe, V. G. 1936. *Man Makes Himself*. London: Watts.
- Childe, V. G. 1944. Archaeological ages as technological stages. *Journal of the Royal Anthropological Institute of Great Britain and Ireland*, 74, 7-24.
- Clark, L. A. 1960. The Fe-As-Se system - phase relations and applications. *Economic Geology*, 55, 1345-1381.
- Coghan, H. H. & Case, H. J. 1957. Early metallurgy of copper in Britain and Ireland. *Proceedings of the Prehistoric Society*, 23, 91-123.
- Cohen, S. M., Arnold, L. L., Eldan, M., Lewis, A. S. & Beck, B. D. 2006. Methylated arsenicals: the implications of metabolism and carcinogenicity studies in rodents to human risk assessment. *Critical Reviews in Toxicology*, 36, 99-133.
- Cooke, S. R. B. & Aschenbrenner, S. 1975. The Occurrence of Metallic Iron in Ancient Copper. *Journal of Field Archaeology*, 2, 251-266.
- Cooper, J., Martínón-Torres, M. & Valcárcel Rojas, R. 2008. American gold and European brass: metal objects and indigenous values in the cemetery of El Chorro de Maíta, Cuba. In: Hofman, C. L., Hoogland, M. L. P. & Van Gijn, A. (eds.) *Crossing the Borders: New Methods and Techniques in the study of material culture in the Caribbean*. 34-42. Tuscaloosa: University of Alabama Press.
- Costin, C. L. 1991. Craft specialization: issues in defining, documenting and explaining the organization of production. *Archaeological Method and Theory*, 3, 1-56.
- Courcier, A. 2012. The metallurgical evidence at Mentesh Tepe: Preliminary results of archaeometallurgical analyses. *Archäologische Mitteilungen aus Iran und Turan*, Deutsches Archäologisches Institut, Eurasien-Abteilung, Aussenstelle Teheran. Berlin: Dietrich Reimer Verlag 109-119.
- Courcier, A. 2014. Ancient metallurgy in the Caucasus from the sixth to the third millennium BCE. In: Roberts, B. & Thornton, C. P. (eds.) *Archaeometallurgy in Global Perspective*. 579-664. New York: Springer.
- Courcier, A., Guliyev, F. & Lyonnet, B. 2012. Metallurgy during the Middle Chalcolithic period in the Southern Caucasus: Insight through recent discoveries at Mentesh-Tepe, Azerbaijan. In: Jett, P., McCarthy, B. & Douglas, J. G. (eds.) *Scientific Research on Ancient Asian Metallurgy: Proceedings of the Fifth Forbes Symposium at the Freer Gallery of Art*. London: Archetype.
- Craddock, P. T. 1995. *Early Metal Mining and Production*. Washington D.C.: Smithsonian Institution.
- Craddock, P. T. 1999. Paradigms of metallurgical innovation in prehistoric Europe. In: Hauptmann, A., Pernicka, E., Rehren, Th. & Yalçın, Ü. (eds.) *The Beginnings of Metallurgy*. 175-192. Bochum: Deutsches Bergbau-Museum.

- Craddock, P. T. 2000. From hearth to furnace: Evidences for the earliest metal smelting technologies in the eastern Mediterranean. *Paléorient*, 26, 151-165.
- Craddock, P. T. & Meeks, N. D. 1987. Iron in ancient copper. *Archaeometry*, 29, 187-204.
- Cui, J. & Wu, X. 2011. An Experimental Investigation on Lead Isotopic Fractionation during Metallurgical Processes. *Archaeometry*, 53, 205-214.
- Çukur, A. & Kuş, S. 1989. Analyses of Tepecik and Tülintepe metal artifacts. *Anatolian Studies*, 39, 113-120.
- Cukur, A. & Kuş, S. 1989. Development of Bronze Production Technologies in Anatolia. *Journal of Archaeological Science*, 16, 225-231.
- Cuenod, A., Bray, P. & Pollard, A.M. 2015. The 'Tin Problem' in the prehistoric Near East – Further insights from a study of chemical datasets on copper alloys from Iran and Mesopotamia. *Iran* 53, 29-48.
- Davis, D. D. 1983. Investigating the diffusion of stylistic innovations. *Advances in Archaeological Method and Theory*, 6, 53-89.
- De Ryck, I., Adriaens, A. & Adams, F. 2003. Microanalytical metal technology study of ancient Near Eastern bronzes from Tell Beydar. *Archaeometry*, 4, 579-590.
- Delibes, G., Fernandez-Miranda, M., Fernandez-Posse, M. D., Martin, C., Montero, I. & Rovira, S. 1991. Almizaraque, Almería, Spain. In: Eluère, C. & Mohen, J.-P. (eds.) *Découverte du Métal*. 303-316. Paris: Picard.
- Dobres, M. 2010. Archaeologies of technology. *Cambridge Journal of Economics*, 34, 103-114.
- Dobres, M. & Hoffman, C. 1994. Social agency and the dynamics of prehistoric technology. *Journal of Archaeological Method and Theory*, 1, 211-258.
- Domanski, M. & Webb, J. 2007. A review of heat treatment research. *Lithic Technology*, 32, 153-194.
- Donald, J. R. 1997. *Surface Interactions between Non-Ferrous Metallurgical Slags and Various Refractory Materials*. Unpublished PhD Thesis from the Department of Metallurgy and Materials Science, University of Toronto.
- Doonan, R. 2006. A storm in an eggcup: enigmatic objects from Broom Quarry, Bedfordshire. *HMS News*, 62, 4.
- Doonan, R. & Day, P. 2007. Mixed origins and the origins of mixing. In: Day, P. & Doonan, R. (eds.) *Metallurgy in the Early Bronze Age Aegean*. 1-18. Oxford: Oxbow Books.
- Doonan, R., Day, P. & Dimpoulou-Rethemiotaki, N. 2007. Lame excuses for emerging complexity in Early Bronze Age Crete: the metallurgical finds from Poros Katsambas and their context. In: Day, P. & Doonan, R. (eds.) *Metallurgy in the Early Bronze Age Aegean*. 98-122. Oxford: Oxbow Books.
- Dousova, B., Fuitova, L., Kolousek, D., Lhotka, M., Grygar, T. M. & Spurna, P. 2014. Stability of iron in clays under different leaching conditions. *Clays and Clay Minerals*, 62, 145-152.
- Dungworth, D. 1997. Roman copper alloys: analysis of artefacts from Northern Britain. *Journal of Archaeological Science*, 24, 901-910.
- Dussubieux, L. & Walder, H. 2015. Identifying American native and European smelted coppers with pXRF: a case study of artifacts from the Upper Great Lakes region. *Journal of Archaeological Science*, 59, 179-178.
- Earl, B. & Adriaens, M. 2000. Initial experiments on arsenical bronze production. *Journal of Metallurgy*, 52, 14-16.
- Eaton, E. A. 1980. Aspects of early metallurgy. *British Museum Occasional Papers*, 17, 159-168.
- Eaton, E. R. & Mckerrell, H. 1976. Near Eastern alloying and some textual evidence for the early use of arsenical copper. *World Archaeology*, 8, 169-191.
- Eisenhüttenleute, V. D. (ed.) 1995. *Slag Atlas*, Düsseldorf: Verlag Stahleisen.
- Enstitüsü, M. T. V. A. 1970. *Arsenic, Mercury, Antimony, and Gold Deposits of Turkey*. Ankara: Maden Tetkik ve Arama Enstitüsü.

- Esin, U. 1967. *Kuantitatif spektral analiz yardimiyla Anadolu'da başlangicindan Asur kolonileri çağına kadar bakir ve tunç madenciliği (Metin, kataloglar, resim ve haritalar)*. Istanbul: Taş Matbaasi.
- Esin, U. 1969. *Kuantitatif Spektral Analiz Yardimiyla Anadolu da Baslangicindan Asur Kolonileri Çağına Kadar Bakir ve Tunç Madenciliği*. Istanbul: University of Istanbul.
- Esin, U. 1976. Die anfänger de metallverwendung und bearbeitung in Anatolien (7500-2000 v. Chr). In: Müller-Karpe, H. (ed.) *Les Débuts de la Métallurgie. IXe Congres, Union Nationales des des Sciences Préhistoriques et Protohistoriques*. 199-242. Nice: Centre national de la recherche scientifique.
- Fernández-Miranda, M., Fernández-Posse, M. D., Martín, C., Montero, I. & Rovira, S. 1996. Changes in Bronze Age metallurgy as depicted by laboratory analysis: The "La Mancha" model, Spain. In: Demirci, Ş., Özer, A. M. & Summers, G. D. (eds.) *Archaeometry 94: The Proceedings of the 29th International Symposium on Archaeometry*. 23-34. Ankara: TÜBİTAK.
- Forbes, R. J. 1964. *Metallurgy in antiquity, part 2; Copper and bronze, tin, arsenic, antimony and iron*. Leiden: Brill.
- Frahm, E. & Doonan, R. 2013. The technological versus methodological revolution of portable XRF in archaeology. *Journal of Archaeological Science*, 40, 1425-1434.
- Frame, L. 2010. Metallurgical Investigations at Godin Tepe, Iran, Part I: The Metal Finds. *Journal of Archaeological Science*, 37, 1700-1715.
- Frame, L. D. 2009. *Technological Change in Southwestern Asia: Metallurgical Production Styles and Social Values during the Chalcolithic and Early Bronze Age*. Unpublished PhD dissertation, University of Arizona.
- Frame, L. D. 2012. Reconstructing ancient technologies: Chalcolithic crucible smelting at Tali Iblis, Iran. In: Jett, P., McCarthy, B. & Douglas, J. G. (eds.) *Scientific Research on Ancient Asian Metallurgy*. 183-204. London: Archetype.
- Frangipane, M. 1985. Early developments of metallurgy in the Near East. In: Liverani, M., Palmieri, A. M. & Peroni, R. (eds.) *Studi di Paleologia in Onore di S.M. Puglisi*. 215-228. Rome: Università di Roma.
- Frangipane, M. 1993. Local components in the development of centralized societies in Syro-Anatolian regions. In: Frangipane, M., Hauptmann, H., Liverani, M., Matthiae, P. & Mellink, M. (eds.) *Between Rivers and Over the Mountains*. 133-61. Rome: Università di Roma "La Sapienza".
- Frangipane, M. 2001. Centralization processes in Greater Mesopotamia: Uruk 'expansion' as the climax of systemic interactions among areas of the Greater Mesopotamian region. In: Rothman, M. S. (ed.) *Uruk Mesopotamia and its Neighbors. Cross-Cultural Interactions in the Era of State Formation*. 307-347. Santa Fe: School of American Research Press.
- Frangipane, M. 2012. Fourth millennium Arslantepe: The development of a centralised society without urbanisation. *Origini*, 34, 19-40.
- Frank, C. & Pernicka, E. 2012. Copper artefacts of the Mondsee Group and their possible sources. In: Midgley, M. S. & Sanders, J. (eds.) *Lake Dwellings after Robert Munro. Proceedings from the Munro International Seminar: The Lake Dwellings of Europe 22nd and 23rd October 2010, University of Edinburgh*. 113-138. Leiden: Sidestone Press.
- Freestone, I. 1989. Refractory materials and their procurement. In: Hauptmann, A. (ed.) *Old World Archaeometallurgy: Proceedings of the International Symposium "Old World Archaeometallurgy", Heidelberg 1987*. 155-162. Bochum: Der Anschnitt Beiheft 7.
- Gal, Z., Smithline, H. & Shalem, D. 1996. A Chalcolithic burial cave in Peqi'in. *Qadmoniot*, 111, 19-24.
- Gale, N. H. 2009. A response to the paper of A.M. Pollard: What a long, strange trip it's been: lead isotopes in archaeology. In: Shortland, A. J., Freestone, I. & Rehren, Th. (eds.)

- From Mine to Microscope: Advances in the Study of Ancient Technology*. 191-196. London: Oxbow.
- Gale, N. H., Bachmann, H.-G., Rothenberg, B., Stos-Gale, Z. A. & Tylecote, R. F. 1990. The Adventitious production of iron in the smelting of copper. In: Rothenberg, B. (ed.) *Researches in the Arabah 1959-1984, Vol. 2, The Ancient Metallurgy of Copper*. 182-191. London: Institute for Archaeo-Metallurgical Studies.
- Gale, N. H., Papastamataki, A., Stos-Gale, Z. A. & Leonis, K. 1985a. Copper sources and copper metallurgy in the Aegean Bronze Age. In: Craddock, P. T. & Hughes, M. J. (eds.) *Furnaces and Smelting Technology in Antiquity*. 81-101. London: British Museum Occasional Paper 48.
- Gale, N. H. & Stos-Gale, Z. A. 1989. Some aspects of early Cycladic copper metallurgy. In: Domergue, C. (ed.) *Mineria y Metalurgia en las Antiguas Civilizaciones Mediterraneas y Europeas* 21-37. Madrid: Ministerio de Cultura.
- Gale, N. H., Stos-Gale, Z. A. & Gilmore, G. R. 1985b. Alloy types and copper sources of Anatolian copper alloy artefacts. *Anatolian Studies*, 35, 143-173.
- Gale, N. H., Stos-Gale, Z. A. & Gilmore, G. R. 1985c. Alloy types and copper sources of Anatolian copper alloy artifacts. *Anatolian Studies*, 35, 143-173.
- Gale, R. & Cutler, D. 2000. *Plants in Archaeology*. Westbury and London: Royal Botanic Gardens Kew.
- Gebel, T. W. 2001. Genotoxicity of arsenical compounds. *International Journal of Hygiene and Environmental Health*, 203, 249-62.
- Georgakopoulou, M. 2013. Metal artefacts and metallurgy. In: Renfrew, C., Philaniotou, O., Brodie, N., Gavalas, G. & Boyd, M. (eds.) *The Settlement of Dhaskalio - The Sanctuary on Keros and the Origins of Aegean Ritual Practice: the Exvations of 2006-2008 Volume I*. 667-692. London: Oxbow Books.
- Georgakopoulou, M., Bassiakos, Y. & Philaniotou, O. 2011. Seriphos surfaces: A study of copper slag heaps and copper sources in the context of Early Bronze Age Aegean metal production. *Archaeometry*, 53, 123-145.
- Gilchrist, J. 1989. *Extractive Metallurgy*. Oxford: Pergamon Press.
- Golden, J., Levy, T. E. & Hauptmann, A. 2001. Recent discoveries concerning Chalcolithic metallurgy at Shiqmim, Israel. *Journal of Archaeological Science*, 28, 951-963.
- Golden, J. M. 2009. New Light on the development of Chalcolithic metal technology in the Southern Levant. *Journal of World Prehistory*, 22, 283-300.
- Golden, J. M. 2010. *Dawn of the Metal Age: Technology and Society during the Levantine Chalcolithic*. London: Equinox.
- Gopher, A. & Tsuk, T. 1996. *The Nahal Qanah Cave: Earliest Gold in the Southern Levant*. Monograph Series of the Institute of Archaeology. Tel Aviv: Tel Aviv University.
- Gubenko, N. & Ronen, A. 2014. More from Yiftahel (PPNB), Israel. *Paléorient*, 40, 149-158.
- Görsdorf, J. 2011. Radiocarbon datings in Arisman. In: Vatandoust, A., Parzinger, H. & Helwing, B. (eds.) *Early Mining and Metallurgy on the Central Iranian Plateau. Report on the first five years of research of the Joint Iranian-German Research Project.*, 370-375. Mainz: Archäologie in Iran und Turan 9.
- Hakemi, A. 1992. The copper smelting furnace of the Bronze Age at Shahdad. In: Jarrige, J.-F. (ed.) *South Asian Archaeology 1989*. 119-132. Monographs in Old World Archaeology 14: Madison.
- Hamuyuni, J., Taskinen, P., Akdogan, G. & Bradshaw, S. M. 2012. Measurement of surface tension of molten matte phases by an improved sessile drop method. *Mineral Processing and Extractive Metallurgy*, 121, 173-177.
- Hanning, E., Gauß, R. & Goldenberg, G. 2011. Metal for Zambujal: experimentally reconstructing a 5000-year-old technology. *Trabajos de Prehistoria*, 67, 287-304.
- Hansen, M. 1958. *Consitution of Binary Alloys*. New York: McGraww Hill.

- Hanson, D. & Marryat, C. 1927. Investigation of the effects of impurities on copper part III. The effect of arsenic on copper. *Journal of the Institute of Metals*, 37, 121-148.
- Harper, M. 1987. Possible toxic metal exposure of prehistoric bronze workers. *British Journal of Industrial Medicine*, 44, 652-656.
- Hauptmann, A. 1989. Copper metallurgy in Feinan, Jordan. In: Hauptmann, A., Pernicka, E. & Wagner, G. A. (eds.) *Old World Archaeometallurgy*. 119-135. Bochum: Der Anschnitt.
- Hauptmann, A. 2007. *The Archaeometallurgy of Copper: Evidence from Faynan, Jordan*. Berlin: Springer.
- Hauptmann, A. 2014. The investigation of archaeometallurgical slag. In: Roberts, B. & Thornton, C. P. (eds.) *Archaeometallurgy in Global Perspective*. 91-105. London: Springer.
- Hauptmann, A., Begemann, F., Heitkemper, R., Pernicka, E. & Schmitt-Strecker, S. 1992. Early copper produced in Feinan, Wadi Araba, Jordan: the composition of ores and copper. *Archaeomaterials*, 6, 1-33.
- Hauptmann, A., Rehren, Th. & Schmitt-Strecker, S. 2003. Early Bronze Age copper metallurgy at Shahr-i Sokhta (Iran), reconsidered. In: Stöllner, T., Körlin, G., Steffens, G. & Cierny, J. (eds.) *Man and Mining: Mensch und Bergbau: Studies in Honour of Gerd Weisgerber on the Occasion of his 65th Birthday*. 197-213. Bochum: Deutsches Bergbau-Museum.
- Hauptmann, A., Schmitt-Strecker, S., Begemann, F. & Palmieri, A. M. 2002. Chemical composition and lead isotopy of metal objects from the "Royal" tomb and other related finds at Arslantepe, Eastern Anatolia. *Paléorient*, 28, 43-69.
- Hauptmann, A. & Wagner, I. 2007. Prehistoric copper production at Timna: thermoluminescence (TL) dating and evidence from the East. In: La Niece, S., Hook, D. & Craddock, P. T. (eds.) *Metals and Mines: Studies in Archaeometallurgy*. 67-75. London: Archetype Publications.
- Hauptmann, A. & Weisgerber, G. 1980. The Early Bronze Age copper metallurgy of Shahr-i Sokhta (Iran). *Paléorient*, 6, 120-127.
- Hauptmann, A. & Weisgerber, G. 1996. The early production of metal in the Near East. In: Bagolini, B. & Lo Schiavo, F. (eds.) *The Copper Age in the Near East*. 95-101. Rome: A.B.A.C.O. Edizioni.
- Hauptmann, H. 1982. Norşuntepe Kazıları, 1974. *Keban Project 1974-1975 Activities*. 15-40. Ankara: Middle East Technical University.
- Hauptmann, H. 1993. Ein Kultgebäude in Nevali Çori. In: Frangipane, M., Hauptmann, H., Liverani, M., Matthiae, P. & Mellink, M. (eds.) *Between the Rivers and Over the Mountains: Archaeologica Anatolica et Mesopotamica Alba Palmieri Dedicata*. 37-70. Roma: Gruppo Editoriale Interni.
- Hauptmann, H. & Pernicka, E. 2004. *Die Metallindustrie Mesopotamiens von den Anfängen bis zum 2. Jahrtausend v. Chr.* Rahden: Verlag Marie Leidorf GmbH.
- Healy, J. F. 1978. *Mining and Metallurgy in the Greek and Roman World*. London: Thames and Hudson.
- Heginbotham, A., Basset, J., Bourgarit, D., Eveleigh, C., Glinsman, L., Hook, D., Smith, D., Speakman, R.J., Shugar, A. & Van Langh, R. 2015. The copper CHARM set: A new set of certified reference materials for the standardization of quantitative x-ray fluorescence analysis of heritage copper alloys. *Archaeometry*, 15, 5, 856-868.
- Heidersbach, R. 2011. Dealloying. In: Revie, R. W. (ed.) *Uhlig's Corrosion Handbook*. 145-150. New Jersey: Wiley.
- Hein, A., Karatasios, I., Müller, N., Kilikoglou, V. 2013. Heat transfer properties of pyrotechnical ceramics used in ancient metallurgy. *Thermochimica Acta*, 573, 87-94.
- Helmig, D., Jackwerth, E. & Hauptmann, A. 1989. Archaeometallurgical fieldwork and the use of a portable X-ray spectrometer. *Archaeometry* 31, 181-191.

- Helwing, B. 2005. Early mining and metallurgy on the western Iranian Plateau: First results of the Iranian-German archaeological research at Arisman 2000-2004. *Archäologische Mitteilungen aus Iran und Turan*, 37, 423-434.
- Helwing, B. 2006. The rise and fall of Bronze Age centers around the Central Iranian desert - A comparison of Tappe Hesar II and Arisman. *Archäologische Mitteilungen aus Iran und Turan*, 38, 35-48.
- Helwing, B. 2008. Early metallurgy in Highland Iran, on the basis of the Joint Iranian-German excavations at Arisman. In: Weeks, L. R. (ed.) Conference paper presented at: *The 2007 Early Iranian Metallurgy Workshop at the University of Nottingham*. *Iran*, 46, 335-345.
- Helwing, B. 2011a. Archaeological comments on the radiocarbon dating. In: Vatandoust, A., Parzinger, H. & Helwing, B. (eds.) *Early Mining and Metallurgy on the Western Central Iranian Plateau: The First Five Years of Work*. 374-375. Mainz: Verlag Philipp Von Zabren.
- Helwing, B. 2011b. Conclusions: The Arismān copper production in a wider context. In: Vatandoust, A., Parzinger, H. & Helwing, B. (eds.) *Early Mining and Metallurgy on the Western Central Iranian Plateau: The First Five Years of Work*. 523-531. Mainz: Verlag Philipp Von Zabren.
- Helwing, B. 2011c. Proto-Elamite pottery from areas A, C, D, and E. In: Vatandoust, A., Parzinger, H. & Helwing, B. (eds.) *Early Mining and Metallurgy on the Western Central Iranian Plateau: The First Five Years of Work*. 196-253. Mainz: Verlag Philipp Von Zabren.
- Helwing, B. 2011d. The small finds from Arisman. In: Vatandoust, A., Parzinger, H. & Helwing, B. (eds.) *Early Mining and Metallurgy on the Western Central Iranian Plateau: The First Five Years of Work*. 254-327. Mainz: Verlag Philipp Von Zabren.
- Heskel, D. L. 1983. A model for the adoption of metallurgy in the ancient Middle East. *Current Anthropology*, 24, 362-366.
- Heskel, D. L. & Lamberg-Karlovsky, C. C. 1980. An alternative sequence for the development of metallurgy: Tepe Yahya, Iran. In: Wertime, S. F. & Muhly, J. D. (eds.) *The Coming of the Age of Iron*. 229-266. New Haven: Yale University Press.
- Heyding, R. D. & Despault, G. J. G. 1960. The copper/arsenic system and copper arsenide minerals. *Canadian Journal of Chemistry*, 38, 2477-2481.
- Hirao, Y., Enomoto, J. & Tachikawa, H. 1995. Lead isotope ratios of copper, zinc and lead minerals in turkey - In relation to the provenance study of artefacts. In: Prince, H. I. H. & Mikasa, T. (eds.) *Essays on Ancient Anatolia and its Surrounding Civilizations*. 89-114. Wiesbaden: Harrassowitz Verlag.
- Hole, F. 1977. *Studies in the Archaeological History of the Deh Luran Plain: The Excavation at Chagha Sefid*. Ann Arbor: University of Michigan.
- Honeycome, R. W. K. 1985. *The Plastic Deformation of Metals*. London: Edward Arnold.
- Hook, D., Arribas, A., Craddock, P. T., Molina, F. & Rothenberg, B. 1987. Copper and silver in Bronze Age Spain. In: Waldren, W. H. & Keenard, R. C. (eds.) *Bell Beakers of the Western Mediterranean*. 147-172. Oxford: BAR International Series 331 (1).
- Hook, D., Freestone, I., Meeks, N. D., Craddock, P. T. & Moreno, A. 1991. The early production of copper-alloys in South-East Spain. In: Pernicka, E. & Wagner, G. A. (eds.) *Archaeometry '90*. 65-76. Berlin: Birkhäuser Verlag Basel.
- Hopper, K. & Wilkinson, T. J. 2013. Population and settlement trends in south-west Iran and neighbouring areas. In: Petrie, C. A. (ed.) *Ancient Iran and its Neighbours: Local Developments and Long-range Interactions in the Fourth Millennium BC*. 35-49. Oxford: Oxbow Books.
- Höppner, B., Bartelheim, M., Huijsmans, M., Krauss, R., Martinek, K.-P., Pernicka, E. & Schwab, R. 2005. Prehistoric copper production in the Inn Valley (Austria), and the earliest copper in Central Europe. *Archaeometry*, 47, 293-315.

- Horejs, B., Mehofer, M. & Pernicka, E. 2010. Metallhandwerker im frühen 3. Jt. v. Chr. - Neue Ergebnisse vom Çukuriçi Höyük. *Istanbul Mitteilungen*, 60, 7-37.
- Hosler, D. 1988. The metallurgy of ancient west Mexico. In: Maddin, R. (ed.) *The Beginning of the Use of Metals and Alloys*. 328–343. Cambridge: MIT Press.
- Hosler, D. 1994. *The Sounds and Colors of Power: The Sacred Metallurgical Technology of Ancient West Mexico*. Cambridge: MIT Press.
- Huebner, J. S. & Turnock, A. C. 1980. The melting relations at one bar of pyroxenes composed largely of Ca-, Mg-, and Fe-bearing components. *The American Mineralogist*, 65, 225-271.
- Hughes, M. F., Beck, B. D., Chen, Y., Lewis, A. S. & Thomas, D. J. 2011. Arsenic exposure and toxicology: a historical perspective. *Toxicol Sci*, 123, 305-32.
- Hultgren, R., Desai, P., Hawkins, D., Gleiser, M. & Kelley, K. 1973. *Selected Values of the Thermodynamic Properties of Binary Alloys*. Ohio: American Society for Metals.
- Hume-Rothery, W. 1949-50. Discussion on the paper by Owen and Morris. *Journal of the Institute of Metals*, 76, 682.
- Hunt-Ortiz, M. A. 2003. *Prehistoric mining and metallurgy in south west Iberia*. Oxford: Archaeopress.
- I-Tu, S. J. & Hsueh-Chuan, S. 1966. *Thien-Kung Khai-Wu, Chinese Technology in the 17th Century, by Sung Ying-Hsing*. Philadelphia: Pennsylvania State University.
- Ixer, R. A. & Patrick, R. a. D. 2003. Copper-arsenic ores and Bronze Age mining and metallurgy with special references to the British Isles. In: Craddock, P. T. & Lang, J. (eds.) *Mining and Metal Production through the Ages*. 9-20. London: British Museum Press.
- Jones, D. (ed.) 2001. *Archaeometallurgy*, Swindon: English Heritage.
- Juleff, G. 1996. An ancient wind-powered iron smelting technology in Sri Lanka. *Nature*, 379, 60-63.
- Kakoulli, I., Prikhodko, S. V., Fischer, C., Cilluffo, M., Uribe, M., Bechtel, H. A., Fakra, S. C. & Marcus, M. A. 2014. Distribution and chemical speciation of arsenic in ancient human hair using synchrotron radiation. *Analytical Chemistry*, 86, 521-526.
- Kanaya, K. & Okayama, S. 1972. Penetration and energy-loss theory of electrons in solid targets. *Journal of Physical D: Applied Physics*, 5, 43-58.
- Karydas, A. G. 2007. Application of a portable XRF spectrometer for the noninvasive analysis of museum metal artefacts. *Annali di Chimica*, 97, 419-432.
- Kassianidou, V. 1998. Was silver actually recovered from speiss in antiquity? In: Rehren, Th., Hauptmann, A. & Muhly, J. D. (eds.) *Metallurgica Antiqua*. 69-76. Bochum: Der Anschnitt, Beiheft 8. Deutsches Bergbau-Museum.
- Keesman, I., Moreno-Onorato, A. & Kronz, A. 1991-1992. Investigaciones científicas de la metalurgia de El Malagon y Los Millares, en el Sureste de Espana. *Cuadernos de Prehistoria de la Universidad de Granada*, 16-17, 247–302.
- Kienlin, T.L., Bischoff, E., Opielka, H. Copper and bronze during the Eneolithic and Early Bronze Age: a metallographic examination of axes from the Northalpine Region. *Archaeometry*, 48, 3, 453-468.
- Killick, D. & Gordon, R. B. 1988. The mechanism of iron production in the bloomery furnace. In: Farquhar, R. M., Hancock, R. G. V. & Pavlish, L. A. (eds.) *Proceedings of the 26th International Archaeology Symposium*. 120-123. Toronto: University of Toronto.
- Krimer, M., Töchterle, Goldenberg, G., Tropper, P., & Vavtar, F. 2012. Mineralogical and petrological investigations of Early Bronze Age copper-smelting remains from the Kiechlberg (Tyrol, Austria). *Archaeometry*, 55, 5, 923-945.
- Kroeber, A. L. 1940. Stimulus diffusion. *American Anthropologist, New Series*, 42, 1-20.
- Kunç, Ş. 1986. Analyses of İkiztepe metal artifacts. *Anatolian Studies*, 36, 99-101.
- Kunç, Ş. & Çukur, A. 1987. Bakı buluntularında iz element dağılımı. *Arkeometri Sonuçları Toplantısı*, 3, 97-105.

- La Niece, S. & Carradice, I. 1989. White copper: The arsenical coinage of the Libyan revolt 241-238 BC. *Historical Metallurgy*, 23, 9-15.
- Lechtman, H. 1977. Style in technology: Some early thoughts. In: Lechtman, H. & Merrill, R. S. (eds.) *Material Culture: Style, Organization, and Dynamics of Technology*. 3-20. New York: West Publishing.
- Lechtman, H. 1981. Cu-As Bronzes from the north coast of Peru. *Annals of the New York Academy of Sciences*, 376, 77-121.
- Lechtman, H. 1991. The production of copper-arsenic alloys in the Central Andes: Highland ores and coastal smelters? *Journal of Field Archaeology*, 18, 43-76.
- Lechtman, H. 1996. Arsenic bronze: dirty copper or chosen alloy? A view from the Americas. *Journal of Field Archaeology*, 23, 477-514.
- Lechtman, H. & Klein, S. 1999. The production of copper-arsenic alloys (arsenic bronze) by cosmelting: modern experiment, ancient practice. *Journal of Archaeological Science*, 26, 497-526.
- Lehner, J. 2012. A preliminary report on the microstructure and microanalysis of metal from Boğazköy. In: Schachner, A. (ed.) *Die Ausgrabungen in Boğazköy-Hattuša 2011*. 57-64. Archäologischer Anzeiger: Archäologischer Anzeiger.
- Lehner, J. 2015. *Cooperation, the Craft Economy, and Metal Technology during the Bronze and Iron Ages in Central Anatolia*. Unpublished PhD thesis. University of California.
- Lehner, J. & Yener, A. 2014. Organization and specialization of early mining and metal technologies in Anatolia. In: Roberts, B. & Thornton, C. P. (eds.) *Archaeometallurgy in Global Perspective*. 529-557. New York: Springer.
- Lehner, J., Yener, A. & Burton, J. 2009. Lead Isotope Analysis and Chemical Characterization of Metallic Residues of an Early Bronze Age Crucible from Goltepe Using ICP-MS. *Türkiye Bilimler Akademisi Arkeoloji Dergisi (TUBA-AR)*, 165-174.
- Lemmonier, P. 1989. Bark, capes, arrowheads and Concorde: On social representations of technology. In: Hodder, I. (ed.) *The Meaning of Things: Material Culture and Symbolic Expression*. 156-171. London: Unwin Hyman.
- Lemmonier, P. 1993. *Technological Choices: Transformations in Material Cultures since the Neolithic*. London: Routledge.
- Leroi-Gourhan, A. 1943. *Evolution et Technique, Vol. 2: Milieu et Technique*. Paris: Albin Michel.
- Levy, T. E. 1995. Cult, metallurgy & rank societies. In: Levy, T. E. (ed.) *Archaeology of Society in the Holy Land*. 226-243. London: Leicester University Press.
- Levy, T. E. & Shalev, S. 1989. Prehistoric metalworking in the Southern Levant: Archaeometallurgical and social perspectives. *World Archaeology*, 20, 352-372.
- Liu, S., Rehren, Th., Pernicka, E. & Hausleiter, A. 2015. Copper processing in the oases of northwest Arabia: technology, alloys and provenance. *Journal of Archaeological Science*, 53, 492-503.
- Lorenzen, W. 1966. Notes concerning copper smelting. *Historical Metallurgy*, 1, 13-19.
- Lutz, J., Wagner, G. & Pernicka, E. 1994. Chalkolithische Kupferverhüttung in Murgul, Ostanatolien. In: Wartke, R. B. (ed.) *Handwerk und Technologie im Alten Orient*. 60-66. Mainz: Philipp von Zabern.
- Luyken, W. & Heller, L. 1938. Arsen in eisenerzen und die möglichkeit seiner austreibung vor der verhüttung. *Archiv für das Eisenhüttenwesen*, 11, 475-479.
- Lyonnet, B. & Guliyev, F. 2012. Mentesh Tepe. In: Helwing, B. & Boroffka, N. (eds.) *Archäologische Mitteilungen aus Iran und Turan*. 86-97. Berlin: Dietrich Reimer Verlag.
- Mackenzie, W. S. & Adams, A. E. 2011. *A Colour Atlas of Rocks and Minerals in Thin Section*. London: Manson Publishing.

- Maddin, R., Muhly, J. D. & Stech, T. 1999. Early metalworking at Çayönü. In: Hauptmann, A., Pernicka, E., Rehren, Th. & Yalçın, Ü. (eds.) *The Beginnings of Metallurgy*. 37-44. Bochum: Deutsches Bergbau-Museum.
- Maddin, R., Wheeler, T. S. & Muhly, J. D. 1980. Distinguishing Artifacts Made of Native Copper. *Journal of Archaeological Science*, 211-225.
- Majidzadeh, Y. 1979. An early coppersmith workshop at Tepe Ghabristan. *Akten des VII. Internationalen Kongresses für Iranische Kunst und Archäologie, München 7-10 September 1976.*, 82-92. Berlin: Dietrich Reimer.
- Majidzadeh, Y. 1989. An early industrial proto-urban center on the central plateau of Iran: Tepe Ghabristan. In: Leonard, A. J. & Williams, B. B. (eds.) *Essays in Ancient Civilization Presented to Helene J. Kantor*. 157-166. Chicago: Oriental Institute of the University of Chicago
- Malfoy, J.-M. & Menu, M. 1987. la métallurgie du cuivre à Suse aux IVe et IIIe millénaires: analyses en laboratoire. In: Tallon, F. (ed.) *Métallurgie Susienne I: De la fondation de Suse au XVIIIe avant J.-C.* Notes et documents des musées de France 15. Paris: Musée du Louvre, Département des Antiquités orientales.
- Mansour, G. 2013. *The Economic Geology of Iran: Mineral Deposits and Natural Resources*. Netherlands: Springer.
- Marechal, J. R. C. P. T. 1985. Methods of ore roasting and the furnaces used. *Furnaces and Smelting Technology in Antiquity*. 29-42. London: The British Museum.
- Marsh, B. 2010. Geoarchaeology of the human landscape at Boğazköy-Hattuša. In: Schachner, A., Üstündağ, H., Dittman, R., Röttger, U., Wilhelm, G., Schoop, U.-D., Marsh, B., Rehren, Th. & Radivojević, M. (eds.) *Die Ausgrabungen in Boğazköy-Hattuša 2009*. 201-207. Archäologischer Anzeiger.
- Martinon-Torres, M., Valcárcel Rojas, R., Guerra, M. F. & Saenz Samper, J. 2012. Metallic encounters in Cuba: The technology, exchange and meaning of metals before and after Columbus. *Journal of Anthropological Archaeology*, 31, 439-454.
- Matthews, R. & Fazeli, H. 2004. Copper and complexity: Iran and Mesopotamia in the fourth millennium B.C. *Iran*, 42, 61-75.
- Mckerrell, H. & Tylecote, R. F. 1972. The working of copper-arsenic alloys in the Early Bronze Age and the effect on the determination of provenance. *Proceedings of the Prehistoric Society*, 38, 209-218.
- Meeks, N. 1993. Surface characterization of tinned bronze, high tin bronze, tinned iron and arsenical bronze. In: La Niece, S. & Craddock, P. T. (eds.) *Metal Plating and Patination*. 245-275. London: Butterworth.
- Mehofer, M. 2014. Metallurgy during the Chalcolithic and the beginning of the Early Bronze Age in Western Anatolia. In: Horejs, B. & Mehofer, M. (eds.) *Western Anatolia Before Troy: Proto-Urbanisation in the 4th Millennium BC*. 463-490. Vienna: Austrian Academy of Science Press.
- Mehofer, M. 2016. Çukuriçi Höyük – Ein Metallurgiezentrum des frühen 3. Jts. v. Chr. in der Westtürkei. In: Horejs, B. (ed.) *Oriental and European Archaeology Volume 3*. 359-373. Rahden: Verlag Marie Leidorf GmbH.
- Mei, J. 2012. Recent research on early bronze metallurgy in Northwest China. In: Jett, P., McCarthy, B. & Douglas, J. G. (eds.) *Scientific Research on Ancient Asian Metallurgy: Proceedings of the Fifth Forbes Symposium at the Freer Gallery of Art*. 37-46. London: Archetype.
- Meliksetian, K., Pernicka, E. & Badalyan, R. 2007. Compositions and some considerations on the provenance of Armenian Early Bronze Age copper artefacts. *Archaeometallurgy in Europe: 2nd International Conference, Aquileia, Italy, 17-21 June 2007*. Milano: Associazione Italiana di Metallurgia.

- Merkel, J. 1990. Experimental reconstruction of Bronze Age copper smelting based on archaeological evidence from Timna. In: Rothenberg, B. (ed.) *The Ancient Metallurgy of Copper*. 78-122. London: IAMS.
- Merkel, J. & Shimada, I. 1988. Arsenical copper smelting at Batán Grande, Peru. *IAMS*, 12, 4-7.
- Merkel, J., Shimada, I., Swann, C. P. & Doonan, R. 1994. Pre-Hispanic copper production at Batán Grande, Peru: Interpretation of the analytical data from ore samples. In: Scott, D. A. & Meyers, P. (eds.) *Archaeometry of Pre-Columbian Sites and Artifacts*. 199-228. Los Angeles: The Getty Conservation Institute.
- Mighal, T. M., Abrahams, P. W., Grattan, J. P., Hayes, D., Timberlake, S. & Forsyth, S. 2002. Geochemical evidence for atmospheric pollution derived from prehistoric copper mining at Copa Hill, Cwmystwyth, mid-Wales, UK. *The Science of the Total Environment*, 292, 69-80.
- Milevski, I. 2013. The transition from the Chalcolithic to the Early Bronze Age of the Southern Levant in socio-economic context. *Paléorient*, 39, 193-208.
- Miller, H. M.-L. 2007. *Archaeological Approaches to Technology*. London: Academic Press.
- Montero, I. 1994. *El origen de la Metalurgia en el Sureste Peninsula*. Instituto de Estudios Almerienses.
- Moorey, P. R. S. 1988. The chalcolithic hoard from Nahal Mishmar, Israel, in context. *World Archaeology*, 20, 170-189.
- Moorey, P. R. S. 1999. *Ancient Mesopotamian Materials and Industries: the Archaeological Evidence*. Oxford: Clarendon Press.
- Muhly, J. D. 1973. Copper and tin. The distribution of mineral resources and the nature of the metals trade in the Bronze Age. *Transactions of the Connecticut Academy of Arts and Sciences*, 43, 155-355.
- Muhly, J. D. 1979. The evidence for sources of and trade in Bronze Age tin. In: Franklin, A. D., Olin, J. S. & Wertime, T. A. (eds.) *The Search for Ancient Tin, Washington D.C.: A Seminar Organized by Theodore A. Wertime and held at the Smithsonian Institution and the National Bureau of Standards*. 43-48. Washington D.C.
- Muhly, J. D. 1985. Sources of tin and the beginnings of bronze metallurgy. *Journal of American Archaeology*, 89, 275-291.
- Muhly, J. D. 1988. The beginnings of metallurgy in the Old World. In: Maddin, R. (ed.) *The Beginnings of the Use of Metals and Alloys*. 2-20. Cambridge: MIT Press.
- Muhly, J. D. 1999. Copper and bronze in Cyprus and the Eastern Mediterranean. In: Pigott, V. C. (ed.) *The Archaeometallurgy of the Asian Old World*. 15-25. Philadelphia: Museum University of Pennsylvania.
- Muhly, J. D. 2006. Chrysokamino in the history of early metallurgy. *Hesperia Supplements*, 36, 155-177.
- Muhly, J. D., Maddin, R., Stech, T. & Özgen, E. 1985. Iron in Anatolia and the nature of the Hittite iron industry. *Anatolian Studies*, 35, 67-84.
- Müller, R., Goldenberg, G., Bertelheim, M., Kunst, M. & Pernicka, E. 2007. Zambajul and the beginnings of metallurgy in southern Portugal. In: La Niece, S., Hook, D. & Craddock, P. T. (eds.) *Metals and Mines: Studies in Archaeometallurgy*. 15-26. London: Archetype Publications.
- Müller, R., Rehren, Th. & Rovira, S. 2004. Almizaraque and the early copper metallurgy of southeast Spain: New data. *Madrid Mitteilungen*, 45, 33-56.
- Neef, R. 2011. Charcoal from the ovens: Botanical remains of Arisman. In: Vatandoust, A., Parzinger, H. & Helwing, B. (eds.) *Early Mining and Metallurgy on the Western Central Iranian Plateau: The First Five Years of Work*. 383-399. Mainz: Verlag Philipp Von Zabren.
- Nezafati, N., Momenzadeh, M. & Pernicka, E. 2008a. New insights into the ancient mining and metallurgical researches in Iran. In: Yalçin, Ü., Özbal, H. & Paşamehmetoğlu, A.

- G. (eds.) *Ancient Mining in Turkey and the Eastern Mediterranean*. 307-328. Ankara: Atilim University.
- Nezafati, N. & Pernicka, E. 2006. The smelters of Sialk: Outcomes of the first stage of archaeometallurgical researches at Tappeh Sialk. In: Shahmirzadi, S. M. (ed.) *The Fishermen of Sialk. Archaeological Monograph Series 7*. 79-102. Tehran: Iranian Center for Archaeological Research.
- Nezafati, N., Pernicka, E. & Shahmirzadi, S. M. 2008b. Evidence on the ancient mining and metallurgy at Tappeh Sialk. In: Yalçın, Ü., Özbal, H. & Paşamehmetoğlu, A. G. (eds.) *Ancient Mining in Turkey and the Eastern Mediterranean*. 329-349. Ankara: Atilim University.
- Northover, J. P. 1989. Properties and uses of arsenical copper alloys. In: Hauptmann, A., Pernicka, E. & Wagner, G. A. (eds.) *Old World Archaeometallurgy*. 111-117. Bochum: Deutsches Bergbau-Museum.
- Northover, P. 1983. The exploration of the long-distance movement of bronze in Bronze and Early Iron Age Europe. *Bulletin of the Institute of Archaeology*, 19, 45-72.
- O'Brien, W. 1999. Arsenical copper in early Irish metallurgy. In: Young, S. M., Pollard, A. M., Budd, P. & Ixer, R. A. (eds.) *Metals in Antiquity*. 33-42. Oxford: Archaeopress.
- O'Brien, W. 2014. *Prehistoric Copper Mining in Europe, 5500 - 500 BC*. Oxford: Oxford University Press.
- Oakberg, K., Levy, T. & Smith, P. 2000. A method for skeletal arsenic analysis, applied to the chalcolithic copper smelting site of Shiqmim, Israel. *Journal of Archaeological Science*, 27, 895-901.
- Oates, J. 1993. Trade and power in the Fifth and Fourth Millennia B.C.: New evidence from Northern Mesopotamia. *World Archeology*, 24, 403-22.
- Olausson, D. 1986. Intrasite spatial analysis in Scandinavian Stone Age research. *Papers of the Archaeological Institute University of Lund*, 6, 5-24.
- Orton, C. 2000. *Sampling in Archaeology*. Cambridge: Cambridge University Press.
- Ottaway, B. S. 2001. Innovation, production and specialization in early prehistoric copper metallurgy. *European Journal of Archaeology*, 4, 87-112.
- Ottaway, B. S. 2001. Innovation, production and specialization in early prehistoric copper metallurgy. *European Journal of Archaeology*, 4, 87-112.
- Özbal, H. 1986. Tepecik ve Tülintepe metal, filiz ve curuf analizleri sonuçları. *Arkeometri Ünitesi Bilimsel Toplantısı Bildireleri III*, 203-218.
- Özbal, H., Adriaens, A. & Earl, B. 1999. Hacinebi metal production and exchange. *Paléorient*, 25, 57-65.
- Özbal, H., Adriaens, A., Earl, B. & Gedik, B. 2002. Minor metallic components associated with Anatolian copper and bronze artifacts: Indications of the utilization of polymetallic ores. In: Jerem, E. & Biró, K. T. (eds.) *Archaeometry 98: Proceedings of the 31st symposium, Budapest, April 26 - May 3 1998*. 433-438. Oxford: Archaeopress.
- Özbal, H., Pehlivan, N., Adriaens, M., Uluocak, B. G. & Earl, B. 2008. Metal technologies during the Late Chalcolithic and Early Bronze Age in North Central Anatolia: İkiztepe a case study. In: Yalçın, Ü., Özbal, H. & Paşamehmetoğlu, A. G. (eds.) *Ancient Mining in Turkey and the Eastern Mediterranean*. 65-85. Ankara: Atilim University.
- Özdemir, K., Erdal, Y. S. & Demirci, Ş. 2010. Arsenic accumulation on the bones in the Early Bronze Age İkiztepe Population, Turkey. *Journal of Archaeological Science*, 37, 1033-1041.
- Özdoğan, M. & Özdoğan, A. 1999. Archaeological evidence on the early metallurgy at Çayönü tepesi. *The beginnings of metallurgy: proceedings of the International Conference "The Beginnings of Metallurgy", Bochum, 1995*. Bochum: Deutsches Bergbau-Museum.
- Palmieri, A. M., Frangipane, M., Hauptmann, A. & Hess, K. 1999. Early metallurgy at Arslantepe during the Late Chalcolithic and the Early Bronze Age IA-IB periods. In:

- Hauptmann, A., Pernicka, E., Rehren, Th. & Yalçın, Ü. (eds.) *The Beginnings of Metallurgy*. 141–149. Bochum: Deutsches Bergbau-Museum.
- Palmieri, A. M., Hauptmann, A., Hess, K. & Sertok, K. 1996a. 1995 archaeometallurgical campaign at Arslantepe. *Arkeometri Sonuçları Toplantısı*, XII, 57-63.
- Palmieri, A. M., Hauptmann, A., Hess, K. & Sertok, K. 1996b. The composition of ores and slags found at Arslantepe, Malatya. In: Demirci, S., Özer, A. M. & Summers, G. D. (eds.) *Archaeometry 94. The Proceedings of the 29th International Symposium on Archaeometry*. 447-449. Ankara: Tübitak.
- Palmieri, A. M. & Sertok, K. 1993. Minerals in and around Arslantepe. *Arkeometri Sonuçları Toplantısı*, IX, 119-152.
- Palmieri, A. M., Sertok, K. & Chernykh, E. 1992. Archaeometallurgical research at Arslantepe. *Arkeometri Sonuçları Toplantısı*, VIII, 391-398.
- Palmieri, A. M., Sertok, K. & Chernykh, E. 1993. From Arslantepe metalwork to arsenical copper technology in Eastern Anatolia. In: Frangipane, M., Hauptmann, H., Liverani, M., Matthiae, P. & Mellink, M. (eds.) *Between the River and Over the Mountains: Archeologica Antaolica et Mesopotamica Alba Palmieri Dedicata*. 573-599. Roma: Gruppo Editoriale Internazionale.
- Papadimitriou, G. 2001. Simulation study of ancient bronzes: their mechanical and metalworking properties. In: Bassiakos, Y., Aloupi, E. & Facorellis, Y. (eds.) *Archaeometry Issues in Greek Prehistory and Antiquity*. 713-733. Athens.
- Papadopoulou, I. & Bogaard, A. 2013. A preliminary study of the charred macrobotanical assemblage from Çamlıbel Tarlası, North-Central Anatolia. In: Schachner, A. (ed.) *Die Ausgrabungen in Boğazköy-Hattuša 2009*. 123-132. Archäologischer Anzeiger: Archäologischer Anzeiger.
- Paulin, A., Spaic, S., Heath, D. J. & Trampuz-Orel, N. 2000. Analysis of Late Bronze Age speiss. *Bulletin of the Metals Museum*, 32, 29-41.
- Pazuchin, V. A. 1964. О происхождении древней мышьяковистой меди. *Известия Академии Наук СССР - Металлургия и горное Дело*, 1, 151-165.
- Penhallurick, R. D. 1986. *Tin in Antiquity: its Mining and Trade Throughout the Ancient World with Particular Reference to Cornwall*. London: The Institute of Metals.
- Pereira, F., Silva, R. J. C., Monge Soares, A. M. & Araújo, M. F. 2013. The role of arsenic in Chalcolithic copper artefacts – insights from Vila Nova de São Pedro (Portugal). *Journal of Archaeological Science*, 40, 2045-2056.
- Pernicka, E. 1999. Trace element fingerprinting of ancient copper: a guide to technology or provenance? In: Young, S. M., Pollard, A. M., Budd, P. & Ixer, R. A. (eds.) *Metals in Antiquity*. 43-52. Oxford: Archaeopress.
- Pernicka, E. 2004. Copper and Silver in Arisman and Tappeh Sialk and the Early Metallurgy in Iran. In: Stöllner, T., Slotta, R. & Vatandoust, A. (eds.) *Persia's Ancient Splendour; Mining, Handicraft and Archaeology*. Bochum: Deutsches Bergbau-Museum.
- Pernicka, E. 2008. Archaeometallurgical Research in Central Iran. In: Weeks, L. R. (ed.) Conference paper presented at: *The 2007 Early Iranian Metallurgy Workshop at the University of Nottingham. Iran*, 46, 335-345.
- Pernicka, E. 2010. *RE: Discussion on Arisman's Area A*. Type to Boscher, L.
- Pernicka, E. 2014. Provenance Determination of Archaeological Metal Objects. 239-268.
- Pernicka, E., Begemann, F., Schmitt-Strecker, S. & Wagner, G. A. 1993. Eneolithic and Early Bronze Age copper artefacts from the Balkans and their relation to Serbian copper ores. *Praehistorische Zeitschrift*, 68, 1-54.
- Pernicka, E., Momenzadeh, M., Vatandoust, A., Adam, K., Böhme, M., Hezarkhani, Z., Nezafati, N., Schreiner, M. & Winterholler, B. 2011. Archaeometallurgical research on the western Central Iranian Plateau. In: Vatandoust, A., Parzinger, H. & Helwing, B. (eds.) *Early Mining and Metallurgy on the Western Central Iranian Plateau: The First Five Years of Work*. 633-687. Mainz: Verlag Philip Von Zabern.

- Pfaffenberger, B. 1992. Social anthropology of technology. *Annual Review of Anthropology*, 21, 491-516.
- Pickard, C. & Schoop, U.-D. 2013. Characterization of Late Chalcolithic micro-beads from Çamlıbel Tarlası, North-Central Anatolia. *Archaeometry*, 55, 14-32.
- Pigott, V. C. 1989. Archaeo-metallurgical investigations at Bronze Age Tappeh Hesar, 1976. In: Dyson, R. H. & Howard, S. M. (eds.) *Tappeh Hesar: Reports of the Restudy Project, 1976*. 25-34. Firenze: Case Editrice le Lettere.
- Pigott, V. C. 1999a. The development of metal production on the Iranian Plateau: an archaeometallurgical perspective. In: Pigott, V. C. (ed.) *The Archaeometallurgy of the Asian Old World*. 215-236. Philadelphia: Museum University Philadelphia.
- Pigott, V. C. 1999b. A heartland of metallurgy: Neolithic/Chalcolithic metallurgical origins on the Iranian Plateau. In: Hauptmann, A., Pernicka, E., Rehren, Th. & Yalçın, Ü. (eds.) *The Beginnings of Metallurgy*. 107-120. Bochum: Deutsches Bergbau-Museum.
- Pigott, V. C. 1999c. Introductory Comments. In: Pigott, V. C. (ed.) *The Archaeometallurgy of the Asian Old World*. 1-13. Philadelphia: Museum University of Pennsylvania.
- Pigott, V. C. 2004. On the importance of Iran in the study of prehistoric copper-base metallurgy. In: Stöllner, T., Slotta, R. & Vatandoust, A. (eds.) *Persia's Ancient Splendour; Mining, Handicraft and Archaeology*. Bochum: Deutsches Bergbau-Museum Bochum.
- Pigott, V. C. 2008. Banesh Period metallurgy at Tal-e Malyan. In: Weeks, L. R. (ed.) Conference paper presented at: *The 2007 Early Iranian Metallurgy Workshop at the University of Nottingham. Iran*, 46, 335-345.
- Pigott, V. C. 2012. Looking East: The coming of tin bronze in the context of Bronze Age trans-Eurasian exchange - An overview. In: Jett, P., McCarthy, B. & Douglas, J. G. (eds.) *Scientific Research on Ancient Asian Metallurgy: Proceedings of the Fifth Forbes Symposium at the Freer Gallery of Art*. 85-100. London: Archetype.
- Pigott, V. C., Howard, S. M. & Epstein, S. M. 1982. Pyrotechnology and culture change at Bronze Age Tepe Hissar (Iran). In: Wertime, T. A. & Wertime, S. F. (eds.) *Early Pyrotechnology: The Evolution of the First Fire-Using Industries*. 215-236. Washington D.C.: Smithsonian Institution Press.
- Pigott, V. C. & Lechtman, H. 2003. Chalcolithic copper based metallurgy on the Iranian Plateau: a new look at old evidence from tal-i Iblis. In: Pots, T., Roaf, M. & Stein, D. (eds.) *Culture Through Objects: Ancient Near Eastern Studies in Honour of P.R.S. Moorey*. 291-312. Oxford: Grifit Institute.
- Pollard, A. M. 2009. What a long strange trip it's been: Lead isotopes in archaeology. In: Shortland, A. J., Freestone, I. & Rehren, Th. (eds.) *From Mine to Microscope: Advances in the Study of Ancient Technology*. 181-189. London: Oxbow.
- Pollard, A. M., Batt, C., Stern, B. & Young, S. M. M. 2007. *Analytical Chemistry in Archaeology*. Cambridge: Cambridge University Press.
- Pollard, A. M., Bray, P., Gosden, C., Wilson, A. & Hamerow, H. 2015. Characterising copper-based metals in Britain in the first millennium AD: a preliminary quantification of metal flow and recycling. *Antiquity*, 89, 697-713.
- Pollard, A. M. & Heron, C. 1996. *Archaeological Chemistry*. Cambridge: Royal Society of Chemistry.
- Pollard, A. M., Thomas, R. G. & Williams, P. A. 1991. Some experiments concerning the smelting of arsenical copper. In: Budd, P., Chapman, C., Jackson, C. M., Janaway, R. & Ottaway, B. S. (eds.) *Archaeological Sciences 1989: Proceedings of a Conference on the Application of Scientific Techniques to Archaeology, Bradford, September 1989*. 169-174. Oxford: Oxbow Books.
- Ponting, M. 2002. Keeping up with the Romans? Romanisation and copper alloys in First Revolt Palestine. *Institute for Archaeo-Metallurgical Studies*, 22, 3-6.
- Potts, P. J. 1987. *A Handbook of Silicate Rock Analysis*. Netherlands: Springer.

- Pryce, T. O. 2011. A flux that binds? The Southeast Asian lead isotope project. In: Jett, P., McCarthy, B. & Douglas, J. G. (eds.) *Scientific Research on Ancient Asian Metallurgy*. 113-121. London: Archetype.
- Pryce, T. O., Bassiakos, Y., Catapotis, M. & Doonan, R. C. 2007. 'De Caerimoniae' Technological choices in copper-smelting furnace design at Early Bronze Age Chrysikamino, Crete. *Archaeometry*, 49, 543-557.
- Quinn, P. S. (ed.) 2009. *Interpreting Silent Artefacts: Petrographic Analysis of Archaeological Ceramics*, Oxford: Archaeopress.
- Rademakers, F. 2015. *Into the Crucible: Methodological Approaches to Reconstructing Crucible Metallurgy, from New Kingdom Egypt to Late Roman Thrace*. Unpublished PhD thesis, Institute of Archaeology, University College London.
- Radivojević, M., Rehren, Th., Pernicka, E., Šljivar, D., Brauns, M. & Borić, D. 2010. On the origins of extractive metallurgy: new evidence from Europe. *Journal of Archaeological Science*, 37, 2775-2787.
- Radivojević, M. & Rehren, Th. 2015. Paint it Black: The Rise of Metallurgy in the Balkans. *Journal of Archaeological Method and Theory*, online, 1-38.
- Radivojević, M., Rehren, Th., Kuzmanović-Cvetković, J., Jovanović, M. & Northover, J. P. 2013. Tainted ores and the rise of tin bronzes in Eurasia, c. 6500 years ago. *Antiquity*, 87, 1030-1045.
- Raghavan, V. 1988. *Phase Diagrams of Ternary Iron Alloys Part 2: Ternary Systems Containing Iron and Sulphur*. Calcutta: Indian Institute of Metals.
- Ramdohr, P. 1969. *The Ore Minerals and their Integrowth*. Translated by C. Amstutz. Germany: Akademie-Verlag GmbH.
- Rapp, G. J. 1988. On the origins of copper and bronze alloying. In: Maddin, R. (ed.) *The Beginning of the Use of Metals and Alloys*. 21-27. London: MIT Press.
- Ravich, I. G. & Ryndina, N. V. 1984. Изучение свойств и микроструктуры сплавов медь — мышьяк в связи с их использованием в древности. *Художественное наследие*, 9, 114-124.
- Reedy, C. L. 2008. *Thin-Section Petrography of Stone & Ceramic Materials*. London: Archetype.
- Rehder, J. E. 1994. Blowpipes versus bellows in ancient metallurgy. *Journal of Field Archaeology*, 21, 345-350.
- Rehren, Th. 1991. Selenium and tellurium in Mediterranean copper ingots. In: Gale, N. H. (ed.) *Bronze Age Trade in the Mediterranean. Papers presented at the Conference held at Rewley House, Oxford, in December 1989*. 240-247. Jonsered: Åström.
- Rehren, Th. 1999. Small size, large scale: Roman brass production in Germania Inferior. *Journal of Archaeological Science*, 26, 1083-1087.
- Rehren, Th., Asderaki, E., Skafida, E. & Kranava, A. 2013. Bronze Age crucibles from the Kastro-Palaia settlement, Volos, Greece – a contradiction of form and function. *Historical Metallurgy*, 47, 111-124.
- Rehren, Th., Boscher, L. & Pernicka, E. 2012. Large scale smelting of speiss and arsenical copper at Early Bronze Age Arisman, Iran *Journal of Archaeological Science*, 39, 1717-1727.
- Rehren, Th. & Martínón-Torres, M. 2014. Technical ceramics. In: Roberts, B. & Thornton, C. P. (eds.) *Archaeometallurgy in Global Perspective: Methods and Syntheses*. 107-131. London: Springer.
- Rehren, Th. & Pernicka, E. 2008. Coins, artefacts and isotopes - archaeometallurgy and archaeometry. *Archaeometry*, 50, 232-248.
- Rehren, Th. & Radivojević, M. 2010. A preliminary report on the slag samples from Çamlıbel Tarlası. In: Schachner, A. (ed.) *Die Ausgrabungen in Boğazköy-Hattuša 2009*. 207-216. Archäologischer Anzeiger: Archäologischer Anzeiger.

- Rehren, Th., Schneider, J. & Bartels, C. 1999. Medieval lead-silver smelting in the Siegerland, West Germany. *Historical Metallurgy*, 33, 73-84.
- Renfrew, C. 1972. *The Emergence of Civilization*. London: Methuen.
- Renzi, M. 2013. *La Fonteta (Guardamar del Segura, Alicante) y la Metalurgia Fenicia de Epoca Arcaica en la Peninsula Iberica*. Universidad Complutense de Madrid.
- Rice, P. M. 1987. *Pottery Analysis: A Sourcebook*. Chicago: University of Chicago Press.
- Roberts, B. W. 2009. Production networks and consumer choice in the earliest metal of Western Europe. *Journal of World Prehistory*, 22, 461-481.
- Roberts, B. W., Thornton, C. P. & Pigott, V. C. 2009. Development of metallurgy in Eurasia. *Antiquity*, 83, 1012-1022.
- Robinson, R. H. 1918. The calcium arsenates. *Oregon Agricultural College Experiment Station Bulletin*, 131, 1-15.
- Rosenberg, M. & Davis, M. K. 1992. Hallan Çemi Tepesi, an early aceramic Neolithic site in eastern Anatolia. *Anatolica*, 18, 1-18.
- Rosenqvist, T. 1983. *Principles of Extractive Metallurgy*. New York: McGraw-Hill.
- Rostoker, W. & Dvorak, J. 1991. Some experiments with co-smelting to copper alloys. *Archeomaterials*, 5, 5-20.
- Rostoker, W., Pigott, V. C. & Dvorak, J. 1989. Direct reduction to copper metal by oxide/sulfide mineral interaction. *Archeomaterials*, 3, 69-87.
- Rothenberg, B. 1988. *The Egyptian Mining Temple at Timna*. London: Institute for Archaeo-Metallurgical Studies.
- Rothenberg, B. 1989. Arsenical copper ore in the newly discovered Copper-Age mine ALS2 in Almeria, South-east Andalusia (Spain) - a correction. *Institute for Archaeo-Metallurgical Studies News*, 14, 7.
- Roux, V., Mille, B., & Pelegrin, J. 2014. Innovations céramiques, métallurgiques et lithiques au Chalcolithique : mutations sociales, mutations techniques. In : *Transitions, ruptures et continuité en préhistoire : XXVIIe congrès préhistorique de France, Bordeaux-Les Eyzies, 31 mai - 5 juin 2010*. 61-73. Paris : Société Préhistorique Française.
- Rovira, S. 2003. Early copper metallurgy slags at Kargaly (Orenburg, Russia). *Archaeometallurgy in Europe*. 479-486. Milan: Associazione Italiana di Metallurgia.
- Ryndina, N. V. & Kolosova, V. 1999. Copper production from polymetallic sulphide ores in North-eastern Balkan Eneolithic Culture. *Journal of Archaeological Science*, 26, 1059-1068.
- Sabatini, B. J. 2015. The As-Cu-Ni system: A chemical thermodynamic model for ancient recycling. *The Journal of the Minerals, Metals & Materials Society*, 67, 2984-2992.
- Salje, G. & Feller-Kniepmeier 1978. The diffusion and solubility of iron in copper. *Journal of Applied Physics*, 49, 229-232.
- Sayre, E. V., Joel, E. C., Blackman, M. J., Yener, K. A. & Özbek, H. 2001. Stable lead isotope studies of Black Sea Anatolian ore sources and related Bronze Age and Phrygian artefacts from nearby archaeological sites. *Archaeometry*, 43, 77-115.
- Scheftelowitz, B. & Oren, E. 1997. Givat Ha'oranim (Nahal Barequet). *New Antiquities: Recent Discoveries from Archaeological Excavations in Israel*. 20. Jerusalem: The Israel Museum.
- Schmitt-Strecker, S., Begemann, F. & Pernicka, E. 1992. Chemische Zusammensetzung und Bleisotopenverhältnisse der Metallfunde vom Hassek Höyük. In: Behm-Blancke, M. (ed.) *Hassek Höyük – Naturwissenschaftliche Beiträge*. 108-123. Istanbul: Istanbulischer Forschungen 38.
- Schoen, A., Beck, B., Sharma, R. & Dube, E. 2004. Arsenic toxicity at low doses: epidemiological and mode of action considerations. *Toxicol Appl Pharmacol*, 198, 253-67.

- Schoop, D.-T. 2011. Çamlıbel Tarlası, ein metallverarbeitender Fundplatz des vierten Jahrtausends v. Chr. im nördlichen Zentralanatolien. In: Yalçın, Ü. (ed.) *Anatolian Metal V*. 53-68. Bochum: Der Anschnitt, Beiheft 24.
- Schoop, U.-D. 2009. Ausgrabungen in Çamlıbel Tarlası 2008. In: Schachner, A. (ed.) *Die Ausgrabungen in Boğazköy-Hattuša 2008*. 56-67. Archäologischer Anzeiger 2009.
- Schoop, U.-D. 2010a. Ausgrabungen in Çamlıbel Tarlası 2009. In: Schachner, A., Üstündağ, H., Dittman, R., Röttger, U., Wilhelm, G., Schoop, U.-D., Marsh, B., Rehren, Th. & Radivojević, M. (eds.) *Die Ausgrabungen in Boğazköy-Hattuša 2009*. 191-201. Archäologischer Anzeiger.
- Schoop, U.-D. 2010b. The chalcolithic on the plateau. In: Steadman, S. R. & McMahon, G. (eds.) *The Oxford Handbook of Ancient Anatolia - 10,000 - 323 BCE*. 150-173. Oxford: Oxford University Press.
- Schoop, U.-D. Year. Some thoughts on social and economic development in Western Anatolia during the fourth and third millennia BC. In: Bilgen, A. N., Von Den Hoff, R., Sandalci, S. & Silek, S., eds. *Archaeological Research in Western Central Anatolia, 2010c Kütahya, Turkey*. 29-45.
- Schoop, U.-D. forthcoming. Çamlıbel Tarlası and the Late Chalcolithic Period in North-Central Anatolia.
- Schoop, U.-D., Grave, P., Kealhofer, L. & Jacobsen, G. 2009. Radiocarbon dates from Chalcolithic Çamlıbel Tarlası. In: Schachner, A. (ed.) *Die Ausgrabungen in Boğazköy-Hattuša 2008*. 66-67. Archäologischer Anzeiger, Vol. 6,.
- Schreiner, M., Heimann, R. B. & Pernicka, E. 2003. Mineralogical and geochemical investigations into prehistoric smelting slags from Tepe Sialk, Central Iran. *Archaeometallurgy in Europe*. 487-496. Milan: Associazione Italiana di Metallurgia.
- Scott, D. A. 1991. *Metallography and Microstructure of Ancient and Historic Metals*. California: J. Paul Getty Museum.
- Scott, D. A. 2002. *Copper and Bronze in Art: Corrosion, Colorants, Conservation*. Los Angeles: Getty Publications.
- Selimkhanov, I. R. 1982. Arsenical Copper Age in HH Cohlan's works: and investigations in the laboratory of the Institute of History of the Academy of Sciences of Azerbaijan SSR. *Historical Metallurgy*, 16, 50-57.
- Shalev, S. 1996. Archaeometallurgy in Israel: The impact of the material on the choice of shape, size and color of ancient products. In: Demirci, Ş., Özer, A. M. & Summers, G. D. (eds.) *Archaeometry 94: The Proceedings of the 29th International Symposium on Archaeometry*. 11-15. Ankara: Tübitak.
- Shalev, S. 1999. Recasting the Nahal Mishmar Hoard: Experimental archaeology and metallurgy. In: Hauptmann, A., Pernicka, E., Rehren, Th. & Yalçın, Ü. (eds.) *The Beginnings of Metallurgy*. 295-300. Bochum: Der Anschnitt Beiheft 9.
- Shalev, S. & Northover, P. J. 1987. Chalcolithic metal and metal working from Shiqmim. In: Levy, T. E. (ed.) *Shiqmim I*. 357-371. Oxford: BAR International Series 356.
- Shalev, S. & Northover, P. J. 1993. The metallurgy of the Nahal Mishmar Hoard reconsidered. *Archaeometry*, 35, 35-47.
- Shalev, S., Shilstein, S. S. & Yekutieli, Y. 2006. XRF study of archaeological and metallurgical material from an ancient copper-smelting site near Ein-Yahav, Israel. *Talanta*, 70, 909-913.
- Shennan, S. 1998. *Quantifying Archaeology*. Edinburgh: Edinburgh University Press.
- Shennan, S. 1999. Cost, benefit and value in the organization of early European copper production. *Antiquity*, 79, 352-363.
- Shortland, A. J. 2004. Hopeful monsters? Invention and innovation in the archaeological record. In: Bourriau, J. P. & Sharon, J. (eds.) *Invention and Innovation: the Social Context of Technological Change*. 1-11. Oxford: Oxbow Books.

- Shugar, A. 2003. Reconstructing the Chalcolithic metallurgical process at Abu Matar, Israel. *Archaeometallurgy in Europe*. 449-458. Milan: Associazione Italiana di Metallurgia.
- Shugar, A. N. 2000. *Archaeometallurgical Investigation of the Chalcolithic Site of Abu Matar, Israel: A Reassessment of Technology and its Implications for the Ghassulian Culture*. Doctor of Philosophy in Archaeology, UCL.
- Sillar, B. & Tite, M. 2000. The challenge of 'technological choices' for material science approaches in archaeology. *Archaeometry*, 42, 2-20.
- Smith, C. M. & Murray, C. W. 1931. The composition of commercial calcium arsenate. *The Journal of Industrial and Engineering Chemistry*, 23, 207-208.
- Smith, C. S. 1969. Analysis of the copper bead from Ali Kosh. In: Hole, F., Flannery, K. V. & Neely, J. A. (eds.) *Prehistory and Human Ecology of the Deh Luran Plain: An Early Village Sequence from Khuzistan, Iran. Memoirs of the Museum of Anthropology*. 427-428. Michigan: Ann Arbor.
- Smith, C. S. 1973. An examination of the arsenic-rich coating on a bronze bull from Horoztepe. In: Young, W. J. (ed.) *Application of Science in Examination of Works of Art*. 96-102. Boston: Museum of Fine Arts.
- Stech, T. 1990. Neolithic copper metallurgy in Southwest Asia. *Archaeomaterials*, 4, 55-61.
- Stein, G. J. 1999. *Rethinking World Systems. Diasporas, Colonies, and Interaction in Uruk Mesopotamia*. Tuscon: University of Arizona Press.
- Stein, G. J. & Wattenmaker, P. 1990. On the Uruk expansion. *Current Anthropology*, 31, 66-67.
- Steiniger, D. 2011. Excavations in the slagheaps in Arisman. In: Vatandoust, A., Parzinger, H. & Helwing, B. (eds.) *Early Mining and Metallurgy on the Western Central Iranian Plateau: The First Five Years of Work*. 69-99. Mainz: Verlag Philipp Von Zabren.
- Stöllner, T. 2011. Archaeological survey of ancient mines on the western Central Plateau. In: Vatandoust, A., Parzinger, H. & Helwing, B. (eds.) *Early Mining and Metallurgy on the Western Central Iranian Plateau: The First Five Years of Work*. 621-629. Mainz: Verlag Philipp Von Zabren.
- Stöllner, T., Mireskanderi, M. & Roustaei, K. 2011a. Mining archaeology in Iran - Investigations at Vešnāve. In: Vatandoust, A., Parzinger, H. & Helwing, B. (eds.) *Early Mining and Metallurgy on the Western Central Iranian Plateau: The First Five Years of Work*. 535-608. Mainz: Verlag Philipp Von Zabren.
- Stöllner, T., Samashev, Z., Berdenov, S., Cierny, J., Doll, M., Garner, J., Gontscharov, A., Gorelik, A., Hauptmann, A., Herd, R., Kusch, G. A., Merz, V., Riese, T., Sikorski, B. & Zickgraf, B. 2011b. Tin from Kazakhstan—Steppe tin for the West? In: Yalçın, Ü. (ed.) *Anatolian metal V*. 231–252. Bochum: Deutsches Bergbau-Museum.
- Stos-Gale, Z. A. 1989. Cycladic copper metallurgy. In: Hauptmann, A., Pernicka, E. & Wagner, G. A. (eds.) *Old World Archaeometallurgy*. 279-291. Bochum: Deutsches Bergbau-Museum.
- Stos-Gale, Z. A. & Gale, N. H. 2011. Bronze Age metal artefacts found on Cyprus - metal from Anatolia and the Western Mediterranean. *Trabajos de Prehistoria*, 67, 389-403.
- Stos, Z. A. 2009. Across the wine dark seas... sailor tinkers and royal cargoes in the Late Bronze Age eastern Mediterranean. In: Shortland, A. J., Freestone, I. & Rehren, Th. (eds.) *From Mine to Microscope: Advances in the Study of Ancient Technology*. 164-180. London: Oxbow.
- Subramanian, P. R. & Laughlin, D. E. 1988. The As-Cu (arsenic-copper) system. *Bulletin of Alloy Phase Diagrams*, 9, 605-617.
- Summers, G. D. 1993. The Chalcolithic Period in Central Anatolia. In: Georgieva, P. (ed.) *The Fourth Millennium B.C.: Proceedings of the International Symposium, Nessebur, 28-30 August 1992*. 29-33. Sofia: Edition of New Bulgarian University.
- Summers, G. D. 2002. Concerning the identification, location and distribution of the Neolithic and Chalcolithic settlements in Central Anatolia. In: Gérard, F. & Thissen, L. (eds.) *The*

- Neolithic of Central Anatolia. Internal Developments and External Relations During the 9th-6th Millennia Cal BC.* 131-137. Istanbul: Proceedings of the International CANeW Table Ronde, 23-24 November 2001.
- Tadmor, M., Begemann, F., Hauptmann, A., Pernicka, E. & Schmitt-Strecker, S. 1995. The Nahal Mishmar hoard from the Judean Desert : Technology, composition, and provenance. *Atiqot*, 27, 95-148.
- Tallon, F. 1987. *Métallurgie Susienne I. De la fondation de Suse au XVIIIe avant J.-C.* Paris: Notes et Documents des Musées de France 15. Ministère de la culture et de la communication : Editions de la Réunion des musées nationaux.
- Thomas, J. T. 2009. Approaching specialisation: Craft production in Late Neolithic/Copper Age Iberia. *Papers from the Institute of Archaeology*, 19, 1-12.
- Thomsen, C. J. 1836. *Ledetraad til Nordisk Oldkundskab.* Copenhagen: Nordiske Oldskrift-Selskab.
- Thornton, C. P. 2010. The rise of arsenical copper in southeastern Iran. *Iranica Antiqua*, XLV, 1-20.
- Thornton, C. P., Lamberg-Karlovsky, C. C., Liezers, M. & Young, S. M. M. 2002. On pins and needles: tracing the evolution of copper-base alloying at Tepe Yahya, Iran, via ICP-MS analysis of common-place items. *Journal of Archaeological Science*, 29, 1451-1460.
- Thornton, C. P. & Rehren, Th. 2009. A truly refractory crucible from fourth millennium Tepe Hissar, Northeast Iran. *Journal of Archaeological Science*, 36, 2700-2712.
- Thornton, C. P., Rehren, Th. & Pigott, V. C. 2009. The production of speiss (iron arsenide) during the Early Bronze Age in Iran. *Journal of Archaeological Science*, 36, 308-316.
- Thornton, C. P. & Roberts, B. W. 2009. Introduction: the beginnings of metallurgy in global perspective. *Journal of World Prehistory*, 22, 181-184.
- Tite, M. S., Hughes, M. J., Freestone, I., Meeks, N. D. & Bimson, M. 1990. Technological characterisation of refractory ceramics from Timna. In: Rothenberg, B. (ed.) *The Ancient Metallurgy of Copper.* 158-175. London: UCL Institute of Archaeo-Metallurgical Studies.
- Trigger, B. 1989. *A History of Archaeological Thought.* Cambridge: Cambridge University Press.
- Tylecote, R. F. 1962. *Metallurgy in archaeology: a prehistory of metallurgy in the British Isles.* London: Edward Arnold.
- Tylecote, R. F. 1976. *A History of Metallurgy.* London: Metals Society.
- Tylecote, R. F. 1980. Furnaces, crucibles, and slags. In: Wertime, T. A. & Muhly, J. D. (eds.) *The Coming of the Age of Iron.* 183-228. London: Yale University Press.
- Tylecote, R. F. 1982. Metallurgical crucibles and crucible slags. In: Franklin, A. & Olin, J. (eds.) *Archaeological Ceramics.* Washington D.C.: Smithsonian Institution Press.
- Tylecote, R. F. 1987. *The Early History of Metallurgy in Europe.* New York: Longman.
- Tylecote, R. F. 1991. Early copper base alloys; natural or man-made. In: Eluère, C. & Mohen, J.-P. (eds.) *Découverte du Métal.* 213-222. Paris: Picard.
- Tylecote, R. F. & Boydell, P. J. 1978. Experiments on copper smelting based on early furnaces found at Timna. In: Rothenberg, B. (ed.) *Chalcolithic Copper Smelting.* 27-49. London: Institute for Archaeo-Metallurgical Studies.
- Tylecote, R. F., Ghaznavi, H. A. & Boydell, P. J. 1977. Partitioning of trace elements between the ores, fluxes, slags and metal during the smelting of copper. *Journal of Archaeological Science*, 4, 305-333.
- Vahidnia, A., Van Der Voet, G. B. & De Wolff, F. A. 2007. Arsenic neurotoxicity - a review. *Human & Experimental Toxicology*, 26, 823-832.
- Vatandoust, A. 1999. A view on prehistoric Iranian metalworking: elemental analyses and metallographic examinations. In: Hauptmann, A., Pernicka, E., Rehren, Th. & Yalçin,

- Ü. (eds.) *The Beginnings of Metallurgy*. 121-140. Borchum, Germany: Deutsches Bergbau-Museum.
- Vatandoust, A., Parzinger, H. & Helwing, B. 2011a. Early mining and metallurgy on the western Central Iranian Plateau: An introduction to the research project. In: Vatandoust, A., Parzinger, H. & Helwing, B. (eds.) *Early Mining and Metallurgy on the Western Central Iranian Plateau: The First Five Years of Work*. 1-7. Mainz: Verlag Philip Von Zabren.
- Vatandoust, A., Parzinger, H. & Helwing, B. (eds.) 2011b. *Early Mining and Metallurgy on the Western Central Iranian Plateau: The First Five Years of Work*, Mainz: Verlag Philip Von Zabern.
- Veldhuijzen, H. A. 2003. 'Slag_Fun' - A new tool for archaeometallurgy: Development of an analytical (P)ED-XRF method for iron-rich materials *Papers from the Institute of Archaeology*, 14, 102-118.
- Wagner, G. A. & Öztunalı, Ö. 2000. Prehistoric copper sources in Turkey. In: Yalçın, Ü. (ed.) *Anatolian Metal I*. Bochum: Deutsches Bergbau-Museum.
- Wagner, G. A., Pernicka, E., Seeliger, T. C., Lorenz, I. B., Begemann, F., Schmitt-Strecker, S., Eibner, C. & Öztunalı, Ö. 1986. Geochemische und Isotopische Charakteristika Früher Rohstoffquellen für Kupfer, Blei, Silber und Gold in der Türkei. *Jahrbuch des Römisch-Germanisches Zentralmuseum Mainz*, 33, 723-752.
- Weeks, L. 2013. Iranian metallurgy of the 4th Millennium BC in its wider technological and cultural contexts. In: Petrie, C. A. (ed.) *Ancient Iran and its Neighbours: Local Developments and Long-range Interactions in the Fourth Millennium BC*. 277-291. Oxford: Oxbow Books.
- Weeks, L., Keall, E., Pashley, V., Evans, J. & Stock, S. 2009. Lead Isotope Analyses of Bronze Age Copper-Base Artefacts from Al-Midamman, Yemen: Towards the Identification of an Indigenous Metal Production and Exchange System in the Southern Red Sea Region. *Archaeometry*, 51, 576-597.
- Weeks, L., Schoop, U.-D. & Faber, E. forthcoming. Çamlıbel Tarlası artefacts - Summary of analyses.
- Weeks, L. R. 2003. *Early Metallurgy of the Persian Gulf: Technology, Trade, and the Bronze Age World*. Boston: Brill.
- Weisgerber, G. & Pernicka, E. 1995. Ore mining in prehistoric Europe: An overview. In: Morteani, G. & Northover, P. J. (eds.) *Prehistoric Gold in Europe*. 159-182. Netherlands: Kluwer Academic Publishers.
- Wertime, T. A. 1964. Man's first encounter with metallurgy: man's discovery of ores and metals heaped to shape his sense of science, technology, and history. *Science*, 146, 1257-67.
- Wertime, T. A. 1968. A metallurgical expedition through the Persian desert. *Science*, 159, 927-935.
- Wheeler, M. 1983. Greenstone amulets. In: Kenyon, K. M. & Holland, T. A. (eds.) *Excavations at Jericho, vol V*. 781-788. London: British Academy.
- Whitbread, I. K. 1995. *Greek Transport Amphorae: A Petrological and Archaeological Study*. British School at Athens: Fitch Laboratory Occasional Paper 4.
- White, J. C. & Pigott, V. C. 1996. From community craft to regional specialization: intensification of copper production in pre-state Thailand. In: Wailes, B. (ed.) *Craft Specialization and Social Evolution: In Memory of V. Gordon Childe*. 151-175. Philadelphia: University Museum Publications.
- Willis, G. M. & Toguri, J. M. 2009. Yazawa's diagram. *The AusIMM Metallurgical Society Special Paper*. 1-8.
- Wilson, L. & Pollard, A. M. 2001. The Provenance Hypothesis. In: Brothwell, D. R. & Pollard, A. M. (eds.) *Handbook of Archaeological Sciences*. 507-517. Chichester: Wiley.

- Witter, W. 1936. Die technische verwendung von kupfer-arsenlegierungen im altertum. *Metall und Erz*, 33, 118-120.
- Wyckoff, D. 1967. *Albertus Magnus: Book of Minerals*. Oxford: Clarendon Press.
- Yalçın, Ü. 2008. Ancient metallurgy in Anatolia. In: Yalçın, Ü., Özbal, H. & Paşamehmetoğlu, A. G. (eds.) *Ancient Mining in Turkey and the Eastern Mediterranean*. 15-40. Ankara: Atılım University.
- Yalçın, Ü. & Pernicka, E. 1999. Frühneolithische metallurgie von Aşıklı Höyük. In: Hauptmann, A., Pernicka, E., Rehren, Th. & Yalçın, Ü. (eds.) *The Beginnings of Metallurgy*. 45-54. Bochum: Deutsches Bergbau-Museum.
- Yalçın, Ü. & Yalçın, H. G. 2009. Evidence for early use of tin at Tülintepe in Eastern Anatolia. *TUBA-AR*, 12, 123-142.
- Yener, A., Geçkinli, E. & Özbal, H. 1996. A brief survey of Anatolian metallurgy prior to 500 BC. In: Demirci, Ş., Özer, A. M. & Summers, G. D. (eds.) *Archaeometry 94: The Proceedings of the 29th International Symposium on Archaeometry*. 375-390. Ankara: Tübitak.
- Yener, A., Özbal, H., Earl, B. & Adriaens, A. 2003. Analyses of metalliferous residues, crucible fragments, experimental smelts, and ores from Kestel tin mine and the tin processing site of Göltepe. In: Craddock, P. T. & Lang, J. (eds.) *Mining and Metal Production through the Ages*. 181-197. London: British Museum.
- Yener, A. & Vandiver, P. 1993. Tin processing at Göltepe, and Early Bronze Age site in Anatolia. *Journal of American Archaeology*, 97, 207-238.
- Yener, K. A. 2000. *The Domestication of Metals: the Rise of Complex Metal Industries in Anatolia*. Leiden: Brill.
- Yener, K. A. 2008. Revisiting Kestel mine and Göltepe. In: Yalçın, Ü., Özbal, H. & Paşamehmetoğlu, A. G. (eds.) *Ancient Mining in Turkey and the Eastern Mediterranean*. 57-64. Ankara: Atılım University.
- Yener, K. A., Sayre, E. V., Joel, E. C., Ozbal, H., Barnes, I. L. & Brill, R. H. 1991. Stable lead isotope studies of Central Taurus ore sources and related artifacts from Eastern Mediterranean Chalcolithic and Bronze Age sites. *Journal of Archaeological Science*, 18, 541-577.
- Zimmermann, T. 2007. Anatolia and the Balkans, once again - Ring-shaped idols from Western Asia and a critical reassessment of some 'Early Bronze Age' items from İkiztepe, Turkey. *Oxford Journal of Archaeology*, 26, 25-33.
- Zwicker, U. 1980. Investigations on the extractive metallurgy of Cu/Sb/As ore and excavated smelting products from Norşun-Tepe (Keban) on the Upper Euphrates (3500-2800 B.C.). In: Oddy, W. A. (ed.) *Aspects of Early Metallurgy*. 13-36. London: British Museum.
- Zwicker, U. 1991. Natural copper-arsenic alloys and smelted arsenic bronzes in early metal production. In: J.-P., M. & Eluère, C. (eds.) *Découverte du Métal*. 331-340. Paris: Picard.

Appendices

Appendix A SEM-EDS Analysis of CRMs and RMs

Basalt

BIR-2G - Reykjavik doleritic basalt. Oxide composition in w.t%. Not measured: P₂O₅, K₂O, and trace elements.

	Na ₂ O	MgO	Al ₂ O ₃	SiO ₂	P ₂ O ₅	K ₂ O	CaO	TiO ₂	FeO	Mn (ppm)	Total
Measurement 1	1.72	9.5	15.04	46.81	-	-	13.11	0.99	9.96	1900	97.32
Measurement 2	1.7	9.42	15.19	47.32	-	-	13.16	1.02	10.15	1500	98.1
Measurement 3	1.75	9.51	15.42	47.6	-	-	13.3	1.01	10.06	1800	98.83
Measurement 4	1.73	9.45	15.27	46.9	-	-	13.16	0.99	10.01	2000	97.71
Measurement 5	1.73	9.62	15.41	47.94	-	-	13.36	1.01	10.21	1900	99.48
Obtained mean	1.73	9.50	15.27	47.31	-	-	13.22	1.00	10.08	1820	98.29
Certified USGS values	1.82	9.70	15.50	47.96	0.02	0.03	13.30	0.96	10.40	-	99.69
δ	0.09	0.20	0.23	0.65	-	-	0.08	0.04	0.32	-	-
% δ	5.16	2.06	1.51	1.35	-	-	0.62	4.58	3.10	-	-

BCR-2G – Columbia River basalt. Oxide composition in wt%. Not measured: trace elements.

	Na ₂ O	MgO	Al ₂ O ₃	SiO ₂	P ₂ O ₅	K ₂ O	CaO	TiO ₂	FeO	Mn (ppm)	Total
Measurement 1	3.25	3.74	13.94	56.31	0.36	1.89	7.25	2.35	12.48	2000	101.77
Measurement 2	3.22	3.62	13.7	55.08	0.35	1.81	7.1	2.41	12.11	2500	99.64
Measurement 3	3.22	3.81	14.02	56.7	0.39	1.9	7.3	2.42	12.6	2000	102.56
Measurement 4	3.24	3.79	14.3	57.4	-	1.87	7.34	2.45	12.54	2300	103.17
Measurement 5	3.21	3.78	13.91	56.38	0.3	1.87	7.29	2.43	12.44	1600	101.77
Obtained mean	3.23	3.75	13.97	56.37	0.35	1.87	7.26	2.41	12.43	2100	101.78
Certified USGS values	3.16	3.59	13.50	54.10	0.35	1.79	7.12	2.26	12.42	1520	98.44
δ	0.07	0.16	0.47	2.27	0.00	0.08	0.14	0.15	0.02	580	-
% δ	2.15	4.40	3.51	4.20	0.00	4.36	1.91	6.73	0.13	38	-

BHOV-2G - Hawaiian basalt. Oxide composition in wt%. Not measured: trace elements.

	Na ₂ O	MgO	Al ₂ O ₃	SiO ₂	P ₂ O ₅	K ₂ O	CaO	TiO ₂	FeO	Mn (ppm)	Total
Measurement 1	2.04	6.95	13	48.46	0.32	0.52	11.3	2.77	10.86	1900	96.43
Measurement 2	2.12	7.01	13.12	49.26	-	0.53	11.27	2.83	10.89	1700	97.21
Measurement 3	2.08	7.03	13.3	49.28	0.29	0.54	11.55	2.9	11.02	1600	98.13
Measurement 4	2.07	6.94	13.04	48.5	-	0.53	11.3	2.76	10.89	1700	96.19
Measurement 5	2.15	7.06	13.27	49.54	0.33	0.54	11.49	2.87	11.11	1400	98.5
Obtained mean	2.09	7.00	13.15	49.01	0.31	0.53	11.38	2.83	10.95	1700	97.29
Certified USGS values	2.18	7.23	13.50	49.80	0.27	0.51	11.40	2.75	10.80	-	98.44
δ	0.09	0.23	0.35	0.79	0.04	0.02	0.02	0.08	0.16	-	-
% δ	4.04	3.21	2.62	1.59	16.05	4.31	0.16	2.76	1.45	-	-

Metal

36X CuAs3A – Arsenical copper chill cast. Elemental composition in wt%. Not measured: Pb, Fe, Ni, Cd, In, and trace elements.

	Cu	As	Pb	Fe	Ni	Sn	Cd	In	Total
Measurement 1	94.6	3.2	-	-	-	0.6	-	-	98.4
Measurement 2	94.6	3.1	-	-	-	0.4	-	-	98.1
Measurement 3	94.6	3.1	-	-	-	0.4	-	-	98.1
Measurement 4	94.9	3.1	-	-	-	0.5	-	-	98.5
Measurement 5	95.4	3.1	-	-	-	0.5	-	-	99.0
Measurement 6	96.1	3.0	-	-	-	0.5	-	-	99.6
Measurement 7	94.9	3.0	-	-	-	0.4	-	-	98.3
Measurement 8	95.0	2.9	-	-	-	0.4	-	-	98.4
Measurement 9	95.3	3.0	-	-	-	0.4	-	-	98.7
Obtained mean	95.1	3.1	-	-	-	0.5	-	-	98.6
Reported MBH values	-	2.9	0.012	0.001	0.007	0.009	0.003	0.0054	-
δ	-	0.15	-	-	-	0.46	-	-	-
% δ	-	5.17	-	-	-	5060.49	-	-	-

Note: Following discussion between myself, Thilo Rehren, the certifying body (Chris Eveleigh, MBH), and the team who commissioned the CHARM set (Heginbotham et al. 2014), it has been established that tin's officially reported values are likely under-reported and that the results obtained by SEM-EDS during this research are probably more accurate. This is because the element was present in the alloy as SnO₂ (tin being used in many castings as a deoxidant), which is a highly refractory compound that can easily be brought out of solution during wet chemical dissolution. It is expected that analyses dependent on the use of solutes would be less likely to report the sample's original tin content. The presence of tin oxide was confirmed by spot analyses of small exsolved phases by SEM-EDS and the element is therefore most definitely present in some quantity.

Since most of the laboratories used for the analysis rely on ICP-AES and FAAS, both of which are based on the use of solutes, tin content results obtained through those analyses are therefore probably too low.

Indeed, after discussing the large disparity with other colleagues and MBH, it was discovered that OE and other ED-XRF techniques which analyse a solid surface all reported much higher tin content, in agreement with the results identified here. Although SEM-EDS is by no means a fully quantitative instrument, bulk area analyses here are much better reflections of the original casting composition in regards to tin than wet chemistry-based techniques.

Appendix B Camlibel

B.1 Technical ceramics

Mean bulk composition of crucible ceramic fabrics. All results in wt% and normalized to 100%. Numbers in parentheses next to the sample name refer to the number of bulk analyses.

Sample	Phase	Na ₂ O	MgO	Al ₂ O ₃	SiO ₂	K ₂ O	CaO	TiO ₂	FeO	As ₂ O ₃
107-6457 (4)	CBT IV	1.9	3.4	14.2	62.1	2.5	9.0	b.d.l.	7.0	b.d.l.
Std. Dev.		0.3	0.2	0.7	1.6	0.0	2.6	b.d.l.	0.8	b.d.l.
Min.		1.6	3.2	13.5	60.5	2.4	6.7	b.d.l.	6.5	b.d.l.
Max.		2.2	3.6	15.1	63.5	2.5	11.2	b.d.l.	8.1	b.d.l.
133-6376 (3)	CBT IV	1.5	5.5	13.7	58.9	2.1	9.1	0.7	7.0	1.4
Std. Dev.		0.3	0.6	0.8	1.6	0.3	0.8	0.7	0.8	2.3
Min.		1.2	4.9	12.7	57.2	1.9	8.3	b.d.l.	6.6	b.d.l.
Max.		1.9	6.2	14.3	60.2	2.4	9.6	1.3	7.9	4.1
136-6325 (3)	CBT IV	1.1	7.9	11.8	53.9	1.3	13.0	1.6	9.4	b.d.l.
Std. Dev.		0.1	1.1	1.2	6.0	0.2	7.1	0.2	0.6	b.d.l.
Min.		1.0	7.0	10.4	47.0	1.1	8.8	1.4	8.8	b.d.l.
Max.		1.3	9.1	12.6	57.6	1.4	21.2	1.7	10.1	b.d.l.
242-6470 (3)	CBT III	1.7	6.6	13.9	61.2	1.3	4.3	1.4	9.6	b.d.l.
Std. Dev.		0.3	0.5	0.4	2.0	0.2	1.1	0.3	0.5	b.d.l.
Min.		1.4	6.2	13.5	58.2	1.1	3.5	1.1	9.1	b.d.l.
Max.		2.0	7.3	14.3	62.3	1.5	6.0	1.8	10.2	b.d.l.
62-6450 (3)	CBT III	1.7	5.8	14.3	61.6	1.7	3.9	1.5	9.6	b.d.l.
Std. Dev.		0.2	0.5	0.8	0.4	0.1	0.2	0.1	0.1	b.d.l.
Min.		1.5	5.3	13.9	61.1	1.5	3.7	1.4	9.5	b.d.l.
Max.		1.9	6.2	15.2	61.8	1.8	4.1	1.5	9.7	b.d.l.
79-6471 (3)	CBT II/III	1.6	5.7	13.7	61.3	2.0	4.9	1.2	9.6	b.d.l.
Std. Dev.		0.1	0.5	0.9	0.2	0.1	1.7	0.1	0.6	b.d.l.
Min.		1.6	5.1	12.8	61.1	1.9	3.7	1.1	9.1	b.d.l.
Max.		1.7	6.1	14.5	61.5	2.2	6.8	1.3	10.3	b.d.l.
956-6202 (3)	CBT II	1.4	6.4	15.1	59.4	2.2	3.6	1.4	10.4	b.d.l.
Std. Dev.		0.3	0.5	0.8	0.6	0.1	0.9	0.3	0.4	b.d.l.
Min.		1.3	6.0	14.2	58.9	2.1	2.8	1.1	10.0	b.d.l.
Max.		1.7	7.0	15.7	60.1	2.3	4.6	1.6	10.9	b.d.l.

Mean bulk composition of residues on the inner surface of Camlibel crucibles.

	Sample	Phase	Na ₂ O	MgO	Al ₂ O ₃	SiO ₂	P ₂ O ₅	SO ₃	Cl	K ₂ O	CaO	TiO ₂	MnO	FeO	CuO	As ₂ O ₃	Br
Ca-rich arsenate	133-6376 (3)	CBT IV	b.d.l.	2.58	0.00	0.52	2.17	0.77	b.d.l.	0.67	37.85	b.d.l.	b.d.l.	0.06	3.90	51.48	b.d.l.
	136-6325 (6)	CBT IV	b.d.l.	0.25	0.94	5.14	0.17	0.30	1.70	0.74	46.19	b.d.l.	0.61	1.21	0.00	42.47	b.d.l.
	242-6470 (8)	CBT III	1.10	3.03	0.49	4.88	4.53	1.01	b.d.l.	0.55	40.00	b.d.l.	b.d.l.	2.46	0.87	41.08	b.d.l.
	62-6450 (3)	CBT III	b.d.l.	2.24	1.11	13.52	3.28	0.54	b.d.l.	1.24	32.57	0.25	0.30	2.90	4.20	34.91	2.66
	79-6471 (2)	CBT II/III	b.d.l.	1.86	5.25	18.15	3.86	0.68	1.10	0.68	32.74	b.d.l.	b.d.l.	4.37	0.00	31.18	b.d.l.
	MEAN		0.22	1.99	1.56	8.44	2.80	0.66	0.56	0.78	37.87	0.05	0.18	2.20	1.79	40.22	b.d.l.
	Std. Dev.		0.49	1.06	2.11	7.18	1.71	0.26	0.80	0.27	5.66	0.11	0.27	1.64	2.09	7.79	1.19
	Min.		b.d.l.	0.25	0.00	0.52	0.17	0.30	b.d.l.	0.55	32.57	b.d.l.	0.00	0.06	0.00	31.18	b.d.l.
Max.		1.10	3.03	5.25	18.15	4.53	1.01	1.70	1.24	46.19	0.25	0.61	4.37	4.20	51.48	2.66	
Mg-rich arsenate	107-6457 (8)	CBT IV	0.61	15.86	b.d.l.	3.09	2.04	b.d.l.	b.d.l.	2.47	14.00	b.d.l.	b.d.l.	2.51	12.39	47.04	b.d.l.
	133-6376 (5)	CBT IV	b.d.l.	17.47	b.d.l.	2.14	0.45	b.d.l.	b.d.l.	2.76	18.40	b.d.l.	b.d.l.	1.35	6.08	51.35	b.d.l.
	MEAN		0.30	16.67	b.d.l.	2.61	1.25	b.d.l.	b.d.l.	2.61	16.20	b.d.l.	b.d.l.	1.93	9.24	49.19	b.d.l.
	Std. Dev.		0.4	1.1	b.d.l.	0.7	1.1	b.d.l.	b.d.l.	0.2	3.1	b.d.l.	b.d.l.	0.8	4.5	3.0	b.d.l.
	Min.		b.d.l.	15.86	b.d.l.	2.14	0.45	b.d.l.	b.d.l.	2.47	14.00	b.d.l.	b.d.l.	1.35	6.08	47.04	b.d.l.
	Max.		0.61	17.47	b.d.l.	3.09	2.04	b.d.l.	b.d.l.	2.76	18.40	b.d.l.	b.d.l.	2.51	12.39	51.35	b.d.l.

B.2 Bowl hearths

Composition of stratigraphic layers from bowl hearth features as determined by pXRF in soils mode. Elemental composition in ppm.

Sample		P	Cl	K	Ca	Ti	Cr	Mn	Fe	Co	Ni	Cu	Zn	As	Rb	Sr	Zr	Sb	Ba	Pb
FURNACE 10	Top fill	b.d.l.	b.d.l.	8435	79797	8076	656	1119	70689	685	706	94	80	b.d.l.	19	253	138	b.d.l.	336	5
	Bottom fill	b.d.l.	7787	7836	67425	3841	728	1016	54126	568	1035	48	67	b.d.l.	27	155	97	b.d.l.	201	7
	Clay surface	b.d.l.	b.d.l.	7631	90124	3355	524	983	44871	581	917	79	64	b.d.l.	24	216	101	b.d.l.	141	7
	Clay	b.d.l.	5953	9291	96733	3634	441	990	37403	376	655	48	61	b.d.l.	31.5	169	92	b.d.l.	175	7
	Natural soil	b.d.l.	b.d.l.	7762	102663	7054	624	967	59067	536	638	79	88	b.d.l.	20	337	133	b.d.l.	273	7
FURNACE 11	Top fill	b.d.l.	b.d.l.	8202	71406	8958	699	1166	76530	745	689	102	81	b.d.l.	17	233	142	b.d.l.	376	4
	Bottom fill	b.d.l.	b.d.l.	8058	87089	7688	626	1049	69557	701	676	102	83	b.d.l.	16	275	133	b.d.l.	291	5
	Clay surface	28958	9719	14044	87078	6014	548	1086	54614	637	536	70	94	5	38	324	181	b.d.l.	330	10
	Clay	b.d.l.	b.d.l.	7610	121923	3955	384	744	39729	419	472	80	72	3	21.2	436	111	b.d.l.	189	b.d.l.
	Natural soil	28068	b.d.l.	11861	91551	5784	645	1053	51207	555	589	80	84	4	23	330	120	37	276	5
FURNACE 12	Top fill	b.d.l.	b.d.l.	8923	82040	5790	490	1020	58036	603	687	92	99	b.d.l.	27	268	125	b.d.l.	268	5
	Bottom fill	32827	b.d.l.	9586	87092	7783	544	1180	64122	679	769	81	71	b.d.l.	25	224	130	b.d.l.	354	7
	Clay surface	53636	b.d.l.	9876	202918	4697	351	794	48317	568	497	95	69	5	31	361	147	b.d.l.	242	8
	Clay	b.d.l.	b.d.l.	13084	43985	6138	326	1246	52228	362	425	78	80	6	35	348	179	b.d.l.	361	12
	Natural soil	51426	6481	11344	118045	4754	398	858	43030	489	489	79	84	4	26	429	113	b.d.l.	240	5
FURNACE 5	Top fill	b.d.l.	b.d.l.	6499	213458	4118	441	646	37964	428	468	99	66	b.d.l.	18	378	96	b.d.l.	170	5
	Clay surface	38841	7483	10379	154257	5273	416	1156	52768	641	347	302	104	5	40	350	137	b.d.l.	343	7
	Clay	26155	6323	14927	67537	7071	410	1076	60201	573	454	99	100	7	39	345	194	b.d.l.	400	12
	Natural soil	38230	7494	6449	90266	6657	599	1106	58260	665	628	155	87	4	17	320	126	b.d.l.	281	6
FURNACE 3	Top fill	b.d.l.	b.d.l.	5581	192452	6619	574	900	58113	594	638	93	68	b.d.l.	15	267	120	b.d.l.	241	6
	Narural soil		b.d.l.	2564	60595	10857	877	1350	92078	877	852	114	83	b.d.l.	6	200	152	b.d.l.	417	b.d.l.
FURNACE 4	Clay surface	51527	7904	11405	90210	7610	733	1164	66192	648	521	112	118	6	31	289	163	b.d.l.	400	9
	Natural soil	37493	b.d.l.	8812	79914	7389	717	1129	62768	678	775	100	96	b.d.l.	26	221	132	b.d.l.	308	6

B.3 Other metallurgical ceramics

Mean bulk composition of other metallurgical ceramic fabrics. All results in wt% and normalized to 100%. Numbers in parentheses next to the sample name refer to the number of bulk analyses.

	Phase	Na ₂ O	MgO	Al ₂ O ₃	SiO ₂	P ₂ O ₅	SO ₃	Cl	K ₂ O	CaO	TiO ₂	CrO	MnO	FeO	NiO	CoO	CuO	ZnO
108-6857 (3)	CBT IV	1.9	4.2	17.2	60.9	0.2	0.2	0.1	3.1	2.9	1.0	b.d.l.	0.2	8.1	b.d.l.	b.d.l.	b.d.l.	b.d.l.
Std. Dev.		0.1	0.4	1.2	2.5	0.0	0.1	0.0	0.1	0.4	0.1	N/A	0.1	0.5	N/A	N/A	N/A	N/A
Min.		1.8	3.9	16.2	58.2	0.2	0.1	0.1	2.9	2.6	1.0	b.d.l.	0.1	7.5	b.d.l.	b.d.l.	b.d.l.	b.d.l.
Max.		2.0	4.6	18.5	63.1	0.2	0.3	0.1	3.2	3.3	1.1	b.d.l.	0.3	8.4	b.d.l.	b.d.l.	b.d.l.	b.d.l.
147-6832 (3)	CBT IV	1.7	6.4	15.2	59.8	1.0	b.d.l.	0.1	1.8	2.7	1.2	b.d.l.	0.2	10.1	b.d.l.	b.d.l.	b.d.l.	b.d.l.
Std. Dev.		0.3	0.9	1.0	1.2	0.5	b.d.l.	0.0	0.1	0.2	0.2	N/A	0.0	0.5	N/A	N/A	N/A	N/A
Min.		1.5	5.4	14.1	58.6	0.5	b.d.l.	0.1	1.7	2.4	1.1	b.d.l.	0.1	9.6	b.d.l.	b.d.l.	b.d.l.	b.d.l.
Max.		2.0	7.2	16.0	61.0	1.6	b.d.l.	0.1	1.9	2.9	1.4	b.d.l.	0.2	10.6	b.d.l.	b.d.l.	b.d.l.	b.d.l.
228-6870 (3)	CBT IV	0.7	9.9	12.8	55.3	0.2	0.3	0.1	1.4	7.2	1.6	b.d.l.	0.2	10.2	b.d.l.	b.d.l.	b.d.l.	b.d.l.
Std. Dev.		0.0	0.6	0.6	1.4	0.0	0.0	0.0	0.3	0.4	0.1	N/A	0.2	0.3	N/A	N/A	N/A	N/A
Min.		0.6	9.3	12.3	54.3	0.2	0.3	0.1	1.2	7.0	1.5	b.d.l.	0.1	9.9	b.d.l.	b.d.l.	b.d.l.	b.d.l.
Max.		0.7	10.4	13.5	56.9	0.3	0.3	0.2	1.7	7.6	1.7	b.d.l.	0.4	10.6	b.d.l.	b.d.l.	b.d.l.	b.d.l.
616-6922 (3)	CBT IV	1.7	7.4	14.6	58.1	0.3	0.3	0.1	1.7	3.7	1.2	0.1	0.3	10.5	b.d.l.	b.d.l.	0.1	b.d.l.
Std. Dev.		0.4	0.3	0.8	0.2	0.1	0.1	0.0	0.4	0.9	0.1	0.0	0.1	0.8	N/A	N/A	0.1	N/A
Min.		1.3	7.1	13.9	57.9	0.2	0.2	0.1	1.5	3.1	1.1	0.1	0.2	9.8	b.d.l.	b.d.l.	b.d.l.	b.d.l.
Max.		2.1	7.7	15.5	58.2	0.3	0.4	0.1	2.2	4.7	1.4	0.1	0.4	11.4	b.d.l.	b.d.l.	0.2	b.d.l.
720-5879 (3)	SPEU	1.8	6.5	15.7	58.1	0.3	0.2	0.2	1.8	3.7	1.4	b.d.l.	0.3	10.2	b.d.l.	b.d.l.	b.d.l.	b.d.l.
Std. Dev.		0.2	0.3	0.2	0.9	0.0	0.0	0.0	0.2	0.0	0.1	N/A	0.1	0.4	N/A	N/A	N/A	N/A
Min.		1.6	6.3	15.5	57.2	0.2	0.2	0.1	1.7	3.7	1.3	b.d.l.	0.2	9.9	b.d.l.	b.d.l.	b.d.l.	b.d.l.
Max.		1.9	6.8	15.8	59.0	0.3	0.2	0.2	2.1	3.8	1.5	b.d.l.	0.4	10.6	b.d.l.	b.d.l.	b.d.l.	b.d.l.
819-7020 (3)	CBT III	0.8	10.1	12.5	53.2	b.d.l.	b.d.l.	0.1	1.1	10.5	1.5	0.1	0.2	9.9	b.d.l.	b.d.l.	b.d.l.	b.d.l.
Std. Dev.		0.0	0.2	0.3	0.3	N/A	N/A	0.0	0.0	1.0	0.2	0.0	0.1	0.5	N/A	N/A	N/A	N/A
Min.		0.8	9.9	12.2	52.8	b.d.l.	b.d.l.	0.1	1.1	9.4	1.3	0.1	0.1	9.6	b.d.l.	b.d.l.	b.d.l.	b.d.l.
Max.		0.8	10.3	12.8	53.5	b.d.l.	b.d.l.	0.1	1.1	11.4	1.7	0.1	0.2	10.4	b.d.l.	b.d.l.	b.d.l.	b.d.l.

Mean bulk composition of other metallurgical ceramic's purple-stained surface layers. All results in wt% and normalized to 100%. Numbers in parentheses next to the sample name refer to the number of bulk analyses.

	Phase	Na ₂ O	MgO	Al ₂ O ₃	SiO ₂	P ₂ O ₅	SO ₃	Cl	K ₂ O	CaO	TiO ₂	CrO	MnO	FeO	NiO	CoO	CuO	ZnO	
108-6857 (8)	CBT IV	b.d.l.	1.4	0.1	1.0	b.d.l.	b.d.l.	0.0	0.0	0.1	0.0	b.d.l.	0.2	69.3	0.1	b.d.l.	27.8	b.d.l.	
Std. Dev.		N/A	1.1	0.2	0.9	N/A	N/A	0.0	0.1	0.1	0.1	N/A	0.3	2.4	0.1	N/A	2.2	b.d.l.	
Min.		b.d.l.	b.d.l.	b.d.l.	b.d.l.	b.d.l.	b.d.l.	b.d.l.	b.d.l.	b.d.l.	b.d.l.	b.d.l.	b.d.l.	b.d.l.	67.0	0.0	b.d.l.	24.4	b.d.l.
Max.		b.d.l.	3.0	0.6	2.9	b.d.l.	b.d.l.	b.d.l.	0.1	0.1	0.3	0.3	b.d.l.	0.6	72.7	0.3	b.d.l.	30.5	b.d.l.
147-6832 (3)	CBT IV	b.d.l.	b.d.l.	b.d.l.	0.4	b.d.l.	b.d.l.	b.d.l.	b.d.l.	0.1	b.d.l.	b.d.l.	b.d.l.	89.2	b.d.l.	1.7	8.5	b.d.l.	
Std. Dev.		N/A	b.d.l.	b.d.l.	0.1	N/A	N/A	N/A	N/A	0.0	N/A	N/A	N/A	3.1	N/A	0.7	2.7	N/A	
Min.		b.d.l.	b.d.l.	b.d.l.	0.3	b.d.l.	b.d.l.	b.d.l.	b.d.l.	0.1	b.d.l.	b.d.l.	b.d.l.	86.1	b.d.l.	0.9	6.2	b.d.l.	
Max.		b.d.l.	b.d.l.	b.d.l.	0.6	b.d.l.	b.d.l.	b.d.l.	b.d.l.	0.2	b.d.l.	b.d.l.	b.d.l.	92.4	b.d.l.	2.3	11.6	b.d.l.	
228-6870 (2)	CBT IV	b.d.l.	0.6	5.3	7.8	b.d.l.	0.2	0.1	0.3	0.3	1.2	b.d.l.	0.5	36.0	b.d.l.	b.d.l.	47.7	b.d.l.	
Std. Dev.		N/A	0.1	3.6	2.2	N/A	0.0	0.0	0.2	0.0	0.4	N/A	0.4	4.9	N/A	N/A	2.1	N/A	
Min.		b.d.l.	0.5	2.8	6.2	b.d.l.	0.1	0.1	0.2	0.3	0.9	b.d.l.	0.3	32.5	b.d.l.	b.d.l.	46.3	b.d.l.	
Max.		b.d.l.	0.6	7.8	9.4	b.d.l.	0.2	0.1	0.5	0.4	1.5	b.d.l.	0.8	39.4	b.d.l.	b.d.l.	49.2	b.d.l.	
616-6922 (7)	CBT IV	b.d.l.	1.6	3.2	6.1	0.0	0.1	0.0	0.1	0.3	0.3	b.d.l.	0.1	73.6	b.d.l.	b.d.l.	14.4	b.d.l.	
Std. Dev.		N/A	2.0	3.1	7.6	0.1	0.2	0.0	0.2	0.3	0.3	N/A	0.2	11.8	N/A	N/A	9.6	N/A	
Min.		b.d.l.	0.0	0.0	0.0	0.0	0.0	0.0	0.0	0.0	0.0	b.d.l.	0.0	59.7	b.d.l.	b.d.l.	1.3	b.d.l.	
Max.		b.d.l.	5.8	8.4	22.2	0.3	0.4	0.1	0.6	0.9	0.7	b.d.l.	0.4	90.9	b.d.l.	b.d.l.	29.7	b.d.l.	
720-5879 (2)	SPEU	b.d.l.	2.1	b.d.l.	0.6	b.d.l.	b.d.l.	b.d.l.	b.d.l.	0.3	b.d.l.	b.d.l.	b.d.l.	70.3	b.d.l.	b.d.l.	26.7	b.d.l.	
Std. Dev.		N/A	0.3	b.d.l.	0.2	N/A	N/A	N/A	N/A	0.2	N/A	N/A	N/A	0.7	N/A	N/A	1.0	N/A	
Min.		b.d.l.	1.9	b.d.l.	0.4	b.d.l.	b.d.l.	b.d.l.	b.d.l.	0.2	b.d.l.	b.d.l.	b.d.l.	69.8	b.d.l.	b.d.l.	26.0	b.d.l.	
Max.		b.d.l.	2.3	b.d.l.	0.7	b.d.l.	b.d.l.	b.d.l.	b.d.l.	0.5	b.d.l.	b.d.l.	b.d.l.	70.8	b.d.l.	b.d.l.	27.4	b.d.l.	
819-7020 (4)	CBT III	b.d.l.	2.7	5.3	11.2	0.3	0.3	0.1	0.4	0.5	0.8	b.d.l.	b.d.l.	45.1	0.4	b.d.l.	32.3	0.7	
Std. Dev.		N/A	3.9	2.4	11.5	0.2	0.3	0.1	0.5	0.2	0.3	N/A	N/A	7.7	0.3	N/A	12.6	0.5	
Min.		b.d.l.	0.5	3.1	4.2	0.2	0.2	0.1	0.2	0.3	0.4	b.d.l.	b.d.l.	34.3	0.1	b.d.l.	14.3	0.3	
Max.		b.d.l.	8.6	8.5	28.4	0.6	0.7	0.2	1.2	0.8	1.0	b.d.l.	b.d.l.	50.6	0.7	b.d.l.	42.5	1.3	

B.4 Slags

Mean bulk composition of copper smelting slags. All results in wt% and normalized to 100%. Numbers in parentheses next to the sample name refer to the number of bulk analyses.

Sample	Phase	Na ₂ O	MgO	Al ₂ O ₃	SiO ₂	P ₂ O ₅	SO ₃	Cl	K ₂ O	CaO	TiO ₂	CrO	MnO	FeO	CuO	As ₂ O ₃	ZnO	BaO	NiO	ZrO	MoO
527-4329 (3)	Surface	b.d.l.	12.6	4.0	45.7	1.1	1.2	b.d.l.	1.5	11.4	0.4	b.d.l.	b.d.l.	20.4	2.0	b.d.l.	b.d.l.	b.d.l.	b.d.l.	b.d.l.	b.d.l.
Std. Dev		N/A	1.4	0.4	5.6	0.1	0.3	N/A	0.7	2.2	0.3	N/A	N/A	2.1	0.3	N/A	N/A	N/A	N/A	N/A	N/A
Min.		b.d.l.	10.9	3.7	39.3	1.0	1.0	b.d.l.	1.0	9.2	b.d.l.	b.d.l.	b.d.l.	18.4	1.7	b.d.l.	b.d.l.	b.d.l.	b.d.l.	b.d.l.	b.d.l.
Max.		b.d.l.	13.5	4.5	49.4	1.2	1.5	b.d.l.	2.3	13.6	0.5	b.d.l.	b.d.l.	22.6	2.2	b.d.l.	b.d.l.	b.d.l.	b.d.l.	b.d.l.	b.d.l.
846-5515 (3)	Surface	b.d.l.	3.8	0.5	47.7	b.d.l.	0.7	b.d.l.	b.d.l.	17.2	b.d.l.	b.d.l.	0.5	26.0	3.6	b.d.l.	b.d.l.	b.d.l.	b.d.l.	b.d.l.	b.d.l.
Std. Dev		N/A	0.1	0.1	0.5	N/A	0.1	N/A	N/A	0.5	N/A	N/A	0.1	2.0	1.8	N/A	N/A	N/A	N/A	N/A	N/A
Min.		b.d.l.	3.6	0.4	47.2	b.d.l.	1.1	b.d.l.	b.d.l.	16.6	b.d.l.	b.d.l.	0.4	24.1	2.4	b.d.l.	b.d.l.	b.d.l.	b.d.l.	b.d.l.	b.d.l.
Max.		b.d.l.	3.9	0.6	48.2	b.d.l.	1.2	b.d.l.	b.d.l.	17.7	b.d.l.	b.d.l.	0.6	28.0	5.6	b.d.l.	b.d.l.	b.d.l.	b.d.l.	b.d.l.	b.d.l.
846-5528a (3)	Surface	b.d.l.	8.0	2.4	36.9	0.8	1.5	b.d.l.	1.1	8.9	0.1	b.d.l.	b.d.l.	39.3	0.9	b.d.l.	b.d.l.	b.d.l.	b.d.l.	b.d.l.	b.d.l.
Std. Dev		N/A	0.5	0.3	0.5	0.1	0.2	N/A	0.1	0.2	0.2	N/A	N/A	0.8	0.2	N/A	N/A	N/A	N/A	N/A	N/A
Min.		b.d.l.	7.6	2.1	36.4	0.7	1.3	b.d.l.	1.0	8.8	b.d.l.	b.d.l.	b.d.l.	38.4	0.8	b.d.l.	b.d.l.	b.d.l.	b.d.l.	b.d.l.	b.d.l.
Max.		b.d.l.	8.5	2.8	37.5	0.9	1.7	b.d.l.	1.2	9.1	0.4	b.d.l.	b.d.l.	40.0	1.2	b.d.l.	b.d.l.	b.d.l.	b.d.l.	b.d.l.	b.d.l.
846-5528b (3)	Surface	b.d.l.	4.2	0.7	46.9	b.d.l.	1.4	b.d.l.	b.d.l.	16.4	b.d.l.	b.d.l.	0.3	28.6	1.6	b.d.l.	b.d.l.	b.d.l.	b.d.l.	b.d.l.	b.d.l.
Std. Dev		N/A	0.3	0.2	0.8	N/A	0.3	N/A	N/A	1.5	N/A	N/A	0.2	1.0	0.4	N/A	N/A	N/A	N/A	N/A	N/A
Min.		b.d.l.	3.9	0.4	46.1	b.d.l.	1.1	b.d.l.	b.d.l.	14.8	b.d.l.	b.d.l.	b.d.l.	27.6	1.2	b.d.l.	b.d.l.	b.d.l.	b.d.l.	b.d.l.	b.d.l.
Max.		b.d.l.	4.4	0.9	47.7	b.d.l.	1.6	b.d.l.	b.d.l.	17.8	b.d.l.	b.d.l.	0.4	29.4	1.9	b.d.l.	b.d.l.	b.d.l.	b.d.l.	b.d.l.	b.d.l.
222-326A (3)	CBT IV	b.d.l.	9.4	1.8	41.4	1.0	1.2	b.d.l.	1.0	19.7	0.2	b.d.l.	0.7	23.2	0.4	b.d.l.	b.d.l.	b.d.l.	b.d.l.	b.d.l.	b.d.l.
Std. Dev		N/A	1.2	0.4	3.4	0.2	0.2	N/A	0.0	7.4	0.1	N/A	0.0	4.7	0.2	N/A	N/A	N/A	N/A	N/A	N/A
Min.		b.d.l.	8.0	1.4	38.4	0.8	1.0	b.d.l.	1.0	11.2	0.1	b.d.l.	0.6	19.6	0.1	b.d.l.	b.d.l.	b.d.l.	b.d.l.	b.d.l.	b.d.l.
Max.		b.d.l.	10.3	2.2	45.2	1.2	1.4	b.d.l.	1.1	24.2	0.2	b.d.l.	0.7	28.5	0.6	b.d.l.	b.d.l.	b.d.l.	b.d.l.	b.d.l.	b.d.l.
222-326B (3)	CBT IV	b.d.l.	1.6	6.5	28.3	0.4	3.4	b.d.l.	0.2	1.8	0.4	b.d.l.	b.d.l.	55.5	1.6	b.d.l.	0.3	b.d.l.	b.d.l.	b.d.l.	b.d.l.
Std. Dev		N/A	1.1	3.9	1.3	0.3	0.7	N/A	0.1	1.0	0.4	N/A	N/A	4.1	0.3	N/A	0.0	N/A	N/A	N/A	N/A
Min.		b.d.l.	1.0	3.8	27.0	0.2	2.8	b.d.l.	0.1	0.7	0.2	b.d.l.	b.d.l.	50.8	1.3	b.d.l.	0.2	b.d.l.	b.d.l.	b.d.l.	b.d.l.
Max.		b.d.l.	2.9	11.0	29.6	0.7	4.1	b.d.l.	0.3	2.8	0.8	b.d.l.	b.d.l.	58.5	1.8	b.d.l.	0.3	b.d.l.	b.d.l.	b.d.l.	b.d.l.

Sample	Phase	Na ₂ O	MgO	Al ₂ O ₃	SiO ₂	P ₂ O ₅	SO ₃	Cl	K ₂ O	CaO	TiO ₂	CrO	MnO	FeO	CuO	As ₂ O ₃	ZnO	BaO	NiO	ZrO	MoO
443-3708 (3)	CBT IV	b.d.l.	6.6	17.3	30.7	0.2	5.7	b.d.l.	0.3	4.5	1.5	b.d.l.	0.3	29.2	3.7	b.d.l.	b.d.l.	b.d.l.	b.d.l.	b.d.l.	b.d.l.
Std. Dev		N/A	0.5	1.0	3.5	0.0	1.2	N/A	0.0	0.8	0.5	N/A	0.1	2.4	0.9	N/A	N/A	N/A	N/A	N/A	N/A
Min.		b.d.l.	6.2	16.2	27.4	0.2	4.7	b.d.l.	0.3	3.6	1.0	b.d.l.	0.3	26.4	2.9	b.d.l.	b.d.l.	b.d.l.	b.d.l.	b.d.l.	b.d.l.
Max.		b.d.l.	7.2	17.9	34.4	0.2	7.1	b.d.l.	0.4	5.0	1.9	b.d.l.	0.4	30.9	4.7	b.d.l.	b.d.l.	b.d.l.	b.d.l.	b.d.l.	b.d.l.
443-3710A (3)	CBT IV	b.d.l.	9.7	2.3	30.7	0.8	1.8	b.d.l.	0.8	12.2	0.2	b.d.l.	0.2	40.1	1.4	b.d.l.	b.d.l.	b.d.l.	b.d.l.	b.d.l.	b.d.l.
Std. Dev		N/A	0.2	0.1	0.1	0.1	0.2	N/A	0.1	0.3	0.0	N/A	0.0	0.1	0.2	N/A	N/A	N/A	N/A	N/A	N/A
Min.		b.d.l.	9.5	2.2	30.6	0.7	1.6	b.d.l.	0.8	11.9	0.2	b.d.l.	0.2	40.0	1.2	b.d.l.	b.d.l.	b.d.l.	b.d.l.	b.d.l.	b.d.l.
Max.		b.d.l.	9.8	2.4	30.8	0.8	2.0	b.d.l.	0.9	12.4	0.2	b.d.l.	0.2	40.1	1.6	b.d.l.	b.d.l.	b.d.l.	b.d.l.	b.d.l.	b.d.l.
443-3710B (4)	CBT IV	b.d.l.	1.8	3.3	42.8	b.d.l.	0.9	b.d.l.	0.2	8.3	0.3	b.d.l.	b.d.l.	41.1	1.4	b.d.l.	b.d.l.	b.d.l.	b.d.l.	b.d.l.	b.d.l.
Std. Dev		N/A	0.2	0.5	2.6	N/A	0.4	N/A	0.1	1.0	0.0	N/A	N/A	2.1	0.8	N/A	N/A	N/A	N/A	N/A	N/A
Min.		b.d.l.	1.5	2.8	40.5	b.d.l.	0.4	b.d.l.	0.1	7.1	0.2	b.d.l.	b.d.l.	38.9	0.5	b.d.l.	b.d.l.	b.d.l.	b.d.l.	b.d.l.	b.d.l.
Max.		b.d.l.	1.9	4.0	46.4	b.d.l.	1.2	b.d.l.	0.3	9.4	0.3	b.d.l.	b.d.l.	43.1	2.1	b.d.l.	b.d.l.	b.d.l.	b.d.l.	b.d.l.	b.d.l.
445-3716 (4)	CBT IV	b.d.l.	4.2	8.6	51.9	b.d.l.	0.5	b.d.l.	0.2	12.6	0.7	b.d.l.	0.2	20.9	0.2	b.d.l.	b.d.l.	b.d.l.	b.d.l.	b.d.l.	b.d.l.
Std. Dev		N/A	0.2	0.6	1.4	N/A	0.2	N/A	0.1	2.1	0.0	N/A	0.0	2.9	0.1	N/A	N/A	N/A	N/A	N/A	N/A
Min.		b.d.l.	3.9	7.8	50.3	b.d.l.	0.4	b.d.l.	0.1	11.4	0.7	b.d.l.	0.2	16.7	0.1	b.d.l.	b.d.l.	b.d.l.	b.d.l.	b.d.l.	b.d.l.
Max.		b.d.l.	4.5	9.1	53.7	b.d.l.	0.8	b.d.l.	0.3	15.7	0.7	b.d.l.	0.3	23.4	0.3	b.d.l.	b.d.l.	b.d.l.	b.d.l.	b.d.l.	b.d.l.
446-3722 (3)	CBT IV	b.d.l.	4.3	1.1	45.1	0.1	0.8	b.d.l.	0.1	17.4	b.d.l.	b.d.l.	0.6	27.9	2.6	b.d.l.	b.d.l.	b.d.l.	b.d.l.	b.d.l.	b.d.l.
Std. Dev		N/A	0.2	0.1	0.5	0.1	0.1	N/A	0.0	0.1	N/A	N/A	0.1	0.5	0.5	N/A	N/A	N/A	N/A	N/A	N/A
Min.		b.d.l.	4.2	1.0	44.5	0.1	0.6	b.d.l.	0.1	17.3	b.d.l.	b.d.l.	0.5	27.4	2.0	b.d.l.	b.d.l.	b.d.l.	b.d.l.	b.d.l.	b.d.l.
Max.		b.d.l.	4.6	1.1	45.5	0.2	0.9	b.d.l.	0.2	17.5	b.d.l.	b.d.l.	0.6	28.3	2.9	b.d.l.	b.d.l.	b.d.l.	b.d.l.	b.d.l.	b.d.l.
466-4118 (3)	CBT IV	b.d.l.	3.0	0.4	50.9	b.d.l.	1.4	b.d.l.	b.d.l.	15.6	b.d.l.	b.d.l.	0.5	25.8	2.4	b.d.l.	b.d.l.	b.d.l.	b.d.l.	b.d.l.	b.d.l.
Std. Dev		N/A	0.2	0.1	1.8	N/A	0.5	N/A	N/A	0.8	N/A	N/A	0.1	2.2	1.0	N/A	N/A	N/A	N/A	N/A	N/A
Min.		b.d.l.	2.8	0.3	48.8	b.d.l.	0.8	b.d.l.	b.d.l.	14.8	b.d.l.	b.d.l.	0.4	24.2	1.4	b.d.l.	b.d.l.	b.d.l.	b.d.l.	b.d.l.	b.d.l.
Max.		b.d.l.	3.3	0.6	52.1	b.d.l.	1.8	b.d.l.	b.d.l.	16.4	b.d.l.	b.d.l.	0.6	28.2	3.5	b.d.l.	b.d.l.	b.d.l.	b.d.l.	b.d.l.	b.d.l.

Sample	Phase	Na ₂ O	MgO	Al ₂ O ₃	SiO ₂	P ₂ O ₅	SO ₃	Cl	K ₂ O	CaO	TiO ₂	CrO	MnO	FeO	CuO	As ₂ O ₃	ZnO	BaO	NiO	ZrO	MoO
629-3860 (3)	CBT IV	b.d.l.	10.0	2.9	47.6	0.9	b.d.l.	b.d.l.	1.3	4.8	0.3	0.1	b.d.l.	27.1	5.0	b.d.l.	b.d.l.	b.d.l.	b.d.l.	b.d.l.	b.d.l.
Std. Dev		N/A	3.7	0.8	3.3	0.3	N/A	N/A	0.6	2.1	0.1	0.2	N/A	4.2	1.3	N/A	N/A	N/A	N/A	N/A	N/A
Min.		b.d.l.	6.1	2.0	45.7	0.6	b.d.l.	b.d.l.	0.6	2.3	0.4	b.d.l.	b.d.l.	22.3	3.8	b.d.l.	b.d.l.	b.d.l.	b.d.l.	b.d.l.	b.d.l.
Max.		b.d.l.	13.5	3.5	51.4	1.1	b.d.l.	b.d.l.	1.7	6.2	0.5	0.4	b.d.l.	30.2	6.4	b.d.l.	b.d.l.	b.d.l.	b.d.l.	b.d.l.	b.d.l.
630-3865 (3)	CBT IV	b.d.l.	5.5	13.2	34.3	0.2	2.7	b.d.l.	0.1	10.7	1.1	b.d.l.	b.d.l.	29.4	2.6	b.d.l.	b.d.l.	b.d.l.	b.d.l.	0.3	b.d.l.
Std. Dev		N/A	1.3	0.6	2.1	0.3	0.2	N/A	0.2	3.5	0.2	N/A	N/A	0.7	2.1	N/A	N/A	N/A	N/A	0.6	N/A
Min.		b.d.l.	4.0	12.7	32.1	b.d.l.	2.5	b.d.l.	b.d.l.	6.9	0.9	b.d.l.	b.d.l.	29.0	1.0	b.d.l.	b.d.l.	b.d.l.	b.d.l.	b.d.l.	b.d.l.
Max.		b.d.l.	6.6	13.8	36.3	0.6	3.0	b.d.l.	0.3	14.0	1.3	b.d.l.	b.d.l.	30.2	4.9	b.d.l.	b.d.l.	b.d.l.	b.d.l.	1.0	b.d.l.
630-3866 (3)	CBT IV	b.d.l.	1.2	2.5	68.2	b.d.l.	0.9	b.d.l.	0.2	4.9	b.d.l.	b.d.l.	b.d.l.	21.5	0.5	b.d.l.	b.d.l.	b.d.l.	b.d.l.	b.d.l.	b.d.l.
Std. Dev		N/A	0.2	0.4	3.0	N/A	0.1	N/A	0.2	0.9	N/A	N/A	N/A	2.4	0.8	N/A	N/A	N/A	N/A	N/A	N/A
Min.		b.d.l.	1.0	2.0	64.7	b.d.l.	0.8	b.d.l.	b.d.l.	4.0	b.d.l.	b.d.l.	b.d.l.	19.7	b.d.l.	b.d.l.	b.d.l.	b.d.l.	b.d.l.	b.d.l.	b.d.l.
Max.		b.d.l.	1.4	2.8	69.9	b.d.l.	1.0	b.d.l.	0.5	5.7	b.d.l.	b.d.l.	b.d.l.	24.3	1.5	b.d.l.	b.d.l.	b.d.l.	b.d.l.	b.d.l.	b.d.l.
637-4219 (3)	CBT IV	b.d.l.	12.0	1.4	34.7	0.7	1.6	b.d.l.	0.3	13.8	0.2	b.d.l.	0.5	32.5	2.4	b.d.l.	0.1	b.d.l.	b.d.l.	b.d.l.	b.d.l.
Std. Dev		N/A	0.9	0.1	2.4	0.1	0.2	N/A	0.0	2.2	0.0	N/A	0.1	0.4	0.7	N/A	0.1	N/A	N/A	N/A	N/A
Min.		b.d.l.	11.1	1.4	33.0	0.6	1.4	b.d.l.	0.3	11.5	0.1	b.d.l.	0.4	32.0	1.6	b.d.l.	b.d.l.	b.d.l.	b.d.l.	b.d.l.	b.d.l.
Max.		b.d.l.	12.8	1.5	37.4	0.7	1.9	b.d.l.	0.3	15.8	0.2	b.d.l.	0.5	32.7	2.8	b.d.l.	0.2	b.d.l.	b.d.l.	b.d.l.	b.d.l.
637-4221A (4)	CBT IV	b.d.l.	9.4	3.4	48.7	0.2	0.5	b.d.l.	0.5	12.2	b.d.l.	b.d.l.	b.d.l.	21.9	1.6	b.d.l.	1.6	b.d.l.	b.d.l.	b.d.l.	b.d.l.
Std. Dev		N/A	0.6	0.2	2.1	0.0	0.1	N/A	0.3	1.3	N/A	N/A	N/A	1.0	0.6	N/A	0.2	N/A	N/A	N/A	N/A
Min.		b.d.l.	8.5	3.1	47.1	0.2	0.4	b.d.l.	0.3	10.3	b.d.l.	b.d.l.	b.d.l.	20.4	1.0	b.d.l.	1.4	b.d.l.	b.d.l.	b.d.l.	b.d.l.
Max.		b.d.l.	9.7	3.6	51.8	0.3	0.6	b.d.l.	0.9	13.0	b.d.l.	b.d.l.	b.d.l.	22.5	2.5	b.d.l.	1.9	b.d.l.	b.d.l.	b.d.l.	b.d.l.
637-4225 (3)	CBT IV	b.d.l.	4.4	0.4	46.1	b.d.l.	3.1	b.d.l.	b.d.l.	15.7	b.d.l.	b.d.l.	b.d.l.	27.8	2.5	b.d.l.	b.d.l.	b.d.l.	b.d.l.	b.d.l.	b.d.l.
Std. Dev		N/A	0.1	0.7	1.7	N/A	2.1	N/A	N/A	1.1	N/A	N/A	N/A	2.1	0.5	N/A	N/A	N/A	N/A	N/A	N/A
Min.		b.d.l.	4.3	b.d.l.	44.8	b.d.l.	1.6	b.d.l.	b.d.l.	14.7	b.d.l.	b.d.l.	b.d.l.	26.5	1.9	b.d.l.	b.d.l.	b.d.l.	b.d.l.	b.d.l.	b.d.l.
Max.		b.d.l.	4.4	1.2	48.0	b.d.l.	5.5	b.d.l.	b.d.l.	17.0	b.d.l.	b.d.l.	b.d.l.	30.2	3.0	b.d.l.	b.d.l.	b.d.l.	b.d.l.	b.d.l.	b.d.l.

Sample	Phase	Na ₂ O	MgO	Al ₂ O ₃	SiO ₂	P ₂ O ₅	SO ₃	Cl	K ₂ O	CaO	TiO ₂	CrO	MnO	FeO	CuO	As ₂ O ₃	ZnO	BaO	NiO	ZrO	MoO
637-4226a (3)	CBT IV	b.d.l.	3.2	0.7	45.5	b.d.l.	0.3	b.d.l.	b.d.l.	16.0	b.d.l.	b.d.l.	0.6	31.8	1.9	b.d.l.	b.d.l.	b.d.l.	b.d.l.	b.d.l.	b.d.l.
Std. Dev		N/A	0.0	0.1	0.7	N/A	0.5	N/A	N/A	0.8	N/A	N/A	0.1	1.2	0.9	N/A	N/A	N/A	N/A	N/A	N/A
Min.		b.d.l.	3.1	0.6	44.7	b.d.l.	b.d.l.	b.d.l.	b.d.l.	15.2	b.d.l.	b.d.l.	0.5	31.1	0.9	b.d.l.	b.d.l.	b.d.l.	b.d.l.	b.d.l.	b.d.l.
Max.		b.d.l.	3.2	0.8	46.2	b.d.l.	0.8	b.d.l.	b.d.l.	16.8	b.d.l.	b.d.l.	0.8	33.2	2.8	b.d.l.	b.d.l.	b.d.l.	b.d.l.	b.d.l.	b.d.l.
637-4226B (3)	CBT IV	0.4	4.0	3.3	26.8	0.7	1.2	b.d.l.	1.3	6.4	0.3	b.d.l.	0.3	52.6	2.4	b.d.l.	b.d.l.	b.d.l.	0.2	b.d.l.	b.d.l.
Std. Dev		0.2	0.3	0.2	0.2	0.0	0.3	N/A	0.3	1.0	0.1	N/A	0.1	0.5	1.4	N/A	N/A	N/A	0.1	N/A	N/A
Min.		0.2	3.7	3.2	26.6	0.7	1.0	b.d.l.	1.0	5.3	0.2	b.d.l.	0.2	52.2	1.6	b.d.l.	b.d.l.	b.d.l.	0.1	b.d.l.	b.d.l.
Max.		0.5	4.2	3.5	26.9	0.8	1.5	b.d.l.	1.5	7.1	0.3	b.d.l.	0.3	53.1	4.0	b.d.l.	b.d.l.	b.d.l.	0.3	b.d.l.	b.d.l.
637-4456 (3)	CBT IV	b.d.l.	11.3	2.4	38.9	0.7	1.5	b.d.l.	0.6	13.6	0.1	b.d.l.	b.d.l.	30.3	0.8	b.d.l.	b.d.l.	b.d.l.	b.d.l.	b.d.l.	b.d.l.
Std. Dev		N/A	0.5	0.1	0.9	0.1	0.1	N/A	0.1	1.0	0.2	N/A	N/A	1.9	0.5	N/A	N/A	N/A	N/A	N/A	N/A
Min.		b.d.l.	11.0	2.4	38.3	0.6	1.4	b.d.l.	0.4	12.5	b.d.l.	b.d.l.	b.d.l.	28.4	b.d.l.	b.d.l.	b.d.l.	b.d.l.	b.d.l.	b.d.l.	
Max.		b.d.l.	11.9	2.5	39.9	0.8	1.6	b.d.l.	0.7	14.3	0.4	b.d.l.	b.d.l.	32.2	0.9	b.d.l.	b.d.l.	b.d.l.	b.d.l.	b.d.l.	b.d.l.
646-4500 (3)	CBT IV	b.d.l.	3.1	1.6	46.3	b.d.l.	0.5	b.d.l.	0.2	15.9	b.d.l.	b.d.l.	0.6	30.3	1.6	b.d.l.	b.d.l.	b.d.l.	b.d.l.	b.d.l.	b.d.l.
Std. Dev		N/A	0.3	0.0	2.2	N/A	0.1	N/A	0.1	1.1	N/A	N/A	0.1	0.2	0.9	N/A	N/A	N/A	N/A	N/A	N/A
Min.		b.d.l.	2.8	1.6	44.9	b.d.l.	0.5	b.d.l.	0.0	14.8	b.d.l.	b.d.l.	0.5	30.0	0.8	b.d.l.	b.d.l.	b.d.l.	b.d.l.	b.d.l.	b.d.l.
Max.		b.d.l.	3.3	1.6	48.8	b.d.l.	0.6	b.d.l.	0.2	17.0	b.d.l.	b.d.l.	0.6	30.5	2.5	b.d.l.	b.d.l.	b.d.l.	b.d.l.	b.d.l.	b.d.l.
722-4629 (7)	SPEU	b.d.l.	2.3	2.3	55.8	b.d.l.	2.6	b.d.l.	0.7	2.6	b.d.l.	b.d.l.	b.d.l.	30.3	2.6	b.d.l.	0.4	b.d.l.	b.d.l.	b.d.l.	0.2
Std. Dev		N/A	3.1	2.2	16.5	N/A	2.6	N/A	0.7	1.4	N/A	N/A	N/A	17.6	1.1	N/A	0.6	N/A	N/A	N/A	0.6
Min.		b.d.l.	b.d.l.	1.1	37.8	b.d.l.	b.d.l.	b.d.l.	b.d.l.	1.0	b.d.l.	b.d.l.	b.d.l.	12.2	1.0	b.d.l.	b.d.l.	b.d.l.	b.d.l.	b.d.l.	b.d.l.
Max.		b.d.l.	7.7	6.5	74.1	b.d.l.	6.1	b.d.l.	1.7	4.4	b.d.l.	b.d.l.	b.d.l.	49.1	4.0	b.d.l.	1.3	b.d.l.	b.d.l.	b.d.l.	1.4
55-440 (10)	CBT III	b.d.l.	4.1	0.2	49.8	b.d.l.	0.8	b.d.l.	b.d.l.	18.9	b.d.l.	b.d.l.	0.5	25.2	0.6	b.d.l.	b.d.l.	b.d.l.	b.d.l.	b.d.l.	b.d.l.
Std. Dev		N/A	1.6	0.4	2.5	N/A	0.9	N/A	N/A	1.8	N/A	N/A	0.1	4.7	0.5	N/A	N/A	N/A	N/A	N/A	N/A
Min.		b.d.l.	2.6	b.d.l.	45.5	b.d.l.	b.d.l.	b.d.l.	b.d.l.	16.3	b.d.l.	b.d.l.	0.4	19.9	b.d.l.	b.d.l.	b.d.l.	b.d.l.	b.d.l.	b.d.l.	b.d.l.
Max.		b.d.l.	7.3	1.0	53.0	b.d.l.	2.4	b.d.l.	b.d.l.	21.3	b.d.l.	b.d.l.	0.6	33.0	1.5	b.d.l.	b.d.l.	b.d.l.	b.d.l.	b.d.l.	b.d.l.

Sample	Phase	Na ₂ O	MgO	Al ₂ O ₃	SiO ₂	P ₂ O ₅	SO ₃	Cl	K ₂ O	CaO	TiO ₂	CrO	MnO	FeO	CuO	As ₂ O ₃	ZnO	BaO	NiO	ZrO	MoO
60-3094 (6)	CBT III	b.d.l.	2.5	14.4	38.7	b.d.l.	5.1	b.d.l.	0.9	1.8	0.5	b.d.l.	b.d.l.	34.7	1.4	b.d.l.	b.d.l.	b.d.l.	b.d.l.	b.d.l.	b.d.l.
Std. Dev		N/A	2.5	4.9	6.3	N/A	2.8	N/A	0.4	1.5	0.6	N/A	N/A	3.8	1.6	N/A	N/A	N/A	N/A	N/A	N/A
Min.		b.d.l.	b.d.l.	9.8	32.8	b.d.l.	2.4	b.d.l.	0.4	0.3	0.0	b.d.l.	b.d.l.	31.2	b.d.l.	b.d.l.	b.d.l.	b.d.l.	b.d.l.	b.d.l.	b.d.l.
Max.		b.d.l.	5.6	19.8	44.9	b.d.l.	8.8	b.d.l.	1.2	3.5	1.2	b.d.l.	b.d.l.	39.7	2.8	b.d.l.	b.d.l.	b.d.l.	b.d.l.	b.d.l.	b.d.l.
440-3566 (3)	CBT III	b.d.l.	11.4	3.0	40.1	0.8	1.9	b.d.l.	1.1	19.2	0.2	b.d.l.	b.d.l.	21.8	0.4	b.d.l.	b.d.l.	b.d.l.	b.d.l.	b.d.l.	b.d.l.
Std. Dev		N/A	3.4	0.9	1.4	0.2	0.6	N/A	0.2	2.8	0.2	N/A	N/A	0.6	0.7	N/A	N/A	N/A	N/A	N/A	N/A
Min.		b.d.l.	9.3	2.5	38.7	0.6	1.3	b.d.l.	0.9	16.5	b.d.l.	b.d.l.	b.d.l.	21.1	b.d.l.	b.d.l.	b.d.l.	b.d.l.	b.d.l.	b.d.l.	b.d.l.
Max.		b.d.l.	15.3	4.1	41.6	0.9	2.5	b.d.l.	1.3	22.2	0.3	b.d.l.	b.d.l.	22.3	1.3	b.d.l.	b.d.l.	b.d.l.	b.d.l.	b.d.l.	b.d.l.
440-3567A (3)	CBT III	0.2	10.0	2.7	37.9	0.8	1.3	b.d.l.	1.2	22.5	0.2	b.d.l.	0.3	22.7	0.2	b.d.l.	b.d.l.	b.d.l.	b.d.l.	b.d.l.	b.d.l.
Std. Dev		0.0	0.3	0.1	1.3	0.0	0.1	N/A	0.1	1.1	0.0	N/A	0.0	2.6	0.1	N/A	N/A	N/A	N/A	N/A	N/A
Min.		0.2	9.7	2.6	36.4	0.8	1.2	b.d.l.	1.0	21.4	0.2	b.d.l.	0.3	20.7	0.1	b.d.l.	b.d.l.	b.d.l.	b.d.l.	b.d.l.	b.d.l.
Max.		0.3	10.4	2.7	39.0	0.9	1.3	b.d.l.	1.3	23.6	0.3	b.d.l.	0.4	25.7	0.3	b.d.l.	b.d.l.	b.d.l.	b.d.l.	b.d.l.	b.d.l.
440-3567B (4)	CBT III	0.2	11.1	3.0	39.1	0.9	1.2	b.d.l.	1.3	20.7	0.3	b.d.l.	0.3	21.8	0.2	b.d.l.	b.d.l.	b.d.l.	b.d.l.	b.d.l.	b.d.l.
Std. Dev		0.1	1.3	0.3	0.3	0.1	0.1	N/A	0.1	0.4	0.0	N/A	0.0	0.4	0.0	N/A	N/A	N/A	N/A	N/A	N/A
Min.		0.2	10.0	2.8	38.8	0.8	1.1	b.d.l.	1.2	20.4	0.2	b.d.l.	0.2	21.5	0.2	b.d.l.	b.d.l.	b.d.l.	b.d.l.	b.d.l.	b.d.l.
Max.		0.4	12.3	3.5	39.6	0.9	1.4	b.d.l.	1.4	21.3	0.3	b.d.l.	0.3	22.4	0.3	b.d.l.	b.d.l.	b.d.l.	b.d.l.	b.d.l.	b.d.l.
643-4264 (3)	CBT III	b.d.l.	13.7	2.2	39.1	0.8	1.7	0.0	0.4	7.6	0.3	b.d.l.	0.4	33.4	0.8	b.d.l.	b.d.l.	b.d.l.	b.d.l.	b.d.l.	b.d.l.
Std. Dev		N/A	3.1	0.3	0.7	0.1	1.3	b.d.l.	0.2	1.5	0.2	N/A	0.2	2.4	0.1	N/A	N/A	N/A	N/A	N/A	N/A
Min.		b.d.l.	10.2	1.8	38.5	0.8	0.3	N/A	0.2	6.2	0.0	b.d.l.	0.0	30.9	0.6	b.d.l.	b.d.l.	b.d.l.	b.d.l.	b.d.l.	b.d.l.
Max.		b.d.l.	16.2	2.4	39.9	0.9	2.9	b.d.l.	0.6	9.1	0.3	b.d.l.	0.4	35.6	0.9	b.d.l.	b.d.l.	b.d.l.	b.d.l.	b.d.l.	b.d.l.
890-5774 (3)	CBT III	b.d.l.	5.5	0.6	25.2	0.3	1.0	b.d.l.	0.3	2.2	b.d.l.	b.d.l.	b.d.l.	59.6	5.1	b.d.l.	b.d.l.	0.2	b.d.l.	b.d.l.	b.d.l.
Std. Dev		N/A	0.7	0.2	1.3	0.1	0.2	N/A	0.1	0.6	N/A	N/A	N/A	2.6	1.4	N/A	N/A	0.1	N/A	N/A	N/A
Min.		b.d.l.	4.7	0.4	24.2	0.2	0.8	b.d.l.	0.2	1.6	b.d.l.	b.d.l.	b.d.l.	57.9	4.0	b.d.l.	b.d.l.	0.1	b.d.l.	b.d.l.	b.d.l.
Max.		b.d.l.	6.0	0.8	26.6	0.3	1.1	b.d.l.	0.3	2.7	b.d.l.	b.d.l.	b.d.l.	62.7	6.6	b.d.l.	b.d.l.	0.4	b.d.l.	b.d.l.	b.d.l.

Sample	Phase	Na ₂ O	MgO	Al ₂ O ₃	SiO ₂	P ₂ O ₅	SO ₃	Cl	K ₂ O	CaO	TiO ₂	CrO	MnO	FeO	CuO	As ₂ O ₃	ZnO	BaO	NiO	ZrO	MoO
777-5161 (3)	FPEU	b.d.l.	16.5	2.8	37.0	0.7	1.8	b.d.l.	0.8	14.4	b.d.l.	b.d.l.	b.d.l.	25.6	1.3	b.d.l.	b.d.l.	b.d.l.	b.d.l.	b.d.l.	b.d.l.
Std. Dev		N/A	1.2	0.1	0.7	0.1	1.0	N/A	0.1	2.1	N/A	N/A	N/A	1.3	0.8	N/A	N/A	N/A	N/A	N/A	N/A
Min.		b.d.l.	15.6	2.7	36.5	0.6	1.3	b.d.l.	0.7	11.9	b.d.l.	b.d.l.	b.d.l.	24.1	b.d.l.	b.d.l.	b.d.l.	b.d.l.	b.d.l.	b.d.l.	b.d.l.
Max.		b.d.l.	17.8	2.9	37.8	0.8	3.0	b.d.l.	0.9	15.8	b.d.l.	b.d.l.	b.d.l.	26.4	1.3	b.d.l.	b.d.l.	b.d.l.	b.d.l.	b.d.l.	b.d.l.
836-4860 (4)		CBT II	b.d.l.	3.8	0.8	44.4	b.d.l.	1.8	b.d.l.	b.d.l.	14.6	b.d.l.	b.d.l.	0.5	32.3	1.9	b.d.l.	b.d.l.	b.d.l.	b.d.l.	b.d.l.
Std. Dev	N/A		0.5	0.2	1.0	N/A	1.0	N/A	N/A	1.2	N/A	N/A	0.0	0.4	1.2	N/A	N/A	N/A	N/A	N/A	N/A
Min.	b.d.l.		3.1	0.6	43.2	b.d.l.	1.0	b.d.l.	b.d.l.	12.8	b.d.l.	b.d.l.	0.5	31.7	1.1	b.d.l.	b.d.l.	b.d.l.	b.d.l.	b.d.l.	b.d.l.
Max.	b.d.l.		4.3	1.0	45.2	b.d.l.	3.2	b.d.l.	b.d.l.	15.4	b.d.l.	b.d.l.	0.6	32.6	3.6	b.d.l.	b.d.l.	b.d.l.	b.d.l.	b.d.l.	b.d.l.
842-4890 (3)	CBT II		b.d.l.	1.2	6.0	37.6	b.d.l.	3.0	b.d.l.	0.3	2.1	0.6	b.d.l.	b.d.l.	48.8	0.4	b.d.l.	b.d.l.	b.d.l.	b.d.l.	b.d.l.
Std. Dev		N/A	0.2	0.6	0.2	N/A	0.4	N/A	0.0	0.2	0.1	N/A	N/A	1.1	0.1	N/A	N/A	N/A	N/A	N/A	N/A
Min.		b.d.l.	1.1	5.6	37.3	b.d.l.	2.6	b.d.l.	0.3	1.9	0.5	b.d.l.	b.d.l.	47.8	0.3	b.d.l.	b.d.l.	b.d.l.	b.d.l.	b.d.l.	b.d.l.
Max.		b.d.l.	1.4	6.8	37.8	b.d.l.	3.4	b.d.l.	0.3	2.2	0.6	b.d.l.	b.d.l.	50.0	0.5	b.d.l.	b.d.l.	b.d.l.	b.d.l.	b.d.l.	b.d.l.
97-3588		CBT I/II	0.3	9.4	2.7	40.5	0.8	b.d.l.	b.d.l.	1.0	4.3	0.3	b.d.l.	0.2	38.3	2.1	b.d.l.	b.d.l.	b.d.l.	0.2	b.d.l.
Std. Dev	0.0		1.2	0.2	0.3	0.0	N/A	N/A	0.1	0.3	0.0	N/A	0.0	0.4	0.2	N/A	N/A	N/A	0.1	N/A	N/A
Min.	0.3		8.0	2.6	40.2	0.7	b.d.l.	b.d.l.	1.0	4.1	0.3	b.d.l.	0.1	37.8	1.9	b.d.l.	b.d.l.	b.d.l.	0.1	b.d.l.	b.d.l.
Max.	0.4		10.2	2.9	40.8	0.8	b.d.l.	b.d.l.	1.1	4.6	0.3	b.d.l.	0.2	38.6	2.3	b.d.l.	b.d.l.	b.d.l.	0.3	b.d.l.	b.d.l.
210-299 (4)	CBT I		b.d.l.	3.8	0.7	45.9	b.d.l.	1.3	b.d.l.	b.d.l.	17.0	b.d.l.	b.d.l.	0.5	28.9	1.9	b.d.l.	b.d.l.	b.d.l.	b.d.l.	b.d.l.
Std. Dev		N/A	0.8	0.3	2.0	N/A	0.7	N/A	N/A	0.6	N/A	N/A	0.1	1.7	0.6	N/A	N/A	N/A	N/A	N/A	N/A
Min.		b.d.l.	3.2	0.5	43.6	b.d.l.	0.7	b.d.l.	b.d.l.	16.3	b.d.l.	b.d.l.	0.4	26.5	1.1	b.d.l.	b.d.l.	b.d.l.	b.d.l.	b.d.l.	b.d.l.
Max.		b.d.l.	5.0	1.1	48.5	b.d.l.	2.0	b.d.l.	b.d.l.	17.7	b.d.l.	b.d.l.	0.6	30.2	2.6	b.d.l.	b.d.l.	b.d.l.	b.d.l.	b.d.l.	b.d.l.
251-984 (3)		CBT I	b.d.l.	13.0	4.8	43.4	0.7	0.4	b.d.l.	0.7	14.3	0.4	b.d.l.	b.d.l.	17.6	4.7	b.d.l.	b.d.l.	b.d.l.	b.d.l.	b.d.l.
Std. Dev	N/A		0.6	0.1	0.6	0.1	0.2	N/A	0.0	1.7	0.0	N/A	N/A	0.3	2.3	N/A	N/A	N/A	N/A	N/A	N/A
Min.	b.d.l.		12.3	4.7	43.0	0.6	0.5	b.d.l.	0.7	12.4	0.4	b.d.l.	b.d.l.	17.3	3.1	b.d.l.	b.d.l.	b.d.l.	b.d.l.	b.d.l.	b.d.l.
Max.	b.d.l.		13.4	4.9	44.1	0.7	0.8	b.d.l.	0.7	15.6	0.4	b.d.l.	b.d.l.	17.8	7.3	b.d.l.	b.d.l.	b.d.l.	b.d.l.	b.d.l.	b.d.l.

B.5 Copper prills in slag

Composition of copper prills in copper smelting slag from Çamlıbel as determined by WDS. Each result is the mean of several point analyses of individual prills larger than 10 µm. All results in wt%. Numbers in parentheses next to the sample name refer to the number of analyses.

	Se	Zn	Cu	As	Fe	Ag	O	Ni	Cl	Al	Co	Sn	Sr	Sb	Bi	Pb	Mn	Au	S	Hg	Ti	Si	Total
629-3860 (11)	b.d.l	b.d.l	96.712	0.005	3.464	0.010	0.064	0.008	0.015	0.001	0.005	0.004	b.d.l	0.002	0.019	b.d.l	0.015	0.024	0.013	b.d.l	0.024	0.013	100.396
Std. dev.	N/A	N/A	0.335	0.009	0.381	0.004	0.058	0.008	0.008	0.002	0.004	0.007	N/A	0.005	0.020	N/A	0.010	0.020	0.012	N/A	0.005	0.022	0.386
Min.	b.d.l	b.d.l	96.311	b.d.l	2.956	0.004	0.001	b.d.l	b.d.l	b.d.l	b.d.l	b.d.l	b.d.l	b.d.l	b.d.l	b.d.l	b.d.l	b.d.l	b.d.l	b.d.l	0.016	b.d.l	99.849
Max.	b.d.l	b.d.l	97.243	0.027	4.116	0.018	0.178	0.021	0.023	0.007	0.012	0.022	b.d.l	0.015	0.064	b.d.l	0.038	0.062	0.040	b.d.l	0.031	0.074	100.949
722-4629 (12)	b.d.l	0.092	96.299	0.010	2.796	0.017	0.219	0.004	0.016	0.012	0.000	0.004	b.d.l	0.002	0.022	b.d.l	0.004	0.011	0.046	b.d.l	0.015	0.128	99.697
Std. dev.	N/A	0.067	0.840	0.016	0.408	0.006	0.140	0.005	0.011	0.018	0.001	0.004	N/A	0.003	0.029	N/A	0.007	0.014	0.097	N/A	0.007	0.146	0.981
Min.	b.d.l	0.041	94.667	b.d.l	2.162	0.007	b.d.l	b.d.l	b.d.l	b.d.l	b.d.l	b.d.l	b.d.l	b.d.l	b.d.l	b.d.l	b.d.l	b.d.l	0.003	b.d.l	0.002	0.018	98.028
Max.	b.d.l	0.216	97.334	0.051	3.244	0.026	0.464	0.012	0.038	0.058	0.002	0.013	b.d.l	0.010	0.068	b.d.l	0.024	0.045	0.347	b.d.l	0.029	0.524	101.249

B.6 Ore minerals and tailings

Mean bulk composition of mineral ores and tailings. All results in wt% and normalized to 100%. Numbers in parentheses next to the sample name refer to the number of bulk analyses.

Sample	Na ₂ O	MgO	Al ₂ O ₃	SiO ₂	P ₂ O ₅	SO ₃	K ₂ O	CaO	TiO ₂	CrO	MnO	FeO	CuO
637-4218 (3)	b.d.l.	1.0	2.1	77.1	b.d.l.	4.7	b.d.l.	0.2	0.2	b.d.l.	b.d.l.	11.9	2.8
Std. Dev.	N/A	0.9	1.9	2.2	N/A	5.8	N/A	0.3	0.3	N/A	N/A	4.8	1.9
Min.	b.d.l.	b.d.l.	b.d.l.	74.7	b.d.l.	1.1	b.d.l.	b.d.l.	b.d.l.	b.d.l.	b.d.l.	6.3	1.1
Max.	b.d.l.	1.6	3.6	79.2	b.d.l.	11.4	b.d.l.	0.5	0.6	b.d.l.	b.d.l.	15.0	4.9
753-5028 (3)	b.d.l.	5.1	b.d.l.	11.8	b.d.l.	b.d.l.	b.d.l.	b.d.l.	b.d.l.	b.d.l.	b.d.l.	83.1	b.d.l.
Std. Dev.	N/A	2.7	N/A	4.9	N/A	N/A	N/A	N/A	N/A	N/A	N/A	7.5	N/A
Min.	b.d.l.	3.4	b.d.l.	8.7	b.d.l.	b.d.l.	b.d.l.	b.d.l.	b.d.l.	b.d.l.	b.d.l.	74.4	b.d.l.
Max.	b.d.l.	8.1	b.d.l.	17.4	b.d.l.	b.d.l.	b.d.l.	b.d.l.	b.d.l.	b.d.l.	b.d.l.	87.9	b.d.l.
838-4870 (3)	b.d.l.	33.3	1.9	48.5	b.d.l.	b.d.l.	b.d.l.	0.4	b.d.l.	0.7	0.2	13.2	1.9
Std. Dev.	N/A	0.7	0.3	0.9	N/A	N/A	N/A	0.3	N/A	0.1	0.3	1.4	0.1
Min.	b.d.l.	32.5	1.6	47.7	b.d.l.	b.d.l.	b.d.l.	b.d.l.	b.d.l.	0.6	b.d.l.	12.1	1.8
Max.	b.d.l.	33.8	2.2	49.5	b.d.l.	b.d.l.	b.d.l.	0.6	b.d.l.	0.8	0.6	14.7	2.0
727-4659 (6)	b.d.l.	13.3	6.9	49.7	b.d.l.	b.d.l.	0.5	5.3	1.3	b.d.l.	b.d.l.	8.8	14.2
Std. Dev.	N/A	1.6	1.0	1.3	N/A	N/A	0.3	0.7	0.2	N/A	N/A	1.1	5.6
Min.	b.d.l.	11.3	5.9	47.7	b.d.l.	b.d.l.	b.d.l.	4.3	1.0	b.d.l.	b.d.l.	7.2	7.8
Max.	b.d.l.	15.2	8.1	51.4	b.d.l.	b.d.l.	0.8	6.0	1.5	b.d.l.	b.d.l.	10.4	20.4
799-5218 (5)	b.d.l.	b.d.l.	3.1	41.2	b.d.l.	21.1	5.6	1.3	b.d.l.	b.d.l.	b.d.l.	27.8	b.d.l.
Std. Dev.	N/A	N/A	2.6	21.3	N/A	8.3	2.6	1.5	N/A	N/A	N/A	9.7	N/A
Min.	b.d.l.	b.d.l.	b.d.l.	10.6	b.d.l.	13.7	3.2	b.d.l.	b.d.l.	b.d.l.	b.d.l.	17.1	b.d.l.
Max.	b.d.l.	b.d.l.	6.5	63.6	b.d.l.	34.3	9.5	3.0	b.d.l.	b.d.l.	b.d.l.	43.2	b.d.l.
934-5409 (3)	b.d.l.	b.d.l.	b.d.l.	15.6	b.d.l.	29.6	7.6	b.d.l.	b.d.l.	b.d.l.	b.d.l.	47.2	b.d.l.
Std. Dev.	N/A	N/A	N/A	12.7	N/A	4.3	1.4	N/A	N/A	N/A	N/A	9.6	N/A
Min.	b.d.l.	b.d.l.	b.d.l.	3.0	b.d.l.	25.0	5.9	b.d.l.	b.d.l.	b.d.l.	b.d.l.	33.9	b.d.l.
Max.	b.d.l.	b.d.l.	b.d.l.	32.4	b.d.l.	34.3	8.8	b.d.l.	b.d.l.	b.d.l.	b.d.l.	56.2	b.d.l.
257-3130 (3)	b.d.l.	0.2	b.d.l.	6.4	b.d.l.	4.2	0.9	0.5	b.d.l.	b.d.l.	0.2	84.1	3.7
Std. Dev.	N/A	0.4	N/A	0.8	N/A	2.4	0.9	0.1	N/A	N/A	0.4	2.5	0.4
Min.	b.d.l.	b.d.l.	b.d.l.	5.5	b.d.l.	2.1	b.d.l.	0.4	b.d.l.	b.d.l.	b.d.l.	81.4	3.3
Max.	b.d.l.	0.7	b.d.l.	7.1	b.d.l.	6.8	1.7	0.5	b.d.l.	b.d.l.	0.6	86.3	4.1
637-4222 (3)	b.d.l.	3.6	7.2	43.7	b.d.l.	6.9	b.d.l.	b.d.l.	1.4	b.d.l.	0.6	33.1	3.9
Std. Dev.	N/A	0.7	1.1	6.0	N/A	1.7	N/A	N/A	0.2	N/A	0.3	3.1	0.6
Min.	b.d.l.	2.9	5.9	38.9	b.d.l.	5.6	b.d.l.	b.d.l.	1.1	b.d.l.	b.d.l.	29.6	3.3
Max.	b.d.l.	4.2	8.0	50.5	b.d.l.	8.8	b.d.l.	b.d.l.	1.5	b.d.l.	0.6	35.2	4.4
877-5695 (3)	2.2	5.4	12.1	33.2	0.4	0.7	1.8	0.6	2.1	b.d.l.	b.d.l.	41.5	b.d.l.
Std. Dev.	1.3	0.8	2.1	5.5	0.1	0.5	0.4	0.2	0.3	N/A	N/A	9.3	N/A
Min.	1.0	4.6	10.1	27.2	0.4	0.3	1.4	0.5	1.8	b.d.l.	b.d.l.	32.7	b.d.l.
Max.	3.5	6.2	14.3	38.1	0.5	1.3	2.1	0.8	2.2	b.d.l.	b.d.l.	51.3	b.d.l.
585-4328A (3)	b.d.l.	0.8	0.2	6.7	0.4	0.5	b.d.l.	1.4	b.d.l.	b.d.l.	0.3	89.4	0.5
Std. Dev.	N/A	0.1	N/A	0.4	0.2	0.1	N/A	0.7	N/A	N/A	0.1	0.6	0.1
Min.	b.d.l.	0.7	0.2	6.3	0.2	0.4	b.d.l.	0.7	b.d.l.	b.d.l.	0.2	88.8	0.4
Max.	b.d.l.	0.8	0.2	7.0	0.5	0.6	b.d.l.	2.0	b.d.l.	b.d.l.	0.5	90.1	0.5

Sample	Na ₂ O	MgO	Al ₂ O ₃	SiO ₂	P ₂ O ₅	SO ₃	K ₂ O	CaO	TiO ₂	CrO	MnO	FeO	CuO
585-4328B (3)	b.d.l.	7.3	0.2	17.8	0.4	0.4	b.d.l.	0.7	b.d.l.	0.5	b.d.l.	72.5	0.3
Std. Dev.	N/A	6.5	0.0	9.7	0.1	0.1	N/A	0.3	N/A	0.2	N/A	16.0	0.1
Min.	b.d.l.	0.6	0.1	6.9	0.3	0.4	b.d.l.	0.4	b.d.l.	0.3	b.d.l.	59.1	0.2
Max.	b.d.l.	13.5	0.2	25.7	0.5	0.5	b.d.l.	1.0	b.d.l.	0.7	b.d.l.	90.2	0.4
619-3497 (3)	b.d.l.	b.d.l.	0.4	6.1	b.d.l.	0.9	N/A	0.5	b.d.l.	b.d.l.	b.d.l.	70.1	21.9
Std. Dev.	N/A	N/A	0.4	3.4	N/A	0.5	N/A	0.1	N/A	N/A	N/A	3.6	7.3
Min.	b.d.l.	b.d.l.	b.d.l.	3.1	b.d.l.	0.5	b.d.l.	0.4	b.d.l.	b.d.l.	b.d.l.	65.1	14.5
Max.	b.d.l.	b.d.l.	0.8	9.2	b.d.l.	1.5	b.d.l.	0.6	b.d.l.	b.d.l.	b.d.l.	73.7	30.7
637-4221B (4)	b.d.l.	b.d.l.	0.1	39.6	b.d.l.	9.9	b.d.l.	0.2	b.d.l.	b.d.l.	b.d.l.	41.2	8.9
Std. Dev.	N/A	N/A	0.0	13.8	N/A	2.7	N/A	0.1	N/A	N/A	N/A	9.6	1.9
Min.	b.d.l.	b.d.l.	0.1	32.0	b.d.l.	6.3	b.d.l.	0.1	b.d.l.	b.d.l.	b.d.l.	27.1	6.1
Max.	b.d.l.	b.d.l.	0.2	60.3	b.d.l.	12.7	b.d.l.	0.3	b.d.l.	b.d.l.	b.d.l.	47.5	9.9
Karakaya (3)	b.d.l.	28.7	12.2	41.0	b.d.l.	b.d.l.	b.d.l.	b.d.l.	0.6	0.2	b.d.l.	15.6	1.7
Std. Dev.	b.d.l.	0.8	1.2	1.6	b.d.l.	b.d.l.	b.d.l.	b.d.l.	0.5	0.3	b.d.l.	0.9	0.6
Min.	b.d.l.	27.9	10.9	39.4	b.d.l.	b.d.l.	b.d.l.	b.d.l.	b.d.l.	b.d.l.	b.d.l.	14.7	1.1
Max.	b.d.l.	29.5	13.2	42.7	b.d.l.	b.d.l.	b.d.l.	b.d.l.	1.0	0.5	b.d.l.	16.5	2.2

B.7 Lead isotopes

Lead isotope ratios of copper alloy objects, minerals, and slag. Results were obtained by LA-MC-ICP-MS for samples submitted to NIGL while samples sent to CEZA were prepared through wet chemical dissolution before analysis by MC-ICP-MS.

Sample	Type	Phase	Laboratory	Lead (ppm)	²⁰⁸ Pb/ ²⁰⁶ Pb mean	²⁰⁸ Pb/ ²⁰⁶ Pb 2σ	²⁰⁷ Pb/ ²⁰⁶ Pb mean	²⁰⁷ Pb/ ²⁰⁶ Pb 2σ	²⁰⁸ Pb/ ²⁰⁴ Pb mean	²⁰⁸ Pb/ ²⁰⁴ Pb 2σ	²⁰⁷ Pb/ ²⁰⁴ Pb calc mean	²⁰⁷ Pb/ ²⁰⁴ Pb calc 2σ	²⁰⁶ Pb/ ²⁰⁴ Pb calc mean	²⁰⁶ Pb/ ²⁰⁴ Pb calc 2σ
523-3368	Needle	Surface	NIGL	>0.15	2.0892	0.001	0.847	0.0001	38.422	0.0666	18.389	0.0321	18.389	0.0321
624-3828	Perforator	Surface	NIGL	<0.01	-	-	-	-	-	-	-	-	-	-
624-3831	Perforator	Surface	NIGL	<0.02	-	-	-	-	-	-	-	-	-	-
632-4621	Droplet	CBT IV	CEZA	9	2.0774	± 0.0001	0.83858	± 0.00003	38.756	± 0.010	15.645	± 0.004	18.656	± 0.005
709-4551	Needle	CBT III	CEZA	22	2.0692	± 0.0001	0.83074	± 0.00004	39.075	± 0.010	15.688	± 0.004	18.884	± 0.006
543-3670	Pin	CBT III	CEZA	b.d.l.	-	-	-	-	-	-	-	-	-	-
773-5138	Perforator	FPEU	CEZA	b.d.l.	-	-	-	-	-	-	-	-	-	-
909-5313	Lead Wire	CBT II	CEZA	lead	2.0717	± 0.0002	0.83526	± 0.00006	38.753	± 0.008	15.624	± 0.004	18.706	± 0.002
877-5692	Perforator	CBT I	CEZA	b.d.l.	-	-	-	-	-	-	-	-	-	-
637-4221B	Mineral	CBT IV	CEZA	36.9	2.1191	± 0.0001	0.86955	± 0.00003	37.671	± 0.013	15.458	± 0.006	17.777	± 0.006
585-4328	Mineral	CBT II	CEZA	1.4	1.6924	± 0.0001	0.70155	± 0.00004	37.856	± 0.007	15.692	± 0.002	22.368	± 0.003
753-5028	Mineral	CBT II	CEZA	2.2	1.4874	± 0.0001	0.62234	± 0.00002	37.845	± 0.006	15.835	± 0.002	25.444	± 0.004
934-5409	Mineral	CBT I	CEZA	0.8	2.1078	± 0.0001	0.85957	± 0.00004	37.938	± 0.001	15.471	± 0.001	17.999	± 0.001
karakaya	Mineral	Surface	CEZA	0.4	-	-	-	-	-	-	-	-	-	-
222-326B	Slag	CBT IV	CEZA	0.9	2.1223	± 0.0001	0.86881	± 0.00005	37.809	± 0.006	15.478	± 0.003	17.815	± 0.004
443-3708	Slag	CBT IV	CEZA	2.3	2.0986	± 0.0001	0.85319	± 0.00004	38.228	± 0.007	15.542	± 0.003	18.216	± 0.003
637-4219	Slag	CBT IV	CEZA	17.3	2.1209	± 0.0003	0.86622	± 0.00008	37.852	± 0.007	15.459	± 0.001	17.847	± 0.004
643-4264	Slag	CBT III	CEZA	4.8	2.1193	± 0.0001	0.86497	± 0.00002	37.902	± 0.004	15.469	± 0.001	17.884	± 0.001
440-3567	Slag	CBT III	CEZA	0.5	-	-	-	-	-	-	-	-	-	-
842-4890	Slag	CBT II	CEZA	15.7	2.1167	± 0.0001	0.87697	± 0.00001	37.605	± 0.003	15.580	± 0.001	17.766	± 0.001
836-4860	Slag	CBT II	CEZA	1.9	2.0736	± 0.0001	0.84309	± 0.00003	38.374	± 0.009	15.602	± 0.004	18.506	± 0.004
210-299	Slag	CBT I	CEZA	1.7	2.0701	± 0.0003	0.83923	± 0.00007	38.587	± 0.009	15.643	± 0.002	18.640	± 0.001

B.8 Objects

Results were determined by WDS on a JEOL-JXA8200 electron microprobe. All values are normalized to 100 wt%. Elements below the minimum detection limit are indicated by "MDL" in the dark grey cells. Cells with light grey shading indicate values at 1-3 times the minimum detection limit. Values just above calculated MDLs are questionable, and those less than 3 times the MDL are likely to be relatively imprecise. Unpublished results provided by Lloyd Weeks.

Sample	Type	Phase	Point Count	Cu	As	Ag	Zn	Ni	S	Pb	Fe	Sn	Au	Hg	Si	Cl	Total	Pre-norm Total
523-3368	Awl (bent)	unknown	5	93.6	4.41	0.059	0.037	1.87	MDL	MDL	MDL	MDL	MDL	MDL	MDL	0.007	100	95.4
442-3596	Blade	CBT IV	5	96	3.73	0.067	0.067	MDL	0.015	MDL	MDL	MDL	MDL	0.063	MDL	0.003	100	99.2
624-3828	Awl (bent)	CBT IV	5	94.7	5.04	0.084	0.065	MDL	MDL	MDL	0.028	MDL	MDL	MDL	MDL	0.005	100	90.4
624-3831	Awl (bent)	CBT IV	5	96.6	2.88	0.038	0.063	MDL	0.014	MDL	MDL	MDL	0.019	MDL	0.339	0.013	100	93.1
624-3847	Awl	CBT IV	8	95.4	4.19	0.031	0.074	0.133	0.026	MDL	MDL	MDL	0.019	MDL	MDL	0.047	100	80.7
632-4621	Droplet	CBT IV	10	98.5	1.21	0.034	0.028	0.169	MDL	MDL	MDL	0.007	MDL	MDL	MDL	0.006	100	98.1
740-4936	Perforator	SPEU	7	94.4	5.25	0.045	0.1	MDL	0.169	MDL	MDL	0.013	MDL	MDL	MDL	0.004	100	98.8
740-4970	Needle	SPEU	10	96	3.48	0.064	0.035	MDL	MDL	MDL	MDL	MDL	MDL	MDL	0.42	0.005	100	98.4
543-63670	Awl (bent)	CBT III	7	95.8	3.86	0.143	0.062	MDL	MDL	MDL	MDL	MDL	MDL	0.051	MDL	0.037	100	96
709-4551	Needle	CBT III	10	97.6	2.15	0.035	MDL	0.108	0.082	MDL	MDL	0.018	MDL	MDL	MDL	0.004	100	97.6
748-4994	Needle	CBT III	10	97.3	2.5	0.063	0.026	MDL	0.01	MDL	MDL	0.016	MDL	MDL	MDL	0.01	100	97.1
773-5138	Point	FPEU	10	95.9	3.82	0.05	0.023	MDL	0.188	MDL	MDL	0.013	MDL	MDL	MDL	0.004	100	98.2
774-5144	Perforator	FPEU	10	95.8	3.95	0.072	0.021	MDL	0.008	MDL	MDL	0.008	0.021	MDL	0.083	0.003	100	99
777-5160	Needle	FPEU	10	93.8	5.99	0.04	MDL	0.009	MDL	MDL	0.041	0.015	MDL	MDL	MDL	0.004	100	97.4
837-4865	Needle	CBT II	10	97.5	2.33	0.04	0.014	MDL	0.012	MDL	MDL	0.014	MDL	0.054	MDL	0.005	100	97.5
909-5313	Wire	CBT II	5	0.11	MDL	MDL	MDL	MDL	MDL	99.71	0.024	0.017	MDL	0.074	MDL	0.066	100	100.5
950-6119	Point	CBT II	10	97.1	2.71	0.038	0.04	MDL	MDL	MDL	MDL	0.012	MDL	0.057	MDL	0.004	100	98.9
976-6127	Needle	CBT II	9	95.3	4.39	0.043	0.013	0.143	0.016	MDL	MDL	0.013	MDL	MDL	MDL	0.004	100	98.5
843-4900	Perforator	CBT I	8	94.9	4.61	0.073	0.034	MDL	MDL	MDL	MDL	MDL	MDL	MDL	0.343	0.003	100	98.9
877-5692	Perforator	CBT I	10	96.3	3.64	0.024	0.026	MDL	0.008	MDL	MDL	0.015	MDL	MDL	MDL	0.009	100	96.6
877-5707	Needle	CBT I	10	96.6	2.92	0.054	0.039	0.038	MDL	MDL	MDL	0.016	MDL	MDL	0.268	0.007	100	98.6
972-6091	Needle	CBT I	10	95.1	4.62	0.035	0.022	0.211	MDL	MDL	MDL	0.01	MDL	MDL	0.082	0.004	100	98.6
Avg. MDL (ppm)				131±7	229±14	92±5	110±6	77±4	79±6	194±8	123±5	68±3	131±6	488±31	43±4	37±2		

Appendix C Arisman

C.1 Technical ceramics

Mean bulk composition of crucible and furnace fabrics. All results in wt% and normalized to 100%. Numbers in parentheses next to the sample name refer to the number of bulk analyses.

		Area	Na ₂ O	MgO	Al ₂ O ₃	SiO ₂	P ₂ O ₃	SO ₃	Cl	K ₂ O	CaO	TiO ₂	MnO	FeO	CuO	As ₂ O ₃	SrO		
Crucible	Copper	FG-030116B (3)	A	2.3	2.9	13.1	53.7	b.d.l.	0.3	0.4	2.7	17.7	0.5	b.d.l.	5.9	0.1	0.4	b.d.l.	
		Std. Dev.		0.3	0.3	0.8	3.0	N/A	0.5	0.1	0.4	3.6	0.1	N/A	0.1	0.2	0.2	N/A	
		Min.		2.1	2.6	12.5	50.3	b.d.l.	b.d.l.	0.4	2.3	15.0	0.6	b.d.l.	5.7	b.d.l.	0.2	b.d.l.	
		Max.		2.6	3.2	14.0	55.5	b.d.l.	0.9	0.5	3.0	21.8	0.8	b.d.l.	6.0	0.3	0.5	b.d.l.	
	Speiss	unknown	FG-011993 (6)	unknown	2.1	3.4	13.9	52.0	0.4	0.5	0.3	3.0	17.8	0.6	0.1	5.4	b.d.l.	0.6	b.d.l.
			Std. Dev.		0.4	0.5	1.1	3.1	0.2	0.1	0.1	0.3	3.1	0.1	0.0	0.7	N/A	0.3	N/A
			Min.		1.7	2.9	12.1	48.5	0.2	0.3	0.1	2.4	11.8	0.5	0.1	4.4	b.d.l.	0.2	b.d.l.
			Max.		2.8	4.0	15.4	57.3	0.6	0.6	0.5	3.3	20.1	0.9	0.2	6.1	b.d.l.	1.0	b.d.l.
		A	FG-030119A (5)	A	1.5	3.4	12.4	45.8	b.d.l.	7.8	0.6	2.2	19.4	0.1	b.d.l.	5.3	b.d.l.	1.0	b.d.l.
			Std. Dev.		0.5	0.2	1.7	3.7	N/A	6.0	0.1	0.7	1.9	0.3	N/A	0.4	N/A	2.2	N/A
			Min.		0.8	3.2	10.3	39.9	b.d.l.	b.d.l.	0.4	1.3	17.3	b.d.l.	b.d.l.	4.7	b.d.l.	b.d.l.	b.d.l.
			Max.		2.0	3.7	14.7	49.1	b.d.l.	16.3	0.7	2.9	22.2	0.6	b.d.l.	5.8	b.d.l.	5.0	b.d.l.
	A	FG-030119B (3)	A	2.9	3.9	14.6	54.0	b.d.l.	b.d.l.	b.d.l.	1.3	14.3	0.8	b.d.l.	7.4	b.d.l.	0.7	b.d.l.	
		Std. Dev.		0.1	0.2	0.2	0.8	N/A	N/A	N/A	0.3	1.4	0.1	N/A	0.3	N/A	0.4	N/A	
		Min.		2.8	3.8	14.4	53.5	b.d.l.	b.d.l.	b.d.l.	1.1	13.3	0.7	b.d.l.	7.2	b.d.l.	0.4	b.d.l.	
		Max.		3.0	4.1	14.7	54.6	b.d.l.	b.d.l.	b.d.l.	1.5	15.2	0.8	b.d.l.	7.7	b.d.l.	1.0	b.d.l.	

		Area	Na ₂ O	MgO	Al ₂ O ₃	SiO ₂	P ₂ O ₃	SO ₃	Cl	K ₂ O	CaO	TiO ₂	MnO	FeO	CuO	As ₂ O ₃	SrO	
Furnace	Copper	FG-012235A (6)	unknown	1.9	4.2	14.2	51.0	0.4	2.7	0.5	3.3	10.6	0.7	0.1	5.7	0.3	4.3	b.d.l.
		Std. Dev.		0.9	0.6	1.2	1.5	0.1	2.0	0.1	0.6	1.9	0.1	0.0	1.1	0.2	1.5	N/A
		Min.		1.1	3.3	12.9	49.4	0.2	1.0	0.2	2.6	7.5	0.5	0.1	4.5	0.1	2.0	b.d.l.
		Max.		3.0	4.9	15.7	53.9	0.6	6.7	0.4	4.2	13.3	0.8	0.2	7.0	0.6	6.0	b.d.l.
		FG-030113 (6)	unknown	1.9	3.5	13.8	59.9	b.d.l.	b.d.l.	0.3	2.8	9.1	0.8	b.d.l.	5.9	1.3	0.7	b.d.l.
		Std. Dev.		0.1	0.6	0.6	1.4	N/A	N/A	0.0	0.2	2.2	0.2	N/A	1.2	1.6	0.7	N/A
		Min.		1.7	2.8	13.1	58.0	b.d.l.	b.d.l.	0.0	2.7	6.6	0.6	b.d.l.	4.7	0.0	0.0	b.d.l.
		Max.		2.0	4.4	14.8	62.5	b.d.l.	b.d.l.	0.0	3.1	11.6	1.0	b.d.l.	7.9	3.8	1.5	b.d.l.
		FG-030665 (3)	A	2.9	3.1	14.5	66.7	b.d.l.	b.d.l.	0.2	3.2	3.3	0.6	b.d.l.	5.6	b.d.l.	b.d.l.	b.d.l.
		Std. Dev.		0.4	0.2	0.5	2.6	N/A	N/A	0.0	0.4	0.4	0.1	N/A	0.7	N/A	N/A	N/A
		Min.		2.7	2.9	14.2	63.7	b.d.l.	b.d.l.	0.2	2.8	2.8	0.6	b.d.l.	5.0	b.d.l.	b.d.l.	b.d.l.
		Max.		3.4	3.3	15.1	68.3	b.d.l.	b.d.l.	0.3	3.6	3.7	0.7	b.d.l.	6.3	b.d.l.	b.d.l.	b.d.l.
	FG-030669 (3)	unknown	2.5	2.4	14.4	63.8	b.d.l.	b.d.l.	0.3	3.7	5.6	0.7	b.d.l.	6.5	b.d.l.	b.d.l.	b.d.l.	
	Std. Dev.		0.4	0.9	0.8	1.8	N/A	N/A	0.1	1.7	2.2	0.1	N/A	0.7	N/A	N/A	N/A	
	Min.		2.1	1.4	13.6	62.2	b.d.l.	b.d.l.	0.2	2.5	3.3	0.7	b.d.l.	5.7	b.d.l.	b.d.l.	b.d.l.	
	Max.		2.8	3.1	15.1	65.8	b.d.l.	b.d.l.	0.5	5.6	7.7	0.9	b.d.l.	6.9	b.d.l.	b.d.l.	b.d.l.	
	FG-030670 (3)	unknown	2.4	4.5	15.7	51.6	b.d.l.	b.d.l.	0.3	1.3	16.9	0.7	b.d.l.	6.7	b.d.l.	b.d.l.	b.d.l.	
	Std. Dev.		0.1	0.1	0.4	1.1	N/A	N/A	0.0	0.3	0.9	0.0	N/A	0.2	N/A	N/A	N/A	
	Min.		2.3	4.5	15.4	50.7	b.d.l.	b.d.l.	0.3	1.0	16.0	0.7	b.d.l.	6.5	b.d.l.	b.d.l.	b.d.l.	
	Max.		2.5	4.6	16.2	52.7	b.d.l.	b.d.l.	0.4	1.6	17.7	0.8	b.d.l.	6.9	b.d.l.	b.d.l.	b.d.l.	
	FG-030671 (3)	unknown	2.1	4.5	16.5	53.5	b.d.l.	b.d.l.	0.2	1.6	13.9	0.7	0.2	6.8	b.d.l.	b.d.l.	b.d.l.	
	Std. Dev.		0.1	0.1	0.3	0.8	N/A	N/A	0.1	0.2	0.6	0.0	0.0	0.1	N/A	N/A	N/A	
	Min.		2.0	4.4	16.3	52.6	b.d.l.	b.d.l.	0.2	1.4	13.3	0.7	0.2	6.7	b.d.l.	b.d.l.	b.d.l.	
	Max.		2.2	4.6	16.8	54.1	b.d.l.	b.d.l.	0.3	1.7	14.5	0.8	0.2	6.8	b.d.l.	b.d.l.	b.d.l.	
	FG-030672A (3)	unknown	2.6	2.5	14.4	68.5	b.d.l.	b.d.l.	0.2	3.0	2.2	0.6	b.d.l.	6.1	b.d.l.	b.d.l.	b.d.l.	
	Std. Dev.		0.1	0.2	0.8	1.8	N/A	N/A	0.0	0.2	0.3	0.1	N/A	0.6	N/A	N/A	N/A	
	Min.		2.5	2.3	13.6	66.5	b.d.l.	b.d.l.	0.1	2.9	1.9	0.6	b.d.l.	5.6	b.d.l.	b.d.l.	b.d.l.	
	Max.		2.8	2.7	15.3	70.1	b.d.l.	b.d.l.	0.2	3.1	2.6	0.7	b.d.l.	6.7	b.d.l.	b.d.l.	b.d.l.	

		Area	Na ₂ O	MgO	Al ₂ O ₃	SiO ₂	P ₂ O ₃	SO ₃	Cl	K ₂ O	CaO	TiO ₂	MnO	FeO	CuO	As ₂ O ₃	SrO
Furnace	Copper	FG-030672B (3)	2.5	2.6	14.8	67.7	b.d.l.	b.d.l.	b.d.l.	3.2	1.9	0.7	b.d.l.	6.6	0.3	b.d.l.	b.d.l.
		Std. Dev.	0.1	0.1	0.0	1.0	N/A	N/A	N/A	0.1	0.3	0.0	N/A	0.6	0.2	N/A	N/A
		Min.	2.4	2.4	14.8	66.8	b.d.l.	b.d.l.	b.d.l.	3.1	1.5	0.7	b.d.l.	6.0	0.0	b.d.l.	b.d.l.
		Max.	2.6	2.7	14.8	68.8	b.d.l.	b.d.l.	b.d.l.	3.3	2.1	0.7	b.d.l.	7.1	0.3	b.d.l.	b.d.l.
		FG-993152A (3)	2.2	2.9	13.8	55.1	0.2	0.4	0.2	2.7	15.6	0.6	0.2	5.7	0.2	0.3	b.d.l.
		Std. Dev.	0.1	0.1	0.4	3.6	0.1	0.0	0.0	0.0	2.6	0.0	0.0	0.6	0.1	0.1	N/A
		Min.	2.1	2.8	13.6	52.4	0.2	0.3	0.2	2.6	12.7	0.6	0.1	5.1	0.1	0.3	b.d.l.
		Max.	2.3	3.0	14.3	59.2	0.3	0.4	0.2	2.7	17.3	0.6	0.2	6.3	0.2	0.4	b.d.l.
		FG-993152B (3)	1.9	2.3	13.1	49.8	b.d.l.	1.3	0.1	2.4	7.0	0.7	0.3	17.0	3.7	0.5	b.d.l.
		Std. Dev.	0.6	0.8	1.9	4.1	N/A	0.7	0.1	0.9	1.4	0.1	0.2	10.0	2.4	0.1	N/A
		Min.	1.4	1.6	11.3	46.9	b.d.l.	0.5	0.1	1.6	5.7	0.6	0.2	5.8	2.1	0.4	b.d.l.
		Max.	2.5	3.2	15.1	54.5	b.d.l.	1.9	0.2	3.3	8.4	0.7	0.5	24.8	6.4	0.6	b.d.l.
Furnace	Speiss	FG-012232 (3)	2.4	3.5	13.3	53.9	0.3	0.8	0.6	3.3	16.1	0.7	0.2	5.0	b.d.l.	b.d.l.	b.d.l.
		Std. Dev.	0.0	0.2	0.3	3.4	0.1	0.3	0.1	0.3	2.2	0.1	0.0	0.2	N/A	N/A	N/A
		Min.	2.4	3.3	13.0	50.8	0.2	0.5	0.5	2.9	13.7	0.6	0.1	4.8	b.d.l.	b.d.l.	b.d.l.
		Max.	2.4	3.7	13.5	57.5	0.4	1.0	0.7	3.5	18.1	0.7	0.2	5.2	b.d.l.	b.d.l.	b.d.l.
		FG-012234 (3)	2.4	2.7	15.3	66.0	b.d.l.	b.d.l.	0.1	3.3	2.4	0.8	b.d.l.	7.0	b.d.l.	b.d.l.	b.d.l.
		Std. Dev.	0.1	0.1	1.3	1.8	N/A	N/A	0.1	0.4	0.5	0.1	N/A	0.1	N/A	N/A	N/A
		Min.	2.4	2.6	14.0	64.2	b.d.l.	b.d.l.	0.2	3.1	2.0	0.7	b.d.l.	6.8	b.d.l.	b.d.l.	b.d.l.
		Max.	2.6	2.8	16.7	67.8	b.d.l.	b.d.l.	0.3	3.8	2.9	0.9	b.d.l.	7.1	b.d.l.	b.d.l.	b.d.l.
		FG-030117 (3)	1.7	3.1	11.5	56.3	b.d.l.	b.d.l.	b.d.l.	2.6	18.9	b.d.l.	b.d.l.	5.2	b.d.l.	0.7	b.d.l.
		Std. Dev.	0.1	0.2	0.5	2.7	N/A	N/A	N/A	0.2	2.7	N/A	N/A	0.8	N/A	0.4	N/A
		Min.	1.6	2.9	11.2	54.0	b.d.l.	b.d.l.	b.d.l.	2.3	17.2	b.d.l.	b.d.l.	4.5	b.d.l.	0.4	b.d.l.
		Max.	1.9	3.3	12.0	59.3	b.d.l.	b.d.l.	b.d.l.	2.8	22.1	b.d.l.	b.d.l.	6.1	b.d.l.	1.1	b.d.l.

Mean bulk composition of lime plaster erroneously categorised as technical ceramic. All results in wt% and normalized to 100%. Numbers in parentheses next to the sample name refer to the number of bulk analyses.

			Area	Na ₂ O	MgO	Al ₂ O ₃	SiO ₂	P ₂ O ₃	SO ₃	Cl	K ₂ O	CaO	TiO ₂	MnO	FeO	CuO	As ₂ O ₃	SrO
Other	Lime	FG-000117D (1)	surface	b.d.l.	2.2	0.5	1.4	b.d.l.	0.7	b.d.l.	b.d.l.	94.7	b.d.l.	b.d.l.	0.3	b.d.l.	b.d.l.	0.4

C.2 Minerals

Mean bulk composition of two minerals recovered from Arisman which were thought to have been ores. All results in wt% and normalized to 100%. Numbers in parentheses next to the sample name refer to the number of bulk analyses.

	Area	Al ₂ O ₃	SiO ₂	P ₂ O ₃	SO ₂	Cl	CaO	TiO ₂	MnO	FeO	CuO	As ₂ O ₃
FG-011992 (1)	Unknown	19.7	30.5	b.d.l.	b.d.l.	b.d.l.	27.7	0.8	0.4	20.9	b.d.l.	b.d.l.
FG-030125 (3)	Unnknown	0.7	3.3	0.3	0.7	0.1	0.3	b.d.l.	b.d.l.	94.3	0.1	0.3
Std. Devl		0.1	0.1	0.0	0.1	0.0	0.1	N/A	N/A	0.2	0.1	0.1
Min.		0.7	3.2	0.2	0.6	0.1	0.3	b.d.l.	b.d.l.	94.1	0.0	0.3
Max.		0.9	3.4	0.3	0.8	0.1	0.4	b.d.l.	b.d.l.	94.4	0.2	0.4

C.3 Slags

Mean bulk composition of copper and arsenical copper smelting slags. All results in wt% and normalized to 100%. Numbers in parentheses next to the sample name refer to the number of bulk analyses.

	Area	Na ₂ O	MgO	Al ₂ O ₃	SiO ₂	P ₂ O ₅	SO ₃	Cl	K ₂ O	CaO	TiO ₂	Mn	FeO	CuO	ZnO	As ₂ O ₃	BaO	PbO
FG-030121 (10)	unknown	0.7	1.4	4.7	40.3	0.1	0.4	b.d.l.	1.4	7.1	b.d.l.	b.d.l.	42.2	1.7	b.d.l.	b.d.l.	b.d.l.	b.d.l.
Std. dev.		0.5	0.5	1.5	9.5	0.2	1.0	N/A	0.5	3.5	N/A	N/A	11.7	1.9	N/A	N/A	N/A	N/A
Min.		0.0	0.6	2.1	21.3	b.d.l.	b.d.l.	b.d.l.	0.4	1.2	b.d.l.	b.d.l.	35.4	b.d.l.	b.d.l.	b.d.l.	b.d.l.	b.d.l.
Max.		1.5	2.2	6.5	52.6	0.6	3.0	b.d.l.	2.0	11.0	b.d.l.	b.d.l.	69.1	6.3	b.d.l.	b.d.l.	b.d.l.	b.d.l.
FG-030120 (5)	A	1.2	2.2	9.6	47.2	b.d.l.	b.d.l.	0.3	2.6	13.6	0.4	0.2	20.2	2.6	b.d.l.	b.d.l.	b.d.l.	b.d.l.
Std. dev.		0.2	0.2	0.3	1.3	N/A	N/A	0.2	0.2	0.4	0.2	0.3	1.5	0.4	N/A	N/A	N/A	N/A
Min.		1.0	2.0	9.3	45.5	b.d.l.	b.d.l.	b.d.l.	2.3	13.1	b.d.l.	b.d.l.	18.2	2.2	b.d.l.	b.d.l.	b.d.l.	b.d.l.
Max.		1.5	2.4	10.1	48.9	b.d.l.	b.d.l.	0.4	2.9	14.2	0.5	0.5	22.3	3.2	b.d.l.	b.d.l.	b.d.l.	b.d.l.
FG-000115 (3)	A	1.8	2.6	8.5	39.6	b.d.l.	b.d.l.	0.1	1.9	13.2	0.3	b.d.l.	29.1	2.9	b.d.l.	0.1	b.d.l.	b.d.l.
Std. dev.		0.1	0.1	0.3	1.3	N/A	N/A	0.2	0.1	0.4	0.3	N/A	1.3	0.6	N/A	0.2	N/A	N/A
Min.		1.7	2.5	8.1	38.1	b.d.l.	b.d.l.	b.d.l.	1.8	12.8	b.d.l.	b.d.l.	27.8	2.3	b.d.l.	b.d.l.	b.d.l.	b.d.l.
Max.		1.9	2.7	8.7	40.3	b.d.l.	b.d.l.	0.3	1.9	13.5	0.5	b.d.l.	30.4	3.4	b.d.l.	0.3	b.d.l.	b.d.l.
FG-000119 (3)	A	1.1	2.5	8.4	39.9	0.6	b.d.l.	0.3	1.3	15.1	0.2	2.4	27.2	1.0	b.d.l.	0.1	b.d.l.	b.d.l.
Std. dev.		0.7	0.2	0.2	0.7	0.4	N/A	0.2	0.1	0.3	0.3	0.1	1.0	0.5	N/A	0.2	N/A	N/A
Min.		b.d.l.	2.3	8.1	39.2	b.d.l.	b.d.l.	b.d.l.	1.2	14.8	b.d.l.	2.3	26.0	0.6	b.d.l.	b.d.l.	b.d.l.	b.d.l.
Max.		1.5	2.7	8.6	40.7	0.9	b.d.l.	0.4	1.5	15.4	0.5	2.6	28.2	1.8	b.d.l.	0.3	b.d.l.	b.d.l.
FG-030114 (3)	A	2.5	2.3	8.2	42.6	b.d.l.	0.2	0.3	2.3	14.4	0.4	0.5	23.6	2.4	b.d.l.	0.3	b.d.l.	b.d.l.
Std. dev.		0.2	0.0	0.3	0.5	N/A	0.3	0.1	0.1	0.9	0.3	0.1	0.4	0.3	N/A	0.1	N/A	N/A
Min.		2.3	2.3	7.8	42.0	b.d.l.	0.0	0.3	2.2	13.4	0.0	0.4	23.4	2.1	b.d.l.	0.3	b.d.l.	b.d.l.
Max.		2.7	2.4	8.4	43.1	b.d.l.	0.5	0.4	2.3	15.0	0.6	0.5	24.0	2.8	b.d.l.	0.4	b.d.l.	b.d.l.
FG-000117A (3)	unknown	3.0	1.9	10.3	47.2	0.4	b.d.l.	b.d.l.	2.9	13.9	0.4	0.3	16.7	2.2	b.d.l.	0.8	b.d.l.	b.d.l.
Std. dev.		0.8	0.3	0.5	0.3	0.1	N/A	N/A	0.0	0.2	0.1	0.0	0.5	0.8	N/A	0.8	N/A	N/A
Min.		2.4	1.6	9.7	47.0	0.3	b.d.l.	b.d.l.	2.9	13.7	0.3	0.2	16.1	1.6	b.d.l.	0.2	b.d.l.	b.d.l.
Max.		3.8	2.1	10.6	47.6	0.5	b.d.l.	b.d.l.	2.9	14.1	0.4	0.3	17.1	3.1	b.d.l.	0.7	b.d.l.	b.d.l.

	Area	Na ₂ O	MgO	Al ₂ O ₃	SiO ₂	P ₂ O ₅	SO ₃	Cl	K ₂ O	CaO	TiO ₂	Mn	FeO	CuO	ZnO	As ₂ O ₃	BaO	PbO
FG-000117B (3)	unknown	1.8	2.2	8.4	37.4	0.3	0.3	0.1	2.2	13.8	0.4	0.3	32.4	0.4	b.d.l.	b.d.l.	b.d.l.	b.d.l.
Std. dev.		0.1	0.1	0.1	0.3	0.0	0.1	0.0	0.1	0.3	0.0	0.0	0.6	0.1	N/A	N/A	N/A	N/A
Min.		1.7	2.1	8.3	37.1	0.3	0.3	0.1	2.2	13.5	0.4	0.3	31.9	0.3	b.d.l.	b.d.l.	b.d.l.	b.d.l.
Max.		1.9	2.3	8.5	37.6	0.3	0.4	0.1	2.3	14.0	0.5	0.3	33.0	0.4	b.d.l.	b.d.l.	b.d.l.	b.d.l.
FG-000117C (3)	unknown	1.4	2.1	6.4	41.6	0.2	0.2	0.6	1.5	16.8	0.3	0.9	25.6	2.3	b.d.l.	b.d.l.	b.d.l.	b.d.l.
Std. dev.		0.2	0.0	0.2	0.8	0.0	0.2	0.1	0.1	0.8	0.0	0.0	0.9	0.6	N/A	N/A	N/A	N/A
Min.		1.2	2.0	6.2	40.7	0.2	0.1	0.5	1.4	16.0	0.3	0.9	24.6	1.9	b.d.l.	b.d.l.	b.d.l.	b.d.l.
Max.		1.6	2.1	6.6	42.3	0.3	0.5	0.7	1.6	17.7	0.4	1.0	26.4	3.0	b.d.l.	b.d.l.	b.d.l.	b.d.l.
FG-000118A (3)	A	1.2	2.0	5.2	41.5	b.d.l.	b.d.l.	0.1	0.9	10.7	b.d.l.	b.d.l.	36.0	2.4	b.d.l.	b.d.l.	b.d.l.	b.d.l.
Std. dev.		0.3	0.1	0.2	0.5	N/A	N/A	0.0	0.2	0.3	N/A	N/A	0.6	0.4	N/A	N/A	N/A	N/A
Min.		0.9	1.9	5.0	40.9	b.d.l.	b.d.l.	0.1	0.7	10.4	b.d.l.	b.d.l.	35.4	2.1	b.d.l.	b.d.l.	b.d.l.	b.d.l.
Max.		1.4	2.1	5.3	41.8	b.d.l.	b.d.l.	0.2	1.0	11.0	b.d.l.	b.d.l.	36.5	2.8	b.d.l.	b.d.l.	b.d.l.	b.d.l.
FG-000123 (3)	unknown	0.8	2.0	8.8	41.9	b.d.l.	b.d.l.	0.1	2.0	14.2	0.4	0.4	26.0	2.2	0.3	0.9	b.d.l.	b.d.l.
Std. dev.		0.1	0.1	0.3	1.1	N/A	N/A	0.0	0.1	0.3	0.1	0.0	0.8	0.4	0.1	0.2	N/A	N/A
Min.		0.7	1.9	8.4	40.8	b.d.l.	b.d.l.	0.1	1.9	14.0	0.4	0.3	25.3	1.9	0.1	0.7	b.d.l.	b.d.l.
Max.		1.0	2.2	9.2	42.9	b.d.l.	b.d.l.	0.1	2.0	14.5	0.5	0.4	27.1	2.7	0.4	1.2	b.d.l.	b.d.l.
FG-012260A (3)	unknown	1.1	2.2	6.3	34.4	b.d.l.	0.3	0.3	1.2	11.2	0.3	2.8	37.3	2.1	0.5	b.d.l.	b.d.l.	b.d.l.
Std. dev.		0.0	0.1	0.2	1.7	N/A	0.1	0.1	0.1	0.8	0.1	0.1	1.9	0.8	0.0	N/A	N/A	N/A
Min.		1.1	2.1	6.1	33.0	b.d.l.	0.1	0.2	1.1	10.5	0.2	2.6	34.6	1.3	0.5	b.d.l.	b.d.l.	b.d.l.
Max.		1.2	2.4	6.6	36.6	b.d.l.	0.3	0.4	1.3	12.2	0.4	2.9	38.7	2.8	0.6	b.d.l.	b.d.l.	b.d.l.
FG-012260B (3)	unknown	1.0	2.1	6.3	33.7	b.d.l.	0.4	0.3	1.2	10.4	0.3	2.9	38.9	2.0	0.5	b.d.l.	b.d.l.	b.d.l.
Std. dev.		0.0	0.0	0.2	0.7	N/A	0.0	0.1	0.0	0.7	0.1	0.0	1.6	0.4	0.0	N/A	N/A	N/A
Min.		1.0	2.1	6.1	32.9	b.d.l.	0.4	0.2	1.2	9.9	0.2	2.9	37.1	1.6	0.5	b.d.l.	b.d.l.	b.d.l.
Max.		1.1	2.1	6.4	34.3	b.d.l.	0.5	0.4	1.3	11.1	0.3	2.9	40.2	2.4	0.5	b.d.l.	b.d.l.	b.d.l.

	Area	Na ₂ O	MgO	Al ₂ O ₃	SiO ₂	P ₂ O ₅	SO ₃	Cl	K ₂ O	CaO	TiO ₂	Mn	FeO	CuO	ZnO	As ₂ O ₃	BaO	PbO
FG-030115 (3)	A	1.9	3.7	12.1	41.9	0.3	b.d.l.	0.1	3.1	14.1	0.6	0.2	20.0	1.7	b.d.l.	0.3	b.d.l.	b.d.l.
Std. dev.		0.4	0.4	0.6	1.1	0.0	N/A	0.0	0.1	0.8	0.0	0.0	1.1	0.3	N/A	0.0	N/A	N/A
Min.		1.6	3.3	11.4	40.7	0.3	b.d.l.	0.1	3.0	13.5	0.6	0.2	18.9	1.4	b.d.l.	0.2	b.d.l.	b.d.l.
Max.		2.4	4.0	12.5	42.9	0.4	b.d.l.	0.1	3.2	14.9	0.6	0.3	21.1	1.9	b.d.l.	0.3	b.d.l.	b.d.l.
FG-030122B (4)	A	1.7	2.9	8.0	43.9	0.5	b.d.l.	0.2	2.0	15.3	0.5	0.3	23.9	0.6	0.2	0.0	b.d.l.	b.d.l.
Std. dev.		0.2	0.1	0.1	0.6	0.0	N/A	0.0	0.1	0.4	0.0	0.0	0.9	0.2	0.1	0.0	N/A	N/A
Min.		1.5	2.8	7.9	43.1	0.4	b.d.l.	0.1	2.0	14.7	0.5	0.3	23.2	0.4	0.2	b.d.l.	b.d.l.	b.d.l.
Max.		1.9	2.9	8.2	44.5	0.5	b.d.l.	0.2	2.1	15.7	0.6	0.3	25.3	0.8	0.3	0.1	b.d.l.	b.d.l.
FG-030123A (4)	A	0.9	1.6	5.9	44.1	0.4	b.d.l.	0.4	1.0	8.1	0.2	0.2	35.7	0.7	b.d.l.	b.d.l.	0.7	b.d.l.
Std. dev.		0.1	0.2	0.1	1.1	0.1	N/A	0.1	0.1	0.1	0.1	0.0	1.5	0.1	N/A	N/A	0.1	N/A
Min.		0.8	1.3	5.8	42.5	0.4	b.d.l.	0.4	0.9	8.1	0.1	0.1	34.7	0.6	b.d.l.	b.d.l.	0.6	b.d.l.
Max.		1.0	1.7	6.0	44.9	0.5	b.d.l.	0.5	1.1	8.2	0.3	0.2	37.8	0.9	b.d.l.	b.d.l.	0.9	b.d.l.
FG-030124A (3)	A	1.2	4.0	6.9	42.0	b.d.l.	b.d.l.	0.3	1.6	12.9	0.3	b.d.l.	28.6	2.2	b.d.l.	b.d.l.	b.d.l.	b.d.l.
Std. dev.		0.1	0.7	1.3	3.5	N/A	N/A	0.2	0.5	1.2	0.1	N/A	5.8	0.8	N/A	N/A	N/A	N/A
Min.		1.2	3.4	6.2	38.1	b.d.l.	b.d.l.	0.2	1.3	11.9	0.2	b.d.l.	23.4	1.4	b.d.l.	b.d.l.	b.d.l.	b.d.l.
Max.		1.4	4.8	8.5	44.8	b.d.l.	b.d.l.	0.5	2.1	14.2	0.5	b.d.l.	34.9	3.1	b.d.l.	b.d.l.	b.d.l.	b.d.l.
FG-030124B (3)	A	1.8	2.3	7.7	38.5	0.4	b.d.l.	0.2	1.9	13.3	0.4	0.4	29.2	2.9	b.d.l.	0.6	0.5	b.d.l.
Std. dev.		0.1	0.1	0.4	1.2	0.1	N/A	0.1	0.1	0.6	0.1	0.0	1.2	0.3	N/A	0.3	0.1	N/A
Min.		1.6	2.3	7.1	37.4	0.3	b.d.l.	0.1	1.8	12.4	0.3	0.3	28.5	2.6	b.d.l.	0.4	0.4	b.d.l.
Max.		1.9	2.4	8.0	40.3	0.4	b.d.l.	0.4	2.0	13.8	0.4	0.4	31.0	3.2	b.d.l.	0.9	0.6	b.d.l.
FG-030664 (3)	unknown	1.1	1.8	4.7	27.9	b.d.l.	0.9	0.2	0.9	16.6	0.3	b.d.l.	41.9	3.1	0.2	0.3	b.d.l.	b.d.l.
Std. dev.		0.0	0.4	0.8	0.9	N/A	0.2	0.2	0.1	4.6	0.1	N/A	4.2	0.6	0.0	0.2	N/A	N/A
Min.		1.1	1.4	4.1	27.1	b.d.l.	0.7	0.1	0.8	11.3	0.3	b.d.l.	37.8	2.5	0.2	0.2	b.d.l.	b.d.l.
Max.		1.2	2.2	5.6	28.9	b.d.l.	1.2	0.5	1.0	19.9	0.4	b.d.l.	46.1	3.6	0.3	0.5	b.d.l.	b.d.l.

	Area	Na ₂ O	MgO	Al ₂ O ₃	SiO ₂	P ₂ O ₅	SO ₃	Cl	K ₂ O	CaO	TiO ₂	Mn	FeO	CuO	ZnO	As ₂ O ₃	BaO	PbO
FG-030673 (4)	unknown	1.5	2.4	6.4	33.1	b.d.l.	0.6	b.d.l.	1.4	23.0	0.3	b.d.l.	30.2	0.7	b.d.l.	b.d.l.	0.3	b.d.l.
Std. dev.		0.2	0.2	1.0	2.4	N/A	0.2	N/A	0.2	2.4	0.0	N/A	6.0	0.3	N/A	N/A	0.3	N/A
Min.		1.2	2.2	4.9	29.5	b.d.l.	0.5	b.d.l.	1.1	19.4	0.2	b.d.l.	26.8	0.5	b.d.l.	b.d.l.	0.1	b.d.l.
Max.		1.7	2.6	7.1	34.4	b.d.l.	0.8	b.d.l.	1.6	24.4	0.3	b.d.l.	39.1	1.2	b.d.l.	b.d.l.	0.7	b.d.l.
FG-030974A (3)	unknown	3.1	3.4	8.9	41.5	0.3	0.2	b.d.l.	3.2	17.0	0.4	0.1	17.1	4.3	b.d.l.	0.3	b.d.l.	b.d.l.
Std. dev.		0.1	0.0	0.2	0.2	0.1	0.0	N/A	0.1	0.3	0.0	0.0	0.5	0.2	N/A	0.2	N/A	N/A
Min.		3.0	3.4	8.7	41.2	0.3	0.1	b.d.l.	3.1	16.7	0.4	0.1	16.7	4.0	b.d.l.	0.1	b.d.l.	b.d.l.
Max.		3.3	3.5	9.1	41.8	0.4	0.2	b.d.l.	3.2	17.3	0.5	0.2	17.9	4.5	b.d.l.	0.5	b.d.l.	b.d.l.
FG-030974B (3)	unknown	2.7	2.6	10.3	48.5	0.6	0.3	b.d.l.	2.4	12.8	0.6	0.2	18.7	0.3	b.d.l.	b.d.l.	b.d.l.	b.d.l.
Std. dev.		0.2	0.1	0.4	0.6	0.0	0.1	N/A	0.1	0.6	0.1	0.0	1.6	0.2	N/A	N/A	N/A	N/A
Min.		2.5	2.5	9.8	47.9	0.6	0.3	b.d.l.	2.3	12.2	0.5	0.2	17.7	0.2	b.d.l.	b.d.l.	b.d.l.	b.d.l.
Max.		2.9	2.7	10.5	49.1	0.6	0.4	b.d.l.	2.5	13.3	0.7	0.2	20.5	0.5	b.d.l.	b.d.l.	b.d.l.	b.d.l.
FG-030974E (3)	unknown	1.9	4.6	13.3	52.1	0.4	b.d.l.	0.0	3.0	16.1	0.7	0.2	7.0	0.5	b.d.l.	b.d.l.	b.d.l.	b.d.l.
Std. dev.		0.1	0.1	0.5	0.8	0.0	N/A	0.0	0.1	0.5	0.1	0.0	0.6	0.1	N/A	N/A	N/A	N/A
Min.		1.8	4.5	13.0	51.0	0.4	b.d.l.	0.2	2.9	15.4	0.6	0.2	6.2	0.4	b.d.l.	b.d.l.	b.d.l.	b.d.l.
Max.		1.9	4.7	14.0	52.9	0.4	b.d.l.	0.3	3.2	16.5	0.7	0.3	7.7	0.6	b.d.l.	b.d.l.	b.d.l.	b.d.l.
FG-993152C (3)	unknown	1.2	2.1	7.0	37.9	0.4	0.1	0.6	1.4	9.9	0.3	0.3	35.1	3.3	b.d.l.	0.2	b.d.l.	b.d.l.
Std. dev.		0.5	0.1	0.1	0.4	0.0	0.0	0.1	0.1	0.2	0.0	0.0	0.8	0.5	N/A	0.0	N/A	N/A
Min.		0.9	2.0	6.9	37.7	0.4	0.1	0.5	1.3	9.8	0.3	0.3	34.2	2.8	b.d.l.	0.2	b.d.l.	b.d.l.
Max.		1.8	2.2	7.2	38.4	0.5	0.1	0.7	1.5	10.2	0.4	0.3	35.8	3.7	b.d.l.	0.2	b.d.l.	b.d.l.
FG-993152D (3)	unknown	2.2	1.9	7.8	41.4	0.4	0.5	0.2	2.2	14.7	0.3	0.2	24.4	1.8	b.d.l.	0.5	1.5	b.d.l.
Std. dev.		0.0	0.0	0.3	0.6	0.1	0.4	0.1	0.1	0.2	0.1	0.0	0.9	0.7	N/A	0.1	0.2	N/A
Min.		2.2	1.8	7.6	40.8	0.3	0.2	0.1	2.1	14.4	0.3	0.2	23.5	1.2	b.d.l.	0.4	1.3	b.d.l.
Max.		2.3	1.9	8.1	42.0	0.4	0.9	0.4	2.2	14.9	0.4	0.3	25.3	2.5	b.d.l.	0.5	1.6	b.d.l.
FG-993155 (3)	unknown	1.4	4.1	7.7	38.8	0.3	b.d.l.	0.8	1.6	15.6	0.5	0.4	23.5	5.0	b.d.l.	0.3	b.d.l.	b.d.l.
Std. dev.		0.1	0.3	0.2	1.0	0.0	N/A	0.2	0.1	0.1	0.1	0.0	0.6	1.1	N/A	0.0	N/A	N/A
Min.		1.4	3.7	7.5	38.1	0.2	b.d.l.	0.5	1.5	15.5	0.4	0.4	22.8	3.5	b.d.l.	0.3	b.d.l.	b.d.l.
Max.		1.6	4.4	8.0	40.3	0.3	b.d.l.	1.0	1.8	15.7	0.5	0.5	24.0	6.1	b.d.l.	0.4	b.d.l.	b.d.l.

Mean bulk composition of copper and arsenical copper smelting slags with attached technical ceramic. All results in wt% and normalized to 100%. Numbers in parentheses next to the sample name refer to the number of bulk analyses.

	Area	Na ₂ O	MgO	Al ₂ O ₃	SiO ₂	P ₂ O ₅	SO ₃	Cl	K ₂ O	CaO	TiO ₂	Mn	FeO	CuO	ZnO	As ₂ O ₃	BaO	PbO
FG-030113 (4)	A	1.4	2.4	14.2	43.1	0.5	0.1	0.1	2.3	9.9	0.3	0.5	24.6	0.5	b.d.l.	b.d.l.	b.d.l.	b.d.l.
Std. dev.		0.1	0.1	0.3	0.4	0.1	0.1	b.d.l.	b.d.l.	0.5	b.d.l.	b.d.l.	0.4	0.2	N/A	N/A	N/A	N/A
Min.		1.4	2.4	13.8	42.7	0.4	0.1	0.1	2.3	9.7	0.3	0.4	24.1	0.3	b.d.l.	b.d.l.	b.d.l.	b.d.l.
Max.		1.5	2.5	14.5	43.5	0.5	0.2	0.1	2.3	10.7	0.3	0.5	25.2	0.8	b.d.l.	b.d.l.	b.d.l.	b.d.l.
FG-030665 (3)	unknown	1.7	3.4	9.9	42.2	0.4	0.2	0.0	1.7	21.9	0.5	0.3	16.3	0.6	b.d.l.	0.9	b.d.l.	b.d.l.
Std. dev.		0.5	1.0	1.5	2.8	0.2	0.1	0.0	0.2	3.6	0.1	0.2	5.7	0.3	N/A	1.0	N/A	N/A
Min.		1.0	2.4	8.1	38.3	0.2	0.0	0.0	1.6	18.7	0.5	0.1	10.9	0.2	b.d.l.	b.d.l.	b.d.l.	b.d.l.
Max.		2.1	4.5	11.7	44.9	0.7	0.3	0.0	2.0	27.1	0.7	0.4	23.8	1.0	b.d.l.	2.0	b.d.l.	b.d.l.
FG-030670 (3)	unknown	1.0	6.7	6.0	44.6	b.d.l.	b.d.l.	b.d.l.	1.4	10.6	0.3	0.8	24.9	2.0	0.2	b.d.l.	b.d.l.	1.5
Std. dev.		0.3	1.3	2.1	0.9	N/A	N/A	N/A	0.6	4.8	0.1	0.2	6.9	0.4	0.1	N/A	N/A	0.1
Min.		0.7	5.8	3.6	43.6	b.d.l.	b.d.l.	b.d.l.	0.7	5.1	0.2	0.7	20.5	1.7	0.1	b.d.l.	b.d.l.	1.3
Max.		1.2	8.2	7.4	45.3	b.d.l.	b.d.l.	b.d.l.	1.8	13.5	0.4	1.0	32.9	2.4	0.2	b.d.l.	b.d.l.	1.5
FG-030672A (3)	unknown	2.2	3.1	11.6	49.0	b.d.l.	b.d.l.	b.d.l.	2.6	17.5	0.7	0.1	13.1	0.2	b.d.l.	b.d.l.	b.d.l.	b.d.l.
Std. dev.		0.0	0.3	0.9	1.5	N/A	N/A	N/A	0.2	0.7	0.1	0.0	3.6	0.0	N/A	N/A	N/A	N/A
Min.		2.1	2.8	10.6	47.2	b.d.l.	b.d.l.	b.d.l.	2.4	16.7	0.6	0.1	10.9	0.2	b.d.l.	b.d.l.	b.d.l.	b.d.l.
Max.		2.2	3.3	12.1	50.0	b.d.l.	b.d.l.	b.d.l.	2.7	18.0	0.7	0.2	17.2	0.2	b.d.l.	b.d.l.	b.d.l.	b.d.l.
FG-030672B (3)	unknown	1.4	1.5	5.0	29.8	0.2	0.8	0.2	1.1	17.1	b.d.l.	b.d.l.	41.3	1.6	b.d.l.	b.d.l.	b.d.l.	b.d.l.
Std. dev.		0.1	0.2	0.6	1.2	0.0	0.3	0.2	0.1	0.7	N/A	N/A	1.9	0.5	N/A	N/A	N/A	N/A
Min.		1.4	1.4	4.4	28.4	0.2	0.4	0.1	1.0	16.6	b.d.l.	b.d.l.	39.9	1.0	b.d.l.	b.d.l.	b.d.l.	b.d.l.
Max.		1.6	1.7	5.6	30.5	0.2	1.1	0.4	1.3	17.9	b.d.l.	b.d.l.	43.4	2.1	b.d.l.	b.d.l.	b.d.l.	b.d.l.
FG-993152A (3)	unknown	1.6	3.8	13.1	52.5	0.3	b.d.l.	b.d.l.	2.7	17.0	0.8	0.2	6.3	1.7	b.d.l.	b.d.l.	b.d.l.	b.d.l.
Std. dev.		0.2	0.2	1.3	2.7	0.1	N/A	N/A	0.2	1.2	0.1	0.0	1.1	2.2	N/A	N/A	N/A	N/A
Min.		1.4	3.6	11.6	49.4	0.2	b.d.l.	b.d.l.	2.4	16.0	0.7	0.2	5.5	0.2	b.d.l.	b.d.l.	b.d.l.	b.d.l.
Max.		1.7	4.0	13.9	54.2	0.4	b.d.l.	b.d.l.	2.8	18.4	0.8	0.3	7.6	4.3	b.d.l.	b.d.l.	b.d.l.	b.d.l.
FG-993152B (5)	unknown	1.5	3.6	14.4	51.6	b.d.l.	0.3	0.1	2.7	16.5	0.7	0.2	8.2	0.3	b.d.l.	b.d.l.	b.d.l.	b.d.l.
Std. dev.		0.3	0.9	0.9	3.2	N/A	0.1	0.7	0.5	3.7	0.1	0.1	3.8	4.1	N/A	N/A	N/A	N/A
Min.		0.9	1.9	13.2	46.0	b.d.l.	0.1	0.1	1.7	8.4	0.6	0.1	6.1	0.2	b.d.l.	b.d.l.	b.d.l.	b.d.l.
Max.		1.6	4.1	15.3	53.6	b.d.l.	0.5	1.5	2.9	17.6	0.9	0.3	15.2	9.4	b.d.l.	b.d.l.	b.d.l.	b.d.l.

Mean bulk composition of speiss smelting slags. All results in wt% and normalized to 100%. Numbers in parentheses next to the sample name refer to the number of bulk analyses.

	Area	Na ₂ O	MgO	Al ₂ O ₃	SiO ₂	P ₂ O ₅	SO ₃	Cl	K ₂ O	CaO	TiO ₂	MnO	FeO	Cu ₂ O	ZnO	As ₂ O ₃
FG-030116A (9)	B	2.2	1.2	9.2	43.8	b.d.l.	b.d.l.	b.d.l.	2.4	14.4	0.4	1.0	24.2	b.d.l.	b.d.l.	1.2
Std. dev.		0.9	0.7	1.8	6.2	N/A	N/A	N/A	1.4	4.8	0.3	0.4	4.1	N/A	N/A	1.0
Min.		1.5	0.0	8.4	39.7	b.d.l.	b.d.l.	b.d.l.	1.6	2.1	0.0	0.0	13.8	b.d.l.	b.d.l.	0.1
Max.		4.4	1.8	14.0	59.8	b.d.l.	b.d.l.	b.d.l.	6.1	17.0	0.6	1.5	27.8	b.d.l.	b.d.l.	3.4
FG-030117 (3)	A	2.3	1.8	8.5	39.6	b.d.l.	b.d.l.	b.d.l.	1.6	14.9	b.d.l.	0.9	28.9	b.d.l.	b.d.l.	1.4
Std. dev.		0.8	0.1	0.7	3.6	N/A	N/A	N/A	0.1	0.6	N/A	0.3	5.3	N/A	N/A	0.3
Min.		1.5	1.7	7.8	37.1	b.d.l.	b.d.l.	b.d.l.	1.5	14.2	b.d.l.	0.7	22.9	b.d.l.	b.d.l.	1.2
Max.		1.5	1.7	7.8	37.1	b.d.l.	b.d.l.	b.d.l.	1.5	14.2	b.d.l.	0.7	22.9	b.d.l.	b.d.l.	1.2
FG-030119A (3)	A	1.9	2.3	10.5	48.3	b.d.l.	b.d.l.	b.d.l.	2.5	16.1	0.5	1.1	15.7	b.d.l.	b.d.l.	1.1
Std. dev.		0.2	0.2	0.2	0.6	N/A	N/A	N/A	0.1	0.2	0.0	0.2	0.5	N/A	N/A	0.2
Min.		1.7	2.2	10.4	47.7	b.d.l.	b.d.l.	b.d.l.	2.4	15.9	0.5	0.9	15.2	b.d.l.	b.d.l.	0.9
Max.		2.1	2.5	10.7	48.9	b.d.l.	b.d.l.	b.d.l.	2.6	16.3	0.6	1.3	16.2	b.d.l.	b.d.l.	1.3
FG-030119B (6)	A	2.3	1.5	7.8	38.7	b.d.l.	b.d.l.	b.d.l.	1.6	19.1	b.d.l.	1.2	23.7	b.d.l.	b.d.l.	3.4
Std. dev.		0.5	1.0	1.0	4.4	N/A	N/A	N/A	0.6	8.1	N/A	0.4	4.9	N/A	N/A	3.9
Min.		1.7	0.0	6.9	35.5	b.d.l.	b.d.l.	b.d.l.	0.9	5.6	b.d.l.	0.5	17.2	b.d.l.	b.d.l.	0.7
Max.		3.3	2.6	9.5	47.3	b.d.l.	b.d.l.	b.d.l.	2.6	28.9	b.d.l.	1.6	30.7	b.d.l.	b.d.l.	11.0
FG-040919 (6)	A	2.1	1.8	9.2	43.3	b.d.l.	0.6	b.d.l.	2.2	19.3	0.6	0.5	19.5	b.d.l.	b.d.l.	0.8
Std. dev.		0.3	0.1	0.5	2.3	N/A	0.3	N/A	0.2	1.0	0.1	0.2	2.0	N/A	N/A	0.2
Min.		1.8	1.7	8.7	42.0	b.d.l.	0.0	b.d.l.	2.0	17.4	0.6	0.0	15.5	b.d.l.	b.d.l.	0.5
Max.		2.5	2.0	10.2	48.1	b.d.l.	0.9	b.d.l.	2.6	19.9	0.7	0.7	20.7	b.d.l.	b.d.l.	1.0
FG-040919B (3)	A	2.0	1.6	8.0	35.8	b.d.l.	b.d.l.	b.d.l.	1.8	14.5	0.4	b.d.l.	34.1	b.d.l.	b.d.l.	1.6
Std. dev.		0.3	0.1	0.5	2.3	0.2	0.3	N/A	0.2	1.0	0.1	0.2	2.0	N/A	N/A	0.2
Min.		1.8	1.7	8.7	42.0	0.0	0.0	b.d.l.	2.0	17.4	0.6	0.0	15.5	b.d.l.	b.d.l.	0.5
Max.		2.5	2.0	10.2	48.1	0.6	0.9	b.d.l.	2.6	19.9	0.7	0.7	20.7	b.d.l.	b.d.l.	1.0

	Area	Na ₂ O	MgO	Al ₂ O ₃	SiO ₂	P ₂ O ₅	SO ₃	Cl	K ₂ O	CaO	TiO ₂	MnO	FeO	Cu ₂ O	ZnO	As ₂ O ₃
FG-011993 (3)	unknown	2.0	2.1	8.3	35.9	0.4	0.6	0.1	2.1	20.4	0.5	0.4	26.9	b.d.l.	b.d.l.	0.5
Std. dev.		0.1	0.0	0.3	0.7	0.0	0.0	0.0	0.1	1.0	0.0	0.0	1.3	N/A	N/A	0.1
Min.		1.9	2.1	7.9	35.2	0.4	0.6	0.1	1.9	19.3	0.4	0.4	25.4	b.d.l.	b.d.l.	0.4
Max.		2.0	2.1	8.5	36.7	0.4	0.6	0.1	2.2	21.3	0.5	0.4	27.7	b.d.l.	b.d.l.	0.6
FG-012232 (3)	D	1.8	3.3	12.6	49.2	0.3	b.d.l.	0.1	2.5	16.0	0.8	0.2	12.8	b.d.l.	b.d.l.	0.5
Std. dev.		0.2	0.1	0.9	2.4	0.1	N/A	0.0	0.4	1.5	0.0	0.0	4.5	N/A	N/A	0.1
Min.		1.6	3.1	11.8	47.4	0.2	b.d.l.	0.0	2.1	14.6	0.8	0.2	8.8	b.d.l.	b.d.l.	0.4
Max.		2.0	3.4	13.5	52.0	0.3	b.d.l.	0.1	2.8	17.6	0.8	0.3	17.7	b.d.l.	b.d.l.	0.6
FG-012234 (3)	D	3.7	2.0	9.0	37.1	0.4	0.7	0.1	1.5	22.1	0.4	0.2	22.2	0.1	b.d.l.	0.5
Std. dev.		0.3	0.2	0.4	0.6	0.0	0.1	0.0	0.2	1.8	0.0	0.0	3.3	0.1	N/A	0.1
Min.		3.4	1.8	8.7	36.5	0.4	0.6	0.1	1.3	20.6	0.4	0.2	18.4	b.d.l.	b.d.l.	0.5
Max.		4.0	2.2	9.5	37.6	0.4	0.8	0.2	1.7	24.1	0.4	0.2	24.3	0.3	b.d.l.	0.6
FG-000116A (3)	B	2.0	2.6	7.9	48.0	0.5	0.5	0.1	2.0	22.6	0.4	0.1	12.8	b.d.l.	b.d.l.	0.4
Std. dev.		0.5	0.0	0.8	1.7	0.1	0.1	0.0	0.5	1.7	0.1	0.0	1.1	N/A	N/A	0.1
Min.		1.7	2.6	7.1	46.4	0.4	0.4	0.1	1.5	21.2	0.3	0.1	11.6	b.d.l.	b.d.l.	0.3
Max.		2.7	2.7	8.7	49.8	0.5	0.6	0.1	2.6	24.6	0.5	0.2	13.7	b.d.l.	b.d.l.	0.5
FG-000116B (3)	B	3.2	3.5	9.2	38.9	0.6	0.8	b.d.l.	1.7	28.9	0.5	0.2	12.2	b.d.l.	b.d.l.	0.4
Std. dev.		0.6	0.1	0.3	1.1	0.1	0.1	N/A	0.2	0.6	0.0	0.0	2.5	N/A	N/A	0.1
Min.		2.8	3.4	8.8	37.8	0.5	0.7	b.d.l.	1.6	28.2	0.4	0.2	10.0	b.d.l.	b.d.l.	0.3
Max.		3.9	3.6	9.4	39.9	0.6	0.8	b.d.l.	1.9	29.4	0.5	0.2	14.9	b.d.l.	b.d.l.	0.5
FG-030118 (4)	A	2.9	1.6	10.6	40.0	0.5	0.3	0.1	1.7	13.2	0.6	0.2	27.8	b.d.l.	b.d.l.	0.4
Std. dev.		0.1	0.1	0.2	0.5	0.0	0.0	0.0	0.1	0.2	0.0	0.0	0.9	N/A	N/A	0.0
Min.		2.8	1.6	10.5	39.6	0.4	0.3	0.1	1.6	12.9	0.6	0.2	26.9	b.d.l.	b.d.l.	0.3
Max.		3.1	1.7	10.9	40.7	0.5	0.3	0.2	1.7	13.5	0.7	0.3	28.6	b.d.l.	b.d.l.	0.4

	Area	Na ₂ O	MgO	Al ₂ O ₃	SiO ₂	P ₂ O ₅	SO ₃	Cl	K ₂ O	CaO	TiO ₂	MnO	FeO	Cu ₂ O	ZnO	As ₂ O ₃
FG-030123B (4)	A	2.2	1.9	9.2	39.7	0.3	0.3	0.2	2.1	18.6	0.5	0.5	23.0	b.d.l.	b.d.l.	1.5
Std. dev.		0.1	0.2	0.2	0.4	0.0	0.1	0.1	0.1	0.9	0.0	0.0	0.6	N/A	N/A	0.3
Min.		2.1	1.6	8.9	39.5	0.3	0.2	0.1	1.9	18.0	0.5	0.5	22.3	b.d.l.	b.d.l.	1.2
Max.		2.2	2.1	9.3	40.4	0.4	0.4	0.2	2.2	19.9	0.6	0.6	23.6	b.d.l.	b.d.l.	1.8
FG-040920A (6)	D	2.4	1.3	7.6	34.2	0.6	0.5	0.3	1.8	20.7	0.4	0.5	29.3	b.d.l.	b.d.l.	0.5
Std. dev.		0.1	0.1	0.2	0.5	0.0	0.1	0.2	0.1	1.0	0.0	0.0	1.4	N/A	N/A	0.3
Min.		2.3	1.2	7.3	33.4	0.5	0.4	0.0	1.6	19.4	0.3	0.5	27.3	b.d.l.	b.d.l.	0.2
Max.		2.5	1.4	7.8	34.7	0.6	0.7	0.3	1.9	22.2	0.4	0.6	31.3	b.d.l.	b.d.l.	0.9
FG-993154 (3)	unknown	2.2	1.5	9.1	40.7	0.4	0.4	0.1	2.0	16.1	0.5	0.6	26.1	b.d.l.	b.d.l.	0.4
Std. dev.		0.2	0.0	0.1	0.5	0.0	0.0	0.0	0.0	0.2	0.0	0.0	0.2	N/A	N/A	0.0
Min.		2.0	1.5	9.0	40.1	0.4	0.3	0.1	1.9	15.9	0.5	0.6	25.8	b.d.l.	b.d.l.	0.4
Max.		2.5	1.6	9.2	41.0	0.4	0.4	0.2	2.0	16.3	0.5	0.7	26.2	b.d.l.	b.d.l.	0.5
FG-010506 (4)	A	2.7	1.4	8.7	35.1	0.5	0.4	0.1	1.7	14.3	0.4	0.3	33.4	b.d.l.	b.d.l.	0.9
Std. dev.		0.2	0.1	0.2	0.6	0.0	0.0	0.0	0.0	0.4	0.0	0.0	0.5	N/A	N/A	0.1
Min.		2.4	1.3	8.6	34.6	0.5	0.4	0.1	1.7	13.9	0.4	0.3	32.9	b.d.l.	b.d.l.	0.8
Max.		2.9	1.6	9.0	36.0	0.5	0.5	0.2	1.7	14.7	0.4	0.4	34.1	b.d.l.	b.d.l.	1.0

Mean bulk composition of 'black' slags. All results in wt% and normalized to 100%. Numbers in parentheses next to the sample name refer to the number of bulk analyses.

	Area	Na ₂ O	MgO	Al ₂ O ₃	SiO ₂	P ₂ O ₅	SO ₃	Cl	K ₂ O	CaO	TiO ₂	MnO	FeO	CuO	ZnO	As ₂ O ₃
FG-030116B (3)	A	3.2	3.5	9.2	38.9	0.6	0.8	b.d.l.	1.7	28.9	0.5	0.2	12.2	b.d.l.	b.d.l.	0.4
Std. dev.		0.6	0.1	0.3	1.1	0.1	0.1	N/A	0.2	0.6	0.0	0.0	2.5	N/A	N/A	0.1
Min.		2.8	3.4	8.8	37.8	0.5	0.7	b.d.l.	1.6	28.2	0.4	0.2	10.0	b.d.l.	b.d.l.	0.3
Max.		3.9	3.6	9.4	39.9	0.6	0.8	b.d.l.	1.9	29.4	0.5	0.2	14.9	b.d.l.	b.d.l.	0.5
FG-010505 (12)	A	2.4	2.2	10.5	48.5	0.2	0.1	b.d.l.	2.6	17.2	0.6	0.1	15.2	0.2	b.d.l.	0.4
Std. dev.		0.3	0.1	0.7	1.9	0.3	0.2	N/A	0.3	0.7	0.1	0.2	2.4	0.2	N/A	0.3
Min.		1.9	2.1	9.6	46.1	0.0	0.0	b.d.l.	2.3	15.6	0.4	0.0	9.4	0.0	b.d.l.	0.0
Max.		3.0	2.6	12.3	52.9	0.7	0.5	b.d.l.	3.3	18.0	0.7	0.5	18.5	0.5	b.d.l.	0.9
FG-012007A (3)	unknown	1.8	2.8	10.9	47.3	0.4	0.2	0.1	2.5	19.0	0.6	0.4	13.7	b.d.l.	b.d.l.	0.3
Std. dev.		0.0	0.0	0.3	1.8	0.0	0.0	0.0	0.1	0.5	0.0	0.0	1.6	N/A	N/A	0.1
Min.		1.7	2.8	10.7	46.1	0.4	0.2	0.1	2.5	18.4	0.6	0.3	11.8	b.d.l.	b.d.l.	0.2
Max.		1.8	2.8	11.2	49.4	0.4	0.3	0.1	2.6	19.4	0.7	0.4	14.8	b.d.l.	b.d.l.	0.4
FG-012254 (3)	D	2.2	2.2	9.8	42.0	0.3	0.2	0.1	2.0	22.3	0.6	0.6	16.8	b.d.l.	b.d.l.	0.8
Std. dev.		0.0	0.1	0.2	0.5	0.0	0.0	0.0	0.1	0.6	0.0	0.0	0.2	N/A	N/A	0.1
Min.		2.1	2.1	9.6	41.5	0.3	0.2	0.2	1.9	22.0	0.6	0.6	16.6	b.d.l.	b.d.l.	0.8
Max.		2.2	2.3	10.0	42.3	0.4	0.3	0.2	2.1	23.0	0.6	0.6	17.0	b.d.l.	b.d.l.	0.9
FG-030704A (3)	unknown	3.0	3.5	9.0	41.0	0.4	0.2	b.d.l.	3.1	16.6	0.5	b.d.l.	17.9	4.6	b.d.l.	0.2
Std. dev.		0.1	0.0	0.6	1.0	0.0	0.1	N/A	0.1	0.3	0.1	N/A	1.3	0.1	N/A	0.0
Min.		2.9	3.5	8.6	40.2	0.3	0.1	b.d.l.	3.0	16.3	0.4	b.d.l.	16.6	4.6	b.d.l.	0.2
Max.		3.1	3.5	9.7	42.1	0.4	0.2	b.d.l.	3.1	17.0	0.5	b.d.l.	19.3	4.8	b.d.l.	0.2
FG-030704B (3)	unknown	2.5	2.4	9.2	51.3	0.5	b.d.l.	b.d.l.	2.2	12.3	0.6	0.2	18.4	0.3	b.d.l.	b.d.l.
Std. dev.		0.2	0.2	0.8	3.8	0.0	N/A	N/A	0.1	1.1	0.1	0.0	2.5	0.1	N/A	N/A
Min.		2.3	2.2	8.5	48.4	0.5	b.d.l.	b.d.l.	2.1	11.7	0.5	0.2	15.9	0.3	b.d.l.	b.d.l.
Max.		2.7	2.6	10.1	55.6	0.6	b.d.l.	b.d.l.	2.3	13.6	0.7	0.2	20.8	0.4	b.d.l.	b.d.l.

	Area	Na ₂ O	MgO	Al ₂ O ₃	SiO ₂	P ₂ O ₅	SO ₃	Cl	K ₂ O	CaO	TiO ₂	MnO	FeO	CuO	ZnO	As ₂ O ₃
FG-030704C (3)	unknown	1.9	3.1	13.1	51.2	b.d.l.	b.d.l.	0.1	2.8	16.3	0.8	0.2	10.1	0.1	b.d.l.	0.3
Std. dev.		0.1	0.0	0.0	0.4	N/A	N/A	0.0	0.1	0.5	0.0	0.0	0.1	0.1	N/A	0.1
Min.		1.8	3.1	13.1	50.9	b.d.l.	b.d.l.	0.1	2.8	15.7	0.8	0.2	10.0	0.1	b.d.l.	0.3
Max.		2.0	3.1	13.1	51.7	b.d.l.	b.d.l.	0.1	3.0	16.7	0.8	0.2	10.2	0.2	b.d.l.	0.4
FG-030974C (3)	unknown	2.1	2.9	12.3	49.2	0.4	0.3	0.1	2.5	18.1	0.7	0.3	10.7	0.1	b.d.l.	0.3
Std. dev.		0.2	0.2	0.5	1.2	0.0	0.2	0.0	0.2	2.3	0.0	0.0	0.8	0.1	N/A	0.0
Min.		1.9	2.7	11.9	47.9	0.4	0.2	0.1	2.3	16.1	0.7	0.2	9.9	0.1	b.d.l.	0.3
Max.		2.3	3.2	12.8	50.3	0.5	0.5	0.1	2.7	20.6	0.7	0.3	11.3	0.2	b.d.l.	0.3
FG-030974D (3)	unknown	1.2	2.8	8.9	45.4	0.4	b.d.l.	0.2	1.5	15.8	0.6	0.3	21.6	1.3	b.d.l.	0.1
Std. dev.		0.2	0.1	0.2	0.5	0.0	N/A	0.1	0.1	0.3	0.0	0.0	1.6	0.3	N/A	0.0
Min.		1.0	2.6	8.6	44.8	0.4	b.d.l.	0.2	1.4	15.6	0.5	0.3	20.2	1.0	b.d.l.	0.1
Max.		1.4	2.9	9.1	45.8	0.4	b.d.l.	0.3	1.6	16.1	0.6	0.4	23.4	1.7	b.d.l.	0.2
FG-012255 (3)	D	2.1	2.5	10.2	42.8	0.5	0.4	0.1	2.3	22.1	0.6	0.3	15.7	b.d.l.	b.d.l.	0.6
Std. dev.		0.0	0.0	0.1	0.3	0.0	0.0	0.0	0.0	0.1	0.0	0.0	0.4	N/A	N/A	0.1
Min.		2.1	2.4	10.1	42.5	0.5	0.4	0.1	2.2	22.0	0.5	0.3	15.3	b.d.l.	b.d.l.	0.5
Max.		2.2	2.5	10.3	43.1	0.5	0.4	0.1	2.3	22.2	0.6	0.3	16.0	b.d.l.	b.d.l.	0.7

Mean bulk composition of matte droplets. All results in wt% and normalized to 100%. Numbers in parentheses next to the sample name refer to the number of bulk analyses.

	Area	O	S	Fe	Ni	Cu	Zn	As	Pb
FG-030974F (1)	unknown	b.d.l.	21.6	b.d.l.	b.d.l.	78.4	b.d.l.	b.d.l.	b.d.l.
FG-030689 (3)	unknown	3.5	21.6	0.9	0.3	60.2	1.9	7.4	4.4
Std. dev.		0.4	0.8	0.4	0.1	4.8	0.9	3.2	0.6
Min.		3.0	20.9	0.5	0.2	53.1	1.4	5.6	3.7
Max.		3.8	22.7	1.3	0.3	62.9	3.3	12.1	4.9

C.4 Lead isotopes

Lead isotope ratios of copper droplets and slag. Results were obtained by MC-ICP-MS at CEZA and are published in Pernicka et al. (2011). Assessment of what constituted speiss or copper slag was mostly based on newly obtained compositional analyses by SEM-EDS. In cases where no new analyses were conducted, the samples were sorted according to bulk Cu and As contents obtained from the same publication determined by ED-XRF.

Sample	Type	Context	208pb/206pb	207Pb/206Pb	206Pb/204Pb
FG-010505	Black slag	A	2.0856	0.84531	18.563
FG-010506	Speiss slag	A	2.1206	0.87299	17.961
FG-012233B	Speiss slag	A	2.0854	0.84434	18.553
FG-000119	Copper slag	A	2.0925	0.85149	18.655
FG-010476C	copper slag	A	2.0827	0.84383	18.799
FG-010484	copper slag	A	2.0816	0.84258	18.615
FG-012256-A	copper slag	A	2.0861	0.84298	18.567
FG-012269B	copper slag	C	2.0914	0.84588	18.500
FG-012270A	copper slag	C	2.0929	0.84420	18.652
FG-012270B	copper slag	C	2.0876	0.84261	18.590
FG-010504A	copper slag	D	2.0928	0.84516	18.568
FG-010504	copper slag	D	2.0922	0.85162	18.492
FG-012275	copper slag	A	2.0936	0.84594	18.534
FG-010501A	copper slag	Arisman 2	2.0833	0.84129	18.620
FG-010501	copper slag	Arisman 2	2.0854	0.84816	18.606
FG-000118	copper slag	near the qanat	2.0964	0.84777	18.503
FG-012257	Copper prill	A	2.1216	0.87237	17.979
FG-012244	Copper prill	A	2.0968	0.85253	18.379
FG-012247	Copper prill	A	2.1139	0.86659	18.108
FG-012246	Copper prill	A	2.1077	0.86197	18.190
FG-012245	Copper prill	A	2.0946	0.84708	18.519
FG-012250	Copper prill	A	2.0871	0.84474	18.522